

2009 Condensed Phase and Interfacial Molecular Science Research Meeting



**Airlie Conference Center
Warrenton, Virginia
October 18-21, 2009**



U.S. DEPARTMENT OF
ENERGY

Office of
Science

Office of Basic Energy Sciences
Chemical Sciences, Geosciences &
Biosciences Division

Foreword

This volume summarizes the scientific content of the 2009 Research Meeting on Condensed Phase and Interfacial Molecular Science (CPIMS) sponsored by the U. S. Department of Energy (DOE), Office of Basic Energy Sciences (BES). The research meeting is held annually for the DOE laboratory and university principal investigators within the BES CPIMS Program to facilitate scientific interchange among the PIs and to promote a sense of program identity.

FY2009 has been exciting for BES, including the funding of forty-six new Energy Frontier Research Centers (EFRCs). Since its founding, the CPIMS Contractors' Meeting has fostered connections across BES research programs. In keeping with that notion, we have invited two investigators who receive funding from EFRCs: Emily Carter (Princeton University) will speak about the EFRC on Combustion Science, and Peter Rossky (University of Texas at Austin) will speak about the EFRC on Understanding Charge Separation and Transfer at Interfaces in Energy Materials and Devices.

During the past year, 95 Single Investigator and Small Group Research (SISGR) proposals have been selected for funding, with five of these new awards being managed as part of the CPIMS program. The CPIMS 2009 meeting includes presentations by three of these new projects. The past year also brought new funding for proposals in Theoretical and Computational Chemistry, resulting in 15 new grants. CPIMS 2009 will include presentations from several principal investigators who receive funding from these grants.

We are deeply indebted to the members of the scientific community who have contributed valuable time toward the review of proposals and programs. These thorough and thoughtful reviews are central to the continued vitality of the CPIMS Program. We appreciate the privilege of serving in the management of this research program. In carrying out these tasks, we learn from the achievements and share the excitement of the research of the many sponsored scientists and students whose work is summarized in the abstracts published on the following pages.

This year's speakers are most gratefully acknowledged for their investment of time and for their willingness to share their ideas with the meeting participants. Thanks to the staff of the Oak Ridge Institute for Science and Education, in particular Margaret Lyday, Connie Lansdon, and to the Airlie Conference Center for assisting with the meeting. We also thank Diane Marceau, Robin Felder, and Michaelene Kyler-King in the Chemical Sciences, Biosciences, and Geosciences Division for their indispensable behind-the-scenes efforts in support of the CPIMS program. Finally, we acknowledge Larry Rahn for his expert help in assembling this volume.

Gregory J. Fiechtner and Mark R. Pederson
Fundamental Interactions Team
Chemical Sciences, Geosciences and Biosciences Division
Office of Basic Energy Sciences

Cover art courtesy of Diane Marceau, Office of Basic Energy Sciences, Chemical Sciences, Geosciences, and Biosciences Division.

This document was produced under contract number DE-AC05-06OR23100 between the U.S. Department of Energy and Oak Ridge Associated Universities.

The research grants and contracts described in this document are supported by the U.S. DOE Office of Science, Office of Basic Energy Sciences, Chemical Sciences, Geosciences and Biosciences Division.

Agenda

**U. S. Department of Energy
Office of Basic Energy Sciences
2009 Meeting on Condensed Phase and Interfacial Molecular Sciences**

Sunday, October 18

3:00-6:00 pm **** Registration ****
6:00 pm **** Reception (Whistling Swan Pub, No Host) ****
7:00 pm **** Dinner (Airlie Room) ****

Monday, October 19

7:30 am **** Breakfast (Airlie Room) ****
8:30 am *Introductory Remarks*
Eric Rohlfing, DOE Basic Energy Sciences
Gregory J. Fiechtner, DOE Basic Energy Sciences
Mark Pederson, DOE Basic Energy Sciences
Session I *Chair: Scott Anderson*, University of Utah
9:15 am *Electronically Non-adiabatic Interactions in Molecule Metal-surface Scattering:
Can We Trust the Born-Oppenheimer Approximation in Surface Chemistry?*
Alec Wodtke, University of California at Santa Barbara
9:45 am *Chemical Imaging and Dynamical Studies of Reactivity and Emergent
Behavior in Complex Interfacial Systems*
Steven Sibener, University of Chicago
10:15 am *An Exploration of Catalytic Chemistry on Au/Ni(111)*
Sylvia Ceyer, MIT
10:45 am **** Break ****
11:00 am *Spectroscopy of Organometallic Radicals*
Michael D. Morse, University of Utah
11:30 am *Manipulating Light with Transition Metal Clusters and Dyes*
Serdar Ogut, University of Illinois-Chicago
12:00 noon *Overview of the Combustion Energy Frontier Research Center (CEFRC)*
Emily Carter, Princeton University
12:30 pm **** Lunch (Airlie Room) ****

- Session II** Chair: **Chris Mundy**, Pacific Northwest National Laboratory
- 4:00 pm *Overview of the DOE Energy Frontier Research Center: Understanding Charge Separation and Transfer at Interfaces in Energy Materials and Devices*
Peter Rossky, University of Texas
- 4:30 pm *Correlating Electronic and Nuclear Motions During Photoinduced Charge Transfer Processes using Multidimensional Femtosecond Spectroscopies and Ultrafast X-ray Absorption Spectroscopy*
Munira Khalil, University of Washington
- 5:00 pm *Optimizing Interfacial Charge Transfer in Photocatalytic Water Splitting Devices*
Marivi Fernandez-Serra, SUNY Stony Brook
- 5:30 pm *Nucleation: From Vapor Phase Clusters to Crystals in Solution*
Shawn Kathmann, Pacific Northwest National Laboratory
- 6:00 pm ***** Reception (No Host, Jefferson Room) *****
- 6:30 pm ***** Dinner (Airlie Room) *****

Tuesday, October 20

- 7:30 am ***** Breakfast (Airlie Room) *****
- Session III** Chair: **Richard Osgood**, Columbia University
- 8:30 am *Optical Manipulation of Ultrafast Electron and Nuclear Motion on Metal Surfaces*
Hrvoje Petek, University of Pittsburgh
- 9:00 am *Imaging Mass Spectrometry, Aerosol Chemistry and Biomolecule Energetics with VUV Radiation*
Musahid Ahmed, Lawrence Berkeley National Laboratory
- 9:30 am *The Quest for Ultimate Sensitivity in Nonlinear Optical Imaging*
Sunney Xie, Harvard University
- 10:00 am ***** Break *****
- 10:30 am *Fluctuations in Macromolecules Studied Using Time-Resolved, Multi-spectral Single Molecule Imaging*
Carl Hayden, Sandia National Laboratories
- 11:00 am *Reactions of Ions and Radicals in Aqueous Systems*
Marat Valiev, Pacific Northwest National Laboratory
- 11:30 am *Radiolysis of Water Adsorbed on Ceramic Oxides*
Jay LaVerne, Notre Dame Radiation Laboratory
- 12:00 noon ***** Lunch (Airlie Room) *****

- Session IV** Chair: **John Miller**, Brookhaven National Laboratory
- 4:00 pm *Reactive Intermediates in the Condensed Phase: Radiation and Photochemistry*
Robert Crowell, Brookhaven National Laboratory
- 4:30 pm *Ion Solvation in Nonuniform Aqueous Environments*
Phillip Geissler, Lawrence Berkeley National Laboratory
- 5:00 pm *Computational Studies of Radiolytic Species and Processes in Water*
Daniel Chipman, Notre Dame Radiation Laboratory
- 5:30 pm *DFT Calculations on Carotenoid-porphyrin-C₆₀ Light-harvesting Molecular Triad*
Tunna Baruah, University Texas-El Paso
- 6:00 pm **** Reception (No Host, Jefferson Room) ****
- 6:30 pm **** Banquet Dinner (Jefferson Room) ****

Wednesday, October 21

- 7:30 am **** Breakfast (Airlie Room) ****
- Session V** Chair: **Kenneth B. Eisenthal**, Columbia University
- 9:00 am *Plasmonic Field Effects on the Proton Pump System of Bacteriorhodopsin*
Mostafa El-Sayed, Georgia Institute of Technology
- 9:30 am *From Charge Transfer to Coupled Charge Transport: A Multiscale Approach
for Complex Systems*
Jessica Swanson, University of Utah
- 10:00 am *Solution Reactivity of Nitrogen Oxides, Oxoacids, and Oxoanions*
Sergei Lymar, Brookhaven National Laboratory
- 10:30 am *Electronic Structure of Transition Metal Clusters and Actinide Complexes and
Their Reactivity*
Krishnan Balasubramanian, California State University-East Bay
- 11:00 am *Closing Remarks*
Greg Fiechtner, DOE Basic Energy Sciences
- 11:30 am **** Lunch (Airlie Room) ****

Table of Contents

Table of Contents

Foreword.....	i
Agenda	iii
Table of Contents	vii
Guest Speaker Abstracts	1
Emily Carter – Overview of the Combustion Energy Frontier Research Center (CEFRC).....	1
Peter Rossky – Overview of the DOE Energy Frontier Research Center: Understanding Charge Separation and Transfer at Interfaces in Energy Materials and Devices...3	
CPIMS Principal Investigator Abstracts	5
Musahid Ahmed – Imaging Mass Spectrometry, Aerosol Chemistry and Biomolecule Energetics with VUV Radiation.....	5
Scott Anderson – Model Catalysis by Size-Selected Cluster Deposition.....	9
K. Balasubramanian – Electronic Structure of Transition Metal Clusters and Actinide Complexes and Their Reactivity	13
David M. Bartels, John Bentley and Daniel M. Chipman – Influence of Medium on Radical Reactions	17
Tunna Baruah – DFT Calculations on Carotenoid-porphyrin-C ₆₀ Light-harvesting Molecular Triad.....	21
Ian Carmichael, David M. Bartels, Daniel M. Chipman and Jay A. Laverne – Electron-Driven Processes in Condensed Phases	23
A. W. Castleman, Jr. – Development of Structure-Reactivity Relationships within Heterogeneous Catalysts through Gas-Phase Cluster Investigations	27
Sylvia T. Ceyer – An Exploration of Catalytic Chemistry on Au/Ni(111)	31
David Chandler – Theory of Dynamics of Complex Systems.....	35
Daniel M. Chipman – Computational Studies of Radiolytic Species and Processes in Water	39
Andrew R. Cook and John R. Miller – Fast Reactions Investigated With Picosecond Electron Pulses	43
James P. Cowin – Chemical Kinetics and Dynamics at Interfaces; Solvation / Fluidity on the Nanoscale and in the Environment	47
Robert A. Crowell – Reactive Intermediates in the Condensed Phase: Radiation and Photochemistry.....	51
Liem X. Dang – Computational Studies of X-ray Reflectivity Liquid Interfaces, Reorientation Mechanism of Hydroxide Ions in Water and CO ₂ Capture	55
Michael A. Duncan – Transition Metal-Molecular Interactions Studied with Cluster Ion Infrared Spectroscopy.....	59
Michel Dupuis – Electronic Structure and Reactivity Studies for Aqueous Phase Chemistry ..	63
Kenneth B. Eisenthal – Photochemistry at Interfaces	65
G. Barney Ellison – Interfacial Oxidation of Complex Organic Molecules	69
Mostafa A. El-Sayed – Plasmonic Field Effects on the Proton Pump System of Bacteriorhodopsin	73

Jim Evans – Statistical Mechanical and Multiscale Modeling of Surface Reaction Processes ..	77
Michael D. Fayer – Liquid and Chemical Dynamics in Nanoscopic Environments.....	81
Marivi Fernandez-Serra – Optimizing Interfacial Charge Transfer in Photocatalytic Water Splitting Devices.....	85
John L. Fulton – Chemical Kinetics and Dynamics at Interfaces	89
Phillip L. Geissler – Ion Solvation in Nonuniform Aqueous Environments.....	93
Mark S. Gordon – Theoretical Studies of Surface Science, Heterogeneous Catalysis, and Intermolecular Interactions	97
Charles B. Harris – Dynamics of Electrons at Interfaces on Ultrafast Timescales	101
Ian Harrison – Catalysis at Metal Surfaces Studied by Non-Equilibrium and STM Methods	105
Carl Hayden – Fluctuations in Macromolecules Studied Using Time-Resolved, Multi- Spectral Single Molecule Imaging.....	107
Wayne P. Hess – Chemical Kinetics and Dynamics at Interfaces: Laser Induced Reactions in Solids and at Surfaces.....	111
So Hirata – Breakthrough Design and Implementation of Electronic and Vibrational Many- Body Theories	115
Wilson Ho – Spectroscopic Imaging toward Space-Time Limit	119
Bret E. Jackson – Theory of the Reaction Dynamics of Small Molecules on Metal Surfaces.....	123
Caroline Chick Jarrold and Krishnan Raghavachari – Probing Catalytic Activity in Defect Sites in Transition Metal Oxides and Sulfides Using Cluster Models: A Combined Experimental and Theoretical Approach.....	127
Ken D. Jordan and Mark A. Johnson – Coordinating Experiment and Theory to Understand how Excess Electrons are Accommodated by Water Networks Through Model Studies in the Cluster Regime	131
Shawn M. Kathmann – Nucleation: From Vapor Phase Clusters to Crystals in Solution.....	135
Bruce D. Kay – Chemical Kinetics and Dynamics at Interfaces: Structure and Reactivity of Ices, Oxides, and Amorphous Materials	139
Munira Khalil – Correlating Electronic and Nuclear Motions during Photoinduced Charge Transfer Processes using Multidimensional Femtosecond Spectroscopies and Ultrafast X-ray Absorption Spectroscopy.....	143
Greg A. Kimmel – Chemical Kinetics and Dynamics at Interfaces: Non-Thermal Reactions at Surfaces and Interfaces	145
Jay A. LaVerne – Radiolysis of Water Adsorbed on Ceramic Oxides.....	149
Jay A. LaVerne, Dan Meisel, Ian Carmichael and Daniel M. Chipman – Radiation Effects in Heterogeneous Systems and at Interfaces	153
H. Peter Lu – Single-Molecule Interfacial Electron Transfer	157
Sergei V. Lymar – Solution Reactivity of Nitrogen Oxides, Oxoacids, and Oxoanions.....	161
Michael D. Morse – Spectroscopy of Organometallic Radicals.....	165
Christopher J. Mundy – <i>Ab initio</i> Approach to Interfacial Processes in Hydrogen Bonded Fluids	169
Serdar Ogut – Manipulating Light with Transition Metal Clusters and Dyes	173
Richard Osgood – Laser Dynamic Studies of Photoreactions on Nanostructured Surfaces...	177
Hrvoje Petek – Optical Manipulation of Ultrafast Electron and Nuclear Motion on Metal Surfaces.....	181
Richard J. Saykally – X-Ray Spectroscopy of Volatile Liquids and their Surfaces.....	185

Gregory K. Schenter – Molecular Theory & Modeling: Development of Statistical Mechanical Techniques for Complex Condensed-Phase Systems	189
Steven J. Sibener – Chemical Imaging and Dynamical Studies of Reactivity and Emergent Behavior in Complex Interfacial Systems	193
Timothy C. Steimle – Generation, Detection and Characterization of Gas-Phase Transition Metal Containing Molecules	197
Jessica M.J. Swanson – From Charge Transfer to Coupled Charge Transport: A Multiscale Approach for Complex Systems.....	201
Ward H. Thompson – Understanding Nanoscale Confinement Effects in Solvent-Driven Chemical Reactions	203
Andrei Tokmakoff – Structural Dynamics in Complex Liquids Studied with Multidimensional Vibrational Spectroscopy	207
John C. Tully – The Role of Electronic Excitations on Chemical Reaction Dynamics at Metal, Semiconductor and Nanoparticle Surfaces	211
Marat Valiev and Bruce C. Garrett – Reactions of Ions and Radicals in Aqueous Systems	215
Xue-Bin Wang – Chemical Kinetics and Dynamics at Interfaces: Gas Phase Investigation of Condensed Phase Phenomena	219
Michael G. White – Surface Chemical Dynamics.....	223
James F. Wishart – Ionic Liquids: Radiation Chemistry, Solvation Dynamics and Reactivity Patterns	227
Alec M. Wodtke – Electronically Non-adiabatic Interactions in Molecule Metal-surface Scattering: Can We Trust the Born-Oppenheimer Approximation in Surface Chemistry?	231
Sotiris S. Xantheas – Molecular Level Understanding of Hydrogen Bonding Environments.	235
Sunney Xie – The Quest for Ultimate Sensitivity in Nonlinear Optical Imaging	239
Author Index	241
List of Participants	243

Guest Speaker Abstracts

Overview of the Combustion Energy Frontier Research Center (CEFRC)
Director: Chung K. Law
Lead Institution: Princeton University

Emily A. Carter, CEFRC Co-Director
Department of Mechanical and Aerospace Engineering
Princeton University, Princeton, NJ 08544-5263
eac@princeton.edu

Energy sustainability and security, along with imminent global warming, have created the need to develop renewable transportation fuels. Predictive tools relating the fuel constituent composition and operational characteristics of energy conversion systems are needed over the next few decades as the world transitions away from conventional, petroleum-derived transportation fuels. Empirical approaches to developing new engines and certifying new fuels have led to only incremental improvements, and as such they cannot meet future challenges in a timely, cost-effective manner. Achieving the required rate of innovation will depend strongly upon computer-aided design, as is currently used to design the aerodynamically efficient air frame of advanced commercial aircraft. The diversity of alternative fuels and the corresponding variation in their physical and chemical properties, coupled with simultaneous changes in the design/control strategies of energy conversion devices to improve efficiency and reduce emissions, pose immense technical challenges. These challenges are particularly daunting since energy conversion efficiencies and exhaust emissions are governed by coupled chemical and transport processes at multiple length scales ranging from the electronic structure of molecules to molecular interactions and rearrangements to nanoscale particulate formation to turbulent fuel/air mixing. Fortunately, recent advances in quantum chemistry, chemical kinetics, reactive flow simulation, scientific computation, and experimental flame diagnostics suggest that first-principles-based predictive tools for optimum integration of energy conversion and control methodologies and new fuel compositions are possible. Figure 1 shows the calculated turbulent flame structure of an ethylene-air jet flame using direct numerical simulation (DNS) and a realistic model of the chemistry.

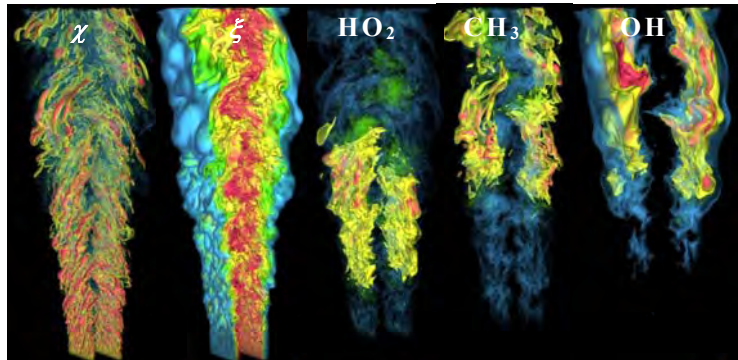


Figure 1: DNS of a lifted ethylene-air jet flame in a heated coflow at a Reynolds number of 10,000. Instantaneous volume rendering from left to right: scalar dissipation rate, mixture fraction, and mass fractions of HO₂, CH₃, and OH.

Motivated by the above challenges and opportunities, the research goals of the Combustion-EFRC are:

- 1) To advance fundamental understanding and practice of combustion and fuel science. This includes the development of quantum mechanical methods for thermochemistry and kinetics at high pressures, the development of nonequilibrium transport models and models of nanoscale particulate inception, growth and oxidation, and the discovery and modeling of new phenomena of near-limit laminar and turbulent combustion.

- 2) To create experimental validation platforms and databases for kinetics, thermochemistry, transport processes, and flame structure through application of advanced extractive and in situ diagnostic methods.
- 3) To enable automated kinetic model generation and reduction.
- 4) To implement validated, multi-scale, quantitative prediction methods for novel energy conversion design/control concepts tailored to physical and chemical properties of non-petroleum-based fuels.

Combustion Energy Frontier Research Center (C-EFRC)

Princeton University	C.K. Law (Director) , E.A. Carter (Co-Director), F.L. Dryer, Y. Ju
Argonne National Laboratory	S.J. Klippenstein
Cornell University	S.B. Pope
Massachusetts Institute of Technology	W.H. Green
Sandia National Laboratories	J.H. Chen, N. Hansen, J.A. Miller
Stanford University	R.K. Hanson
University of Connecticut	C.J. Sung
University of Minnesota	D.G. Truhlar
University of Southern California	F.N. Egolfopoulos, H. Wang

Contact: Professor Chung K. (Ed) Law
 Department of Mechanical and Aerospace Engineering
 Princeton University
 cklaw@princeton.edu; efrc@princeton.edu
 609-258-5271 (voice); 609-258-6233 (fax)

**Overview of the DOE Energy Frontier Research Center:
*Understanding Charge Separation and Transfer
at Interfaces in Energy Materials and Devices*
(Paul F. Barbara, Director)**

Peter J. Rossky

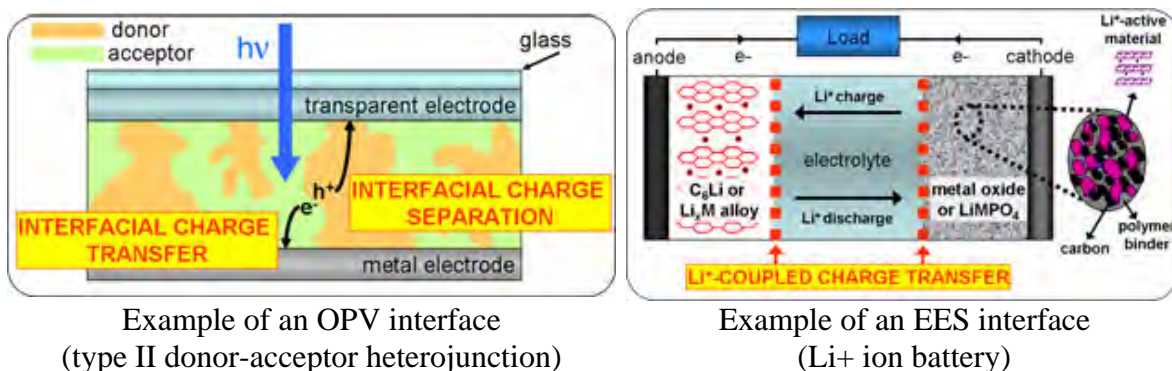
Director, Center for Computational Molecular Sciences

Institute for Computational Engineering and Sciences, University of Texas at Austin

1 University Sta C0200, Austin, TX 78712

<rossky@ices.utexas.edu>

In this talk, I will outline the scientific investigations and their motivations for the title EFRC, with emphasis on the area of organic photovoltaic materials. The vision of this EFRC is to establish a broadly collaborative and highly synergistic chemical sciences research program that will lead to major breakthroughs in the molecular-level understanding of critical interfacial charge separation and transfer processes. It is these that underpin the potential for practical function of highly promising and innovative nanostructured *molecular* materials for organic photovoltaic (OPV) and electrical-energy-storage (EES) applications. The interfaces of interest are those occurring at the molecular and nanoscale, as illustrated below, and the processes to be elucidated are those elemental molecular-scale processes associated with charge separation on this scale.



A distinguishing element of the Center is to target the development of structure-function relationships at the nano and molecular scales, using both theory and experiment to bridge the knowledge gap which exists between molecular and materials processes. This strategy features coordinated projects which focus on unique *interfacial prototypes* of increasing molecular complexity starting from well-defined molecular and crystalline interfaces that are accessible to both theory and to state-of-the-art imaging and sub-ensemble measurement methods (e.g., single particle spectroscopy). This strategy allows correlated measurements of structure and charge separation/transfer processes as well as meaningful theoretical investigations on the same interfacial systems.

For a complete list of senior investigators, go to <http://www.nano.utexas.edu/efrc thrusts.html> . This center is funded by the DOE through the 2009 American Recovery and Reinvestment Act.

CPIMS
Principal Investigator
Abstracts
(Alphabetical by last name)

“Imaging Mass Spectrometry, aerosol chemistry, cluster and biomolecule energetics with VUV radiation”

Musahid Ahmed, Kevin R. Wilson and Stephen R. Leone
Chemical Dynamics Beamline, MS 6R-2100, 1 Cyclotron road
Lawrence Berkeley National Laboratory, University of California, Berkeley, CA 94720
mahmed@lbl.gov

The Chemical Dynamics Beamline at the Advanced Light Source (ALS), is a synchrotron user facility dedicated to state-of-the-art investigations in chemical physics and physical chemistry using tunable vacuum ultraviolet light for excitation or detection. Key scientific problems addressed at the beamline with support from CPIMS include imaging mass spectrometry, aerosol chemistry and fundamental studies of laser ablation and desorption processes, cluster and biomolecule energetics.

Imaging Mass Spectrometry-

In this program a technique to perform chemical imaging on surfaces using a novel mass spectrometry method is being developed, wherein ion-sputtered neutrals are photoionized with high fluxes of tunable synchrotron VUV radiation. To achieve the goals of imaging aerosols, combustion products and biological systems, a systematic approach to understanding the VUV photoionization of surface neutrals is required. In addition, fine tuning the performance of the instrument as well as understanding of fundamental sputtering mechanisms is a necessary first step. Neutral parent VUV-secondary neutral mass spectrometry (SNMS) also provides fundamental insight into the energy partitioning within ion-sputtered molecular species. Ion-sputtered neutral clusters from GaAs and gold exhibit ionization onsets shifted by ~ 0.3 eV towards lower photon energies, while sputtered atoms exhibit no shift that would be indicative of electronic excitation.¹

VUV-SNMS has been observed for various polycyclic aromatic hydrocarbons (PAHs) like coronene and chrysene, as well as the DNA bases thymine, adenine, and cytosine. These studies have yielded information on molecular sputtering energetics and images of chemical localization. Preliminary analysis of the data from these organic molecules indicate that ion-sputtered organics have ionization onsets shifted by a few tenths of an eV, which may indicate that the neutral organics leave the surface with internal energies on the order of 1 eV.

A major thrust with the imaging program is to image organic molecules prevalent in plants and organisms that are being considered for biofuel development. Lignin is the second most abundant organic biopolymer in nature, and its association with cellulose places critical limitations on the rate, productivity and cost efficiency of sugar extraction from cellulosic biomass. Despite its importance, the details of the biosynthesis of lignin remain unknown, and the specific chemical changes that occur after genetically modifying plants are not completely clear. It is therefore important to be able to image the spatial localization of lignin and its key intermediates. Lignin is made up of three primary subunits, or monolignols (sinapyl alcohol, coniferyl alcohol and p-coumaroyl alcohol). Although further studies are necessary to determine precisely how sensitive VUV-SNMS is to these species, initial analyses of sinapyl alcohol and coniferyl alcohol have shown promising signs of intact parent molecules with VUV-SNMS. Phenylalanine, a key molecular precursor to these molecules, has shown a distinct neutral fragment. These results suggest that it is possible to quantitatively determine the relative abundances and spatial localizations of different types of lignin and their precursors within single-cell systems.

In the coming year there will be ongoing instrumental optimization and the imaging system will be integrated with other imaging/mass spectrometric techniques. Collaborations with an IR beamline at the ALS are underway to allow cellulose-degrading bacterial communities to be analyzed via IR microscopy, with subsequent chemical analysis at the higher-spatial resolution of the VUV-SNMS technique. A high repetition rate (5 KHz) desorption laser has also been recently coupled to the SNMS instrument to allow imaging on

larger length scales. These additions will extend the scale and scope of VUV-SNMS so that a broader range of systems can be studied.

Biomolecule Energetics-

Fundamental studies of photoionization processes of biomolecules are necessary for their implementation in imaging mass spectrometry. Furthermore determinations of ionization energies and other properties of biomolecules in the gas phase are not trivial. We have developed a thermal vaporization technique coupled with supersonic molecular beams that provides a gentle way to transport these species into the gas phase. Judicious combination of source gas and temperature allows for formation of dimers and higher clusters of the DNA bases. Extensive theoretical electronic structure and thermodynamic calculations performed in collaboration with Anna Krylov (USC) and co-workers allow for novel insights into the thermodynamics and photoionization properties of DNA base monomers and dimers.

We have performed experimental and theoretical characterization of the photoionization dynamics of gas-phase AA, TT, AT, CC, GG, and GC dimers. These are the first experimental measurements of the ionization energies of these dimers. The focus of this particular work is on the effects of noncovalent interactions, i.e., hydrogen bonding, stacking, and electrostatic interactions, on the IEs of the individual nucleobases. The changes in electronic structure upon clustering (i.e., hole localization) induced by these interactions are being analyzed.

The differences in tautomer population for guanine upon thermal vaporization and laser desorption was investigated.² The guanine generated by each method is entrained in a molecular beam, single photon ionized with tunable VUV synchrotron radiation, and analyzed using reflectron mass spectrometry. The recorded PIE curves show a dramatic difference for experiments performed via thermal vaporization compared to laser desorption. The calculated vertical and adiabatic ionization energies for the eight lowest lying tautomers of guanine suggest the experimental observations arise from different tautomers being populated in the two different experimental methods.

In recent work we have successfully adapted an experimental apparatus to perform mass analyzed threshold ionization (MATI) at the synchrotron.³ This opens up a novel way to perform spectroscopy at the beamline and improve resolution in ionization onset measurements as well as generate structural information of the cation. The idea is to have access to spectroscopy that is typically available in photoelectron spectroscopy but with mass resolution. This would be invaluable in studying mixtures of molecules, conformers and isomers, and clusters. MATI spectrum was recorded for a number of molecules. In future experiments, we plan to incorporate our aerosol VUV mass spectrometer to MATI to be able to record vibrationally resolved photoionization spectra of fragile biomolecules. In parallel, we are developing 2 color IR-VUV experiments to allow structural identification of the molecules prevalent in our molecular beams. We are in collaboration with Cheuk Ng (UC Davis) is developing a IR-OPO system that has a rep-rate up to 25 kHz and will access wavelengths up to 5 μm .

Aerosol Chemistry-

The heterogeneous reactivity of small radicals, such as OH, at the surface of organic particles or droplets has important implications for the combustion and auto-oxidation of fuel sprays, the formation and destruction of aerosols in the atmosphere and the chemical aging of soot in urban environments. In particular, the hydroxyl radical (OH) plays a critical role both in the oxidation of soot formed in high temperature combustion as well as subsequent atmospheric transformations that these particles undergo as they are emitted into the environment and exposed to tropospheric oxidants. To examine the fundamental reactivity of free radicals at surfaces, the heterogeneous reaction of OH radicals with sub-micron squalane particles, in the presence of O₂, is used as a model system to explore the reaction rate and oxidation mechanisms that control the chemical transformation of the particle produced after a surface reaction. Detailed kinetic measurements combined with elemental mass spectrometric analysis reveal that the

reaction proceeds sequentially by adding an average of one oxygenated functional group per reactive loss of squalane. Based on a comparison between the measured particle mass and model predictions it appears that significant volatilization of a reduced organic particle would be extremely slow in the real atmosphere. However, as the droplets become more oxygenated, volatilization becomes a significant loss channel for organic material in the particle phase. Together these results provide a chemical framework in which to understand how heterogeneous chemistry transforms the physicochemical properties of particle phase organic matter exposed to small gas phase free radicals.^{4,5}

A new theme of probing nucleation phenomenon continues with photoionization using tunable VUV radiation on sprays, cluster beams, and under atmospheric pressure. The idea for these exploratory experiments is to perform fundamental studies to probe ionization processes in atmospheric pressure photoionization (APPI) and also undertake gas phase cluster ion experiments applicable to interpret nucleation phenomena. New instrumentation to perform these studies has recently been acquired at the beamline. A high-resolution hybrid quadrupole-TOF mass spectrometer combined with nanospray liquid chromatography and orthogonal laser desorption in conjunction with VUV photoionization is being developed.

Nucleation phenomenon, heterogeneous chemistry and subsequent growth of particles are crucial in the field of materials chemistry, fluid dynamics, aerosol physics and atmospheric chemistry. We are developing an experimental strategy for understanding the role of small ions or neutrals as a “seed” for condensation phenomenon. A differential pumping arrangement is implemented to allow synchrotron radiation to directly access the high pressure (10^{-4} mbar) source region of a molecular beams apparatus. Photoionization is performed at four distances between the nozzle and the VUV light beam. It is observed that at far distances (45 mm) the methanol seeded in an Ar beam is behaving as a typical neutral cluster beam,⁶ however at the closest distance (15 mm) two processes are occurring. This suggests that the initially formed ion is being solvated by neutral methanol molecules leading to large protonated methanol clusters. There are also interesting ion-molecule reactions going on in the system – water elimination gives rise to protonated dimethyl-ether methanol clusters while dimethyl-ether elimination gives rise to protonated methanol–water clusters. These results are being analyzed and new experiments to interpret nucleation behavior are being proposed.

Laser ablation and cluster studies-

In this project, molecules and clusters are generated by laser ablation and photoionized by tunable VUV allowing elucidation of ionization energies and thermodynamic properties.

The thermodynamic properties of organosilicon molecules are of paramount importance in understanding the formation of silicon-bearing nanostructures together with their precursors from the ‘bottom up’ in the interstellar medium, in our Solar System, and in chemical vapor deposition processes. Towards this end we have started performing reactivity studies of Si clusters generated by laser ablation with a variety of hydrocarbons and oxidizing molecules. We were successful in generating gas phase SiO_2 *in situ* via laser ablation of silicon in a beam with added CO_2 . Photoionization efficiency (PIE) curves are recorded for SiO and SiO_2 and ionization energies are derived from the measurements.⁷ Under optimized conditions, the same source was used to produce a series of Si_n clusters. The ionization energies of Si_n ($n=1-7$) have been measured and analysis is under way. While the IE for the dimer is reasonably well known, those for the higher clusters are less reliable and these results provide for a better value and error limits. By changing the carrier gas to C_2H_2 , a series of Si insertion reactions takes place leading to the formation of a rich mixture of organo-silicon compounds. A mass spectral analysis suggests that a number of species are formed in the ablation setup – C_4H_2 , C_6H_2 , C_8H_2 , C_{10}H_2 , SiC_2H , SiC_2H_2 , $\text{Si}_2\text{C}_2\text{H}$, $\text{Si}_2\text{C}_2\text{H}_2$, Si_2C_n , ($n=1-6$), $\text{Si}_2\text{C}_4\text{H}$, $\text{Si}_2\text{C}_4\text{H}_2$, $\text{Si}_2\text{C}_6\text{H}$, $\text{Si}_2\text{C}_6\text{H}_2$, Si_3C , Si_3C_2 , Si_4C_2 . Ionization energies were measured for each species, and collaborations with Alex Mebel (Florida International) and Ralf Kaiser (U. Hawaii) are underway to interpret the thermodynamic and kinetic pathways that lead to this rich chemistry in the silicon vapor plume.

Ricardo Metz (U Mass. Amherst) in collaboration with beamline staff continues to study the photoionization of metal systems and their reactive products. $IE(\text{PtC})=9.45\pm 0.05$ eV, $IE(\text{PtO})=10.0\pm 0.1$ eV and $IE(\text{PtO}_2)=11.35\pm 0.05$ eV were reported.⁸ The values for the oxides are ~ 0.5 eV higher than IE's derived from the existing neutral and ion bond strengths. This independent measurement provides an excellent check on the accuracy of the measured bond strengths. This work has been extended to tantalum oxides and PIE's for TaO_x ($x=2-6$) have been measured. The ionization onsets are sharp, and the IE's increase with x , up to $x=4$, indicating that up to four oxygen atoms bind to the metal. Larger complexes have lower IE's with a broad onset, indicating O_2 binding to a TaO_{x-2} core. Ionization energies of H-Pt-H, PtCH_2 , H-Pt- CH_3 , $\text{Pt}(\text{C}_2\text{H}_2)$ and $\text{Pt}(\text{C}_2\text{H}_4)$ formed by reacting laser-ablated platinum atoms with CH_4 , C_2H_4 and C_2H_6 were measured. The photoionization studies observe the H-Pt- CH_3 reaction intermediate formed by Pt insertion into the C-H bond in methane. It has been predicted by calculations, and postulated to be responsible for the high termolecular rate for $\text{Pt} + \text{CH}_4$ clustering. Combining the photoionization results with guided ion beam measurements of the $\text{Pt}^+ + \text{CH}_4$ potential energy surface allows for a derivation of a potential energy surface for the *neutral* reaction.

References (DOE sponsored publications 2007-present) –

1. L. Takahashi, J. Zhou, K. R. Wilson, S. R. Leone and M. Ahmed, "Imaging with Mass Spectrometry: A Secondary Ion and VUV-Photoionization Study of Ion-Sputtered Atoms and Clusters from GaAs and Au" *J. Phys. Chem. A* **113**, 4035 (2009)
2. J. Zhou, O. Kostko, C. Nicolas, X. Tang, L. Belau, M. S. de Vries, and M. Ahmed, "The direct observation of guanine tautomers using VUV photoionization" *J. Phys. Chem. A* **113**, 4829 (2009)
3. O. Kostko, S.K. Kim, S.R. Leone, and M. Ahmed, "Mass-Analyzed Threshold Ionization (MATI) Spectroscopy of Atoms and Molecules using VUV Synchrotron Radiation" *J. Phys. Chem. A* (In press)
4. J. D. Smith, J. H. Kroll, C. D. Cappa, D. L. Che, M. Ahmed, S. R. Leone, D. R. Worsnop, and K. R. Wilson. "The heterogeneous reaction of hydroxyl radicals with sub-micron squalane particles: a model system for understanding the oxidative aging of ambient aerosols" *Atmos. Chem. Phys.* **9**, 3209 (2009)
5. D.L. Che, J. D. Smith, S. R. Leone, M. Ahmed and K. R. Wilson, "Quantifying the Reactive Uptake of OH by Organic Aerosols in a Continuous Flow Stirred Tank Reactor" *PCCP* (In press)
6. O. Kostko, L. Belau, K.R. Wilson and M. Ahmed. "Vacuum-ultraviolet (VUV) photoionization of small methanol and methanol-water clusters" *J. Phys Chem. A* **112**, 9555 (2008)
7. O. Kostko, M. Ahmed, and R. B. Metz, "A VUV photoionization measurement and ab-initio calculation of the ionization energy of gas phase SiO_2 " *J. Phys. Chem. A* **113**, 1225 (2009)
8. M. Citir, R.B. Metz, L. Belau, and M. Ahmed. "Direct determination of the ionization energies of PtC, PtO and PtO_2 with VUV radiation" *J. Phys. Chem. A* **112**, 9584 (2008)
9. L. Belau, K. R. Wilson, S. R. Leone and M. Ahmed, "Vacuum Ultraviolet (VUV) photoionization of small water clusters" *J. Phys. Chem A.* **111**, 10075 (2007)
10. L. Belau, S. E. Wheeler, B. W. Ticknor, M. Ahmed, S. R. Leone, W. D. Allen, H. F. Schaefer III, and M. A. Duncan, "Ionization Thresholds of Small Carbon Clusters: Tunable VUV Experiments and Theory." *J. Am. Chem. Soc.* **129** 10229 (2007)
11. K. R. Wilson, S. Zou, J. Shu, E. Rühl, S. R. Leone, G. C. Schatz and M. Ahmed, "Size-Dependent Angular Distributions of Low Energy Photoelectrons emitted from NaCl Nanoparticles" *Nano Letters* **7**, 2014 (2007)
12. L. Belau, K. R. Wilson, S. R. Leone, and M. Ahmed, "Vacuum-Ultraviolet photoionization studies of the micro-hydration of DNA bases (Guanine, Cytosine, Adenine and Thymine)," *J. Phys. Chem. A.* **111**, 7562 (2007)
13. R. I. Kaiser, L. Belau, S. R. Leone, M. Ahmed, Y. Wang, B. J. Braams, and J. M. Bowman, "A combined experimental and computational study on the ionization energies of the cyclic and linear C_3H isomers," *ChemPhysChem* **8**, 1236 (2007)
14. M. Ahmed, "Photoionization of desorbed neutrals from surfaces." *Encyclopedia of Mass Spectrometry*, Vol. 6, 264 Elsevier (2007)

Model Catalysis by Size-Selected Cluster Deposition

Scott Anderson, Chemistry Department, University of Utah, 315 S. 1400 E. Rm. 2020, Salt Lake City, UT 84112. anderson@chem.utah.edu

Program scope: The activity of supported catalysts is determined by the inherent properties of the supported metal as modified by cluster size effects, by interaction with the support, and by binding of adsorbates. We examine such effects for model catalysts prepared by depositing size-selected cluster ions on well defined substrates in ultra-high vacuum. Tools available include a variety of pulsed and temperature-programmed mass spectrometric techniques, x-ray photoelectron spectroscopy (XPS), Auger electron spectroscopy (AES), ion scattering (ISS), and infrared reflection absorption spectroscopy (IRAS). The goal is to understand the complex interplay between the effects of cluster size, interaction with supports, and with adsorbates, and to develop methods to probe these complicated samples.

Recent Progress

For the past ~1.5 years our effort has focused on the Pd_n/alumina and Pd_n/TiO₂(110) systems, which provide interesting comparisons allowing the effects of support and cluster size to be observed. To enable these studies, a new dosing/mass spectrometry station was constructed for our UHV system, with about 4 times the pumping speed, improving both background level and the time response for TPD and pulsed dosing. The new arrangement has 6 gas dosing tubes (SS or glass-lined SS), and an additional port for backfill dosing or other purposes. Each dosing port is served by a separate inlet manifold, dedicated to a particular gas, thereby minimizing background reactions in the inlet system. Gas doses can be controlled by either continuous leak valves or pulsed valves. When the sample is in the dosing position ~2 mm from the aperture in the skimmer cone, the (calibrated) gas flux from the dosing tubes onto the surface is equivalent to that from a backfill exposure at ~10 times greater chamber pressure, minimizing the effect of gas doses on the chamber background. Overall, the sensitivity of the system is ~10 times higher than the previous arrangement.

Pd/alumina: The alumina support in this case is a 5Å thick alumina layer grown on NiAl(110), which is a very commonly used alumina model support. Some studies on sapphire Al₂O₃ (0001) were also attempted, however, the conductivity is too low to allow ion beam deposition with useful currents.

Low temperature oxidation: XPS was used to probe the oxidation state of different size Pd_n deposited at 10% ML-equivalent coverage on alumina/NiAl(110) at room temperature, then cooled to 100 K. For the as-deposited clusters, the binding energies (BEs) for the 3d_{5/2} component range from 336.9 eV for Pd₁ to 336.1 eV for Pd₁₀ - all significantly shifted to higher energy compared to the BE for bulk Pd metal (335.1 eV). (1) The shift, relative to the bulk value is shown in Fig. 1 - note that the convergence on the bulk is not smooth in the small size range. The fact that the as-deposited BEs are quite size dependent is evidence that the deposited clusters do not agglomerate or fragment significantly.

For all samples except Pd₄/alumina, exposure to 180 L of O₂ at 100 K results in additional 0.3 - 0.5 eV shifts to higher BE, indicating that the Pd is being oxidized. The data suggest that the entire particle oxidizes, because the entire peak shifts, rather than broadening or splitting. XPS taken after vacuum annealing the oxidized clusters to 200 K and 300 K for 2 minutes is also quite dependent on the size of Pd_n. For Pd₁, the BE shifts back to the as-deposited value after 200 K annealing. For the larger clusters (n ≥ 7), 200 K annealing has little if any effect, and even after 300 K annealing, the Pd 3d BE is still shifted between the as-deposited and oxidized values. In summary, Pd₁ and Pd₇-Pd₁₃ all oxidize efficiently at 100K, but the resulting oxide is more stable in the larger clusters. Pd₄ is inert.

The inertness of Pd₄ at 100 K appears to be an

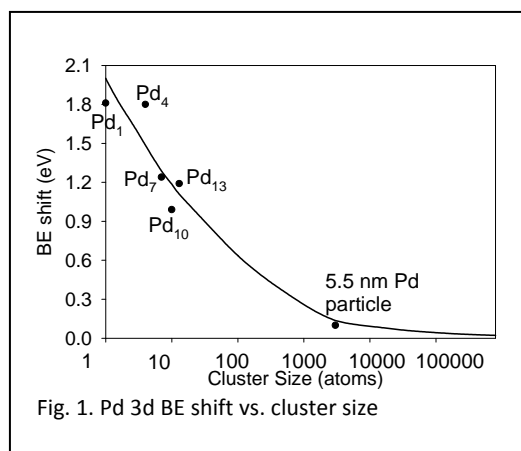


Fig. 1. Pd 3d BE shift vs. cluster size

electronic effect, relating to a particularly stable valence structure. The evidence for this conclusion comes from the as-deposited XPS BE shifts in Fig.1. In addition to our data, I include the shift for ~5.5 nm Pd/alumina/NiAl(110) from Shaikhutdinov et al.(2) Note that Pd₄ has a substantially greater Pd 3d BE than expected from the general trend of decreasing BE with increasing size. The general trend of increasing metal XPS BEs with decreasing metal coverage on oxide supports has been seen in many previous studies, and in some cases correlations with chemical activity have been noted. To our knowledge, this is the first cluster size-resolved measurement showing a correlation between core binding energy and chemical behavior.

High temperature oxidation: Similar experiments carried out with O₂ exposure temperatures of 300, 400 and 500K show no change in the as-deposited Pd BEs, even for exposures as high as 600 L. Note, however, that ion scattering shows that the Pd is covered with adsorbate (presumably oxygen) after the O₂ exposure, but apparently the nature of the bonding does not lead to significant polarization of the Pd. This behavior is consistent with that observed on both Pd/Al₂O₃(0001) and Pd/alumina/NiAl(110) model catalysts for O₂ exposures at elevated temperatures.(2-4) We looked for O₂ desorption and also CO oxidation activity under a wide variety of conditions but neither was observed. Desorption of the CO reactant was observed in two broad features centered at ~230 K and ~400 K, similar to previous studies for larger Pd particles grown by Pd evaporation on alumina/NiAl(110).(5) The explanation seems to be that the alumina layer on NiAl(110) is too thin (~0.5 nm) to completely isolate supported metal particles from the underlying NiAl support, and adsorbed oxygen atoms are evidently scavenged by the support, leaving none to react with CO or to desorb as O₂ in TPD. For future work on alumina, we will grow thicker alumina films.

Pd_n/TiO₂(110): The substrate in this case is the very commonly used near-stoichiometric rutile TiO₂(110) prepared by vacuum annealing, where ~8% of the unit cells have a vacancy in the bridging oxygen row. The conductivity of this surface is sufficient to neutralize clusters upon deposition. Ion scattering shows that deposition of Pd_n⁺ (n≤10) on this surface leads to planar structures where all the Pd atoms are in the surface layer, and a second layer is increasingly populated as the size ranges up to n=25. This behavior is similar to that for Ni_n/TiO₂.

CO oxidation activity was studied by first exposing the samples to O₂ at temperatures ranging from 100 K to 450 K. As with Pd_n/alumina, low temperature (≤200 K) O₂ exposure leads to a shift to higher Pd 3d binding energy, indicating formation of an oxide-like state of Pd. Surprisingly, however, the resulting oxidized Pd does not oxidize subsequently dosed CO either in temperature-programmed or fixed temperature pulsed dosing experiments. In contrast, O₂ exposures at 300 or 400 K result in no shift in Pd 3d BE (Fig. 3, inset), however, the resulting sample does have oxygen adsorbed on Pd which does oxidize CO. This chemistry is observed both in temperature-programmed reaction, and in pulsed dosing experiments at fixed temperatures above 300 K. In the temperature-programmed reaction (TPR), the samples were exposed to O₂ at T≥300K, then to CO at 180K, followed by a temperature ramp from 130K to 530K at 3K/sec while monitoring desorption of both CO₂ product and unreacted CO. The CO₂ product is observed only if the samples are pre-exposed to O₂ for T≥300 K, and desorbs in a broad feature between ~200 and 450 K. With or without O₂-pre-exposure, CO desorbs in three features at ~150K (CO at TiO₂ defects), ~200K and ~430K. The latter two features are associated with Pd, and have roughly equal integrated intensities for clusters (e.g. Pd₂, Pd₂₀) with high activities for CO oxidation. In contrast, the 430 K CO desorption feature is small or absent for relatively unreactive clusters such as Pd₁ and Pd₇. The nature of the two CO binding sites was explored by ion scattering, discussed below.

Fig. 2 shows a key result. This compares the CO oxidation activity (number of CO₂ product molecules per TPR - left axis, solid points) with the shift in as-deposited Pd 3d BE relative to what might be expected from final state charge scaling (right axis, inverted scale, open symbols). The correlation is essentially perfect and does not depend on the assumed form of charge scaling. Cluster sizes (n = 1, 7, 25) with higher-than-expected 3d BEs are relatively unreactive, while sizes (n = 2, 20) with lower than expected 3d BEs are highly reactive. General trends of increasing XPS BEs with decreasing metal coverage (thus decreasing average particle size) have been observed in many previous systems. This is

the first case where cluster size-resolved structure BEs has been seen, and where it can clearly be correlated with chemical behavior.

We used temperature-dependent ion scattering (TD-ISS) and He⁺ sputtering analysis to examine how the two reactants adsorb on the Pd/TiO₂ samples. Example results (for Pd₂₀) summarized in Fig. 3.

The first point shows the as-deposited Pd intensity, which is attenuated by ~80% by 5L CO exposure at 180 K, showing that CO is binding on top of the clusters, blocking the ISS signal. As the sample is heated through the 200 K CO desorption feature, the change in Pd intensity is only that expected from He⁺ sputtering of the CO (straight trend line), indicating that this component of the

adsorbed CO is not bound on top of the Pd (this component also appears to be uninvolved in the CO oxidation). In contrast, as the sample is heated through the 430 K CO desorption feature, the Pd signal recovers nearly to its as-deposited value, indicating that this CO component is bound on top of the Pd clusters. Subsequently, the sample was dosed with O₂ at 300 and 400 K, resulting in significant Pd ISS attenuation, indicating that some oxygen ends up bound on the clusters. As shown in the inset, this oxygen binding is not associated with a shift in the Pd 3d XPS. When the sample is next exposed to CO at 180 K, there is additional attenuation of Pd signal, indicating that some CO also binds on top of the Pd clusters. As the sample is heated (losing CO at 200 K and 430 K, and CO₂ between 200 and 450 K), there is some recovery of Pd signal, but the final value is well below the as-deposited value. This decrease

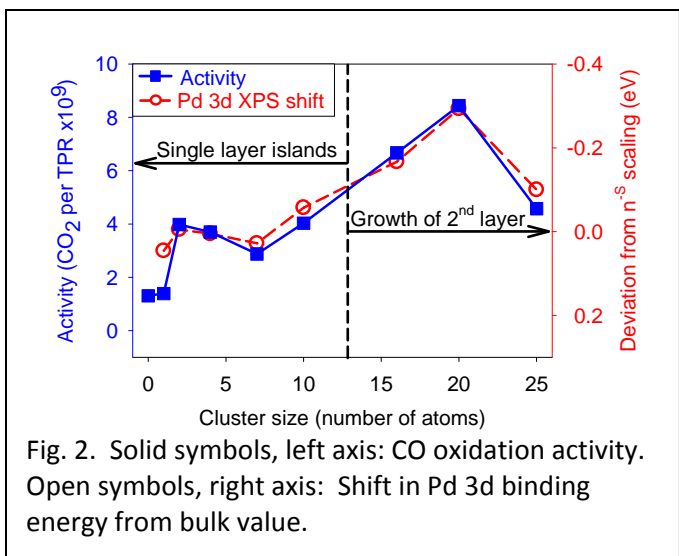


Fig. 2. Solid symbols, left axis: CO oxidation activity. Open symbols, right axis: Shift in Pd 3d binding energy from bulk value.

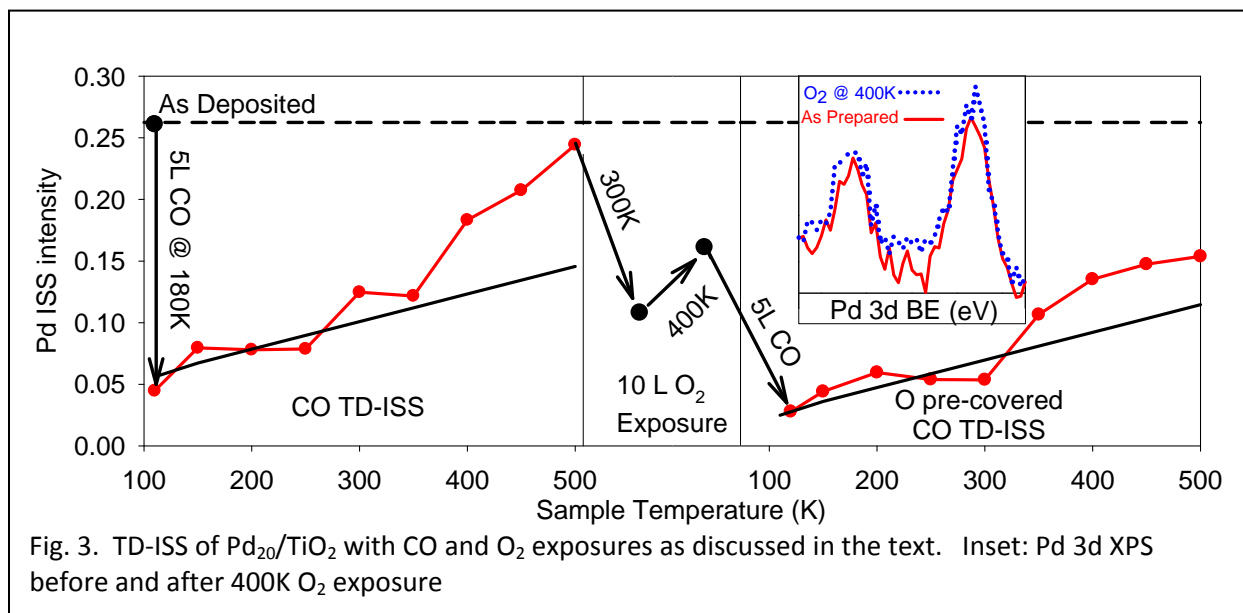
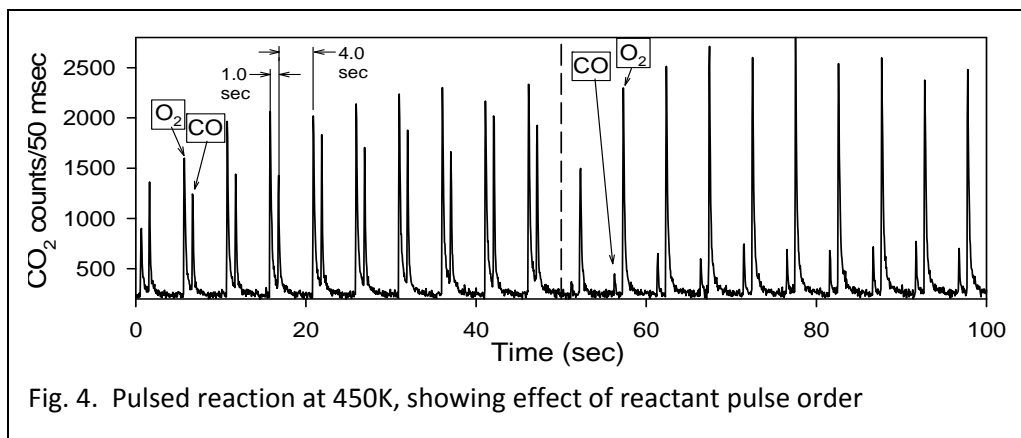


Fig. 3. TD-ISS of Pd₂₀/TiO₂ with CO and O₂ exposures as discussed in the text. Inset: Pd 3d XPS before and after 400K O₂ exposure

suggests that the morphology of the clusters is changed by the cycle of O₂ and CO exposure followed by heating. Indeed, if the TPR experiment is repeated, the amount of CO₂ produced decreased with each cycle, and there is a net shift in Pd XPS to higher binding energy (opposite of what would be expected from simple sintering). Note that if the sample is simply heated after O₂ exposure (without CO), there is no increase in Pd intensity, indicating that CO oxidation is responsible for removing the overlying oxygen.

We are currently examining the temperature dependence and mechanism of this reaction using

both TPR and constant temperature pulsed reaction methods, and also filling in the gaps in the measured size dependence. Pulsed reaction allows us to measure product yields under conditions of



catalytic turnover, and to examine kinetics by varying the pulse timing. For example, Fig. 4 shows the effects of varying the order of O₂ vs. CO exposure. Note that CO₂ is produced during both O₂ and CO pulses when the delay between O₂ and CO exposures is short, whereas a long O₂-CO delay leads to most CO₂ being generated during the O₂ pulse. In essence this tells us about the lifetime of the activated reactant on the surface under the reaction conditions.

We plan to examine other systems for similar correlations between core and valence level spectroscopy and activity, and try to develop a quantitative understanding of photoemission final state effects, and how they vary with cluster size and the nature of the cluster-support interaction. If such an understanding can be developed, it would enhance the utility of XPS as a chemically sensitive surface probe.

References

1. C. D. Wagner *et al.*, *NIST Standard Reference Database 20, Version 3.2 (Web Version)*, (2000).
2. S. Shaikhutdinov *et al.*, *Surf. Sci.* **501**, 270 (2002).
3. S. L. Tait, Ngo, L.T., Yu, Q., Fain S. C. Jr., Campbell, C.T., *J. Chem. Phys.* **122**, 064712 (2005).
4. S. Penner, Bera, P., Pederson S., Ngo, L.T., Harris, J.J.W., Campbell, C. T., *J. Phys. Chem. B* **110**, 24577 (2006).
5. M. Bäumer *et al.*, *Ber. Bunsen-Ges.* **99**, 1381 (1995).

DOE funded publications since 2005

1. "Agglomeration, Support Effects, and CO Adsorption on Au/TiO₂ (110) Prepared by Ion Beam Deposition" Sungsik Lee, Chaoyang Fan, Tianpin Wu, and Scott L. Anderson, *Surf. Sci.* **578** (2005) 5-19
2. "Agglomeration, Sputtering, and Carbon Monoxide Adsorption Behavior for Au/Al₂O₃ Prepared by Au_n⁺ Deposition on Al₂O₃/NiAl(110)", Sungsik Lee, Chaoyang Fan, Tianpin Wu, and Scott L. Anderson, *J. Phys. Chem. B* **109** (2005) 11340-11347
3. "Cluster size effects on CO oxidation activity, adsorbate affinity, and temporal behavior of model Au_n/TiO₂ catalysts", Sungsik Lee, Chaoyang Fan, Tianpin Wu, and Scott L. Anderson, *J. Chem. Phys.* **123** (2005) 124710 13 pages.
4. "Water on rutile TiO₂(110) and Au/TiO₂(110): Effects on Au mobility and the isotope exchange reaction", Tianpin Wu, William E. Kaden and Scott L. Anderson, *J. Phys. Chem. C.*; **2008**; 112(24); 9006-9015. DOI: [10.1021/jp800521q](https://doi.org/10.1021/jp800521q)
5. "Size-dependent oxidation of Pd_n (n ≤ 13) on alumina/NiAl(110): Correlation with Pd core level binding energies." Tianpin Wu, William E. Kaden, William A. Kunkel, and Scott L. Anderson, *Surf. Sci.* **603** (2009) 2764-77.
6. "Electronic Structure Controls Reactivity of Size-Selected Pd Clusters Adsorbed on TiO₂ Surfaces", William E. Kaden, Tianpin Wu, William A. Kunkel, Scott L. Anderson, *Science* (in press 9/09).

**“Electronic Structure of Transition Metal Clusters and Actinide Complexes and Their Reactivity”
DEFG2-05ER15657**

K. Balasubramanian,

California State University East Bay, Hayward CA 94542 kris.bala@csueastbay.edu

Program Scope

Our research is focused on electronic structure of actinide complexes and transitional metal clusters and their reactivity. This research has resulted in 15 completed publications¹⁻¹⁵ since October 2007 and more work is in progress. Our work during this period included both on actinide complexes and transition metal clusters such as W_xO_y clusters and gold clusters all carried out in collaboration with experimental works. As the publications are available online with all of the details of the results, tables and figures, we are providing here only a brief summary of major highlights, in each of the categories.

Electronic Structure of Actinide Complexes and Actinide-nonmaterial Interactions.

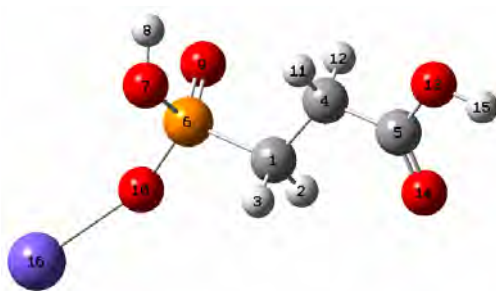
We have carried out a number of actinide complexes in aqueous solution; as such complexes are of considerable importance in our understanding of behavior of actinide species in the environment and high level nuclear wastes. A major highlight of our work during this period is experimental-theoretical collaboration on curium (III) complexes with multidentate ligands with Professor Nitsche and coworkers at LBNL. Our focus was on Cm(III) complexes with ligands that have both carboxylic and phosphoric acid groups so that relative binding strengths of the two ligands can be assessed with varying pH. Experimental studies have revealed intriguing trends that could not be explained. Thus our computational studies have provided valuable insights into the nature of Cm(III) complexes with multidentate ligands. We have also studied aqueous complexes of Cm (III), U(VI), NP(VI) and Pu(VI) with OH^- .

Extensive *ab initio* computations have been carried out to study the equilibrium structure, infrared spectra, and bonding characteristics of a variety of hydrated $NpO_2(CO_3)_m^{q-}$ complexes by considering the solvent as a polarizable dielectric continuum as well as the corresponding anhydrate complexes in the gas-phase. The computed structural parameters and vibrational results at the MP2 level in aqueous solution are in good agreement with Clark et al.'s experiments and provide realistic pictures of the neptunyl complexes in an aqueous environment. We have studied the electronic and spectroscopic properties of plutonyl di and tri carbonate complexes of the types $PuO_2[CO_3]_2$ and $PuO_2[CO_3]_3Ca_3$ using coupled cluster (CC) and other techniques.¹ In particular the structures, and select vibrational spectra, electron density and molecular orbital contour plots of plutonium(VI) complexes of environmental importance. Our computed equilibrium geometries and vibrational spectra of these species agree quite well with the EXAFS and Raman data.

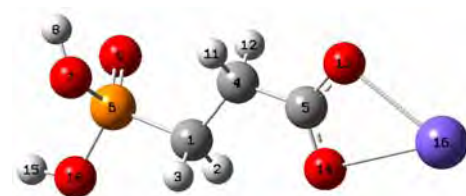
A joint experimental-theoretical study³ was carried out on curium (III) complexes with multidentate ligands such as phosphonic acid (PPA) which has both carboxylic and phosphoric acid groups to explain the observed dramatic variations in the nature of the observed complexes as a function of pH. Theoretical studies of CmH_2PPA^{2+} and $CmHPPA^+$ complexes were carried out in aqueous solution. All possible isomers in the gas phase and aqueous solution have been calculated. The effects of the aqueous solvent in the configuration preferences of CmH_2PPA^{2+} and $CmHPPA^+$ have been investigated. The free energies of solvation were predicted using a self-consistent reaction-field model and a combined discrete-continuum model. Spectroscopic studies on Cm(III) aquoion were carried out by a fluorescence emission spectroscopy at Berkeley, which revealed a band maximum at 593.8 nm. There is a pronounced red-shift of the emission as a result of the complex formation with the PPA molecule, accompanied by an increase in the fluorescence emission lifetime from 65 μs for the Cm(III) aquoion. The TRLFS (time-resolved laser-induced fluorescence spectroscopy) spectra have also been obtained for Cm(III) and PPA species. The PPA molecule can interact with metal ions via the oxygen atoms from the phosphate group and the carboxylate group, thus relative competition of the two groups and their binding propensities with Cm(III) were the central objectives.

Geometries and energy differences of CmH_2PPA^{2+} in aqueous solution were computed in solution. The theoretical results by inclusion of the continuum solvent models produce a relative stabilization of CmH_2PPA^{2+} in aqueous solution. The equilibrium geometries are presented in Fig. 1 and the corresponding geometries of $HPPA^{2-}$ with Cm(III) were also optimized. The solvation free energies, structures and IR spectra of the complexes were computed in solution. The calculation with the SCRf model, surprisingly,

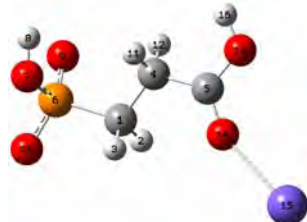
indicates that the most stable structure is the monodentate phosphate complexation (Cm-P, Fig. 1a) which is the least stable structure in the gas phase. The second stable structure is the bidentate carboxylate complexation (Cm-C2, Fig. 1b), followed by bidentate complexation (Cm-CP2, Fig. 1e). The monodentate carboxylate complexation is even higher in energy in aqueous solution, which is not a stable structure in the gas phase. The tridentate complexation which is the most stable structure in the gas phase is 35.3 kcal/mol higher in energy than the monodentate phosphate complexation. We have also optimized geometries of (a) $\text{Cm}[\text{H}_2\text{PPA}]_2^+$ and (b) $\text{Cm}[\text{HPPA}]_2^-$ in aqueous solution.



(a) Cm-P ($\Delta\Delta G_{\text{conf}} = 0.00$ kcal/mol)



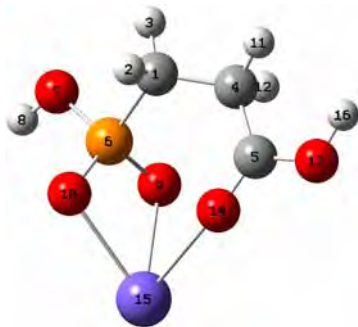
(b) Cm-C2



(c) Cm-C ($\Delta\Delta G_{\text{conf}} = 17.17$ kcal/mol)



(d) Cm-CP ($\Delta\Delta G_{\text{conf}} = 7.09$ kcal/mol)



(e) Cm-CP2 ($\Delta\Delta G_{\text{conf}} = 18.74$ kcal/mol)

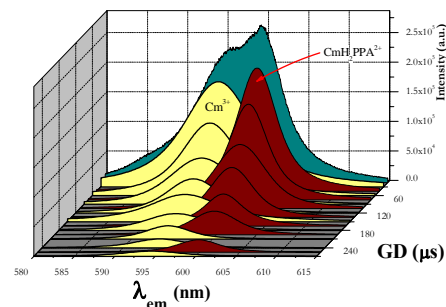
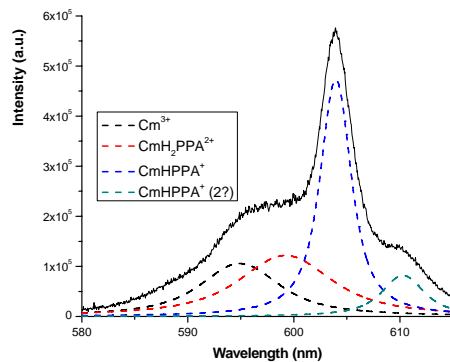


Fig 1 Some Optimized Structures of Cm^{3+} complexes both COO^- And phosphoric acid groups.

TRLFS Of $\text{CmH}_2\text{PPA}^{2+}$ complexes.

We find that the ordering of the calculated conformational Gibbs energies in solution is different from the ordering of energies from the pure continuum model. The tridentate complex Cm-CP2 is the most stable structure in aqueous solution. The next are Cm-P and Cm-C2. Cm-P and Cm-C are not stable structures in the gas phase. Aqueous solution geometries were used in the calculations of gas phase energies. There are significant changes on geometries after solvation in aqueous solution. The conformational Gibbs energy of Cm-P2 is only ca. 6 kcal/mol larger than that of Cm-C2. The carboxylate complexation is capable of displacing the phosphate binding in aqueous solution. Cm-CP is even more unstable. The most stable structure is the tridentate complex Cm-CP2. This might explain the experimental observation that the lifetime of CmHPPA^+ is 160 μs while the lifetime of $\text{CmH}_2\text{PPA}^{2+}$ is 112 μs . CmHPPA^+ binds less coordinated water molecules than $\text{CmH}_2\text{PPA}^{2+}$ in solution.

Extensive *ab initio* calculations have been carried out to study equilibrium structures, vibrational frequencies, and bond characters of hydrated $\text{UO}_2(\text{OH})^+$, $\text{UO}_2(\text{OH})_2$, $\text{NpO}_2(\text{OH})$, and $\text{PuO}_2(\text{OH})^+$ complexes in aqueous solution and the gas phase.⁴ The structures have been further optimized by considering long-range solvent effects as a polarizable continuum dielectric model. Our results reveal that it is necessary to include water molecules bound to the complex for proper treatment of the hydrated complex and the dielectric cavity. Structural reoptimization of the complex in a dielectric cavity seems inevitable to seek subtle structural variations in the solvent and to correlate with the observed spectra. The optimized structure of some of these complexes is not the same in the gas phase and aqueous solution illustrating the importance of carrying out these computations in solution

We have carried out computational studies on actinide mesoporous material interactions in collaboration with ongoing experimental studies carried out by Profs Peidong Yang and H. Nitsche at Berkeley. As a representative we have shown our computed structures for uranyl binding with carbon nanotubes.

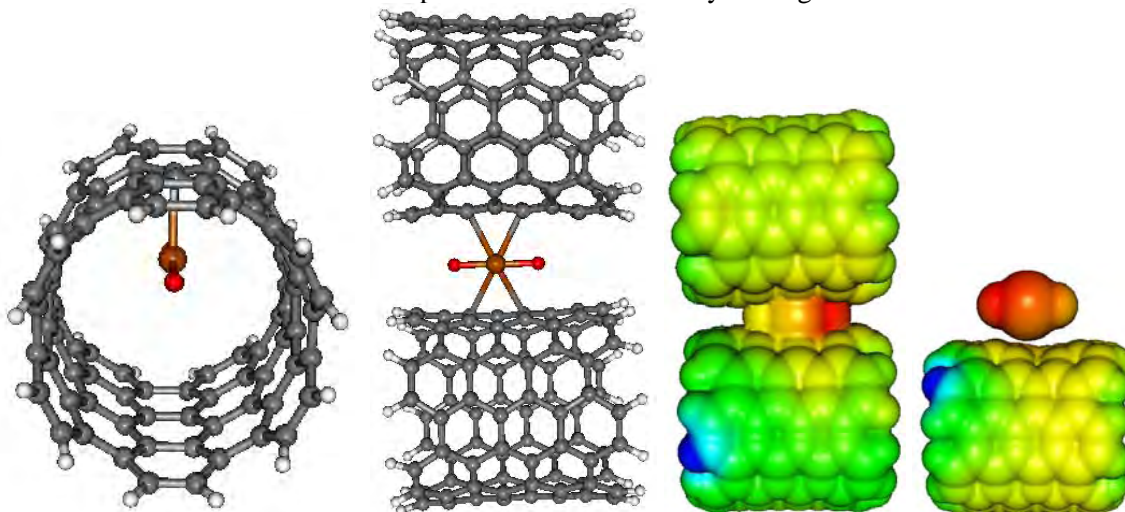


Fig. 2 Optimized Structures of (a) UO_2^{2+} bound to (6,6)SWNT, (b) UO_2^{2+} trapped between SWNT.

There are numerous open questions ranging from the accurate determination of structures and magnetic the nature of reactivity of actinides in various oxidation states. In order to address such questions and to provide reliable predictive computational models, we have carried out computational studies of potential energy surfaces of actinides and its ionic reactions with H_2 and H .

Transition Metal Clusters.

We have carried out joint experimental-computational studies on gas-phase tungsten oxide clusters and gold clusters. Fig 3 shows the experimentally observed relative abundance of W_xO_y anionic clusters and our computed BE/atom both of which confirm the existence of magic numbers for clusters that contain 6 and 13 W atoms.

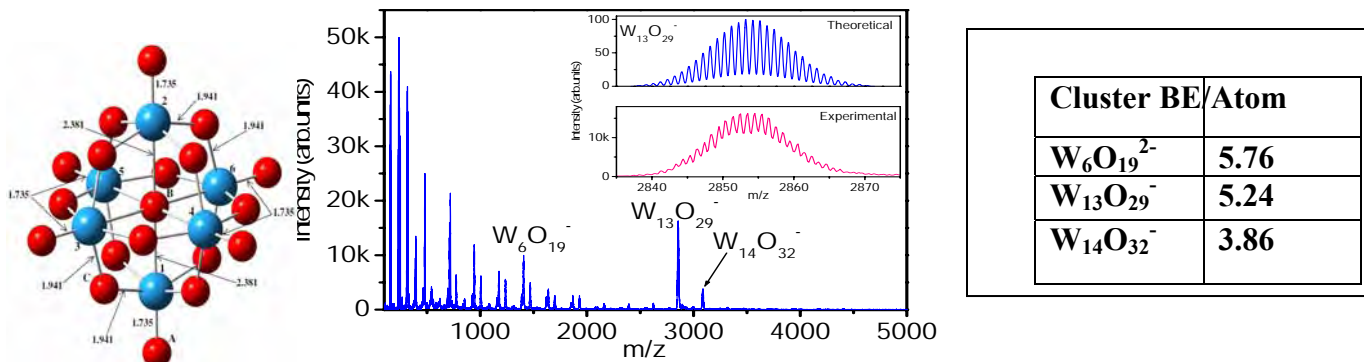


Fig. 3 Optimized structure of $\text{W}_6\text{O}_{19}^{2-}$, LDI mass-spectrum of W_xO_y Clusters show magic numbers for 6 and 13 W atoms; this is confirmed by our computed BE/atom.

Proposed Plan.

We plan to continue our works on environmental actinide complexes and transition metal species. We are investigating Cm(III) complexes with other ligands such as OH⁻ and CO₃²⁻ in collaboration with Professor Nitsche and his coworkers who are carrying out EXAFS and time-resolved x-ray fluorescence studies of such curium(III) complexes in solution. Likewise structures and properties of Bk(III) complexes remain unknown at this time and one often has to rely on analogous lanthanide complexes, which often results in erroneous deductions, as transplutonium complexes tend to behave quite differently from the lanthanide analogs due to relativistic effects. The observed behavior of these complexes as a function of pH is far from understood. Moreover there is a scarcity of thermodynamic solvation energy data on Bk(III) and Am(III) species which occur not only in high level nuclear wastes but also in nuclear reactor reactions during fission process. We would be continuing our recent exciting experimental-theory collaborations on actinide-nonmaterial interactions. At present there are no theoretical studies to provide insight into these species. We also propose to continue our work on transition metal species and actinides with specific focus on spectroscopic properties, geometries, Gibbs Free energies in solutions and potential energy curves.

Recent Publications from the DOE BES Grant

1. K. Balasubramanian, and D. Chaudhuri, "Computational modeling of environmental plutonyl mono-, di- and tricarbonato complexes with Ca counterions: Structures and spectra: PuO₂(CO₃)₂²⁻, PuO₂(CO₃)₂Ca, and PuO₂(CO₃)₃Ca₃, *Chemical Physics Letters*, 450, 196-202, (2008).
2. K. Balasubramanian, and Cao, Z., "Geometries and energy separations of electronic states of In₃N, InN₃, and their ions", *J. Theoretical and Computational Chemistry*, Vol. 7, 751-765 (2008).
3. Z. Cao, Balasubramanian, K., Calvert, M., Nitsche, H., "Solvation effects on the isomeric preference of binding of Curium³⁺ with phosphocarboxylic acid multidentate ligands: CmH₂PPA²⁺ and CmHPPA⁺", *Inorganic Chemistry* (2009).
4. Z. Cao, Balasubramanian, K., "Unusual Structures and Energetics of U(VI), NP(VI) and Pu(VI) complexes with OH⁻ in aqueous solution: UO₂(OH)(H₂O)₄⁺, UO₂(OH)₂(H₂O)₃, NpO₂(OH)(H₂O)₄, and PuO₂(OH)(H₂O)₄⁺ complexes", (2009).
5. Cao, Z., Balasubramanian, K., "Potential Energy Surfaces for the Interaction of Curium and Curium ion with H₂ and H⁺", *Journal of Physical Chemistry*, (2009) in press
6. Balasubramanian, K., "Group Theory and Unusual Nuclear Spin Statistics of Bismuth and Antimony Clusters: Spin-Orbit Versus Jahn-Teller Effects", *Molecular Physics* 107, 797 - 807 (2009)
7. M. Benavides-Gardia and K. Balasubramanian, "Structural Insights into the Binding of Uranyl with Human Serum Protein Apotransferrin-Structure and Spectra of Protein-Uranyl Interactions", *ACS Chemical Research in Toxicology*, (2009) in Press
8. T. Simeon, K. Balasubramanian, and C. Welch, "Computational Studies of Interaction of In and In³⁺ with Stone-Wales Defect Single-Walled Carbon nanotubes", *J. Phys. Chem. Lett.*, (2009) Submitted
9. D. M. David Jaba Singh, T. Pradeep, K. Thirumoorthy and K. Balasubramanian, "Closed-cage Tungsten oxide Clusters in the Gas Phase", (2009), Submitted
10. Z. Cao, K. Thirumoorthy and K. Balasubramanian, "Curium(III) hydroxide Complexes in Aqueous Solution", (2009) Submitted
11. T. Simeon, K. Balasubramanian, J. Leszynski, "New Insights Into the Chemical and Electronic Properties of C₆₉M [M = In⁻, Tl⁻, Sb⁺, Bi⁺] Species", *J. Phys. Chem. A*, 112 12179-12186 (2008)
12. Suo, B.; Balasubramanian, K., Spectroscopic constants and potential energy curves of yttrium carbide (YC). *Journal of Chemical Physics* 126, 224305 (2007) [\[PDF\]](#)
13. Balasubramanian, K and Z. Cao, "Theoretical Studies on Structures of Neptunyl Carbonates: NpO₂(CO₃)_m(H₂O)_n^q (m = 1-3, n = 0-3) in Aqueous Solution", *Inorganic Chemistry*, 46, 10510-10519 (2007)
14. T. Pradeep, Y. Sun and K. Balasubramanian, "Fluorescence Spectra and Computational Studies on Au₈-Containing Clusters", (2009) in preparation.
15. K. Balasubramanian, W. Sikehaus, W. McLean II, "Uranium Hydriding: Mechanisms, Trends and Influence of Impurities", In: Uranium: Compounds, Isotopes and Applications, Chapter 3, 23 pages, ISBN: 978-1-60692-573-7, Editor: Gerhardt H. Wolf, 2009 Nova Science Publishers, Inc.

Influence of medium on radical reactions

David M. Bartels, John Bentley and Daniel M. Chipman
Notre Dame Radiation Laboratory, Notre Dame, IN 46556
e-mail: bartels.5@nd.edu; Bentley.1@nd.edu ; chipman.1@nd.edu

Program definition

This project pursues the use of radiolysis as a tool in the investigation of solvent effects in chemical reactions, particularly the free radicals derived from solvent which are copiously generated in the radiolysis excitation process. Most recently we have focused on radical reactions in high-temperature water, and some of these results are described below. The project has now evolved toward the particular study of solvent effects on reaction rates in supercritical (sc-)fluids where the fluid density becomes a primary variable. One proposed thrust will be the study of solvated electrons under these conditions. Others will focus on small radicals in supercritical water and CO₂. A theoretical component has also recently been joined with this project, which will be directed to support the analysis and interpretation of experimental results.

An anthropomorphic way to think about near-critical phenomena, is that the fluid is trying to decide whether it is a liquid or a gas. The cohesive forces between molecules that tend to form a liquid are just being balanced by the thermal entropic forces that cause vaporization. The result, on a microscopic scale, is the highly dynamic formation and dissipation of clusters and larger aggregates. The fluid is extremely heterogeneous on the microscopic scale. A solute in a supercritical fluid can be classified as either attractive or repulsive, depending on the potential between the solute and solvent. If the solute-solvent potential is more attractive than the solvent-solvent potential, the solute will tend to form the nucleus of a cluster. When the solute-solvent potential is repulsive, one might expect the solute to remain in a void in the fluid as the solvent molecules cluster together. Extremely large partial molal volumes are known for hydrophobic molecules in near-critical water, indicating an effective phase separation. Such variations in local density around the solute will have implications for various spectroscopies and for reaction rates.

The ultimate goal of our study is the development of a predictive capability for free radical reaction rates, even in the complex microheterogeneous critical regime. Our immediate goal is to determine representative free radical reaction rates in sc-fluid and develop an understanding of the important variables to guide development and use of predictive tools. Electron beam radiolysis of water (and other fluids) is an excellent experimental tool with which to address these questions. The primary free radicals generated by radiolysis of water, (e⁻)_{aq}, OH, and H, are respectively ionic, dipolar, and hydrophobic in nature. Their recombination and scavenging reactions can be expected to highlight the effects of clustering (i.e. local density enhancements) and solvent microheterogeneity both in terms of relative diffusion and in terms of static or dynamic solvent effects on the reaction rates.

Recent Progress

As we noted in the 2008 progress report, accurate rate constants for free radical recombination reactions are of utmost importance for modeling reactions in high temperature cooling loops of water-cooled nuclear reactors. In order to measure such second-order recombination reactions, it

is necessary to have a method to determine absolute concentrations of the transient intermediates. The most convenient experiments tend to be transient UV-vis absorption measurements, with either pulse radiolysis or laser photolysis excitation. In either case, accurate extinction coefficients of the transients are required. Last year, we reported a method to determine absolute extinction coefficient for the hydrated electron, by recording its transient absorption as the electron is being scavenged by SF₆. The stable fluoride ion product is measured, and this establishes a direct connection to the transient concentration of solvated electrons, enabling their extinction coefficient to be established. This year the SF₆ measurement has been complemented by scavenging measurements producing methyl viologen radical cation MV⁺, whose extinction coefficient has been measured up to 200°C. The final combined result for hydrated electrons up to 350°C is illustrated in figure 1.

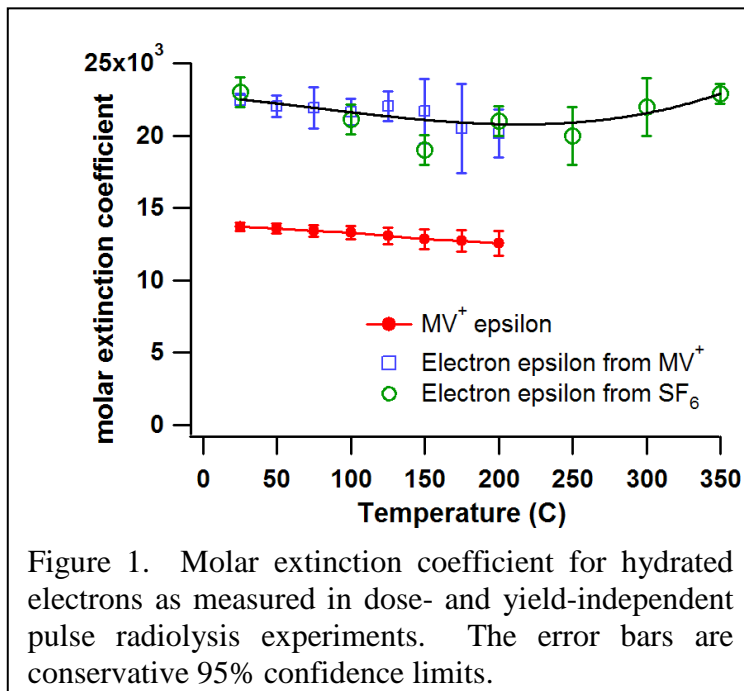
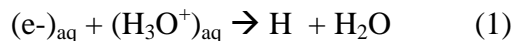


Figure 1. Molar extinction coefficient for hydrated electrons as measured in dose- and yield-independent pulse radiolysis experiments. The error bars are conservative 95% confidence limits.

The methyl viologen experiments were carried out because the room temperature SF₆ measurements had returned a value some 10-20% higher than all previous estimates. The result brings into question the entire system of radiation dosimetry that is commonly used for pulse radiolysis experiments. To understand the origin of this discrepancy we carried out a traditional measurement, directly comparing the transient absorbance of thiocyanate solution to the transient absorbance of hydrated electrons in water, using the same apparatus. This provides a comparison of the product $G \times \epsilon$ for the two samples, where G is yield and ϵ is extinction coefficient. When we carefully fit the $(e^-)_{aq}$ transient to measure the absorbance corresponding to an *escape yield*, the ϵ value deduced for hydrated electron is identical to our independent measurements. Previous workers chose a G value from gamma radiolysis scavenging experiments. The choice of slightly larger G value by other workers completely explains their underestimation of extinction coefficient for the electron. Consequently our measurement confirms by a completely independent route, the pulse radiolysis dosimetry system based on thiocyanate transient absorption, and by extension the validity of most measured free radical extinction coefficients.

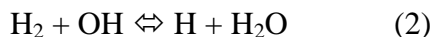
Significant effort in the past year has been put into a review of all high temperature rate constants of importance in nuclear reactor simulation, in collaboration with Atomic Energy of Canada. Ltd. A number of key reactions were identified as requiring more study, and some of these will be addressed in the coming year. Some discrepancies were found in high temperature data for reaction of hydrated electrons with hydronium ions:



Consequently this reaction was remeasured, and earlier data was refit, to produce the Arrhenius plot shown in figure 2. In still higher temperature supercritical water this recombination is

extremely fast due to the coulombic attraction and low dielectric constant. Merely adding acid scavenger gives an incorrect rate constant result because the acid is already ion-paired or undissociated, and the coulomb attraction is absent. Pulse radiolysis measurements are underway to treat the recombination in supercritical water by second order kinetics.

It has been known for some time that the most important reaction in controlling water radiolysis in reactors with “hydrogen water chemistry” is



which converts the oxidizing OH radical into the reducing H atom. Only in the past year was it realized that the equilibrium, including the reverse

reaction of H atoms with water, was of critical importance to the overall problem. The gas phase equilibrium constant changes six orders of magnitude between room temperature and the ca. 300°C operating temperature of pressurized water reactors, making the reverse reaction significant. To calculate the equilibrium constant in the aqueous phase, hydration free energy of all the reactants must be known. Given the very strong similarity of H and H₂ (hydrophobic) solvation, the hydration free energy difference for these species can be assumed zero at all temperatures. The OH radical hydration free energy has been determined by two methods at room temperature, and lies 25% below H₂O and 50% below H₂O₂, when equi-density standard states are used for gas and liquid (see Figure 3). The ratio of hydration free energies of H₂O and H₂O₂ remains approximately constant to 350°C, suggesting that the number of strong hydrogen bonds (four in H₂O and six in H₂O₂) dominates the thermodynamics. Assuming OH radical can make three strong hydrogen bonds, one can estimate the temperature dependence of its hydration free energy. Moreover, the measured value for the H₂O molecule provides hard upper and lower bounds for OH (figure 3). In the end, we are able to estimate the equilibrium constant, and the reverse reaction rate for reaction 2, within a factor of two. Future work should be able to improve upon this estimate of OH radical thermodynamics using ab initio and molecular dynamics techniques.

As a first step in quantitative modeling of OH radicals in water, the hydration of hydroxyl radical has been analyzed in terms of a many-body decomposition of quantum chemical calculations on the interaction energy between OH and water molecules in a wide variety of cluster structures. Works in the literature on water clusters have shown that two-body interactions are of primary importance, three-body effects are smaller but significant, and higher order effects are very small. We find that OH radicals involved in single-donor single-acceptor hydrogen bonding arrangements follow a very similar pattern to the analogous parent water clusters. But surprisingly, OH radicals involved in single-donor double-acceptor hydrogen bonding arrangements display substantial higher order effects, with up to six-body interactions being

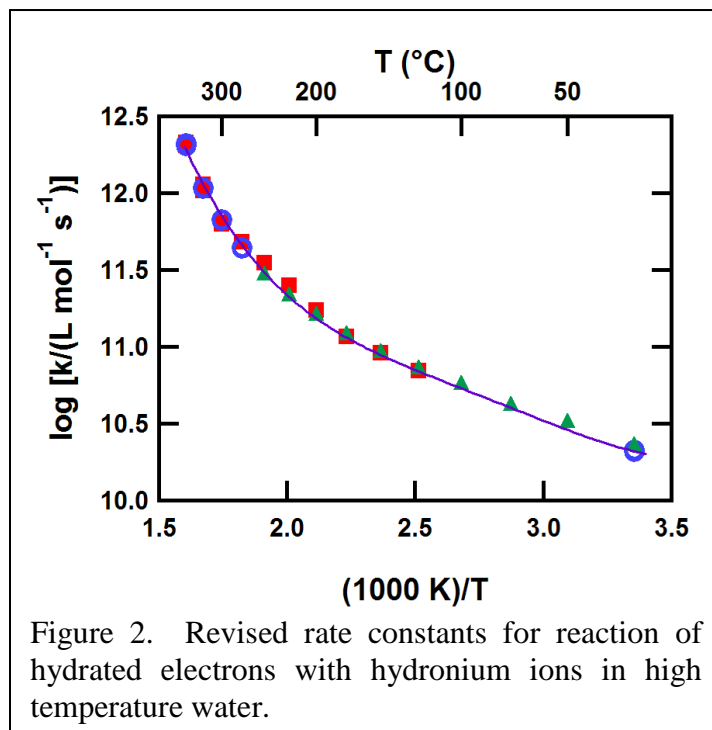


Figure 2. Revised rate constants for reaction of hydrated electrons with hydronium ions in high temperature water.

significant. These results will be used in the future to guide development of a force field suitable for molecular dynamics simulation on the properties of hydroxyl radical in liquid water over a wide range of temperatures and pressures.

Future Plans

Immediate plans are to continue the optical transient absorption measurements of OH radical and hydrated electron reaction rates. A most important target for experimental measurement is the reaction $\text{H}_2 + \text{OH}$ in supercritical water. Mechanisms of prototypical radiolytic reactions in aqueous solution such as $\text{H} + \text{OH} \rightarrow \text{H}_2\text{O}$, $\text{H}_2 + \text{OH} \rightarrow \text{H} + \text{H}_2\text{O}$, $\text{H}_2 + \text{O}^- \rightarrow \text{H} + \text{OH}^-$, $\text{OH} + \text{OH} \rightarrow \text{H}_2\text{O}_2$ and $\text{OH} + \text{OH}^- \rightarrow \text{O}^- + \text{H}_2\text{O}$, as well as the OH/O⁻ equilibrium, will be characterized by ab initio methods as initial steps toward the ultimate goal of understanding their unusual temperature dependences.

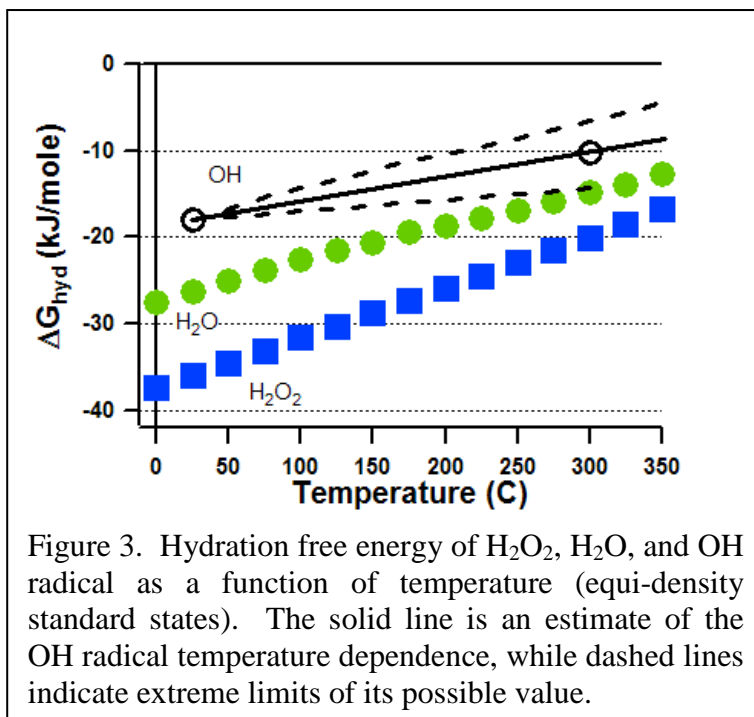


Figure 3. Hydration free energy of H_2O_2 , H_2O , and OH radical as a function of temperature (equi-density standard states). The solid line is an estimate of the OH radical temperature dependence, while dashed lines indicate extreme limits of its possible value.

Publications, 2007-2009

Elliot, A.J.; Bartels, D.M. (2009). *AECL report 153-127160-450-001* The Reaction Set, Rate Constants and g-Values for the Simulation of the Radiolysis of Light Water over the Range 20° to 350°C Based on Information Available in 2008

Bartels, D.M. (2009). *Rad. Phys. Chem.* 78: 191-194. Comment on the possible role of the reaction $\text{H} + \text{H}_2\text{O} \rightarrow \text{H}_2 + \text{OH}$ in the radiolysis of water at high temperatures.

Hare, P. M., Price, E. A., Bartels, D. M., (2008). *J. Phys. Chem. A* 112(30): 6800-6802. Hydrated electron extinction coefficient revisited.

Bonin, J.; Janik, I.; Janik, D.; Bartels, D. M. (2007). *J. Phys. Chem. A* 111(10): 1869-1878. Reaction of the Hydroxyl Radical with Phenol up to Supercritical Conditions.

Du, Y.; Price, E.; Bartels, D. M. (2007). *Chem. Phys. Lett.* 438: 234-237. Solvated electron spectrum in supercooled water and ice.

Janik, I.; Bartels, D. M.; Jonah, C. D. (2007). *J. Phys. Chem. A* 111: 1835-1843. Hydroxyl Radical Self-Recombination Reaction and Absorption Spectrum in Water up to 350°C.

Janik, I.; Marin, T.; Jonah, C. D.; Bartels, D. M. (2007). *J. Phys. Chem. A* 111(1): 79-88. Reaction of O_2 with the Hydrogen Atom in Water up to 350°C.

Marin, T. W.; Takahashi, K.; Jonah, C. D.; Chemerisov, S.; Bartels, D. M. (2007) *J. Phys. Chem. A* 111(45): 11540-11551. Recombination of the Hydrated Electron at High Temperature and Pressure in Hydrogenated Alkaline Water.

DFT calculations on carotenoid-porphyrin-C₆₀ light-harvesting molecular triad

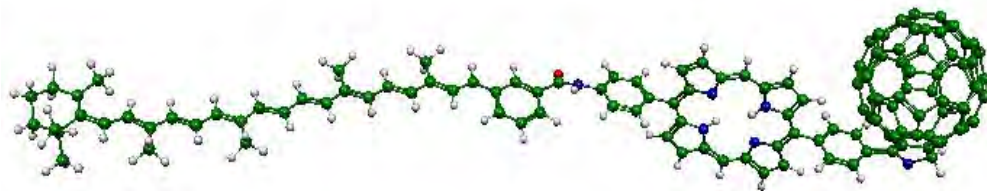
Tunna Baruah
Department of Physics
University of Texas at El Paso

An understanding of the photochemical processes in bio-mimetic light-harvesting molecules gained through quantum mechanical simulations can help in designing efficient and stable organic photovoltaics. One such molecule of interest is a carotenoid-porphyrin-C₆₀ molecular triad synthesized by Liddell et al.[1] over a decade ago. The molecular triad is about 5nm long and upon photo-induced charge separation exhibits a dipole moment of 153 Debye. Quantum mechanical calculations on such a large molecule become prohibitively expensive. We have carried out a density functional theory based calculation on the ground state structure and electronic properties of the triad [2]. The description of the photo-induced charge separation process requires an accurate description of the excited states of the molecule. The failures of TD-DFT in the linear response regime to handle the charge separated states are well documented. We present an efficient although imperfect means for the calculation of the charge transfer energies with DFT [3]. The method is suitable for any mean field theory however for practical reasons it is applied using standard DFT. In this method we use the constraint of orthogonality to the reference ground state. Since the excited states possess large dipole moments, the excited state energies so derived require correction due to the polarization of the solvent/spectator molecules. The correction terms depend on the concentration as well as the polarizabilities of the spectator molecules. Einstein's A and B coefficients are calculated and used in a kinetic Monte Carlo scheme to determine the time to reach a particular state through radiative transitions. It is observed that presence of counter ions can influence such transition times. Future directions to improve the excited state calculations, to include the electron-phonon couplings to determine the reaction coordinates, non-radiative energy transfer processes and spin-forbidden transitions will be discussed.

[1] Liddell et al., J. Am. Chem. Soc., **119**, 1400 (1997).

[2] Baruah et al., J. Chem. Phys. **125**, 164706 (2006).

[2] Baruah et al., J Chem. Theor. Comp. **5**, 834 (2009).



ELECTRON-DRIVEN PROCESSES IN CONDENSED PHASES

PIS: I. CARMICHAEL (carmichael.1@nd.edu), D.M. BARTELS, D.M. CHIPMAN, J.A. LAVERNE
NOTRE DAME RADIATION LABORATORY – NDRL, UNIVERSITY OF NOTRE DAME, NOTRE DAME, IN 46556

SCOPE

Fundamental physicochemical processes in water radiolysis are probed in an experimental program measuring spur kinetics of key radiolytic transients at elevated temperatures and pressures using a novel laser-based detection system with interpretation supported by computer simulations. Related experimental and computational studies focus on the electronic excitation of liquid water, important aqueous radiolytic species, and the significance and mechanism of dissociative electron attachment in the liquid. Radiolytic decay channels in nonaqueous media are investigated, both experimentally, with product analysis under γ and heavy-ion irradiation and transient identification under pulse radiolysis, and theoretically, via kinetic track modeling and electronic structure calculations.

PROGRESS

Preliminary measurements of the UV absorption spectrum of water at elevated temperature and pressure were performed at the Synchrotron Radiation Center (SRC) at the University of Wisconsin, Madison. Due to insufficient monochromaticity of the light available at the SRC, initial experiments produced unexpected results. After installation of an additional vacuum UV monochromator we attempted preliminary measurements of the first absorption maximum of water up to 350 °C. However even at 350 °C, where the density of water is $\sim 0.6 \text{ g cm}^{-3}$, using a 700 nm pathlength cell we were not able to record the peak of the first absorption band, indicating that the extinction coefficient of this band is substantially higher than reported previously in the literature. By modifying the cell and decreasing the pathlength to 350 nm we have obtained the first reliable measurements of the water absorption peak up to 300 °C. Using this much shorter pathlength decreases the flow through the cell (at 100 °C for instance the flow is $\sim 1 \mu\text{l}/\text{min}$) and complicates the measurement because of difficult-to-remove trapped air. Additional challenges arise from temperature shifts in window absorption. Nonetheless, preliminary experiments have revealed that extinction coefficients are higher than originally expected, increasing the temperature up to supercriticality is indeed observed to shift the entire spectrum towards the visible, however the density decrease in supercritical water does not shift the absorption peak towards the blue.

A new theory has been developed for quantum mechanical calculation of solvatochromic shifts within a dielectric continuum model of solvent. Exact and accurate approximate methods are found to treat the oft-neglected but important effects of solvent volume polarization on both the fast and slow solvent responses. The methods have been implemented in a popular electronic structure computer package and calculations have been made on representative solutes. Treatment of volume polarization effects is found to be essential in cases where the excited state charge density is significantly more diffuse than in the ground state.

Critical methodological issues in calculation of the UV absorption spectrum of liquid water related to the accuracy of the theoretical method, system size convergence of the absorption spectrum, and correction of surface effects have been investigated. Due to substantial delocalization of both the valence hole and the excited electron distribution, a supra molecular perspective that considers on the same footing the ground and excited states of a number of explicit quantum molecules is found to be necessary. Based on these investigations, promising schemes have been identified to separately prevent the valence hole and the excited electron

from delocalizing to the surface of any finite size cluster, as they inevitably do in straightforward computational methods, and so to allow for proper investigation of the true bulk behavior.

Isotopic labeling studies have been used to determine the extent of production of H atoms in the radiolysis of water with ions of different linear energy transfer and the experimental results simulated with track model calculations. Different solutes have been used to measure H atom yields and identify its precursor. H atoms readily abstract the D atom from deuterated formate to give HD as a well established direct probe of the H atom yield. Variation of the deuterated formate concentration gives a measure of the time dependence of H atom chemistry. Variation of added nitrate at constant deuterated formate concentration was used to examine H atom dependences on the hydrated electron. H atom production is expected to be due to a combination of hydrated electron reactions and decomposition of the water excited state at very short times. At 1 M nitrate and 1 M deuterated formate concentrations the H atom yield is found to be 0.27, 0.25, and 0.25 molecule/100 eV for γ rays, 5 MeV protons and 5 MeV He ions, respectively. The high solute concentrations result in H atom yields that are representative of direct water decomposition at early times in the radiolysis and with little contribution of the hydrated electron. The results suggest that the yield of the water excited state leading to H atom production is about 0.3 molecule/100 eV. This work gives the first direct experimental evidence that excited state chemistry contributes only about 10% to the total decomposition of liquid water.

Simple aromatic liquids are known to be relatively radiation inert. The main products are H₂ and the appropriate dimer. H₂ yields have been shown to increase significantly with increasing LET. Previous studies with benzene have suggested that most of the H₂ is produced molecularly from the decay of the singlet excited state. Further efforts with pyridine have suggested that high energy states lead to H₂ production in a channel three process. Here we examine the dependence of H₂ production on the energy level of the excited state in several simple aromatics. UV lamps of 254 to 183 nm were used to pump liquid benzene, pyridine, aniline, and toluene to the lowest one or two singlet excited state energy levels and the H₂ production was compared to that observed in gamma radiolysis. H₂ yields were essentially zero with excitation to the lower energy levels. Measureable H₂ yields were only observed with the highest energy excitation suggesting that high-energy singlet excited states are responsible for the production of H₂. These states are short lived, which explains the relatively low H₂ yields. However, these higher energy states certainly make a significant contribution to the radiation decomposition of simple aromatic compounds. The chemistry of high-energy states becomes very important in high LET radiolysis because of the increased probability of second order reactions of lower level excited states to repopulate higher level states, thereby increasing H₂ yields.

As an alternative to cryocooling for prolonging crystal lifetime during X-ray diffraction, the effect of several putative radioprotectants was tested with lysozyme crystals at 293 K. Plots of relative summed intensity against absorbed dose were used as a metric to assess radioprotectant ability. Ascorbate, which scavenges OH radicals about 30 times more effectively than electrons, doubled the dose tolerance of the crystal, whereas 1,4-benzoquinone, which also scavenges both radicals but with similarly high rate constants, produced a ninefold increase in dose tolerance at the dose rates used. Pivotaly, these preliminary results on a limited number of samples show that the two scavengers also induced a striking change in form of the dose dependence of the intensity decay from a first-order to a zeroth-order process. The latter behavior corresponds closely to that characteristically observed at cryotemperatures.

FUTURE PLANS

Advancing our investigation into the temperature dependence of the optical absorption of liquid water, a new cell is under construction that has much smaller dead volume and additionally allows usage of thinner sapphire windows to decrease the effect of unwanted sapphire absorption edge. A review of high-temperature yield information for water radiolysis just completed indicates that spur escape yields of H atoms have been significantly underestimated above 200 °C. Based on this archived data we will undertake new optical absorption measurements to extract this important quantity, key to understanding the high temperature radiolysis mechanism.

The radiation stability of simple aromatic compounds will be examined with high LET radiation in order to determine the relative importance of highly excited states in their decomposition. High LET radiation significantly enhances second order processes and modifications to final product yields can be used in combination with track model calculations and photolysis studies to elucidate radiolytic mechanisms.

The microscopic solvation environments of water molecules, hydroxyl radicals, and hydrogen atoms in liquid water will be determined as a function of temperature and pressure from a computational effort that is closely coupled to the respective experimental program in this laboratory. Clusters containing the solutes together with nearby explicit solvent molecules will be extracted from snapshots of molecular dynamics simulations, and their spectral properties then determined from high level electronic structure calculations that include effects of the bulk solvent from simplified models. The calculated water UV absorption spectra, the hydroxyl UV/vis absorption spectra, and the hydrogen atom EPR spectra will be compared to those determined experimentally in this laboratory. This will allow the experimental data to be interpreted and the quality of the computations to be assessed, which will lead to a much more complete understanding of how water, hydroxyl, and hydrogen atoms solvate in water.

Following proposals to extend the beam wavelength range to be routinely used for macromolecular cryocrystallography at several synchrotron sources, including the NSLS II currently under construction at BNL, efforts are underway to include the effects of previously neglected Compton processes to reliably evaluate the dose deposited by the incident photons. A theoretical understanding of the mechanism(s) that lead to specific radiation damage markers is being developed and mitigation strategies will be proposed.

BES SUPPORTED PUBLICATIONS (2007-9)

Chipman D.M. *J. Chem. Phys.* **2007**, *127*, 194309 Dissociative electron attachment to the hydrogen-bound OH in water dimer through the lowest anionic Feshbach resonance.

Du Y.; Price E.; Bartels D.M. *Chem. Phys. Lett.* **2007**, *438*, 234-7 Solvated electron spectrum in supercooled water and ice.

Enomoto K.; LaVerne J.A.; Araos M.S. *J. Phys. Chem. A* **2007**, *111*, 9-15 Heavy ion radiolysis of liquid pyridine.

Ichino T.; Fessenden R.W. *J. Phys. Chem. A* **2007**, *111*, 2527-41 Reactions of hydrated electron with various radicals: Spin factor in diffusion-controlled reactions.

Janik I.; Bartels D.M.; Jonah C.D. *J. Phys. Chem. A* **2007**, *111*, 1835-43 Hydroxyl radical self-recombination reaction and absorption spectrum in water up to 350 °C.

LaVerne J.A.; Enomoto K.; Araos M.S. *Radiat. Phys. Chem.* **2007**, *76*, 1272-4 Radical yields in the radiolysis of cyclic compounds.

Pimblott S.M.; LaVerne J.A. *Radiat. Phys. Chem.* **2007**, *76*, 1244-7 Production of low energy electrons by ionizing radiation.

Rajesh P.; LaVerne J.A.; Pimblott S.M. *J. Nuclear Material* **2007**, *361*, 10-7 High dose radiolysis of aqueous solutions of chloromethanes: Importance in the storage of radioactive organic wastes.

Southworth-Davies R.J.; Medina M.A.; Carmichael I.; Garman E.F. *Structure* **2007**, *15*, 1531-41 Observation of decreased radiation damage at higher dose rates in room temperature protein crystallography.

Zhao H.; Carmichael I.; Serianni A.S. *J. Org. Chem.* **2007**, *72*, 7071-82 Density functional calculations of $^2J_{\text{COH}}$, $^3J_{\text{HCOH}}$ and $^3J_{\text{CCOH}}$ NMR spin-spin coupling constants in saccharides.

Albarran G.; Schuler R.H. *Talanta* **2008**, *74*, 844-50 Determination of the spectroscopic properties and chromatographic sensitivities of substituted quinones by hexachlorate(IV) oxidation of hydroquinones.

Chipman D.M. *J. Phys. Chem. A* **2008**, *112*, 13372-81 Absorption spectrum of OH radical in water.

Enomoto K.; LaVerne J.A. *J. Phys. Chem. A* **2008**, *112*, 12430-6 Reactions of hydrated electrons with pyridinium salts in aqueous solutions.

Enomoto K.; LaVerne J.A.; Tandon L.; Enriquez A.E.; Matonic J.H. *J. Nuclear Materials* **2008**, *373*, 103-11 The radiolysis of poly(4-vinylpyridine) quaternary salt ion exchange resins.

Hare P.M.; Price E.A.; Bartels D.M. *J. Phys. Chem. A* **2008**, *112*, 6800-2 Hydrated electron extinction coefficient revisited.

Huerta Parajon M.; Rajesh P.; Mu T.; Pimblott S.M.; LaVerne J.A. *Radiat. Phys. Chem.* **2008**, *77*, 1203-7 H atom yields in the radiolysis of water.

Hug G.L.; Mozumder A. *Radiat. Phys. Chem.* **2008**, *77*, 1169-75 Electron localization in liquid hydrocarbons: The Anderson model.

Hull K.L.; Carmichael I.; Noll B.C.; Henderson K.W. *Chem. Eur. J.* **2008**, *14*, 3939 – 53 Homo- and Heterodimetallic Geminal Dianions Derived from the Bisphosphinimine $\{\text{Ph}_2\text{P}(\text{Me}_3\text{Si})\text{N}\}_2\text{CH}_2$ and the Alkali Metals Li, Na and K.

Klepach T.; Carmichael I.; Serianni A.S. *J. Am. Chem. Soc.* **2008**, *130*, 11892-900 ^{13}C -Labeled N-acetyl-neuraminic acid in aqueous solution: Detection and quantification of acyclic keto, hydrate and enol forms by ^{13}C NMR.

Klepach T.; Zhang W.; Carmichael I.; Serianni A.S. *J. Org. Chem.* **2008**, *73*, 4376-87 ^{13}C - ^1H and ^{13}C - ^{13}C NMR J-couplings in ^{13}C -labeled N-acetyl-neuraminic acid: Correlations with molecular structure.

LaVerne J.A.; Carrasco-Flores E.A.; Araos M.S.; Pimblott S.M. *J. Phys. Chem. A* **2008**, *112*, 3345-51 Gas production in the radiolysis of poly(vinyl chloride).

Zhao H.; Carmichael I.; Serianni A.S. *J. Org. Chem.* **2008**, *73*, 3255-7 Oligosaccharide trans-glycoside $^3J_{\text{COCC}}$ Karplus curves are not equivalent: Effects of internal electronegative substituents.

Atinault E.; De Waele V.; Fattahi M.; LaVerne J.A.; Pimblott S.M.; Mostafavi M. *J. Phys. Chem. A* **2009**, *113*, 949-51 Aqueous solution of UCl_3^+ in acidic medium: A perfect system to scavenge all primary radicals in spurs products by irradiation.

Barker A.I.; Southworth-Davies R.J.; Paithankar K.S.; Carmichael I.; Garman E.F. *J. Synchr. Radiat.* **2009**, *16*, 205-16 Room temperature scavengers for MX: Increased lifetimes and modified dose dependence of the intensity decay.

Chipman D.M. *J. Chem. Phys.* **2009**, *131*, 014103 Vertical electronic excitation with a dielectric continuum model of solvation including volume polarization. I. Theory.

Chipman D.M. *J. Chem. Phys.* **2009**, *131*, 014104 Vertical electronic excitation with a dielectric continuum model of solvation including volume polarization. II. Implementation and applications.

Dziewinska K.M.; Peters A.M.; LaVerne J.A.; Martinez P.; Dziewinski J.J.; Davenhall L.; Rajesh P. *Radiochim. Acta* **2009**, *97*, 213-7 In search for an optimum plutonium density measurement fluid.

Lewandowska A.; Hug G.L.; Hörner G.; Carmichael I.; Kazmierczak F.; Marciniak B. *Chem. Phys. Lett.* **2009**, *473*, 348–53 Chiral discrimination in the hydrogen-atom transfer between tyrosine and benzophenone in rigid peptides.

Strzelczak G.; Janeba-Bartoszewicz E.; Carmichael I.; Marciniak B.; Bobrowski K. *Res. Chem. Intermed.* **2009**, *35*, 507–17 Electron paramagnetic resonance (EPR) study of γ -radiation-induced radicals in 1,3,5-trithiane and its derivatives.

Tarabek P.; Liu S.; Haygarth K.; Bartels D.M. *Radiat. Phys. Chem.* **2009**, *78*, 168–72 Hydrogen gas yields in irradiated room temperature ionic liquids.

Watson C.; Janik I.; Zhuang T.; Charvátová O.; Woods R.J.; Sharp J.S. *Analytical Chemistry* **2009**, *81*, 2496-505 Pulsed electron beam water radiolysis for sub-microsecond hydroxyl radical protein footprinting.

Development of Structure-Reactivity Relationships within Heterogeneous Catalysts Through Gas-Phase Cluster Investigations

A. W. Castleman Jr.

Pennsylvania State University
Departments of Chemistry and Physics
104 Chemistry Building
University Park, PA 16802
awc@psu.edu

Program Scope:

Identification of the molecular-level interactions occurring within a heterogeneous catalytic process may provide a method of optimizing the route to production of the desired chemical species. In light of recent economic and environmental events, renewed emphasis has been directed toward the development of alternative fuels, the abatement of pollutants, and the reduction of the energetic requirements for chemical processing. Research in the field of heterogeneous catalysis is directed at attaining these three goals which will contribute directly to the Department of Energy's mission of promoting energy security. An ideal catalyst will have a surface tailor-made to convert reactants directly into products while minimizing the creation of byproducts. A combinatorial method of preparation and testing different materials is commonly utilized for the development of heterogeneous catalysts. This method is inefficient and rarely takes into account the active site specific chemical reactions taking place within a catalytic process. Methods of surface analysis have proven valuable in characterizing the surface structure of catalyst materials and identification of intermediate surface species. However, the occurrence of a large variety of active sites on a sample, as well as other surface inhomogeneities often causes the identification of structure-reactivity relationships to be difficult. It is a necessity to determine such structure-reactivity relationships to enable the directed design of more efficient catalysts.

Our experimental studies aim at determining molecular-level insight of heterogeneous catalytic oxidation processes occurring on transition metal oxide surfaces. A guided ion beam mass-spectrometer is utilized to perform gas-phase reactivity experiments as a model for the interactions occurring at individual active sites. High-level theoretical studies performed by the group of Professor Vlasta Bonačić-Koutecký at the Institut für Chemie, Humboldt Universität zu Berlin provide complementary insight into reaction mechanisms, leading to a more detailed understanding of the reaction. Such experimental and theoretical investigations determine the influence chemical and physical properties of different materials have toward promoting catalytic reactions.

As stated by Muetterties, a molecular-level understanding of catalytic reactions must be developed before the rational design of ideal catalysts can be achieved. Cluster studies aim to acquire this necessary insight. Catalytic reaction is enabled by cluster-like surface chemical bonds involving surface metal and next nearest neighbors according to Somorjai. Sub nanometer sized clusters have also been found to be catalytically active species when deposited on a surface. Thus, in addition to modeling interactions with surface active sites, gas-phase investigations show potential for identifying particles with enhanced activity for deposition onto a surface as the active catalytic material. Mass spectrometric gas-phase reactivity studies are performed on isolated clusters of discrete size, stoichiometry and composition. This capability is pertinent toward nanocatalysis which has exhibited marked differences in catalytic properties due to the addition or removal of a single atom. In addition, investigations are conducted on ionic clusters which may better emulate charged active sites on bulk surfaces that result from electron transfer between the support material and the catalyst. The studies performed in our laboratory provide a fundamental understanding of the catalytic reaction mechanisms occurring for the future tailored design of bulk catalysts.

Recent Progress:

At the beginning of the continuing grant period we investigated gas-phase transition metal oxide clusters to further determine the molecular-level details of heterogeneous oxidation reactions. Zirconium oxide is utilized as

a catalyst support and active phase due to its thermal stability and high resistance to poisoning. Fundamental studies of the active site specific interactions occurring on the catalyst surface need to be conducted to optimize the utility of zirconium oxide as a catalyst material. Previous work in our laboratory determined that species with a $(\text{ZrO}_2)_x^+$ stoichiometry exhibit dominant products consistent with the transfer of an oxygen atom to CO, C_2H_4 , and C_2H_2 due to the existence of a highly localized oxygen radical center on this series of clusters. Charge transfer interactions between catalyst particles and support materials result in pronounced effects on catalytic activity; thus we endeavored to discover the influence charge state has on the activity of zirconium oxide clusters. During the grant period, our studies were extended to anionic zirconium oxide clusters to provide basic understanding of the catalytic mechanisms involved in practical industrial and commercial applications to enable the design of more efficient materials.

The reactivity of anionic zirconium oxide clusters with CO, C_2H_4 , and C_2H_2 were investigated both theoretically and experimentally to determine if an enhanced oxidation pathway can be identified as well as the existence of a radical oxygen species on the clusters. A series of anionic clusters with a $\text{Zr}_x\text{O}_{2x+1}^-$ stoichiometry were found to exhibit dominant oxygen transfer products when reacted with CO, consistent with the formation of CO_2 . The phenomenological rate constants have been calculated for the series to give a qualitative comparison of the relative reactivity of the different clusters ($\text{ZrO}_3^- = 2.1 \times 10^{-12} \text{ cm}^3 \text{ s}^{-1}$, $\text{Zr}_2\text{O}_5^- = 2.2 \times 10^{-13} \text{ cm}^3 \text{ s}^{-1}$, $\text{Zr}_3\text{O}_7^- = 3.4 \times 10^{-13} \text{ cm}^3 \text{ s}^{-1}$, and $\text{Zr}_4\text{O}_9^- = 1.8 \times 10^{-13} \text{ cm}^3 \text{ s}^{-1}$). In comparison with the earlier reported rate constants for the cationic clusters exhibiting enhanced oxidation, the anionic clusters are on average an order of magnitude lower. The calculated ground state structures of these anionic clusters revealed the presence of a highly localized oxygen radical center with an elongated zirconium oxygen bond, thus establishing that the radical oxygen can be found in both charge states. Therefore, by comparing the reactivity of cationic and anionic clusters containing radical oxygen centers it was possible to investigate how ionic charge state influences the oxidation of CO at the active site.

The calculated energy profile for the anionic clusters reveals that the oxidation of CO is initiated through the exothermic binding of the carbon atom of CO to the radical oxygen atom of the cluster. Transfer of charge from the CO_2 subunit back to the cluster involves a surmountable energy barrier and results in the formation of a complex with a linear CO_2 subunit. Emanation of CO_2 requires an available amount of energy making the oxidation of CO exothermic. Comparison of these results with those for the corresponding cationic cluster reveals that while the mechanism for CO oxidation is qualitatively similar between charge states, the energies of the various steps are different. Primarily, the oxidation of CO is more thermodynamically favorable for the cationic cluster than for the anionic species (1.65 eV for cation vs. 0.87 eV for anion). Furthermore, the critical barrier to the transfer of charge from the CO_2 subunit back to the cluster is larger for the anionic cluster than for the cationic species.

To determine whether the anionic $\text{Zr}_x\text{O}_{2x+1}^-$ clusters may be regenerated, and, therefore, promote a full catalytic cycle for the oxidation of CO, oxygen deficient $\text{Zr}_x\text{O}_{2x}^-$ clusters were reacted with N_2O . Each anionic cluster exhibited a strong oxygen addition product consistent with the formation of the original radical containing species. The phenomenological rate constants were determined for the oxidation of each stoichiometric cluster to the active $\text{Zr}_x\text{O}_{2x+1}^-$ and were on the order of high $10^{-13} \text{ cm}^3 \text{ s}^{-1}$ to mid $10^{-12} \text{ cm}^3 \text{ s}^{-1}$. Therefore, both cationic and anionic clusters containing oxygen radical centers promote a full catalytic cycle for the oxidation of CO with subsequent regeneration of the active site.

In contrast to the cationic $(\text{ZrO}_2)_x^+$ clusters that showed strong oxygen transfer products when reacted with C_2H_4 and C_2H_2 , the anionic $\text{Zr}_x\text{O}_{2x+1}^-$ clusters exhibited association products. Molecular dynamics (MD) simulations revealed that both hydrocarbons associate preferentially to an undercoordinated zirconium atom of the cluster. Consequently, in the anionic clusters, the radical oxygen center is located on the opposite side of the cluster to where C_2H_4 and C_2H_2 bind. This initial binding configuration necessitates significant structural rearrangement to enable the hydrocarbons to interact with a radical oxygen atom. The calculated energy profile reveals that the molecular mechanism for the oxidation of C_2H_4 and C_2H_2 involves insurmountable energy barriers. Therefore, association of C_2H_4 and C_2H_2 is observed to be the dominant reaction channel for the anionic clusters and not oxidation. Importantly, these findings suggest that charge state may be used to tune which molecules are oxidized by radical oxygen centers.

The different reactivity observed for cationic and anionic zirconium oxide clusters containing oxygen radical centers may be understood qualitatively from the calculated molecular electrostatic potential (MEP) of the clusters. The anionic $Zr_2O_5^-$ cluster has a negative value of the MEP over the entire cluster surface except in the vicinity of the less coordinated zirconium atom. Therefore, nucleophilic molecules such as acetylene and ethylene will bind preferentially to this site, which is on the opposite side of the cluster to the radical oxygen center. Consequently, oxidation is not observed due to the large energy barriers involved in the structural rearrangement and subsequent hydrogen transfer step. By contrast, the cationic $Zr_2O_4^+$ cluster has a positive MEP over the entire cluster surface, including in the vicinity of the radical oxygen center. Therefore, nucleophilic molecules may bind to the entire surface of the cationic cluster including the radical oxygen center. Oxidation then occurs because the barriers to the hydrogen transfer step are easily surmountable. CO, in contrast to C_2H_2 and C_2H_4 , has a dipole moment and can bind both to the radical center as well as to the less coordinated zirconium atom of the anionic cluster. This collaborative experimental and theoretical investigation of ionic zirconium oxide clusters has provided evidence that charge state directly influences the ability for isolated radical oxygen species to oxidize CO, C_2H_2 , and C_2H_4 .

Future Studies:

Significant progress has been made toward the elucidation of the molecular-level interactions occurring in catalytic processes; yet continued investigation is desirable to identify novel catalytically active species as well as alternatives for currently utilized precious metal catalysts. The remarkable oxidative ability of catalytic materials is due to their capacity to activate oxygen on their surfaces. Activated O_2 units possessing an extra electron, known as superoxides, have been identified on metal oxide surfaces and the catalytic activity of such surfaces are attributed to the presence of the superoxide species. In the gas-phase, the superoxide unit has been identified and a number of theoretical studies have revealed the superoxide structure as the thermodynamically stable metal-oxo species. Investigations will be performed utilizing the GIB-MS technique to probe the reactivity of $Zr_xO_{2x+1}^+$ clusters in an attempt to verify the existence of the superoxide unit. The series of clusters containing a superoxide unit will be reacted with butadiene, propylene, and ethylene. The expected result is to observe an oxidation pathway. Reaction profiles will be calculated by the Bonačić-Koutecký Group to provide mechanistic details of the oxidation process. Phenomenological rate constants will be calculated from the experimental results to facilitate the comparison of the oxidative properties between the radical oxygen and superoxide species. The investigation of zirconium oxide clusters containing isolated superoxide will produce a detailed molecular-level understanding of the reaction mechanism occurring.

Previous studies have investigated the regeneration of the catalytic site by oxidizing the deficient cluster with N_2O . In the case of superoxide, the likely event is that the cluster will react through loss of an oxygen creating a radical oxygen with a localized spin unpaired electron and an elongated zirconium oxygen bond. As has been previously shown, the radical oxygen species is an active site for the oxidation of CO, C_2H_4 , and C_2H_2 . The resultant cluster possessing the stoichiometry $Zr_xO_{2x-1}^+$ will be reacted with O_2 to determine if the superoxide structure is regenerated. This process will represent a full catalytic cycle that will likely occur in an industrial process utilizing O_2 as the oxidizing agent. The molecular-level understanding developed through these investigations will be beneficial toward the future directed design of catalysts either through cluster deposition or tailoring a surface to encompass selected active sites.

Publications Resulting from this Grant (2004 to Present):

570. "Elucidating Mechanistic Details of Catalytic Reactions Utilizing Gas Phase Clusters," M. L. Kimble, D. R. Justes, N. A. Moore, and A. W. Castleman, Jr., *Clusters and Nano-Assemblies: Physical and Biological Systems* (P. Jena, S. N. Khanna, B. K. Rao, Eds.) World Scientific: Singapore, New Jersey, London, 127-134 (2005).
573. "A Kinetic Analysis of the Reaction between $(V_2O_5)_n^+$ and Ethylene," N. A. Moore, R. Mitrić, D. R. Justes, V. Bonačić-Koutecký, and A. W. Castleman, Jr., *J. Phys. Chem. B.* 110, 3015 (2006)
584. "Influence of Charge State on the Mechanism of CO Oxidation on Gold Cluster," N. M. Reilly, G. E. Johnson, M. L. Kimble, A. W. Castleman, Jr., C. Bürgel, R. Mitrić, and V. Bonačić-Koutecký, *J. Am. Chem. Soc.* 130, 1694 (2008)

586. "Clusters: A bridge between disciplines," A. W. Castleman, Jr., *Puru Jena, Proc. Nat. Acad. Sci.* 103, 10552 (2006)
588. "Interactions of CO with $Au_nO_m^-$ ($n \geq 4$)," M. L. Kimble, A. W. Castleman, Jr., C. Bürgel, R. Mitrić, and V. Bonačić-Koutecký, *Int. J. Mass. Spec.* 254, 163 (2006).
592. "Clusters: A bridge across the disciplines of physics and chemistry," *Puru Jena, A. W. Castleman, Jr., Proc. Nat. Acad. Sci.* 103, 10560 (2006)
593. "Clusters: A bridge across the disciplines of environment, materials science, and biology," A. W. Castleman, Jr., *Puru Jena, Proc. Nat. Acad. Sci.* 103, 10554 (2006)
595. "Joint Experimental and Theoretical Investigations of the Reactivity of $Au_2O_n^-$ and $Au_3O_n^-$ ($n=1-5$) with Carbon Monoxide," M. L. Kimble, N. A. Moore, G. E. Johnson, A. W. Castleman, Jr., C. Bürgel, R. Mitrić, and V. Bonačić-Koutecký, *J. Chem. Phys.* 125, 204311 (2006)
599. "Reactivity of Anionic Gold Oxide Clusters Towards CO: Experiment and Theory," M. L. Kimble, N. A. Moore, A. W. Castleman, Jr., C. Bürgel, R. Mitrić, and V. Bonačić-Koutecký, *Eur. Phys. J. D* 43, 205 (2007)
600. "Influence of Charge State on the Reaction of $FeO_3^{+/-}$ with Carbon Monoxide," N. M. Reilly, J. U. Reveles, G. E. Johnson, S. N. Khanna, and A. W. Castleman, Jr., *Chem. Phys. Lett.* 435, 295 (2007)
601. "Recent Advances in Cluster Science," A. W. Castleman, Jr., *Proceedings for the Advances in Mass Spectrometry for the 17th Eur. J. Mass Spectrom.*, 13, 7-11 (2007)
603. "Femtochemistry VII: Fundamental Ultrafast Processes in Chemistry, Physics, and Biology," A. W. Castleman, Jr., and M. L. Kimble, Elsevier, ISBN 0 444 52821 0
606. "Multi-component fitting of cluster dynamics," K. L. Knappenberger, Jr., and A. W. Castleman, Jr., *Femtochemistry VII: Fundamental Ultrafast Processes in Chemistry, Physics, and Biology*, Elsevier, ISBN 0 444 52821 0
610. "Experimental and Theoretical Study of the Structure and Reactivity of $Fe_{1-2}O_{\leq 6}^-$ Clusters with CO," N. M. Reilly, J. U. Reveles, G. E. Johnson, S. N. Khanna, and A. W. Castleman, Jr., *J. Phys. Chem. A* 111, 4158 (2007)
613. "Experimental and Theoretical Study of the Structure and Reactivity of $Fe_{1-2}O_{1-5}^+$ with CO," N. M. Reilly, J. U. Reveles, G. E. Johnson, J. M. del Campo, S. N. Khanna, A. M. Köster, and A. W. Castleman, Jr., *J. Phys. Chem. C*, 111, 19097 (2007)
617. "The Reactivity of Gas Phase Metal Oxide Clusters: Systems for Understanding the Mechanisms of Heterogeneous Catalysts," N. M. Reilly, G. E. Johnson, and A. W. Castleman, Jr., book chapter to be published in, "Model Systems in Catalysis: From Single Crystals and Size-Selected Clusters to Supported Enzyme Mimics"
621. "Oxidation of CO by Aluminum Oxide Cluster Ions in the Gas Phase," G. E. Johnson, E. C. Tyo, and A. W. Castleman, Jr., *J. Phys. Chem. A*, 112, 4732 (2008)
623. "Cluster Reactivity Experiments: Employing Mass Spectrometry to Investigate the Molecular Level Details of Catalytic Oxidation Reactions," G. E. Johnson, E. C. Tyo, and A. W. Castleman, Jr., *Proc. Natl. Acad. Sci.*, 105, 18108 (2008)
624. "Gas-Phase Reactivity of Gold Oxide Cluster Cations with CO," G. E. Johnson, E. C. Tyo, A. W. Castleman, Jr., *J. Phys. Chem. C*, 112, 9730 (2008)
627. "Stoichiometric Zirconium Oxide Cations as Potential Building Blocks for Cluster Assembled Catalysts," G. E. Johnson, E. C. Tyo, A. W. Castleman, Jr., R. Mitrić and V. Bonačić-Koutecký, *J. Am. Chem. Soc.*, 130, 13912 (2009)
628. "Effect of Charged State and Stoichiometry on the Structure and Reactivity of Nickel Oxide Clusters with CO," G. E. Johnson, N. M. Reilly and A. W. Castleman, Jr., *Int. J. Mass Spectrom.*, 280, 93 (2009)
630. "Influence of Stoichiometry and Charge State on the Structure and Reactivity of Cobalt Oxide Clusters with CO," G. E. Johnson, J. U. Reveles N. M. Reilly, E. C. Tyo, S. N. Khanna and A. W. Castleman, Jr., *J. Phys. Chem. A*, 112, 11330 (2008)
632. "Clusters, Superatoms and Building Blocks of New Materials," A. W. Castleman, Jr., and S. N. Khanna, *Invited Featured Article for the J. Phys. Chem. C*, 113, 2664 (2009)
635. "Influence of Charge State on Catalytic Oxidation Reactions at Metal Oxide Clusters Containing Radical Oxygen Centers," G. E. Johnson, E. C. Tyo, A. W. Castleman, Jr., R. Mitrić, M. Nöbner and V. Bonačić-Koutecký, *J. Am. Chem. Soc.*, 131, 5460 (2009)
636. "Cluster-Assembled Materials," S. A. Claridge, A. W. Castleman, Jr., S. N. Khanna, C. B. Murray, A. Sen, and P. S. Weiss, *ACS Nano*, 3, 244 (2009)
637. "Clusters as Model Systems for Investigating Nanoscale Oxidation Catalysis," G. E. Johnson and A. W. Castleman, Jr., *Chem. Phys. Lett.*, 475, 1 (2009)
638. "Large Effect of a Small Substitution: competition of Dehydration with Charge Retention and Coulomb Explosion in Gaseous $[(bipy^R)Au(\mu-O)_2Au(bipy^R)]^{2+}$ Dications," E. C. Tyo, A. W. Castleman, Jr., D. Schröder, P. Milko, J. Roithova, J. M. Ortega, M. A. Cinellu, F. Cocco and G. Minghetti, *J. Am. Chem. Soc.* (submitted 4/8/09)
639. "Reactivity Trends in the Oxidation of CO by Anionic Transition Metal Oxide Clusters," G. E. Johnson, J. U. Reveles, S. N. Khanna and A. W. Castleman, Jr., *J. Phys. Chem.*, (submitted June 2009)

An Exploration of Catalytic Chemistry on Au/Ni(111)
Professor S. T. Ceyer
Department of Chemistry
Massachusetts Institute of Technology, Cambridge, MA 02139
stceyer@mit.edu

Project Scope

This project explores the breadth of catalytic chemistry that can be effected on a Au/Ni(111) surface alloy. A Au/Ni(111) surface alloy is a Ni(111) surface on which less than 60% of the Ni atoms are replaced at random positions by Au atoms. The alloy is produced by vapor deposition of a small amount of Au onto Ni single crystals. The Au atoms do not result in an epitaxial Au overlayer or in the condensation of the Au into droplets. Instead, Au atoms displace and then replace Ni atoms on a Ni(111) surface, even though Au is immiscible in bulk Ni. The two dimensional structure of the clean Ni surface is preserved. This alloy is found to stabilize an adsorbed peroxo-like O₂ species that is shown to be the critical reactant in the low temperature catalytic oxidation of CO and that is suspected to be the critical reactant in other oxidation reactions. These investigations may reveal a new, practically important catalyst for catalytic converters and production of some widely used chemicals.

Recent Progress

To supplement our studies of the catalytic oxidation reactivity, we have carried out a detailed study of the interaction of O₂ with the Au/Ni(111) surface alloy. We find that the adsorption of O₂ is molecular at 77 K. This observation is in stark contrast to the adsorption of O₂ on Ni(111), which is dissociative even at 8 K. This observation is also in stark contrast to the interaction of O₂ with Au(111) because O₂ adsorbs neither molecularly nor dissociatively on Au(111) at or above 100 K. The addition of a small amount of Au to Ni lowers the Fermi level so that the overlap of the Ni 3d electrons with the π^* orbitals of O₂ is less than what it is on pure Ni. It is just enough less to stabilize O₂ from dissociation on the Au/Ni surface alloy but not so little as to preclude adsorption as on Au(111). Molecularly adsorbed O₂ on Au/Ni(111) is characterized by three distinct vibrational frequencies, 790 cm⁻¹, 865 cm⁻¹ and 950 cm⁻¹, as measured by high resolution electron energy loss spectroscopy, and are assigned to the vibration of the O=O bond of molecular oxygen adsorbed on the alloy with its bond axis largely parallel to the surface. Molecular oxygen so adsorbed is considered a peroxo (O₂⁻²) or superoxo (O₂⁻¹) species. The three distinct O₂ vibrational frequencies reflect three distinct binding sites, where the vibrational frequency is inversely proportional to the binding energy. The three sites are populated sequentially as a function of Au coverage. The more strongly

bound O₂, characterized by the lowest vibrational frequency of 790 cm⁻¹, is stabilized on the Au/Ni surface alloy at a low Au coverage, 0.25 ML. At 0.3 ML Au, a feature at 865 cm⁻¹ and a feature at 950 cm⁻¹ appear. The three features grow in intensity until a maximum intensity of the 790 cm⁻¹ feature is achieved at about 0.38 ML Au and a maximum intensity of the 865 cm⁻¹ and 950 cm⁻¹ features is achieved at about 0.45 ML Au. The intensity of all features then decreases as the Au coverage is increased and approaches zero at about 0.65 ML Au. The frequency of the 950 cm⁻¹ feature shifts up to about 1000 cm⁻¹ as the Au coverage increases from 0.45 ML to 0.65 ML.

The peroxy and superoxy species dissociate after heating the surface to 105-120 K as evidenced by the disappearance of their O=O stretch modes and the appearance of two features at 580 and 435 cm⁻¹, attributed to atomically adsorbed O. These features at 580 cm⁻¹ and 435 cm⁻¹ have the same frequency as observed for O atoms bound to Ni(111). Extensive detailed measurements have recently shown that about 10% of the O₂ does not dissociate but rather desorbs molecularly between 105-120 K. Note that there is no evidence for atomically bound O at 77 K.

We have discovered that the peroxy and superoxy species stabilized on the Au/Ni(111) surface alloy efficiently oxidize CO at 70 K. The experiment is carried out in the following manner. Saturation coverage of molecular O₂ is adsorbed on the 0.44 ML Au/Ni surface alloy at 77 K. When a beam of thermal energy CO is directed at the O₂ covered Au/Ni(111) surface alloy held at 70 K, gas phase CO₂ is immediately produced. A control experiment demonstrates that no CO₂ is produced when the CO beam impinges on the crystal mount.

After exposure of the O₂-covered surface alloy at 70 K to CO, two C=O stretch vibrational modes are observed at 2170 and 2110 cm⁻¹, along with the Au/Ni-CO stretch mode at 420 cm⁻¹. The O=O modes at 865 cm⁻¹ and 950 cm⁻¹ are much reduced in intensity, while the feature at 790 cm⁻¹ has maintained its intensity. The decrease in intensities of the 865 cm⁻¹ and 950 cm⁻¹ features is interpreted to mean that most of the molecularly adsorbed O₂ has reacted with CO to form gas phase CO₂. The product remaining from this reaction is an O atom adsorbed to Au, as evidenced by the appearance of a new feature at 660 cm⁻¹. The molecularly adsorbed O₂ that gives rise to the feature at 790 cm⁻¹ appears not to react with CO.

This alloy surface covered with CO and some adsorbed O₂ is heated at 2 K/s while the partial pressures at masses 44 and 28 are monitored. Rapid production and desorption of CO₂ is clearly observed between 105-120 K, along with CO desorption. Production of CO₂ in this temperature range occurs at the same temperature at which O₂ dissociates. This observation suggests that CO₂ formation occurs between CO and a

"hot" O atom that has not yet equilibrated with the surface after bond dissociation. From 120 K to about 250 K, CO₂ is slowly produced by reaction of the adsorbed O atoms represented by 660 cm⁻¹ mode and by the adsorbed O atoms that did not react immediately as a hot O atom upon O₂ dissociation.

These results demonstrate that Au/Ni(111) catalyzes the oxidation of CO at low temperature. Clearly, substitution of a small number of Ni atoms on the Ni(111) surface by Au atoms has dramatically changed the Ni chemistry. The oxidation of CO on Ni has never been observed under UHV laboratory conditions, presumably because both the oxygen atom and CO are too strongly bound, and hence the barrier to their reaction is too large. Introduction of Au into the Ni lattice serves to weaken the bonds between oxygen and CO so as to allow the reaction to proceed. These results also imply that nanosize Au clusters are not a necessary requirement for low temperature CO oxidation in general. Rather, interaction of the Au atoms around the perimeter of the Au nanocluster with the transition metal of the oxide support likely provides the active sites that stabilize the adsorption of molecular O₂ that is necessary for the oxidation of CO.

Current Status

We recently designed and fabricated a new Au source coupled with a quartz crystal microbalance that allowed the production of a more homogenous Au/Ni surface alloy over the entire surface area of the Ni single crystal. This discovery necessitated that the absolute Au coverage be recalibrated. It was found to be a factor of two larger than our previous calibration. The attainment of a more homogeneous alloy enabled the more detailed study of the molecular O₂ vibrational spectrum described above. In addition, we have observed a negative ion resonance at about 2 eV in the high resolution electron energy loss spectra of the adsorbed molecular O₂. The resonance scattering resulted in increased intensity of the vibrational spectra that allows the observation of additional adsorbed O₂ vibrational modes not observed at more typical excitation energies (5 eV). These high resolution vibrational spectra of molecularly adsorbed O₂ on the Au/Ni(111) surface alloy will serve as important benchmarks for the continued development of density functional theory for surface adsorbates.

Additional measurements of the CO₂ production at 77 K as a function of Au coverage show that CO₂ production correlates with molecular O₂ coverage (as measured by the intensity of the adsorbed peroxy species at 950 and 865 cm⁻¹), where the maximum CO₂ production and molecular O₂ coverage occurs at 0.44 ML Au. A Monte Carlo simulation of the molecular O₂ coverage as a function of Au coverage was carried out to probe the site requirements for O₂ adsorption. The best agreement between the simulated and experimental O₂ coverage is observed when O₂ sits in a Ni atom bridge

site of an ensemble of 6 Ni and 4 Au atoms of any hexagonal configuration. Molecular adsorption is blocked when an adsorbed O atom is within 5 Å of the bridge site.

We have also recently discovered that atomically adsorbed O atoms also react with CO at 77 K to produce CO₂ at high Au coverages around 0.5 ML. This experiment was carried out by initially adsorbing O₂ at 77 K, raising the surface temperature to 300 K to dissociate O₂, lowering the temperature to 77 K and then exposing the surface to a beam of CO. The reaction probability of adsorbed O atoms with CO appears to be substantially lower, approximately an order of magnitude, than that of adsorbed molecular O₂. Measurements are presently being carried out to accurately quantify this observation.

Future Plans

A major thrust of this project is to explore the range of reactivity of the O₂ species molecularly adsorbed on the Au/Ni(111) surface alloy. The hypothesis is that our newly observed molecular O₂ adsorbate is the crucial reactant in two oxidation reactions to be studied: the direct synthesis of H₂O₂ from H₂ and O₂ and the epoxidation of propylene to form propylene oxide. In addition, it is planned to investigate whether the Au/Ni surface alloy is also active for the reduction of NO by CO. It is possible that a molecularly adsorbed NO species with a bond order approaching one is the active species in the NO reduction reaction at low temperature on the Au/Ni(111) surface alloy.

Publications

Catalyzed CO Oxidation at 70 K on an Extended Au/Ni Surface Alloy

D. L. Lahr and S. T. Ceyer, *J. Am. Chem. Soc.* **128**, 1800 (2006)

Stabilization of Molecular O₂ Adsorbed on a Au-Ni Surface Alloy

J. G. Lee, J. D. Fischer, D. L. Lahr, C. Leon, in preparation

Oxidation of CO on a Au/Ni Surface Alloy

J. G. Lee, D. L. Lahr, J. D. Fischer, C. Leon, in preparation

Ph.D. Theses

Molecular Oxygen Adsorbates at a Au/Ni(111) Surface Alloy and Their Role in Catalytic CO Oxidation at 70 – 250 K, D. L. Lahr - June, 2006 – MIT

Catalytic Oxidation on Au/Ni(111), J. D. Fischer – February, 2010 - MIT

Patent Application

U.S. Pat. Apl. Ser. No.: 11/335,865. S. T. Ceyer and D. L. Lahr

Theory of Dynamics of Complex Systems

David Chandler

*Chemical Sciences Division, Lawrence Berkeley National Laboratory
and
Department of Chemistry, University of California, Berkeley CA 94720*

DOE funded research in our group concerns the theory of dynamics in systems involving large numbers of correlated particles. Glassy dynamics is a quintessential example. Here, dense molecular packing severely constrains the allowed pathways by which a system can rearrange and relax. The majority of molecular motions that exist in a structural glass former are trivial small amplitude vibrations that couple only weakly to surrounding degrees of freedom. In contrast, motions that produce significant structural relaxation take place in concerted steps involving many particles, and as such, dynamics is characterized by significant heterogeneity in space and time. We have shown how the essential features of this heterogeneity – the decoupling of exchange and persistence – emerge from molecular dynamics of atomistic models [4].¹ An interesting consequence of this decoupling is negative response. For example, the drift velocity in response to a pulling force can on average *decrease* with increasing pulling force [6].

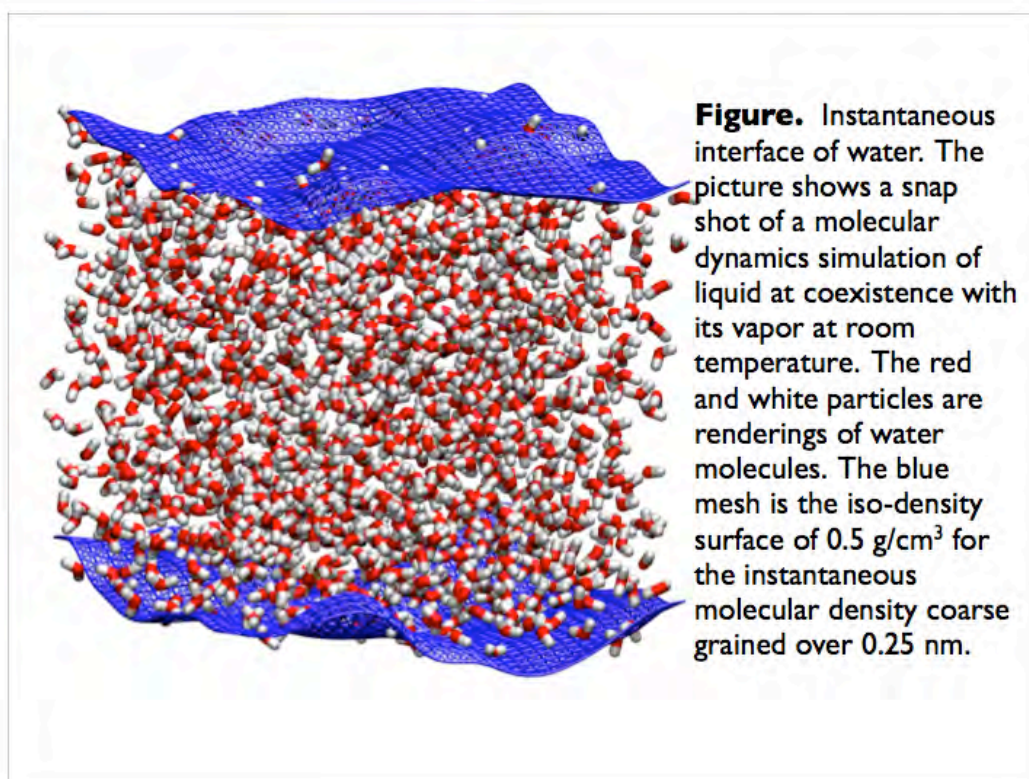
The kinetics of self-assembly is another example of correlated many-particle dynamics. On this topic, we have worked to devise and apply new algorithms for numerical simulation [1,2], and we have carried out trajectory studies of the dynamics of hydrophobic assembly [2,5]. This process is closely related to nucleation of vapor in water and the formation of a water-vapor interface, and it is the nature of this interface that controls the likelihood of solvent fluctuations [9,10] and free energies of solvation [3].

Our current and planned DOE funded research focuses on electron transfer, chemical dynamics and inhomogeneous fluids. We are developing techniques and concepts that should ultimately prove useful in the specific context of combining sunlight and renewable resources to produce transportation fuels, thus interfacing with the LBNL Helios SERC. To reach that point, our DOE support in this program is aimed at basic underlying issues. Applications can then be done with Helios support. The first of these basic issues is the nature of ionic solutions at metal and semiconductor surfaces. In our first paper on the topic, we have demonstrated the dominant effect of fluctuations from mean ionic densities [8], and work is currently underway to describe the correlated nature of water reorganization adjacent to these surfaces. We have found that at these surfaces ensemble-averaged dynamics of water is remarkably slow. Rare or intermittent events that produce reorganization of surface bound water molecules are thus pertinent to any chemical dynamics that might be catalyzed at these surfaces. The second is the

¹ Numbers in square brackets refer to papers cited in **Recent DOE Supported Research Publications**

development of ways to carry out numerical simulations of electronically non-adiabatic transitions. For this topic, we have explored a way to reliably mimic aspects of quantum dynamics with classical computation and used the method to treat the behavior of an electron in a fluid [7], and we are currently considering extensions of this procedure for treating coupled electron-proton transfer reactions. With these techniques in hand, it will be possible to carry out transition path sampling calculations to discover pathways of hydrogen production from water.

We have also developed a new and generally applicable tool for examining liquid interfacial structure and dynamics [10]. In particular, we have found a useful definition of an instantaneous fluid interface as an iso-density surface for molecular density coarse grained over a bulk correlation length. See Figure below. The algorithm we have devised for identifying this surface is easily applied in conditions of arbitrary symmetries. It can therefore be applied to study the role of liquid interfacial fluctuations on the kinetics of various processes, from evaporation to self-assembly to chemical transformations. Studies are underway on each of these topics.



Recent DOE Supported Research Publications

1. Miller, T.F. and C. Predescu, "Sampling diffusive transition paths," *J. Chem. Phys.* **126**, 144102.1-12 (2007) .
2. Miller, T.F., E. Vanden-Eijnden and D. Chandler, "Solvent coarse-graining and the string method applied to the hydrophobic collapse of a hydrated chain," *Proc. Natl. Acad. Sci., USA* **104**, 14559-64, (2007).
3. Maibaum, L. and D. Chandler, "Segue between favorable and unfavorable solvation," *J. Phys. Chem. B* **111**, 9025-9030 (2007).
4. Hedges, L.O., L. Maibaum, D. Chandler and J.P. Garrahan "De-coupling of Exchange and Persistence Times in Atomistic Models of Glass Formers," *J. Chem. Phys.* **127**, 211101.1-4 (2007).
5. Willard, A. P., D. Chandler "The Role of Solvent Fluctuations in Hydrophobic Assembly," *J. Phys. Chem. B* **112**, 6187-6192 (2007).
6. Jack, R.L., D. Kelsey, J.P. Garrahan and D. Chandler, "Negative differential mobility of weakly driven particles in models of glass formers," *Phys. Rev. E* **78**, 011506.1-9 (2008)
7. Miller, T.F., "Isomorphic classical molecular dynamics model for an excess electron in a supercritical fluid," *J. Chem. Phys.* **129**, 194502.1-10 (2008).
8. Willard, A.P., S.K. Reed, P.A. Madden, and D. Chandler, "Water at an electrochemical interface - a simulation study," *Faraday Discuss.* **141**, 423-441 (2009)
9. Willard, A.P., and D. Chandler, "Coarse Grained Modeling of The Interface Between Water and Heterogeneous Surfaces," *Faraday Discuss.* **141**, 209-220 (2009).
10. Willard, A.P., and D. Chandler, "Instantaneous Liquid Interfaces," submitted (2009)

Computational Studies of Radiolytic Species and Processes in Water

Daniel. M. Chipman, Chipman.1@nd.edu
Radiation Laboratory, University of Notre Dame, Notre Dame, IN 46556

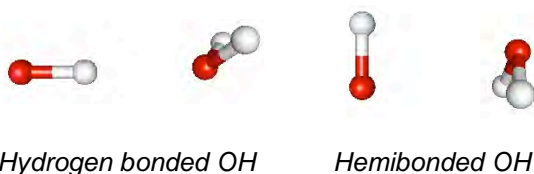
Program Scope

This program provides theoretical and computational support for experimental efforts in various group projects at the Notre Dame Radiation Laboratory that investigate water radiolysis. It particularly focuses on characterizing early events where aqueous radiolytic species are formed and transformed in the fs-ps time domain. The information from such studies is needed to provide initial conditions for Monte Carlo modeling of the subsequent inhomogeneous track chemistry and to understand how solvent influences the mechanisms of the various bimolecular reactions that ensue to produce final products.

Recent Progress

The theoretical basis for quantum mechanical calculation of solvatochromic shifts within a dielectric continuum model of solvent has been extended to develop exact and accurate approximate methods for treatment of the oft-neglected effects of solvent volume polarization in the fast optical and slow inertial solvent responses. These methods have been implemented in the Gamess electronic structure computer package and illustrative calculations have been made on representative solutes. The volume polarization contributions are found to be important when there is a significant change upon excitation in the amount of solute charge that penetrates outside the solute cavity.

The hydroxyl (OH) radical, being the primary oxidizing species produced in water radiolysis, is fundamental to aqueous radiation chemistry, and its chemical reactions are also of great importance in many biological systems. Measurements of rate constants involving the OH radical reacting with various substrates in aqueous solution are often based on monitoring the characteristic UV absorption band of OH, which peaks at about 235 nm. We have investigated the molecular nature of this band with high level electronic structure calculations on OH interacting in various ways with a water molecule, together with a dielectric continuum treatment of remaining bulk effects. The main valence transition of OH occurs at about 306 nm in gas. The wide shoulder in the aqueous spectrum



occurring to the red side of the gas band is found to be mainly due to this transition in the most stable hydrogen bonded arrangement wherein OH donates a hydrogen bond to water. In a less stable

arrangement wherein OH accepts a hydrogen bond from water, this transition occurs near or only slightly to the blue side of the gas phase band. The

characteristic broad absorption peaking at about 235 nm is instead found to be due to a “charge transfer *from* solvent” transition. This transition is somewhat operative in the OH acceptor arrangement, and is mainly operative in hemibonded arrangements between OH and water. The hemibond is a two-center three-electron interaction with a formal bond order of $\frac{1}{2}$. Such hemibonded interactions are attractive between the two partners, but are not local minimum energy structures and so occur only transiently. They contribute to the spectrum far out of proportion to their population due to the huge oscillator strength associated with the charge transfer nature of the transition. This interpretation also serves to qualitatively explain the observed temperature and pressure dependence of the experimental OH spectrum.

Benchmarks have been established for the quantum mechanical treatment of delocalization and charge transfer effects on excited states of small water clusters. These elucidate critical methodological issues in calculation of the UV absorption spectrum of liquid water related to the accuracy of the theoretical method, system size convergence of the absorption spectrum, and correction of surface effects. Due to substantial delocalization of both the valence hole and the excited electron distribution, a supramolecular perspective that considers on the same footing the ground and excited states of a number of explicit quantum molecules is found to be necessary.

Previous experimental and theoretical works have indicated that dissociative electron attachment (DEA) processes are important in the radiolysis of ice, and possibly also of liquid water, but details are poorly understood. To help elucidate how hydrogen bonding may affect the DEA of water in the condensed phase, we have utilized multireference configuration interaction methods to computationally characterize the lowest energy Feshbach resonance state of water dimer anion. The potential energy surface in the analogous state of water monomer anion is known to be repulsive, so that electron attachment leads directly to dissociation of H^- . In contrast, we find for the dimer that an energetic barrier is encountered as the hydrogen-bonded OH moiety is stretched from its equilibrium position toward the hydrogen bond acceptor. The migrating hydrogen can thereby be held near the Franck-Condon region in a quasibound vibrational state for a time long compared to the OH vibrational period. This behavior is found both for the case of an ice-like dimer structure and for a substantial majority of liquid-like dimer structures. These findings raise the possibility that hydrogen bonding in condensed water phases may allow for a localized molecule-centered anionic entity to exist that is metastable both to electron detachment and to bond dissociation, and which may live long enough to be considered as a species affecting DEA processes in water radiolysis.

Changes in the SERS spectra of a *p*-aminothiophenol probe molecule adsorbed on silver nanoparticles were monitored during charging and discharging of the particles. The observed changes were attributed to the effect of the Fermi level position on coupling of the particle’s plasmon band to vibrational levels of the

electronic ground state. This vibrational coupling in turn leads to borrowed intensity due to the existence of a particle-molecule charge-transfer state for the adsorbed molecule. Electronic structure calculations on representative model Ag-molecule species suggest that some significant redistribution of charge between the molecule and the particle is already present in the ground state. This redistribution of charge implies the existence of an adsorbed radical-charged metallic particle in addition to the original molecule-metal particle. Present efforts focus on expanding the metallic surfaces to include other metals, understanding the effect of excitation wavelength on the SERS spectra during irradiation, and performing electronic structure calculations on more realistic, select cluster-molecule or cluster-radical structures in order to predict the vibrational transitions of the molecule (or radical) on the surface.

Future Plans

The microscopic solvation environments of water molecules, hydroxyl radicals, and hydrogen atoms in liquid water will be determined as a function of temperature and pressure from a computational effort that is closely coupled to an experimental program in this laboratory. Clusters containing the solutes together with nearby explicit solvent molecules will be extracted from snapshots of molecular dynamics simulations, and their spectral properties then determined from high level electronic structure calculations that include effects of the bulk solvent from simplified models. The calculated water UV absorption spectra, the hydroxyl UV/vis absorption spectra, and the hydrogen atom EPR spectra will be compared to those determined experimentally in this laboratory. This will allow the experimental data to be interpreted and, at the same time, the quality of the computations to be assessed, which will eventually lead to a much more complete understanding of how water, hydroxyl, and hydrogen solvate in water.

BES Sponsored Publications 2006-2009

D. M. Chipman, *Vertical Electronic Excitation with a Dielectric Continuum Model of Solvation Including Volume Polarization. I. Theory*, J. Chem. Phys. **2009**, *131*, 014103/1-10.

D. M. Chipman, *Vertical Electronic Excitation with a Dielectric Continuum Model of Solvation Including Volume Polarization. II. Implementation and Applications*, J. Chem. Phys. **2009**, *131*, 014104/1-6.

D. M. Chipman, *Absorption Spectrum of OH Radical in Water*, J. Phys. Chem. A **2008**, *112*, 13372-13381.

G. Merga, L. C. Cass, D. M. Chipman, and D. Meisel, *Probing Silver Nanoparticles During Catalytic H₂ Evolution*, J. Am. Chem. Soc. **2008**, *130*, 7067-7076.

D. M. Chipman, *Dissociative Electron Attachment to the Hydrogen-bound OH in Water Dimer Through the Lowest Anionic Feshbach Resonance*, J. Chem. Phys. **2007**, 127, 194309/1-10.

D. M. Chipman, *New Formulation and Implementation for Volume Polarization in Dielectric Continuum Theory*, J. Chem. Phys. **2006**, 124, 224111.

D. M. Chipman and F. Chen, *Cation Electric Field is Related to Hydration Energy*, J. Chem. Phys. **2006**, 124, 144507.

D. M. Chipman, *Stretching of Hydrogen-Bonded OH in the Lowest Excited Electronic State of Water Dimer*, J. Chem. Phys. **2006**, 124, 044305.

Y. Shao, L. F. Molnar, Y. Jung, J. Kussmann, C. Ochsenfeld, S. T. Brown, A. T.B. Gilbert, L. V. Slipchenko, S. V. Levchenko, D. P. O'Neill, R. A. DiStasio Jr, R. C. Lochan, T. Wang, G. J.O. Beran, N. A. Besley, J. M. Herbert, C. Y. Lin, T. Van Voorhis, S. H. Chien, A. Sodt, R. P. Steele, V. A. Rassolov, P. E. Maslen, P. P. Korambath, R. D. Adamson, B. Austin, J. Baker, E. F. C. Byrd, H. Dachsel, R. J. Doerksen, A. Dreuw, B. D. Dunietz, A. D. Dutoi, T. R. Furlani, S. R. Gwaltney, A. Heyden, S. Hirata, C.-P. Hsu, G. Kedziora, R. Z. Khalliulin, P. Klunzinger, A. M. Lee, M. S. Lee, W. Z. Liang, I. Lotan, N. Nair, B. Peters, E. I. Proynov, P. A. Pieniazek, Y. M. Rhee, J. Ritchie, E. Rosta, C. D. Sherrill, A. C. Simmonett, J. E. Subotnik, H. L. Woodcock III, W. Zhang, A. T. Bell, A. K. Chakraborty, D. M. Chipman, F. J. Keil, A. Warshel, W. J. Hehre, H. F. Schaefer III, J. Kong, A. I. Krylov, P. M. W. Gil, and M. Head-Gordon, *Advances in Methods and Algorithms in a Modern Quantum Chemistry Program Package*, Phys. Chem. Chem. Phys. **2006**, 8, 3172.

Fast Reactions Investigated With Picosecond Electron Pulses

Center for Radiation Chemistry Research

Principal Investigators: Andrew R. Cook & John R. Miller

Chemistry Department, Brookhaven National Laboratory

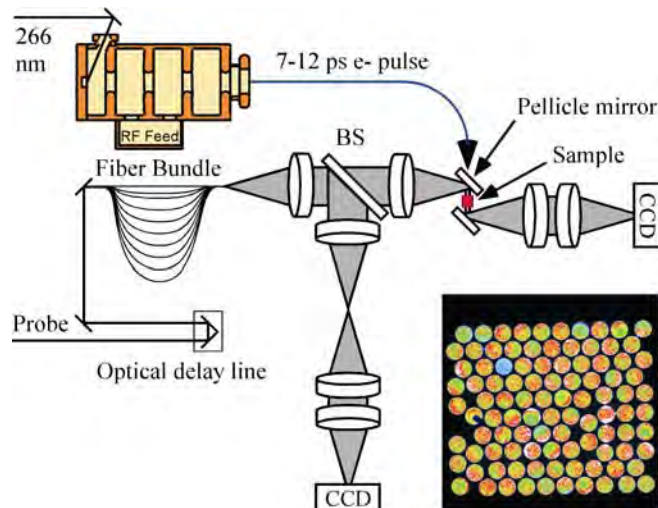
Bldg. 555, Upton NY 11973

acook@bnl.gov, jrmiller@bnl.gov

Program Scope: Short electron pulses provide unique tools to investigate questions important in solar energy conversion. This program develops new tools for such investigations, applies them to chemical questions, and makes them available to the research community.

Optical Fiber Single-Shot (OFSS) detection system at LEAF. The OFSS detection system allows single shot kinetic measurements of transient optical absorption with time resolution of 15 ps and time range of 1.5 ns after single electron pulses from the accelerator. Overlap with data from transient digitizer experiments can be obtained using multiple positions

of an optical delay line. It is a critical new capability for LEAF science studies that makes possible measurements on samples that are available in limited quantities, are too viscous to flow, or are rigid. It is essential in applications such as picosecond pulse radiolysis, where the thousands of pulses per kinetic trace typical in classical pump-probe experiments can damage the sample before useful results could be obtained. Other methods have performed single-shot transient-absorption spectroscopy following laser excitation. This new approach, illustrated at right, utilizes a bundle of optical fibers of varied lengths imaged on a CCD array

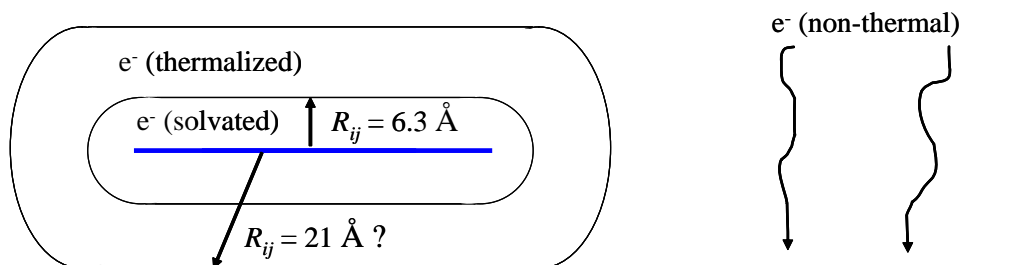


detector. First demonstrated just over three years ago, this detection system produced data only at 800 nm with signal-to-noise adequate for only a limited set of investigations. Two days or more were needed to set it up for use. It was not yet a real research tool. Improvements in this period: 1) Installed a reference CCD camera that reduced noise due to shot-to-shot variations in fiber-to-fiber light intensity. 2) Further enhanced signal-to-noise (S/N) using correction factors that account for the different dose the sample receives at each fiber position. 3) Developed a remote sample changer that reduced the time to switch samples from minutes to seconds, mitigating the effect of slow electron beam drift and the accompanying loss of correction factor efficacy. 4) Added the ability to tune the probe wavelength from 540 – 960 nm using an optical parametric amplifier (OPA). 5) Enabled faster wavelength and sample changes with remotely focusable key optics. 6) Revised the data acquisition software for easier and faster operation as well as improved S/N.

The improved OFSS has enabled new studies of rapid charge capture by molecular wires and electron scavenging in ionic liquids, as well as studies of charge transfer in polyfluorenes, and oligomers of fluorene and platinum acetylides. It has become a powerful research tool providing 15 ps time resolution. Set-up and data reduction are still time consuming; additional improvements in efficiency and S/N are planned.

“Step” capture of electrons by conjugated polymers. In order to study rapid charge transport to pendant acceptor groups on long extended conjugated polymers, it is necessary to understand the rates and numbers of electrons attached following pulse radiolysis. Part of this understanding comes from studies of diffusional capture of electrons, discussed below. However if charge transfer rates are rapid, diffusion is typically too slow due to the limited solubility of such molecules. It was noted last year that substantial numbers of electrons in dilute concentrations of polymers were captured by some rapid sub-15 ps process, presumably pre-solvated electron capture. Recent efforts have refined this thinking and quantified this process. Studies involved both polyfluorene (pF) polymers of different length (~20-114 nm) and different concentrations dissolved in THF. Contributions to the observed 15 ps “step” in the transient absorption due to the formation of pF cations, and excited states were measured and accounted for. At the highest concentrations of different length polymers used (in which the fluorene monomer concentration was the same), it was found that ~30% of electrons produced by pulse radiolysis were captured in < 15 ps.

The mechanism of pre-solvated electron capture has been discussed previously by multiple authors, but has not been definitively determined. Such capture is generally discussed as occurring from one or more states of the electron. The initial ionization event ejects an electron with excess kinetic energy, e^- (non-thermal). The electron is thought to travel large distances, many larger than the Onsager radius depending on the solvent as evidenced by significant free ion yields. Through interactions with the medium, the electron subsequently becomes thermalized. Because they are not yet fully trapped by the solvent, thermalized electrons are characterized by large electronic wavefunctions and high mobilities. Finally, thermalized electrons are localized following relaxation of the environment around them to form solvated electrons. Pre-solvated electron capture may involve both non-thermal and thermalized electrons. For pFs, the mechanisms by which such capture may occur is shown in the figure below:



The greater mobility of thermalized electrons compared to solvated is shown in terms of a radius around the polymer at which electron capture may occur. Previous work determined that electrons that are solvated within 6.3 Å of the polymer are attached promptly. Similarly, if all of the pre-solvated electron capture was due to reactions with thermalized electrons, a reaction distance of 21 Å would be required to describe the volume fraction of the solution within which capture occurs to account for the magnitude of the observed step capture in the case of the highest concentration of polymers. Capture of hot electrons can be understood as occurring when the trajectory of the electron away from the ionization site intercepts the cross-sectional area of the polymer. While knowledge of the proper cross-sectional area is not known, reasonable assumptions can describe a similar electron capture volume as above if the distance the electron travels is ~ 12 Å. This distance is reasonable, especially when it is considered that the trajectory is not straight due to scattering processes, compared to the average distance electrons get away from the parent holes after ionization, which would be a just bit less than the Onsager distance of 7.5 Å in THF to account for the low known free ion yield. Given that both of these pre-solvated electron capture mechanisms are plausible, it is not possible to determine if either dominates step capture in the pF samples.

While some details remain to be worked out, the key conclusion of this work is that large numbers of electrons are attached in pulse radiolysis experiments of conjugated polymers. As noted earlier, this is key to the measurement of expected rapid charge transport in such systems.

The Transient Term and Time-Dependent Rate Coefficients. Classically diffusion-controlled reactions occur on every encounter of the reacting species, so the rate constants depend only on the diffusion coefficients and the reaction radius, with little dependence on specific reactivities. The theory of Smoluchowski produced an equation, the simple form of which has proved to be remarkably durable:

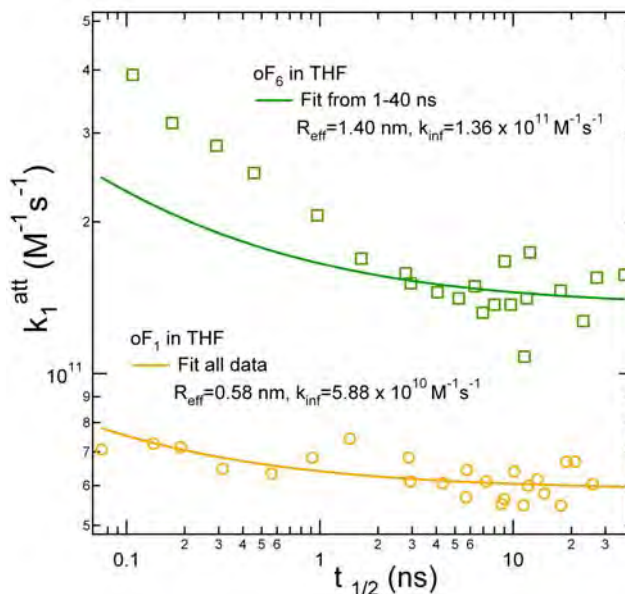
$$k(t) = 4\pi R_{\text{eff}} D N_A (1 + R_{\text{eff}}/(\pi D t))^{1/2} \quad (1)$$

$$k_{\text{inf}} = 4\pi R_{\text{eff}} D N_A \quad (2)$$

Eq 1 gives the rate constant for a bimolecular, diffusion-controlled reaction in terms of just two parameters, the mutual diffusion coefficient $D=(D_A+D_B)$ and the effective reaction radius, R_{eff} . R_{eff} has different meanings: 1) In the Smoluchowski theory for diffusion-controlled reactions of small molecules approximated as spheres, R_{eff} is just the sum of the physical radii of the two reactants. The reaction rate at contact is taken as infinite and zero otherwise. Subsequent more precise theories developed many elaborated forms to deal with finite rate on contact, and complexities that cause deviations from eq 1 have been reviewed. 2) Electron transfer and electronic energy transfer do not require physical contact for reaction and occur over a range of distances so R_{eff} is typically a few to several Å larger than the physical sizes of the reactants at ordinary viscosities. 3) Reactions with non-spherical molecules can be accommodated in the same framework, with R_{eff} representing an average reaction distance. Results reported last year showed that rates of electron attachment to conjugated polymer molecule were in good accord with theories that discussed the diffusional flux to either a 1) prolate spheroid, or 2) a line of spheres. For lengths from one to 133 fluorene repeat units R_{eff} varied from 0.58 to 10.4 nm.

The results also found an that diffusion controlled rate coefficients increase a short times due to the “transient term” in Eq 1. For an oligomer containing one repeat unit, oF_1 , the increases in the attachment rate coefficients are small, but larger increases are seen for the longer oF_6 . Time dependence of electron capture by oF_1 and oF_6 (100, 400 and 970 μM) oligomers in THF determined by competition with DCE. The lines show predictions of Eq 1.

These results and those for the very long pF_{133} are now found to be in excellent accord with Eq 1 when “step capture” of electrons as discussed above (measured by the OFSS detection system), is taken into account. From these we may conclude that 1) there is excellent accord of the measurements, corrected for sudden, “step” capture, with Eq 1 and 2) the rate coefficient is observed to increase by a factor of twenty compared to its limiting value at long time when the transient term in Eq 1 is negligible.



BES supported publications 2005-2009:

- (1) Funston, A.; Kirby, J. P.; Miller, J. R.; Pospisil, L.; Fiedler, J.; Hromadova, M.; Gal, M.; Pecka, J.; Valasek, M.; Zawada, Z.; Rempala, P.; Michl, J. One-electron reduction of an "extended viologen" p-phenylene-bis-4,4'-(1-aryl-2,6-diphenylpyridinium) dication *Journal of Physical Chemistry A* **2005**, *109*, 10862-10869.
- (2) Funston, A. M.; Miller, J. R. Increased yields of radical cations by arene addition to irradiated 1,2-dichloroethane *Radiation Physics and Chemistry* **2005**, *72*, 601-611.
- (3) Paulson, B. P.; Miller, J. R.; Gan, W. X.; Closs, G. Superexchange and sequential mechanisms in charge transfer with a mediating state between the donor and acceptor *Journal of the American Chemical Society* **2005**, *127*, 4860-4868.
- (4) Funston, A. M.; Silverman, E. E.; Schanze, K. S.; Miller, J. R. Spectroscopy and transport of the triplet exciton in a terthiophene end-capped poly(phenylene ethynylene) *Journal of Physical Chemistry B* **2006**, *110*, 17736-17742.
- (5) Takeda, N.; Asaoka, S.; Miller, J. R. Nature and energies of electrons and holes in a conjugated polymer, polyfluorene *Journal of the American Chemical Society* **2006**, *128*, 16073-16082.
- (6) Cardolaccia, T.; Funston, A. M.; Kose, M. E.; Keller, J. M.; Miller, J. R.; Schanze, K. S. Radical ion states of platinum acetylide oligomers *Journal of Physical Chemistry B* **2007**, *111*, 10871-10880.
- (7) Funston, A. M.; Lyman, S. V.; Saunders-Price, B.; Czapski, G.; Miller, J. R. Rate and driving force for protonation of aryl radical anions in ethanol *Journal of Physical Chemistry B* **2007**, *111*, 6895-6902.
- (8) Asaoka, S.; Takeda, N.; Lyoda, T.; Cook, A. R.; Miller, J. R. Electron and hole transport to trap groups at the ends of conjugated polyfluorenes *Journal of the American Chemical Society* **2008**, *130*, 11912-11920.
- (9) Cook, A. R.; Shen, Y. Z. Optical fiber-based single-shot picosecond transient absorption spectroscopy *Review of Scientific Instruments* **2009**, *80*.
- (10) Sreearunothai, P.; Asaoka, S.; Cook, A. R.; Miller, J. R. Length and Time-Dependent Rates in Diffusion-Controlled Reactions with Conjugated Polymers *Journal of Physical Chemistry A* **2009**, *113*, 2786-2795.

Chemical Kinetics and Dynamics at Interfaces

Solvation/Fluidity on the Nanoscale, and in the Environment

James P. Cowin

Fundamental and Computational Sciences Directorate, Pacific Northwest National Laboratory
P.O. Box 999, Mail Stop K8-88, Richland, Washington 99352. jp.cowin@pnl.gov

Program Scope

Interfaces, solid or liquid, have a unique chemistry, unlike that of any bulk phase. Ice interfaces also tend to have adherent liquid brine films in nature. This program explores interfacial effects including changes in fluidity, transport, and solvation. The knowledge gained relates to reactions and transport across two-phase systems: microemulsions, electrochemical systems, cell membranes, enzymes and ion channels, and environmental interfaces at normal humidities, such as the surfaces of atmospheric or soil particles. We explore these systems via re-creating liquid-liquid interfaces using molecular beam epitaxy, and use of a molecular soft landing ion source, and recently TOFSIMS. We also explore fundamental properties of bulk ice, related to proton transport, amorphous ice properties, unique electrical properties and even the effect of ice in formation of planets. True aqueous liquid interfaces are now being explored with a new microfluidic interface to a time-of-flight secondary ion mass spectrometer (TOFSIMS).

Recent Progress (2006-2009)

Mapping the Oil-Water Interface's Solvation Potential [1]

(Richard C. Bell, Kai Wu, Martin J. Iedema,
Gregory K. Schenter, James P. Cowin)

Ions that traverse the junction of water and low dielectric constant materials (air, oil, cell membranes, proteins, etc.) experience a solvation energy that varies strongly according to its location with respect to the interface. Recently much progress in understanding these interfaces was made via computational methods. This study adds important new measurements to the field. Directly measured is the solvation potential for Cs^+ as it approaches the oil-water interface ("oil" = 3-methylpentane), from 0.4 to 4 nm away. The oil-water interfaces with pre-placed ions are created at 40K using molecular beam epitaxy and a soft-landing ion beam. The solvation potential slope was determined at each distance by balancing it against an increasing electrostatic potential made by increasing the number of imbedded ions at that distance, and

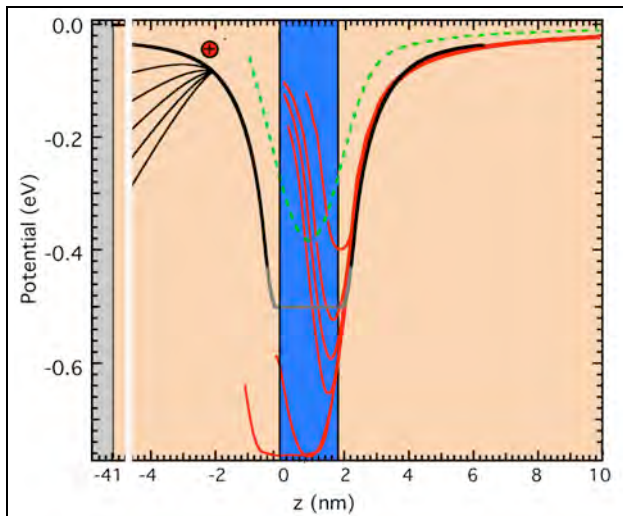


Figure 1 The blue shaded region shows 1.8 nm water film, within a 3-methylpentane film (salmon). The measured solvation chemical potential for a single ion approaching the water film is the heavy black solid line. The red curves are Born calculations for $5\text{\AA} = r_b$, $\epsilon_1=1.9$, $\epsilon_2=100$, and water films 0.15, 0.3, 0.45, 0.6, 1.8, and 3.0 nm (7.1 ML) thick. Green curve is Born model for a 1.8 nm water film with $\epsilon_2=5$.

monitoring the resulting ion motion.

Figure 1 shows the solvation chemical potential (in heavy black lines) for a single ion approaching a 4 monolayer (ML) film of water (shaded blue), immersed in 3-methylpentane (3MP) (salmon). To the far left is a metallic substrate. In a previous work [2], we roughly estimated the well depth of the solvation potential. In more recent work we determine the potential shape. When ions are placed several monolayers away from the oil water interface (left of Figure 1) they add to the solvation potential a collective electric potential. For increasing number of ions, the net potential begins to bend down, eventually reaching (and exceeding) zero slope at the initial ion position. This profoundly alters the ion motion and becomes a direct measure of the slope of the solvation potential at that distance.

Experiments were done for ions placed from 1 to 10 ML away from the water layer, and for water layers ranging from 2 to 30 ML thick, to obtain the solvation potentials, which were then compared to simple Born solvation models. The measured solvation potential is the thick black line in Figure 1. The results show the need for a “k-dependent” dielectric constant Born model. These measurements are a unique, direct bridging of molecular to semi-macroscopic distances.

Dissociation of Water on Pt(111), Buried Under Ice [2] and Proton Segregation at Ice Interfaces [4]

(Yigal Lilach, Martin J. Iedema, James P. Cowin)

Adsorbed water, well studied on metallic surfaces, is largely thought to not dissociate on Pt(111). With thick films of ice on Pt, we show that water does dissociate, probably because of small changes in the kinetic barrier to desorption and/or changing in the relative energy levels of the reactants or products. Careful, 3-step temperature programmed desorption (TPD) and work function measurements show that water dissociates on Pt(111) for T as low as 151K [3][4].

Hydronium segregates to the surface of H₂O (D₂O) ice films grown on Pt(111) above 151K (158K). This is observed as a voltage that develops across the films, utilizing work function measurements. For example 3500 ML D₂O ice films, grown via the tube doser at T_{growth} above 155 to 178K at about 400 ML/s form with a positive voltage (as much as 8V), due to the presence of trapped hydronium ions at the vacuum-ice interface. The H₂O films a threshold temperature of 153K. The coverage dependence of film voltages show that it is initially linear with coverage, then it reaches a saturation value at a coverage of several thousands of monolayers. This, and other evidence indicate that this voltage originates from charges on top of and within the ice films, that originally came from the Pt-ice interface. We found that a simple model fits the data well: Hydronium from the dissociation of water at the Pt-ice interface, at an initial ~0.1 ML concentration had a small probability (~1 %) of being found at the ice-vacuum interface. This was true only for the very first part of the ice growth (<30 ML ?). As the films get thicker, these hydroniums (~ 0.01 ML) at the ice-vacuum interface stay trapped at the ice-vacuum interface in a local minimum. As the film grows, most of these ions will stay on top of the ice film, with a small fraction (≈ 0.02% each new monolayer of ice) becomes trapped in the bulk ice. Since $\Delta G = -RT\ln(K_{\text{equil}})$, this permits the free energy for the charge segregation to the vacuum ice interface, compared to being stranded in the bulk ice to be estimated.

Pyroelectricity of Water Ice [5]

(Richard C. Bell, Kai Wu, Martin J. Iedema, Gregory K. Schenter, James P. Cowin)

Water ice usually is thought to have zero pyroelectricity by symmetry. However, biasing it with ions breaks the symmetry because of the induced partial dipole alignment. This unmasks a large pyroelectricity. Ions were soft-landed upon $1\mu\text{m}$ films of water ice at temperatures greater than 160 K. When cooled below 140-150 K, the dipole alignment locks in. Work function measurements of these films then show high and reversible pyroelectric activity from 30 to 150 . This implies that water has pyroelectric coefficients as large as that of many commercial pyroelectrics, such as lead zirconate titanate (PZT). The pyroelectricity of water ice, not previously reported, is in reasonable agreement with that predicted using harmonic analysis of a model system of SPC ice. The pyroelectricity is observed in crystalline and compact amorphous ice, deuterated or not. This implies that for water ice between 0 and 150 K (such as astrophysical ices), temperature changes can induce strong electric fields (~ 10 MV/m) that can influence their chemistry, ion trajectories, or binding.

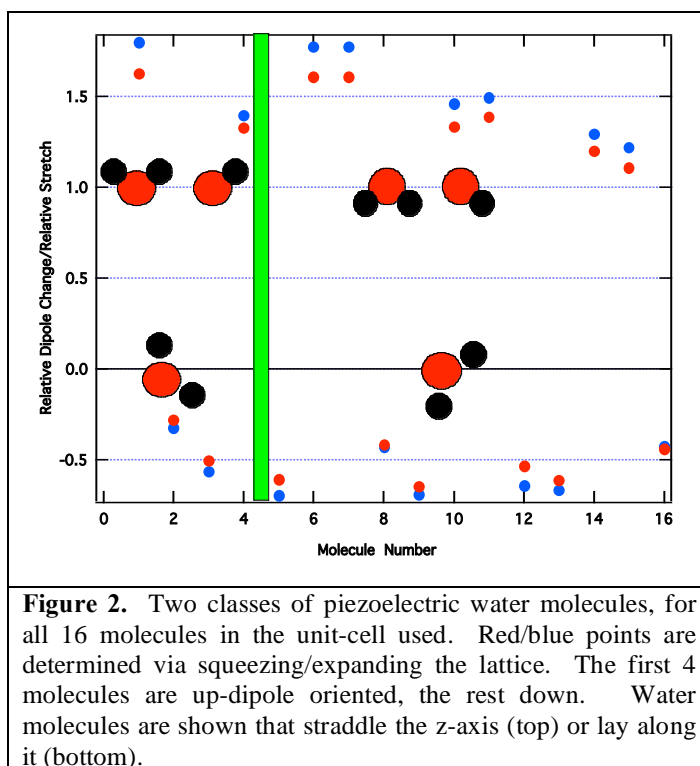


Figure 2. Two classes of piezoelectric water molecules, for all 16 molecules in the unit-cell used. Red/blue points are determined via squeezing/expanding the lattice. The first 4 molecules are up-dipole oriented, the rest down. Water molecules are shown that straddle the z-axis (top) or lay along it (bottom).

The contributions to the total piezoelectricity, when analyzed on a molecule-by-molecule basis (Figure 2), falls in to two very classes. The piezoelectric contributions are very different, depending upon if one of hydrogen-oxygen bond of the water molecule is lined up with the crystal axis under consideration, or straddles it. If lined up, a negative piezo coefficient results. If it straddles it, a positive and 3 times larger magnitude coefficient results. Yet in both cases the magnitude of the dipole aligned up with the z-axis is identical. This leads to the interesting possibility that the piezoelectric properties of ice, or even its sign, may vary substantially upon the preparation or history of the ice.

This work was cited by a Nature highlight [6]

Microfluidic Probe For Time of Flight Secondary Ion Mass Spectrometry (TOFSIMS) of Liquid Interfaces

(Li Yang, Kai Wu, Martin J. Iedema, James P. Cowin)

Probing environmental interfaces under realistic conditions requires techniques that can tolerate the necessary reactive gases and provide adequate sensitivity and chemical resolution. The new EMSL IonToF V TOFSIMS, in combination with a micro-fluidic environmental stage will provide a unique capability, which we will use to explore molecular transport and reactions in the salt-rich liquid films that coat nearly all minerals and environmental ices. This would be also highly applicable to studies of biological films and cells, or catalysts.

The TOFSIMS system lends it self to adding a micron-sized, "open-faced" microfluidic environmental cell to probe true liquids, as the ion sources and analysis systems are differentially pumped. Our approach is to add water vapor and reactive gases via a piezoelectrically positioned microdoser locally. The ions need only traverse a net few microns of vapor. At 25 torr (100% RH at 25C), the ion's mean free path λ is at least 5 microns, and rapidly increases as T and the RH is dropped (brine/salty films permit study at much less than 0 °C, with $\lambda > 50$ microns). The chamber pressure rise is $< 10^{-9}$ torr for water vapor, and $< 10^{-12}$ torr for trace reactive gases. The liquids can be quiescent or rapid flowing, permitting a wide range of liquid and liquid-material studies. To carry this out, we will use a self-contained micro-fluidic-stage, with microliter reservoirs of solutions and electroosmotic fluid injection. This provides great flexibility, protects the TOFSIMS from large fluid leaks.

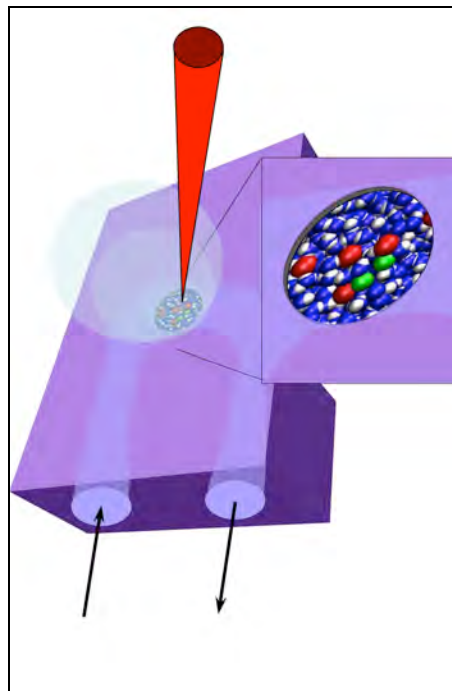


Figure 3. Exposed flowing liquid water surface (3 micron) in a hydrophobic slot, probed by a submicron TOF-SIMS ion beam. A Bi_3 cluster ion beam probes with 120 nm lateral resolution.

References (Papers under BES support from 2006-present, in **Bold**)

- [1] **R. C. Bell, Kai Wu, M. J. Iedema, G. K. Schenter, J. P. Cowin Mapping the Oil-Water Interface's Solvation Potential , J. Amer. Chem. Soc. 131, (2009) 1037–1042**
- [2] K. Wu, M.J. Iedema, J.P. Cowin, "Ion Penetration of the Oil-Water Interface", *Science* 286 (1999) 2482
- [3] **Y Lilach, MJ Iedema, JP Cowin, "Dissociation of Water on Pt(111), Buried Under Ice", *Phys. Rev. Lett.* 98 (2006) 016105**
- [4] **Y. Lilach, M.J. Iedema, J.P. Cowin, "Proton Segregation on a Growing Ice Interface" *Surface Science*, 602, (2008) 2886**
- [5] **H. Wang, RC Bell, MJ Iedema, GK Schenter, K Wu, and JP Cowin. 2008. "Pyroelectricity of Water Ice." *J. of Physical Chemistry B* 112 (2008) 6379**
- [6] **Slicing the ice, *Nature*, 453 (2008)**
- [7] Wang, HF, RC Bell, MJ Iedema, AA Tsekouras, JP Cowin, "Sticky Ice Grains Aid Planet Formation", *Astrophys. J.* 620, 1027 (2005).
- [8] **Lilach, Y. MJ Iedema, JP Cowin, "Reply to Comment on 'Dissociation of Water on Pt(111), Buried Under Ice'", *Phys. Rev. Lett.* 99, 109602 (2007)**
- [9] **Bell RC, K. Wu, MJ Iedema, JP Cowin, "Hydronium ion motion in nanometer 3-methyl-pentane films" *J. Chem. Phys.* 127 024704 (2007)**
- [10] **Hadjar, O. P. Wang, J.H. Futrell, Y. Dessiaterik, Z.H. Zhu, J.P. Cowin, MJ Iedema and J. Laskin Design and performance of an instrument for soft landing of biomolecular ions on surfaces, *J. Analy. Chem.* 79, 6566 (2007)**
- [11] B.C. Garrett, et Al., Role of water in electron-initiated processes and radical chemistry: issues and scientific advances, *Chemical Reviews* 105,355 (2005)

Reactive Intermediates in the Condensed Phase: Radiation and Photochemistry

Robert A. Crowell

Chemistry Department, Brookhaven National Laboratory, P.O. Box 5000, Upton NY, 11973;

crowell@bnl.gov

Scope

The scope of this program is to study and gain an understanding of the fundamental processes associated with the interaction of ionizing radiation and energetic photons within bulk liquids, the liquid/solid and solid/solid interface. Specific emphasis will be placed upon developing detailed knowledge of the role of the solvent, the interface and nano-confinement on charge recombination, electron transfer and ion-radical chemistry and on making the connection to the fields of radiation chemistry solar energy conversion, energy storage and catalysis. One of the most common sources of chemical reactivity is ionizing radiation. Radiation chemists typically study the rapid, energetic reactions that are initiated by the interaction of ionizing radiation, such as high-energy electrons, with matter. The processes that control these reactions are among the most fundamental events that occur in condensed phase chemistry and the related sciences of physics and biology, and are the key steps for efficient energy conversion, catalysis, and energy storage. Understanding of the basic processes that control these reactions impacts many fields including the design of nuclear reactors, radioactive waste management, radiation therapy, polymer processing, and planetary- and astrophysics. While much is now understood about radiation chemistry, there is still a significant gap in our knowledge of the many fundamental processes that lead to radiation damage. Detailed mechanisms for these processes are not known and it is commonly accepted that these (and many other) radiation induced processes involve exotic chemistry that occurs on an ultrafast timescale ($<10^{-10}$ s). This work takes advantage of a variety of DOE user facilities, including LEAF, NSLS and the APS.

Recent Progress

The main focus of our program has been ultrafast laser and x-ray studies of the mechanisms for electron dynamics and solvation and water ionization/dissociation and electron photodetachment from aqueous anions, such as Br^- . Additionally, initial attempts at analogous studies of room temperature ionic liquids have begun.

Excitation-energy dependence and mechanism for 2-photon ionization of liquid water

Tunable laser excitation provides an opportunity to explore the ionization mechanism of liquid water over a wide range (8-12 eV), observe the subsequent dynamics of e^-_{aq} and thereby determine the mean electron ejection path. The latter increases from 0.9 nm at 8.3 eV to 4 nm at 12.4 eV, with the increase taking place most rapidly above 9.5 eV. We connect these results with recent advances in the understanding of the electronic structure of liquid water, interpreting it as a gradual switchover between several ionization mechanisms. The electron ejection length has a similar energy dependence for D_2O , but is consistently shorter than in H_2O by 0.3 nm across the entire range of excitation energies studied. The autoionization plays a major role throughout this range, but the amount of nuclear reorganization of the excited states decreases monotonically as the energy increases towards 11 eV, at which the direct process becomes prevalent. Surprisingly, the isotope effect on the electron thermalization is exactly opposite to that observed in radiolysis, over the entire energy range studied. The cause of this discrepancy remains unclear.

Water ionization vs. dissociation in low-energy (8.3 eV) 2-photon excitation of water .

Following the dynamics of OH radicals (that absorb in the UV), in addition to e^-_{aq} (that absorb in

the near IR), provides a glimpse of the dynamics following water excitation by revealing the branching ratio between ionization and H-OH bond dissociation. We observed that the two processes occur with 1:1 probability for the total excitation energy of 9.3 eV, while the dissociation channel prevails for 8.3 eV excitation. At the lower energy we observed the geminate recombination kinetics of OH radical, and determined that the initial H...OH separation exceeded 0.6 nm, which was in agreement with recent molecular dynamics simulations of dissociating H₂O in amorphous ice. Therefore, this photodissociation yields *hot* H atoms; we found no evidence for caging of the resulting geminate radical pairs (contrary to aqueous H₂O₂ photodissociation). The competition among ionization and dissociation channels reveals important details about the dynamics in the excited electronic states of liquid water, and how the liquid environment changes the behavior of those states relative to the gas phase (which is currently at the center of much attention). Our experiments provide an experimental benchmark for comparison with theoretical results.

Electron photodetachment from aqueous anions. Single - (1 x 6.2 eV) and two - (2 x 3.1 eV) photon excitation of aqueous halide ions in the charge transfer to solvent (CTTS) band was studied. Pairing of the photodetached electron with the residual radical/atom in a solvent cage was observed for all halide and pseudohalide anions; these caged pairs remain in proximity (0.5-0.7 nm) for 4-15 ps and then decay by diffusion out of the cage. There is a considerable barrier for recombination of the caged pairs, ca. 85 meV. For I⁻, 1- and 2-photon processes of the same total energy result in nearly identical electron distributions. For HO⁻, the electron distribution is much broader in the two-photon excitation. The latter is also much less efficient than that of I⁻. We attribute this inefficiency of the 2-photon process to a changeover of the electron wavefunction from *s*- (1-photon excitation) to *p*- (2-photon excitation) and spin-orbital mixing in the heavier anion. Our study indicates that low-energy water ionization does not proceed through electron detachment from the excited hydroxyl anion.

Time-Resolved X-ray Spectroscopy (XAS) of Solvation Structure and Dynamics. We have been studying the photoinduced electron detachment from aqueous bromide. The choice of this anion is dictated by (i) the convenience of XAS detection in the fluorescence mode and relatively large absorption cross-section at the K edge (11.4 keV), (ii) the large absorptivity of bromide at 200 nm with a near-unity photodetachment yield. We have previously studied photodetachment from bromide using ultrafast transient absorption spectroscopy and found that the charge separation proceeds (as is the case for other halide and pseudohalide anions) through the formation of a close (Br⁻:e_{aq}⁻) pair with a life time of 20 ps.

Details about the hydration of halogen atoms are not well known, but XAS is uniquely suited for probing the interaction of the atom with its aqueous environment. The hydration of halogen atoms (X⁰) is very different from the hydration of negatively charged halide anions (X⁻). Whereas the anion forms strong hydrogen bonds with several water molecules in the first solvent shell, hydrophobic effects dominate the solvation of neutral halogen atoms. There is also evidence that halogen atoms interact directly with a single solvent molecule, leading to an ultraviolet charge transfer (CT) absorption band. The CT absorption promotes an electron from the water molecule onto the halogen atom.

Time-resolved XAS has been used to observe the transient species generated by one-photon detachment of an electron from aqueous bromide. The objective is to study the solvation of residual bromine atoms and follow the separation dynamics of the contact pairs comprised of such radicals and e_{aq}⁻ that are caged by the solvent. The *K*-edge spectrum of the short-lived Br⁰

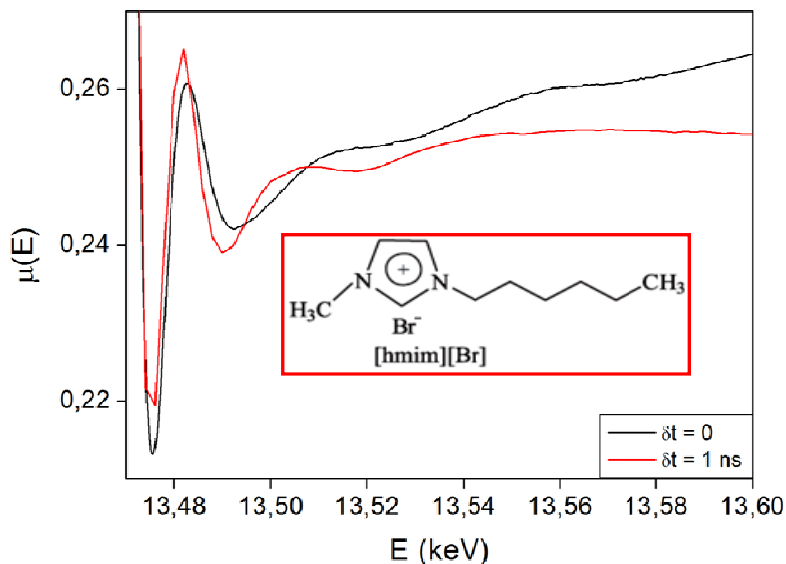


Figure 1. Time resolved XAS of 1-hexyl-3-methylimidazolium bromide following excitation of the bromide charge transfer band

atom exhibits a resonant $1s-4p$ transition that is absent for the Br^- precursor. The strong $1s-4p$ resonance suggests that there is very little charge transfer from the solvent to the open-shell atom, whereas weak oscillations above the absorption edge indicate that the solvent shell around a neutral Br^0 atom is defined primarily by hydrophobic interactions. These conclusions are in agreement with Monte Carlo and quantum chemical simulations of the solvent structure.

In addition to the aqueous studies we have begun experiments on a series of bromide containing room temperature ionic liquids where the solvation times are significantly slower than those in water. We have very recently succeeded in obtaining our first results (Figure 1) of static and time-resolved XAS measurements on 1-hexyl-3-methyl imidazolium bromide and 1-butyl-3-methyl imidazolium bromide from experiments carried out at Sector 7 of the APS.

Future Plans

Future work will focus on two main areas of interest. First, we will continue to study both the photochemistry and solvation dynamics of selected room temperature ionic liquids. Second we will extend our ultrafast laser spectroscopy (both IR and visible), ultrafast pulse radiolysis and our newly developed time resolved XAS technique to studies of the effects of nanoconfinement/interface on basic photochemical and radiation induced reactions. Initial efforts will focus on aqueous systems that have been well characterized in the bulk, e.g. the reaction of solvated electron with protons. To develop of a detailed knowledge of the role of nanoconfinement/interface in radiation and photochemistry we will address the following issues:

1. Develop an accurate description of the properties of nanoconfined/interfacial water and its effect on solvation, particularly at the interface.
2. To study the effect of confinement/interface on reaction kinetics and mechanisms.
3. To understand how nanoconfinement/interface affects ion/radical diffusion and its affect on radiolytic yields.

DOE Publications 2005-present

1. K. Takahashi, K. Suda, T. Seto, Y. Katsumura, R. Katoh, R. A. Crowell, J. F. Wishart "Photo-detrapping of solvated electrons in an ionic liquid," *Rad. Phys. Chem.*, (2009) in press.
2. K. Takahashi, H. Tezuka, T. Sato, Y. Katsumura, M. Watanabe, R. A. Crowell, J. F. Wishart "Kinetic salt effects on an ionic reaction in ionic liquid/methanol mixtures," *Chem. Lett.* 38, 236 (2009)
3. M. Ave, M. Bohacova, B. Buonomo et al. "Spectrally resolved pressure dependence measurements of air fluorescence emission with AIRFLY," *NIMA*, 597, 41 (2008).
4. M. Ave, M. Bohacova, B. Buonomo et al. "Energy dependence of air fluorescence yield measured by AIRFLY," *NIMA*, 597, 46 (2008).
5. M. Ave, M. Bohacova, B. Buonomo et al. "Temperature and humidity dependence of air fluorescence yield measured by AIRFLY," *NIMA*, 597, 50 (2008).
6. M. Ave, M. Bohacova, B. Buonomo et al. "A novel method for the absolute fluorescence yield measurement by AIRFLY," *NIMA*, 597, 55 (2008).
7. C. G. Elles, I. A. Shkrob, R. A. Crowell, D. A. Arms, E. C. Landahl "Transient x-ray absorption spectroscopy hydrated halogen atom," *J. Chem. Phys.* 128, 061102 (2008)
8. C. G. Elles, R. A. Crowell, I. A. Shkrob, S. E. Bradforth "Excited state dynamics of liquid water: Insight from the dissociation reaction following two-photon excitation," *J. Chem. Phys.* 126, 164503 (2007)
9. M. Ave et al, "Measurement of the pressure dependence of air fluorescence emission induced by electrons," *Astrophys.*, 28, 41 (2007).
10. B. Shen, Y. Li, K. Nemeth, H. Shang, R. Soliday, R. A. Crowell, E. Frank, W. Gropp and J. Cary "Triggering wave breaking in a laser plasma bubble by a nanowire," *Phys. Plasma.* 14, 053115 (2007).
11. D. A. Oulianov, R. A. Crowell, D. J. Gosztola, I. A. Shkrob, O. J. Korovyanko, R. C. Rey-de-Castro, "Ultrafast pulse radiolysis using a terawatt laser wakefield accelerator," *J. Appl. Phys.* 101, 053102 (2007).
12. Y. Li and R. A. Crowell, "Shortening of a laser pulse with a self-modulated phase at the focus of a lens," *Opt. Lett.* 32, 93 (2007).
13. I. A. Shkrob, M. C. Sauer, Jr., R. Lian, R. A. Crowell, D. M. Bartels and S. E. Bradforth "Quantum yields and recombination dynamics in electron photodetachment from aqueous anions III. The effect of ionic strength on picosecond dynamics, quantum yields and the escape fraction of hydrated electrons in anion CTTS systems," *J. Phys. Chem. A*, 110, 9071 (2006).
14. C. G. Elles, A. E. Jailaubekov, R. A. Crowell, S. E. Bradforth, "Excitation energy dependence of the mechanism for two-photon ionization of liquid H₂O and D₂O from 8.3 eV to 12.4 eV," *J. Chem. Phys.* 125, 044515 (2006)
15. D. A. Oulianov, R. A. Crowell, D. J. Gosztola, and Y. Li "Ultrafast time-resolved x-ray absorption spectroscopy of solvent-solute transient structures," *Nucl. Instr. and Meth. in Phys. Res. B.* 241, 82 (2005)
16. R. A. Crowell, I. A. Shkrob, D. A. Oulianov, O. Korovyanko, D. J. Gosztola, Y. Li and R. Rey-Castro, "Motivation and development of ultrafast laser based accelerator techniques for chemical physics research," *Nucl. Instr. and Meth. in Phys. Res. B* , 241, 9 (2005).

Computational studies of X-ray reflectivity liquid interfaces, reorientation mechanism of hydroxide ions in water and CO₂ capture

Liem X. Dang

Chemical and Materials Sciences Division

Pacific Northwest National Laboratory

Richland, WA 93352

liem.dang@pnl.gov

Background and significance

Ion distributions at aqueous/vapor interfaces have attracted intensive attention due to their fundamental and practical importance. The traditional view is that the liquid/vapor interface is devoid of ions based on interpretations of surface tension measurements due to the Gibbs adsorption isotherm. This argument is challenged from both theoretical and experimental studies, with an enhancement of anion concentrations at the liquid/vapor interface being observed from both molecular dynamics (MD) simulations and spectroscopy. One recent effort on this topic is the work of Sloutskin et al. (*J. Chem. Phys.* **2007**, *126*, 054704), who used x-ray reflectivity techniques to explore the surface structure of concentrated aqueous salt solutions. Their results are a very important contribution to the understanding of liquid/vapor interfaces, and if they can be reliably interpreted, can bring major improvements to the understanding of interfacial ion behavior.

Molecular modeling approaches, such as molecular dynamics simulations are powerful tools, with the ability to probe the ion behavior at liquid interfaces, providing a strong microscopic understanding of their structures, distributions, and behavior. Unfortunately, observations made from molecular dynamics simulations often cannot be directly compared with experimental measurements, making conclusions extracted from them difficult to verify. Because of this, effort has been put forth to bridge the gap between experimental measurements and molecular dynamics simulations for aqueous salt solutions. For instance, sum frequency generation spectra for salt solutions can be generated from molecular dynamics simulations, but these are somewhat indirect probes of ion distributions, as they primarily describe water vibrations.

X-ray reflectivity spectroscopy, though, probes the structure of interfacial electron density, and recent work has been carried out to compare molecular dynamics simulation results with spectroscopic measurements by Sloutskin et al. However, the molecular dynamics simulations were not performed at the same concentrations for RbBr or with the same cations for SrCl₂ as experiment, requiring the simulation results to be scaled or approximated to correspond with the experiments. Consequently, the outcome of such comparisons cannot be deemed rigorous. Very recently, a direct comparison with x-ray reflectivity experiments using molecular dynamics simulations for concentrated RbBr aqueous solution has been carried out. The ion concentrations were found to be enhanced at the interfaces, and the calculated structure factor reproduced the experimental one qualitatively from simulations with polarizable potential models, while the simulations with non-polarizable potential models showed contrasting results.

Progress Report

Computational studies of aqueous interfaces of SrCl₂ salt solutions

We describe our investigation of the distribution of the SrCl₂ and NaCl ions at the aqueous/vapor interfaces using MD simulations. To the best of our knowledge, this work is the first MD calculation of the x-ray reflectivity of the concentrated divalent salt solutions. In addition to the potential models, the divalent cations provided additional changes due to the strong ion-ion interactions. As a consequence, many body effects will be important in these systems. One of our main goals is to make a direct comparison to the measured data, we also discuss the way to improve the agreement between MD and x-ray reflectivity interpretation of the aqueous salt surfaces. We used both polarizable and non-polarizable potential models and full 3D periodic Ewald summation to investigate the distribution of ions at the aqueous interfaces. Fig.1 shows the calculated $|\Phi(q_z)|^2$ from simulations with polarizable potentials as well as the experimental results. Considering the simulation environment is substantially different from the experimental one, such as the system size, equilibration time etc., the calculated $|\Phi(q_z)|^2$ from the simulations are optimized by a Debye-Waller factor to scale the amplitude to be a better fit to the experiments. Generally, this extra term is small, and will not change the resonance frequency of the structure factor in our calculation. The experimentally calculated $|\Phi(q_z)|^2$ from X-ray reflectivity measurements shows a single peak at $q_z=0.4 \text{ \AA}^{-1}$, and large fluctuations in the high frequency region. The calculated $|\Phi(q_z)|^2$ from the simulations with polarizable potentials qualitatively agrees with the experimental

curve. The same resonance frequency is observed at $q_z=0.4 \text{ \AA}^{-1}$, and the trend of the $|\Phi(q_z)|^2$ corresponding to the frequency follows the experiment reasonably well. However, the peak of simulated $|\Phi(q_z)|^2$ is more abrupt than that of experiment. The simulations with non-polarizable potentials show a much different scenario. Although an experimentally matched resonance frequency can be observed, the shape of the curve is significantly different from the experimental one. This could not be further improved by any choice of Debye-Waller factor. The comparison between the $|\Phi(q_z)|^2$ calculated from simulations and x-ray reflectivity indicates an enhanced distribution of ions at the liquid/vapor interface. However, the simulations with polarizable potentials give over-structured spectra. Our simulations with polarizable potentials provide a direct comparison with experiment for the interfacial structural properties at the molecular level. It is possible that a lower interfacial ion concentration than what is found from our simulations with polarizable potentials would improve agreement with experiment. Further efforts on improving the ion-ion and ion-water interactions should be addressed in the future.

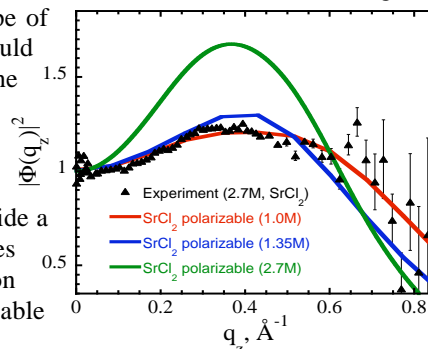


Fig. 1. Simulated $|\Phi(q_z)|^2$ as a function of SrCl₂ salt concentrations.

To understand the role of salt concentration, we carrying out additional simulations at lower concentrations (1.00 M and 1.35 M) of SrCl₂ salt solutions. The simulated X-ray reflectivity results are also presented in Fig. 1. Upon examination of these results, better agreement with experiment can be achieved with the 1.35M SrCl₂ (50% of 2.7M) salt solution. A snapshot taken from the simulation of 1.35 M is shown in Fig. 2. We can conclude that the origin of the over structured X-ray spectra calculated from our MD simulations is likely the result of the surface concentration of SrCl₂ ions being around a factor of two too high. This was both confirmed by the improved agreement between simulation and experiment when the Sr²⁺ contribution to the spectra was halved in a 2.7 SrCl₂ solution, and with the agreement shown when the overall SrCl₂ concentration is halved. The results show that both Sr²⁺ and Cl⁻ are enhanced at the liquid/vapor interface from the simulations with polarizable potential models, and both are depleted from the interface from simulations with non-polarizable potential models. The structure factor calculated from the simulations with non-polarizable potential

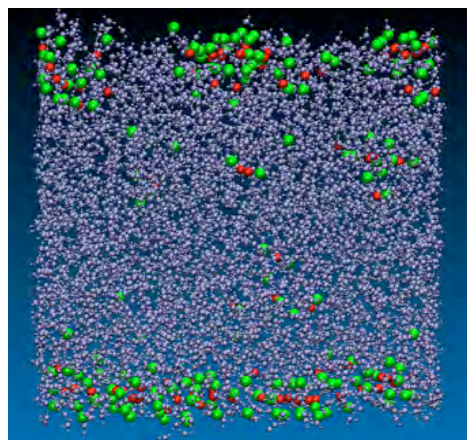


Fig. 2. Snapshot taken from the simulations of 1.35 M

models cannot reproduce the corresponding experimentally calculated, even qualitatively. In addition, this study demonstrated that simulations of NaCl aqueous solution gave significantly different results with the corresponding simulation results of SrCl₂ X-ray reflectivity. We can attribute this finding due to the fact that unlike the monovalent ions, which form solvent separated ion pairs in dilute solutions, Sr²⁺ and Cl⁻ primarily exist as contact ion pairs in the solution due to the large net charge on Sr²⁺.

The reorientation mechanism of hydroxide ions in water: A molecular dynamics study

As one of the two ions formed by water dissociation, hydroxide plays a unique role in chemical and biochemical processes. In contrast to the well-established mechanism for the mobility of hydronium ions in water, the debate over the mechanism of the orientation relaxation of hydroxide ions in solution is still quite active. The traditional view of the transport mechanism for both hydronium and hydroxide ions is similar, namely that the transport of both ions is driven by second solvation shell fluctuations. By breaking one hydrogen bond in the second solvation shell, the coordination number of a first solvation shell water is reduced from 4 to 3 and this under-coordinated hydrogen bonded network will subsequently form either a [H₂O-H-OH₂]⁺ complex with hydronium or a [HO-H-OH]⁻ complex with hydroxide to facilitate the proton transfer between those ions in water. This mechanism is based on a tri-coordinated structure of hydroxide ions that is similar to the structure of hydronium ions. This triply hydrogen bonded complex OH(H₂O)₃ with a tetrahedral arrangement is supported by some theoretical and experimental studies.

For both OH⁻ and H₂O at different temperatures, the decay of the orientational correlation function is described by a single exponential. This observation indicates a successive small angular jump mechanism for the reorientation of both OH⁻ and H₂O. At low temperatures, C(t) shows an anomalous slow decay that was also observed in the CTTS experiments. Figure 3 shows the computed relaxation time of the hydroxide ion reorientation as a function of temperature. The computed relaxation time increases with decreasing temperature in qualitative agreement with the CTTS experimental data.

The reorientation of water was also previously investigated using the same experimental techniques. The two experimentally available orientational relaxation times for water (from NMR and THz measurements) are shown in Figure 3 for comparison. As described in the experimental paper, the THz results were obtained by

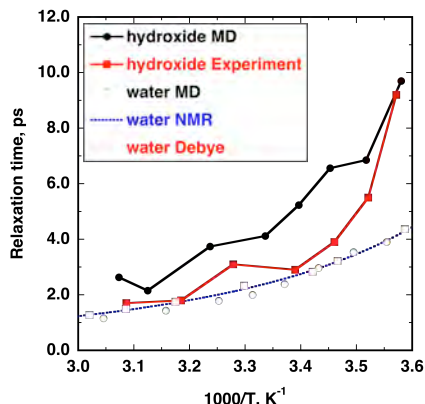


Fig. 3. Computed relaxation time of the hydroxide and water reorientation as a function of temperature.

changes with temperature. It is therefore necessary to investigate the solvation structure of hydroxide ions at different temperatures.

Future plans

Grand Canonical Monte Carlo studies of CO₂ and CH₄ adsorption in *p*-*tert*-butylcalix[4]arene (TBC4)

The current understanding of global warming indicates that CO₂ accumulation in the atmosphere plays an important role, and a significant source of atmospheric CO₂ over recent decades is the combustion of carbon based fuels. In addition to hydrocarbon combustion, CO₂ is generated in the production of some other fuels such as biomethane, green synfuel, and hydrogen. One important approach to minimizing CO₂ emission into the atmosphere is carbon capture and sequestration. Capture of CO₂ from flue gases, or during fuel production is a key component in this strategy.

Grand Canonical Monte Carlo simulations are performed for single component isotherms of CO₂ and CH₄ in the *p*-*tert*-butylcalix[4]arene structure. Comparison with literature data for adsorption used the Peng-Robinson equation of state to map simulated fugacities to experimentally determined pressures. CO₂ binding in the high-pressure structure of TBC4 (TBC4-H) occurs in two distinct waves. The cage sites in TBC4 completely fill, followed by the filling of interstitial sites, resulting in the sum of two Langmuir isotherms being the best way to describe the total absorption isotherms. Our simulation results capture the essential experimental feature that the cage sites are the major contributor to the absorption isotherms, and the contribution of interstitial sites is significantly less. We found that CH₄ does not exhibit the same two site binding characteristic and has a smaller temperature dependence, which

arises from a smaller negative entropy change upon absorption compared with CO₂. Our calculations give higher binding than observed experimentally for the cage site but lower binding for the interstitial site. We also demonstrate that by rescaling the interaction between CO₂ and the lattice, the results can reproduce the experimental data well.

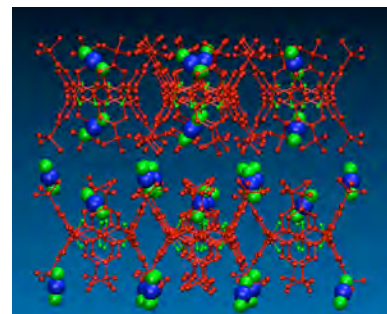


Fig. 4. Distribution of CO₂ in TBC4 molecules.

References to publications of DOE sponsored research (2005-2009)

1. T.-M. Chang and **LXD** "Liquid/Vapor Interface of Methanol-Water Mixtures: A Molecular Dynamics Study" *J. Phys. Chem. B* 109, 5759 (2005).
2. M. M., T. Frigato, L. Levering, H. C. Allen, D. J. Tobias, **LXD** and P. Jungwirth "A unified molecular picture of the surfaces of aqueous acid, base, and salt solutions" *J. Phys. Chem. B* 109, 7617 (2005).
3. V. -A. Glezakou, Y. C. Chen, J. L. Fulton, G. K. Schenter and **LXD** "Electronic Structure, Statistical Mechanical Simulations, and EXAFS Spectroscopy of Aqueous Potassium" *Theoretical Chemistry Accounts* 115 (2-3): 86 (2006).
4. **LXD** and T. M. Chang, "Recent Advances in Molecular Simulations of Ion Solvation at Liquid Interfaces" *Chemical Reviews* 106, 1305 (2006).
5. Wick CD, **LXD** and Jungwirth P. "Simulated Surface Potentials at the Vapor-Water Interface for the KCl Aqueous Electrolyte Solution" *J. Chem. Phys.* 125 (2): Art. No. 024706 (2006).
6. Wick CD and **LXD** "Computational Observation of Enhanced Solvation of the Hydroxyl Radical with Increased NaCl Concentration" *J. Phys. Chem. B* 110, 8917 (2006).
7. Oliver Höfft, Andriy Borodin, Uwe Kahnert, Volker Kempter, **LXD** and Pavel Jungwirth "Surface Segregation of Dissolved Salt Ions" *J. Phys. Chem. B* 110, 11971 (2006).
8. Wick CD and **LXD** "Distribution, Structure, and Dynamics of Cesium and Iodide Ions at the H₂O-CCl₄ and H₂O-Vapor Interfaces" *J. Phys. Chem. B* 110 (13): 6824 (2006).
9. **LXD**, Chang TM, Roeselova M, et al. "On NO₃⁻-H₂O Interactions in Aqueous Solutions and at Interfaces" *J. Chem. Phys.* 124 (6): Art. No. 066101 (2006).
10. **LXD**, G. K. Schenter, J. L. Fulton, V. -A. Glezakou, "Molecular Simulation Analysis and X-ray Absorption Measurement of Ca²⁺, K⁺ and Cl⁻ Ions in Solution" *J. Phys. Chem. B* 110, (2006).
11. John L. Daschbach, Tsun-M. Chang, L. R. Corrales, **LXD** Pete McGrail "Molecular Mechanisms of Hydrogen Loaded Beta-Hydroquinone Clathrate". *J. Phys. Chem. B* 110, 17291 (2006).
12. L. Cwiklik, G. Andersson, **LXD** and P. Jungwirth, *Chemphyschem* 8, 1457 (2007).
13. J. Thomas, J., M. Roeselova, **LXD** and Doug. J. Tobias, "Molecular dynamics simulations of the solution-air interface of aqueous sodium nitrate" *J. Phys. Chem. A* 111, 3091 (2007).
14. John L. Daschbach and Praveen K. Thallapally, Jerry L. Atwood, B. Peter McGrail and **LXD** "Free energies of CO₂/H₂ capture by p-tert-butylcalix[4]arene: A molecular dynamics study. *J. Chem. Phys.* 127, 104703 (2007).
15. Hoeffft, O.; Kahnert, U.; Bahr, S.; Kempter, V.; Jungwirth, P.; **LXD** "Segregation of salt ions at amorphous solid and liquid surfaces. in *Physics and Chemistry of Ice*, ed. W. Kuhs, RSC Publishing, London, 217 (2007).
16. Collin Wick and **LXD**, Molecular Mechanism Of Transporting A Polarizable Iodide Anion Across The Water-CCl₄ Liquid/Liquid Interface. *J. Chem. Phys.* (13): Art. No. 134702 (2007).
17. Collin D. Wick, I-Feng W. Kuo, Christopher J. Mundy, and **LXD** "The Effect of Polarizability for Understanding the Molecular Structure of Aqueous Interfaces. *J. Chem. Theo. Comp.* 3, 2002 (2007).
18. Collin D. Wick and **LXD** "Molecular Dynamics Study of Ion Transfer and Distribution at the Interface of Water and 1,2-Dichloroethane" *J. Phys. Chem. A* 112, 647, (2008).
19. Chang, TM and **LXD** "Computational Studies Of Liquid Water And Diluted Water In Carbon Tetrachloride" *J. Phys. Chem. B* 112, 1694 (2008).
20. Daschbach, JL; Thallapally, PK; McGrail, BP and **LXD** "Dynamics And Free Energies Of CH₄ And CO₂ In The Molecular Solid Of The P-Tert-Butylcalix[4] Arene" *Chem. Phys. Letts.* 453, 123 (2008).
21. Collin D. Wick, **LXD** "Recent Advances In Understanding Transfer Ions Across Aqueous Interfaces" *Chem. Phys. Letts.* 458, 1 (2008).
22. Wick CD and **LXD** "Investigating Hydroxide Anion Interfacial Activity by Classical and Multistate Empirical Valence Bond Molecular Dynamics Simulations" *J. Phys. Chem. A.* 113, 6356 (2009).
23. Sun XQ, Chang TM, Cao Y, **LXD** et al. "Solvation of Dimethyl Succinate in a Sodium Hydroxide Aqueous Solution. A Computational Study" *J. Phys. Chem. B.* 113, 6473 (2009).
24. Daschbach JL, Sun XQ, Chang TM, **LXD** et al. "Computational Studies of Load-Dependent Guest Dynamics and Free Energies of Inclusion for CO₂ in Low-Density p-tert-Butylcalix[4]arene at Loadings up to 2:1" *J. Phys. Chem. A.* 113, 3369 (2009).
25. Sun XQ, **LXD** "Computational studies of aqueous interfaces of RbBr salt solutions" *J. Chem. Phys.* 130, 124709 (2009).
26. Glezakou VA, **LXD** and BP McGrail "Spontaneous Activation of CO₂ and Possible Corrosion Pathways on the Low-Index Iron Surface Fe(100)" *J. Phys. Chem. C.* 113, 3691 (2009).
27. Chang TM, **LXD** "Computational Studies of Structures and Dynamics of 1,3-Dimethylimidazolium Salt Liquids and their Interfaces Using Polarizable Potential Models" *J. Phys. Chem. A* 113, 2127 (2009).

Transition Metal-Molecular Interactions Studied with Cluster Ion Infrared Spectroscopy

DE-FG02-96ER14658

Michael A. Duncan

Department of Chemistry, University of Georgia, Athens, GA 30602-2556

maduncan@uga.edu

Program Scope

Our research program investigates gas phase metal clusters and metal cation-molecular complexes as models for heterogeneous catalysis, metal-ligand bonding and metal cation solvation. The clusters studied are molecular sized aggregates of metal or metal oxides. We focus on the bonding exhibited by "physisorption" versus "chemisorption" on cluster surfaces, on metal-ligand interactions with benzene or carbon monoxide, and on solvation interactions exemplified by complexes with water, acetonitrile, etc. These studies investigate the nature of the metal-molecular interactions and how they vary with metal composition and cluster size. To obtain size-specific information, we focus on ionized complexes that can be mass selected. Infrared photodissociation spectroscopy is employed to measure the vibrational spectroscopy of these ionized complexes. The vibrational frequencies measured are compared to those for the corresponding free molecular ligands and with the predictions of theory to reveal the electronic state and geometric structure of the system. Experimental measurements are supplemented with calculations using density functional theory (DFT) with standard functionals such as B3LYP.

Recent Progress

The main focus of our recent work has been infrared spectroscopy of transition metal cation-molecular complexes with carbon monoxide or water, e.g., $M^+(CO)_n$ and $M^+(H_2O)_n$. These species are produced by laser vaporization in a pulsed-nozzle cluster source, size-selected with a specially designed reflectron time-of-flight mass spectrometer and studied with infrared photodissociation spectroscopy using an IR optical parametric oscillator laser system (OPO). In studies of complexes with a variety of transition metals, we examine the shift in the frequency for selected vibrational modes in the adsorbate molecule that occur upon binding to the metal. The number and frequencies of IR-active modes in multi-ligand complexes reveal the structures of these systems, while sudden changes in vibrational spectra or IR dissociation yields are used to determine the coordination number for the metal ion in these complexes. In some systems, new bands are found at a certain complex size that correspond to intra-cluster reaction products. In small complexes with strong bonding, we use the method of "rare gas tagging" with argon or neon to enhance dissociation yields. In all of these systems, we employ a close interaction with theory to investigate the details of the metal-molecular interactions that best explain the spectroscopy data obtained. We perform density functional theory (DFT) or MP2 calculations (using Gaussian 03W or GAMESS) and when higher level methods are required, we collaborate with local theorists (Profs. P.v.R. Schleyer, H.F. Schaefer) or those at other universities (Prof. Mark Gordon, Iowa State). Our infrared data on these

transition metal ion-molecule complexes provide many examples of unanticipated structural and dynamical information.

A crucial aspect of these studies is the infrared laser system, which is an infrared optical parametric oscillator/amplifier system (OPO/OPA; Laser Vision). This system, which has only become available recently, covers the infrared region of 700-4500 cm^{-1} with a linewidth of about 1.0 cm^{-1} .

$\text{M}^+(\text{H}_2\text{O})_n$ complexes and those tagged with argon have been studied previously in our lab for the metals iron, nickel, cobalt and vanadium. We have recently extended these studies to titanium, manganese, chromium, scandium, copper, silver, gold and zinc. We have studied the noble metal ions copper, silver and gold with one and two water molecules. The gold system prefers a coordination of two ligands, and its O-H stretches are red shifted much more than those of copper and silver. In the vanadium system, we have studied multiple water complexes. Hydrogen bonding bands appear for the first time for the complex with five water molecules, establishing that four water molecules is the coordination for V^+ . Copper and zinc complexes with a single attached water have unexpected vibrational bands at high frequency above the normal region of the symmetric and asymmetric O-H stretches. With the help of theory by Prof. Anne McKoy (Ohio State), we are able to assign these features to combination bands involving the twisting motion of the water. Silver, scandium and chromium complexes were rotationally resolved, providing the H-O-H bond angle in these systems. In very new work, we have been able for the first time to produce multiply charged transition metal cation-water complexes for chromium, manganese and scandium systems tagged with multiple argons. IR spectra of these systems have very different intensity patterns and O-H shifts than those for the singly charged systems, and we are able to study the charge dependence of the cation-water interaction.

$\text{M}^+(\text{CO})_n$ complexes are analogous to well-known species in conventional inorganic chemistry. However, we are able to make these systems without the complicating influences of solvent or counter ions. The C-O stretch in most stable neutral transition metal complexes shifts strongly to the red from free CO, and this vibration often falls below 2000 cm^{-1} . However, we have found that *cation* transition metal complexes have smaller red shifts, and the carbonyl stretches lie in the 2000-2200 cm^{-1} region. We have examined cobalt, vanadium, niobium, tantalum, copper, silver, gold, platinum and manganese systems as a function of the number of carbonyl ligands attached. $\text{Co}^+(\text{CO})_5$ has 18 electrons and is isoelectronic to the well-known neutral complex $\text{Fe}(\text{CO})_5$. The stable coordination is found for the $n=5$ species, as expected, and the carbonyl stretch is hardly shifted from the free-CO value. In $\text{V}^+(\text{CO})_n$ complexes, the $n=7$ species has 18 electrons and had been predicted to be stable by theory. However, we found that the stable coordination is not at $n=7$, but is at the 16 electron species $\text{V}^+(\text{CO})_6$. The CO band shifts for the $n=1-8$ complexes reveal how this system gradually changes from a triplet for the mono-ligand species to a singlet for the $n=6$ species. Niobium and tantalum systems are isoelectronic to vanadium, and also predicted to form seven coordinate carbonyls. Experiments found evidence for *both* six- and seven-coordinate structures for $\text{Nb}^+(\text{CO})_n$ but only the seven-coordinate species was found for $\text{Ta}^+(\text{CO})_n$. This trend of higher coordination for the heavier metals was attributed to the effects of both cation size and the increasing ability to undergo the spin change required to add the seventh ligand. We have also examined so-called non-classical carbonyl complexes of the noble metal and platinum cations. $\text{M}^+(\text{CO})_n$ complexes for these systems have been studied, and they exhibit blue shifts of the carbonyl stretch relative to free CO. The size dependence of these resonances provides insight into the structures of these complexes.

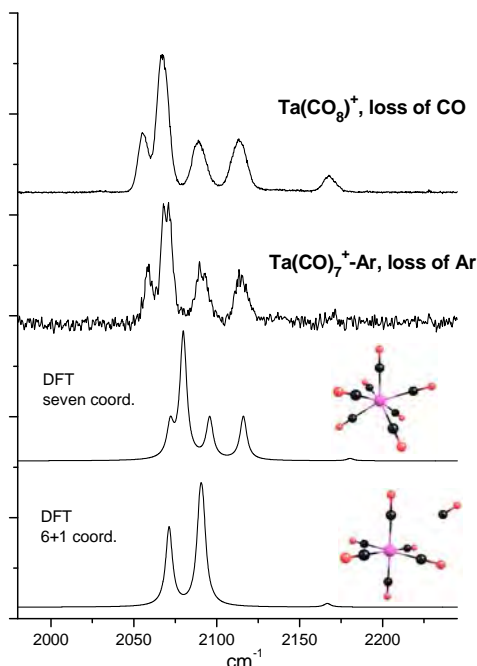


Figure 1. The IR spectra of $\text{Ta}^+(\text{CO})_7$ complexes measured with mass-selected photodissociation.

Future Plans

Future plans for this work include the extension of these IR spectroscopy studies to more ligands and to complexes with multiple metal atoms. These systems should exhibit characteristic IR spectra, and allow us to make better connections with IR spectroscopy on metal surfaces. We have realized that larger metal clusters or their oxides are quite difficult to produce and cool simply by supersonic expansions. We are therefore exploring different designs of cryogenically cooled cluster sources to make these systems and tag them effectively. In all of these studies, we have focused on the qualitative effects of metal-adsorbate interactions and trends for different transition metals interacting with the same ligand. Our theoretical work has revealed that density functional theory has some serious limitations for small metal systems that were not previously recognized. This is particularly evident in metals such as vanadium and iron, where two spin states of the metal lie at low energy. DFT has difficulty identifying the correct relative energies of these spin states, and further examinations of this issue are planned.

Publications (2005-2009) for this Project

1. R.S. Walters, P.v.R. Schleyer, C. Corminboeuf and M.A. Duncan, "Structural Trends in Transition Metal Cation-Acetylene Complexes Revealed Through the C-H Stretch Fundamentals," *J. Am. Chem. Soc.* **127**, 1100 (2005).
2. T.D. Jaeger and M.A. Duncan, "Infrared Photodissociation Spectroscopy of $\text{Ni}^+(\text{benzene})_x$ Complexes," *J. Phys. Chem. A* **109**, 3311 (2005).
3. E.D. Pillai, T.D. Jaeger and M.A. Duncan, "Infrared spectroscopy and density functional theory of small $\text{V}^+(\text{N}_2)_n$ clusters," *J. Phys. Chem. A* **109**, 3521 (2005).

4. R.S. Walters, E.D. Pillai and M.A. Duncan, "Solvation Processes in Ni⁺(H₂O)_n Complexes Revealed by Infrared Photodissociation Spectroscopy," *J. Am. Chem. Soc.* **127**, 16599 (2005).
5. R.S. Walters, E.D. Pillai, P.v.R. Schleyer and M.A. Duncan, "Vibrational spectroscopy of Ni⁺(C₂H₂)_n (n=1-4) complexes," *J. Am. Chem. Soc.* **127**, 17030 (2005).
6. N.R. Walker, R.S. Walters and M.A. Duncan, "Frontiers in the Infrared Spectroscopy of Gas Phase Metal Ion Complexes," *New J. Chem.* **29**, 1495 (2005).
7. E.D. Pillai, T.D. Jaeger and M.A. Duncan, "Infrared Spectroscopy of Nb⁺(N₂)_n Complexes: Coordination, Structures and Spin States," *J. Am. Chem. Soc.* **129**, 2297 (2007).
8. A.C. Scott, N.R. Foster, G.A. Grieves and M.A. Duncan, "Photodissociation of lanthanide metal cation complexes with cyclooctatetraene," *Int. J. Mass Spectrom.* **263**, 171 (2007).
9. V. Kasalova, W.D. Allen, H.F. Schaefer, E.D. Pillai and M.A. Duncan, "Model systems for probing metal cation hydration: The V⁺(H₂O) and V⁺(H₂O)Ar complexes," *J. Phys. Chem. A* **111**, 7599 (2007).
10. L. Belau, S.E. Wheeler, B.W. Ticknor, M. Ahmed, S.R. Leone, W.D. Allen, H.F. Schaefer, and M.A. Duncan, "Ionization Thresholds of Small Carbon Clusters: Tunable VUV Experiments and Theory," *J. Am. Chem. Soc.* **129**, 10229 (2007).
11. J. Velasquez, III, B. Njagic, M. S. Gordon and M. A. Duncan, "IR Photodissociation Spectroscopy and Theory of Au⁺(CO)_n Complexes: Nonclassical Carbonyls in the Gas Phase," *J. Phys. Chem. A* **112**, 1907 (2008).
12. M.A. Duncan, "Structures, energetics and spectroscopy of gas phase transition metal ion-benzene complexes," *Int. J. Mass Spectrom.* **272**, 99 (2008).
13. P. D. Carnegie, B. Bandyopadhyay and M.A. Duncan, "Infrared spectroscopy of Cr⁺(H₂O) and Cr²⁺(H₂O): The role of charge in cation hydration," *J. Phys. Chem. A* **112**, 6237 (2008).
14. J. Velasquez, III and M. A. Duncan, "IR Photodissociation Spectroscopy of Pt⁺(CO)_n Complexes," *Chem. Phys. Lett.* **461**, 28 (2008).
15. A. M. Ricks and M. A. Duncan, "IR spectroscopy of Co⁺(CO)_n complexes in the gas phase," *J. Phys. Chem. A* **113**, 4701 (2009).
16. P. D. Carnegie, A. B. McCoy and M. A. Duncan, "Infrared spectroscopy and theory of Cu⁺(H₂O)Ar₂ and Cu⁺(D₂O)Ar₂: Fundamentals and combination bands," *J. Phys. Chem. A* **113**, 4849 (2009).
17. A. M. Ricks, Z. D. Reed and M. A. Duncan, "Seven-coordinate homoleptic metal carbonyls in the gas phase," *J. Am. Chem. Soc.* **131**, 9176 (2009) (communication; featured in *Chemical & Engineering News*, July 6, 2009 issue).

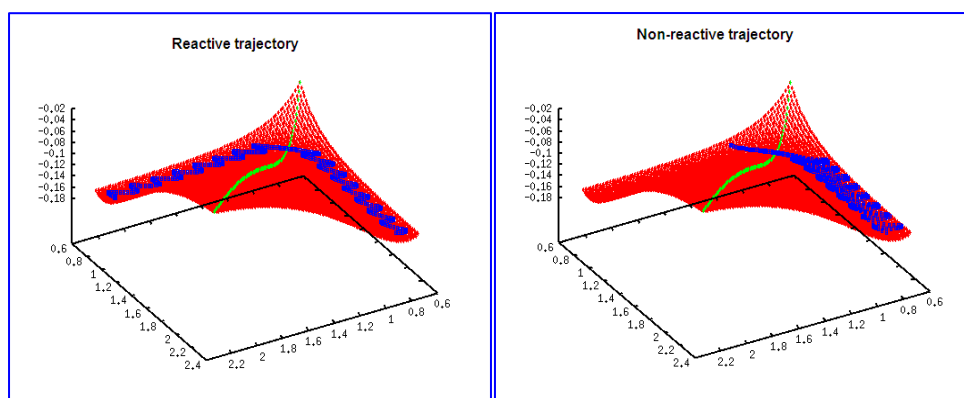
Electronic Structure and Reactivity Studies for Aqueous Phase Chemistry

Michel Dupuis

Chemical and Materials Sciences Division
Pacific Northwest National Laboratory, Richland WA
michel.dupuis@pnl.gov

Program scope[#]: We are interested in the theoretical characterization of thermochemical and spectroscopic properties as well as reaction rates involving molecules and clusters in the aqueous phase and at interfaces for chemistries relevant to DOE missions. In this context, rates of chemical reactions (k) are often calculated using Transition State Theory (TST) whereby it is assumed that reactions proceed along an intrinsic reaction pathway and once the reactive system crosses the transition state, it necessarily evolves into products.

However reactions can be more complex. Calculation of re-crossing factors κ from chemical reaction trajectories across the dividing surface is essential to the improved estimation of reaction rates beyond Transition State Theory (TST), in particular in reactions involving light fragment transfer (for example H atom transfers)^a.



The figures illustrate the appearance of reactive (left) and non-reactive (right) trajectories

Recent pro gress: *Direct Dynamics Calculations of the Reactive Flux Correlation Function (Re-crossing Factor) in Chemical Reactions (with B. Ginovska and G.K. Schenter)*

We are implementing a general and efficient method for the calculation of κ where $\kappa = k/k^{\text{TST}}$ whereby we calculate a Monte Carlo ensemble average of re-crossing factors for trajectories initiated near the reaction transition state over judiciously chosen structures and momenta. The dividing surface separating the reactant and product regions of the reaction is chosen to be the $(3N-7)$ -dimensional hyperplane spanned by the $(3N-7)$ normal modes (expressed in mass-weighted coordinates) perpendicular to the transition state mode at the TS. We sample the configuration space of the structures that belong to the dividing surface, generate an ensemble of initial conditions (atomic momenta), and follow the associated trajectories forward and backward in time. We keep track of crossing and re-crossing and determine whether the trajectories are ‘reactive’ or ‘non-reactive’.

Initial tests of the algorithm have been carried out for collinear, symmetric H-transfer chemical reaction for a variety of mass ratio conditions^b, and for a complex molecular reaction, i.e. the heterolysis rearrangement of protonated pinacolyl alcohol^c $\text{Me}_3\text{C-CHMe-OH}_2^+$ (Me=Methyl) where C-O bond cleavage and a methyl group migration. This latter system was chosen because of the unusual shape of the PES near the TS. This system has been shown to exhibit dynamical mechanistic effects where the reaction trajectories deviate significantly from the intrinsic reaction coordinate (IRC) pathway. The IRC pathway was shown to be consistent with a concerted mechanism of reaction while dynamics trajectories were shown to be indicative of a dynamically step-wise mechanism. This present work aimed to

determine whether the differing character of the dynamics is responsible for an unusual recrossing factor. The functionality has been implemented in HONDO and in NWChem software. The implementation in NWChem is being extended to QM/MM models and using group parallelization for efficiencies. Improved strategies for ensemble averaging of κ are being developed, and the method is being benchmarked for well-studied chemical reactions involving H abstraction in the gas phase and in solution^d.

- a) Truhlar, D.G. and Garrett, B.C. *Acc.Chem.Res.* 13, 440 (1980)
- b) Schenter, G.K., McRae, R.P., and Garrett, B.C. *J.Chem.Phys.* 97,9116 (1992)
- c) Ammal,S.C., Yamataka, H., Aida,M and Dupuis, M. *Science*, 299. (5612), 1555 (2003)
- d) B. Ginovska, D. M. Camaioni, and M. Dupuis, *J. Chem. Phys.* 129, 014506 (2008).

References to publications of DOE Chemical Physics sponsored research (2006-present)

1. S. Du and J.S. Francisco,G.K. Schenter, T.D. Iordanov, B.C. Garrett, **M. Dupuis**, and J. Li, “The OH Radical-H₂O Molecular Interaction Potential”, *J. Chem. Phys.* 124, 224318 (2006).
2. A. Furuham, **M. Dupuis**, and K. Hirao, “Reactions associated with ionization in water: a direct ab initio dynamics study of ionization in (H₂O)₁₇”, *J. Chem. Phys.* 124, 164310 (2006).
3. M. Valiev, B.C. Garrett, M.K. Tsai, K. Kowalski, S. M. Kathman, G. K. Schenter, and **M. Dupuis**, “Hybrid Coupled Cluster Approach for Free Energy Calculations: Application to the Reaction of CHCl₃ and OH⁻ in water”, *J. Chem. Phys.* 127, 051102 (2007).
4. B. Gonovska, D. M. Camaioni, and **M. Dupuis**, “Reaction pathways and excited states in H₂O₂ + OH → HO₂ + H₂O: a New ab initio Investigation”, *J. Chem. Phys.* 127, 084389 (2007).
5. M.K. Tsai, K. Kowalski, M. Valiev, **M. Dupuis**, "Signature OH Absorption Spectrum from Cluster Models of Solvation: A Solvent-to-Solute Charge Transfer State", *J. Phys. Chem. A* 000, 0000 (2007).
6. M. Ohisa, H. Yamataka, **M. Dupuis**, and M. Aida, “Two-Dimensional Free Energy Surface on Exchange Reaction of Alkyl Chloride/Chloride Using QM/MM-MC Method”, *Phys. Chem. Chem. Phys.* 10, 844 (2008)
7. E. Bylaska, **M. Dupuis**, P. Tratnyek, "One-Electron Transfer Reactions of Polychlorinated Ethylenes: Concerted and Stepwise Cleavages", *J. Phys. Chem. C* 112, 3712 (2008)
8. M. Valiev, E. Bylaska, **M. Dupuis**, P. Tratnyek, "Combined Quantum Mechanical and Molecular Mechanics Studies of the Electron Transfer Reactions Involving Carbon Tetrachloride in Solution", *J. Phys. Chem. A* 12, 2713 (2008)
9. A. Furuham, **M. Dupuis**, and K. Hirao, “Application of a kinetic energy partitioning scheme for ab initio molecular dynamics to reactions associated with ionization in water tetramers (H₂O)₄⁺”, *Phys.Chem.Chem.Phys.* 10, 2033 (2008).
10. B. Ginovska, D. M. Camaioni, and **M. Dupuis**, “The H₂O₂+OH → HO₂+H₂O reaction in aqueous solution from a charge-dependent continuum model of solvation”, *J. Chem. Phys.* 129, 014506 (2008).
11. B. Ginovska, D. M. Camaioni, **M. Dupuis**, C. Schwerdtfeger, and Q. Gilcrease, “Charge-Dependent Cavity Radii for an Accurate Dielectric Continuum Model of Solvation with Emphasis on Ions: Aqueous Solutes with Oxo, Hydroxo, Amino, Methyl, Chloro, Bromo and Fluoro Functionalities”, *J. Phys. Chem. A* 000, 0000 (2008).
12. B. Ginovska, M. Dupuis, and G. K. Schenter, “Direct Dynamics Calculations of Re-crossing factors in Chemical Reactions in the Gas Phase and in the Condensed Phase”, in preparation (2009).

[#] This research was performed in part using the Molecular Science Computing Facility in the William R. Wiley Environmental Molecular Sciences Laboratory (EMSL) at the Pacific Northwest National Laboratory (PNNL). The EMSL is funded by DOE's Office of Biological and Environmental Research. PNNL is operated by Battelle for DOE.

Photochemistry at Interfaces
Kenneth B. Eisenthal
Department of Chemistry
Columbia University
New York, NY 10027
eisenth@chem.columbia.edu

A. Effects of Molecular Structure and Reduction Potential on Dynamics of Electron Transfer at Air/Organic-Aqueous Interface

The dynamics of electron transfer from donor N,N-dimethylaniline (DMA) molecules to three different photoexcited coumarin molecules at the DMA/ water interface were obtained from femtosecond pump – SHG probe measurements. Two of the coumarins, C314 and C153, have essentially the same reduction potentials, -1.721 eV and -1.731 eV, but have different substituents on the aromatic ring. The electron transfer times are the same within our experimental error, 14 ± 2 ps and 11 ± 3 ps respectively. This indicates that the structural differences, which could affect the mutual orientation and separation of the reactants and thereby their interaction strength, are essentially the same, and it is their very close reduction potentials that is the key factor. This is more clearly seen in our finding that C152, which has a significantly lower reduction potential, -1.630 than the other coumarins, has a significantly faster electron transfer time constant of 3 ± 0.5 ps. Our calculations of the free energy of reaction for the three coumarins together with our measured rate constants indicate that the electron transfer is in the Marcus normal region. Comparison with known measurements in bulk DMA show that for C152 that the electron transfer is significantly slower, whereas for C153 the interface transfer time is slightly faster.

B. Effects of a Negatively Charged Surface on Molecular Rotation Dynamics at Air/ Water Interface

The in-plane rotational dynamics of the permanent dipole moment axis of C314 at the sodium dodecyl sulfate(SDS)/water interface was measured using the SHG method. At an SDS density of 100 \AA^2 per SDS molecule the surface coverage is that of a homogeneous monolayer. It was found that the in-plane rotation was only 15% slower at the anionic SDS/water interface than at the air/water interface. Similar results were found for the out of plane rotation dynamics. These results were surprising because there was clear information that there are strong interactions of C314 and the SDS monolayer. For example the C314 orientation is $\sim 30^\circ$ more upright at the SDS/water interface than the air/water interface. In addition there are marked changes in the C314 interface spectra, and changes in the SDS phase diagram as well. The relative insensitivity of rotations to the presence of anionic surfactants has implications for molecular rotations at biological cell membrane/water interfaces, most of which contain a significant population of anionic phospholipids.

C. Ultrafast Intermolecular Energy Transfer and Molecular Rotation of D₂O in Bulk D₂O

We report on a study of the vibrational energy relaxation and resonant vibrational (Förster) energy transfer of the OD vibrations of D₂O and mixtures of D₂O and H₂O using femtosecond mid-infrared spectroscopy. We observe the lifetime of the OD vibrations of bulk D₂O to be 400 ± 30 fs. The rate of the Förster energy transfer is measured *via* the dynamics of the anisotropy of the OD vibrational excitation. For a solution of 0.5% D₂O in H₂O, resonant energy transfer is negligible, and the anisotropy shows a single exponential decay with a time constant of 2.6 ± 0.1 ps, representing the time scale of the molecular reorientation. With increasing concentration, the anisotropy decay becomes faster and non-exponential, showing the increased contribution of resonant energy transfer between the OD vibrations. We determine the Förster radius of the OD vibration of HDO in H₂O to be $r_0 = 2.3 \pm 0.2$ Å.

D. Effects of NaBr on the Population and Molecular Motions of Coumarin 314 at the Air/Aqueous Interface

Surface tension measurements indicate that the surface concentration of C314 at the air/aqueous interface is enhanced as the bulk concentration of NaBr is increased from zero to 5M. In apparent contradiction to this finding is the observation that the magnitude of the second harmonic signal generated at the air/aqueous interface decreases as the bulk concentration of NaBr is increased from zero to 5M. The decrease in the SHG signal suggests that the surface concentration of C314 has decreased. The orientation of C314 obtained from measurement of the polarization of the SHG signal was found to be not sensitive to the presence of NaBr, thus eliminating changes in the orientation of C314 as a factor in the observed decrease in the magnitude of the SHG signal when NaBr is present. It was also found that NaBr affected not only the equilibrium properties of C314 but also the dynamics of C314 motions. The rotational relaxation time of C314 was found to be faster in the presence of NaBr. Measurements of the rotational relaxation of C314 in bulk aqueous NaBr solutions are underway. It is of interest to note that studies by M.Fayer on the effects of NaBr on hydrogen bond dynamics in bulk aqueous solution is slower, i.e. the rearrangement of the hydrogen bond structure is slowed down. The orientational relaxation time of an HOD molecule was found to be slower when NaBr is present. At the air/aqueous interface it appears that there is less friction to the rotational motion of C314, suggesting that the dynamics of water rearrangement becomes faster in the presence of NaBr.

Future Plans

SFG and SHG studies of the ultrafast dynamics of the chemical and physical pathways by which molecules in excited electronic states dissipate their energy at vapor/liquid, liquid/liquid, liquid/solid, and liquid/nanoparticle interfaces.

Vibrational and electronic spectroscopy, by SFG and SHG studies, of molecules in excited electronic states at liquid interfaces.

DOE Supported Publications 2005-2009

Rao, Yi; Subir, Mahamud; McArthur, Eric A.; Turro, Nicholas J.; Eienthal, Kenneth B.. **Organic ions at the air/w ater interface.** Chemical Physics Letters (2009), 477(4-6), 241-244.

Rao, Yi; Turro, Nicholas J.; Eienthal, Kenneth B.. **Water structure at air/acetonitrile aqueous solution interfaces.** Journal of Physical Chemistry C (2009), 113(32), 14384-14389.

Piatkowski, L.; Eienthal, K.B.; Bakker, H.J.; **Ultrafast intermolecular energy transfer in heavy water;** Phys.Chem.Chem.Phys. 2009, DOI 10.1039/b908975f

Shang, Xiaoming; Nguyen, Kim; Rao, Yi; Eienthal, Kenneth B.. **In-pla ne mole cular rotational dynamics at a negatively charged surfactan t/aqueous interface.** Journal of Physical Chemistry C (2008), 112(51), 20375-20381.

Liu, Jian; Subir, Mahamud; Nguyen, Kim; Eienthal, Kenneth B.. **Second harmonic studies of ions crossing liposome membranes in real t ime.** Journal of Physical Chemistry B (2008), 112(48), 15263-15266.

Subir, Mahamud; Liu, Jian; Eienthal, Kenneth B.. **Protonation at the aqueous interface of polymer nanoparticles with second harmonic generation.** Journal of Physical Chemistry C (2008), 112(40), 15809-15812.

Rao, Yi; Song, Daohua; Turro, Nicholas J.; Eienthal, Kenneth B.. **Orientalional motions of vibrational chromophores in mole cules at the air/water interface w ith time res olved sum frequency generation.** Journal of Physical Chemistry B (2008), 112(43), 13572-13576.

Eienthal, Kenneth B.. **Laser method to measure th e e ffects of organic and inorganic species on direct and ion channel transport o f ions and other species across lipid bilayers and other interface structures.** PCT Int. Appl. (2006), 38pp.

Nguyen, Kim T.; Shang, Xiaoming; Eienthal, Kenneth B.. **Molecular rotation a t negatively charged surfactant/aqueous interfaces.** Journal of Physical Chemistry B (2006), 110(40), 19788-19792.

Eienthal, Kenneth B.. **Second harmonic spectroscopy of aqueous nano- and microparticle interfaces.** Chemical Reviews (Washington, DC, United States) (2006), 106(4), 1462-1477.

McArthur, Eric A.; Eienthal, Kenneth B.. **Ultrafas t e xcited sta te ele ctron tr ansfer a t a n organic liquid/aqueous interface.** Journal of the American Chemical Society (2006), 128(4), 1068-1069

Rao, Yi; Comstock, Matthew; Eienthal, Kenneth B.. **Absolute or ientation of mo lecules at interfaces.** Journal of Physical Chemistry B (2006), 110(4), 1727-1732.

Fitts, Jeffrey P.; Machesky, Michael L.; Wesolowski, David J.; Shang, Xiaoming; Kubicki, James D.; Flynn, George W.; Heinz, Tony F.; Eienthal, Kenneth B.. **Second-harmonic generation and theoretical studies of protonation at the water/ α -TiO₂ (110) interface.** Chemical Physics Letters (2005), 411(4-6), 399-403.

Fitts, Jeffrey P.; Shang, Xiaoming; Flynn, George W.; Heinz, Tony F.; Eienthal, Kenneth B.. **Electrostatic surface charge at aqueous/ α -Al₂O₃ single crystal interfaces as probed by optical second harmonic generation.** Journal of Physical Chemistry B (2005), 109(16), 7981-7986.

Liu, Jian; Shang, Xiaoming; Pompano, Rebecca; Eienthal, Kenneth B.. **Antibiotic assisted molecular ion transport across a membrane in real time.** Faraday Discussions (2005), 129 291-299.

Garrett, Bruce C; et.al. **Role of water in electron-initiated processes and radical chemistry: issues and scientific advances.** Chemical Reviews (Washington, DC, United States) (2005), 105(1), 355-389.

Interfacial Oxidation of Complex Organic Molecules

G. Barney Ellison — (Grant DE-FG02-93ER14364)

Department of Chemistry, University of Colorado, Boulder, Colorado 80309-0215

Email: barney@jila.Colorado.edu, Web: <http://www.colorado.edu/chem/people/ellisonb.html>

We are studying the interfacial oxidation of organic films that coat water droplets. A main focus of our group is the design and fabrication of a droplet spectrometer to study the formation of peroxy radicals at the droplet/atmosphere interface. We also continue to study the vibrational spectroscopy of complex peroxy radicals isolated in Argon matrices at 20 K. Use of a combination of photoionization mass spectroscopy and matrix infrared spectroscopy has characterized the adduct of propargyl radical and oxygen as $\text{HC}\equiv\text{CCH}_2\text{OO}\cdot$. Finally we have applied the EA/Negative ion cycle to measure the bond energies of two of the most fundamental peracids: performic acid [$\text{HC}(\text{O})\text{OOH}$] and peracetic acid [$\text{CH}_3(\text{O})\text{OOH}$]

When the propargyl radical, $\text{HCCCH}_2\cdot$, and O_2 are co-deposited onto a cold argon matrix, a chemical reaction ensues¹; infrared absorption spectra reveal the formation of the propargyl peroxy radical: $\text{HC}\equiv\text{C}\cdot\text{CH}_2\tilde{\text{X}}^2\text{B}_1 + \text{O}_2 \rightarrow \text{trans-HC}\equiv\text{C-CH}_2\text{OO}\tilde{\text{X}}^2\text{A}''$. We do not observe the isomeric adduct, $\text{CH}_2=\text{C=CHOO}\tilde{\text{X}}^2\text{A}''$. The propargyl radicals are produced by a hyperthermal nozzle

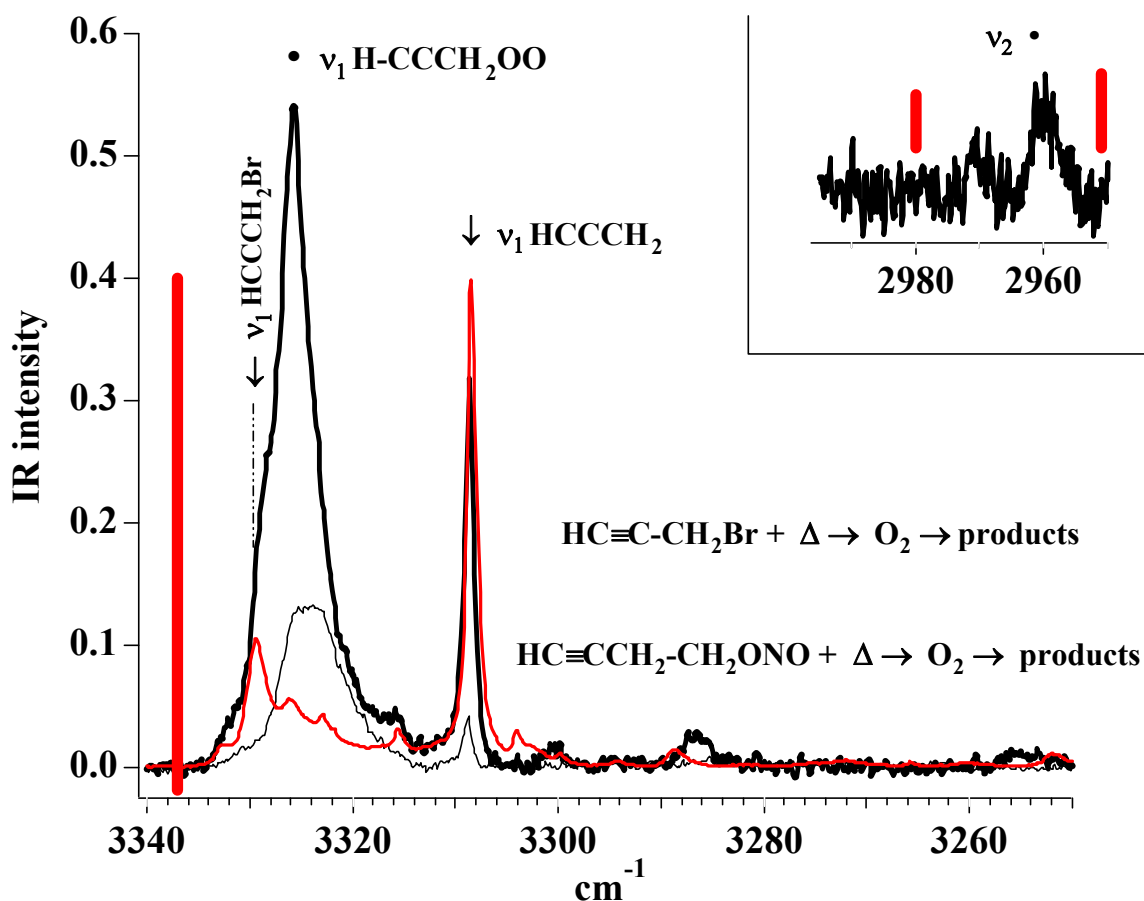


Figure 1. The two black traces are IR spectra (of the CH stretching region) resulting from combination of propargyl radicals with O_2 in a cryogenic matrix. The top black trace uses HCCCH_2Br as the propargyl precursor and the bottom trace uses $\text{HCCCH}_2\text{CH}_2\text{ONO}$ to generate propargyl radical. The red trace is the IR spectrum that results from the thermal cracking of $\text{HC}\equiv\text{C-CH}_2\text{Br}$. The red spectrum provides us with $\nu_1(\text{H-CCCH}_2\text{Br})$ and $\nu_1(\text{H-CCCH}_2)$. The intense red stick is the predicted CCSD(T)/ANO anharmonic transition, ν_1 .

while a second nozzle alternately fires bursts of O₂/Ar at the 20 K matrix. The absorption spectra of the radicals are measured using a Fourier transform infrared spectrometer. We observe 13 of the 18 fundamental infrared bands of the propargyl peroxy radical in an Ar matrix at 20 K. The experimental frequencies (cm⁻¹) of *trans*-HC≡C-CH₂OO \tilde{X}^2A'' are assigned. The a' modes are $\nu_1 = 3326$, $\nu_2 = 2960$, $\nu_3 = 2148$, $\nu_4 = 1440$, $\nu_5 = 1338$, $\nu_6 = 1127$, $\nu_7 = 982$, $\nu_8 = 928$, $\nu_9 = 684$, and $\nu_{10} = 499$ cm⁻¹, while the a'' modes are $\nu_{14} = 1218$, $\nu_{15} = 972$, and $\nu_{16} = 637$ cm⁻¹. Linear dichroism spectra were measured with photooriented HCCCH₂OO radical samples to establish the experimental polarizations of several vibrational bands. The experimental frequencies (ν) for the propargyl peroxy radical are compared to the anharmonic frequencies (ν) resulting from electronic structure calculations. The experimental thermochemistry for C₃H₃ reacting with oxygen has been reanalyzed as: $\Delta_{\text{rxn}}H_{298}(\text{HCCCH}_2 + \text{O}_2 \rightarrow \text{CH}_2=\text{C}=\text{O} + \text{HCO}) = -83 \pm 3$ kcal mol⁻¹; $\Delta_{\text{rxn}}H_{298}(\text{HCCCH}_2 + \text{O}_2 \rightarrow \text{CH}_3\text{CO} + \text{CO}) = -111 \pm 3$ kcal mol⁻¹; $\Delta_{\text{rxn}}H_{298}(\text{HCCCH}_2 + \text{O}_2 \rightarrow \text{CH}_2\text{CHO} + \text{CO}) = -106 \pm 4$ kcal mol⁻¹; $\Delta_{\text{rxn}}H_{298}(\text{HCCCH}_2 + \text{O}_2 \rightarrow \text{HCHO} + \text{HCCO}) = -67 \pm 4$ kcal mol⁻¹; $\Delta_{\text{rxn}}H_{298}(\text{HCCCH}_2 + \text{O}_2 \rightarrow \text{CH}_2\text{CH} + \text{CO}_2) = -105 \pm 3$ kcal mol⁻¹.

The 351.1 nm photoelectron spectra of the both the peroxyformate,² HC(O)OO⁻, and the peroxyacetate anion,³ CH₃C(O)OO⁻, were measured. Photodetachment of mass-selected beams of the performate anion² has been observed: HC(O)OO⁻ + $\hbar\omega_{351\text{nm}}$ → HC(O)OO + e⁻. The photoelectron spectrum displays vibronic features in both the \tilde{X}^2A'' ground state and the \tilde{A}^2A' first excited states of the of the performyl radical, HC(O)OO. Franck-Condon simulations of the spectrum show that the ion is formed exclusively in the *trans*-conformation. The electron affinity (EA) of the peroxyformyl radical was determined to be EA(HC(O)OO) = 2.493 ± 0.006 eV.

Thermochemistry Chart: Peracetic Acid

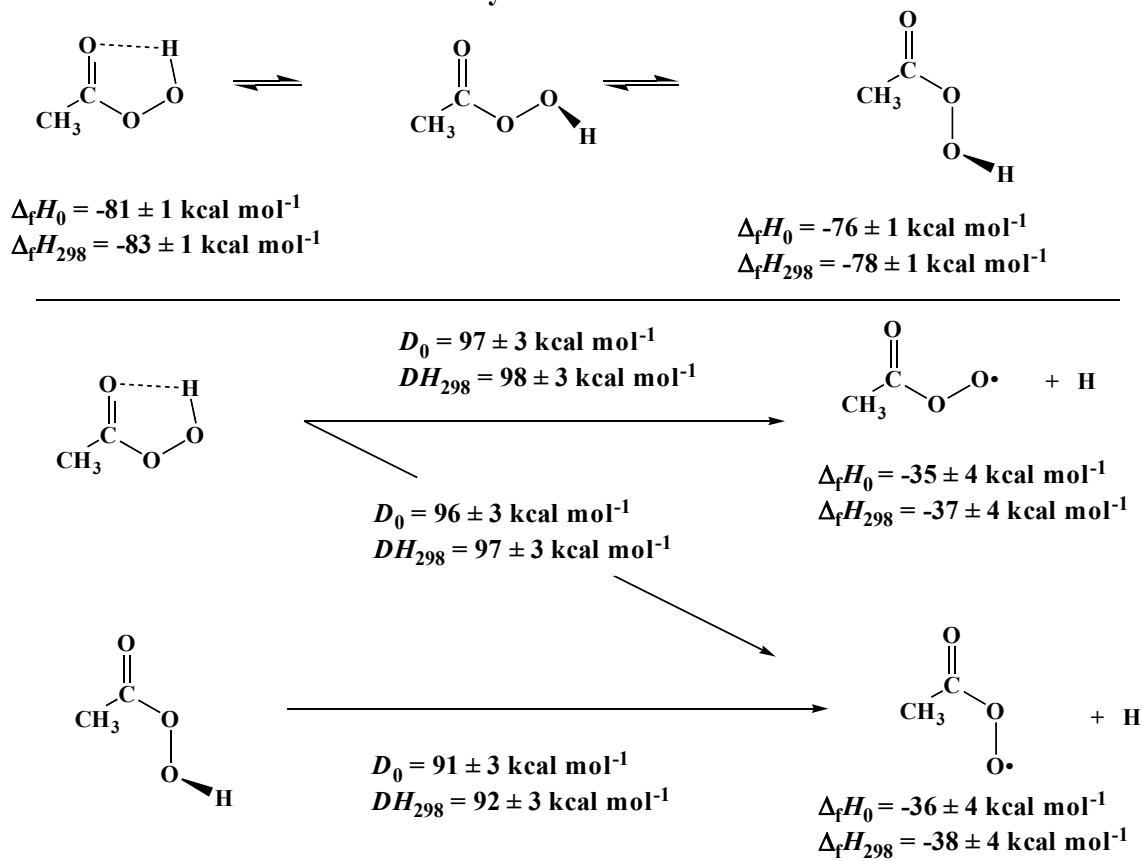
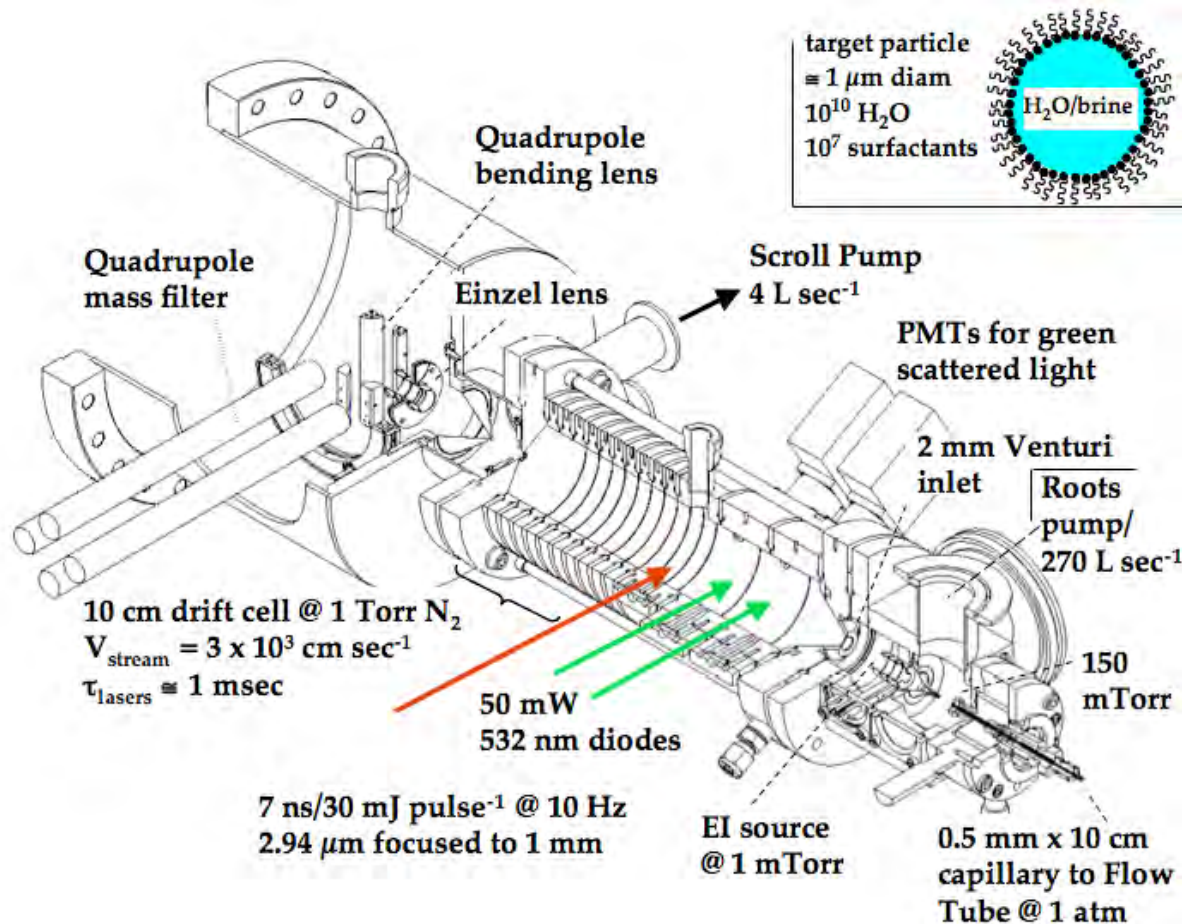


Figure 2. A summary of the thermochemistry of peracetic acid.

The term energy splitting was found to be $T_e(\tilde{A} \leftarrow \tilde{X}) = 0.783 \pm 0.060$ eV. The gas-phase acidity of peroxyformic acid has been determined using an ion-molecule bracketing technique. Based on the size of the *trans*- to *cis*- isomerization barrier, the measured acidity was assigned to the higher energy *trans*-conformer of the acid. The gas-phase acidity of the lower energy *cis*-conformer of peroxyformic acid was found from the measured acidity for the *trans*-form and a calculated energy correction: $\Delta_{\text{acid}}G_{298}(\textit{cis}\text{-peroxyformic acid}) = 347 \pm 3$ kcal mol⁻¹ and $\Delta_{\text{acid}}H_{298}(\textit{cis}\text{-peroxyformic acid}) = 354 \pm 3$ kcal mol⁻¹. Using the negative ion *EA*/acidity thermochemical cycle,^{4,5} the O-H bond dissociation energy of *cis*-peroxyformic acid was determined to be $D_0(\textit{cis}\text{-HC(O)OO-H}) = 97 \pm 3$ kcal mol⁻¹.

In a separate study,³ the photoelectron spectrum of peracetate was studied: $\text{CH}_3\text{C(O)OO}^- + \hbar\omega_{351\text{nm}} \rightarrow \text{CH}_3\text{C(O)OO} + e^-$. The observed spectrum arises almost exclusively from transitions between the *trans*-conformer of the anion and the \tilde{X}^2A'' and \tilde{A}^2A' states of the corresponding radical. The *EA* of *trans*-CH₃C(O)OO is 2.381 ± 0.008 eV and the $T_e(\tilde{A}^2A')$ is 0.691 ± 0.009 eV. The gas-phase acidity of *trans*-peroxyacetic acid was bracketed between the acidity of acetic acid and *tert*-butylthiol. The acidity of *cis*-CH₃C(O)OOH acid was found by adding a calculated energy correction to the acidity of the *trans*-conformer; $\Delta_{\text{acid}}H_{298}(\textit{cis}\text{-CH}_3\text{C(O)OOH}) = 356 \pm 3$ kcal mol⁻¹.

We are fabricating a new experiment to study the oxidation of surfactants coating water droplets.⁶ This instrument is designed to produce a stream of saline-water droplets that are coated with organics, to size-select them, and to inject them into an atmospheric flow tube where they will be dosed with OH radicals. The organic radicals will combine with O₂ and produce a population of peroxy radicals at the droplet/atmospheric interface. The resulting oxidized particles will be



analyzed with a mass spectrometer. A 1 μm saline-water, organic aerosol contains roughly 10^{10} waters in the core and carries about 10^7 surfactant $\text{CH}_3(\text{CH}_2)_{10}\text{CO}_2^-$ ions at the droplet/atmosphere interface. The heat of vaporization of water is 40.7 kJ mol^{-1} so it takes roughly 1 nJ to vaporize a 1 μm aqueous droplet. The LaserVision OPO is pumped by a YAG laser and delivers 30 mJ/7nsec of 2.94 μm (3400 cm^{-1}) radiation focused to a 1 mm spot. The imaginary part of the refractive index of water provides the absorption coefficient and a 1 μm droplet will absorb 18 nJ of the 10 mJ pulse. There are no organic vibrational modes resonant with the 3400 cm^{-1} radiation. The absorption coefficient of water, $\alpha(\text{H}_2\text{O}, 2.93 \mu\text{m})$, is measured to be $0.88 \mu\text{m}^{-1}$ so the optical penetration depth is roughly 1.1 μm . Consequently all of the 18 nJ will be absorbed by the saline-water core of the particle. The surfactant-coated droplet will completely dissociate and release the surfactant negative ions for analysis by a quadrupole mass filter.

References:

1. E. B. Jochnowitz; X. Zhang; M. R. Nimlos; B. A. Flowers; J. F. Stanton; G. B. Ellison, "Infrared Spectrum of the Propargylperoxyl Radical, $\text{HC}\equiv\text{CCH}_2\text{OO}\cdot$ ", *J. Phys. Chem. A*, 2009, (in press, Sept. 2009).
2. S. M. Villano; N. Eyet; S. W. Wren; G. B. Ellison; V. M. Bierbaum; W. C. Lineberger, "Photoelectron Spectroscopy and Thermochemistry of the Peroxyformate Anion", *J. Phys. Chem. A* 2009, (**in press, 2009**).
3. S. M. Villano; N. Eyet; S. W. Wren; G. B. Ellison; V. M. Bierbaum; W. C. Lineberger, "Photoelectron Spectroscopy and Thermochemistry of the Peroxyacetate Anion", *European Mass Spec.*, 2009, (**in press, Sept. 2009**).
4. J. Berkowitz; G. B. Ellison; D. Gutman, "Three Methods to Measure RH Bond Energies", *J. Phys. Chem.*, 1994, **98**, 2744-2765.
5. S. J. Blanksby; G. B. Ellison, "Bond Dissociation Energies of Organic Molecules", *Acc. Chem. Res.*, 2003, **36**, 255-263.
6. L. A. Cuadra-Rodriguez; B. R. Reed; D. E. David; S. E. Barlow; A. Zelenyuk; G. B. Ellison, "Mass spectroscopy of saline-water droplets", *J. Chem. Phys.*, 2010, (in preparation).

DOE supported research (2008-2009)

1. Timothy D'Andrea, Xu Zhang, Evan B. Jochnowitz, Theodore G. Lindeman, C. J. S. M. Simpson, Donald E. David, Thomas J. Curtiss, John R. Morris, and G. Barney Ellison, "Oxidation of Hydrocarbon Films by OH Radical Beams", *J. Phys. Chem. B.*, 112, 535-544 (2008).
2. Shuji Kato, G. Barney Ellison, Veronica M. Bierbaum, Stephen J. Blanksby, "Base-Induced Decomposition of Alkyl Hydroperoxides in the Gas Phase. Part 3. Kinetics and Dynamics in the $\text{HO}\cdot + \text{CH}_3\text{OOH}$, $\text{C}_2\text{H}_5\text{OOH}$, and $\text{tert-C}_4\text{H}_9\text{OOH}$ Reactions", *J. Phys. Chem. A.*, 112, 9516-9525 (2008).
3. John F. Stanton, Bradley A. Flowers, Devin A. Matthews, Asa P. Ware, and G. Barney Ellison, "Gas-phase Vibrational Spectrum of Methylnitrate", *J. Mol. Spectroscopy* 251, 384-393 (2008).
4. AnGayle Vasiliou, Mark R. Nimlos, John W. Daily, and G. Barney Ellison, "Thermal Decomposition of Furan Generates Propargyl Radicals", *J. Phys. Chem. A* 113, 8540-8547 (2009).
5. Stephanie M. Villano, Nicole Eyet, Scott W. Wren, G. Barney Ellison, Veronica M. Bierbaum, and W. Carl Lineberger, "Photoelectron Spectroscopy and Thermochemistry of the Peroxyformate Anion", *J. Phys. Chem. A* (in press, Sept. 2009)
6. Evan B. Jochnowitz, Xu Zhang, Mark R. Nimlos, Bradley A. Flowers, John F. Stanton, and G. Barney Ellison, Infrared Spectrum of the Propargyl Peroxyl Radical, $\text{HC}\equiv\text{CCH}_2\text{OO}\cdot$, *J. Phys. Chem. A*, (in press, Sept. 2009).
7. Stephanie M. Villano, Nicole Eyet, Scott W. Wren, G. Barney Ellison, Veronica M. Bierbaum, and W. Carl Lineberger, "Photoelectron Spectroscopy and Thermochemistry of the Peroxyacetate Anion" *European J. Mass Spectrom.*, (in press, Sept. 2009).

Plasmonic Field Effects on the Proton Pump System of Bacteriorhodopsin

Mostafa A El-Sayed
School of Chemistry and Biochemistry, Georgia Institute of Technology
Atlanta, GA 30332
email: melsayed@gatech.edu

Program Scope:

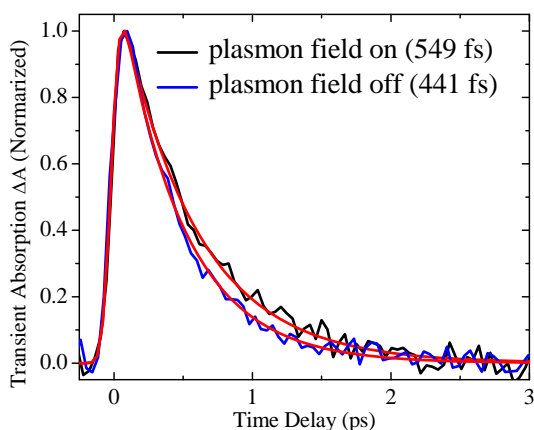
Bacteriorhodopsin (bR) is the other photosynthetic system in nature. The absorption of light by its retinal chromophore leads to its photo-isomerization. This is followed by the formation of a number of intermediates nonradiatively before the formation of the parent bR. As a result, protons are pumped across the cell membranes whose gradients are used to make ATP from ADP. Thus the proton pump process determines bR efficiency of converting solar energy into electric then chemical energy (ATP formation). The scope of this program is to examine the plasmon field effects on the rates of the different steps in the proton pump processes in bR.

Recent Progress:

I. Plasmonic Field Enhancement:

Plasmonic field enhancement of the radiative properties of nearby coupled electronic systems has been known to occur under certain conditions. We are now actively examining the plasmonic field effects on the non-radiative electronic relaxation processes in a number of systems. Figure 1 shows the effect of turning on the plasmonic field of gold nanospheres (A) and nanorods (B) on the primary step of bacteriorhodopsin, the retinal photo-isomerization process.

A.)



B.)

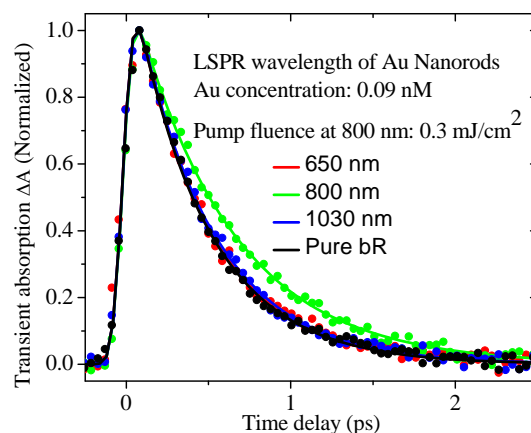


Figure 1: The kinetics of the primary step of bR (the retinal photoisomerization) in presence and absence of the plasmonic field of nanospheres excited at 560 nm (A) and of nanorods of different absorption maxima but all are excited at 800 nm (B).

The exact mechanism(s) involved in this process is not yet understood. Using spheres, the effect could be a result of radiative perturbation as exciting the bR retinal does excite the

plasmon, which can enhance the retinal absorption rate. With rods, where no absorption of bR occurs at the excitation wavelength of the plasmon field, the effect must be totally nonradiative.

Two studies have been carried out recently that shed light on the mechanisms that might be involved in the enhancement of the nonradiative electronic relaxation of the CdTe excitons in CdTe nanorods under the surface plasmon fields of gold nanoshells (see figure 2). In the first study, the dependence of the relaxation rates on the angle between the exciting light polarization direction and the band gap exciton transition moment of the CdTe nanorod was carried out (see figure 2A). In the second study, this dependence was studied as a function of the thickness of the gold nanoshell (Fig. 2; comparing A and C)). The mechanism of enhancing the non-radiative relaxation of the band gap excited electron is proposed to involve either the plasmonic enhancement of the radiative absorption properties of the semiconductor electronic system or the non-radiative electron transfer of the band gap excited electron to the plasmonic nanoshell. The enhancement of the absorption processes could involve either the absorption of the excited electron to the ionization continuum or the ground state electron to the band gap excited state. In the latter case, the absorption process is followed by exciton-exciton annihilation (Auger processes) thus decreasing the excited electronic state lifetime.

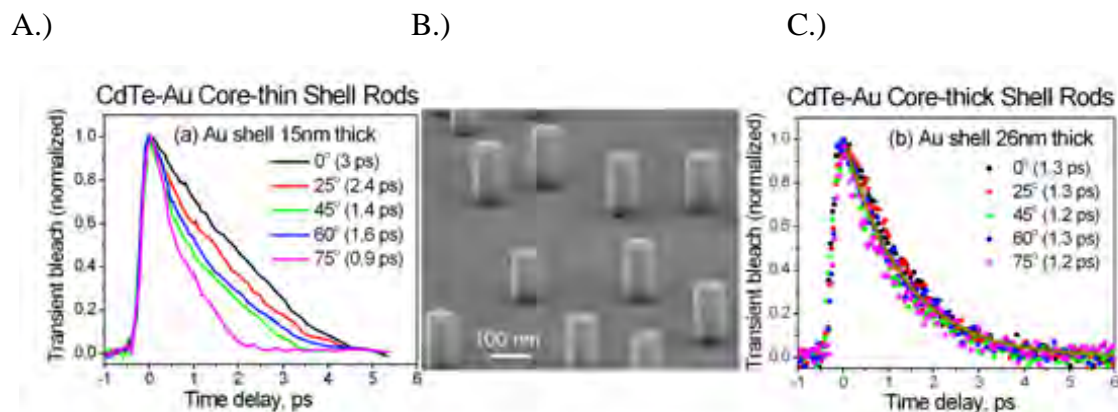


Figure 2: Orientation dependence of the band gap CdTe Exciton decay in CdTe core – gold shell nanorods with a gold shell of 15nm (A) and 26nm (C) thickness. The angle of rotation is the angle between the long axis of the nanorod and the incident light propagation direction. Figure B is an SEM of the CdTe core–gold shell nanorods (Svetlana Neretina et. al, *Nano Letters* **2009**, 9, (3), 1242-1248. and in press.).

When a thin gold nanoshell (15nm) is used to encapsulate a CdTe nanorod, the plasmonic field of the gold nanoshell is found to be polarized along the long axis. As the thickness of the gold nanoshell increases to 26nm, the plasmonic field becomes unpolarized and has a very high scattering to absorption probability ratio. This could explain the independence of the relaxation rate on the relative nanorod orientation with respect to the exciting light polarization direction (Figure 2C). The Auger mechanism becomes less probable as it depends quadratically on the exciton concentration, which depends on the plasmon field enhancement of the absorption rate. This makes the excited electron ionization or transfer to the gold nanoshell the two most likely mechanisms for the enhancement of the relaxation rates in the 26 nm thick gold shell nanorod.

II. Plasmonic Field Effects on the Proton Pump Function of bR:

The proton pump is the most important process in the photosynthesis of bR. It is required to build up proton gradients across the bR membrane needed for the synthesis of ATP from ADP.

Proton pumps are very important processes in biology in general and are the most quantitatively studied in bR. Its efficiency determines the efficiency of the conversion of solar energy into electric and then into chemical energy. If the plasmonic field enhances the rate of this process, the yield of the proton production should increase, leading to better photo-conversion efficiency.

The rates of deprotonation and reprotonation were determined in the presence of the gold nanorods with absorption maximum at 800 nm, which is at longer wavelength than the bR retinal absorption. These rates were measured with and without simultaneously turning on the plasmon field (by exciting the 800 nm absorption of the surface plasmon resonance of the gold nanorods used). Two different kinds of experiments were carried out and these rates were measured at different Plasmon field intensities. In one experiment, the field was changed by changing the intensity of the surface plasmon exciting laser. In the other experiment, the field was changed by changing the gold nanorod concentration. No effects on the rate of the proton dissociation from the protonated schiff base of the retinal are observed. However, a faster rate is observed in the presence of the plasmon field for the reprotonation process.

The plasmonic field effect on the rate of reprotonation can result from enhancing nonradiative process(es), such as photothermal effects resulting from the electron-phonon and phonon-phonon relaxation processes in the plasmonic gold. It can also result from affecting the electronic relaxation processes of other electronic systems within the active site. Temperature rise was measured and calculated and was found to be too small to induce such an increase in the rate, as the activation energy and frequency factors are known for this process. Electromagnetic field coupling requires changes in the electrostatic configuration of protonated schiff base-protein modality with charged ions. Radiative coupling is a very unlikely cause as the laser used has a wavelength around 800 nm (capable of exciting the plasmon) while the bR absorption maximum is ~ 560 nm. Using gold nanorods of absorption maxima at wavelength shorter than the plasmon exciting wavelength (800 nm) but longer than 560nm (the bR exciting wavelength) had no effect on the lifetime as the laser wavelength at 800 nm determines the strength of the plasmonic field. It also suggests that the absorption of bR does not extend far enough near the 800 nm wavelength of the laser. It could be a result of the coupling between the electromagnetic fields and the changes in the electrostatic structure in bR during this process. It is interesting that the deprotonation involves a direct donation of the proton to an attached amino acid while the reprotonation occurs as a result of transferring the proton over a 15 Å long distance. This makes the effect of external perturbations and structural changes very likely to take place in the reprotonation process.

Future Plans:

The addition of small amount of different types of surfactants is found to have effects on the different decays of the different steps in the photocycle depending on whether the surfactant is hydrophobic or hydrophilic in nature. A detailed examination of the plasmonic field effect on the rates of the proton pump in the presence of different amounts of surfactants of different polarity will be carried out. Furthermore, studies of the changes in the enhanced Raman and FTIR spectra during the photocycle upon turning on the Plasmonic field will also be examined. This will allow us to study in details the structured changes and their response to turning on the plasmonic fields. The study of the plasmonic field effects on the rates of the other five known steps in the cycle will also be examined.

Publications Since 2005:

1. Xiaohua Huang, Svetlana Neretina, Mostafa A. El-Sayed. "Gold nanorods: from synthesis to biomedical applications." **Adv. Mater.**, in press. Invited review.
2. Arianna Biesso, Wei Qian, Xiaohua Huang, Mostafa El-Sayed. "Gold nanoparticles surface plasmon field effects on the proton pump process of the bacteriorhodopsin photosynthesis". **J. Am. Chem. Soc. Commun.**, 2009, 131(7), 2442-2443.
3. L.-K. Chu, Mostafa A. El-Sayed, "Bacteriorhodopsin O-state photocycle kinetics: A surfactant study". **Photochem. Photobiol.**, 2009 in press.
4. Jianping Wang, Mostafa A. El-Sayed. "Rapid thermal tuning of chromophore structure in membrane protein". **J. Phys. Chem. B**, 2009, ASAP.
5. Arianna Biesso, Wei Qian, Mostafa A. El-Sayed. "Gold nanoparticle plasmonic field effect on the primary step of the other photosynthetic system in nature, bacteriorhodopsin". **J. Am. Chem. Soc.**, 2008, 130(11), 3258-3259.
6. Erin B. Dickerson, Erik C. Dreaden, Xiaohua Huang, Hunghao Chu, Sujatha Pushpanketh, John F. McDonald and Mostafa A. El-Sayed. "Gold nanorod assisted near-infrared plasmonic photothermal therapy (PPTT) of HSC-3 tumors in mice". **Cancer Lett.**, 2008, 269, 57-66.
7. Prashant K. Jain, Xiaohua Huang, Ivan H. El-Sayed and Mostafa A. El-Sayed. "Noble metals on the nanoscale: optical and photothermal properties and applications in imaging, sensing, biology, and medicine". **Acc. Chem. Res.**, 2008, 41(12), 1578-1586. Invited review.
8. Xiaohua Huang, Ivan H. El-Sayed, Wei Qian and Mostafa A. El-Sayed. "Cancer cells assemble and align gold nanorods conjugated to antibodies to produce highly enhanced, sharp and polarized surface Raman spectra: a potential cancer diagnostic marker". **Nano Letter.**, 2007, 7(6): 1591-1597.
9. Prashant K. Jain, Xiaohua Huang, Ivan H. El-Sayed, Mostafa A. El-Sayed. "Review of some surface plasmon resonance-enhanced properties of noble metal nanoparticles and their applications to biosystems". **Plasmonics**, 2007, 2, 107-118. Invited review.
10. Xiaohua Huang, Prashant K. Jain, Ivan H. El-Sayed and Mostafa A. El-Sayed. "Determination of the minimum Temperature temperature required for selective photothermal destruction of cancer cells using Antibody-Conjugated Immunotargeted gold nanoparticles". **Photochem. Photobiol.**, (2006) <https://passport.gatech.edu/>, 82 (2), 412-417.
10. Sanii, Laurie S.; El-Sayed, Mostafa A. "Effect of Crystallization on the Proton Pump Function of bR". **Israps Bulletin** (2006), 18 (1&2), 52-57.
11. El-Sayed, Ivan H.; Huang, Xiaohua; El-Sayed, Mostafa A. "Surface plasmon resonance scattering and absorption of anti-EGFR antibody conjugated gold nanoparticles in cancer diagnostics: Applications in oral cancer". **Nano Lett.** (2005), 5(5), 829-834.
12. Sanii, Laurie S.; Schill, Alex W.; Moran, Cristin E.; El-Sayed, Mostafa A. "The protonation-deprotonation kinetics of the protonated Schiff base in bicelle bacteriorhodopsin crystals". **Biophys. J.** (2005), 89(1), 444-451.
13. Sanii, Laurie S.; El-Sayed, Mostafa A. "Partial dehydration of the retinal binding pocket and proof for photochemical deprotonation of the retinal Schiff base in bicelle bacteriorhodopsin crystals". **Photochem. Photobiol.** (2005), 81, 1356-1360.
14. Garczarek, Florian; Wang, Jianping; El-Sayed, Mostafa A.; Gerwert, Klaus. "The assignment of the different infrared continuum absorbance changes observed in the 3000-1800-cm-1 region during the bacteriorhodopsin photocycle". **Biophys. J.** (2004), 87(4), 2676-2682.
15. Heyes, Colin D.; Reynolds, Keith B.; El-Sayed, Mostafa A. "Eu³⁺ binding to europium-regenerated bacteriorhodopsin upon delipidation and monomerization". **FEBS Lett.** (2004), 562(1-3), 207-210.

Statistical Mechanical and Multiscale Modeling of Surface Reaction Processes

Jim Evans (PI) and Da-Jiang Liu
Ames Laboratory – USDOE and Department of Mathematics,
Iowa State University, Ames, IA 50011
evans@ameslab.gov

PROGRAM SCOPE:

A major component of the Chemical Physics Program at Ames Laboratory focuses on the modeling of **heterogeneous catalysis and other complex reaction phenomena** at surfaces. This effort integrates *electronic structure analysis, non-equilibrium statistical mechanics and coarse-graining or multi-scale modeling*. The *electronic structure* component includes DFT-VASP analysis of chemisorption and reaction energetics on metal surfaces, as well as application of QM/MM methods in collaboration with **Mark Gordon** (PI) to treat adsorption and reaction phenomena on non-conducting surfaces. The *non-equilibrium statistical mechanics and related studies* of surface phenomena include Kinetic Monte Carlo (KMC) simulation of atomistic models, coarse-graining, and heterogeneous multiscale formulations. One aspect of this effort relates to heterogeneous catalysis on metal surfaces, and considers both reactions on extended crystalline surfaces (including connecting atomistic to mesoscale behavior) as well as nanoscale catalyst systems (exploring the role of fluctuations). Another aspect focuses on modeling of reaction processes on non-conducting surfaces and in mesoporous amorphous oxides. In addition, we are exploring cooperative behavior in general statistical mechanical models for chemical reactions which exhibit non-equilibrium phase transitions and critical phenomena.

RECENT PROGRESS:

CHEMISORPTION AND HETEROGENEOUS CATALYSIS ON METAL SURFACES

(i) Tuning the self-assembly and reactivity of metal nanostructures on surfaces: QSE. A fundamental and general goal in catalysis is to tune the structure of metal surfaces or nanostructures to enhance catalytic activity and selectivity. One strategy is to exploit “quantum size effects (QSE)” of electrons confined in metal overlayers. QSE can lead to selection of preferred film heights and also a strong dependence of surface electronic properties on film thickness. Following previous analysis of the thermodynamics and kinetics of nanostructure formation in specific systems [10,13], we have considered the utility of a general, simple and versatile Free Electron Gas Model in predicting various aspects of QSE for metal nanostructures. Comparison with DFT analysis reveals a considerable degree of success [21].

(iii) Multi-site lattice-gas modeling of CO-oxidation on Pd(100) and Rh(100). A long-standing goal for surface science has been to develop realistic atomistic models for “complete” catalytic reaction processes on metal surfaces. We have continued [22] development and application of realistic multi-site lattice-gas models and efficient KMC simulation algorithms to describe CO-oxidation and related reactions on unreconstructed metal surfaces [2,4-6,9]. Incorporation of multiple adsorption sites with distinct binding for CO (the multi-site feature of the model) is key to describe the relevant “reaction configurations” for CO₂ production in mixed reactant adlayers. Recent modeling elucidates the various reaction configurations which underlie the different CO₂ production peaks in Temperature Programmed Reaction spectra for Pd(100) and Rh(100) [22]. Current developments focus on improved estimation of species energetics,

more realistic and efficient treatment of surface diffusion, and of adsorption-desorption and LH reaction kinetics. Application to analysis of the kinetics of titration reactions is planned.

(iii) Interaction of sulfur with metal surfaces. Metal catalysts are often sensitive to sulfur (S) poisoning. In addition, sulfide formation can occur potentially either reducing or enhancing catalytic activity. Following our previous analysis of self-organized row-dot formation for S/Ag(111) [12], we are considering S/Ag(100) as well as detailed analysis of the effect of additives on metal surface dynamics (and specifically on accelerated nanostructure decay [19]).

FUNDAMENTAL PHENOMENA IN FAR-FROM-EQUILIBRIUM REACTION SYSTEMS

Our general statistical mechanical studies of non-linear reaction-diffusion systems focus on non-equilibrium phase transitions and associated metastability and critical phenomena. The goal is to develop understanding of these phenomena to a level comparable to that for equilibrium systems. Such problems are targeted in the *BESAC Science Grand Challenges* report under the heading *Cardinal Principles of Behavior beyond Equilibrium*, and require advancing from traditional mean-field kinetics models of reactions to atomistic statistical mechanical modeling.

We have thus continued [15,20] our previous analyses [7,8,11] of a statistical mechanical version of Schloegl's second model for autocatalysis and various generalizations of this model. These models display a discontinuous non-equilibrium "catalytic poisoning transition" between reactive and unreactive (extinct or poisoned) states. In dramatic contrast to equilibrium systems, we find a remarkable "generic two-phase coexistence", i.e., both reactive and extinct states are stable for a finite range of control parameter! However, despite this feature, metastability akin to equilibrium systems occurs upon sweeping through this transition. We have focused on analyzing associated nucleation phenomena (e.g., nucleation of the poisoned state from the metastable reactive state) borrowing a variety of concepts from, e.g., KPZ theory for non-equilibrium interfaces [15]. In addition, we have analyzed the nature of the non-equilibrium critical point at which the discontinuous transition disappears [20].

REACTIONS IN MESOPOROUS SYSTEMS AND ON NON-CONDUCTING SURFACES

(i) Catalytic polymerization in surface-functionalized mesoporous silica systems. A lattice model is developed to describe diffusion-mediated polymerization within mesopores, where reaction is enhanced at catalytic sites distributed interior to the pores [18]. Diffusive transport of polymers is one-dimensional, diffusion coefficients decreasing with polymer length. KMC simulation is used to analyze behavior in the "clogging regime" observed in experiments on the formation of PPB in Cu²⁺-functionalized MCM-41 silica by Victor Lin and coworkers. We characterize the growth in mean length of polymer, as well as the spatial and length distributions.

(ii) Self-organization of metal nanostructures during deposition. We continued analysis of the formation of single-atom thick atomic rows or "wires" via a "surface-polymerization reaction" during deposition of Group III metals on Si(100) [16,17]. We utilized both Gordon's QM/MM analysis of adatom binding and diffusion, and KMC simulation of atomistic lattice-gas models. The latter accounted for recently quantified reversibility in row formation for In, and also incorporated the effect of heterogeneous nucleation of rows at C-defects on the surface.

FUTURE PLANS:

CHEMISORPTION AND HETEROGENEOUS CATALYSIS ON METAL SURFACES

(i) Catalytic reactions on Rh, Pd, ... surfaces: higher pressures, nanoscale effects, etc. We will develop further realistic atomistic models for KMC simulation of catalytic reactions on

various metal (111) and (100) surfaces. Such models can elucidate reaction behavior in nanoscale systems (e.g., Field-emitter-tips and supported clusters) [5,6]. New efforts will explore higher-pressure catalysis noting strong evidence that oxide formation does not always dominate behavior, but that mass-transport limitations in the gas phase and non-isothermal effects must be considered. Our models will incorporate input from electronic structure studies.

(ii) Chemisorbed adlayer dynamics; interplay of steps with chemisorption and reaction.

We plan to explore ordering and dynamics in chemisorbed layers on metal surfaces probed by in-situ STM and PEEM: interaction of chalcogens with coinage metals (Thiel - Ames Lab), high-density O on Pt(111) (Imbihl); the dynamics of CO clusters in CO + H on Pd (Salmeron - LBL). We will also explore the interplay of steps with chemisorbed adlayers and with reaction processes. Experiments reveal a strong effect of chemisorbed structures on step fluctuations, e.g., for S/Ag(111) (Thiel - Ames Lab) and for NH₃ on Pt(111) (Imbihl et al). In-situ LEEM indicates that steps on Pt(111) are also strongly modified during NO reduction (Imbihl). We plan to develop models which couple chemisorbed layer dynamics/reaction kinetics to step dynamics.

(ii) Heterogeneous Coupled Lattice-Gas (HCLG) multi-scale modeling of surface reactions.

Our HCLG approach [22] uses continuous-time parallel KMC simulation to provide a realistic atomistic-level description of the reaction process at distinct macroscopic points distributed across a surface. These simulations are coupled accounting for chemical diffusion to describe mesoscale spatiotemporal behavior. Some multi-scale methods take large time-steps tracking just macro-variables (coverages). This assumes local equilibrium so that micro-states can be regenerated from macro-variables (“lifting”). Local equilibrium is often not satisfied in reaction systems, so we plan to develop refined “lifting” procedures accounting for local correlations.

FUNDAMENTAL PHENOMENA IN FAR-FROM-EQUILIBRIUM REACTION SYSTEMS

Analysis will continue of non-equilibrium phase transitions in a variety of statistical mechanical reaction-diffusion models. Issues of metastability and nucleation, and well as critical phenomena, are of fundamental interest for these non-equilibrium systems where the standard thermodynamic framework (i.e., involving a free energy) cannot be applied. The ramifications of anomalous behavior such as “generic two-phase coexistence” will be explored. We are extending these analyses to various ZGB-type surface reaction models, which although too simplistic to describe standard low-pressure reaction behavior, should provide a valuable paradigm for higher-pressure (and coverage) low-effective-surface-mobility fluctuation-dominated reaction systems.

REACTIONS IN MESOPOROUS SYSTEMS AND ON NON-CONDUCTING SURFACES

Additional investigations related to *catalysis in mesoporous systems* will explore both the atomic-scale structure and formation process of the mesoporous amorphous oxide catalyst material, and well as transport and kinetics for specific reactions. For the former, we are implementing a bond-switching Monte Carlo algorithm for a Continuous Random Network (CRN) model of the amorphous material. For the latter, we will analyze atomistic models for polymerization, both exploiting analytic random walk theory to elucidate the polymer length distribution for simple reactions, and applying KMC to treat complex multi-species reactions.

Our modeling of etching, CVD growth, and other *reactions on dynamic stepped surfaces* will focus on development of coarse-grained phase-field type formulations to describe evolution of surface morphology. This approach is versatile, allowing efficient integration of various models for the surface chemistry with a computationally efficient framework to describe complex surface morphologies. DFT and QM/MM will be utilized to provide reliable energetic input.

PUBLICATIONS SUPPORTED BY USDOE CHEM. SCIENCES FOR 2006-PRESENT:

- [1] *Morphological Evolution during Epitaxial Thin Film Growth: Formation of 2D Islands and 3D Mounds*, J.W. Evans, P.A. Thiel, M.C. Bartelt, *Surface Science Reports*, **61**, 1-128 (2006).
- [2] *Atomistic Lattice-Gas Modeling of CO-oxidation on Pd(100): Temperature-Programmed Spectroscopy and Steady-State Behavior*, D.-J. Liu, J.W. Evans, *J. Chem. Phys.* **124**, 154705 (2006).
- [3] *Monotonically Decreasing Size Distributions for Ga Rows on Si(100): Reply to Comment*, M.A. Albao, M. Evans, J. Nogami, D. Zorn, M.S. Gordon, J.W. Evans, *Phys. Rev. B* **74**, 037402 (2006).
- [4] *Chemical Diffusion in Mixed CO+O Adlayers and Reaction Front Propagation in CO-oxidation on Pd(100)*, D.-J. Liu, J.W. Evans, *J. Chem. Phys.* **125**, 054709 (2006).
- [5] *Fronts and Fluctuations in a Tailored Model for CO-oxidation on Unreconstructed Metal(100) Surfaces*, D.-J. Liu, J.W. Evans, *J. Phys.: Cond. Matt.*, **19**, 065129 (2007).
- [6] *Fluctuations and Patterns in Nanoscale Surface Reaction Systems: Influence of Reactant Phase Separation during CO-oxidation*, D.-J. Liu, J.W. Evans, *Phys. Rev. B* **75**, 073401 (2007).
- [7] *Quadratic Contact Process (Schoegl's Model for Autocatalysis): Phase Separation with Interface-Orientation-Dependent Equistability*, D.-J. Liu, X. Guo, J.W. Evans, *Phys. Rev. Lett.*, **98**, 050601 (2007).
- [8] *Generic Two-Phase Coexistence, Relaxation, Kinetics, and Interface Propagation in the Quadratic Contact Process: Simulation Studies*, X. Guo, D.-J. Liu, J.W. Evans, *Phys. Rev. E.*, **75**, 061129 (2007).
- [9] *CO-oxidation on Rh(100): Multi-site LG Modeling*, D.-J. Liu, *J. Phys. Chem. C* **111**, 14698 (2007).
- [10] *Scanning Tunneling Microscopy and Density Functional Theory Study of Initial Bilayer Growth of Ag Films on NiAl(110)*, B. Unal, F. Qin, Y. Han, D.-J. Liu, et al., *Phys. Rev. B*, **76**, 195410 (2007).
- [11] *Generic Two-Phase Coexistence, Relaxation, Kinetics, and Interface Propagation in the Quadratic Contact Process: Analytic Studies*, X. Guo, J.W. Evans, D.-J. Liu, *Physica A*, **387**, 177 (2008).
- [12] *Novel Self-Organized Structure of a Ag-S Complex on the Ag(111) Surface below Room Temperature*, M. Shen, D.-J. Liu, C.J. Jenks, P.A. Thiel, *J. Phys. Chem. C* **112**, 4281 (2008).
- [13] *Quantum Stabilities and Growth Modes of Thin Metal Films: Unsupported and NiAl-supported Ag Films*, Y. Han, J.W. Evans, D.-J. Liu, *Surface Science*, **602**, 2532 (2008).
- [14] *Kinetic Monte Carlo simulation atomistic models for oxide island formation and step pinning during etching by O of vicinal Si(100)*, M. Albao, F.-C. Chuang, J.W. Evans, *Thin Solid Films*, **517**, 1949 (2009).
- [15] *Schloegl's Second Model for Autocatalysis with Particle Diffusion: Lattice-Gas Realization with Generic Two-Phase Coexistence*, X. Guo, D.-J. Liu, J.W. Evans, *J. Chem. Phys.* **130**, 074106 (2009).
- [16] *Binding and diffusion of Al adatoms & dimers on the Si(100)-2x1 surface: hybrid QM/MM embedded cluster study*, D. Zorn, M. Albao, J.W. Evans, M.S. Gordon, *J. Phys. Chem. C* **113**, 7277 (2009).
- [17] *Kinetic Monte Carlo study on the role of defects and detachment of formation and growth of In chains on Si(100)*, M. Albao, J.W. Evans, F.-C. Chuang, *J. Phys.: Cond. Matter*, in press (2009).
- [18] *Statistical mechanical modeling of catalytic polymerization in surface functionalized mesoporous materials*, D.-J. Liu, H.-T. Chen, Victor S.-Y. Lin, J.W. Evans, *Phys. Rev. E* **80**, 011801 (2009).
- [19] *Coarsening of two-dimensional nanoclusters on metal surfaces*, P.A. Thiel, M. Shen, D.-J. Liu, J.W. Evans, *J. Phys. Chem. C*, **113**, 5047-5067 (2009). *Invited Centennial Feature Article*
- [20] *Non-equilibrium criticality in Schloegl's autocatalysis model*, D.-J. Liu, *J. Stat. Phys.* **135**, 77 (2009).
- [21] *Quantum size effects in metal nanofilms: Comparison of an electron-gas model and DFT theory calculations*, Y. Han, D.-J. Liu, *Phys. Rev. B*, in press (2009).
- [22] *Atomistic & multiscale modeling of CO-oxidation on Pd(100) & Rh(100): From nanoscale fluctuations to mesoscale reaction fronts*, D.-J. Liu, J.W. Evans, *Surf. Sci.* **603**, 1706 (2009). *Ertl Nobel Special Issue*

Liquid and Chemical Dynamics in Nanoscopic Environments (DE-FG03-84ER13251)

Michael D. Fayer
Department of Chemistry, Stanford University, Stanford, CA 94305
fayer@stanford.edu

The research group of Michael D. Fayer is investigating topics directed toward understanding how nanoscopic size, interfaces, and nanoconfinement influence the dynamics of water and processes that occur in nanoconfined water, for example, proton transport dynamics. The research is focused on nanoscopic water and water at interfaces because of water's importance in a wide range of chemical, materials, biological processes and technological devices relevant to energy applications. In many systems, water is not found in its bulk form. Our recent work was the first to use ultrafast infrared methods to directly examine the dynamics of nanoscopic water, that is, water confined on a length scale of a few nanometers.

Water can make up to four hydrogen bonds and forms an extended hydrogen bonding network. The network structure is constantly undergoing changes on timescales ranging from tens of femtoseconds to picoseconds. Water's ability to reorganize its hydrogen bonding network and thereby solvate charges and other chemical species gives it its unique importance. The dynamics of water are strongly influenced by charged solutes, for example, salt solutions. When water is confined on nanoscopic distance scales, its hydrogen bond network dynamics change, and these changes influence processes, such as proton transport, that occur in nanoscopic water. To understand the role of nanoconfinement and interfaces on the dynamics and properties of water, a variety of materials are being investigated. These include ionic and non-ionic reverse micelles, Nafion a polyelectrolyte fuel cell membrane, phospholipid multibilayer, lamellar structures, and concentrated salt solutions. The research addresses how such physical constraints on systems influence chemical and physical processes. Proton transport is an important focus particularly in fuel cell membranes. Photoinduced electron transfer has also been investigated.

During the past year, the Fayer group has made major advances in understanding the dynamics of water as it is influenced by charged solutes, at interfaces, and in nanoconfinement, as well as proton transfer in and the properties of the water nanochannels of protonated Nafion fuel cell membranes.

A new method, ultrafast 2D IR vibrational echo chemical exchange spectroscopy was applied to the problem of hydrogen bond switching between a water molecule bonded to an ion and water bonded to another water. Water with concentrated NaBF_4 was studied. In the experiments, the time dependent appearance of off-diagonal peaks in the 2D spectrum permitted a direct measurement of the ion-water – water-water hydrogen bond switching. The time for water to go from being bonded to a BF_4^- to being bonded to another water is 7 ps. The comparable time for hydrogen bond switching in bulk water is 2 ps. This result is in contrast to indirect methods that have suggested that water in the presence of ions may have a reduction of as much as 100 in the time scale for hydrogen bond dynamics.

Proton transfer in protonated Nafion fuel cell membranes was studied using several pyrene derivative photoacids. Proton transfer in the center of the Nafion nanoscopic water channels was probed with the highly charged photoacid HPTS. At high hydration levels, both the time-integrated fluorescence spectrum and the fluorescence kinetics of HPTS permitted the determination of hydronium concentration of the interior of the water channels in Nafion. The proton transfer kinetics of HPTS in protonated Nafion at maximum hydration are identical to the kinetics displayed by HPTS in a 0.5M HCl solution. This is a measurement of the nanoscopic

pH. Previously it has been thought that the interior of protonated Nafion behaves like a superacid. The hydronium concentration near the water interface in Nafion using the chromophore rhodamine-6G was found to be 1.4 M. Thus the proton concentration at the interface is ~3 times greater than in the center of the nanochannel. Excited state proton transfer was followed in the nonpolar side chain regions of Nafion with the photoacid HPTA. Excited state proton transfer of HPTA is possible in protonated Nafion only at the highest hydration level due to a relatively high local pH.

The orientational dynamics of water molecules at the interface of large Aerosol-OT (AOT) reverse micelles were investigated using ultrafast infrared polarization and frequency selective pump-probe spectroscopy of the OD stretch of dilute HOD in H₂O. In large reverse micelles (~9 nm diameter or larger), a significant amount of the nanoscopic water is sufficiently distant from the interface that it displays bulk-like characteristics. However, some water molecules interact with the interface and have vibrational absorption spectra and dynamics distinct from bulk water. The different characteristics of these interfacial waters allowed their contribution to the data to be separated from the bulk. A two component model was developed that simultaneously describes the population relaxation and orientational dynamics of the OD stretch in the spectral region of the interfacial water. The model provided a consistent description of both observables and demonstrated that water interacting with the interface has slower vibrational relaxation and orientational dynamics. The orientational relaxation of interfacial water molecules occurs in 18 ± 3 ps in contrast to the bulk water value of 2.6 ps. These experiments are the first direct measurements of the hydrogen bond dynamics of water at an interface. In addition, AOT lamellar structures (2D slabs of water) were studied. It was found that the water hydrogen bond dynamics at the flat lamellar interface are the same as those at the interface of large reverse micelles.

In the large reverse micelles, the dynamics of water are separable into two ensembles: slow interfacial water and bulk-like core water. However, as the reverse micelle size decreases, the slowing effect of the interface and the collective nature of water reorientation begin to slow the dynamics of the core water molecules. In the smallest reverse micelles, these effects dominate and all water molecules have the same long time reorientational dynamics. To understand and characterize the transition in the water dynamics from two ensembles to collective reorientation, experiments were conducted on the complete range of reverse micelle sizes from a diameter of 1.6 nm to a diameter of 20 nm. The crossover between two ensemble and collective reorientation occurs near a reverse micelle diameter of 4 nm. Below this size, the small number of confined water molecules and structural changes in the reverse micelle interface lead to homogeneous long time reorientation. The intermediate regime (~4 nm) was also found in which there is a distinct core, but its dynamics are slower than the bulk water dynamics seen in the cores of large reverse micelles.

The orientational dynamics of water molecules at a neutral surfactant reverse micelle interface were also measured and the results were compared to orientational relaxation of water interacting with an ionic surfactant interfaces discussed above. Orientational relaxation of water is a result of the hydrogen bond network rearrangement, so the comparison provides insights into the influence of a neutral vs. ionic interface on hydrogen bond dynamics. Measurements were made and analyzed for large reverse micelles (water nanopool 9 nm diameter) made from the nonionic surfactant Igepal CO-520. The results were compared to those from the same size reverse micelles formed with the ionic surfactant AOT discussed above. The results demonstrated that the orientational relaxation times for interfacial water molecules in the two types of reverse micelles are very similar (13 ps for Igepal and 18 ps for AOT) and are significantly slower than that of bulk water (2.6 ps). The comparison of water orientational relaxation at neutral and ionic interfaces shows that the presence of an interface plays the

dominant role in determining the hydrogen bond dynamics while the chemical nature of the interface plays a secondary role.

Publication from DOE Sponsored Research 2005 – present

Nanoconfined, Interfacial, Salt Solutions, and Bulk Water

- (1) “Dynamics of Water Confined on a Nanometer Length Scale in Reverse Micelles: Ultrafast Infrared Vibrational Echo Spectroscopy,” Howe-Siang Tan, Ivan R. Piletic, Ruth E. Riter, Nancy E. Levinger and M. D. Fayer, *Phys. Rev. Lett.* **94**, 057405(4) (2005).
- (2) “Orientational Dynamics of Water Confined on a Nanometer Length Scale in Reverse Micelles,” Howe-Siang Tan, Ivan R. Piletic, and M. D. Fayer, *J. Chem. Phys.* **122**, 174501 (2005).
- (3) “The Dynamics of Nanoscopic Water: Vibrational Echo and IR Pump-probe Studies of Reverse Micelles,” Ivan R. Piletic, Howe-Siang Tan, and M. D. Fayer, *J. Phys. Chem. B* **109**, 21273-21284 (2005).
- (4) “Testing the Core/Shell Model of Nanoconfined Water in Reverse Micelles Using Linear and Nonlinear IR Spectroscopy,” Ivan R. Piletic, David E. Moilanen, D. B. Spry, and Nancy E. Levinger, M. D. Fayer, *J. Phys. Chem. A* **110**, 4985-4999 (2006).
- (5) “Confinement or Properties of the Interface? Dynamics of Nanoscopic Water in Reverse Micelles,” David E. Moilanen, David B. Spry, Nancy E. Levinger, and M. D. Fayer, *J. Am. Chem. Soc.* **129**, 14311-14318 (2007).
- (6) “Water Dynamics – The Effects of Ions and Nanoconfinement,” Sungnam Park, David E. Moilanen, and M. D. Fayer *J. Phys. Chem. B* **112**, 5279-5290 (2008).
- (7) “Tracking Water’s Response to Structural Changes in Nafion Membranes,” David E. Moilanen, Ivan R. Piletic, and M. D. Fayer, *J. Phys. Chem. A* **110**, 9084-9088 (2006).
- (8) “Water Dynamics in Nafion Fuel Cell Membranes: the Effects of Confinement and Structural Changes on the Hydrogen Bonding Network,” David E. Moilanen, Ivan R. Piletic, Michael D. Fayer *J. Phys. Chem. C* **111**, 8884-8891, (2007).
- (9) “Water at the Surfaces of Aligned Phospholipid Multi-Bilayer Model Membranes Probed with Ultrafast Vibrational Spectroscopy,” Wei Zhao, David E. Moilanen, Emily E. Fenn, and M. D. Fayer *J. Am. Chem. Soc.* **130**, 13927-13937 (2008).
- (10) “Hydrogen Bond Dynamics in Aqueous NaBr Solutions,” Sungnam Park and M. D. Fayer, *Proc. Nat. Acad. Sci. U.S.A.* **104**, 16731-16738 (2007).
- (11) “Are Water Simulation Models Consistent With Steady-State and Ultrafast Vibrational Spectroscopy Experiments?” J. R. Schmidt, A. Tokmakoff, M. D. Fayer, and J. L. Skinner *Chem. Phys.* **341**, 143-157 (2007).
- (12) “Water Inertial Reorientation: Hydrogen Bond Strength and the Angular Potential,” David E. Moilanen, Emily E. Fenn, Yu-Shan Lin, J. L. Skinner, B. Bagchi, and M. D. Fayer *Proc. Nat. Acad. U.S.A.* **105**, 5295-5300 (2008).
- (13) “Ultrafast 2D-IR Vibrational Echo Spectroscopy: A Probe of Molecular Dynamics,” Sungnam Park, Kyungwon Kwak, and M. D. Fayer *Laser Phys. Lett.* **4**, 704-718 (2007).
- (14) “Polarization Selective Spectroscopy Experiments: Methodology and Pitfalls,” Howe-Siang Tan, Ivan R. Piletic and M. D. Fayer, *J.O.S.A. B* **22**, 2009-2017 (2005).
- (15) “Ion-Water Hydrogen Bond Switching Observed with 2D IR Vibrational Echo Chemical Exchange Spectroscopy,” David E. Moilanen, Daryl Wong, Daniel E. Rosenfeld, Emily E. Fenn, and M. D. Fayer *Proc. Nat. Acad. Sci. U.S.A.* **106**, 375-380 (2009).
- (16) “Water Dynamics and Interactions in Water-Polyether Binary Mixtures,” Emily E. Fenn, David E. Moilanen, Nancy E. Levinger, and Michael D. Fayer *J. Am. Chem. Soc.* **131**, 5530-5539 (2009).
- (17) “Water Dynamics at the Interface in AOT Reverse Micelles,” David E. Moilanen, Emily E. Fenn, Daryl Wong and M.D. Fayer *J. Phys. Chem. B* **113**, 8560–8568 (2009).

- (18) "Geometry and Nanolength Scales vs. Interface Interactions: Water Dynamics in AOT Lamellar Structures and Reverse Micelles," David E. Moilanen, Emily E. Fenn, Daryl Wong, and M.D. Fayer J. Am. Chem. Soc. 131, 8318-8328 (2009).
- (19) "Water Dynamics in Salt Solutions Studied with Ultrafast 2D IR Vibrational Echo Spectroscopy," M. D. Fayer, David E. Moilanen, Daryl Wong, Daniel E. Rosenfeld, Emily E. Fenn, and Sunnam Park Acc. of Chem. Res. 42, 1210-1219 (2009).
- (20) "Water Dynamics in Large and Small Reverse Micelles: From Two Ensembles to Collective Behavior," David E. Moilanen, Emily E. Fenn, Daryl Wong, and Michael D. Fayer J. Chem. Phys. 131, 014704 (2009).
- (21) "Water Dynamics at Neutral and Ionic Interfaces in Reverse Micelles," Emily E. Fenn, Daryl B. Wong, and M.D. Fayer Proc. Nat. Acad. Sci. U.S.A. 106, 15243-15248 (2009).
- (22) "Solvent Control of the Soft Angular Potential in Hydroxyl- π Hydrogen Bonds: Inertial Orientational Dynamics," Daniel E. Rosenfeld, Zsolt Gengeliczki, and M. D. Fayer J. Phys. Chem. B ASAP (2009).

Proton Transfer and Photoacids in Solution and Nanoconfinement

- (23) "Identification and Properties of the 1L_a and 1L_b States of Pyranine (HPTS)," D. B. Spry, A. Goun, C. B. Bell III, and M. D. Fayer, J. Chem. Phys. 125, 144514-(12) (2006).
- (24) "The Deprotonation Dynamics and Stokes Shift of Pyranine (HPTS)," D. B. Spry, A. Goun, and M. D. Fayer J. Phys. Chem. A 111 230-237 (2007).
- (25) "Proton Transport and the Water Environment in Nafion Fuel Cell Membranes and AOT Reverse Micelles," D. B. Spry, A. Goun, K. Glusac, David E. Moilanen, W. Childs, and M. D. Fayer J. Am. Chem. Soc. 129 8122-8130 (2007).
- (26) "Water Dynamics and Proton Transfer in Nafion Fuel Cell Membranes," David E. Moilanen, D.B. Spry, and M. D. Fayer Langmuir 24, 3690-3698 (2007).
- (27) "Observation of Slow Charge Redistribution Preceding Excited State Proton Transfer," D. B. Spry and M. D. Fayer J. Chem. Phys. 127, 204501 (2007).
- (28) "Charge Redistribution and Photoacidity: Neutral vs. Cationic Photoacids," D. B. Spry and M. D. Fayer J. Chem. Phys. 128, 084508 (2008).
- (29) "Charge Transfer in Photoacids Observed by Stark Spectroscopy," Lisa N. Silverman, D. B. Spry, Steven G. Boxer and M. D. Fayer J. Phys. Chem. A 112, 10244-10249 (2008).
- (30) "Proton Transfer and Proton Concentrations in Protonated Nafion Fuel Cell Membranes," D. B. Spry and M. D. Fayer J. Chem. Phys. B 113, 10210-10221 (2009).

Electron Transfer in Solution and Nanoconfinement

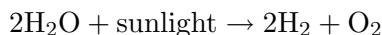
- (31) "Photoinduced Electron Transfer and Geminate Recombination in Liquids on Short Time Scales: Experiments and Theory," Alexei Goun, Ksenija Glusac, and M. D. Fayer, J. Chem. Phys. 124, 084504(11) (2006).
- (32) "Photoinduced Electron Transfer and Geminate Recombination in the Head Group Region of Micelles," Ksenija Glusac, Alexei Goun, and M. D. Fayer, J. Chem. Phys. 125, 054712(12 pages) (2006).
- (33) "Photoinduced Electron Transfer in the Head Group Region of Sodium Dodecyl Sulfate Micelles," J. Nanda, P. K. Behera, H. L. Tavernier and M. D. Fayer, J. Lum. 115, 138-146 (2005).

Optimizing Interfacial Charge Transfer in Photocatalytic Water Splitting Devices

Maria V. Fernandez-Serra

1 Program Scope

The development of a means of efficiently and economically harnessing the energy of the sun is the technological challenge of our time. And the solution, in principle, is quite simple:



Sunlight converts water into hydrogen fuel, with oxygen the only byproduct. The surfaces of semiconductor/metal nanostructures with appropriately-tuned electro-chemical properties provide promising candidates for catalysts of this process. The overall water splitting reaction requires 6 eV of input energy, which can be provided by four solar photons. The energy, $h\nu$, of photons in the visible is between 1.8 and 3.1 eV. A semiconductor with a bandgap tuned near the minimum of this range could absorb the four photons to excite four electron-hole pairs. GaN/ZnO alloy semiconductors have been shown to have desirable properties [1, 2], including a surface at which water dissociates [3]: $2\text{H}_2\text{O} \rightarrow 2\text{H}^+ + 2\text{OH}^-$. If the four holes make it to the water-immersed semiconductor surface, they can take part in the oxidation of oxygen in the water: $4\text{h}^+ + 2\text{OH}^- \rightarrow 2\text{H}^+ + \text{O}_2$. Metallic nanoparticles deposited on the semiconductor surface act as sinks for electrons. And if the four electrons are successfully delivered across the semiconductor-metal and metal-water interfaces, they can take part in the reduction of the H^+ to hydrogen gas: $4\text{e}^- + 4\text{H}^+ \rightarrow 2\text{H}_2$. The hydrogen can then be stored and the energy extracted in the reverse reaction



which yields an entirely carbon-free solar energy cycle.

The problem, of course, is that this process is poorly understood and rather inefficient in current samples. Improving matters will require enhancements in a number of electrical and chemical properties, all in the same device. At present most efforts have focused on improving the catalytic activity of the surfaces. But since incident photons penetrate to a significant depth before being absorbed, it is also essential to optimize the fraction of electrons and holes that are delivered from photon to water.

The photocatalytic activity of a given semiconductor(catalyst)/metal(co-catalyst) complex can be approximated through the rate of photocatalytic reaction, r , which can be expressed in the following oversimplified form:

$$r = \frac{I\Phi k_{\text{red}}C_{\text{red}}}{k_r} \quad (1)$$

where I is the incident light flux, Φ is the photoabsorption efficiency, k_{red} is the rate constant of reaction of electrons and holes with the surface adsorbed active reactants, C_{red} is the surface concentration of the active reactants, and k_r is the rate constant of electron-hole recombination. Hidden behind the simplicity of this equation are complex physical and chemical phenomena of difficult direct experimental characterization. In particular, while it might be possible to estimate I , Φ , and C_{red} by photometry, spectrometry, and adsorption techniques, the ratio k_{red}/k_r can only be measured from the actual reaction rate (or quantum efficiency) [4]. In addition to the adequacy of the catalyst band gap, the crystallinity of the samples has been shown to be a requirement for improved quantum yields. It is clear that the presence of defects in the samples can be responsible

for reduced carrier mobility or concentration, either as sources of resonant backscattering or as centers for electron-hole recombination. It is also well known that for many catalysts, and in particular for GaN:ZnO, the activity is strongly dependent on the co-catalyst material. This dependence must be due to the different Schottky barriers formed at the semiconductor-metal and metal-water interfaces [4,5].

2 Recent Progress: Water/Metal interface

We have performed AIMD simulations of 96 molecules of water confined between two Pd< 111 > interfaces [6]. We observe that metal surface states are strongly affected by the liquid water at the interface. Our detailed studies of the metal/water interface show that the role played by the XC potential is decisive on the organization of water at the metal interface and the electronic structure of the metal is strongly affected by this. Besides, it is also evident that much longer AIMD simulations are needed to see the equilibrium preferential order of the liquid at the interface. The water molecules chemisorbed at the metal surface affect the electronic structure of the metal slab, which can be divided into bulk and surface states. The chemisorption of the water molecules implies an electron (charge) transfer between the two systems [7] the direction of this transfer being dependent on the chemisorption geometry of the molecules. When water molecules are chemisorbed parallel to the surface charge donation from the oxygen lone pair orbitals toward the metal surface states occurs [7]. When hydrogen atoms point toward the surface the charge transfer happens in the opposite direction. Even if we are using localized atomic orbitals as basis sets, it has been shown [8] that when extra layers of “ghost” metal atoms at the surface are systematically added to the calculations, the results are as accurate as plane waves results. Figure 1 shows a snapshot of our Pd/water system. ninety six molecules of water are embedded by periodic repetitions of a Pd< 111 > slab with 4 atomic layers of thickness. The electrostatic potential across the interface is also shown in the figure. No bias potential has been applied to the two Pd slabs, the calculation is done for a neutral system.

Two competing ordering structures of the water molecules on the two metal surfaces occur. One of the two structures has an average dipole pointing toward the metal surface and the other one has an average dipole pointing outward. The potential inside the water region is not constant in average as should happen in pure liquid water, but instead has a slope of 0.2 eV/. This behavior resembles the polarization of a ferroelectric thin film [9]. Indeed, it is possible to apply a model [9] to compute the polarization of the system, assuming some parameters (screening length of Pd, dielectric constant of water). The overall polarization will be the balance between the unexpected spontaneous polarization and the field induced polarization. We have calculated [6] that the total polarization is 0.2 C/m². This is a large number, comparable to some of the most common ferroelectric materials.

3 Future plans

We are currently performing molecular dynamics simulations of water at the GaN <10-10> non polar surface. It is our plan to artificially induce an electron-hole excitation (by a forced occupation of the LUMO state and half emptying the HOMO state) in the molecular dynamics simulation. The electronic structure of this system will be studied as a function of different defect concentrations at the surface. We will also study the electrostatic potential at the water/GaN interface for this non polar surface and at the <0001> polar surface. In parallel we will Time-

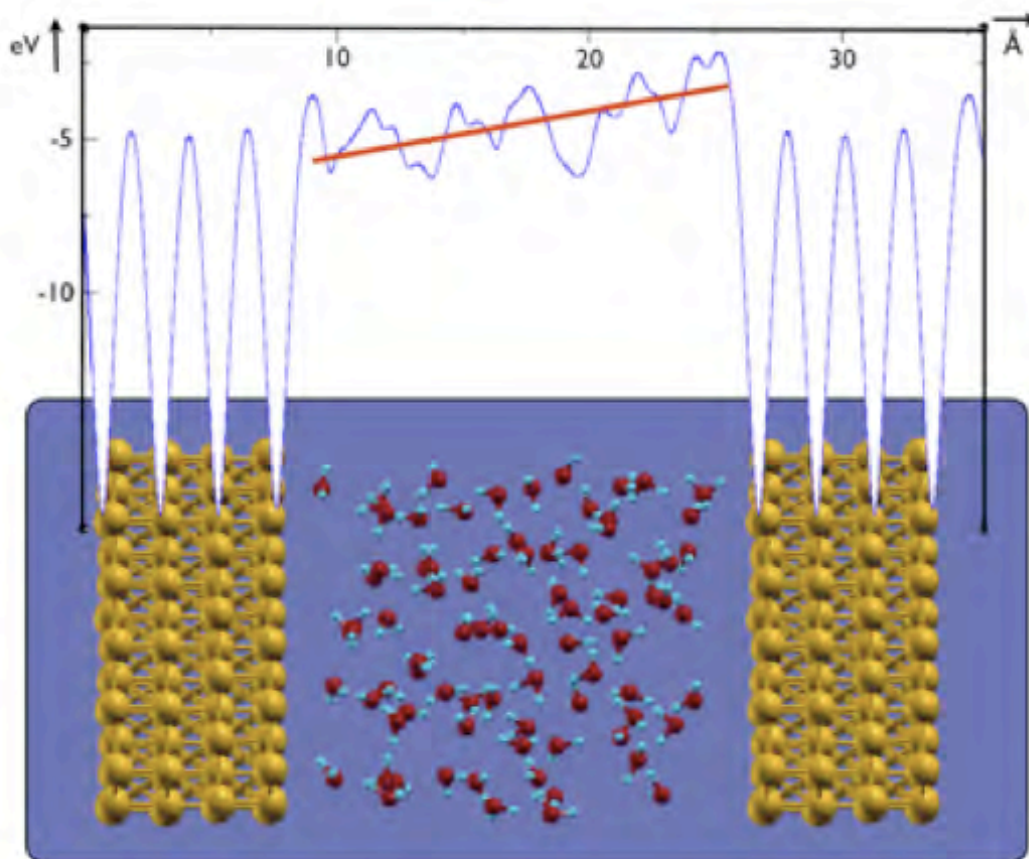


Figure 1: *Results from our AIMD simulations that show the spontaneous electrostatic potential created at the Pd-water-Pd interface.*

Dependent Density functional theory studies of an electron-hole pair excitation in pure GaN with different defects and in the presence of different surfaces.

We will also start implementing the development part of our project. The use of atomic orbitals with finite range as a basis to expand the Kohn-Sham wave functions in DFT allows the building of both the Hamiltonian and Overlap matrices in $O(N)$ operations. The localization of the molecular orbitals of the water molecule in the gas phase offers an excellent intermediate alternative solution between the full $O(N)$ solution and the $O(N^3)$ one. The key to achieve linear scaling is the locality of the wave functions. Water molecular orbitals (MOs) can be used as “support” orbitals to build the Hamiltonian and Overlap matrices. Different ways of calculating these molecular orbitals exist. They could simply be frozen molecular orbitals obtained for the optimized geometry of the molecule in the gas phase. This solution would require a large number of these orbitals to achieve results as converged as the original DZP basis. A more flexible alternative is that of obtaining the MOs of each water molecule at each AIMD step. The total cost of this operation would be that of M total energy calculations of one single water molecule (M being the total number of molecules) plus one calculation of the whole system with a much reduced basis set.

References

- [1] K. Maeda, T. Takata, M. Hara, N. Saito, Y. Inoue, H. Kobayashi, and K. Domen. Gallium zinc oxide solid solution as a photocatalyst for visible-light-driven overall water splitting. *J. Am. Chem. Soc.*, 127:8286, 2005.
- [2] K. Maeda, K. Tamamura, T. Takata, N. Saito, Y. Inoue, and K. Domen. Photocatalyst releasing hydrogen from water. *Nature*, 440:295, 2006.
- [3] Xiao Shen, Philip B. Allen, Mark S. Hybertsen, and James T. Muckerman. Water adsorption on the gallium (1010) nonpolar surface. *J. Phys. Chem. C*, 113(9):3365–3368, 2009.
- [4] B. Ohtani. Preparing articles on photocatalysis—beyond the illusions, misconceptions, and speculation. *Chemistry Letters*, 37:217, 2008.
- [5] F. E. Osterloh. Inorganic materials as catalysts for photochemical splitting of water. *Chem. Mater.*, 20:35–40, 2008.
- [6] Adrien Poissier and M.V. Fernandez-Serra. Spontaneous polarization of water confined by two palladium(111) surfaces. *In preparation*.
- [7] A. Michaelides, V. A. Ranea, P. L. de Andres, and D. A. King. General model for water monomer adsorption on close-packed transition and noble metal surfaces. *Phys. Rev. Lett.*, 90(21):216102, May 2003.
- [8] Sandra García-Gil, Alberto García, Nicolás Lorente, and Pablo Ordejón. Optimal strictly localized basis sets for noble metal surfaces. *Physical Review B (Condensed Matter and Materials Physics)*, 79(7):075441, 2009.
- [9] M. Dawber, K. M. Rabe, and J. F. Scott. Physics of thin-film ferroelectric oxides. *Reviews of Modern Physics*, 77(4):1083, 2005.

Chemical Kinetics and Dynamics at Interfaces
Fundamentals of Solvation under Extreme Conditions

John L. Fulton
Chemical and Materials Sciences Division
Pacific Northwest National Laboratory
902 Battelle Blvd., Mail Stop K2-57
Richland, WA 99354
john.fulton@pnl.gov

Program Scope

The primary objective of this project is to describe, on a molecular level, the solvent/solute structure and dynamics in fluids such as water under extremely non-ideal conditions. The scope of studies includes solute–solvent interactions, clustering, ion-pair formation, and hydrogen bonding occurring under extremes of temperature, concentration and pH. The effort entails the use of spectroscopic techniques such as x-ray absorption fine structure (XAFS) spectroscopy, coupled with theoretical methods such as molecular dynamics (MD-XAFS), and electronic structure calculations in order to test and refine structural models of these systems. In total, these methods allow for a comprehensive assessment of solvation and the chemical state of an ion or solute under any condition. The research is answering major scientific questions in areas related to energy-efficient separations, hydrogen storage and sustainable nuclear energy (aqueous ion chemistry and corrosion). This program provides the structural information that is the scientific basis for the chemical thermodynamic data and models in these systems under non-ideal conditions.

Recent Progress

The hydration of ions and the formation of contact ion pairs underlie processes in a large number of aqueous systems. Direct experimental measurement of ion-ion interactions decoupled from those of ion-water are non-existent from neutron and x-ray diffraction studies and have only recently been reported for XAFS studies. X-ray absorption fine structure (XAFS) spectroscopy, coupled with molecular dynamics (MD-XAFS) are being used to test and refine structural models of these systems. As an example⁴, a clearer picture of hydration of common ions such as Cl⁻, K⁺, and Ca²⁺ has emerged from XAFS that allows one to measure the structure in the first solvation shell about ions including precise measurements of the atomic distances, coordination numbers and oxidation states.

We have developed and demonstrated a new method called symmetry-dependent multiple scattering (SDMS) that can be derived from the K- and L-edge x-ray absorption fine structure (XAFS) spectra. This method provides a much clearer picture of the symmetry of the hydration shell about ions. In this method, different multiple scattering geometries lead to different sets of photoelectron scattering amplitudes and phase shifts for the K-edge (s-electrons) versus the L₂-edge (2p-electrons). This is in contrast to the common expectation that the electronic wavefunction final states for K or L₁ versus L₂ or L₃ edge XAFS only gives rise to a simple π shift factor and thus represent redundant measurements of structure. We discovered that these

scattering characteristics provide two, completely independent measurements of the first shell symmetry. Thus a much clearer picture of the hydration symmetry details can be obtained.

We have used this method successfully for the study of the hydration structure about Ag^+ .⁷ The conventional view is of the pure tetrahedral structure, however this does not match the multiple scattering features. A structure having collinear and 90° O-Ag-O bonds is required to fit the K- and L_2 - edge spectra. Thus for this 2nd row transition metal, the site-specific bonding of water to hybridized valence orbitals of the Ag^+ play a leading role in the hydration structure in contrast to the structure for Na^+ wherein water interactions are purely ionic and there is no local symmetry. For Ag^+ , a distorted octahedral (2+4) model best matches the multiple scattering features, the fitted bond distances, bond disorder and coordination numbers.

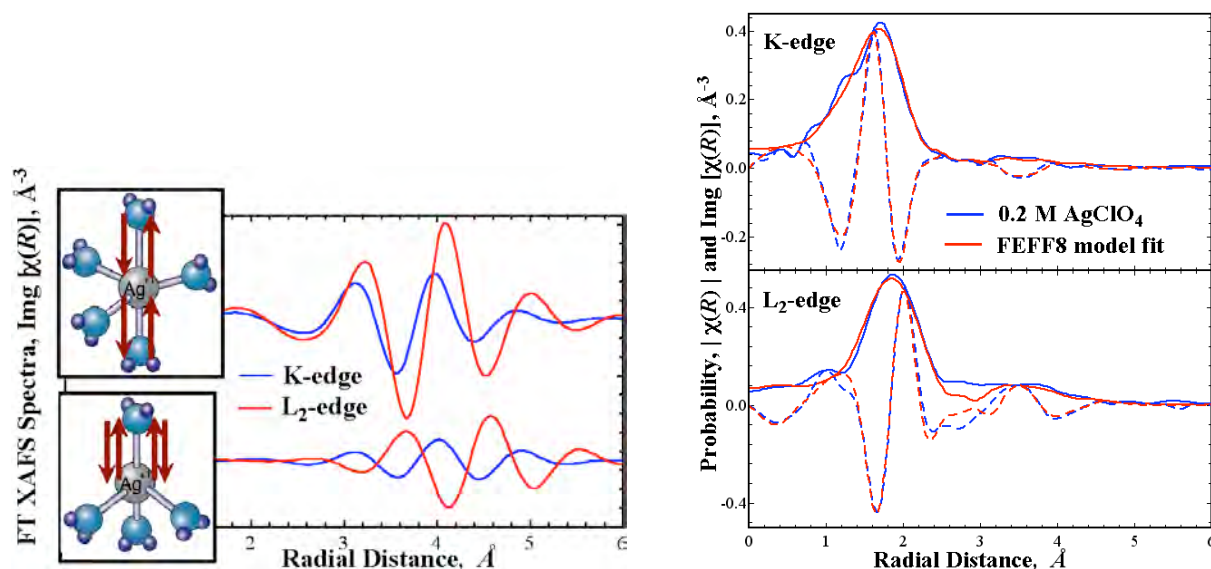


Figure 2. Symmetry-dependent multiple scattering evaluation of Ag^+ hydration structure. Comparison of various $\text{Im}[\tilde{\chi}(R)]$ scattering spectra generated from FEFF8 for aqueous Ag^+ (left). XAFS k^2 -weighted $\chi(k)$ and $\text{Im}[\tilde{\chi}(R)]$ plots for hydrated Ag^+ and the fitted lines for a distorted octahedral (2+4) model (right).

The K- and L_2 - edge spectra can also be used as a rigorous test of a new generation of molecular simulations since the experimental results impose requirements for highly specific symmetries, bond distances and disorder. For Ag^+ we calculated an EXAFS spectrum from an ensemble of molecular configurations generated from a DFT molecular dynamics simulation.⁷ This MD-XAFS method⁴ obviates the need to compare poorly defined entities such as coordination or solvation numbers but rather involves the direct comparison of experimentally measured and simulated spectral quantities. The advantage of MD-EXAFS is that all details of the ion-water structure inherent in the simulations are represented in the MD-EXAFS spectrum. Not only does this lead to a stringent test of the structure of the simulation but it also can provide key insights to the structure of the experimental system. The DFT method generates multiple scattering signals that reproduce some of the features of the experimental Ag^+ spectra, however, the multiple scattering amplitudes are lower than the experimental values. This suggests that the

first-shell water is even more symmetrically oriented about Ag^+ than predicted by the DFT method (PBE/MOLOPT).⁷

Future Plans

We are starting to explore the structure of hydronium (H_3O^+) contact-ion pair formation with halide ions (Cl^- , Br^- , and I^-) in concentrated acids using XAFS. XAFS detects the Cl-O pair distribution function for both H_2O and H_3O^+ in the first shell about the halide ion. This experimental effort compliments ongoing theoretical efforts in the Molecular Interactions and Transformations group. Comparisons will be made to i) electronic structure calculations of small $\text{H}_3\text{O}^+/\text{Cl}^-/\text{H}_2\text{O}$ clusters, ii) newly-developed classical intermolecular potentials for $\text{Cl}^-/\text{H}_3\text{O}^+$ used in a classical molecular dynamics simulation and iii) efforts modeling the chemistry of hydronium using DFT-molecular dynamics methods. The interest in hydronium structure pertains to its role in a large number of biological, chemical, and geochemical systems. No previous experimental studies have directly measured the structure of the $\text{Cl}^-/\text{H}_3\text{O}^+$ contact ion pair.

We have recently developed methods for making XAFS transmission measurements of aqueous systems at very low x-ray energies (Cl K-edge, 2822 eV). As shown in the schematic of Figure 3, preliminary data shows a shortening of the Cl-O distance (from H_3O^+) that is approximately equal to the theoretical value. Thus this study will provide the first direct measure of the $\text{Cl}^-/\text{H}_3\text{O}^+$ distance and provide an excellent comparison to ab initio-based molecular dynamics studies of the same system.



Figure 3. XAFS result for hydronium ion pairing with Cl^- in concentrated HCl solutions (left). The hydronium-chloride structure from Car-Parrinello molecular dynamics simulations of 6.2 m HCl in water. (Heuft, *PCCP* 8, 3116, 2006)

We are also planning to apply the new method of symmetry-dependent multiple scattering analysis to look closely at the hydrated structure/symmetry of several different ions in solution including Dy^{3+} , Tm^{3+} , Nd^{3+} and I^- . The studies would entail collecting both L- and K-edge spectra to capture the multiple scattering regions. There are several existing XAFS studies of the hydration structure of various lanthanide ions. However none of them have evaluated the combined information available from the K- and L- edge multiple scattering features. Our interest is also in benchmarking these spectra against structures from MD simulations. Finally, we will also explore the hydration structure of iodide. Iodide is believed to be asymmetrically hydrated on one side of the ion. From a measure of the coordination numbers, hydration

symmetry and the I-O-H bond angle a much clearer picture of the hydration structure should emerge.

Another objective is to obtain very high quality K-edge spectra of Zn^{2+} . We have calculated DFT-MD structures but they have so far not yet been directly compared to the experimental system using the MD-XAFS method. A careful study of Zn(II) DFT-MD simulation is being completed. Zn(II) is one of the most difficult 1st row transition metals since it is known to have a flexible geometry along with moderately fast ligand exchange processes. The PNNL theory group is also implementing a parallel ab initio molecular dynamics (AIMD) MP2 code (E. Bylaska). The objective then is to compare the experimental Zn(II) results to both AIMD MP2 simulations as well as the DFT-MD results.

Collaborators on this project include G.K Schenter, S. M. Kathmann. Battelle operates Pacific Northwest National Laboratory for the U. S. Department of Energy.

References to publications of DOE sponsored research (CY 2006-present)

1. J. L. Fulton, D. W. Matson, K. H. Pecher, J. E. Ammonette, J. C. Linehan, “Iron-based and Iron Oxide Nanoparticle Synthesis from the Rapid Expansion of Carbon Dioxide Solutions” **Journal of Nanoscience and Nanotechnology**, 6, 562-567 (2006).
2. V. Glezakou, Y. Chen, J. L. Fulton, G. K. Schenter and L. X. Dang. Electronic structure, statistical mechanical simulations, and EXAFS spectroscopy of aqueous potassium. **Theor. Chem. Acc.** 115, 86-99, (2006)
3. “Calcium Ion Hydration and Ion Pairing in Supercritical Water”, J. L. Fulton Y. Chen, S. M. Heald, and M. Balasubramanian, **J. Chem. Phys.**, 125(9), Art. No. 094507, (2006).
4. “Molecular simulation analysis and X-ray absorption measurement of Ca^{2+} , K^+ and Cl^- ions in solution”, Liem X. Dang, Gregory K. Schenter, Vassiliki-Alexandra Glezakou and John L. Fulton, **J. Phys. Chem. B**, 110(47), 23644, (2006)
5. J. L. Fulton, J. C. Linehan, T. Autrey, M. Balasubramanian, Y. Chen, and N. K. Szymczak. When is a Nanoparticle a Cluster? An Operando EXAFS Study of Amine Borane Dehydrocoupling by Rh_{4-6} Clusters. **J. Am. Chem. Soc.**, 129(39), 11936-11949, (2007).
6. R. Rousseau, G.K. Schenter, J.L. Fulton, J.C. Linehan, M.H. Engelhard, T. Autrey. “Defining the Active Catalyst Structure and Reaction Pathways from *Ab initio* Molecular Dynamics and *Operando* XAFS: Dehydrogenation of Dimethylaminoborane by Rhodium Clusters” **J. Am. Chem. Soc.**, 131 (30), 10516–10524, (2009)
7. J. L. Fulton, S. M. Kathmann, G. K. Schenter, M. Balasubramanian, “Hydrated Structure of Ag(I) Ion from Symmetry-Dependent, K- and L-edge XAFS Multiple Scattering and Molecular Dynamics Simulations”, **J. Phys. Chem. A**, in press, (2009)

Ion Solvation in Nonuniform Aqueous Environments

Principal Investigator

Phillip L. Geissler

Faculty Scientist, Chemical Sciences Division

Mailing address of PI:

Lawrence Berkeley National Laboratory

1 Cyclotron Road

Mailstop: HILDEBRAND

Berkeley, CA 94720

Email: plgeissler@lbl.gov

Program Scope

Research in this program applies computational and theoretical tools to determine structural and dynamical features of aqueous salt solutions. It focuses specifically on heterogeneous environments, such as liquid-substrate interfaces and crystalline lattices, that figure prominently in the chemistry of energy conversion. In these situations conventional pictures of ion solvation, though quite accurate for predicting bulk behavior, appear to fail dramatically, e.g., for predicting the spatial distribution of ions near interfaces. We develop, simulate, and analyze models to clarify the chemical physics underlying these anomalies. We also scrutinize the statistical mechanics of intramolecular vibrations in nonuniform aqueous systems, in order to draw concrete connections between spectroscopic observables and evolving intermolecular structure. Together with experimental collaborators we aim to make infrared and Raman spectroscopy a quantitative tool for probing molecular arrangements in these solutions.

Recent Progress

In the past year we have taken several significant steps toward understanding a phenomenon that highlights how profoundly inhomogeneities can influence the physics of solvation. Computer simulations of atomistically detailed models for aqueous solutions suggest that certain small ions (little larger than a solvent molecule) adsorb to air-water interfaces. A variety of experimental data support this notion, and there has been considerable speculation on its relationship to more complex issues (e.g., the role of dissolved salts in protein solubility). Such behavior defies expectations from dielectric theories of solvation, which have proved remarkably accurate for bulk liquids. Put simply, the enormously favorable enthalpy of introducing an ion into highly polarizable environments must be sacrificed in the interfacial region; ion concentrations at the liquid surface should be correspondingly suppressed. In discussions of basic flaws in this reasoning, it has been noted that (i) an ion's polarizability can strongly modulate observed surface enhancement; (ii) charge asymmetry within water molecules generates nonzero average electric fields at the interface with air, which could preferentially bias

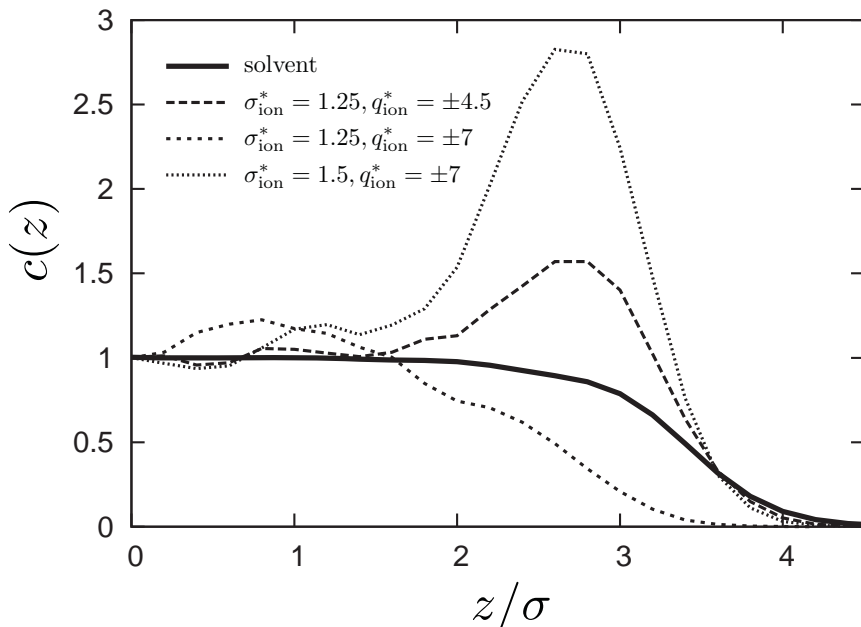


Figure 1. Density profiles for several charged solutes, as well as solvent molecules, in a Stockmayer liquid near its interface with vapor. Average density relative to its value in bulk, $c(z)$, is plotted as a function of vertical distance z from the center of the simulated slab. Modest changes in the solute charge q_{ion}^* or diameter σ_{ion}^* (relative to solvent molecules' diameter σ) are sufficient to substantially enhance or suppress ions' residence at the solution's boundary.

anions toward the vapor; and (iii) that dielectric response at the liquid-vapor interface exhibits considerable nonlinearities omitted in most theoretical descriptions. A thorough understanding of the statistical mechanics of ion adsorption, however, has remained elusive.

We have established several aspects of this behavior that greatly clarify its microscopic underpinnings, and that point to essential elements of a successful theory. Through simulations of ions in schematic polar fluids (namely, a Stockmayer liquid in coexistence with its vapor), we have shown that surface enhancement requires neither molecular polarizability, nor charge asymmetry, nor hydrogen bonding. (See Fig. 1.) The circumstances under which Stockmayer solutions exhibit ion adsorption instead point to a precarious balance between forces associated with dielectric response and with the entropy of creating solute-sized cavities in the liquid. Both can be substantial near the interface, and both can be sensitive to spontaneous fluctuations in interfacial shape. We have confirmed that a similar mechanism operates in aqueous solutions by computing density profiles for fractionally charged ions. Those cases tip the precarious balance described above, generating surface enhancement that is considerable even for cations and dramatic for anions.

For both Stockmayer and aqueous solutions we have more deeply probed the interplay between density and polarization fluctuations near the liquid surface. Probability distributions of electric fields experienced by charged solutes indicate a large but bounded range of Gaussian statistics. This result highlights a basic failing in conventional dielectric continuum theories that idealize the surface as a rigid structure. Presence of the ion induces substantial changes in surface geometry that in effect change

boundary conditions for polarization response, a highly nonlinear effect. Gaussian models are nonetheless sufficient for gauging the much-discussed role of ion polarizability. We have shown how the interaction between a solute's transient dipole and the reaction field induced by its charge can provide an attraction to the interface, provided fluctuations in the liquid's electric field do not attenuate too rapidly as the ion is withdrawn from solution. Interfacial flexibility appears to be key for satisfying this condition.

We have additionally made progress in developing a physical interpretation of the nonlinear spectroscopies that report on solutes' spatial distributions near interfaces. Our simplified expressions for sum-frequency susceptibilities provide fresh insight into their microscopic origins, focusing on the combined roles of fluctuations in molecular orientation and collective electric fields. Recent applications to electrolyte solutions have demonstrated the dominance of long-range polarization response in sum frequency generation. Macroscopic electroneutrality ensures that signals distinct from pure solvent arise only if the surface region is stratified in charge density, i.e., if cations and anions possess different surface affinities. Together with measured spectra, this observation strengthens the experimental case for surface enhancement of anions in water.

Future Plans

These recent results pave the way for a comprehensive theory of solvating simple ions near liquid-vapor interfaces. It is now clear that a successful description must include the physics of interfacial deformations, that the coupling between packing and dielectric response must be explicitly considered, and that linear response models can be usefully employed only in a proper context. Elements of such a theory exist in distinct forms that have individually been explored by others. Work in the next year will focus on assembling them into a working mathematical framework, and on consideration of more complex, multiatomic solutes.

Our work to date on the theory of sum frequency generation has stopped short of predicting measurable susceptibilities, due to complications that will be addressed in the coming years. These difficulties principally involve conventions for breaking symmetry in molecular simulations and realistic molecular response functions for partially solvated molecules.

Articles supported by DOE funding, 2005-2009

1. Geissler, P. L. "Temperature Dependence of Inhomogeneous Broadening: On the Meaning of Isosbestic Points" *J. Am. Chem. Sci.* **2005**, *127*, 13019.
2. Eaves, J. D.; Tokmakoff, A.; Geissler, P. L. "Electric Field Fluctuations Drive Vibrational Dephasing in Water" *J. Phys. Chem. B* **2005**, *109*, 9424.
3. Smith, J. D.; Cappa, C. D.; Wilson, K. R.; Cohen, R. C.; Geissler, P. L.; Saykally, R. J.

“Unified Description of Temperature-Dependent Hydrogen Bond Rearrangements in Liquid Water” *Proc. Natl. Acad. Sci. U.S.A.* **2005**, *102*, 14171.

4. Smith, J.; Saykally, R.; Geissler, P. L. “The Effects of Dissolved Halide Anions on Hydrogen Bonding in Liquid Water” *J. Am. Chem. Soc.* **2007**, *129*, 13847.

5. Noah-Vanhoucke, J.; Smith, J.; Geissler, P.L. “Statistical Mechanics of Sum Frequency Generation Spectroscopy for the Liquid-Vapor Interface of Dilute Aqueous Salt Solutions,” *Chem Phys. Lett.* **2009**, *470*, 21.

6. Noah-Vanhoucke, J.; Smith, J.; Geissler, P.L. “Toward a Simple Molecular Understanding of Sum Frequency Generation at Air-Water Interfaces,” *J. Phys. Chem. B* **2009**, *113*, 4065.

7. Noah-Vanhoucke, J.; Geissler, P.L. “On the Fluctuations that Drive Small Ions Toward, and Away From, Interfaces Between Polar Liquids and Their Vapors,” *Proc. Natl. Acad. Sci. U.S.A.* **2009**, *106*, 15125.

Program Title: Theoretical Studies of Surface Science, Heterogeneous Catalysis, and Intermolecular Interactions

Principal Investigator: Mark S. Gordon, 201 Spedding Hall, Iowa State University and Ames Laboratory, Ames, IA 50011; mark@si.msg.chem.iastate.edu

Program Scope. Our research effort spans the study of a variety of problems in surface science and heterogeneous catalysis using *ab initio* cluster and embedded cluster methods, the development and application of sophisticated model potentials for the investigation of intermolecular interactions, including solvent effects in ground and excited electronic states, the liquid-surface interface, the development and implementation of methods that will take advantage of massively parallel computing systems, and general studies of mechanisms in organometallic chemistry. Many of the surface science studies are in collaboration with Dr. James Evans. Much of the catalysis effort is in collaboration with Drs. Victor Lin, Marek Pruski, and James Evans.

Recent Progress. Several studies of the Si(100) and related surfaces and processes that occur on these surfaces have been completed. Combined kinetic Monte Carlo (KMC)/electronic structure theory studies of the etching of the Si(100) surface and the diffusion of group III metals on the Si(100) surface are ongoing. Several papers in this general area have already been published. SIMOMM studies have also been carried out on the diamond and silicon carbide surface. Of particular interest is the study of metal oxide surfaces (e.g., silica, alumina, titania) in view of their importance in heterogeneous catalysis. In order to study the liquid-surface interface (frequently important in heterogeneous catalysis), an interface has been developed between our effective fragment potential (EFP) and the universal force field (UFF), so one can now do three-layer QM/EFP/UFF calculations in GAMESS.

Because MCSCF calculations are limited with regard to the size of the active space that can be included, extensive studies have been initiated on methods that are designed to significantly increase the sizes of systems that can be realistically treated with this method. Particularly important is the ORMAS (occupation restricted multiple active spaces) method that appears to be very successful for silicon surfaces.

As part of a NERI grant (PI: Francine Battaglia), an extensive series of calculations has been initiated to study the chemical vapor deposition processes of SiC, starting from CH₃SiCl₃ (MTS). The overall mechanism involves more than 100 reactions whose overall reaction energetics and barrier heights and activation energies have been predicted with many body perturbation theory and coupled cluster theory. As part of this effort, it has been demonstrated that the new CR-CCSD(T)_L method is in almost perfect agreement with full configuration interaction (FCI) for breaking a wide variety of single bonds in both closed and open shell molecules. The next step in this effort will be the development of a model for bulk kinetic flow in the MTS system.

Development of the effective fragment potential (EFP) method has continued with the derivation and implementation of a new approach to electrostatic damping and the application to the benzene dimer and an extensive series of substituted benzene dimers, the derivation and implementation of analytic gradients for the most demanding terms in the potential, and the implementation of a scalable EFP algorithm. The equations for the QM-EFP exchange repulsion energy and Fock operator have been derived, coded and tested, and the corresponding gradient expression has been derived. The corresponding expressions for the QM-EFP dispersion have been derived, and the coding is in progress. The EFP method has recently been extended to open shell species. EFP applications have included a study of the aqueous solvation of F⁻ and Cl⁻, to bihalides anions and to the nitrate anion. A new definitive interpretation of the dipole moment of water in the bulk has also been developed and described.

Several studies of non-adiabatic interactions, including spin-orbit coupling have been published, and several papers on advances in high quality electronic structure theory have been completed. Of particular note is a sequence of definitive papers (with K. Ruedenberg) on the F_2 molecule, in which the most accurate potential energy curves and vibrational spectrum for this molecule are presented, together with an interpretation of the long-range tails of the PE curve.

As part of the Ames Laboratory catalysis effort, a detailed study of the nitroaldol reaction, both in the gas phase and in solution, has been completed.

Future Plans. In order to significantly expand the sizes of clusters that can realistically be modeled with MCSCF wavefunctions, the ORMAS method mentioned above is being tested on clusters of increasing size and compared with the full CASSCF calculations. This initial study is nearing completion. An exhaustive study of the diffusion of one and two Ga atoms on the Si(100) surface, using ORMAS to greatly expand the size of the MCSCF cluster that can be used, is in progress. The etching of the Si(100) surface by O was studied previously. This system is being revisited, partially to explore the importance of using larger basis sets and better levels of theory, and partially to study the diffusion of O along the surface. The energetics and structural information obtained for these processes will then be incorporated into the kinetic Monte Carlo analyses performed by the Evans group. The SIMOMM method is being extended to more complex species, such as silica. A primary motivation for this is to model the catalysis of various reactions in silica-based MSM pores.

The fragment molecular orbital (FMO) method has been developed to greatly expand the sizes of molecular systems that can be treated with accurate electronic structure methods. The FMO approach was originally developed to study molecules of importance in biology; however, it has recently been applied successfully to zeolites. We are in the process of assessing the efficacy of the FMO method for silica. If this effort is successful, and preliminary indications are that it will be, the silica pores of importance to the Ames Laboratory catalysis effort will be accessible to fully quantum studies.

The EFP method is currently being interfaced with both the CI singles and CI singles with perturbative doubles [CIS(D)], as well as with multi-reference perturbation theory, equations of motion coupled cluster, and time dependent density functional theory (TDDFT) methods, so that solvent-induced shifts in electronic spectra can be investigated. Improved methods for treating weak intermolecular interactions, such as dispersion, will be developed and implemented, and then applied to important problems. A preliminary molecular dynamics (MD) code for the EFP method and a combined *ab initio* EFP MD code has been implemented, and more robust algorithms are being developed. Several studies of the aqueous solvation of ions and electrolytes, including Na^+ , OH^- , and $NaOH$ are underway. This includes a systematic study of the solvated structures (internal vs. external ions) and the convergence of ionization potentials and electron affinities to their gas phase values. The EFP method will also be used in extensive investigations of atmospheric aerosols, including the structures and reaction clusters of H_2SO_4 , HNO_3 , and their ions with water molecules. The latter study is in collaboration with Theresa Windus (Iowa State) and Shawn Kathmann (PNNL) and is supported by a generous computer grant from PNNL.

Ruedenberg and Bytautas have developed the very excited CEEIS (Correlation Energy Extrapolation with Intrinsic Scaling) that facilitates the prediction of the exact wavefunction (full CI at the complete basis set limit) for small molecules. This method has been shown to provide essentially exact energies for diatomic molecules (e.g., F_2). We will now move on to address more complex species, most notably the ground and excited state potential energy surfaces of O_3 .

Analytic gradients and Hessians for the Klobukowski model core potentials (MCP) have been derived and implemented into GAMESS. Combined with the correlation consistent basis sets, this provides a powerful approach to study mechanisms of reactions in transition metal organometallic

chemistry, in collaboration with the Ames Laboratory catalysis group, especially Andreja Bakac, and studies of uranium complexes with Theresa Windus (Ames) and Bert de Jong (PNNL).

In collaboration with Francine Battaglai and Rodney Fox, the NERI project will continue with the incorporation of the thermodynamic and rate constant data discussed above into bulk kinetic models, such as ChemKin. This will provide important insights to our experimentalist colleagues at ORNL.

Finally, as part of the End Station project, we have initiated the development of a broad array of electronic structure methods that are designed for use on graphical processing units (GPUs). The first step has been to develop a novel approach for two-electron integrals that involve high angular momentum basis functions. This will be incorporated into GPU-based Hartree-Fock and density functional theory codes, before moving on to correlated methods.

References to publications of DOE sponsored research, 2006-present.

- [1] *Theoretical Study of the Formation and Isomerization of Al₂H₂*, T. J. Dudley and M. S. Gordon, *Mol. Phys.*, **104**, 751 (2006)
- [2] *Dissociation Potential Curves of Low-Lying States in Transition Metal Hydrides. III. Hydrides of Groups 6 and 7*, S. Koseki, T. Matsushita, and M.S. Gordon, *J. Phys. Chem*, **A110**, 2560 (2006).
- [3] *Parallel Coupled Perturbed CASSCF Equations and Analytic CASSCF Second Derivatives*, T. J. Dudley, R. M. Olson, M. W. Schmidt and M. S. Gordon, *J. Comp. Chem.* **27**, 353 (2006).*
- [4] *Gradients of the Exchange-Repulsion Energy in the Effective Fragment Potential Method*, H. Li and M. S. Gordon, *Theor. Chem. Accts.*, **115**, 385 (2006).
- [5] *Scalable Implementation Of Analytic Gradients For Second-Order Z-Averaged Perturbation Theory Using The Distributed Data Interface*, C.M. Aikens and M.S. Gordon, *J. Chem. Phys.*, **124**, 014107 (2006).
- [6] *Gradients of the Polarization Energy in the Effective Fragment Potential Method*, H. Li, H.M. Netzloff, and M.S. Gordon, *J. Chem. Phys.*, **125**, 194103 (2006).
- [7] *Reinvestigation of SiC₃ with Multi-reference Perturbation Theory*, J. M. Rintelman, M. S. Gordon, G. D. Fletcher, and J. Ivanic, *J. Chem. Phys.*, **124**, 034303 (2006).
- [8] *Reply to Comment on monotonically decreasing size distributions for one-dimensional Ga rows on Si(100)*, M.A. Albao, M.M.R. Evans, J. Nogami, D. Zorn, M.S. Gordon, and J.W. Evans, *Phys. Rev. B*, **74**, 037402 (2006).
- [9] *Electrostatic Energy in the Effective Fragment Potential (EFP) Method. Theory and Application to Benzene Dimer*, L. Slipchenko and M.S. Gordon, *J. Comp. Chem.*, **28**, 276 (2007)
- [10] *Theoretical Study of the Pyrolysis of Methyltrichlorosilane in the Gas Phase. I. Thermodynamics*, Y. Ge, M.S. Gordon, F. Battaglia, and R.O. Fox, *J. Phys. Chem.*, **A111**, 1462 (2007).
- [11] *Theoretical Study of the Pyrolysis of Methyltrichlorosilane in the Gas Phase. II. Reaction Paths and Transition States*, Y. Ge, M.S. Gordon, F. Battaglia, and R.O. Fox, *J. Phys. Chem.*, **A111**, 1475 (2007).
- [12] *Multiterminal Nanowire Junctions of Silicon: A Theoretical Prediction of Atomic Structure and Electronic Properties*, P.A. Avramov, L.A. Chernozatonskii, P.B. Sorokin, and M.S. Gordon, *Nano Letters*, **7**, 2063 (2007).
- [13] *Breaking Bonds with the Left Eigenstate Completely Renormalized Coupled Cluster Method*, Y. Ge, M.S. Gordon, and P. Piecuch, *J. Chem. Phys.*, *J. Chem. Phys.*, **127**, 174106 (2007).
- [14] *Polarization Energy Gradients in Combined Quantum Mechanics, Effective Fragment Potential and Polarizable Continuum Model Calculations*, H. Li and M.S. Gordon, *J. Chem. Phys.*, **126**, 124112 (2007).*
- [15] *Accurate ab initio potential energy curve of F₂. I. Non-relativistic full valence CI energies by the CEEIS method*, L. Bytautas, T. Nagata, M. S. Gordon, and K. Ruedenberg, *J. Chem. Phys.*, **127**, 164317 (2007).
- [16] *Accurate ab initio potential energy curve of F₂. II. Core-valence correlations, relativistic contributions and long-range interactions, Core-valence correlations, relativistic contributions and long-range interactions*, L. Bytautas, N. Matsunaga, T. Nagata, M. S. Gordon, and K. Ruedenberg, *J. Chem. Phys.*, **127**, 204301 (2007).
- [17] *Accurate ab initio potential energy curve of F₂. III. The Vibration rotation spectrum*, L. Bytautas, N. Matsunaga, T. Nagata, M. S. Gordon, and K. Ruedenberg, *J. Chem. Phys.*, **127**, 204301 (2007).

- [18] *Atomic and electronic structure of new hollow-based symmetric families of silicon nanoclusters*, P.V. Avramov, D.G. Fedorov, P.V. Sorokin, L.A. Chernozatonskii, and M.S. Gordon, *J. Phys. Chem C*, 111, 18824 (2007).
- [19] *An Interpretation of the Enhancement of the Water Dipole Moment Due to the Presence of Other Water Molecules*, D. D. Kemp and M.S. Gordon, *J. Phys. Chem.*, A112, 4885 (2008).
- [20] *Modeling π - π interactions with the effective fragment potential method: The benzene dimer and substituents*, T. Smith, L.V. Slipchenko, and M.S. Gordon, *J. Phys. Chem. A*, 112, 5286 (2008).
- [21] *Comparison of Nitroaldol Reaction Mechanisms Using Accurate Ab Initio Calculations*, D. Zorn, V. S.-Y. Lin, M. Pruski, and M.S. Gordon, *J. Phys. Chem.* A112, 10635 (2008).
- [23] *An Interface Between the Universal Force Field and the Effective Fragment Potential Method*, D. Zorn, V.S.-Y. Lin, M. Pruski and M.S. Gordon, *J. Phys. Chem.* B112, 12753 (2008)
- [24] *Breaking bonds of open-shell species with the restricted open-shell size extensive left eigenstate completely renormalized coupled-cluster method*, Y. Ge, M.S. Gordon, P. Piecuch, M. Wloch, and J.R. Gour, *J. Chem. Phys.*, 106, 11873 (2008).

Dynamics of Electrons at Interfaces on Ultrafast Timescales

Charles B. Harris P.I.
Chemical Sciences Division
Lawrence Berkeley National Lab
1 Cyclotron Road, Mail Stop Latimer
Berkeley, CA 94720
CBHarris@berkeley.edu

Program Scope:

The electronic structure and dynamics of ultrathin films are known to differ from their bulk properties. Our research under this program is aimed at elucidating and quantifying the behavior of electrons in ultrathin films of organic molecules at metallic surfaces. Interfacial band structure, band bending, Fermi level pinning, charge localization and polaron formation, and morphologies imposed by a metal/molecule junction are a sample of the processes which we are studying in these systems.

We use two photon photoemission (2PPE) in order to investigate the electronic properties of these interfacial regions. This technique is a pump-probe style technique in which the kinetic energy of the photo-electrons are measured rather than the differential absorption of a light probe. Ultrafast pulses are required because the lifetime of electrons at a metal interface range from 20 to 10,000 femtosecond (fs). In a 2PPE experiment, one pulse excites an interfacial electron, and after some time, Δt , a second laser pulse photoemits the excited electron. The energy of both the pump and the probe beam are kept below the workfunction of the material so that all of the photo-electrons must have been excited by interaction with both the pump and the probe beam. The kinetic energy of photo-electron is measured by time of flight, and the binding energy of the electron is then determined by subtracting the photon energy of the probe pulse. This allows us access to both occupied and unoccupied states, which transient absorption and time resolved fluorescence cannot do. By varying the energy of the two pulses and measuring the workfunction, we can accurately pin the exact energy of a given electron with respect to the Fermi level.

In addition to measuring the energy levels, we can also pick off specific momentum slices by varying the angle of our sample with the respect to the detector. Angle resolved photo-emission spectroscopy (ARPES) is an established technique for measuring the band structure of occupied states in a crystalline system. Here, we apply the same technique to the unoccupied states, which allow us to measure the momentum of excited state electrons from 0 to 0.3 \AA^{-1} . For crystalline systems with strong orbital overlap, the electronic energy levels will mix to form dispersive bands. For many organic molecules at metal surfaces, excited electronic levels are initially delocalized dispersive states, but over time the electrons will interact with their surrounding material and become self trapped into a small polaron.

We are using 2PPE to study two broad classes of electronic states at organic/metal interfaces. The first state is the image potential state, which is derived from high polarizability of nearly free electrons contained in the metal. These states have been shown to be excellent probes of the dielectric and solvating properties of molecular adsorbates. The second class of states we are investigating are the molecular orbital derived band from organic semiconductors on metal surfaces. In these systems we are investigating the barriers to charge injection, exciton separation, and metal to molecule charge transfer events.

Recent Progress:

Morphology-dependent Photo-conductivity of Organic Semiconductors : Photoconductivity in organic semiconductors has garnered considerable research attention in the search for sustainable

energy sources. In particular, the factors for consideration in optimizing these devices, which include the efficiency of photogeneration and the carrier dynamics at an interface, merit a close investigation of the physical chemistry at the interface. Using 2PPE, we have probed the dynamics of charge carriers at the interface of Ag(111) and PTCDA, a widely-studied planar aromatic hydrocarbon. By varying the morphology of the surface, we have quantitatively examined the role of crystallinity versus structural disorder in affecting the carrier dynamics and electronic structure at an interface. High substrate temperatures (> 400 K) cause the growth of a wetting layer with islands, and the exposed wetting layer inhibits the evolution of the vacuum level and valence band to bulk PTCDA values. In the layer-by-layer growth of low substrate temperatures, we observe the transition of molecular state energies from monolayer to bulk values. Effective masses of the conduction band and the $n = 1$ image potential state varied from 2.1 me and 1.4 me, resp., in disordered PTCDA layers to 0.5 me and 1.1 me in the most crystalline layers. Decay constants were obtained for electrons excited into the conduction band and into image potential states at different layer thicknesses and morphologies. Decay constants for the LUMO in crystalline systems were mediated by electron transfer back to the surface and were on the order of 100 fs, whereas layer-by-layer amorphous growth resulted in exponential decays with time constants of picoseconds present in films thicker than ~ 7 monolayers.

DMSO: In electrochemically relevant systems, interfacial capacitance affects electrochemical signal collection and heterogeneous charge transfer. At noble metal electrodes, dimethyl sulfoxide (DMSO), a common electrochemical solvent, exhibits an uncharacteristically low interfacial capacitance of 7–10 $\mu\text{F}/\text{cm}^2$ over a 1.5 V range which includes the potential of zero charge. This stands in contrast to similar, polar, high-dielectric constant electrochemical solvents, e.g., 50 $\mu\text{F}/\text{cm}^2$ for acetonitrile under identical experimental conditions. Si and Gewirth have proposed that hindered rotation of the DMSO dipole at the surface lowers its interfacial capacitance and reduces the response of interfacial DMSO to changes in potential [1]. We directly tested this hypothesis with 2PPE by modeling the injected electron as a planar charge outside a capacitive layer. We measured a much weaker solvation response in a monolayer than multilayer coverages, which we attribute to hindered dipole rotation in the monolayer. The solvation responses were then interpreted as a comparison of the dielectric response of the monolayer with those of various multilayer coverages.

Current and Ongoing Work

Solvation in Room Temperature Ionic Liquids: The electrochemical interface found at a liquid immersed electrode is found throughout the chemistry where there is charge injection or capacitance. The behavior of the device is strongly influenced by the solvation and localization of an excited electron at the interface. An electron injected into a solvent can initially be found at an often well defined energy and location, bound backwards to the interface by the image charge potential. The recent development and application of room temperature ionic liquids (RTIL's) has given us new room for study as steric hindrance allows them to remain as a viscous liquid to temperatures lower than that of other solvents. Meanwhile their large size and charge strongly decrease their vapor pressure, allowing studies to be performed on ionic liquids in a liquid form under vacuum. We have produced some initial results on the solvation behavior of these materials.

Preliminary TPPE data shows the presence of an unoccupied state in the RTIL's above the Fermi level of Ag(111). This state, currently assigned to a conduction band electron, has an appreciable lifetime and shows notable solvation of the injected excess charge over the course of hundreds of femtoseconds. Solvation rate and magnitude of this state both show strong temperature dependence over the range of 130-325K. The solvation magnitude, measured as a function of the difference in the energy of the state between initial and final times, decreases steadily from 325 down to below 250K. The solvation rate, measured as a fit to the dynamic shifting of the peak center, shows an apparent discontinuous jump near 250K. This is one of few instances that have shown a measurable change in either the timescale or the magnitude of

solvation as a function of temperature. Both the time and energy dynamics suggest a possible phase transition at a sample temperature of approximately 250K. Below this temperature, translational and rotational motions may be frozen out and librational dynamics likely dominate solvation.

Electronic States in Chemically Substituted Phthalocyanines: Phthalocyanines and their derivatives offer a model system well suited characterizing band structure of surface states. Phthalocyanines, which have served as model systems in devices engineering due to the size of their bandgap and high stability, have well characterized surface structures. These molecules can be grown in highly ordered flat lying lattices when grown epitaxially on noble metal surfaces. While the high mobility found in bulk phthalocyanines results from a large pi-pi intermolecular overlap, flat lying molecules have little or no intermolecular overlap. Molecules lying flat on the surface have pi-orbitals separated by a large distance due to the presence of carbon-hydrogen or carbon-halogen bonds at the edges of each molecule. The unusually small intermolecular coupling that results in this type of configuration provides a unique material for examining how the degree of intermolecular pi-overlap affects two-dimensional band structure and mobility.

One of the simplest ways to model a perturbation of a wavefunction caused by the introduction of a nearby model is to treat the interaction as a tunneling barrier between the two molecules. By then assuming in this case the tunneling barrier between molecules is large as compared to the potential energy corrugation within a single molecule, and picturing that barrier as a simple square well tunneling barrier, one can obtain an lattice of potentials extending in two dimensions that approximates the two-dimensional potential experienced by an electron at the interface. This is exactly the potential first treated by Kronig and Penny in the theoretical development of understanding the nature of semiconductor crystals. This model predicts sigmoidal electronic bands separated by a small band gap. Comparing predictions of this simple model to unoccupied surface band structure highlights the importance of this tunneling barrier in describing the mobility of two dimensional electrons.

Preliminary results have been collected comparing different metalated and halogenated phthalocyanines. Copper phthalocyanine has an epitaxial crystal structure consisting of flat lying molecules on the surface. Growth of subsequent layers results in molecules that stack directly on top of one another. This results in a picture similar to the one above, in which wavefunctions are strongly coupled perpendicular to the plane of the molecule but only weakly coupled parallel to the plane of the molecule. As predicted by the Kronig-Penney type tunneling model, this results in a deviation from the rydberg series energies and parabolic band structure typically predicted for image potential state electrons. Because of the large size of individual molecules, this two-dimensional band gap becomes small, on the order of only a couple hundred meV. The splitting of the image potential state, which is less than the spacing between individual image potential states, results in the addition of new observed states coming from higher order Brillouin zones in the tunneling model. Also, as predicted by the model, momentum resolved measurements of the band structure reveal sigmoidal bands rather than the typical free-electron-like parabolic bands. This work has highlighted the importance of intermolecular coupling in two dimensional systems in semiconductor band structure. Continuing work on this project is aimed at examining the change in tunneling barriers between molecules with small changes in the crystal structure and molecular identity.

Articles Supported by DOE Funding from 2005-2009

[1] J. E. Johns, E. Muller, S. Garrett-Roe, M. Strader. "Image Potential Dynamics for Complex Molecules Adsorbed to Metal Surfaces." Chapter in Dynamics at Solid State Surfaces and Interfaces. Ed. Uwe Bovensiepe. Wiley. In press.

[2] K.R. Sawyer, R.P. Steele, E.A. Glascoe, J.F. Cahoon, J.P. Schlegel, M. Head-Gordon, C.B. Harris, "Direct observation of photoinduced bent nitrosyl excited-state complexes" J. Phys. Chem. A, **112**, 8505-8514 (2008). Funded by NSF using DOE equipment.

- [3] J.F. Cahoon, M.F. Kling, K.R. Sawyer, L.K. Andersen, C.B. Harris, "DFT and Time-resolved IR Investigation of Electron Transfer between Photogenerated 17- and 19-electron organometallic radicals" *J. Mol. Struct.* (honor issue for F. Albert Cotton), **890**, 328-338 (2008). Funded by NSF using DOE equipment.
- [4] K.R. Sawyer, E.A. Glascoe, J.F. Cahoon, J.P. Schlegel, C.B. Harris, "The mechanism of iron-catalyzed alkene isomerization in solution" *Organometallics*, **27**, 4370-4379 (2008). Funded by NSF using DOE equipment.
- [5] J.F. Cahoon, K.R. Sawyer, J.P. Schlegel, C.B. Harris, "Determining Transition-state Geometries in Liquids Using 2D-IR" *Science* **319**, 1820-1823 (2008). Funded by NSF using DOE equipment.
- [6] M.L. Strader, S. Garrett-Roe, P. Szymanski, S.T. Shipman, J.E. Johns, A. Yang, E. Muller, C.B. Harris. "The ultrafast dynamics of image potential state electrons at the dimethylsulfoxide/Ag(111) interface" *J. Phys. Chem. C*, **112**, 6880-6886, (2008).
- [7] A. Yang, S.T. Shipman, S. Garrett-Roe, J. Johns, M. Strader, P. Szymanski, E. Muller, C. Harris. "Two-photon photoemission of ultrathin film PTCA morphologies on Ag(111)" *J. Phys. Chem. C*, **112**, 2506-2513, (2008).
- [8] E. A. Glascoe, M. F. Kling, J. E. Shanoski, J. R. A. DiStasio, C. K. Payne, B. V. Mork, T. D. Tilley, and C. B. Harris. "Photoinduced beta-hydrogen elimination and radical formation with CpW(CO)₃(CH₂CH₃): Ultrafast IR and DFT studies." *Organometallics*, **26**, 1424 (2007). Funded by NSF using DOE equipment.
- [9] E. A. Glascoe, K. R. Sawyer, J. E. Shanoski, and C. B. Harris. "The influence of the metal spin state in the iron-catalyzed alkene isomerization reaction studied with ultrafast infrared spectroscopy." *J. Phys. Chem. C*, **111**, 8789 (2007). Funded by NSF using DOE equipment.
- [10] J. F. Cahoon, M. F. Kling, K. R. Sawyer, H. Frei, and C. B. Harris. "19-electron intermediates in the ligand substitution of CpW(CO)₃ with a Lewis base." *J. Am. Chem. Soc.*, **128**, 3152 (2006). Funded by NSF using DOE equipment.
- [11] E. A. Glascoe, M. F. Kling, J. E. Shanoski, and C. Harris. "Nature and role of bridged carbonyl intermediates in the ultrafast photoinduced rearrangement of Ru₃(CO)₁₂." *Organometallics*, **25**(775) (2006). Funded by NSF using DOE equipment.
- [12] J. E. Shanoski, E. A. Glascoe, and C. Harris. "Ligand rearrangement reactions of Cr(CO)₆ in alcohol solutions: Experiment and theory." *J. Phys. Chem. B*, **110**(996) (2006). Funded by NSF using DOE equipment.
- [13] S. Shipman, S. Garrett-Roe, P. Szymanski, A. Yang, M. Strader, and C. B. Harris. "Determination of band curvatures by angle-resolved two-photon photoemission in thin films of C₆₀ on Ag(111)." *J. Phys. Chem. B*, **110**, 10002 (2006).
- [14] J. F. Cahoon, M. F. Kling, S. Schmatz, and C. B. Harris. "19-electron intermediates and cage-effects in the photochemical disproportionation of [CpW—(CO)₃]₂ with Lewis bases." *J. Am. Chem. Soc.*, **127**(12555) (2005). Funded by NSF using DOE equipment.
- [15] S. Garrett-Roe, S. T. Shipman, P. Szymanski, M. L. Strader, A. Yang, and C. B. Harris. "Ultrafast electron dynamics at metal interfaces: Intraband relaxation of image state electrons as friction." *J. Phys. Chem. B*, **109**, 20370 (2005).
- [16] J. E. Shanoski, C. K. Payne, M. F. Kling, E. A. Glascoe, and C. B. Harris. "Ultrafast infrared mechanistic studies of the interaction of 1-hexyne with group 6 hexacarbonyl complexes." *Organometallics*, **24**(1852) (2005). Funded by NSF using DOE equipment.
- [17] P. T. Snee, J. E. Shanoski, , and C. B. Harris. "Mechanism of ligand exchange studied using transition path sampling." *J. Am. Chem. Soc.*, **127**(1286) (2005). Funded by NSF using DOE equipment.
- [18] P. Szymanski, S. Garrett-Roe, and C. B. Harris. "Time- and angle-resolved two-photon photoemission studies of electron localization and solvation at interfaces." *Prog. Surf. Sci.*, **78**, 1 (2005).

Catalysis at Metal Surfaces Studied by Non-Equilibrium and STM Methods

Ian Harrison

Department of Chemistry, University of Virginia

Charlottesville, VA 22904-4319

harrison@virginia.edu

Program Scope:

This research program aims to employ non-equilibrium techniques to investigate the nature of the transition states for activated dissociative chemisorption of small molecules on catalytic metal surfaces. Two separate approaches/ideas are under investigation. In the first, we posit that dissociative chemisorption reactions on metal surfaces are primarily surface mediated electron transfer reactions for many hard-to-activate small molecules. Accordingly, the lowest lying affinity levels of these adsorbates, which are accessible by surface photochemistry and scanning tunneling microscopy (STM), will play a key electronic structure role in determining barrier heights for dissociative chemisorption. Electron transfer excitation into these adsorbate affinity levels followed by image potential acceleration towards the surface and rapid quenching may leave the adsorbate in the “transition state region” of the ground state potential relevant to thermal catalysis from where desorption and/or dissociation may ultimately occur. Using low temperature scanning tunneling microscopy (STM) and surface science techniques we have been investigating the thermal, electron, & photon induced chemistry of CH_3Br ,¹ CO_2 , and CH_4 on Pt(111). In our second approach towards probing surface transition states, we dose hot gas-phase molecules on to a cold surface and measure dissociative sticking coefficients macroscopically^{2,3} via Auger electron spectroscopy (AES) or microscopically by imaging chemisorbed fragments via low T_s STM. A local hot spot, microcanonical unimolecular rate theory (MURT) model of gas-surface reactivity³⁻⁷ can be used to extract transition state characteristics for dissociative chemisorption. An important long-range goal of our research is to microscopically characterize the different transition states for dissociative chemisorption occurring at metal terrace sites as compared to step sites – a goal of long-standing interest to the catalysis and electronic structure theory communities.⁸

Recent Progress & Future Plans:

We have been working towards using low T_s STM in conjunction with heated effusive molecular beam measurements to *microscopically* characterize the transition states for CH_4 dissociation on terraces and at step edges on a Pt(111) surface. Our ambition is to explore the site resolved activation of small alkanes, alcohols, and CO_2 for a range of catalytic metal surfaces.

DOE Publications (2005-):

T.C. Schwendemann, I. Samanta, T. Kunstmann, and I. Harrison, "CH₃Br Structures on Pt(111): Kinetically Controlled Self-Assembly of Dipolar and Weakly Adsorbed Molecules," J. Phys. Chem. C, 1347-1354 (2007).

References:

- 1 T.C. Schwendemann, I. Samanta, T. Kunstmann, and I. Harrison, "CH₃Br Structures on Pt(111): Kinetically Controlled Self-Assembly of Dipolar and Weakly Adsorbed Molecules," *J. Phys. Chem. C*, 1347-1354 (2007).
- 2 K. M. DeWitt, L. Valadez, H. L. Abbott, K. W. Kolasinski, and I. Harrison, "Using effusive molecular beams and microcanonical unimolecular rate theory to characterize CH₄ dissociation on Pt(111)," *J. Phys. Chem. B* **110**, 6705-6713 (2006).
- 3 K. M. DeWitt, L. Valadez, H. L. Abbott, K. W. Kolasinski, and I. Harrison, "Effusive molecular beam study of C₂H₆ dissociation on Pt(111)," *J. Phys. Chem. B* **110**, 6714-6720 (2006).
- 4 A. Bukoski, D. Blumling, and I. Harrison, "Microcanonical unimolecular rate theory at surfaces. I. Dissociative chemisorption of methane on Pt(111)," *J. Chem. Phys.* **118**, 843-871 (2003).
- 5 H. L. Abbott and I. Harrison, "Microcanonical transition state theory for activated gas-surface reaction dynamics: Application to H₂/Cu(111) with rotation as a spectator," *J. Phys. Chem. A* **111**, 9871-9883 (2007).
- 6 H. L. Abbott and I. Harrison, "Activated dissociation of CO₂ on Rh(111) and CO oxidation dynamics," *J. Phys. Chem. C* **111**, 13137-13148 (2007).
- 7 H. L. Abbott and I. Harrison, "Methane dissociative chemisorption on Ru(0001) and comparison to metal nanocatalysts," *J. Catal.* **254**, 27-38 (2008).
- 8 F. Abild-Pedersen, O. Lytken, J. Engbaek, G. Nielsen, I. Chorkendorff, and J. K. Nørskov, "Methane activation on Ni(111): Effects of poisons and step defects," *Surf. Sci.* **590**, 127 (2005).

Fluctuations in Macromolecules Studied Using Time-Resolved, Multi-spectral Single Molecule Imaging

Carl Hayden
Sandia National Laboratories
P. O. Box 969, MS 9055
Livermore, CA 94551-0969
cchayde@sandia.gov

Haw Yang
Department of Chemistry
Princeton University
Princeton NJ 08544
hawyang@princeton.edu

Program Scope

In this research program we use simultaneous, time-resolved measurements of multiple fluorescence properties of probe fluorophores to study conformational and local chemical environment fluctuations in single macromolecules. A time-resolved, multi-spectral confocal microscope at Sandia National Laboratories, records the wavelength (λ), and emission time relative to excitation (τ) for each detected fluorescence photon along with its absolute detection time (Δ) so that correlations among all the fluorescence properties are maintained. The ability to also record polarization (p) is currently being added to the apparatus. Fully correlated photon records of λ , p , τ , and Δ improve the capability of fluorescence measurements to characterize local chemical environments. The record of fluorescence photon emission provides detailed information on chemical processes, including energy transfer and conformational changes, on time scales from picoseconds to minutes. The capabilities of this apparatus are complemented by state-of-the-art single-molecule Förster-type resonance energy transfer (FRET) intensity measurements on a microscope at Princeton University optimized to operate at the maximum possible photon collection rate to record dynamics on the shortest possible time scales. These experimental approaches are combined with the development of rigorous analysis based on maximum information methods to allow us to more clearly resolve the fluctuations of macromolecules and the chemical environments around them.

Recent Progress:

High resolution FRET studies of poly-L-proline peptides

Poly-L-proline peptides have long been considered to favor an all trans, type-II helix,^{1,2} which is thought to behave as rigid rod on short length scales. However, it has been found that these molecules are not perfectly rigid; deviations from fully extended forms are seen in many studies. There is still no consensus on the length scale²⁻⁴ or on the physical basis for the apparent flexibility of poly-prolines in room-temperature solution. FRET experiments have been linked with poly-proline since short proline peptides were first used to demonstrate the $1/R^6$ distance dependence for energy transfer.⁵ In recent years, poly-proline experiments have been revisited with advanced ensemble^{6,7} and single-molecule fluorescence techniques.^{3,4,8,9} In many of these experiments, the distances measured were consistently shorter than predicted by a perfectly rigid, all-trans poly-proline. These deviations have been attributed to non-ideal energy transfer for very short poly-prolines,^{6,8,10} flexibility in the proline helix,^{3,6,8} or the presence of cis-isomers.^{4,7,9}

These questions have not been answered by measurements of the mean end-to-end distances alone because the mean distances from a series of poly-L-proline peptides can be fit equally well by different models of the flexibility of their structure. The freely jointed chain (FJC) model describes a polymer with discrete kinks such as a trans-proline helix with interspersed cis-isomers. The worm-like chain (WLC) model is analogous to the model of proline flexibility in which the all-trans helix is flexible due to torsional flexibility along the backbone. In order to test their applicability, one needs a means of comparing the entire probability distribution of conformations measured experimentally to those predicted by the models.

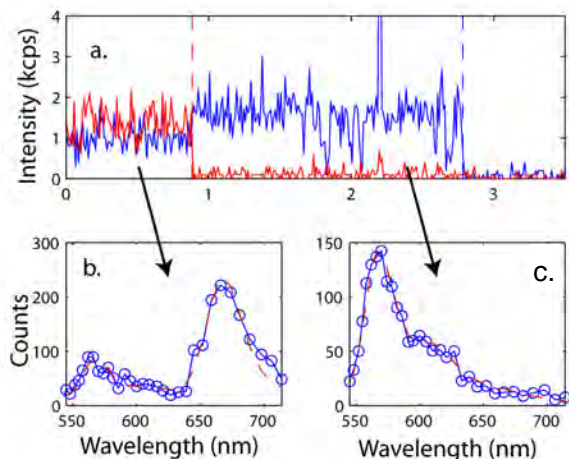


Figure 1 – Single-molecule spectra for a sample trajectory. Acceptor emission is red while donor emission is blue. Spectral data for the FRET region of the trajectory is displayed in (b) with a fit to bulk spectra. Donor spectra (c) obtained after acceptor bleaching. All agree with their bulk counterparts.

immobilized single molecules to allow accurate absolute calibration of the FRET measurements. These measurements show the donor and acceptor spectra are relatively constant and match the bulk spectra quite well (Figure 1). The donor lifetimes, measured using donor only samples, have a substantially asymmetric distribution and must be considered in the data analysis (Figure 2). To follow dynamics on the shortest time scales measurements were made with our FRET system that is optimized for maximum photon collection rate. Single-molecule intensity vs. time traces were converted to distance vs. time profiles with the maximum information method and probability distributions for the separation of the two dyes were constructed using the maximum entropy method, which allows unbiased deconvolution of the noise from the distributions.

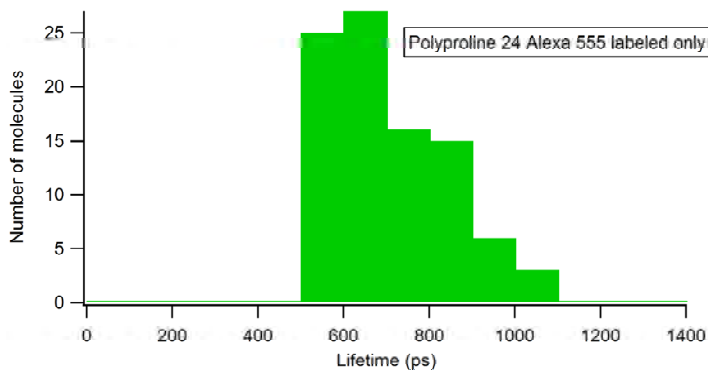


Figure 2. Donor lifetime histogram

The comparison of statistical polymer models can be extended beyond the ensemble averaged picture since the conformational probability distribution function (PDF) for each poly-proline sample has been measured through single-molecule experiments. The experimental distributions are very narrow for P₈ and broaden progressively as the length of the peptide increases. The WLC model predicts a relatively narrow distance distribution which is generally skewed towards longer distances than the experimental results. The skewed shape predicted by the WLC model is only similar to the poly-proline-P₂₄ experimental data set whereas the rest of the experimental data sets are quite symmetric. The FJC predicts a very broad, symmetric distribution of distances which are a poor fit to experimental data. Thus, neither of these models is appropriate for describing the behavior of short poly-proline peptides and a more detailed molecular picture is required to understand conformational distributions observed in single-molecule experiments.

Protein-lipid membrane binding using metal chelating lipids

Many functions of proteins occur in association with lipid membranes, so it is important to develop methods for single-molecule studies of proteins on membranes. We have developed an approach to attaching proteins to membranes applicable to single-molecule studies. The attachment method uses lipids that selectively chelate Cu⁺² which then strongly binds his-tags commonly used on recombinant proteins to purify them after expression. Two forms of the copper chelating lipid have been synthesized by a collaborator, Dr. Darryl Sasaki, at Sandia National Labs. Both forms use an iminodiacetic acid headgroup to bind copper, but one lipid, DSIDA, forms a gel phase membrane while the other, DOIDA, forms a fluid phase membrane. The availability of gel and fluid phase lipids provides great flexibility in the mobility of attached proteins in contrast to the commercially available fluid phase nickel chelating NTA lipids.

We have studied membranes made from mixtures of a fluid phase lipid POPC and DSIDA and found that upon Cu⁺² addition submicron gel phase membrane domains form that are extremely high affinity sites for his-tagged protein binding.¹⁴ His-tagged proteins were immobilized indefinitely on these domains. We have also studied mixtures of POPC and DOIDA to form completely fluid phase membranes. These membranes uniformly bind his-tagged proteins that freely diffuse on the surface. Membrane fluorescence correlation spectroscopy (FCS) measurements of the diffusion of dye-labeled proteins on a POPC/DOIDA membrane show the homogeneous nature of this membrane.

Ongoing Work and Future Plans:

Protein immobilization with lipid systems

The capability of doing single-molecule studies of proteins on membranes makes possible a range of new experiments. The membrane surface is a different environment than the PEG coated surfaces we usually use for protein immobilization and for many proteins more closely approximates the native environment. By comparing results on PEG and on membranes we will study how different surfaces affect protein function. Using fluid phase membranes we can observe individual dye labeled molecules diffuse through the excitation laser spot. This motion produces a burst of fluorescence photons similar to photon burst experiments performed on freely diffusing molecules in liquids. However, since the diffusion is much slower on the membrane than it would be in solution we can observe the molecule for a much longer time, increasing the signal-to-noise ratio. With this approach we can rapidly sample large numbers of molecules to identify subpopulations such as conformers that that persist longer than the diffusion time scale. Since proteins can readily be expressed with his-tags this technique will be

very generally applicable. Our first experiments will be to compare structural dynamics of small peptides on membranes to results with our current mobilization methods.

Conformational dynamics of ligand binding proteins

We have an ongoing investigation of the conformational dynamics of MBP from *E.Coli* using single molecule FRET. The two lobes of this protein close around the maltose ligand upon binding. Our experiments are to determine the fraction of open versus closed states in the presence and absence of the ligand. To detect the open and closed states we have performed single molecule experiments using FRET to measure the time dependent distance changes between the two lobes of the protein. An unexpected result we are investigating further is that in the absence of the ligand the open and closed states are nearly equally probable. The open state was expected to dominate when no ligand is bound.

Aptamer binding of small molecules

To extend our studies of ligand binding by macromolecules we will investigate DNA aptamer binding of small molecules. Aptamers for a number of small molecules have been identified. Of interest in these systems is whether the aptamer is prefolded to recognize the ligand or whether it folds into its binding configuration in response to the ligand.

References:

1. Cowan, P. M.; McGavin, S. *Nature*, **1955**, *176*, 501-503.
2. Schimmel, P. R.; Flory, P. J. *Proc. Natl. Acad. Sci. U.S.A.*, **1967**, *58*, 52-59.
3. Schuler, B.; Lipman, E. A.; Steinbach, P. J.; Kumke, M.; Eaton, W. A. *Proc. Natl. Acad. Sci. U.S.A.*, **2005**, *102*, 2754-2759.
4. Watkins, L. P.; Chang, H.; Yang, H. *J. Phys. Chem. A* **2006**, *110*, 5191-5203.
5. Stryer, L.; Haugland, R. P. *Proc. Natl. Acad. Sci. U.S.A.*, **1967**, *58*, 719-726.
6. Sahoo, H.; Roccatano, D.; Hennig, A.; Nau, W. M. *J. Am. Chem. Soc.*, **2007**, *129*, 9762-9772.
7. Doose, S.; Neuweiler, H.; Barsch, H.; Sauer, M. *Proc. Natl. Acad. Sci. U.S.A.*, **2007**, *104*, 17400-17405.
8. Rüttinger, S.; Macdonald, R.; Krämer, B.; Koberling, F.; Roos, M.; Hildt, E. *Journal of Biomedical Optics* **2006**, *11*.
9. Best, R. B.; Merchant, K. A.; Gopich, I. V.; Schuler, B.; Bax, A.; Eaton, W. A. *Proc. Natl. Acad. Sci. U.S.A.* **2007**, *104*, 18964-18969.
10. Dolgih, E.; Ortiz, W.; Kim, S.; Krueger, B. P.; Krause, J. L.; Roitberg, A. E. *J. Phys. Chem. A* **2009**, *113*, 4639-4646.
11. Watkins, L. P.; Yang, H. *Biophysical Journal* **2004**, *86*, 4015-4029.
12. Hanson, J. A.; Duderstadt, K.; Watkins, L. P.; Bhattacharyya, S.; Yang, H. *Proc. Natl. Acad. Sci. U.S.A.* **2007**, *104*, 18055-18060.
13. Luong, A.K.; Gradinaru, C.C.; Chandler, D.W. and Hayden, C.C. *J. Phys. Chem. B*, **2005**, *109*, 15691.
14. Hayden, C.C.; Hwang, J.S.; Abate, E.A.; Kent, M.S. and Sasaki, D.Y. *J. Am. Chem. Soc.*, **2009**, *131*, 8728.

DOE sponsored publications, 2007-2009

1. C. S. Xu, H. Kim, H. Yang and C. C. Hayden, "Multiparameter Fluorescence Spectroscopy of Single Quantum Dot-Dye FRET Hybrids," *J. Am. Chem. Soc.*, **129** (36), 11008 -11009, 2007.
2. C. S. Xu, H. Kim, C. C. Hayden and H. Yang, "Joint Statistical Analysis of Multi-Channel Time Series from Single Quantum Dot-(Cy5)_n Constructs," *J. Phys. Chem. B*, *112* (19), 5917-5923, 2008.
3. H. Liu, G. D. Bachand, H. Kim, C. C. Hayden, E. A. Abate, and D. Y. Sasaki, "Lipid Nanotube Formation from Streptavidin-Membrane Binding," *Langmuir*, **24** (8), 3686 -3689, 2008.
4. C. C. Hayden, J. S. Hwang, E. A. Abate, M. S. Kent and D. Y. Sasaki, "Directed Formation of Lipid Membrane Microdomains as High Affinity Sites for His-Tagged Proteins," *J. Am. Chem. Soc.*, **131** (25), 8728-8729, 2009.

Chemical Kinetics and Dynamics at Interfaces

Laser induced reactions in solids and at surfaces

Wayne P. Hess (PI), Alan G. Joly and Kenneth M. Beck

Chemical and Materials Sciences Division
Pacific Northwest National Laboratory
P.O. Box 999, Mail Stop K8-88,
Richland, WA 99352, USA
wayne.hess@pnl.gov

Additional collaborators include A.L. Shluger, P.V. Sushko, N. Govind, K. Kowalski, J.T. Dickinson, K. Tanimura, G. Xiong, J.M. White, M. Henyk and O. Diwald

Program Scope

The chemistry and physics of electronically excited solids and surfaces is relevant to the fields of photocatalysis, radiation chemistry, and solar energy conversion. Irradiation of solid surfaces by UV, or higher energy photons, produces energetic species such as core holes and free electrons, that relax to form electron-hole pairs, excitons, and other transient species capable of driving surface and bulk reactions. These less energetic secondary products induce the transformations commonly regarded as radiation damage. The interaction between light and nanoscale oxide materials is fundamentally important in catalysis, microelectronics, sensor technology, and materials processing. Photo-stimulated desorption, of atoms or molecules, provides a direct window into these important processes and is particularly indicative of electronic excited state dynamics. Excited state chemistry in solids is inherently complex and greater understanding is gained using a combined experiment/theory approach. We therefore collaborate with leading solid-state theorists who use *ab initio* calculations to model results from our laser desorption and photoemission experiments.

Approach:

Photon energies are chosen to excite specific surface structural features that lead to particular desorption reactions. The photon energy selective approach takes advantage of energetic differences between surface and bulk exciton states and probes the surface exciton directly. We measure velocities and state distributions of desorbed atoms or molecules from ionic crystals using resonance enhanced multiphoton ionization and time-of-flight mass spectrometry. Application of this approach to controlling the yield and state distributions of desorbed species requires detailed knowledge of the atomic structure, optical properties, and electronic structure. To date we have thoroughly demonstrated surface-selective excitation and reaction on alkali halides. However, technological applications of alkali halides are limited compared to oxide materials. Oxides serve as dielectrics in microelectronics and form the basis for exotic semi- and super-conducting materials. Although the electronic structure of oxides differs considerably from alkali halides, it now appears possible to generalize the exciton model for laser surface reactions to these interesting new materials. Our recent studies have explored nanostructured samples grown by chemical vapor deposition or thin films grown by reactive ballistic deposition (RBD) in addition to cleaved single-crystal surfaces. We have demonstrated that desorbed atom product states can be selected by careful choice of laser wavelength, pulse duration, and delay between laser pulses. Recently, we have applied the technique of photoemission electron microscopy

(PEEM) to these efforts. In particular, we are developing a combined PEEM two-photon photoemission approach to probe spatially-resolved excited electronic state dynamics in nanostructured materials.

Recent Progress

Calculations indicate that it is possible to excite preferentially either the surface or bulk of ionic materials (crystals) and induce surface or bulk specific reactions. We have excited low-coordinated surface sites (e.g. corners, steps and terraces) using sub-bandgap photons and induced hyperthermal neutral atom emission. In parallel experiments we excited bulk transitions using above bandgap photon energies and induce only thermal neutral atom emission. The kinetic energy distributions provide a signature for the surface or bulk origin of the desorption mechanism. In the particular case of rough CaO films, we irradiate nanostructured CaO samples using tunable UV laser pulses and observe hyperthermal O-atom emission indicative of a surface excited-state desorption mechanism. The O-atom yield increases dramatically with photon energy, between 3.75 and 5.4 eV, well below the bulk absorption threshold. The peak of the kinetic energy distribution does not increase with photon energy in this energy range. When the data are analyzed, in the context of a laser desorption model developed previously for nanostructured MgO samples, the results are consistent with desorption induced by exciton localization at corner-hole trapped surface sites following electronic energy transfer from higher coordinated surface sites. In a study of nanostructured MgO thin films, neutral magnesium atom emission is induced using two-color nanosecond laser excitation. We find that combined visible/UV excitation, for single-color pulse energies below the desorption threshold, induces neutral Mg-atom emission with hyperthermal kinetic energies in the range of 0.1 – 0.2 eV. The observed metal atom emission is consistent with a mechanism involving rapid electron transfer to 3-coordinated Mg surface sites. The two-color Mg-atom signal is significant only for parallel laser polarizations and temporally overlapped laser pulses indicating that intermediate excited states are short-lived and likely of sub-nanosecond duration.

Future Directions

Since it is possible to selectively excite terrace, step, or corner surface sites, we have explored various sample preparation techniques that produce high concentrations of low-coordinated surface sites such as 4-coordinated steps and 3-coordinated corner or kink sites. In particular, we have employed reactive ballistic deposition (a technique developed in Bruce Kay's lab) to grow very high surface area MgO and CaO thin films. These films have been thoroughly characterized using XPS, SEM, TEM, and XRD techniques. Similarly, we have also studied laser desorption of MgO and CaO nano-powders grown by a chemical vapor deposition technique (in collaboration with Oliver Diwald of the Technical University of Vienna). The MgO nano-powders show cubic structure and edge lengths ranging between 3 and 10 nm (through TEM analysis).

If exciton-based desorption can be generalized from alkali halides to metal oxides then selective excitation of specific surface sites could lead to controllable surface modification, on an atomic scale, for a general class of technologically important materials. While exciton-based desorption is plausible for MgO and CaO, we note that the higher valence requires a more complex mechanism. With the aid of DFT calculations we have developed such a hyperthermal desorption mechanism that relies on the combination of a surface exciton with a three-coordinated surface-trapped hole, a so-called "hole plus exciton" mechanism. In every instance we have studied, a hyperthermal O-atom KE distribution can be linked to an electronic surface excited state desorption mechanism. In contrast, a thermal O-atom KE distribution clearly indicates a bulk derived origin for desorption. In analogy to alkali halide thermal desorption, we have considered

a bulk-based thermal desorption mechanism involving trapping of two holes at a three-coordinated site (a “two-hole localization” mechanism). Our calculations, however, do not indicate that two-hole localization is likely without invoking a dynamical trapping process. The details of these mechanisms need to be further delineated and confirmed by demonstrating control of the various desorption processes.

Most recently we have observed formation of zinc nanoparticles on the surface of ZnO crystals following intense 6.4 eV laser excitation. Zinc metal forms following preferential removal of oxygen hyperthermal neutral Zn-atom desorption. This is a novel method for preparation of 10 nm metal particles. We plan to grow and study several other oxide surfaces in the near term including ZrO₂, BaO, and TiO₂. Future plans include femtosecond PEEM to study Plasmon resonant photoemission from noble metal nanostructures and pulse-pair PEEM to probe dynamics of oxide nanostructures on surfaces. We are also presently developing capabilities to perform energy-resolved two-photon photoemission using a hemispherical analyzer XPS instrument. In combination we expect these two techniques will provide the first *spatially-resolved* electronic state dynamics of nanostructured oxide materials.

References to publications of DOE BES sponsored research (2006 to present)

1. “Site-specific laser modification of MgO nano-clusters: Towards atomic scale surface structuring.” KM Beck, M Henyk, C Wang, PE Trevisanutto, PV Sushko, WP Hess, and AL Shluger, *Phys. Rev. B* **74**, 045404 (2006).
2. “Carrier Dynamics in α -Fe₂O₃ Thin-films and Single Crystals Probed by Femtosecond Transient Absorption and Reflectivity.” AG Joly, JR Williams, SA Chambers, G Xiong, WP Hess, and DM Laman, *J. Appl. Phys.* **99**, 1 (2006).
3. “Introduction to Photoelectron Emission Microscopy: Principles and Applications.” G Xiong, AG Joly, WP Hess, M Cai, and JT Dickinson, *J. Chin. Elec. Microsc. Soc.* **25**, 16 (2006).
4. “In-situ photoemission electron microscopy study of thermally-induced martensitic transformation in CuZnAl shape memory alloy.” G Xiong, AG Joly, KM Beck, WP Hess, M Cai, SC Langford, and JT Dickinson, *Appl. Phys. Lett.* **88**, 091910 (2006).
5. “Two-hole localization mechanism for electronic bond rupture of surface atoms by laser-induced valence excitation of semiconductors.” K Tanimura, E Inami, J Kanasaki, and WP Hess *Phys. Rev. B* **74**, 035337 (2006).
6. “Excited carrier dynamics of α -Cr₂O₃/ α -Fe₂O₃ core-shell nanostructures.” G Xiong, AG Joly, WP Hess, G Holtom, CM Wang, DE McCready, and KM Beck, *J. Phys. Chem. B* **110**, 16937 (2006).
7. “Probing electron transfer dynamics at MgO surfaces by Mg-atom desorption.” A.G. Joly, M Henyk, KM Beck, PE Trevisanutto, PV Sushko, WP Hess, and AL Shluger, *J. Phys. Chem. B Lett.* **110**, 18093 (2006).
8. “Laser-induced oxygen vacancy formation and diffusion on TiO₂ (110) surfaces probed by photoemission electron microscopy.” G Xiong, AG Joly, KM Beck, WP Hess, *Phys. Stat. Sol. (c)* **3**, 3598 (2006).

9. "Study of martensitic phase transformation in a NiTiCu thin film shape memory alloy using photoelectron emission microscopy." M Cai, SC Langford, JT Dickinson, MJ Wu, WM Huang, G Xiong, TC Droubay, AG Joly, KM Beck, and WP Hess, *Adv. Funct. Mater.* **17**, 161 (2007).
10. "An *In-situ* Study of the Martensitic Transformation in Shape Memory Alloys using Photoemission Electron Microscopy," M Cai, SC Langford, JT Dickinson, G Xiong, TC Droubay, AG Joly, KM Beck and WP Hess, *J. Nuc. Mater.* **361**, 306 (2007).
11. "Study of copper diffusion through a ruthenium thin film by photoemission electron microscopy." W. Wei, S. L. Parker, Y.-M. Sun, and J. M. White, G Xiong, AG Joly, KM Beck, and WP Hess, *Appl. Phys. Lett.* **90**, 111906 (2007).
12. "Synthesis and photoexcited charge carrier dynamics of β -FeOOH nanorods." AG Joly, G Xiong, C Wang, DE McCready, KM Beck, and WP Hess, *Appl. Phys. Lett.* **90**, 103504 (2007).
13. "Photoemission electron microscopy of TiO₂ anatase films embedded with rutile nanocrystals." G Xiong, R Shao, TC Droubay, AG Joly, KM Beck, SA Chambers, and WP Hess, *Adv. Funct. Mater.* **17**, 2133 (2007).
14. "Proceedings of the Eighth International Conference on Laser Ablation (COLA 05)." WP Hess, PR Herman, D Bäuerle, and H Koinuma, Editors, *Journal of Physics: Conference Series*, Vol. **59**, pages 1 -729 (2007).
15. K.M. Beck, A.G. Joly, O. Diwald, S. Stankic, P.E. Trevisanutto, P.V. Sushko, A.L. Shluger, and W.P. Hess, "Energy and site selectivity in O-atom photodesorption from nanostructured MgO," *Surf. Sci.* **602**, 1968 (2008).
16. A.G. Joly, K.M. Beck, and W.P. Hess, "Electronic energy transfer on CaO surfaces," *J. Chem. Phys.* **129**, 13 (2008).
17. P.E. Trevisanutto, P.V. Sushko, A.L. Shluger, K.M. Beck, A.G. Joly, and W.P. Hess, "Excitation, ionization, and desorption: how sub-band-gap photons modify the electronic properties and atomic structure of oxide nanoparticles," *J. Phys. Chem. C* **113**, 1274 (2009).
18. E.H. Khan, S.C. Langford, J.T. Dickinson, L.A. Boatner, and W.P. Hess, "Photoinduced Formation of Zinc Nanoparticles by UV Laser Irradiation of ZnO," *Langmuir*, **25**, 1930 (2009).
19. Govind, P. V. Sushko W. P. Hess, M. Valiev, K. Kowalski, "Excitons in insulators: a study using embedded time-dependent density functional theory and equation-of-motion coupled cluster methods," *Chem. Phys. Lett.* **470**, 353 (2009).
20. K.M. Beck, A.G. Joly, and W.P. Hess, "Two-color laser desorption of nanostructured MgO thin films," *Appl. Surf. Sci.* (published online).

Breakthrough Design and Implementation of Electronic and Vibrational Many-Body Theories

So Hirata (principal investigator: DE-FG02-04ER15621)

Quantum Theory Project and The Center for Macromolecular Science and Engineering,
Departments of Chemistry and Physics, University of Florida, Gainesville, FL 32611

hirata@qtp.ufl.edu

Program Scope

Predictive chemical computing requires hierarchical many-body methods of increasing accuracy for both electronic and vibrational problems. Such hierarchies are established, at least conceptually, as configuration-interaction (CI), many-body perturbation (PT), and coupled-cluster (CC) methods for electrons and for vibrations, which all converge at the exact limit with increasing rank of a hierarchical series. These methods can generate results of which the convergence with respect to various parameters of calculations can be demonstrated and which can be predictive in the absence of experimental information.

The progress in these methods and their wide use are, however, hindered by (1) the immense complexity and cost of designing and implementing some of the high-rank members of the hierarchical methods and by (2) the extremely slow convergence of electronic energies and wave functions with respect to one-electron basis set sizes, which is compounded with the high-rank polynomial or even exponential molecular size dependence of the computational cost of these methods.

The overarching goal of our research is to address both difficulties for electrons and vibrations. We will eradicate the first difficulty for electrons by developing a computerized symbolic algebra system that completely automates the mathematical derivations of electron-correlation methods and their implementation. For vibrations, the vibrational SCF (VSCF) and CI (VCI) codes will be developed in the general-order algorithm that is applicable to polyatomic molecules and allows us to include anharmonicity and vibrational mode-mode couplings to any desired extent. We address the second difficulty by radically departing from the conventional Gaussian basis set and introduce a new hierarchy of converging electron-correlation methods with completely flexible but rational (e.g., satisfying asymptotic decay and cusp conditions) basis functions such as numerical basis functions on interlocking multicenter quadrature grids and explicit r_{12} (inter-electronic distance) dependent basis functions. They, when combined with high-rank electron-correlation methods, can in fact achieve the exact solutions of the Schrödinger equation. Also, these predictive electronic and vibrational methods based on MP2, CC, VSCF, and VMP2 are extended to large molecules such as polymers and molecular crystals.

Recent Progress

Significant progress has been made in the last year. Capitalizing upon the developments made in the previous year,^{16,19} we have implemented^{8,13} complete explicitly correlated CC methods including up to connected quadruple excitation operator, namely, F12-CCSDT and F12-CCSDTQ as well as explicitly-correlated combined CC and PT methods such as F12-CCSD(T), F12-CCSD(2)_T, F12-CCSD(2)_{TQ}, F12-CCSD(3)_T, F12-CCSDT(2)_Q, etc. Together with the F12-CCSD method reported by us,¹⁶ these methods form a hierarchy of systematic approximations that are most rapidly converging toward the exact solutions of the Schrödinger equations of general polyatomic molecules. In Ref. 13, we have demonstrated that a combination of these methods can predict the exact eigenvalue solutions of the Schrödinger equation of small polyatomic molecules such as hydrogen fluoride and water within a few kcal/mol without resorting to statistical treatments or empirical extrapolations. While one is rarely interested in total energies, our ability to compute them with such high accuracy will have a great impact on all areas of chemistry.

We have also extended electronic and vibrational many-body methods to solids. In Ref. 12, we applied rigorous electron-correlation treatments such as second-order Møller–Plesset (MP2) and CC singles and doubles (CCSD) as well as perturbative triples [CCSD(T)] to energies, structures, and phonon dispersions as well as phonon densities of solid hydrogen fluoride. Our linear-scaling, localized-basis scheme¹⁴ underlying this application is only loosely coupled with the periodic boundary conditions and can obtain the frequencies of the phonons that lift the periodic symmetry. Furthermore, not only harmonic frequencies but also anharmonic frequencies of infrared- and/or Raman-active phonons have been obtained by *vibrational* MP2 in the two-mode coupling and the Γ approximations (see below) to provide accurate predictions. We have also introduced¹¹ a

new approximation that brings about one to two orders of magnitude speedup in the MP2 crystalline orbital (CO) method for energies and quasi-particle energy bands. We have applied⁷ this to computationally reproduce the (angle-resolved) photoelectron spectra of polyacetylenes and polyethylene and predict the spectra of polydiacetylene.

We have performed chemical applications of vibrational many-body methods on 7 key species of hydrocarbon combustion, interstellar, and/or atmospheric chemistry¹⁰ as well as on the guanine–cytosine base pair.⁹ The latter application has shed light on the nature of vibrational energy dissipation in base pairs (and hydrogen-bonded complexes in general) as a DNA photoprotection mechanism. We have also derived⁶ an important, general conclusion on the errors due to the Born–Oppenheimer approximation and its diagonal corrections applying a BO-like separation between light and heavy particle motion in the anharmonic vibrations of FHF⁻.

Since the 2008 DOE Research Meeting (CPIMS), 10 papers^{4–13} have been published including 2 invited articles and 3 book chapters. In total, 37 publications^{1–37} have resulted from this grant in 2006–09. In 2008–09, the PI has been an invited speaker at 20 conferences and university seminars. The PI has also been selected to receive National Science Foundation’s CAREER Award and Camille Dreyfus Teacher-Scholar Award and his students working on the DOE project have won two best poster awards, a best contributed lecture award, a Japan Society for Promotion of Science fellowship, a dissertation award, an ACS Graduate Student Award in Computational Chemistry, a physical chemistry division award, and an alumni fellowship. The PI has also been invited to contribute reviews or perspectives to *Annual Reports of Computational Chemistry* and *Physical Chemistry Chemical Physics*.

Higher-order explicitly correlated CC methods^{13,16} and combined CC and PT methods⁸ Efficient computer codes for the explicitly correlated CC (R12- or F12-CC) methods with up to quadruple excitations and explicitly correlated combined CC and PT methods, which take account of the spin, Abelian point-group, and index-permutation symmetries and are based on complete diagrammatic equations,²⁴ have been implemented with the aid of the computerized symbolic algebra SMITH. Together with the explicitly correlated CCSD (F12-CCSD) method reported earlier,¹⁶ they form a hierarchy of systematic approximations [F12-CCSD, F12-CCSD(T), F12-CCSD(2)_T, F12-CCSD(3)_T, F12-CCSDT, F12-CCSD(2)_{TQ}, F12-CCSDT(2)_Q, F12-CCSDTQ] that converge most rapidly toward the exact solutions of the polyatomic Schrödinger equations with respect to both the highest excitation rank and basis-set size. Using the Slater-type function $1 - \exp(-\eta r_{12})$ as a correlation function, a F12-CC method can provide the aug-cc-pV5Z-quality results of the conventional CC method of the same excitation rank using only the aug-cc-pVTZ basis set. Combining these F12-CC methods with the grid-based, numerical Hartree–Fock equation solver,²² the exact solutions (eigenvalues) of the Schrödinger equations of neon, boron hydride, hydrogen fluoride, and water at their equilibrium geometries have been obtained as -128.9377 ± 0.0004 , -25.2892 ± 0.0002 , -100.459 ± 0.001 , and $-76.437 \pm 0.003 E_h$, respectively, without resorting to complete-basis-set extrapolations. These absolute total energies or the corresponding correlation energies agree within the quoted uncertainty with the accurate, nonrelativistic, Born–Oppenheimer values derived experimentally and/or computationally. These studies^{8,13,16,24} have been the focus of our review on explicitly correlated CC methods that is to be published in *Annual Reports of Computational Chemistry*⁴ and also a part of our book chapter.²

CC and MP 2 study of energies, structures, and phonons of solid hydrogen fluoride¹² With the binary-interaction method,¹⁴ we have optimized the geometry and obtained the phonon dispersion curves of solid hydrogen fluoride at the CCSD/aug-cc-pVDZ and BSSE-corrected MP2/aug-cc-pVTZ levels. The predicted geometries have been in quantitative agreement with the diffraction data. The calculated frequencies of the infrared- and/or Raman-active phonons do not agree with the observed, with the largest errors exceeding a few hundred cm^{-1} (Fig. 1). The errors are not due to the electronic structure treatment, but are caused by strong anharmonicity in the potential energy surfaces of this hydrogen-bonded solid. When we perform a vibrational MP2 calculation in the Γ approximation using the potential energy surface scanned by the binary-interaction method, vastly improved agreement is achieved between the first-principles theory and experiments (Fig. 1). The bands in the observed inelastic neutron scattering

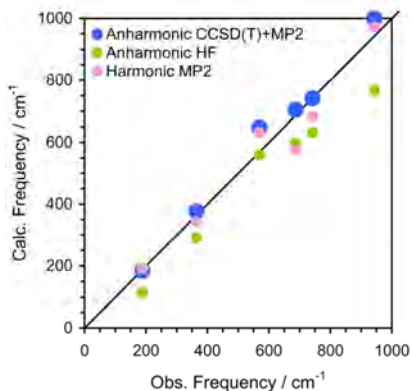


Fig.1 Calculated and observed phonon frequencies of solid hydrogen fluoride.

from solid hydrogen fluoride have also been straightforwardly assignable to the peaks in the hydrogen-amplitude-weighted phonon density of states (harmonic).

Efficient Brillouin-zone integrations in MP2 for extended systems of one-dimensional periodicity.^{7,11} The validity and accuracy of various ways of drastically reducing the number of k -points in the Brillouin zone integrations occurring in MP2 calculations of one-dimensional solids has been investigated. The most promising approximation can recover correlation energies of polyethylene and polyacetylene within 1% of converged values at less than a tenth of usual computational cost. The quasi-particle energy bands have also been reproduced quantitatively with the same approximation. In the most drastic approximation, in which only one zone-center k -point (Γ point) in the BZ is sampled (the Γ approximation), the correlation energies are recovered within 10% of the converged values with a speedup by a factor of 80–100. The (angle-resolved) photoelectron spectra of *trans*- and *cis*-polyacetylenes, polyethylene, and polydiacetylene have been reproduced accurately or predicted by MP2 with this scheme (Fig. 2).

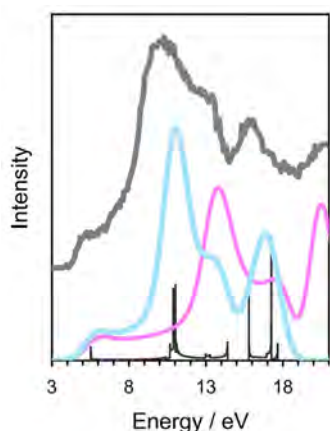


Fig. 2 Photoelectron spectra of *trans*-polyacetylene. The grey curves: experiment; red curves: HF/6-31G*; blue curves: MP2/6-31G*; black histogram: MP2/6-31G* density of states.

Anharmonic vibrational frequencies and vibrationally averaged structures of key species in hydrocarbon combustion.¹⁰ A general scheme to predict anharmonic vibrational frequencies and vibrationally averaged structures and rotational constants of molecules is proposed with applications to HCO^+ , HCO , HNO , HOO , HOO^- , CH_3^+ , and CH_3 . A combination of CCSD, CCSD with a second-order perturbation correction in the space of triples and in the space of triples and quadruples, and a correlation-consistent basis set series has been employed to achieve the complete-correlation, complete-basis-set limits of the potential energy surfaces of these species near equilibrium geometries. A new representation of potential energy surfaces that combines two existing representations, namely, a fourth-order Taylor expansion and numerical values on a rectilinear grid, has been proposed and shown to yield accurate frequencies, when combined with vibrational general-order configuration-interaction method. The mean absolute deviation in the predicted frequencies is 11 cm^{-1} .

First-principles quantum anharmonic dynamics simulations on the guanine-cytosine base pair.⁹ The origin of extremely broad features in the $2800\text{--}3800\text{-cm}^{-1}$ region of the infrared spectrum of the guanine-cytosine (GC) base pair remains a mystery. Unraveling this is crucial in understanding the ultrafast relaxation (< 100 femtoseconds) of the NH stretching vibrational energy that is believed to help protect DNA against a UV damage. We have carried out a full 81 dimensional quantum anharmonic vibrational calculations combined with *ab initio* potential energy surface to study the spectrum and dynamics of the GC base pair. A strong vibrational resonance among fundamental tones of intermolecular NH stretching modes (red-shifted by hydrogen bonds) and various overtones and combination tones of fingerprint modes is shown to play a vital role in the manifestation of the observed phenomena.

The nature of the Born–Oppenheimer (BO) approximation.⁶ In 2006, Takahashi and Takatsuka [*J. Chem. Phys.* **124**, 144101 (2006)] concluded that the errors in the BO approximation are proportional to the $3/2$ power of the mass ratio of light to heavy particles (m/M). We have revisited this problem and on the basis of both analytical and numerical investigations revised their conclusion. The correct scaling is $(m/M)^1$. The errors decrease and are proportional to $(m/M)^{3/2}$ and $(m/M)^2$, respectively, when the diagonal BO corrections are included either in the first-order perturbation theory or variationally.

Future Plans

Important extensions of the F12-CC methods include a new ansatz for accelerating the basis-set convergence of the connected triples contributions in CC energies, a treatment of ionization and electron-attachment energies, and an extension to extended systems. The combinations of the F12-CC methods with the vibrational many-body methods as well as the binary-interaction method for molecular clusters and crystals are being examined. The latter methods are being extended to covalently bonded macromolecules. The k -point downsampling will be applied to CCSD for polymers. A new and even more efficient downsampling scheme is being implemented. A whole array of vibrational many-body methods for anharmonic lattice vibrations is formulated and some preliminary applications are being carried out.

References to Publications of DOE Sponsored Research (2006–Present)

1. **Book chapter:** S. Hirata, O. Sode, M. Keçeli, and T. Shimazaki, "Electron correlation in solids: delocalized and localized orbital approaches," in *Accurate Condensed-Phase Quantum Chemistry* (in press, Taylor & Francis, 2009).
2. **Book chapter:** S. Hirata, T. Shiozaki, E. F. Valeev, and M. Noijien, "Eclectic electron-correlation methods," in *Recent Progress in Coupled-Cluster Methods: Theory and Application* (in press, Springer, 2009).
3. **Book chapter:** S. Hirata *et al.*, "Computational interstellar chemistry," in *Recent Advances in Spectroscopy: Astrophysical, Theoretical and Experimental Perspective* (in press, Springer, 2009).
4. **Invited article:** T. Shiozaki, E. F. Valeev, and S. Hirata, *Annual Reports of Computational Chemistry* (in press, 2009), "Explicitly correlated coupled-cluster methods."
5. **Invited article:** S. Hirata, *Physical Chemistry Chemical Physics* [Perspective] (in press, 2009), "Quantum chemistry of macromolecules and solids."
6. S. Hirata, E. B. Miller, Y.-Y. Ohnishi, and K. Yagi, *The Journal of Physical Chemistry A* [Pitzer Special Issue] (in press, 2009), "On the validity of the Born-Oppenheimer separation and the accuracy of diagonal corrections in anharmonic molecular vibrations."
7. S. Hirata and T. Shimazaki, *Physical Review B* **80**, 085118 (2009) (7 pages), "Fast second-order many-body perturbation method for extended systems."
8. T. Shiozaki, S. Hirata, and E. F. Valeev, *The Journal of Chemical Physics* **131**, 044118 (2009) (12 pages), "Explicitly correlated combined coupled-cluster and perturbation methods."
9. K. Yagi, H. Karasawa, S. Hirata, and K. Hirao, *ChemPhysChem* **10**, 1442–1444 (2009), "First-principles quantum vibrational simulations of the guanine-cytosine base pair."
10. M. Keçeli, T. Shiozaki, K. Yagi, and S. Hirata, *Molecular Physics* [Schaefer Special Issue] **107**, 1283–1301 (2009), "Anharmonic vibrational frequencies and vibrationally-averaged structures of key species in hydrocarbon combustion: HCO^{*}, HCO, HNO, HOO, HOO^{*}, CH₃⁺, and CH₃."
11. T. Shimazaki and S. Hirata, *International Journal of Quantum Chemistry* [Harris Special Issue] **109**, 2953–2959 (2009), "On the Brillouin-zone integrations in second-order many-body perturbation calculations for extended systems of one-dimensional periodicity"
12. O. Sode, M. Keçeli, S. Hirata, and K. Yagi, *International Journal of Quantum Chemistry* [Hirao Special Issue] **109**, 1928–1938 (2009), "Coupled-cluster and many-body perturbation study of energies, structures, and phonon dispersions of solid hydrogen fluoride."
13. T. Shiozaki, M. Kamiya, S. Hirata, and E. F. Valeev, *The Journal of Chemical Physics* **130**, 054101 (2009) (10 pages), "Higher-order explicitly correlated coupled-cluster methods."
14. S. Hirata, *The Journal of Chemical Physics* **129**, 204104 (2008) (11 pages), "Fast electron-correlation methods for molecular crystals: An application to the α , β_1 , and β_2 modifications of solid formic acid."
15. **Invited article:** S. Hirata and K. Yagi, *Chemical Physics Letters* **464**, 123–134 (2008) [a Frontiers article], "Predictive electronic and vibrational many-body methods for molecules and macromolecules."
16. T. Shiozaki, M. Kamiya, S. Hirata and E. F. Valeev, *The Journal Chemical Physics (Communications)* **129**, 071101 (2008) (4 pages), "Explicitly correlated coupled-cluster singles and doubles method based on complete diagrammatic equations."
17. **Book chapter:** S. Hirata, P.-D. Fan, T. Shiozaki, and Y. Shigeta, *Radiation Induced Molecular Phenomena in Nucleic Acid: A Comprehensive Theoretical and Experimental Analysis* edited by Jerzy Leszczynski and Manoj Shukla (Springer, 2008), "Single-reference methods for excited states in molecules and polymers."
18. S. Hirata, K. Yagi, S. A. Perera, S. Yamazaki, and K. Hirao, *The Journal of Chemical Physics* **128**, 214305 (2008) (9 pages), "Anharmonic vibrational frequencies and vibrationally averaged structures and nuclear magnetic resonance parameters of FHF^{*}."
19. **Invited article:** T. Shiozaki, M. Kamiya, S. Hirata, and E. F. Valeev, *Physical Chemistry Chemical Physics* **10**, 3358–3370 (2008) [in the issue on "Explicit-R12 correlation methods and local correlation methods"], "Equations of explicitly-correlated coupled-cluster methods."
20. K. Yagi, S. Hirata, and K. Hirao, *Physical Chemistry Chemical Physics* **10**, 1781–1788 (2008), "Vibrational quasi-degenerate perturbation theory: Application to Fermi resonances in CO₂, H₂CO, and C₆H₆."
21. M. Kamiya, S. Hirata, and M. Valiev, *The Journal of Chemical Physics* **128**, 074103 (2008) (11 pages), "Fast electron correlation methods for molecular clusters without basis set superposition errors."
22. T. Shiozaki and S. Hirata, *Physical Review A (Rapid Communications)* **76**, 040503(R) (2007) (4 pages), "Grid-based numerical Hartree–Fock solutions of polyatomic molecules."
23. K. Yagi, S. Hirata, and K. Hirao, *The Journal of Chemical Physics* **127**, 034111 (2007) (7 pages), "Efficient configuration selection scheme for vibrational second-order perturbation theory."
24. T. Shiozaki, K. Hirao, and S. Hirata, *The Journal of Chemical Physics* **126**, 244106 (2007) (11 pages), "Second- and third-order triples and quadruples corrections to coupled-cluster singles and doubles in the ground and excited states."
25. M. Kamiya and S. Hirata, *The Journal of Chemical Physics* **126**, 134112 (2007) (10 pages), "Higher-order equation-of-motion coupled-cluster methods for electron attachment."
26. P.-D. Fan, M. Kamiya, and S. Hirata, *The Journal of Chemical Theory and Computation* **3**, 1036–1046 (2007), "Active-space equation-of-motion coupled-cluster methods through quadruple excitations for excited, ionized, and electron-attached states."
27. V. Rodriguez-Garcia, S. Hirata, K. Yagi, K. Hirao, T. Taketsugu, I. Schweigert, and M. Tasumi, *The Journal of Chemical Physics* **126**, 124303 (2007) (6 pages), "Fermi resonance in CO₂: A combined electronic coupled-cluster and vibrational configuration-interaction prediction."
28. K. Yagi, S. Hirata, and K. Hirao, *Theoretical Chemistry Accounts* **118**, 681–691 (2007) [Fraga special issue], "Multiresolution potential energy surfaces for vibrational state calculations."
29. S. Hirata, T. Yanai, R. J. Harrison, M. Kamiya, and P.-D. Fan, *The Journal of Chemical Physics* **126**, 024104 (2007), "High-order electron-correlation methods with scalar relativistic and spin-orbit corrections."
30. **Invited article:** S. Hirata, *Journal of Physics: Conference Series* **46**, 249–253 (2006), "Automated symbolic algebra for quantum chemistry."
31. M. Kamiya and S. Hirata, *The Journal of Chemical Physics* **125**, 074111 (2006), "Higher-order equation-of-motion coupled-cluster methods for ionization processes."
32. **Invited article:** S. Hirata, *Theoretical Chemistry Accounts* **116**, 2–17 (2006) [a part of the special issue "New Perspective in Theoretical Chemistry"], "Symbolic algebra in quantum chemistry."
33. V. Rodriguez-Garcia, K. Yagi, K. Hirao, S. Iwata, and S. Hirata, *The Journal of Chemical Physics* **125**, 014109 (2006) [selected as an article in *Virtual Journal of Biological Physics Research*, July 15 (2006)], "Franck–Condon factors based on anharmonic vibrational wave functions of polyatomic molecules."
34. **Invited article:** Y. Shao, *et al.* *Physical Chemistry Chemical Physics* **8**, 3172–3191 (2006), "Advances in methods and algorithms in a modern quantum chemistry package."
35. P.-D. Fan and S. Hirata, *The Journal of Chemical Physics* **124**, 104108 (2006), "Active-space coupled-cluster methods through connected quadruple excitations."
36. Y. Shigeta, K. Hirao, and S. Hirata, *Physical Review A (Rapid Communications)* **73**, 010502(R) (2006), "Exact-exchange time-dependent density-functional theory with the frequency-dependent kernel."
37. **Invited article:** P. Piecuch, S. Hirata, K. Kowalski, P.-D. Fan, and T. L. Windus, *International Journal of Quantum Chemistry* **106**, 79–97 (2006), "Automated derivation and parallel computer implementation of renormalized and active-space coupled-cluster methods."

Spectroscopic Imaging Toward Space-Time Limit

Wilson Ho

Department of Physics & Astronomy and Department of Chemistry
University of California, Irvine
Irvine, CA 92697-4575 USA

wilsonho@uci.edu

Program Scope:

The ability to probe changes in real time with sub-Ångström spatial resolution would open a new window for viewing the inner machinery of matter. A promising approach involves the combination of laser with the scanning tunneling microscope (STM). Diffraction limited spatial resolution has been defeated through the demonstration of sub-Ångström resolution in spectroscopic, optical imaging, and photo-induced electron transfer. Thermal effects due to laser irradiation have been controlled. Current research aims at reaching an additional goal in the time domain by pushing spectroscopic imaging toward the simultaneous limits of sub-Ångström and <50 femtoseconds. Four focused activities have been identified, and all are designed to probe and image the dynamic properties in the interior of single molecules and artificially created nanostructures: 1. Spatially, spectroscopically, and temporally resolved photon imaging, 2. Direct measurement of photo-induced tunneling current, 3. Photo-induced electron tunneling in the time domain, and 4. Multi-electron induced light emission. These experiments would lead to a fundamental understanding of matter by revealing them in previously unattainable regimes of space and time. Furthermore, knowledge of the coupling of light to nanoscale objects bring us one step closer toward the realization of efficient conversion of sun light to energy, broad range of optoelectronics and plasmonics, and economically competitive photocatalysis.

Recent Progress:

Fermi's Golden Rule is one of the pivotal principles that are being taught in every course on quantum mechanics. The Rule enables the calculation of the rate of transition between two states of a system. This rate is invariably integrated over the spatial coordinates in the matrix element. Using the scanning tunneling microscope (STM), it has become possible to obtain a spatially resolved image of the transition rate and obtain results that are hidden and averaged in the integration. The STM is used to manipulate individual Ag atoms to form an atomic chain that exhibits properties of a one-dimensional particle-in-a-box. An electron from the tip of the STM is injected at a specific location into an excited state of the 1-D box and a photon is emitted and detected when the electron decays to a lower lying state of the box. The simplicity of the wavefunctions for the 1-D box leads to photon emission images that are easy to interpret, visualize, and grasp. Such images provide a picture of the integrand in the matrix element, the spatially dependent, inner ingredients of the Fermi's Golden Rule. These "textbook" results not only lead to direct visualization of a quantum mechanical rule, they also shed new light on optical phenomena at the sub-nanometer scale.

The role of the spatially oscillating electronic states of a chain of 10 Ag atoms (Ag_{10}) in the optical transitions is determined from imaging of the photon emission. Photon imaging of different emission energies at a fixed bias of 3.45 V allows investigation of final states effects. Not every final state could be probed because of the limited photon detection window of the CCD (1.3 eV to 3.0 eV) and spectral range of the plasmon modes. For 3.45 V bias, final states from the first five states of the 1-D particle-in-the-box states can be accessed (Fig. 1). With emission energies from 2.85 eV to 1.55 eV, photon images show 0 (nearly no signal), 1, 2, 3, and 4 bright maxima. A comparison with the corresponding final-states $dI/dV_{(f)}$ images reveals that the number of emission maxima is equivalent to the number of nodes. Furthermore, the distributions of emission maxima directly coincide with the positions of nodes in $dI/dV_{(f)}$ images. The entire emission spectrum was recorded at each pixel of the x-y image. The different images correspond to integrated energy slices within each spectrum. These results are consistent for different chain lengths, scanning directions, and biases. We can completely exclude any influence on the photon emission images from feedback or tip movement.

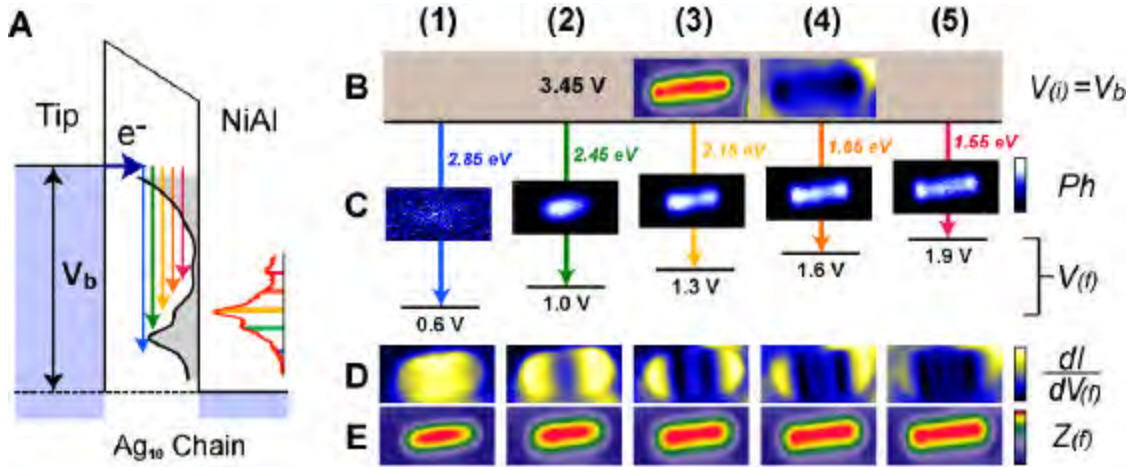


Fig. 1: (A) Schematic representation of radiative transitions in Ag_{10} . Electrons undergo transitions between the silver chain states (black curve, dI/dV at center of Ag_{10}), and the corresponding photon emission spectrum (red curve, emission at center of Ag_{10}). Horizontal arrow indicates the injection of tunneling electron. Five vertical arrows of different colors show transitions into the LDOS of Ag_{10} . (B) Topography (left) and simultaneous dI/dV image (right) at 3.45 V, which is the initial state of all the transitions shown below. (C) Photon emission (Ph) for different energies from transitions between the same initial state $V_{(i)}$ to five different final states at $V_{(f)}$. The photon images shown here are $3.6 \text{ nm} \times 1.8 \text{ nm}$ (96×48 pixels) and accumulated under 6 nA tunneling current, and 1 second spectral accumulation at each pixel. The range for the integrated intensity is $\pm 0.2 \text{ eV}$. (As an example, we integrate the spectrum at each pixel from 1.28 eV to 1.32 eV for the photon image at 1.3 eV.) The photon images show 0, 1, 2, 3, and 4 maxima as the photon energy decreases from 2.85 eV to 1.55 eV. Each photon image is displayed over the full range of intensity for the shown palette so the intensity cannot be compared from one to another. (D) $dI/dV_{(f)}$ images for the five final states showing 0, 1, 2, 3, and 4 nodes (dark bands) for the ground state, first, second, third, and fourth excited states of the particle-in-a-box. Note that the positions of the emission maxima coincide with the nodes in $dI/dV_{(f)}$ images. (E) Topographic images ($Z_{(f)}$) of the Ag_{10} chain at biases corresponding to different final states, $V_{(f)}$. The images of this chain yield a length of 2.9-3.4 nm, with the variation due to the dependence of the image on bias voltage. Images for (B), (D), and (E) have the same size: $3.9 \text{ nm} \times 1.95 \text{ nm}$ (64×32 pixels), taken at 1 nA tunneling current.

Future Plans:

The detection of spatially and vibronically resolved fluorescence from single molecules provides information on the vibrational and electronic states involved in the radiative transition. With time resolution of the fluorescence signal, the dynamics of the radiative transition is measured as a function of the position in the molecule. Thus the measurement is in 4-dimensions: intensity, space, time, and energy (wavelength of the emitted photon). In addition, the other variables that will also be in the measurements are: sample bias, tunneling current, and photon energy.

The first experiment is to demonstrate laser induced fluorescence via photo-induced tunneling from Mg-porphine adsorbed on 5 Å thick alumina film grown on the NiAl(110) surface since this system has shown to be photoactive on the surface and has been fully characterized. The demonstration of laser induced fluorescence with sub-Å spatial resolution leads directly into time resolved fluorescence measurements where for the first time it will be possible to achieve spectroscopic imaging with simultaneous temporal (10-100 ps) and spatial limit (sub-Å).

To reach the ultimate spatial resolution of sub-Å, the plasmon enhanced light field needs to couple to the tunneling process. Irradiation of the tunnel junction with light raises the question on the stability of the STM since the absorption of light inputs thermal energy to the junction, causing the STM to drift. We have found solutions to this problem of junction heating using two methods. One of our goals is to measure directly the magnitude and time dependence of photo-induced current, thus providing the gateway to experiments probing dynamics at the simultaneous space-time limit.

Nonlinear optics such as two-photon induced fluorescence can reveal properties of the system that are different than those probed by one photon absorption followed light emission. In order to observe two-photon process, the intensity of the irradiation has to be sufficiently high so that there is likelihood that two photons can be absorbed simultaneously.

Two photon induced fluorescence was observed not long after the invention of the pulsed laser in the 1960's, with the theoretical prediction of two-photon excitation advanced 30 years earlier. A similar question can be posed in the possibility of two-electron induced fluorescence in addition to the one-electron process. The high current density achievable in the STM junction makes it possible to reach the condition for two-electron induced light emission, a nonlinear process with sub-Å spatial resolution since the electrons are still confined by the tunneling process.

Experiments are desirable to answer questions such as the following. Are there any differences, either obvious or subtle, in the spectral features (intensity and position of peaks)? How do the spatial images of the photon emission related to the surface geometric structure in one-electron versus two-electron processes? Why are the exponents in the multi-electron process differ from integer values? Can we extract dynamic information from the magnitude of the current where two-electron induced processes become prominent? Note that for 10 microA of current, electrons arrive on the average once every 16 fs, i.e. a time scale in the order of hot

electron relaxation time. How do the two electrons interact to give rise to the high energy photons that are emitted? Can an impurity or an adsorbed species in the tunnel junction affect the one-electron and two-electron induced light emission? How does an island or monolayer of adsorbed metal atoms affect the light emission processes?

References to Publications of DOE Sponsored Research (2005-present):

- [1] H.J. Lee, J.H. Lee, and W. Ho, “*Vibronic Transitions in Single Metalloporphyrins*”, *ChemPhysChem* **6**, 971-975 (2005).
- [2] G.V. Nazin, X.H. Qiu, and W. Ho, “*Vibrational Spectroscopy of Individual Doping Centers in a Monolayer Organic Crystal*”, *J. Chem. Phys.* **122**, 181105-1-4 (2005).
- [3] G.V. Nazin, S.W. Wu, and W. Ho, “*Tunneling Rates in Electron Transport Through Double-Barrier Molecular Junctions in a Scanning Tunneling Microscope*”, *Proc. Nat. Acad. Sci.* **102**, 8832-8837 (2005).
- [4] J.R. Hahn and W. Ho, “*Orbital Specific Chemistry: Controlling the Pathway in Single-Molecular Dissociation*”, *J. Chem. Phys.* **122**, 244704-1-3 (2005).
- [5] G.V. Nazin, X.H. Qiu, and W. Ho, “*Charging and Interaction of Individual Impurities in a Monolayer Organic Crystal*”, *Phys. Rev. Lett.* **95**, 166103-1-4 (2005).
- [6] J.R. Hahn and W. Ho, “*Direct Observation of C₂ Hydrocarbon-Oxygen Complexes on Ag(110) With a Variable-Low-Temperature Scanning Tunneling Microscope*”, *J. Phys. Chem. B* **109**, 20350-20354 (2005).
- [7] J.R. Hahn and W. Ho, “*Chemisorption and Dissociation of Single Oxygen Molecules on Ag(110)*”, *J. Chem. Phys.* **123**, 214702-1-6 (2005).
- [8] J.R. Hahn and W. Ho, “*Imaging and Vibrational Spectroscopy of Single Pyridine Molecules on Ag(110) Using a Low-Temperature Scanning Tunneling Microscope*”, *J. Chem. Phys.* **124**, 204708-1-4 (2006).
- [9] S.W. Wu, N. Ogawa, and W. Ho, “*Atomic Scale Coupling of Photons to Single-Molecule Junction*”, *Science* **312**, 1362-1365 (2006).
- [10] S.W. Wu, N. Ogawa, G.V. Nazin, and W. Ho, “*Conductance Hysteresis and Switching in Single-Molecule Junction*”, *J. Phys. Chem. C* **112**, 5241-5244 (2008).
- *** Figure from this paper appeared on the cover of this issue of the *J. Phys. Chem. C*.
- [11] S.W. Wu, G.V. Nazin, and W. Ho, “*Intramolecular Photon Emission From a Single Molecule in a Scanning Tunneling Microscope*”, *Phys. Rev. B* **77**, 205430-1-5 (2008).
- [12] C. Chen, C.A. Bobisch, and W. Ho, “*Visualization of Fermi’s Golden Rule Through Imaging of Light Emission from Atomic Silver Chain*”, *Science* **325**, 981-985 (2009).

THEORY OF THE REACTION DYNAMICS OF SMALL MOLECULES ON METAL SURFACES

Bret E. Jackson

Department of Chemistry
701 LGRT
710 North Pleasant Street
University of Massachusetts
Amherst, MA 01003
jackson@chem.umass.edu

Program Scope

Our objective is to develop realistic theoretical models for molecule-metal interactions important in catalysis and other surface processes. The dissociative adsorption of molecules on metals, Eley-Rideal and Langmuir-Hinshelwood reactions, recombinative desorption and sticking are all of interest. To help elucidate the experiments that study these processes, we examine how they depend upon the nature of the molecule-metal interaction, and experimental variables such as substrate temperature, beam energy, angle of impact, and the internal states of the molecules. Electronic structure methods based on Density Functional Theory (DFT) are used to compute the molecule-metal potential energy surfaces. Both time-dependent quantum scattering techniques and quasi-classical methods are used to examine the reaction dynamics. Effort is directed towards developing improved quantum methods that can accurately describe reactions, as well as include the effects of temperature (lattice vibration) and electronic excitations.

Recent Progress

In an earlier study of H atom recombination on Ni(100), we allowed the lattice atoms to move, necessitating the construction of a potential energy surface (PES) based upon the instantaneous positions of the lattice atoms and the adsorbates. We avoided the usual problems associated with pairwise potentials by using ideas from embedded atom theory, and fit the PES to our DFT calculations. More recently we used this potential to study the sputtering of Ni surfaces by Ar beams [1]. We found that this PES accurately described the energy required to severely distort the lattice or to remove one or more Ni atoms. Agreement of sputtering yields and threshold energies with experiments was greatly improved over earlier models.

We completed our studies of H-graphite reactions, important in the formation of molecular Hydrogen on graphitic dust grains in interstellar space, and in the etching of graphite walls in fusion reactors. Our earlier DFT studies demonstrated that an H atom could chemisorb onto a graphite terrace carbon, with the C atom puckering out of the surface plane by several tenths of an Å. We computed the PES for the Eley-Rideal (ER) reaction of a gas phase H atom with this chemisorbed H, and our scattering calculations showed that the reaction cross sections should be very large – on the order of 10 \AA^2 . This was later confirmed experimentally by the Küppers group (Bayreuth). More recent work has focused on why the measured sticking probabilities of H on graphite are so large, roughly 0.4. Given the significant lattice distortion required for chemisorption, this is surprising. We used DFT to map out the H-graphite interaction as a function of the position of the bonding carbon, and found a barrier to chemisorption of about 0.2 eV, in excellent agreement with recent experiments. A PES for trapping and sticking was constructed, and a collinear quantum study of the trapping process was

implemented [2]. We found that the bonding carbon puckers in about 50 fs, and suggested that sticking proceeds via a trapping resonance, which relaxes by dissipating energy into the substrate. We then computed the full three-dimensional PES, and used classical mechanics to compute sticking cross sections [4]. However, when averaged over the experimental incident energy distribution, the sticking probability was only about 0.1. An improved model that included a large dynamical graphite lattice provided a more accurate (and converged) description of the relaxation of the C-H bond, but the sticking probability was still small [7]. We then computed the PESs for addition of H atoms to Carbon sites adjacent to chemisorbed H atoms. For several of these sites the barrier to H sticking is small, and the binding energy is large [7]. Thus, while the initial (zero coverage) sticking may indeed be small, as we computed, the addition of subsequent H atoms in preferred locations relative to the initial adsorbates can happen with a large probability. This preferred clustering of H adsorbates on graphite has now been observed in two STM studies. In addition, the Küppers group has now measured sticking down to (true) zero coverage, finding that probabilities decrease to around 0.1. Thus, theory and experiment now agree.

In interstellar space much of the ER-reactive adsorbed H is likely physisorbed. To estimate the rates for H₂ formation via this pathway, one must know the sticking probability of H into the physisorption well. We have developed a powerful approach to these types of problems based on the reduced density matrix, which allows us to evolve a quantum system weakly coupled to a bath over a relatively long time. Thus, we can not only compute, quantum mechanically, the scattering into free and bound states, we can observe the relaxation and/or desorption from these states over long times. We tested this approach in a study of He scattering and trapping/desorption on corrugated metal surfaces over timescales of 100's of ps [8]! In a study of H physisorption on graphite, and we demonstrated that sticking is enhanced at low energies due to diffraction mediated trapping states that relax into the substrate vibrations [8].

We concluded our studies of the H(g) + Cl/Au(111) reaction, where experiments observed strong H atom trapping and a thermal Langmuir-Hinshelwood channel for HCl formation, as well as ER and hot atom (HA) channels. The ER reaction cross section was much larger than for H(g) + H/metal reactions, due to a steering mechanism arising from the relatively large distance of the adsorbed Cl above the metal. There were interesting variations of ER reactivity with the Cl vibrational state, and an exchange pathway was observed, in which the H remains bound while the Cl desorbs. Quasi-classical trajectories were used to study this reaction at large Cl coverages [3]. We found that HA reactions dominated the formation of HCl, and that significant energy loss into the substrate excitations, perhaps into electron hole pair excitations, was necessary in order to explain the experiments.

Most of our efforts these past few years have focused on the dissociative adsorption of methane on metals, in an attempt to understand how methane reactivity varies with the temperature of the metal, and from metal to metal. Starting with Ni(111), we used DFT to compute the barrier and explore the PES for reaction, and have examined how it changes due to lattice motion. We found that at the transition state for dissociation, the Ni atom over which the molecule dissociates would prefer to pucker out of the surface by 0.23 Å. Put another way, when this Ni atom vibrates in and out of the plane of the surface, the barrier to dissociation increases and decreases, respectively. This should lead to a strong variation in the reactivity with temperature, though it is not clear that a metal atom would have time to move or relax during the collision. To explore these issues, high dimensional quantum scattering calculations were implemented, which allowed for the inclusion of several key methane degrees of freedom (DOF), as well as the motion of the metal atom over which the reaction occurs. We found that the reactivity was significantly larger than for the static lattice case, even at 0 K, and strongly

increased with temperature [5,6]. We also compared our results with the surface oscillator model, used for many years to explain the temperature dependence of these reactions. We clearly demonstrated that when lattice relaxation occurs at the transition state, the effects of lattice motion are very different from what has long been assumed [5, 6], and are not well described by earlier models. We also examined recent experiments by the Utz group (Tufts) of CD_3H dissociation on Ni(111). They were able to significantly enhance reactivity by laser exciting the C-H stretch of the molecule. We showed that vibrationally excited molecules can make significant contributions to the “laser off” reactivity, particularly at lower incident energies where the ground vibrational state is “below the barrier”[6].

We have similarly explored methane dissociation on several other metals. Recent experiments by the Beck group (EPFL) showed that the reactivity of methane on Pt(111) was significantly larger than on Ni(111), with an apparent difference in activation energies of 0.29 eV. Using DFT, we found that the static surface barrier to reaction was only 0.13 eV lower on the Pt surface [9]. We then constructed DFT-based PESs for these metals, much improved over our previous work, and quantum scattering studies were implemented. While the forces for lattice puckering are similar on the two metals, the heavier Pt is much less able to move during the reaction. While we are able to explain the Ni(111) reactivity well, we underestimate the reactivity on Pt(111), particularly at lower energies [9]. We believe this is due to the way we treat the motion of the methyl group in our model, or errors in the DFT energies. More recently, we completed a comparison of the energetics of methane dissociation on Ni(100), Ni(111), Pt(100), Pt(111) and Pt(110)-(1x2). For all 5 surfaces the barrier varies with lattice motion. However, there are interesting metal to metal variations in both the barrier height and the magnitude of these effects. A simple model was developed for a temperature-dependent “activation energy”, using only data from DFT studies of the transition state. This activation energy can be several tenths of an eV lower than the static surface barrier height.

In an attempt to better understand the role of lattice motion, we implemented a variety of mixed quantum-classical models. We found that treating only the lattice classically did not work well, and that the best approach was to treat both the lattice motion and the molecular center of mass motion classically, and the remaining molecular DOF quantum mechanically. While this model did lose some tunneling contributions from motion normal to the surface, it did allow us to directly observe the motion of the lattice at a given collision energy. We found that the majority of the reaction probability came from collisions where the lattice atom was at its outer turning point, where the barrier is lowest, during the collision. Moreover, most of the reactions occurred for lattice atoms that were “hot”; i. e., on the tail of the Boltzmann distribution, and there was only a small recoil of the metal atom. This led to the development of a sudden model, where quantum calculations were implemented for frozen lattice configurations, Monte Carlo sampled at the substrate temperature. Because the heavy metal atom was not explicitly included, and non-reactive lattice configurations were easily identified and excluded, this very accurate model required two orders of magnitude less computer time.

Future Plans

Experiments have shown that exciting different vibrational states of methane can significantly promote reaction, but to varying degrees. In order to explain these vibrational efficacies, and to more accurately describe methane reactivity in general, we need a model with more molecular DOF. Thus, during the past 6 months we have explored the use of a reaction path Hamiltonian. In this approach, one locates (using DFT, in our case) the minimum energy path (MEP) for reaction, and implements a normal mode analysis at several points along this MEP.

This leads to a PES including all 15 molecular DOF. Two studies are already in progress. In the first, we computed this PES for methane dissociation on Ni(100), and found that the ν_1 mode (symm stretch) significantly softens at the transition state, and is strongly coupled to the reaction coordinate. One expects a large vibrational efficacy for this mode, and that has been observed. In order to better understand how different vibrational states couple to each other and the reaction coordinate, we are developing a close-coupled wave packet treatment of the reaction dynamics using this Hamiltonian. In a second study, we are revisiting our comparison of Ni(111) and Pt(111). On both metals, the transition state is over the top site. However, on Ni, the methyl group moves towards a hollow site during the reaction, while on Pt the methyl remains at the top site. In the mass-weighted coordinates of our MEP, this leads to a broadening of the barrier and a lowering of the reactivity for Ni relative to Pt, as the heavy methyl group does not tunnel as effectively as the H. Thus far, we have only computed the MEPs on Ni(111) and Pt(111), without the normal mode analysis, but a rough semiclassical calculation of the reactivity reproduces the apparent difference in activation energies of about 0.3 eV. We plan to continue and extend these studies over the next year or two, and are also working on a purely classical study of the dynamics on this PES.

Over the past year we have derived a fully quantum model for the time evolution of a reacting, scattering, or adsorbed molecule coupled to the electronic excitations of the metal substrate, using reduced density matrix methodologies. We have recently obtained a computer program from a collaborator (Mats Persson) that will allow us to compute the electronically non-adiabatic coupling, and hope to implement a study of H atom sticking over the coming year.

The development of our sudden model for lattice motion allows us to significantly extend our quantum scattering models by including more molecular DOF. In particular, we are looking at ways to average over impact sites and accurately describe vibration. We should be able to accurately model CD_3H and CH_2D_2 reactions by treating the less reactive C-D bonds as frozen. Our goal is to be able to directly compute state-resolved temperature-dependent reaction probabilities that can be compared directly with experiment.

References

- [1]. Z. B. Guvenc, R. Hippler and B. Jackson, "Bombardment of Ni(100) surface with low-energy argons: molecular dynamics simulations, *Thin Solid Films* 474, 346-357 (2005).
- [2]. X. Sha, B. Jackson, D. Lemoine and B. Lepetit, "Quantum studies of H Atom Trapping on a graphite surface," *J. Chem. Phys.* 122, 014709, 1-8 (2005).
- [3]. J. Quattrucci and B. Jackson, "Quasi-classical study of Eley-Rideal and Hot Atom reactions of H atoms with Cl adsorbed on a Au(111) surface, *J. Chem. Phys.* 122, 074705, 1-13 (2005).
- [4]. J. Kerwin, X. Sha and B. Jackson, "Classical studies of H atom trapping on a graphite surface," *J. Phys. Chem. B* 110, 18811-18817 (2006).
- [5]. S. Nave and B. Jackson, "Methane dissociation on Ni(111): the role of lattice reconstruction," *Phys. Rev. Lett.* 98, 173003, 1-4 (2007).
- [6]. S. Nave and B. Jackson, "Methane dissociation on Ni(111): The effects of lattice motion and relaxation on reactivity," *J. Chem. Phys.* 127, 224702-1 - 11 (2007).
- [7]. J. Kerwin and B. Jackson, "The sticking of H and D atoms on a graphite (0001) surface: the effects of coverage and energy dissipation", *J. Chem. Phys.* 128, 084702-1 - 7 (2008).
- [8]. Z. Medina and B. Jackson, "Quantum studies of light particle trapping, sticking and desorption on metal surfaces, *J. Chem. Phys.* 128, 114704-1 - 9 (2008).
- [9]. S. Nave and B. Jackson, "Methane dissociation on Ni(111) and Pt(111): Energetic and dynamical studies," *J. Chem. Phys.* 130, 054701-1 - 14 (2009).

Probing catalytic activity in defect sites in transition metal oxides and sulfides using cluster models: A combined experimental and theoretical approach

Caroline Chick Jarrold and Krishnan Raghavachari
*Indiana University, Department of Chemistry, 800 East Kirkwood Ave.
Bloomington, IN 47405*
cjarrold@indiana.edu, kraghava@indiana.edu

I. Program Scope

Attempts to fully understand the molecular scale interactions that result in desirable catalytic properties of metal oxide-based heterogeneous catalytic systems are complicated by the complex nature of these systems. Better properties are achieved with highly defective material deposited on a high surface area support structure. Because of the complexity of these systems, experimental reproducibility and theoretical modeling is difficult. Our research program approaches the problem from the bottom-up. We use cluster models for both experimental and computational investigations of catalyst-substrate interactions, with the primary focus on transition metal (TM) oxides and sulfides. The strategy of this project is to determine the defect structures that exhibit the essential balance between structural stability and electronic activity necessary to be simultaneously robust and catalytically active, and to find trends and patterns in activity that can lead to improving applied catalytic systems. Bonding in metal oxides and sulfides is localized because of its ionic nature. What is learned from small cluster interactions can therefore be more rationally related to applied supported particulate catalysts.

Both experimental and computational methods are used in these studies on transition metal oxides and sulfides and their reactivity and interaction with simple substrate molecules. Experimentally, the bare metal oxide and sulfide clusters are produced using a laser ablation/pulsed molecular beam cluster source, and the mass distribution of the negative ions is measured using mass spectrometry. Anions are of particular interest because of the propensity of metal oxide and sulfides to accumulate electrons in applied systems. Cluster structures are probed using a combination of mass-specific anion photoelectron (PE) spectroscopy and calculations. Clusters are then exposed to a variety of reagents relevant in a range of catalytic applications, including H₂O, CH₄, CO, and CO₂. Simple kinetic measurements on the reactions are made by measuring cluster and product intensities as a function of reactant number density in a high-pressure fast flow reactor. Reaction products are probed mass spectrometrically and with PE spectroscopy, and detailed studies of the mechanisms and energetics of the reactions are done computationally.

II. Recent Progress

A. Kinetics of reactions between water and $W_xO_y^-$, $Mo_xO_y^-$:

Tungsten trioxide, WO₃, has been identified as a material that could be used for the photocatalytic decomposition of water, and several studies on supported WO₃, particularly in nanoscale forms, have borne this out. However, it is difficult to separate the properties of the WO₃ from the various support materials. To better understand the intrinsic properties of the tungsten-oxygen bond, we have undertaken a series of kinetic studies of tungsten suboxide clusters with H₂O and D₂O. We have further extended these studies to the group 6 analogs, Mo_xO_y⁻ clusters, which have yielded several unexpected results.

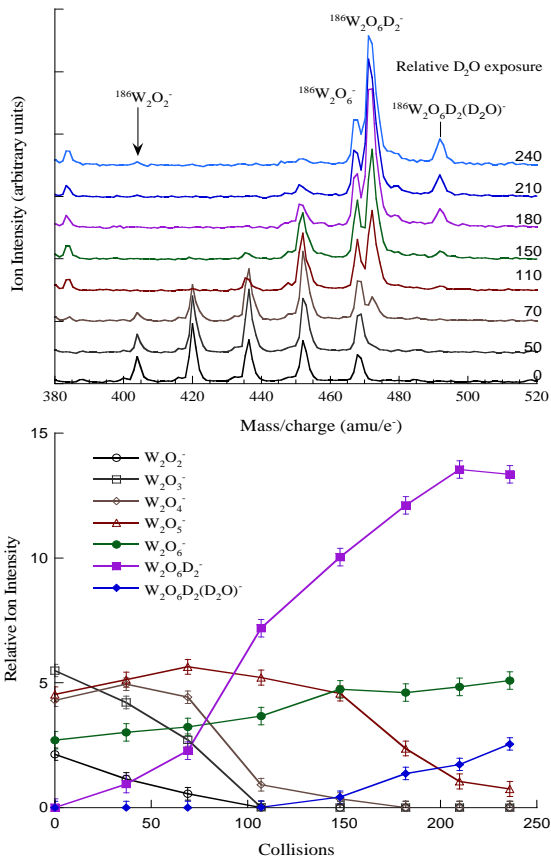


Figure 1. Mass spectra (above) and integrated intensities (below) of $W_2O_y^-$ ions as a function of average number of D_2O collisions.

different from the $W_xO_y^-$ reactions. Figure 2 shows an example of this. Analysis of the lower panel indicates that $Mo_3O_6^-$ is essentially unreactive toward water, while $W_3O_6^-$ is highly reactive.

B. Computational studies of water/cluster reactions combined with spectroscopy of reaction intermediates

In order to understand how the sequential oxidation of the group 6 oxide clusters add water with a clear indication of H_2 evolution, and to potentially explore a spectroscopic means for regenerating the lower and more reactive suboxide species after water exposure, a detailed computational study on the interactions between water and the clusters was done. The first focus has been on $W_2O_4^- + H_2O \rightarrow W_2O_5^- + H_2$ and $W_2O_5^- + H_2O \rightarrow W_2O_6^- + H_2$, both of which were determined to be strongly energetically favored. The question raised in the studies was, therefore, why $W_2O_6H_2^-$ is observed experimentally.

The results on the kinetic measurements on $W_2O_y^-$ clusters can be found in the second publication listed in Section IV below. What was observed was fast sequential oxidation of suboxide clusters via $W_2O_y^- + H_2O \rightarrow W_2O_{y+1}^- + H_2$, and that there was no difference in rate constants determined for reactions with H_2O versus D_2O . Figure 1 shows an example of how the cluster intensities change with number of D_2O collisions. There was, as would be expected, a drop in rate constant as y increases, and for the $W_2O_y^-$ cluster series, this reaction appeared to terminate with $W_2O_5^- + H_2O \rightarrow W_2O_6H_2^-$. However, in larger cluster series, the reaction appears to similarly terminate at lower average oxidation states, suggesting a strong *local* structural component in the termination.

Results from $Mo_xO_y^- + H_2O/D_2O$ studies showed a strikingly different effect. First, the rate constants for the sequential oxidation reactions increase very slightly as the average oxidation state of the cluster increases. Second, evidence that some form of oxidation carriers on beyond the dominant $Mo_2O_6H_2^-$ trap is observed: $Mo_2O_7H^-$ and $Mo_2O_8^-$ species appear with water addition. This is counterintuitive, because the Mo–O bond is substantially weaker than the W–O bond, so there would be less internal energy to drive the $Mo_2O_y^-$ sequential oxidation reactions to higher oxidation states. Finally, the larger $Mo_xO_y^- + H_2O$ reactions appear to terminate at oxidation states that are

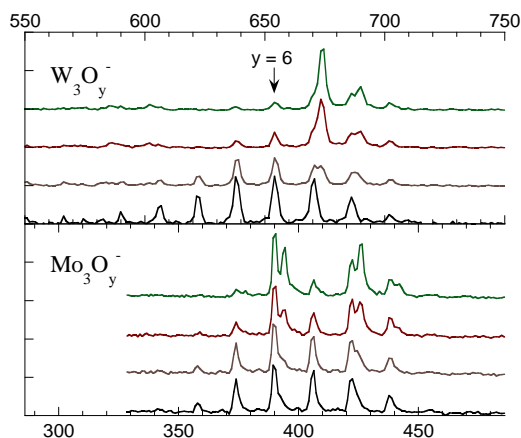


Figure 2. Evolution of $W_3O_y^-$ and $Mo_3O_y^-$ cluster distributions with increasing D_2O concentration.

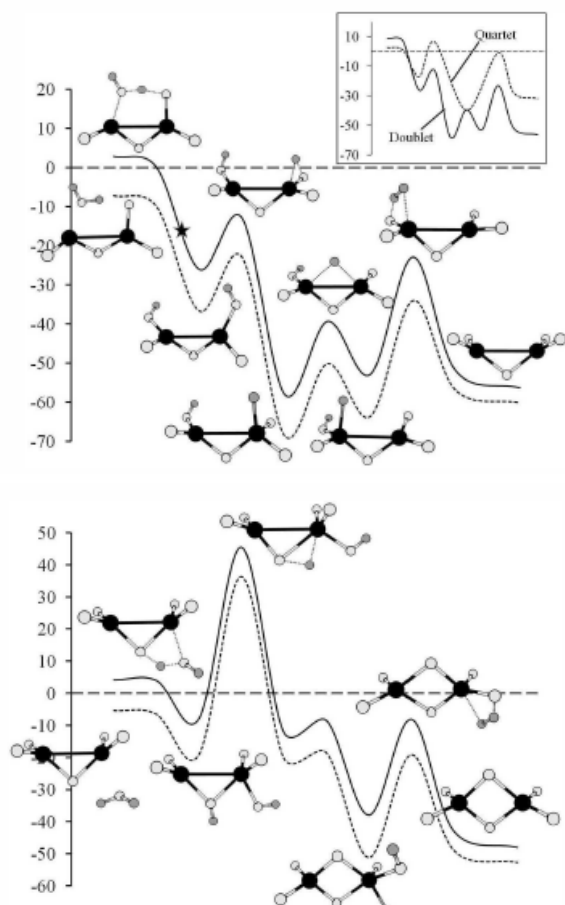


Figure 3. Example of a reaction path for $W_2O_4^- + H_2O$ (top) and $W_2O_5^- + H_2O$ (bottom). A change in spin state occurs in the $W_2O_4^-$ reaction, indicated in the inset.

in which one of the hydroxides is a hypervalent bridge hydroxide. This coincides with the structure shown in the lower panel of Fig.3, which could be trapped by the substantial barrier to hydroxide-hydride formation.

This study exemplifies the synergy of the experimental and computation efforts of our combined groups: The reactivity studies drive the computational studies which are subsequently supported by additional reactivity studies. A detailed description of these can be found in the third and fourth papers listed in Section IV.

C. Kinetics of CO_2 oxidation of group 6 oxide cluster anions, and the discovery of an unusually stable cluster, $Mo_3O_6^-$:

Water is a very strong oxidizing agent toward the group 6 suboxide cluster anions. However, we have also observed sequential oxidation reactions using CO_2 as the oxidizing agent, though with rate constants three orders of

Several general features of the cluster-water interactions have emerged from the calculations. First, interactions resulting in dihydroxide formation are lower barrier than interactions resulting in hydroxide-hydride formation. Second, interactions that involve both tungsten centers are lower barrier than those involving a single tungsten center. For $W_2O_4^-$, the two-center di-hydroxide and hydroxide-hydride complexes both were predicted to have very low barrier to formation.

Starting from cluster-water complexes predicted to form with the lowest barriers, we calculated that reaction paths for subsequent structural rearrangement to form W–OH and W–H groups in close proximity, which is required for H_2 evolution. Two examples of low-entrance barrier paths are shown in Figure 3. The feature that emerged with these profiles was that $W_2O_5^-$ was unique in that it had a profile in which a subsequent barrier to reorganization exceeded the internal energy gained in the formation of an intermediate.

To evaluate the validity of these calculations, the spectrum of $W_2O_6D_2^-$ was obtained and compared to an extensive set of possible structural isomers of $W_2O_6H_2^-$. Based on the spectroscopic parameters calculated for the eight minima found on the anion surface (scaled appropriately to compare –H and –D analogs), the best match between calculated structures and the spectrum was found with a dihydroxide structure,

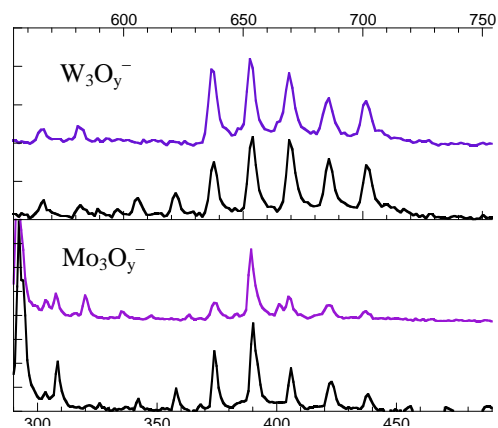


Figure 4. $W_3O_y^-$ and $Mo_3O_y^-$ cluster distributions before (black trace) and after (purple trace) CO_2 exposure.

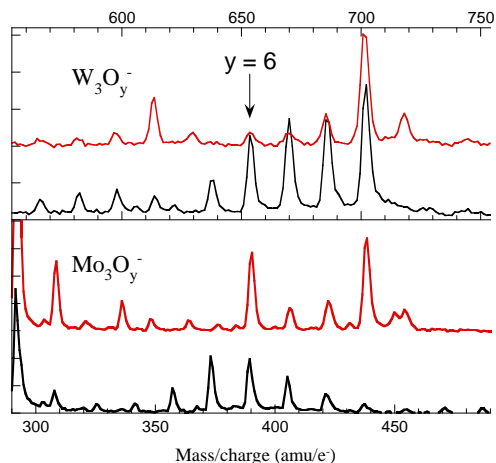


Figure 5. $W_3O_y^-$ and $Mo_3O_y^-$ cluster distributions without (black trace) and with (red trace) CO_2 seeded in carrier gas.

magnitude lower than for H_2O . Again, counterintuitive results are apparent in comparing $W_xO_y^- + CO_2$ with $Mo_xO_y^- + CO_2$ product distributions. Figure 4 shows how the sequential oxidation of the $Mo_3O_y^-$ suboxide clusters carries on to higher y-values than for $W_3O_y^-$, though based on the stronger W–O bond, we would expect the opposite to occur. There is also evidence of CO_2 addition to several of the lower oxides: A mass assigned to $Mo_3O_4^-(CO_2)$ is observed, though we have not yet performed the necessary spectroscopic and computational investigation to determine whether this is a dissociative addition or a cluster.

A surprising result that is consistent with water reactivity studies is that $Mo_3O_6^-$ does not undergo any significant oxidation. This holds true when CO_2 is introduced to the clusters under much more violent conditions by seeding CO_2 in the carrier gas present at the point of laser ablation in which the clusters are initially formed. This is shown in Figure 5. The structures and

electronic states predicted for $Mo_3O_6^-$ and $W_3O_6^-$ are the same, and there is so far no clue why the reactivity of these species are so different.

III. Future Plans

Computational studies on $Mo_xO_y^- + H_2O$ reactions are being initiated to determine why the weaker Mo–O bond does not prevent sequential oxidation of the clusters at higher average oxidation states. Oxidation of the group 6 clusters by CO_2 will also be explored computationally. The modes of CO_2 –cluster interaction are expected to be very different from the charge-dipole interactions that figure into the initial barrier for complex formation in the water-cluster systems.

Experimentally, cluster and complex anion excited state spectroscopy and photodissociation studies will be done to explore the role of excited states in both reactivity and cluster “regeneration.” Metal sulfide reactivity will also be initiated.

IV. References to publications of DOE sponsored research that have appeared in 2004–present or that have been accepted for publication

1. “Electronic structure of coordinatively unsaturated molybdenum and molybdenum oxide carbonyls,” Ekram Hossain and Caroline Chick Jarrold, *J. Chem. Phys.* **130** 064301 (2009).
2. “Unusual products observed in gas-phase $W_xO_y^- + H_2O$ and D_2O reactions,” David W. Rothgeb, Ekram Hossain, Angela T. Kuo, Jennifer L. Troyer, Caroline Chick Jarrold, Nicholas J. Mayhall, and Krishnan Raghavachari, *J. Chem. Phys.* **130**, 124314 (2009).
3. “Water reactivity with tungsten oxides: H_2 production and kinetic traps,” Nicholas J. Mayhall, David W. Rothgeb, Ekram Hossain, Caroline Chick Jarrold and Krishnan Raghavachari, accepted for publication, *J. Chem. Phys.* (2009).
4. “Termination of the $W_2O_y^- + H_2O/D_2O \rightarrow W_2O_{y+1}^- + H_2/D_2$ reaction: Kinetic versus thermodynamic effects,” David W. Rothgeb, Ekram Hossain, Nicholas J. Mayhall, Krishnan Raghavachari, and Caroline Chick Jarrold, revised manuscript resubmitted for publication, *J. Chem. Phys.* (2009).

Two manuscripts are currently in preparation.

**Coordinating experiment and theory to understand how excess electrons are accommodated by water networks through model studies in the cluster regime
DE-FG02-06ER15800**

**K. D. Jordan (jordan@pitt.edu), Dept. of Chemistry, University of Pittsburgh, Pittsburgh, PA 15260
and M. A. Johnson (mark.johnson@yale.edu), Dept. of Chemistry, Yale University, New Haven, CT 06520**

We seek to build a predictive understanding for how hydrogen-bonded networks rearrange to accommodate solutes of importance in radiation chemistry and aqueous chemistry in general. Toward this end, we are primarily interested in elucidating the factors that control water network behavior not only in its familiar morphologies (e.g., tetrahedral H-bonded, hexagonal, etc.) but also in environments far from those explored by saturated H-bonding configurations. Our role in this endeavor is to integrate theoretical and experimental methods that exploit size-selected clusters as model systems that can be used to expose the peculiar properties of water from a “bottom-up” approach. The focus of our work is to understand the cooperative mechanics governing the interaction of an excess electron with well-defined networks of water molecules using the unique properties of size-selected ionic clusters. In the smallest size regime, clusters containing fewer than 10 or so water molecules, the advantage of this approach is that the entire cluster can be treated both experimentally and theoretically as a “supermolecule” in the sense that spectra can be effectively assigned to vibrational modes associated with particular minimum energy structures. Challenges for the field are now to increase the scope of the cluster-based studies to capture more of the complexity at play in the condensed phase.

This involves working with larger systems with finite (and controlled) internal energy content, where isomerization among many local minima begins to control the macroscopic properties of the ion ensemble.

During the past year, we have used theoretical methods to begin the exploration of the extended potential landscapes available to clusters with significant internal energy. As a starting point, we focused on the nature of the isomers observed experimentally in the hexamer anion when formed by electron

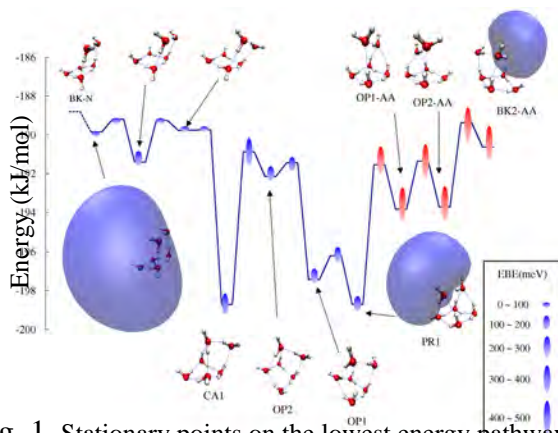


Fig. 1. Stationary points on the lowest energy pathway between the book form of $(\text{H}_2\text{O})_6$ and the AA forms of the hexamer anion, where the lengths of the markers are proportional to the vertical electron binding energies, and the letters designate the network types: CA = cage, BK = book, PR = prism, and OP = open prism, with one broken H-bond. AA denotes anions with a double acceptor monomer, and PR-N and BK-N denote, respectively, the lowest energy prism and book forms of the neutral cluster.

capture by the “book” form of the neutral. The key issues here are to identify the local minima and transition states leading to the anionic structures identified by vibrational spectroscopy and photoelectron spectroscopy. The results of this exercise are summarized in Ref. 8 and illustrated in Fig. 1. One emerging puzzle of the theoretical results is that the experimentally observed cluster anions are dominated by high electron binding species with the characteristic double H-bond acceptor (AA) water molecule with both its dangling protons pointing toward the excess electron cloud, while theory predicts that there are more isomers which do not display this motif, but which bind the excess

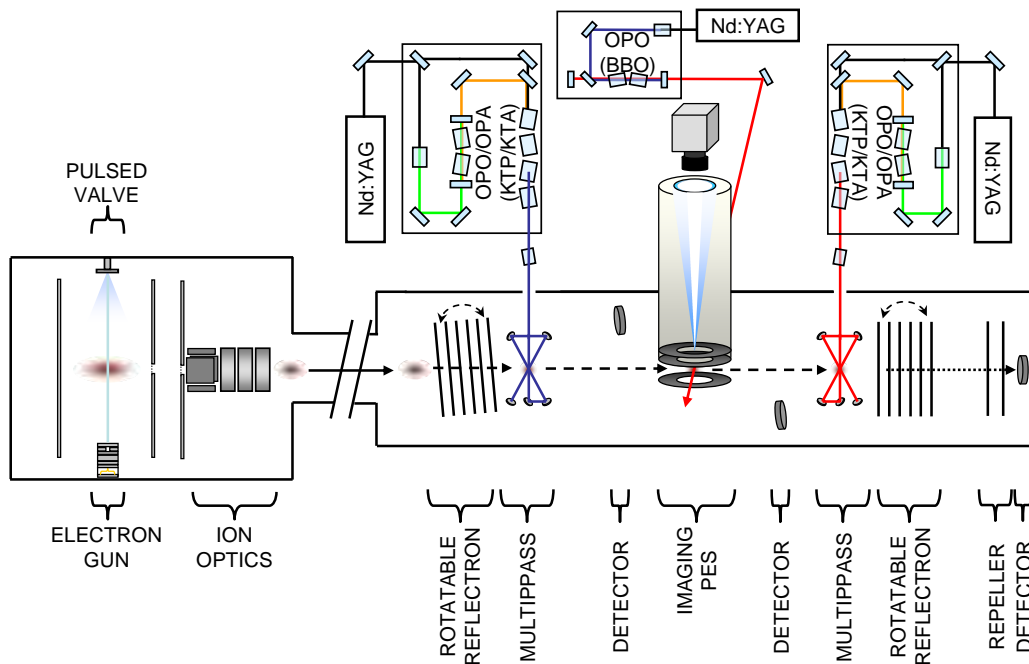


Fig. 2. Schematic layout of the present multi-stage photofragmentation and velocity-map photoelectron imaging spectrometer at Yale. This consists of two independently tunable infrared lasers in an ms-ms-ms arrangement for size- and isomer-selective spectroscopies.

electron much more weakly. This has motivated us to modify our experimental arrangement as illustrated in Fig. 2, where we now have the ability to follow not only isomer-selective vibrational and photoelectron spectroscopy, but also photochemical isomerization of various species prepared in the supersonic jet ion source.

The modified instrument has already delivered isomer-selective predissociation spectra of the water heptamer anion (Ref. 4) as well as a comprehensive survey of the relative roles of photofragmentation and electron autodetachment for the two more strongly electron binding isomers of the hexamer anion (Ref. 3). We have also demonstrated its ability to follow vibration-induced isomerization using both photoelectron (Ref. 5) and vibrational predissociation spectroscopies to selectively excite a particular isomer and follow the formation of new isomers in the photoproducts generated after the internal energy is quenched by successive evaporation of Ar atoms attached to the initially excited species. Interestingly, the first series of experiments indicated that the high electron binding isomers (type I or “AA”-based) are more stable

than the type II forms, indicating that the non-AA isomers formed in the jet are not those predicted to occur lowest in energy from theory. Thus, a major thrust of our efforts for the next year will be directed toward following the generality of this behavior in other clusters as well as attempting to prepare clusters in other ways (e.g., changing carrier gas, isotopic mixture, etc.) to see if there are indeed more species available than those routinely observed. We note the approaches used so far would fail to detect anions produced by isomerization if electron ejection were to occur more rapidly than Ar-atom evaporation.

A particularly exciting and powerful development over the past year involves the application of hole-burning double resonance spectroscopy on isotopomers created by selective incorporation of just one

D₂O molecule in an otherwise homogeneous H₂O-based cluster. This

promises the opportunity to follow

how the label moves from one site to another after vibrational excitation,

thus establishing how labile these

clusters are at various degrees of

internal excitation. A first application of the method is illustrated in Fig. 3,

where we use double resonance to

establish the spectrum yielded by the particular isotopomer in which D₂O

occupies the site closest to the excess electron. This was carried out by

setting a probe laser on the

intramolecular D₂O bending vibration associated with the AA water

molecule (see inset in Fig. 3), and

scanning the hole-burning laser

through the entire range of the higher

energy OD stretches (trace A in Fig.

3). Most importantly, this

unambiguously establishes that the

strongest resonances in the OD

region, which are also most red-

shifted from the position of the free OD in the isolated molecule, are in fact the

transitions associated with the AA water molecule. Although this information was

inferred from earlier, indirect measurements, this represents the first critical test of that

hypothesis and thus provides a firm foundation for the next round of experiments where

we will follow how the AA site evolves in the large cluster regime.

In spite of the huge strides that have been made in characterizing (H₂O)_n⁻ clusters,

both experimentally and theoretically, little is known about the rate of interchange of

molecules in the clusters as a function of excess energy. In principle this question is

addressable theoretically, but for the results to be meaningful it is essential to have

accurate energetics, and also to include nuclear quantum effects, in particular zero point

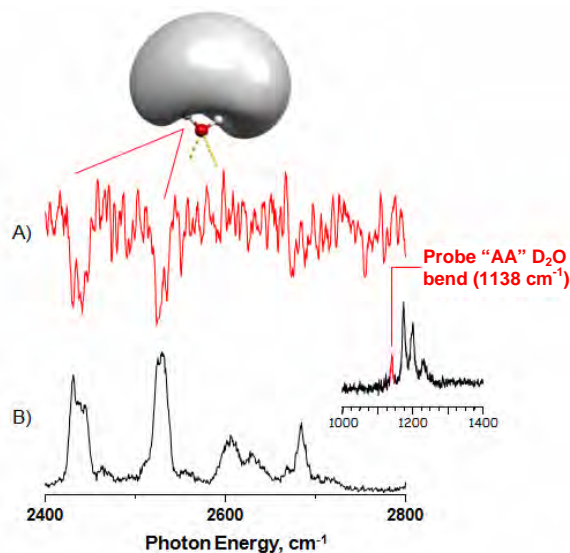


Fig. 3. Application of the double-resonance method to the heptamer anion formed by incorporation of an intact D₂O molecule into the hexamer anion. The lower trace (B) corresponds to the resonances associated with the various isotopomers of the labeled heptamer, while the upper trace (A) is obtained when the same spectral region is filtered using double resonance to isolate the spectrum arising from the isotopomer in which the label occupies the “AA” binding site closest to the excess electron.

energies. Only now do we have a theoretical model that is accurate enough and sufficiently fast computationally, to undertake such simulations with nuclear quantum effects being included via path integral methods. We will initially undertake such calculations on the $(\text{H}_2\text{O})_6^-$ and $(\text{H}_2\text{O})_7^-$ clusters for which there is the most experimental data.

Publications acknowledging DOE support

1. **“Model potential approaches for describing the interactions of excess electrons with water clusters: incorporation of long-range correlation effects”**, T. Sommerfeld, A. DeFusco, and K. D. Jordan, feature article for *J. Phys. Chem. A*, **112**, 11021-11035 (2008). (feature article, cover art).
2. **“Structural Evolution of the $[(\text{CO}_2)_n(\text{H}_2\text{O})]^-$ Cluster Anions: Quantifying the Effect of Hydration on the Excess Charge Accommodation Motif”**, A. Muraoka, Y. Inokuchi, N. I. Hammer, J.-W. Shin, T. Nagata, and M. A. Johnson, *J. Phys. Chem. A*, **113**, 8942–8948 (2009).
3. **“Photoelectron imaging study of vibrationally mediated electron autodetachment in the type I isomer of the water hexamer anion”**, B. M. Elliott, L. R. McCunn and M. A. Johnson, *Chem. Phys. Lett.*, **467**, 32-36, (2008).
4. **“Exploring the correlation between network structure and electron binding energy in the $(\text{H}_2\text{O})_7^-$ cluster through isomer photoselected vibrational predissociation spectroscopy and ab initio calculations: Addressing complexity beyond types I-III”**, J. R. Roscioli, N. I. Hammer, M. A. Johnson, K. Diri and K. D. Jordan, *J. Chem. Phys.*, **128**, 104314 (2008).
5. **“Probing isomer interconversion in anionic water clusters using an Ar-mediated pump-probe approach: Combining vibrational predissociation and velocity-map photoelectron imaging spectroscopies”**, L. R. McCunn, G. H. Gardenier, T. L. Guasco, B. M. Elliott, J. C. Bopp, R. A. Relph, and M. A. Johnson *J. Chem. Phys.*, **128**, 234311 (2008).
6. **“Site-specific addition of D_2O to the $(\text{H}_2\text{O})_6^-$ “hydrated electron” cluster: Isomer interconversion and substitution at the double H-bond acceptor (AA) electron-binding site”**, Laura R. McCunn, Jeffrey M. Headrick and M. A. Johnson, *Phys. Chem. Chem. Phys.*, **10**, 3118 (2008).
7. **“Parallel tempering Monte Carlo simulations of the water heptamer anion”**, A. DeFusco, T. Sommerfeld, K. D. Jordan”, *Chem. Phys. Lett.*, **455**, 135-138 (2008).
8. **“Potential Energy Landscape of the $(\text{H}_2\text{O})_6^-$ Cluster”**, T.-H. Choi and K. D. Jordan, *Chem. Phys. Lett.*, **475**, 293-297 (2009).
9. **“Vibrational predissociation spectroscopy of the $(\text{H}_2\text{O})_{6-21}^-$ clusters in the OH stretching region: Evolution of the excess electron-binding signature into the intermediate cluster size regime,”** N. I. Hammer, J. R. Roscioli, J. C. Bopp, J. M. Headrick and M. A. Johnson, *J. Chem. Phys.*, **123**, 244311, 2005.
10. **“Infrared spectrum and structural assignment of the water trimer anion,”** N. I. Hammer, J. R. Roscioli, M. A. Johnson, E. M. Myshakin and K. D. Jordan, *J. Phys. Chem. A*, **109**, 11526-11530, 2005.
11. **“An infrared investigation of the $(\text{CO}_2)_n^-$ clusters: Core ion switching from both the ion and solvent perspectives,”** J.-W. Shin, N. I. Hammer, M. A. Johnson, H. Schneider, A. Glob and J. M. Weber, *J. Phys. Chem. A*, **109**, 3146-3152, 2005.
12. **“Identification of two distinct electron binding motifs in the anionic water clusters: A vibrational spectroscopic study of the $(\text{H}_2\text{O})_6^-$ isomers,”** N. I. Hammer, J. R. Roscioli and M. A. Johnson, *J. Phys. Chem. A*, **109**, 7896-7901, 2005.
13. **“Infrared spectroscopy of water cluster anions, $(\text{H}_2\text{O})_{n=3-24}^-$ in the HOH bending region: Persistence of the double H-bond acceptor (AA) water molecule in the excess electron binding site of the class I isomers,”** J. R. Roscioli, N. I. Hammer and M. A. Johnson, *J. Phys. Chem. A*, **110**, 517-7520, 2006.
14. **“Low-lying isomers and finite temperature behavior of $(\text{H}_2\text{O})_6^-$,”** T. Sommerfeld, S. D. Gardner, A. DeFusco, and K. D. Jordan, *J. Chem. Phys.*, **125**, 174309 (2006).
15. **“Infrared multiple photon dissociation of the hydrated electron clusters $(\text{H}_2\text{O})_{15-50}^-$,”** K. R. Asmis, G. Santambrogio, J. Zhou, E. Garand, J. Headrick, D. Goebbert, M. A. Johnson, D. M. Neumark, *J. Chem. Phys.*, **126**, 191105 (2007).
16. **“Isomer-specific spectroscopy of the $(\text{H}_2\text{O})_8^-$ cluster anion in the intramolecular bending region by selective photodepletion of the more weakly electron binding species (isomer II),”** J. R. Roscioli and M. A. Johnson, *J. Chem. Phys.*, **126**, 024307, 2007.

Nucleation: From Vapor Phase Clusters to Crystals in Solution

Shawn M. Kathmann
Chemical and Material Sciences Division
Pacific Northwest National Laboratory
902 Battelle Blvd.
Mail Stop K1-83
Richland, WA 99352
shawn.kathmann@pnl.gov

Program Scope

The objective of this work is to develop an understanding of the chemical physics governing nucleation. The thermodynamics and kinetics of the embryos of the nucleating phase are important because they have a strong dependence on size, shape and composition and differ significantly from bulk or isolated molecules. The technological need in these areas is to control chemical transformations to produce specific atomic or molecular products without generating undesired byproducts, or nanoparticles with specific properties. Computing reaction barriers and understanding condensed phase mechanisms is much more complicated than those in the gas phase because the reactants are surrounded by solvent molecules and the configurations, energy flow, and electronic structure of the entire statistical assembly must be considered.

Recent Progress

Understanding $(\text{Ag}^+)_{aq}$ from EXAFS and *ab initio* Molecular Dynamics

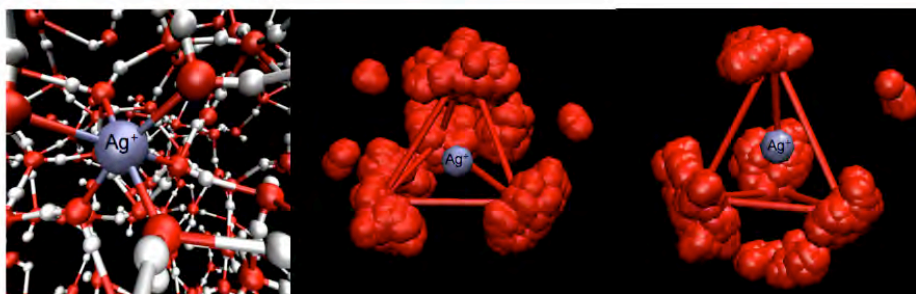
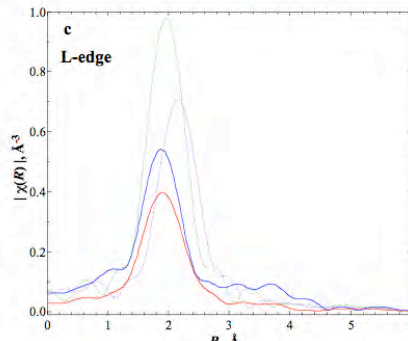
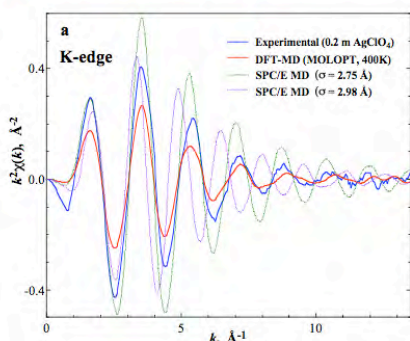


Figure 1. (Top left) Aqueous solvation of silver cation (Ag^+). (Top right) showing the sensitivity of the Ag-O symmetries to different basis sets. (Bottom) Comparison between the measured EXAFS and the Fourier transform of the absorption fine structure from *ab initio* molecular dynamics for the K and L-edge absorptions.



Understanding the nucleation of ions in solution is one of the most difficult topics in chemical physics. Charge transfer effects are important in dictating the difference between salts of AgCl versus NaCl . To this end, we calculated EXAFS signals using electronic structure and *ab initio* dynamics of an Ag^+ ion in water to test the validity of the interactions and statistical mechanical sampling. We

find coordination numbers between 4-5 water molecules, that the multiple scattering peaks are better reproduced by DFT/PBE but not so for the classical interaction potentials, and that the symmetry around the Ag^+ ion is more accurately represented by a distorted trigonal bi-pyramidal structure (shown in Figure 1) compared to the tetrahedral symmetry that is commonly assumed. Future work will address limitations on the DFT functional and the basis sets.

Electric Fields and Potentials in the Condensed Phase

The surface potential of the vapor-liquid interface of pure water is relevant to electrochemistry, solvation thermodynamics of ions, and interfacial reactivity. Indirect determinations of the surface potential have been experimentally attempted many times, yet there has been little agreement as to its magnitude and sign (-1.1 to +0.5 V). We performed the first computation of the surface potential of water using *ab initio* molecular dynamics (Figure 2 – left) and find that explicit treatment of the electronic density makes a dramatic contribution to the electric properties of the vapor-liquid interface of water. Accurate inclusion of electronic effects, charge transfer, polarization, etc. are essential to understand the extreme differences found in crystallization thermodynamics and kinetics between NaCl and AgCl. As an example, the potential arising from a gaussian distribution (with σ^2 variance) becomes equal to that of a delta function point charge ($\phi = q/r$) as long as the potential is evaluated at $r > 3\sigma$ (red vertical line in Figure 2 – right). The question then becomes, what is the extent of the charge distributions, intra- and intermolecular potentials and electric fields in condensed phase systems? To this end, we are computing the interfacial potential and internal electric fields experienced between ions and water as the ions move from aqueous solvation to the crystal phase.

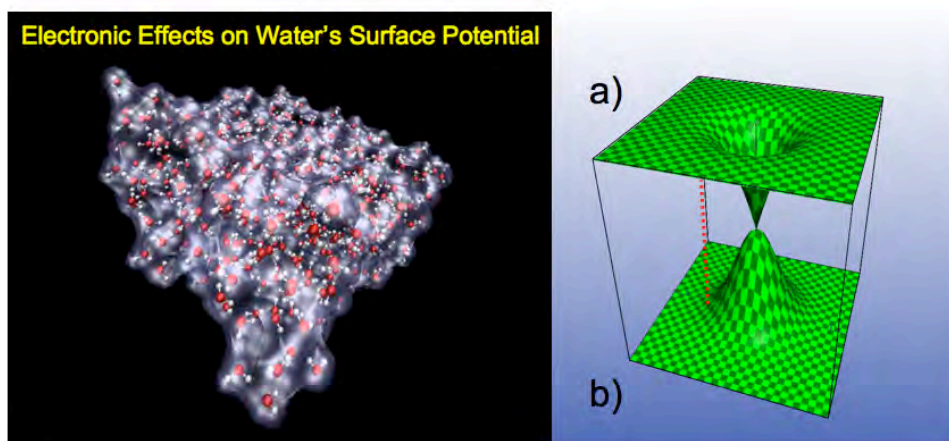


Figure 2. (Left) Does the representation of the charge distribution in aqueous phases influence their electric properties? (Right) Plot of a gaussian distribution of charge (b) compared to the $\text{erf}[r/\sigma/2]$ function (a) found in the electric potential arising from a Gaussian distribution of charge: $\phi = (q/r)\text{erf}[r/\sigma/2]$.

Future Plans

Crystalloluminescence

It has been known since the 1700's that the crystallization of certain substances from solution is accompanied by the emission of light - *crystalloluminescence*. It is found that in the early stages of crystal nucleation of NaCl a burst of some 10^5 photons of blue light is emitted (about 2.7eV).

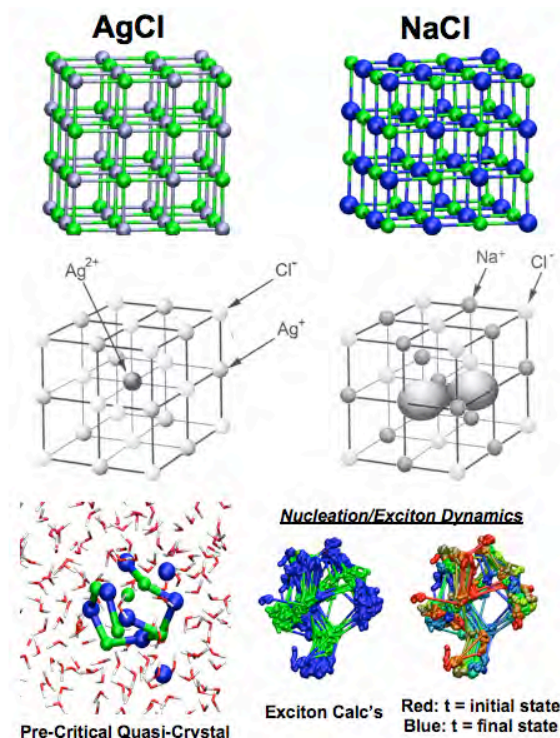


Figure 3. (Top) Bulk crystals of AgCl and NaCl. AgCl has a direct band gap $E_g=5.13\text{eV}$ and an indirect gap $E_{g,\text{ind}}=3.25\text{eV}$. NaCl has an $E_g=8.97\text{eV}$. (Middle) Both AgCl and NaCl crystals admit self-trapped hole (STH) states, however, the AgCl STH is an Ag^{2+} state and the NaCl STH is a Cl_2^- state. (Bottom) Dynamics must sample relevant pre-critical quasi-crystal configurations. The electronic states of these configurations can be analyzed during the crystallization event to sample the density of states to compare with the bulk band gap.

Crystalloluminescence may act as a direct probe of the nucleation event since it is not seen as a consequence of simply growing a crystal. This opens the possibility that during crystallization, the electronic states are strongly coupled to the formation of the quasi-crystal lattice, which can lead to the formation of self-trapped Frenkel excitons (STE). These excitons can then radiatively recombine to emit photons at the observed crystalloluminescent wavelengths. Bulk AgCl shows a luminescence of its STE of $E_{\text{STE}} = 2.5\text{eV}$ (green-blue light) whereas bulk NaCl luminescence occurs at $E_{\text{STE}} = 3.4\text{eV}$ (UV light) – see Figure 3. The non-stoichiometry of pre-critical quasi-crystals is being considered in the mechanism for the formation of the self-trapped Frenkel exciton state – perhaps arising from transient electron transfer from the Cl^- anions on one cluster to a Na^+ cation on a nearby cluster. As these adjacent clusters combine into larger clusters the electrons can recombine with the self-trapped holes to emit blue light – see Figure 4. In order to quantify the creation of excitonic states in aqueous solution accurately, condensed phase electronic structure methods must be used that reproduce known bulk crystal band gaps and bulk exciton states before any confidence is placed on calculations in solution.

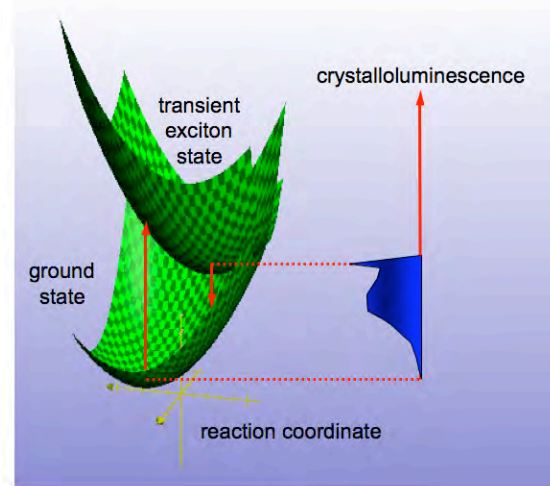


Figure 4. Schematic of the formation and radiative recombination of STEs underlying the mechanism of crystalloluminescence. Along the reaction coordinate, the system is driven (upward vertical arrow) into a localized excited state – a STE, which relaxes, and then through radiative recombination (downward arrow) emits a blue photon.

Direct collaborators on this project include A. Shluger, P. Sushko, G.K. Schenter, C.J. Mundy, S.S. Xantheas, L.X. Dang, and B.C. Garrett. I would also like to thank collaborators Will Kuo, Niri Govind, Marat Valiev, Michel Dupuis, and Karol Kowalski.

Acknowledgement: This research was performed in part using the Molecular Science Computing Facility in the Environmental Molecular Sciences Laboratory located at PNNL and the BES NERSC facility. Battelle operates PNNL for DOE.

Publications of DOE Sponsored Research (2006-present)

1. **Invited Article:** Understanding the Chemical Physics of Nucleation, S.M. Kathmann, A New Perspectives Issue: *Theoretical Chemistry Accounts*, **116**, 169-182, (2006).
2. The Use of Processor Groups in Molecular Dynamics Simulations to Sample Free Energy States, B.J. Palmer, S.M. Kathmann, M. Krishnan, V. Tipparaju, and J. Nieplocha, *Journal of Chemical Theory and Computation*, **3**, 583 (2006).
3. The Critical Role of Anharmonicity in the Aqueous Ionic Clusters Relevant to Nucleation, S.M. Kathmann, G.K. Schenter, and B.C. Garrett, *Journal of Physical Chemistry B*, **111**, 4977 (2007).
4. Comment on “Quantum Nature of the Sign Preference in Ion-Induced Nucleation”, S.M. Kathmann, G.K. Schenter, and B.C. Garrett, *Physical Review Letters*, **98**, 109603 (2007).
5. Activation Energies and Potentials of Mean Force for Water Cluster Evaporation, S.M. Kathmann, B.J. Palmer, G.K. Schenter, and B.C. Garrett, *Journal of Chemical Physics*, **128**, 064306 (2007).
6. **Invited Article:** “Water, The Wellspring of Life”, C.J. Mundy, S.M. Kathmann, G.K. Schenter, *Natural History*, November, **116**(9) (2007).
7. Hybrid Coupled Cluster Approach for Free Energy Calculations: Application to the reaction of CHCl_3 and OH^- in Water, M. Valiev, B.C. Garrett, M-K. Tsai, K. Kowalski, S.M. Kathmann, G.K. Schenter, M. Dupuis, *Journal of Chemical Physics*, **127**, 051102 (2007).
8. **Invited Article:** The Impact of Molecular Interactions on Atmospheric Aerosol Radiative Forcing, S.M. Kathmann, G.K. Schenter, and B.C. Garrett, *Advances in Quantum Chemistry: Applications of Theoretical Methods to Atmospheric Sciences*, **55**, Chapter 20, 429 (2008).
9. **Letter** - On the Determination of Monomer Dissociation Energies of Small Water Clusters from Photoionization Experiments, S.M. Kathmann, G.K. Schenter, and S.S. Xantheas, *Journal of Physical Chemistry A - Letter*, **112**, 1851 (2008).
10. **Invited Article** - High Performance Computations using Dynamical Nucleation Theory, T.L. Windus, S.M. Kathmann, and L.D. Crosby, *Journal of Physics: Conference Series*, **125**, 012017 (2008).
11. **Invited Article** - A Molecular Approach to Understanding Complex Systems: Computational Statistical Mechanics Using State-of-the-Art Algorithms on Tera-Scale Computational Platforms, C.J. Mundy, R. Rousseau, A. Curioni, S.M. Kathmann, and G.K. Schenter, *Journal of Physics: Conference Series*, **125**, 012014 (2008).
12. Electronic Effects on the Surface Potential at the Vapor-Liquid Interface of Water, S. M. Kathmann, I.F. Kuo, and C.J. Mundy, *Journal of the American Chemical Society*, **130**, 16556 (2008).
13. Implementation of Dynamical Nucleation Theory with Quantum Potentials, L.D. Crosby, S.M. Kathmann, and T.L. Windus, *Journal of Computational Chemistry*, **30**, 743 (2009).
14. **Invited Cover Article** – Thermodynamics and Kinetics of Nanoclusters Controlling Gas-to-Particle Nucleation, S. M. Kathmann, G.K. Schenter, B.C. Garrett, B. Chen, and J.I. Siepmann, *Journal of Physical Chemistry C*, **113**, 10354 (2009).
15. Hydrated Structure of Ag(I) Ion from Symmetry-Dependent, K- and L-edge XAFS Multiple Scattering and Molecular Dynamics Simulations, J.L. Fulton, S.M. Kathmann, G.K. Schenter, M. Balasubramanian, *Journal of Physical Chemistry A*, **in press**, (2009).

Chemical Kinetics and Dynamics at Interfaces

Structure and Reactivity of Ices, Oxides, and Amorphous Materials

Bruce D. Kay (PI), R. Scott Smith, and Zdenek Dohnálek

Chemical and Materials Sciences Division
Pacific Northwest National Laboratory
P.O. Box 999, Mail Stop K8-88
Richland, Washington 99352
bruce.kay@pnl.gov

Additional collaborators include P. Ayotte, C. T. Campbell, T. R. Engstrom, J. Kim, G. A. Kimmel, J. Matthiesen, C. B. Mullins, C. J. Mundy, N. G. Petrik, J. M. White, and T. Zubkov

Program Scope

The objective of this program is to examine physiochemical phenomena occurring at the surface and within the bulk of ices, oxides, and amorphous materials. The microscopic details of physisorption, chemisorption, and reactivity of these materials are important to unravel the kinetics and dynamic mechanisms involved in heterogeneous (i.e., gas/liquid) processes. This fundamental research is relevant to solvation and liquid solutions, glasses and deeply supercooled liquids, heterogeneous catalysis, environmental chemistry, and astrochemistry. Our research provides a quantitative understanding of elementary kinetic processes in these complex systems. For example, the reactivity and solvation of polar molecules on ice surfaces play an important role in complicated reaction processes that occur in the environment. These same molecular processes are germane to understanding dissolution, precipitation, and crystallization kinetics in multiphase, multicomponent, complex systems. Amorphous solid water (ASW) is of special importance for many reasons, including the open question over its applicability as a model for liquid water, and fundamental interest in the properties of glassy materials. In addition to the properties of ASW itself, understanding the intermolecular interactions between ASW and an adsorbate is important in such diverse areas as solvation in aqueous solutions, cryobiology, and desorption phenomena in cometary and interstellar ices. Metal oxides are often used as catalysts or as supports for catalysts, making the interaction of adsorbates with their surfaces of much interest. Additionally, oxide interfaces are important in the subsurface environment; specifically, molecular-level interactions at mineral surfaces are responsible for the transport and reactivity of subsurface contaminants. Thus, detailed molecular-level studies are germane to DOE programs in environmental restoration, waste processing, and contaminant fate and transport.

Our approach is to use molecular beams to synthesize “chemically tailored” nanoscale films as model systems to study ices, amorphous materials, supercooled liquids, and metal oxides. In addition to their utility as a synthetic tool, molecular beams are ideally suited for investigating the heterogeneous chemical properties of these novel films. Modulated molecular beam techniques enable us to determine the adsorption, diffusion, sequestration, reaction, and desorption kinetics in real-time. In support of the experimental studies, kinetic modeling and Monte Carlo simulation techniques are used to analyze and interpret the experimental data.

Recent Progress and Future Directions

Effect of Incident Energy on the Phase, Crystallization Kinetics, and Porosity of Vapor Deposited Amorphous Solid Water Water vapor deposited on a cold substrate ($T < 130$ K) is known to form an amorphous solid known as amorphous solid water (ASW). ASW is a solid phase of water that is thermodynamically metastable with respect to the stable crystalline phase. There is great interest in ASW because of questions regarding its thermodynamic relationship to supercooled and liquid water, its applicability as a model for liquid water, and its prevalence in cometary and other astrophysical ices. Whether a vapor deposited material grows as an amorphous or crystalline solid depends on the ability of an incident molecule to explore the multidimensional energy landscape to find the crystalline minimum.

Heuristically, one expects that the ability of the system to find the thermodynamically favored crystalline configuration will depend on the incident flux, incident energy, incident angle, substrate temperature, and other factors related to the dynamics of energy transfer between the incoming molecule and the substrate. Upon collision, the issue is whether the molecule has enough residual energy to reorient into the crystalline configuration prior to thermally equilibrating with the substrate.

To address this issue, we used molecular beam techniques to grow water films on Pt(111) with incident collision energies from 5 to 205 kJ/mole. The effect of the incident collision energy on the phase of vapor deposited water films and their subsequent crystallization kinetics were studied using temperature programmed desorption and infrared spectroscopy. We find that for films deposited at substrate temperatures below 110 K, the incident kinetic energy, up to 205 kJ/mole, had no effect on the initial phase of the deposited film or its crystallization kinetics. Above 110 K, the substrate temperature does affect the phase and crystallization kinetics of the deposited films but this result is also independent of the incident collision energy. These results suggest that the crystallization of amorphous solid water requires cooperative motion of several water molecules.

While it is clear that the incident kinetic energy has no effect on the crystallinity or crystallization kinetics of ASW films, more recent work demonstrates that the incident energy dramatically affects film porosity. We have previously shown that the porosity and morphology of vapor-deposited materials can be controlled by varying the incident deposition angle. In particular, vapor deposition at large incident angles from normal can result in high surface area, highly porous materials. This approach has been used to grow highly porous films for a wide range of materials including ASW, metals (Au, Pd), and metal oxides (MgO, TiO₂). The success of the technique for such a wide variety of materials is because the fundamental mechanism is based on a simple physical principle that can be described using a ballistic deposition model. The term “ballistic deposition” refers to a statistical growth model where incident particles (atoms or molecules) “stick” where they “hit”. If the incident particles “hit and stick”, then a simple shadowing picture can be used to understand the dependence of morphology on the growth angle. Inherent in the above description is that incident particles truly do hit and stick or at least have limited mobility. If this were not the case, particle mobility/diffusion could act to fill the void regions thereby reducing the film porosity.

The effect of the incident angle and collision energy (up to 205 kJ/mole) on the porosity and surface area of the vapor-deposited water films was studied using nitrogen physisorption and infrared spectroscopy. At low incident energy (5 kJ/mol), the dangling OH bond infrared spectra, which provide a direct measure of the surface area, show that the surface area increases with incident angle and levels off at angles > 65°. This is in contrast to the nitrogen uptake data, which display a maximum near 65° because of the decrease in nitrogen condensation in the larger pores that develop at high incident angles. Both techniques show that the morphology of vapor-deposited water films depends strongly on the incident kinetic energy. These observations are consistent with a ballistic deposition shadowing model used to describe the growth of highly porous materials at glancing angle. The dependence of film morphology on incident energy may have important implications for the growth of porous materials via glancing angle deposition. Effusive metal evaporators are often used to deposit metal atoms for the growth of metal and metal oxide porous films. The temperature needed to sublime a metal will vary with the material and, as such, so will the average kinetic energy of the incident metal atoms and thus affect the morphology of the film. Future work may require that the incident deposition energy be considered when creating and characterizing highly porous materials via vapor deposition at off normal angles.

Using Rare Gas Permeation to Probe Methanol Diffusion near the Glass Transition Temperature

Glassy or amorphous materials are widespread in both nature and technology. Understanding the formation of a glass through the extraordinary viscous slow-down that accompanies the supercooling of a liquid is a major current scientific challenge. Studying the properties of the supercooled liquid just above the glass transition temperature (T_g) is important for the understanding of this phenomenon.

We have previously studied deeply supercooled liquid diffusion using both isotopically labeled water and binary layers methanol and ethanol of nanoscale amorphous films. In those experiments the intermixing

rate of the layered films was determined using the molecular desorption rate from the film's outer layer. However, this method only works for systems where there is an experimentally measurable desorption rate prior to crystallization, which is not always the case.

To avoid this problem, we have employed a new approach in which the mobility of deeply supercooled liquid methanol is probed at temperatures near its glass transition (103 K). The technique uses the permeation of rare-gas atoms through nanoscale amorphous methanol films. Specifically, a monolayer of Kr is deposited onto a graphene substrate and then capped with methanol layers of varying thickness. At 25 K, methanol is deposited as an amorphous solid which is heated and then, at temperatures where the amorphous solid becomes a supercooled liquid, the Kr permeates through the overlayer. The diffusion rates were obtained using a one-dimensional diffusion model in which Kr diffusion was represented by a series of discrete hops between potential minima between adjacent methanol layers.

The extracted rare-gas diffusion coefficients together with the available literature diffusion data for methanol self-diffusion are well-fit by a Vogel-Fulcher-Tamann (VFT) equation. The VFT equation is often used to describe markedly non-Arrhenius behavior and is indicative of collective complex motion on a rugged energy landscape rather than the physical crossing of a single barrier characteristic of a normal liquid above its melting point. These new measurements provide clear evidence that methanol is a fragile liquid near the glass transition temperature. It is interesting to compare the kinetic parameters for diffusion in the normal liquid and in deeply supercooled liquid methanol. The apparent activation energy changes from 12.0 to 81.2 kJ/mol, i.e. by almost a factor of seven, as the temperature decreases from 292 to 100 K. This very clearly shows the non-Arrhenius temperature dependence of the diffusivity. An apparent diffusion activation energy of 81.2 kJ/mole, exceeds the vaporization energy, 41.8 kJ/mole, of the supercooled liquid and thus provides evidence of multi-molecular, cooperative motion as being required for diffusion near T_g .

The gas permeation method allows for diffusivity data to be obtained in temperature regimes where data was previously unattainable, dramatically increasing both the temperature and dynamic range of the diffusion measurements. Temperature dependent diffusivity data as presented here, especially near T_g , are requisite to address many of the questions related to supercooled liquids and amorphous materials. Further work is needed to test whether the approach presented here will be widely applicable to a wide range of other chemical systems.

Observation of a Metastable Hydrophobic Wetting Two-Layer Ice on Graphene The structure of water at interfaces is crucial in areas as diverse as protein folding, the structure of living cells, and heterogeneous catalysis. Water's interactions at interfaces span the range from strongly hydrophobic to strongly hydrophilic. For hydrophilic substrates, it is obvious that the strong binding of the water to the substrate can influence the structure of the water film near the substrate. However, even very hydrophobic substrates can have a profound influence on the structure of water in the vicinity because of the tendency for substrates to induce stratification in the water near the interface. The lack of bonding to a hydrophobic substrate, in conjunction with the stratification, can lead to significant distortions away from ice's preferred tetrahedral bonding geometry. For example, molecular dynamics (MD) simulations have predicted the existence of quasi-two-dimensional crystalline and amorphous ices between planar hydrophobic walls, which have distinctive properties such as nontetrahedral bonding geometries, novel phase transitions and anomalous self-diffusion. To date, these structures have not been observed experimentally. A closely related topic, the structure and dynamics of water confined in nonplanar geometries such as carbon nanotubes, is also of great current interest.

In a combined experimental (Kimmel, Kay PIs) and theoretical (Mundy PI) effort we have observed and characterized a metastable, quasi-two-dimensional crystalline ice grown on a planar hydrophobic substrate, graphene on Pt(111), with a unique, nontetrahedral bonding geometry. This new ice polymorph consists of two *flat* hexagonal sheets of water molecules in which the hexagons in each sheet are stacked directly on top of each other. Each molecule forms three hydrogen bonds with its neighbors within a given layer with oxygen-oxygen-oxygen bond angles, θ_{OOO} , of 120° and a fourth hydrogen bond with a molecule in the other sheet, with $\theta_{OOO} = 90^\circ$. In this arrangement, the number of hydrogen bonds is

maximized and there are no dangling OH's or lone pair electrons on either surface of the ice film (i.e., these ice surfaces are expected to be hydrophobic). The two-layer ice, which grows at low temperatures (<100-135 K), has been characterized experimentally with low energy electron diffraction (LEED), reflection-absorption infrared spectroscopy (RAIRS), and rare-gas temperature programmed desorption (TPD), and theoretically with ab initio MD simulations. The results lend support to the previous simulations predicting the existence of two-layer ices in the confined hydrophobic geometries that are relevant to protein folding. Furthermore, the unusual bonding geometry exhibited in the two-layer ice may also play a role in liquid water at hydrophobic interfaces. Future work will continue characterization of the structural and physical properties of this unique form of water. In addition, we are currently investigating the structure of the ice films for coverages greater than 2 ML.

References to Publications of DOE sponsored Research (CY 2006- present)

1. Smith RS, T Zubkov, and **BD Kay**. 2006. "The Effect of the Incident Collision Energy on the Phase and Crystallization Kinetics of Vapor Deposited Water Films." *Journal of Chemical Physics* 124(11): Art. No. 114710.
2. Dohnálek Z, J Kim, O Bondarchuk, JM White, and **BD Kay**. 2006. "Physisorption of N₂, O₂, and CO on Fully Oxidized TiO₂(110)." *Journal of Physical Chemistry B* 110(12):6229-6235.
3. Z Dohnálek, J.Kim and **BD Kay** 2006 "Growth of Epitaxial Pd(111) Films on Pt(111) and Oxygen Terminated FeO(111) Surfaces." *Surface Science* **600**: 3461
4. Kimmel GA, NG Petrik, Z Dohnálek, and **BD Kay**. 2006. "Layer-by-Layer Growth of Thin Amorphous Solid Water Films on Pt(111) and Pd(111)." *Journal of Chemical Physics* 125(4): Art. No. 044713.
5. Tait SL, Z Dohnálek, CT Campbell, and **BD Kay**. 2006. "*n*-Alkanes on Pt(111) and on C(0001)/Pt(111): Chain Length Dependence of Kinetic Desorption Parameters." *Journal of Chemical Physics* 125(23): Art. No. 234308.
6. Kimmel GA, NG Petrik, Z Dohnálek, and **BD Kay**. 2007. "Crystalline Ice Growth on Pt(111) and Pd(111): Nonwetting Growth on a Hydrophobic Water Monolayer." *Journal of Chemical Physics* 126(11): Art. No. 114702.
7. Flaherty DW, Z Dohnálek, A Dohnálková, BW Arey, DE McCreedy, N Ponnusamy, CB Mullins, and **BD Kay**. 2007. "Reactive Ballistic Deposition of Porous TiO₂ Films: Growth and Characterization." *Journal of Physical Chemistry C* 111(12):4765-4773.
8. Smith RS, P Ayotte, and **BD Kay**. 2007. "Formation of Supercooled Liquid Solutions from Nanoscale Amorphous Solid Films of Methanol and Ethanol." *Journal of Chemical Physics* 127(24): Art. No. 244705.
9. Zubkov T, RS Smith, TR Engstrom, and **BD Kay**. 2007. "Adsorption, Desorption and Diffusion of Nitrogen in a Model Nanoporous Material: I.: Surface Limited Desorption Kinetics in Amorphous Solid Water." 2007. *Journal of Chemical Physics* 127(18): Art. No. 184707.
10. Zubkov T, RS Smith, TR Engstrom, and **BD Kay**. 2007. "Adsorption, Desorption and Diffusion of Nitrogen in a Model Nanoporous Material: II.: Diffusion Limited Kinetics in Amorphous Solid Water." *Journal of Chemical Physics* 127(18): Art. No. 184708.
11. Dohnalek Z, J Kim and **BD Kay**. 2008. "Understanding How Surface Morphology and Hydrogen Dissolution Influence Ethylene Hydrogenation on Palladium." *Journal of Physical Chemistry* **112**, 15796.
12. Smith RS, T Zubkov, Z Dohnálek and **BD Kay**. 2009. "The Effect of the Incident Collision Energy on the Porosity of Vapor Deposited Amorphous Solid Water Films." *Journal of Physical Chemistry B* **113**, 4000.
13. Cholette F, T Zubkov, RS Smith, Z Dohnálek, **BD Kay** and P Ayotte. 2009. "Infrared Spectroscopy and Optical Constants of Porous Amorphous Solid Water." *Journal of Physical Chemistry B* **113**, 4131.
14. Parkinson GS, Z Dohnálek, RS Smith, and **BD Kay**. 2009. "Reactivity of Fe⁰ atoms and clusters with D₂O over FeO(111)." *Journal of Physical Chemistry C* **113**, 44960.
15. Kimmel GA, J Matthiesen, M Baer, CJ Mundy, NG Petrik, RS Smith, Z Dohnálek, and **BD Kay**. 2009. "No Confinement Needed: Observation of a Metastable Hydrophobic Wetting Two-Layer Ice on Graphene." *Journal of The American Chemical Society*, (Accepted August 2009).

Correlating electronic and nuclear motions during photoinduced charge transfer processes using multidimensional femtosecond spectroscopies and ultrafast x-ray absorption spectroscopy

Munira Khalil

University of Washington, Department of Chemistry, Box 351700, Seattle, WA 98115

Email: mkhalil@chem.washington.edu

The goal of this recently funded DOE program is to measure coupled electronic and nuclear motions during photoinduced charge transfer processes in mixed valence transition metal complexes by developing and using novel femtosecond spectroscopies. In this program, we will use a unique two-pronged experimental approach to relate commonly measured kinetic parameters in transient photochemical experiments to the time-evolving distributions of molecular and electronic structures of the reactants and products and their interactions with the solvent bath. This study will focus on transition metal mixed- valence dimers and trimers of the form: $[(\text{CN})_5\text{M}^{\text{II}} - \text{CN} - \text{M}^{\text{III}}(\text{NH}_3)_5]^-$ and $[(\text{NC})_5\text{M}^{\text{II}} - \text{CN} - \text{Pt}^{\text{IV}}(\text{NH}_3)_4 - \text{NC} - \text{M}^{\text{II}}(\text{CN})_5]^{4-}$, where M=Fe, Os and Ru.

One part of the research program will focus on the development of novel three-dimensional visible-infrared experiments employing a sequence of visible and infrared fields to directly correlate electronic and vibrational motion during ultrafast photochemical reactions. These experiments will measure time-dependent anharmonic vibrational couplings of the high-frequency solute vibrations with the low-frequency solvent and solute degrees of freedom, time-dependent vibronic couplings, and elucidate the role of incoherent and coherent vibrational relaxation and transfer pathways during electron transfer.

The other half of the experimental program will consist of performing ultrafast transient x-ray experiments at the Advanced Light Source using tunable 200 fs x-rays to measure changes in local electronic and atomic structure surrounding the transition metal species with high spatial and temporal resolution following intervalence charge transfer excitation. A self-consistent analysis of the data from these experiments will provide intricate molecular details on intervalence charge transfer chemistry.

In the past year, we have built and tested a multidimensional IR spectrometer to obtain equilibrium and non-equilibrium 2D IR spectra of various chemical systems in solution. We have also made progress in synthesizing the mixed valence compounds listed above and are starting to characterize the vibrational dynamics of the cyanide ligands using nonlinear IR spectroscopy.

Presently we are studying the photochemical dynamics of sodium nitroprusside (SNP) in solution. Upon metal-to-ligand charge transfer photoexcitation, the nitrosyl group in SNP undergoes linkage isomerism where the ground state (GS) Fe-N-O bonding is changed to an η^2 side-on configuration and an Fe-O-N linear configuration in the metastable states referred to as MS2 and MS1 respectively. The crystal structures of the metastable states have been obtained from x-ray crystallography, however there has been no time-resolved work done on this system in solution at room temperature. We have recently obtained evidence of photoinduced linkage isomerism in SNP on the picosecond timescale in solution using transient infrared spectroscopy. We have also performed 2D

IR experiments to gain insight into the solvation dynamics of SNP dissolved in methanol using the nitrosyl and cyanide stretching frequencies as probes of their local environment.

Future work will focus on developing 3D spectroscopies using a combination of visible and infrared pulses. We have competed successfully to obtaining beamtime for performing ultrafast x-ray experiments at the Advanced Light Source in collaboration with Robert Schoenlein's group. In the next year, we plan to perform transient x-ray experiments at the Fe and Ru K-edges to study the local structural rearrangements following ultrafast charge transfer processes.

Chemical Kinetics and Dynamics at Interfaces

Non-Thermal Reactions at Surfaces and Interfaces

Greg A. Kimmel (PI) and Nikolay G. Petrik

Chemical and Materials Sciences Division

Pacific Northwest National Laboratory

P.O. Box 999, Mail Stop K8-88

Richland, WA 99352

gregory.kimmel@pnl.gov

Program Scope

The objectives of this program are to investigate 1) the thermal and non-thermal reactions at surfaces and interfaces, and 2) the structure of thin adsorbate films and how this influences the thermal and non-thermal chemistry. The fundamental mechanisms of radiation damage to molecules in the condensed phase are of considerable interest to a number of scientific fields ranging from radiation biology to astrophysics. In nuclear reactor design, waste processing, radiation therapy, and many other situations, the non-thermal reactions in aqueous systems are of particular interest. Since the interaction of high-energy radiation (gamma-rays, alpha particles, etc.) with water produces copious amounts of low-energy secondary electrons, the subsequent reactions of these low-energy electrons are particularly important. The general mechanisms of electron-driven processes in homogeneous, dilute aqueous systems have been characterized in research over the last several decades. More recently, the structure of condensed water and its interactions with electrons, photons, and ions have been extensively studied and a variety of non-thermal reaction mechanisms identified. However, the complexity of the electron-driven processes, which occur over multiple length and time scales, has made it difficult to develop a detailed molecular-level understanding of the relevant physical and chemical processes.

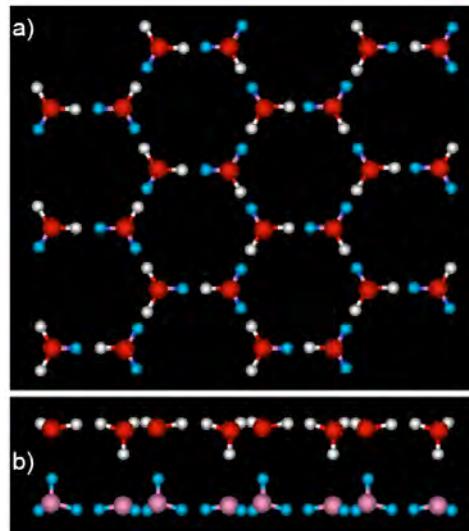
We are focusing on low-energy, electron-stimulated reactions in thin water films. Our approach is to use a molecular beam dosing system to create precisely controlled thin films of amorphous solid water (ASW) and crystalline ice (CI). Using isotopically layered films of D₂O, H₂¹⁶O and H₂¹⁸O allows us to explore the spatial relationship between where the incident electrons deposit energy and where the electron-stimulated reactions subsequently occur within the films. Furthermore, working with thin films allows us to explore the role of the substrate in the various electron-stimulated reactions.

Recent Progress:

No Confinement Needed: Observation of a Hydrophobic Wetting Two-Layer Ice on Graphene

The structure of water at interfaces is crucial in areas as diverse as protein folding, the structure of living cells, and heterogeneous catalysis. Water's interactions at interfaces span the range from strongly hydrophobic to strongly hydrophilic. For hydrophilic substrates, it is obvious that the strong binding of the water to the substrate can influence the structure of the water film near the substrate. However, even very hydrophobic substrates can have a profound influence on the structure of water in the vicinity because of the tendency for substrates to induce stratification in the water near the interface. The lack of bonding to a hydrophobic substrate, in conjunction with the stratification, can lead to significant distortions away from ice's preferred tetrahedral bonding geometry. For example, molecular dynamics (MD) simulations have predicted the existence of quasi-two-dimensional crystalline and amorphous ices confined between planar hydrophobic walls, which have distinctive properties such as nontetrahedral bonding geometries, novel phase transitions and anomalous self-diffusion. To date, these structures have not been observed experimentally. A closely related topic, the structure and dynamics of water confined in nonplanar geometries such as carbon nanotubes, is also of great current interest.

In a combined experimental (Kimmel, Kay PIs) and theoretical (Mundy PI) effort we have observed and characterized a metastable, quasi-two-dimensional crystalline ice grown on a planar hydrophobic substrate, graphene on Pt(111), with a unique, nontetrahedral bonding geometry [17]. This new ice polymorph consists of two *flat* hexagonal sheets of water molecules in which the hexagons in each sheet are stacked directly on top of each other (see the figure at the right). Each molecule forms three hydrogen bonds with its neighbors within a given layer with oxygen-oxygen-oxygen bond angles, θ_{OOO} , of 120° and a fourth hydrogen bond with a molecule in the other sheet, with $\theta_{\text{OOO}} = 90^\circ$. In this arrangement, the number of hydrogen bonds is maximized and there are no dangling OH's or lone pair electrons on either surface of the ice film (i.e., these ice surfaces are expected to be hydrophobic). The two-layer ice, which grows at low temperatures ($<100\text{-}135\text{ K}$), has been characterized experimentally with low energy electron diffraction (LEED), reflection-absorption infrared spectroscopy (RAIRS), and rare-gas temperature programmed desorption (TPD), and theoretically with ab initio MD simulations. The results lend support to the previous simulations predicting the existence of two-layer ices in the confined hydrophobic geometries that are relevant to protein folding. Furthermore, the unusual bonding geometry exhibited in the two-layer ice may also play a role in liquid water at hydrophobic interfaces. Future work will continue characterization of the structural and physical properties of this unique form of water. In addition, we are currently investigating the structure of the ice films for coverages greater than 2 ML.



Electron-Stimulated Reactions and O₂ production in Methanol-Covered Amorphous Solid Water Films

Non-thermal reactions in aqueous systems, including frozen aqueous systems (“ices”), are relevant for several areas of fundamental and practical interest ranging from photocatalysis to radiation biology. Since water is so important, the reactions in pure liquid water and water ices have been the most extensively studied. Outside of the laboratory however, other species are always present and understanding how various factors, such as the chemical composition and the local structure of aqueous mixtures, influence the non-thermal chemistry is essential. Ionizing radiation plays a significant role in the production of a wide variety of molecules in extraterrestrial environments where water ices are present and since methanol is among the most abundant molecules found there, the non-thermal reactions in methanol-water ices are relevant for astrochemistry. Non-thermal reactions in methanol and water are also important in radiation biology, nuclear technology, and atmospheric chemistry.

We have investigated the low-energy (100 eV), electron-stimulated reactions in multilayer ASW films capped with thin films of methanol for methanol coverages, θ_{MeOH} , ranging from less than a monolayer to a few monolayers [15]. We examined the influence of the ASW “substrate” on the reactions in the methanol adlayer, the influence of the methanol on the reactions in the ASW, and energy transfer from the ASW to the methanol adlayers. We find that the electron-stimulated desorption (ESD) yields from thin methanol layers on ASW are similar to those for thick methanol films, and there is little evidence for energy transfer from the ASW films to the methanol adlayers. The molecular oxygen, hydrogen and water ESD yields from the ASW film are suppressed by the methanol adlayers. The suppression of the water ESD products by methanol is consistent with the non-thermal reactions occurring preferentially at or near the ASW/vacuum interface and not in the bulk of the water film. The molecular water and hydrogen ESD yields from the ASW decrease exponentially versus θ_{MeOH} with $1/e$ constants of $\sim 0.6 \times 10^{15}\text{ cm}^{-2}$ and $1.6 \times 10^{15}\text{ cm}^{-2}$, respectively. In contrast, the O₂ ESD is suppressed by an order of magnitude lower methanol coverage ($1/e \sim 6.5 \times 10^{13}\text{ cm}^{-2}$). The suppression of the O₂ ESD by small amounts of methanol is

primarily due to reactions between OH radicals (which are precursors to the O₂) and methanol. We present a kinetic model, which was previously developed to account for the O₂ ESD in neat and H₂O₂/ASW films, that has been modified to include the relevant reactions in the methanol-ASW films. The model semi-quantitatively accounts for the observations.

Non-thermal water splitting on Rutile TiO₂: Electron-stimulated production of H₂ and O₂ in Amorphous Solid Water films on TiO₂(110)

TiO₂ is an important catalyst for a variety of applications including the photocatalytic destruction of organic pollutants, and potentially for photocatalytic water splitting to produce hydrogen. The applications of TiO₂ have motivated extensive research on the thermal and photon-stimulated reactions on single crystals, particles and aqueous suspensions. Since many of the uses of TiO₂ for catalysis involve aqueous solutions, the thermal and non-thermal reactions of water with TiO₂ are particularly important. These reactions have been investigated with a wide variety of techniques. However, despite intensive scrutiny, fundamental aspects of the reactions of water and other molecules on TiO₂ surfaces remain to be addressed.

We have investigated the electron-stimulated reactions in amorphous solid water (ASW) films on TiO₂(110) leading to the production of H₂ and O₂ and the desorption of H₂O as function of water coverage, θ , and isotopic composition [14]. For 100 eV incident electrons, H₂ and O₂ ESD yields have maxima at $\theta \sim 20$ ML, while the H₂O ESD yield increases monotonically with water coverage. All the products reach a coverage-independent yield for $\theta > 40 - 50$ ML. Experiments using layered films of H₂O and D₂O demonstrate that molecular hydrogen is produced in reactions that occur preferentially at or near both the ASW/TiO₂ interface and the ASW/vacuum interface, but not in the interior of the ASW films. The energy for the reactions, however, is absorbed from the incident electrons in the interior of the films creating electronic excitations and/or ionic defects which subsequently migrate to the interfaces where they drive the reactions. The TiO₂(110) surface becomes hydrogenated after irradiation of multilayer ASW films on TiO₂(110). In particular bridge-bonded hydroxyls are formed, but they do not contribute to the H₂ produced near the ASW/TiO₂(110) interface. Instead, the results suggest that the H₂ is produced from a stable precursor that is trapped on the TiO₂(110) or in the water near the substrate. The proposed mechanism for the H₂ production near the ASW/TiO₂(110) interface is supported by a kinetic model that semi-quantitatively reproduces the main features of the non-thermal reactions.

Future Directions:

Important questions remain concerning the factors that determine the structure of thin water films on various substrates. We plan to continue investigating the structure of thin water films on non-metal surfaces, such as oxides, and on metals where the first layer of water does not wet the substrate. For the non-thermal reactions in water films, we will use FTIR spectroscopy to characterize the electron-stimulated reaction products and precursors. The mechanisms of the non-thermal precursor migration through ASW films need to be further explored. We will also investigate the non-thermal reactions at lower electron energies (i.e. closer to the ionization threshold for water). Finally, we plan to investigate the lifetimes of excited states in ASW and CI using pump-probe fluorescence measurements.

References to publications of DOE sponsored research (FY 2005 – present)

- [1] Nikolay G. Petrik and Greg A. Kimmel, "Electron-stimulated sputtering of thin amorphous solid water films on Pt(111)," *J. Chem. Phys.* **123**, 054702 (2005).
- [2] Bruce C. Garrett, et al., "Role of Water in Electron-Initiated Processes and Radical Chemistry: Issues and Scientific Advances," *Chem. Rev.* **105**, 355 (2005).
- [3] Greg A. Kimmel, Nikolay G. Petrik, Zdenek Dohnálek and Bruce D. Kay, "Crystalline ice growth on Pt(111): Observation of a hydrophobic water monolayer," *Phys. Rev. Lett.* **95** (2005) 166102.

- [4] Nikolay G. Petrik, Alexander Kavetsky and Greg A. Kimmel, "Electron-Stimulated Production of Molecular Oxygen in Amorphous Solid Water," *J. Phys. Chem. B.* **110**, 2723 (2006).
- [5] Greg A. Kimmel, Nikolay G. Petrik, Zdenek Dohnálek and Bruce D. Kay, "Layer-by-layer growth of thin amorphous solid water films on Pt(111) and Pd(111)," *J. Chem. Phys.* **125**, 044713 (2006).
- [6] Nikolay G. Petrik, Alexander Kavetsky and Greg A. Kimmel, "Electron-stimulated production of molecular oxygen in amorphous solid water on Pt(111): Precursor transport through the hydrogen bonding network," *J. Chem. Phys.* **125**, 124702 (2006).
- [7] Greg A. Kimmel, Nikolay G. Petrik, Zdenek Dohnálek and Bruce D. Kay, "Crystalline ice growth on Pt(111) and Pd(111): Non-wetting growth on a hydrophobic water monolayer," *J. Chem. Phys.* **126**, 114702 (2007).
- [8] Christopher D. Lane, Nikolay G. Petrik, Thomas M. Orlando, and Greg A. Kimmel, "Electron-stimulated oxidation of thin water films adsorbed on TiO₂(110)," *J. Phys. Chem. C* **111**, 16319 (2007).
- [9] Nikolay G. Petrik and Greg A. Kimmel, "Hydrogen bonding, H/D exchange and molecular mobility in thin water films on TiO₂(110)," *Phys. Rev. Lett.* **99**, 196103 (2007).
- [10] Christopher D. Lane, Nikolay G. Petrik, Thomas M. Orlando, and Greg A. Kimmel, "Site-dependent electron-stimulated reactions in water films on TiO₂(110)," *J. Chem. Phys.* **127**, 224706 (2007).
- [11] Greg A. Kimmel and Nikolay G. Petrik, "Tetraoxygen on reduced TiO₂(110): Oxygen adsorption and reactions with oxygen vacancies," *Phys. Rev. Lett.* **100**, 196102 (2008).
- [12] G. A. Grieves, N. Petrik, J. Herring-Captain, B. Olanrewaju, A. Aleksandrov, R. G. Tonkyn, S. A. Barlow, G. A. Kimmel, and T. M. Orlando, "Photoionization of Sodium Salt Solutions in a Liquid Jet," *J. Phys. Chem. C* **112**, 8359 (2008).
- [13] Zhenrong Zhang, Yingge Du, Nikolay G. Petrik, Greg A. Kimmel, Igor Lyubinetsky, and Zdenek Dohnálek, "Water as a Catalyst: Imaging Reactions of O₂ with Partially and Fully Hydroxylated TiO₂(110)," *J. Phys. Chem. (C)* **113**, 1908 (2009).
- [14] Nikolay G. Petrik and Greg A. Kimmel, "Non-thermal water splitting on Rutile TiO₂: Electron-stimulated production of H₂ and O₂ in Amorphous Solid Water films on TiO₂(110)," *J. Phys. Chem. (C)* **113**, 4451 (2009).
- [15] Minta C. Akin, Nikolay G. Petrik and Greg A. Kimmel, "Electron-Stimulated Reactions and O₂ production in Methanol-Covered Amorphous Solid Water Films," *J. Chem. Phys.* **130**, 104710 (2009).
- [16] Nikolay G. Petrik, Zhenrong Zhang, Yingge Du, Zdenek Dohnálek, Igor Lyubinetsky, and Greg A. Kimmel, "The Chemical Reactivity of Reduced TiO₂(110): The dominant role of surface defects in oxygen chemisorption," *J. Phys. Chem. (C)* **113**, 12407 (2009).
- [17] Greg A. Kimmel, Jesper Matthiesen, Marcel Baer, Christopher J. Mundy, Nikolay G. Petrik, R. Scott Smith, Zdenek Dohnálek, and Bruce D. Kay, "No Confinement Needed: Observation of a Metastable Hydrophobic Wetting Two-Layer Ice on Graphene," *J. Am. Chem. Soc.* **131**, 12838 (2009).

Radiolysis of Water Adsorbed on Ceramic Oxides

Jay A. LaVerne
Radiation Laboratory, University of Notre Dame
Notre Dame, IN 46556
laverne.1@nd.edu

Program Scope

A variety of experimental techniques are being used to elucidate the mechanism for the radiolytic decomposition of water adsorbed on the surface of ceramic oxides. The research focuses on the radiation chemistry of the water and how it is affected by the solid interface. Water adsorbed on or very near to a ceramic oxide surface has very different properties than normal bulk water. Dissociative adsorption and strong hydrogen bonding are expected with most of the ceramic oxides, which will affect the water decomposition. Transport of energy or matter through the interface will influence the initial yields and subsequent kinetics. Variation in gas evolution, particularly molecular hydrogen, is used as one of the probes of the chemistry occurring at the water – solid interface. Molecular hydrogen is the primary stable reducing species formed in the radiolysis of liquid water and its production is extremely important in nuclear power plant operation and in radioactive waste cleanup and management. A variety of spectroscopic techniques are used to examine the formation or loss of species at the water – ceramic oxide interface. The goal is to obtain information about the intermediate species involved and the mechanisms for product formation under conditions commonly encountered in typical applications involving liquid – solid interfaces in radiation fields. The fundamental physical and chemical information obtained in this program will find wide application in a wide variety of science and technology fields including: nano-technology, nuclear power plant operation, radioactive waste cleanup and management, environmental remediation, and health physics.

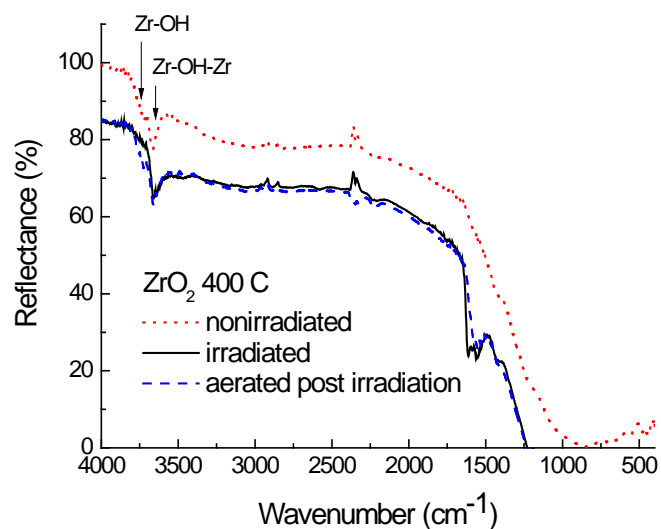
Recent Progress

Experimental studies have determined H₂ production in the gamma radiolysis of water adsorbed on CeO₂, ZrO₂, and UO₂ particles,^{1,2} and more recently on SiO₂, HfO₂, TiO₂, Al₂O₃, ZnO, MgO, CaO, and BeO. The amount of water in these studies varied from a few to about 30 monolayers of physisorbed water. A few monolayers of water on a particle of 100 nm diameter amounts to only about one percent of the total weight. Energy absorbed by each component of a system is essentially equal to its fraction of electron density so virtually all of the energy is located initially in the solid particle. The radiolysis of liquid water alone would result in a H₂ yield of 0.45 molecule/100 eV absorbed, but this value is expected to be two orders of magnitude lower, i.e. 0.0045 molecule/100 eV, if only 1 percent of the energy is initially deposited in the water. Experiments with ZrO₂ give a H₂ yield of 0.08 molecule/100 eV of energy deposited in the entire water – oxide system. This extremely high yield suggests that a significant fraction of the energy initially deposited within the solid oxide reaches the surface leading to an excess production of H₂. Variations of the H₂ yields with the amount of physisorbed water show that H₂ can be observed down to the lowest water loading suggesting that surface reactions of chemisorbed water are responsible for a significant portion of the H₂ production.^{1,2}

The more recent studies have focused on examining the properties of the ceramic oxides that are responsible for the excess production of H₂. The results from previous efforts using a variety of dopants suggest that energy transport in the oxide involves the

migration of excitons to the surface followed by their coupling to bound surface water.³ Coupling between surface water and the oxide band gap is suggested to occur with a resonant energy of about 5 eV. The nature of this resonance or even its existence is unclear, but such a property would be extremely valuable for understanding the mechanism of water decomposition and for predicting H₂ yields. A variety of oxides were examined for H₂ production to determine if other oxides with band gaps near 5 eV exhibited similar excesses in H₂ yields and if oxides of much different band gaps could give excessive H₂ yields. Several ceramic oxides with band gaps significantly greater than 5 eV give yields of H₂ equivalent to or greater than that for ZrO₂. For instance, the yield of H₂ with water adsorbed on BeO with a band gap energy of 10.4 eV results in a H₂ yield of 0.11 molecule/100 eV of energy adsorbed in the entire system. In general, many oxides with high band gap energies give excess H₂ production. However, high band gap energy is not a sufficient condition for excess H₂ production and other conditions must be satisfied.

Several experimental studies suggest that surface water is responsible for H₂ production so an effort was made to directly examine variations in the surface of ceramic oxides with radiolysis. Physisorbed water gives a broad IR band at about 3400 cm⁻¹ due to the OH stretch that masks the underlying chemisorbed species. A high temperature diffuse reflectance infrared Fourier transform, DRIFT, cell was modified to fit on the exit window of a 3 MeV electron accelerator. Increasing the ceramic oxide temperature to 400 C results in the loss of the physisorbed water to reveal the OH species bound to the surface cations. Water dissociatively chemisorbes to most ceramic oxides to give isolated and bridged OH groups at the surface as shown in the figure for ZrO₂. Radiolysis of the oxide *in situ* shows a decrease in the terminal OH group at 3500 cm⁻¹ suggesting that this species is responsible for H₂ production. Peaks are formed at 1600 cm⁻¹ with increasing irradiation. These peaks are located where OH bending motions are expected. The exact nature of the species has not been determined, but it could be the oxidizing species that complements the H₂ production.



DRIFT spectra of γ -irradiated water on ZrO₂ particles at 400 C.

Future Plans

Many oxides have been examined for H₂ production and a number of these have been found to be very efficient.⁴ The most recent set of experiments seem to indicate that band gap alone is not responsible for excess H₂ production so some other parameter must also have an effect. Several possible factors can contribute to H₂ formation including: number or type of bound OH sites, the amount of water loading, the associated hydrogen bonding, and the particle size. The effects of these parameters on H₂ production will be

examined in future studies.

Recent IR examinations of the interfacial species produced in the radiolysis of chemisorbed water observed the loss of the terminal OH group with increasing irradiation. However, a direct correlation between the loss of this species and the formation of H₂ has not been established. Only a few number of oxides have been examined and the technique will be further refined to examine a wider variety of ceramic oxides. An examination of the formation of H₂ under the same conditions as used in the IR experiments will be especially important to establish its dependence on OH moieties. Emphasis will be placed on ZrO₂, TiO₂, and Al₂O₃ because of their importance as construction materials and because they have the most ancillary information on processes occurring at their surface. Other studies will focus on the radiolysis of BeO and HfO₂ because of their relatively large production of H₂.

In all of the experimental studies performed to date, H₂ production is not accompanied by the formation of stoichiometric O₂. This result suggests that oxygen species remain on the particle surface. Identification of these species will aid in determination of the water decomposition mechanism, which is also of extreme technological importance. For instance, adsorbed oxygen species may affect the water chemistry of reactors or it may incorporate into the surface leading to radiation induced corrosion or dissolution. EPR and IR spectroscopic techniques will be used to examine the ceramic oxide surfaces for oxygen species produced in radiolysis.

References

- (1) LaVerne, J. A.; Tandon, L. *J. Phys. Chem. B* **2002**, *106*, 380.
- (2) LaVerne, J. A.; Tandon, L. *J. Phys. Chem. B* **2003**, *107*, 13623.
- (3) Petrik, N. G.; Alexandrov, A. B.; Vall, A. I. *J. Phys. Chem. B* **2001**, *105*, 5935.
- (4) Aleksandrov, A. B.; Byakov, A. Y.; Vall, A. I.; Petrik, N. G. *Russ. J. Phys. Chem.* **1991**, *65*, 847.

DOE Sponsored Publications in 2005-2009

- La Verne, J. A., Ryan, M. R. and Mu, T. **2009**, "Hydrogen Production in the Radiolysis of Halide Solutions", *Radiat. Phys. Chem.* **in press**,
- Dziewinska, K. M., Peters, A. M., LaVerne, J. A., Martinez, P., Dziewinski, J. J., Davenhall, L. B. and Rajesh, P. **2009**, "In Search of an Optimum Plutonium Density Measurement Fluid", *Radiochim. Acta* **97**, 213-217.
- Atinault, E., De Waele, V., Fattahi, M., La Verne, J. A., Pimblott, S. M. and Mostafavi, M. **2009**, "Aqueous Solution of UCl₆²⁻ in O₂ Saturated Acidic Medium: An Efficient System to Scavenge All Primary Radicals in Spurs Produced by Irradiation", *J. Phys. Chem. A* **113**, 949-951.
- La Verne, J. A., Carrasco-Flores, E. A., Araos, M. S. and Pimblott, S. M. **2008**, "Gas Production in the Radiolysis of Poly(vinyl chloride)", *J. Phys. Chem. A* **112**, 3345-3351.
- Huerta Parajon, M., Rajesh, P., Mu, T., Pimblott, S. M. and La Verne, J. A. **2008**, "H Atom Yields in the Radiolysis of Water", *Radiat. Phys. Chem.* **77**, 1203-1207.

- Enomoto, K. and La Verne, J. A. **2008**, "Reactions of Hydrated Electrons with Pyridinium Salts in Aqueous Solutions", *J. Phys. Chem. A* **112**, 12430-12436.
- Pimblott, S. M. and La Verne, J. A. **2007**, "Production of Low-Energy Electrons by Ionizing Radiation", *Radiat. Phys. Chem.* **76**, 1244-1247.
- La Verne, J. A., Enomoto, K. and Araos, M. S. **2007**, "Radical Yields in the Radiolysis of Cyclic Compounds", *Radiat. Phys. Chem.* **76**, 1272-1274.
- Enomoto, K., LaVerne, J. A. and Araos, M. S. **2007**, "Heavy Ion Radiolysis of Liquid Pyridine", *J. Phys. Chem. A* **111**, 9-15.
- Carrasco-Flores, E. A. and La Verne, J. A. **2007**, "Surface Species Produced in the Radiolysis of Zirconia Nanoparticles", *J. Chem. Phys.* **127**, 234703.
- Enomoto, K., LaVerne, J. A. and Pimblott, S. M. **2006**, "Products of the Triplet Excited State Produced in the Radiolysis of Liquid Benzene", *J. Phys. Chem. A* **110**, 4124-4130.
- Enomoto, K., La Verne, J. A., Seki, S. and Tagawa, S. **2006**, "Formation and Decay of the Triplet Excited State of Pyridine", *J. Phys. Chem. A* **110**, 9874-9879.
- Milosavljevic, B. M. and LaVerne, J. A. **2005**, "Pulse Radiolysis of Aqueous Thiocyanate Solution", *J. Phys. Chem. A* **109**, 165-168.
- LaVerne, J. A., Tandon, L., Knippel, B. C. and Montoya, V. M. **2005**, "Heavy Ion Radiolysis of Methylene Blue", *Radiat. Phys. Chem.* **72**, 143-147.
- LaVerne, J. A., Stefanic, I. and Pimblott, S. M. **2005**, "Hydrated Electron Yields in the Heavy Ion Radiolysis of Water", *J. Phys. Chem. A* **109**, 9393-9401.
- LaVerne, J. A., Stefanic, I. and Pimblott, S. M. **2005**, "Hydrated Electron Yields in the Proton Radiolysis of Water", *Jpn. J. Radiat. Chem.* **79**, 9-12.
- LaVerne, J. A., Carmichael, I. and Araos, M. S. **2005**, "Radical Production in the Radiolysis of Liquid Pyridine", *J. Phys. Chem. A* **109**, 461-465.
- LaVerne, J. A. **2005**, "H₂ Formation from the Radiolysis of Liquid Water with Zirconia", *J. Phys. Chem. B* **109**, 5395-5397.
- Hiroki, A. and LaVerne, J. A. **2005**, "Decomposition of Hydrogen Peroxide at Water-Ceramic Oxide Interfaces", *J. Phys. Chem. B* **109**, 3364-3370.

Radiation Effects in Heterogeneous Systems and at Interfaces

Jay A. LaVerne, Dan Meisel, Ian Carmichael, Daniel M. Chipman

Radiation Laboratory, University of Notre Dame, Notre Dame, IN 46556

laverne.1@nd.edu, dani@nd.edu, carmichael.1@nd.edu, chipman.1@nd.edu

Program Scope

Fundamental chemical processes induced by the passage of ionizing radiation are being examined in heterogeneous systems and at interfaces using a combination of experimental and theoretical methods. Experimental studies of systems ranging from aqueous dispersions of nanoparticles to hydroxide monolayers are focusing on the transport of charge carriers through interfaces and the identity and reactivity of species bound to interfaces. These studies are coupled with model calculations on the stability of transient and interfacial species to give a complete description of the radiolytic processes. Interfaces provide the opportunity for the transfer of energy and charge between two phases and are relevant to many practical technological problems of importance to the Department of Energy. Heterogeneous systems are frequently encountered in the management of nuclear materials and nuclear waste, and in nuclear power plant infrastructure.

Recent Progress

Surface enhanced Raman spectroscopy, SERS, has been used to probe changes at the surface of metallic nanoparticles. We adopted the same method described previously for silver to the synthesis of gold particles and are now trying to generate alloys and core-shell particles that would broaden the range of useful metals and supports without compromising their catalytic activity while maintaining their SERS enhancement. All of these particles are free of any stabilizers or counter ions and contain only the metal, water and their corresponding ions. Following our earlier observations from silver and using the same reporting probe molecule, *p*-aminothiophenol, estimates of the overpotential during the catalytic hydrogen evolution on gold particles were determined from the dependence of the SERS spectra on the solution parameters. However, due to the higher work function of gold and the corresponding position of the Fermi level, the pattern of spectra on Au and Ag are very different.

To demonstrate the power of SERS in unraveling mechanistic aspects of radiation effects on catalytic processes we are examining another redox process, the conversion of nitroaromatic compounds, specifically *p*-nitrothiophenol to its amine analog. This process competes with hydrogen evolution in the presence of a nitro-substrate, which is readily initiated by excitation of the silver (but not gold) particles. Surprisingly we find that the equivalent radiolytic reaction does not proceed to generate the amine. We show that the reason for the difference between its behavior in a radiolytic compared to a photolytic environment is the radical stage that is circumvented in the photolysis. While the photolytic process undergoes a multi-electron transfer step following excitation of the particles (or a particle-substrate complex at the surface) the radiolytic system requires charging of the particles with electrons from the reducing donor radicals. At this single-electron transfer stage the substrate molecule competes with the particles for the electrons. Using radiation chemical techniques we have shown the direct reaction of the nitrothiophenol with the reducing radicals leads to the one-electron reduced radical, which does

not proceed to the amine. Thus, once the electron is captured by the molecule its reduction is diverted from the nitro-center to the aromatic ring and the catalytic process essentially stops. We were able to outline kinetic considerations to direct the reaction towards the catalytic multi-electron reduction pathway. We are now measuring the effect of charge density in these particles, which is controlled by the injection of electrons from reducing particles (Ag and Au), on their extinction spectra in an effort to correlate it with intensity patterns of SERS of a few probes rather than rely on scarce electrochemical data. The implications of the radiolysis to photolysis comparison are further discussed in our Future Plans section.

The production of H₂ from the radiolysis of water adsorbed on ceramic oxide interfaces has been examined. A variety of ceramic oxides were examined in order to determine the effects of band gap on H₂ production. The literature suggests that the H₂ yield is enhanced significantly for oxides with band gaps of about 5 eV. However, virtually no H₂ production was observed in the radiolysis of water on anatase or rutile TiO₂ (band gap 3.4 eV) AlTi₂O₃ (band gap 3.6) and SrTiO₃ (band gap 3.4 eV). These oxides are typically used in photochemical studies because the band gap is readily accessible by solar radiation. However, these results show that they are extremely poor producers of H₂ in radiolysis. On the other hand, HfO₂ (band gap 5.5 eV) and BeO (band gap 10.4 eV) both have H₂ yields of up to double than that of ZrO₂, which has been the most prolific producer of H₂ of the oxides studied at Notre Dame. The results with BeO clearly show that an oxide with a band gap of greater than 5 eV is capable of inducing large yields of H₂ and that band gap alone is insufficient to predict radiolytic response. The dependence of H₂ yields with several other types of ceramic oxides and on different water loadings is currently under investigation.

Modifications to the dissociated water layer on the surface of a variety of ceramic oxide surfaces have been examined using diffuse reflection Fourier transform infrared (DRIFT). Water dissociatively adsorbs on the surface of ceramic oxides to give a monolayer of OH groups. Different OH entities can exist depending on the near neighbors. For instance, OH can be bound to a single Zr cation of ZrO₂ to give an isolated group or it can be bound to two Zr cations to give a bridged group. Studies have shown that the OH layer or the few monolayers of ice-like water immediately above this layer is responsible for much of the H₂ production in radiolysis. A device has been constructed for radiolysis of ceramic oxides with *in situ* spectroscopy and heating. Heating to 400 C is required to drive off the physisorbed water overlayers that obscure the surface. The DRIFT spectra show that the isolated OH group in ZrO₂ and in CeO₂ depletes faster than the bridged OH group. Similarly, of the two OH groups observed on TiO₂ one is much more radiation resistant than the other. The identities of the OH groups in TiO₂ are not known and are currently being investigated. Further studies are underway to measure the relative H₂ production from the OH layer and the overlayer of ice-like water.

A chamber for the *in situ* examination of water adsorbed on ceramic oxides has been constructed to examine radiation effects occurring at water – ceramic oxide interfaces. Water can be adsorbed on clean oxide surfaces at low temperatures and pressures in the chamber. Radiolysis effects induced by low energy electrons will be monitored using IR reflection spectroscopy. The face of the oxide can be rotated within the chamber for water deposition, IR monitoring, or low energy electron radiolysis thereby maintaining the integrity of the sample. Techniques for water adsorption and characterization of the ice layers formed are currently underway.

The •-Al₂O₃(0001) surface is well-known to become hydroxylated in the presence of water, and this hydroxylation is important to subsequent alumina surface chemistry. We have

used plane-wave, supercell density functional theory to examine the progression of multiple water dissociation steps from the hydrogen-free stoichiometric surface to the fully hydroxylated, gibbsite-like surface. Consistent with earlier reports, we find that water molecules adsorb and dissociate exothermically and with a small activation barrier at unhydroxylated and coordinatively unsaturated surface Al_s sites and that the formation energy of these hydroxylated Al_s is coverage-independent. Subsequent water dissociations at a singly hydroxylated Al_s site, steps necessary to liberate Al_s and reach the fully hydroxylated surface, are approximately thermoneutral at any surface hydroxyl coverage. Further, within the pathways we are able to identify, these subsequent dissociation steps proceed along more complex reaction coordinates and have higher activation energies than the first water dissociation step. Although the fully hydroxylated surface is the thermodynamic ground state in the presence of water, the actual $\bullet\text{-Al}_2\text{O}_3(0001)$ surface composition under any particular set of conditions may exhibit strong dependence on sample history.

Future Plans

Two different approaches will be used for *in situ* examination of the processes occurring in the radiolysis of water – ceramic oxide interfaces. A 3 MeV electron accelerator will be used to irradiate powders in a controlled atmosphere chamber configured for inclusion in a spectrometer for DRIFT measurements. Samples will be evacuated or purged with selected gases while undergoing controlled heating to remove adsorbed water overlayers so surface species can be observed. The second technique will make use high vacuum chamber with integrated infrared spectrometer and an electron gun of a few keV energy. This device will allow for preparation of samples with controlled amounts of adsorbed water followed by radiolysis. Optical variations of the ceramic oxide surfaces will be coupled with stable product formation such as H_2 and theoretical predictions of interfacial species in order to elucidate the radiation induced reactions at interfaces.

Minimum energy paths linking the various locally-stable structures for water absorption onto the $\bullet\text{-Al}_2\text{O}_3(0001)$ surface will be elucidated and kinetically accessible transformations characterized. Calculations will be extended to encompass more relevant ceramic oxides such as zirconia.

The observation described above of a photolytic process at the surface of metallic particles is of much interest. Since the major mechanism for SERS enhancement is the large optically-induced electric field near the curved surface other field dependent processes may also be enhanced at that surface. Two obvious candidates are enhancement of fluorescence and of photochemical processes and both were predicted theoretically. The former competes with metal-induced quenching but due to the different dependence on distance from the surface reports on fluorescence enhancement near the metallic surface do appear in the literature. Reports of enhanced photochemistry, however, have only recently appeared primarily in the context of photo-induced growth of metallic, specifically silver, particles in the presence of stabilizers. Our ability to generate the same particles without any stabilizer provides a unique opportunity to determine the effect of the stabilizer on the particles. Using the arsenal of time-domain techniques available at the NDRL we will study the effect of stabilizers on the dynamics of relaxation processes following the particles excitation. We will use the plasmon band of the particle itself, possible appearance of light absorbing products (radicals or molecules), and perhaps SERS signatures to follow this reactions. Most interest in this context is the competition between cooling of the particles, be it electron-electron, electron-phonon or relaxation to the

medium, and the photochemical redox reaction. At this time we have no information on positioning the photochemistry along the relaxation time scale.

Publications Sponsored by this DOE Program, 2007-2009

La Verne, J. A., Ryan, M. R. and Mu, T. **2009**, "Hydrogen Production in the Radiolysis of Halide Solutions", *Radiat. Phys. Chem.* **in press**,

Atinault, E., De Waele, V., Fattahi, M., La Verne, J. A., Pimblott, S. M. and Mostafavi, M. **2009**, "Aqueous Solution of UCl_6^{2-} in O_2 Saturated Acidic Medium: An Efficient System to Scavenge All Primary Radicals in Spurs Produced by Irradiation", *J. Phys. Chem. A* **113**, 949-951.

Enomoto K.; LaVerne J.A.; Tandon L.; Enriquez A.E.; Matonic J.H. **2008**, "The radiolysis of poly(4-vinylpyridine) quaternary salt ion exchange resins," *J. Nucl. Mater.* **373**, 103-111.

Hull K.L.; Carmichael I.; Noll B.C.; Henderson K.W. **2008**, "Homo- and heterodimetallic geminal dianions derived from the bisphosphinimine $\{\text{Ph}_2\text{P}(\text{Me}_3\text{Si})\text{N}\}_2\text{CH}_2$ and the alkali metals Li, Na and K," *J. Am. Chem. Soc.* **130**, 3939-3953.

LaVerne J.A.; Carrasco-Flores E.A.; Araos M.S.; Pimblott S.M. **2008**, "Gas production in the radiolysis of poly(vinyl chloride)," *J. Phys. Chem. A* **112**, 3345-3351.

Sehayek, T.; Meisel, D.; Vaskevich, A.; Rubinstein, I. **2008**, "Laterally Controlled Template Electrodeposition of Polyaniline," *Israel J. Chem.* **48**, 359-66.

Merga G.; Cass L.C.; Chipman D.M.; Meisel D. **2008**, "Probing silver nanoparticles during catalytic H_2 evolution," *J. Amer. Chem. Soc.* **130**, 7067-7076.

Ranea V.A.; Schneider W.F.; Carmichael I. **2008**, "DFT characterization of coverage dependent molecular water absorption on $\bullet\text{-Al}_2\text{O}_3(0001)$," *Surf. Sci.* **602**, 268-275.

Zhang Z.; Meisel D.; Kamat P.V.; Kuno M. **2008**, "Layer-by-layer self-assembly of colloidal gold-silica multilayers," *Chem. Educator* **13**, 153-157.

Benoit R.; Saboungi M.-L.; Tréguer-Delapierre M.; Milosavljevic B.H.; Meisel D. **2007**, "Reactions of radicals with hydrolyzed bismuth(III) ions. A pulse radiolysis study," *J. Phys. Chem. A* **111**, 10640-10645.

Carrasco-Flores E.A.; LaVerne J.A. **2007**, "Surface species produced in the radiolysis of zirconia nanoparticles," *J. Chem. Phys.* **127**, 234703.

Merga, G.; Wilson, R.; Lynn, G.; Milosavljevic, B. H.; Meisel, D. **2007**, "Redox Catalysis on "Naked" Silver Nanoparticles," *J. Phys. Chem. C* **111**, 12220-12226.

Pimblott S.M.; LaVerne J.A. **2007**, "Production of low energy electrons by ionizing radiation," *Radiat. Phys. Chem.* **76**, 1244-1247.

Rajesh P.; LaVerne J.A.; Pimblott S.M. **2007**, "High dose radiolysis of aqueous solutions of chloromethanes: Importance in the storage of radioactive organic wastes," *J. Nucl. Mater.* **361**, 10-17.

Zidki, T.; Cohen, H.; Meyerstein, D.; Meisel, D. **2007**, "Effect of silica-supported silver nanoparticles on dihydrogen yields from irradiated aqueous solutions," *J. Phys. Chem. C* **111**, 10461-10466.

Single-Molecule Interfacial Electron Transfer

H. Peter Lu

Bowling Green State University
Department of Chemistry and Center for Photochemical Sciences
Bowling Green, OH 43403
hplu@bgsu.edu

Program Scope

Our research is focused on the use of single-molecule high spatial and temporal resolved techniques to understand molecular dynamics in condensed phase and at interfaces, especially, the complex reaction dynamics associated with electron and energy transfer rate processes. The complexity and inhomogeneity of the interfacial ET dynamics often present a major challenge for a molecular level comprehension of the intrinsically complex systems, which calls for both higher spatial and temporal resolutions at ultimate single-molecule and single-particle sensitivities. Single-molecule approaches are unique for heterogeneous and complex systems because the static and dynamic inhomogeneities can be identified, characterized, and/or removed by studying one molecule at a time. Single-molecule spectroscopy reveals statistical distributions correlated with microscopic parameters and their fluctuations, which are often hidden in ensemble-averaged measurements. Single molecules are observed in real time as they traverse a range of energy states, and the effect of this ever-changing "system configuration" on chemical reactions and other dynamical processes can be mapped. In our research, we have been integrating two complementary methodologies; single-molecule spectroscopy and scanning probe microscopy (STM and AFM) to study interfacial electron transfer dynamics in solar energy conversion, environmental redox reactions, and photocatalysis. The goal of our project is to integrate and apply these techniques to measure the energy flow and electron flow between molecules and substrate surfaces as a function of surface site geometry and molecular structure. We have been primarily focusing on studying electron transfer under ambient condition and electrolyte solution involving both single crystal and colloidal TiO₂ and related substrates. The resulting molecular level understanding of the fundamental interfacial electron transfer processes will be important for developing efficient light harvesting systems and broadly applicable to problems in interface chemistry and physics.

Recent Progress

1. Correlate d topographic and spec troscopic i maging of single-molecule interfacial electron transfer at TiO₂-electrolyte interface. We have demonstrated and applied single-molecule spectroscopy combined with AFM/STM imaging at room temperature under electrolyte solution to single-molecule studies of photo-induced interfacial ET processes in porphyrin-TiO₂ nanoparticle systems, as a model (Fig. 1A and 1B). We have demonstrated STM imaging of single-molecule porphyrin derivative molecules under electrolyte solution on an Au surface, and the redox states of the molecules can be controlled by a potential applied to the substrate surface (Fig. 1C), and we have obtained both single-molecule fluorescence images and topographic images (Fig. 1C, Fig. 2 and 3) from porphyrin derivative molecules (Fig. 1D). Fluorescence intensity trajectories of individual dye molecules adsorbed on TiO₂ NP surface showed fluorescence fluctuations and blinking, with time constants distributed from milliseconds to seconds (Fig. 2B). We have also demonstrated the single-molecule measurements of interfacial electron transfer rate processes

by recording the photon stamping single-molecule fluorescence trajectories, probing single photon arrival times and the photon delay times between photon to photon.

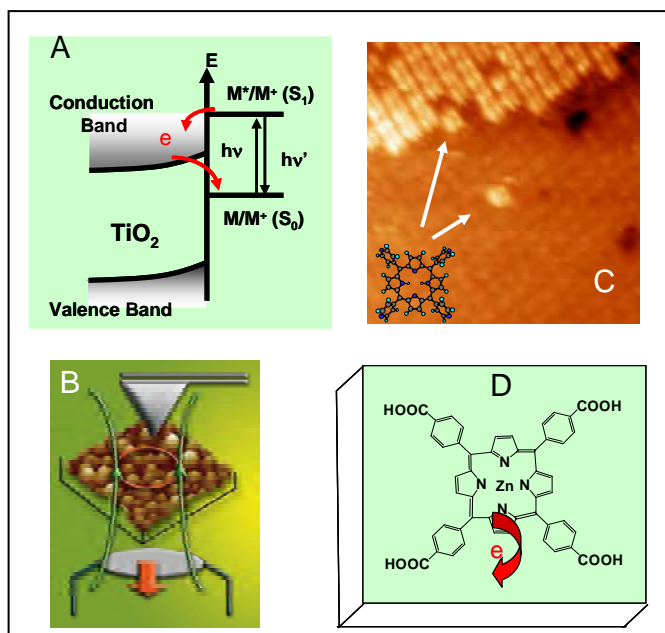


Fig. 1. Correlated single-molecule scanning probe microscopy imaging and spectroscopic imaging of porphyrin/TiO₂ interfacial electron transfer dynamics under ambient conditions. **(A)** Schematic description of the interfacial electron transfer dynamics involved with both forward and backward electron transfers: Forward electron transfer from the excited state of the porphyrin derivative molecules to the conduction band or energetically-accessible surface states of TiO₂ single-crystals and nanoparticles; and backward electron transfer from TiO₂ to surface adsorbed porphyrin derivative molecule cations. **(B)** Correlated AFM/STM single-molecule imaging and single-molecule

fluorescence imaging microscopy. The AFM/STM microscope and single-molecule fluorescence imaging microscope are coupled in an over-and-under configuration for imaging the same nanoscale local sample area with single-molecule topographic and spectroscopic sensitivity, respectively. The features on the image are TiO₂ nanoparticles (~12±4 nm). **(C)** STM imaging (150 Å X 150 Å) of single-molecule porphyrin derivative molecules on an Au surface at a potential of 0.09 V_{SCE} and under 100 mM H₂SO₄ solution. The STM imaging can also identify the redox state of the single-molecules. **(D)** Molecular structure of the porphyrin derivative molecules that involve interfacial electron transfer on TiO₂ surfaces.

2. Probing single-molecule interfacial electron transfer dynamics of porphyrin on TiO₂ nanoparticles. Single-molecule interfacial electron transfer (ET) dynamics has been studied in real time by using single-molecule fluorescence spectroscopy and microscopic imaging. In this work, real-time interfacial ET dynamics have been studied based on single-molecule zinc-tetra(4-carboxyphenyl) porphyrin (ZnTCPP)/TiO₂ nanoparticle system by using single-molecule fluorescence imaging and photon-stamping technique (Fig. 2). For the single-molecule ZnTCPP)/TiO₂ nanoparticle system, the single-molecule fluorescence trajectories show strong fluctuation and blinking between bright and dark states (Fig. 2). Based on a series of control experiments, we have identified that the single-molecule fluorescence intensity fluctuation is not due to triplet state or single-molecule rotational or translational motions during the measurements. The intermittency and fluctuation of the single-molecule fluorescence are attributed to the variation of the reactivity of interfacial electron transfer. We attributed the fluorescence fluctuations to the interfacial ET reaction rate fluctuations in competing with the nanosecond excited-state relaxation of the dye molecules, associating redox reactivity intermittency with the fluctuations of molecule-TiO₂ electronic and vibronic coupling. The non-exponential autocorrelation function and the power-law distribution of the probability density of dark times imply the dynamic and static inhomogeneity of the interfacial ET dynamics. On the basis of the power-law analysis, the variation of single-

molecule interfacial ET reactivity is analyzed as a fluctuation according to the Lévy statistics. According this work and our previously reported work, the highly inhomogeneous ET dynamics is common for the interfacial chemical reactions that strongly regulated by the molecular interaction between adsorbed molecules and substrate surfaces. The spontaneous thermal fluctuations of the local environment and the molecular interactions occur at a wide time-scale at room temperature, resulting in the interfacial ET reaction-rate fluctuation and inhomogeneous dynamics. Our single-molecule spectroscopy analysis provides detailed information about the inhomogeneity of the interfacial electron transfer, which is novel but not obtainable from the conventional ensemble-averaged experiments.

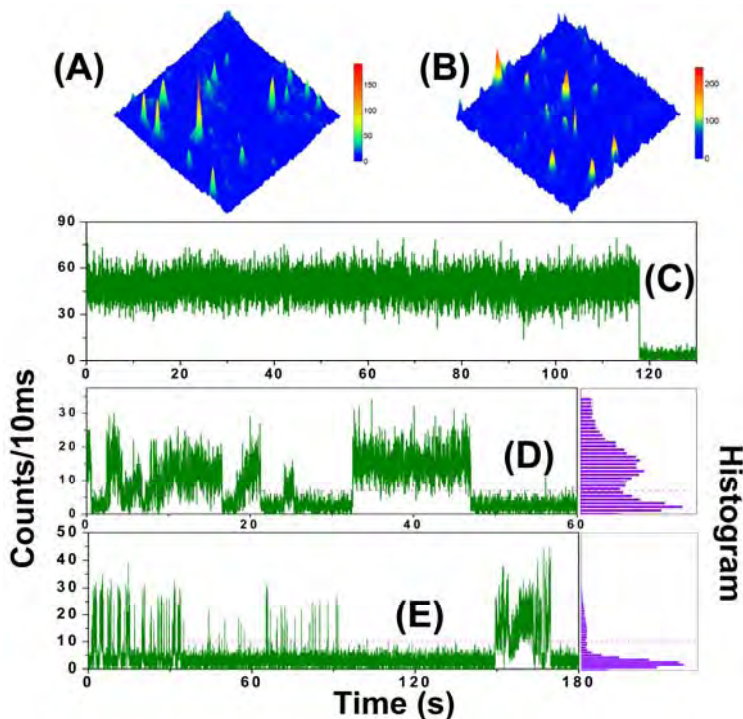


Fig. 2. (A) and (B) are fluorescence images for single ZnTCPP molecules on a cover glass and a TiO₂ nanoparticle covered glass surface (10μm×10μm). A typical single-molecule fluorescence emission trajectory of ZnTCPP on a cover glass surface is shown in (C). (D) and (E) show the typical single-molecule fluorescence emission trajectories of ZnTCPP on TiO₂ NP surface. The binning time is 10 ms. Histograms of the emission intensity are given to determine the threshold for dark states and bright states.

3. Probing single-molecule interfacial electron-cation geminate recombination dynamics. Both forward electron transfer (FET) and backward electron transfer (BET) processes are involved in the photo-induced electron transfer at the dye/semiconductor interface. Previously, there has been no demonstration of measuring single-molecule BET across the molecule-TiO₂ substrate interfaces. We have probed BET dynamics for zinc-tetra (4-carboxyphenyl) porphyrin (ZnTCPP)/TiO₂ nanoparticle system at single-molecule level by precisely recording and analyzing photon-to-photon pair times. It is significant that the fluorescence trajectory from ZnTCPP/TiO₂ shows strong fluctuation with dark time at sub-seconds to seconds time scale. Demonstrating triplet blinking, cation emission and molecule rotation are not responsible for the fluctuation, we have suggested that the dark state is due to dominated ET process with high activity and bright state is due to monotonous fluorescence emission cycles from $S_0 \rightarrow S_1 \rightarrow S_0$ or low active ET process (mixed with fluorescence cycles). By deconvolution, the BET time of ZnTCPP/TiO₂ system is deduced to be inhomogeneous from molecule to molecule and span a broad range from sub-ms to ms time scale. The inhomogeneity implies the non-exponential BET dynamics in ensemble-averaged measurements and complexity of the electron-cation recombination process, which is

associated with excess electron trapping, detrapping and non-Brownian diffusion motions in TiO₂.

Future Research Plans

Intermittent interfacial ET dynamics of individual molecules, beyond the conventional kinetic scope, could be a characteristic of the surface chemical reactions strongly involved with and regulated by molecule-surface interactions. The fluorescence fluctuation dynamics were found to be inhomogeneous from molecule to molecule and from time to time, showing significant static and dynamic disorders in the interfacial ET reaction dynamics. The intermittent interfacial reaction dynamics that likely occur among single molecules in other interfacial and surface chemical processes can typically be observed by single-molecule studies, but not by conventional ensemble-averaged experiments. To decipher the underlying mechanism of the intermittent interfacial electron transfer dynamics, we plan to study porphyrin interfacial electron transfer on single crystal TiO₂ surfaces by using ps and sub-ps pump-probe ultrafast single-molecule spectroscopy. Our study will focus on understanding the interfacial electron transfer dynamics at specific crystal sites (kinks, planes, lattices, and corners) with high-spatially and temporally resolved topographic/spectroscopic characterization at individual molecule basis.

Publications of DOE sponsored research (FY2006-2009)

1. Yuanmin Wang, H. Peter Lu, "Single-molecule interfacial electron transfer fluctuation of porphyrin on Ag nanoparticles," *Submitted*, 2009.
2. Yuanmin Wang, Xuefei Wang, and H. Peter Lu, "Probing single-molecule interfacial geminate electron-cation recombination dynamics," *J. Am. Chem. Soc.* **131**, 9020–9025 (2009).
3. Yuanmin Wang, Xuefei Wang, Sujit Kumar Ghosh, H. Peter Lu, "Probing single-molecule interfacial electron transfer dynamics of porphyrin on TiO₂ nanoparticles," *J. Am. Chem. Soc.* **131**, 1479-1487 (2009).
4. Xuefei Wang, and H. Peter Lu, "2D Regional Correlation Analysis of Single-Molecule Time Trajectories," *J. Phys. Chem. B.* **112**, 1492--14926 (2008).
5. Duohai Pan, Dehong Hu, Ruchuan Liu, Xiaohua Zeng, Samuel Kaplan, H. Peter Lu, "Fluctuating Two-State Light Harvesting in a Photosynthetic Membrane," *J. Phys. Chem. C*, **111**, 8948-8956 (2007).
6. V. Biju, D. Pan, Yuri A. Gorby, Jim Fredrickson, J. Mclean, D. Saffarini and H. Peter Lu, "Correlated Spectroscopic and Topographic Characterization of Nanoscale Domains and Their Distributions of a Redox Protein on Bacterial Cell Surfaces," *Langmuir* **23**, 1333-1338 (2007).
7. Duohai Pan, Nick Klymyshyn, Dehong Hu, and H. Peter Lu, "Tip-enhanced near-field Raman spectroscopy probing single dye-sensitized TiO₂ nanoparticles," *Appl. Phys. Lett.*, **88**, 093121(2006).
8. Duohai Pan, Dehong Hu, and H. Peter Lu, "Probing Inhomogeneous Vibrational Reorganization Energy Barriers of Interfacial Electron Transfer," *J. Phys. Chem. B*, **109**, 16390-16395 (2005).
9. Dehong Hu and H. Peter Lu, "Single-Molecule Triplet-State Photon Antibunching at Room Temperature," *J. Phys. Chem. B*, **109**, 9861-9864 (2005).
10. H. Peter Lu, invited review article, "Site-Specific Raman Spectroscopy and Chemical Dynamics of Nanoscale Interstitial Systems," *J. Physics: Condensed Matter*, **17**, R333-R355 (2005).

Solution Reactivity of Nitrogen Oxides, Oxoacids, and Oxoanions

Sergei V. Lymar

Chemistry Department, Brookhaven National Laboratory, Upton, NY 11973-5000

e-mail: lymar@bnl.gov

Program Scope

This program investigates the physical chemistry of nitrogen oxides and their congeneric oxoacids and oxoanions which are at the core of classical inorganic chemistry. They play an essential role in environmental chemistry, particularly in the terrestrial nitrogen cycle, pollution, bioremediation, and ozone depletion. Nitrogen-oxygen intermediates are also central to the radiation-induced reactions that occur in nuclear fuel processing and within attendant nuclear waste. Over 60 million gallons of this highly radioactive, nitrate/nitrite-rich waste is currently in the DOE custody. Redox and radical chemistry of the nitrate/nitrite system mediates the most of radiation-induced transformations in these environments. Equally important are the biological roles of nitrogen oxides.

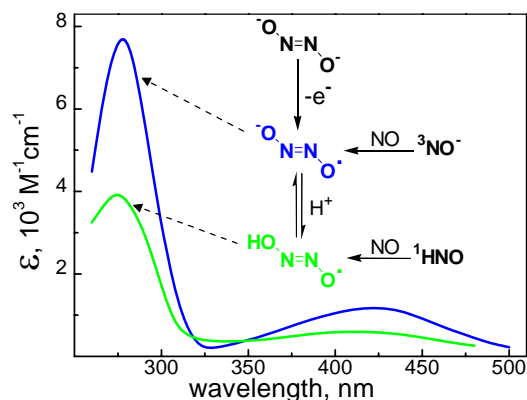
Despite a long history, the inorganic chemistry of nitrogen, which includes a large number of metastable compounds, is far from being fully understood. This research program applies time-resolved techniques (primarily pulse radiolysis and flash photolysis) for elucidation of the prospective reactions in terms of their thermodynamics, rates and mechanisms, focusing on the positive nitrogen oxidation states, whose chemistry is of the greatest current interest.

Progress

The nearest redox neighbors of NO are nitroxyl (H-N=O) and its conjugate NO⁻ anion. Little quantitative information exists on the reactivity of these species and their adducts. Among the latter, prominent are the hyponitrite radical (HN₂O₂[•]/N₂O₂^{•-}) and the so-called NONOates, the compounds of the general structure X[N(O)NO]⁻, where X is a strongly nucleophilic group, such as aminyl (R₂N) or oxyl (O⁻).

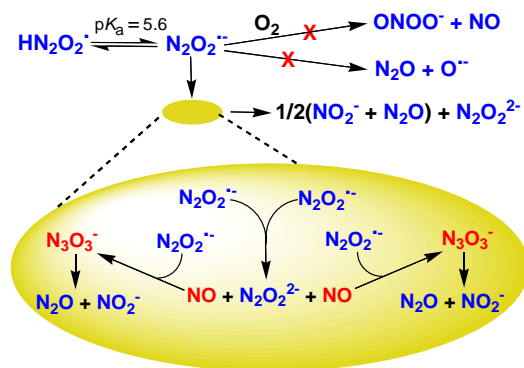
One-electron reduction of aqueous NO by the hydrated electrons and hydrogen atoms has been investigated by pulse radiolysis.¹ The hydrated electrons and hydrogen atoms yield the ground state triplet ³NO⁻ and singlet ¹HNO, respectively, which further concatenate two NO producing the N₃O₃⁻ anion. These reactions occur much more rapidly than the spin-forbidden acid-base equilibration of ³NO⁻ and ¹HNO under all experimentally accessible conditions.

Properties, reactivity, and decay pathways for the hyponitrite radicals (HN₂O₂[•]/N₂O₂^{•-}), an



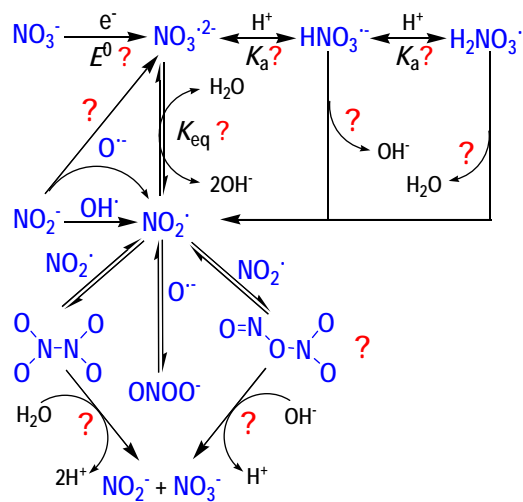
important intermediate in the aqueous redox chemistry of NO, have been investigated.^{2,3} This radical is formed either by one-electron oxidation of hyponitrite³ (N₂O₂²⁻) or by one-electron reduction of NO (figure to the left);^{1,4,5} in which case, the precursor can be either nitroxyl (¹HNO) or nitroxyl anion (³NO⁻) in their respective singlet and triplet ground states. The HN₂O₂[•] and N₂O₂^{•-} radicals exhibit absorption spectra that differ drastically from those reported,^{4,5} suggesting the radical misassignment in prior work. The radicals are

estimated to be both strongly oxidizing and moderately reducing and orders of magnitude more stable to elimination of NO than suggested previously. Although the radical decay conforms to simple second-order kinetics, its mechanism is complex, comprising a short chain of NO release-consumption steps (scheme below with intermediates in red). In the first, rate-determining step, two $\text{N}_2\text{O}_2^{\cdot-}$ radicals disproportionate regenerating $\text{N}_2\text{O}_2^{2-}$ and releasing two NO. This occurs either by electron transfer or, more likely, through radical recombination-dissociation. Each NO so-produced rapidly adds to another $\text{N}_2\text{O}_2^{\cdot-}$ yielding the N_3O_3^- ion, which slowly decomposes to the final $\text{N}_2\text{O} + \text{NO}_2^-$ products. The $\text{N}_2\text{O}_2^{\cdot-}$ radical protonates with $\text{p}K_a = 5.6$, and the neutral $\text{HN}_2\text{O}_2^{\cdot}$ radical decays by an analogous mechanism but over 10 times more rapidly. The $\text{N}_2\text{O}_2^{\cdot-}$ radical shows surprisingly low reactivity toward O_2 . The previously reported,^{5,6} rapid dissociation of $\text{N}_2\text{O}_2^{\cdot-}$ into N_2O and OH^{\cdot} does not occur, contrary to the suggestions^{7,8} on the role of hyponitrite radical as OH-releasing species in biological environments.



Photochemical decomposition of NONOates ($\text{X}[\text{N}(\text{O})\text{NO}]^-$, where X is aminyl or oxyl), have been investigated. The $[\text{N}(\text{O})\text{NO}]^-$ group is photosensitive, decomposing upon illumination. This process has been investigated⁹ by laser kinetic spectroscopy to evaluate the application of these compounds for controlled photochemical release of nitroxyl and/or nitric oxide. The photolysis generates a NONOate-specific spectrum of primary products including the ground state triplet ($^3\text{NO}^-$) and singlet (^1HNO) nitroxyl species, and NO. These findings are significant because NO and HNO have been reported to produce distinctly different biological effects. Kinetic analysis reveals a novel, rapid, spin-forbidden combination reaction, $^3\text{NO}^- + ^1\text{HNO}$, and its rate is determined by competition with the reduction of methylviologen by $^3\text{NO}^-$; the latter reaction yielding the stable, colored product is useful for detection of $^3\text{NO}^-$.

Redox and radical chemistry in the nitrate/nitrite system. This chemistry encompasses much of the nitrogen(III), (IV) and (V) reactivity in important environmental and biological processes. It also mediates the most of radiation-induced transformations in highly alkaline Hanford nuclear waste containing large concentrations of nitrate and nitrite. The literature data on radiation chemistry in this system points to a complex set of radical reactions, with major intermediated being the NO_2^{\cdot} and $\text{NO}_3^{\cdot 2-}$ radicals that are generated from the hydrated electron and $\text{OH}^{\cdot}/\text{O}^{\cdot-}$ (scheme to the right). However, accounts of the formation pathways, properties, and reactivity of NO_2^{\cdot} and $\text{NO}_3^{\cdot 2-}$ differ substantially both qualitatively and quantitatively, and no coherent picture emerges. We are seeking such a picture by addressing the major unresolved issues, which include: (1) Rate and branching in the $\text{NO}_2^{\cdot} + \text{O}^{\cdot-}$ reaction. Is it a redox reaction producing an oxidant (NO_2^{\cdot}) or an addition generating a reductant ($\text{NO}_3^{\cdot 2-}$)?



Conflicting evidence exists on this question.^{10,11} (2) Reduction potential and free energy of formation of $\text{NO}_3^{\bullet 2-}$. The literature values $E^0(\text{NO}_3^-/\text{NO}_3^{\bullet 2-}) = -0.76^{12}$ and -0.89 V^{13} predict that the equilibrium $\text{NO}_2^{\bullet} + 2\text{OH}^- = \text{NO}_3^{\bullet 2-} + \text{H}_2\text{O}$ should lie to the right even at modest alkalinities ($[\text{OH}^-] > 0.01 - 0.1 \text{ M}$). However, our recent observations do not support this conclusion, suggesting a significantly more negative potential. (3) Acid-base equilibration and hydrolysis of $\text{NO}_3^{\bullet 2-}$. The earlier studies^{14,15} asserted that $\text{NO}_3^{\bullet 2-}$ behaves as a normal base and protonates with $\text{p}K_a$ of 7.5 and 4.8 to yield $\text{HNO}_3^{\bullet -}$ and $\text{H}_2\text{NO}_3^{\bullet}$ with lifetimes on the microsecond time scale, but later works^{10,13,16} question the existence of these species suggesting that $\text{NO}_3^{\bullet 2-}$ behaves as a Lewis acid and is hydrolyzed by donating O^{2-} to water or general acids. Our studies of ionic strength dependence and kinetic isotope effect of the hydrolysis rate are consistent with proton transfer from water to $\text{NO}_3^{\bullet 2-}$ being a rate-determining step. These results strongly disfavor the O^{2-} transfer mechanism, but also suggest that the $\text{HNO}_3^{\bullet -}$ radical has only fleeting existence and the $\text{H}_2\text{NO}_3^{\bullet}$ radical probably does not exist at all.

Future Plans

The reactions of $^3\text{NO}^-$ with O_2 and ^1HNO and of $^1\text{HNO}/^3\text{NO}^-$ with NO remain the only nitroxyl reactions measured directly despite the expectations of the rich chemistry for nitroxyl, which is simultaneously a Lewis acid and base, a hydrogen atom donor, and a redox agent. This chemistry will be explored along with the properties and reactivity of the most consequential adducts of nitroxyl.

Pathways and energetics of NO reduction will be investigated with the purposes to develop new methods of generating nitroxyl and to establish its thermochemistry. With respect to the former, reduction of NO by the $\text{CO}_2^{\bullet -}$ radical is of interest. All present estimates for the reduction potentials for NO and $\text{p}K_a$ for HNO involve significant assumptions spreading a range of $\sim 0.2 \text{ V}$ and $\sim 4 \text{ p}K_a$ units; we will attempt determination of nitroxyl thermochemistry by measuring its redox equilibria.

Spin-forbidden bond breaking/making reactions involving nitroxyl will be investigated. The first is protonation of $^3\text{NO}^-$ by Brønsted acids. The second spin-forbidden reaction of interest is the addition of $^3\text{O}_2$ to ^1HNO , which could directly lead to peroxyxynitrite, ONOO^- , and is potentially very significant because it replaces mildly reducing HNO by strongly oxidizing ONOO^- .

Energetics of $\text{NO}_3^{\bullet 2-}$ radical will be studied through examining its equilibrium $\text{NO}_3^{\bullet 2-} + \text{H}_2\text{O} = \text{NO}_2^{\bullet} + 2\text{OH}^-$ at high alkalinities, which should yield the reduction potential provided it is not below about -1.1 V . If it is, we will attempt obtaining or bracketing the potential from equilibrating $\text{NO}_3^-/\text{NO}_3^{\bullet 2-}$ couple with the reference redox couples.

Dimerization/hydrolysis of NO_2^{\bullet} radical will be explored. It is widely held that the hydrolysis of occurs through the intermediacy of its symmetric N-N bonded dimer.^{17,18} We question this mechanism and conjecture that the hydrolysis involves the higher-energy N-O bonded asymmetric dimer (scheme above), while the N-N bonded dimer is an unreactive bystander.

Collaborators on this project include V. Shafirovich (NYU) and H. Schwarz (BNL, emeritus); past contribution from G. A. Poskrebyshev is acknowledged. Other pulse radiolysis work on solvent protonation of aryl radical anions and on intermediates in water oxidation catalysis has been done in collaboration with J. Miller¹⁹ and J. K. Hurst.²⁰

References (DOE sponsored publications in 2005-present are marked with asterisk)

- (1*) Lymar, S. V.; Shafirovich, V.; Poskrebyshev, G. A. *Inorg. Chem.* **2005**, *44*, 5212-5221.
- (2*) Poskrebyshev, G. A.; Shafirovich, V.; Lymar, S. V. *J. Phys. Chem. A* **2008**, *112*, 8295-8302.
- (3) Poskrebyshev, G. A.; Shafirovich, V.; Lymar, S. V. *J. Am. Chem. Soc.* **2004**, *126*, 891-899.
- (4) Grätzel, M.; Taniguchi, S.; Henglein, A. *Ber. Bunsen-Ges. Phys. Chem.* **1970**, *74*, 1003-1010.
- (5) Seddon, W. A.; Fletcher, J. W.; Sopchyshyn, F. C. *Can. J. Chem.* **1973**, *51*, 1123-1130.
- (6) Chazotte-Aubert, L.; Oikawa, S.; Gilibert, I.; Bianchini, F.; Kawanishi, S.; Ohshima, H. *J. Biol. Chem.* **1999**, *274*, 20909-20915.
- (7) Ohshima, H.; Gilibert, I.; Bianchini, F. *Free Radic. Biol. Med.* **1999**, *26*, 1305-1313.
- (8) Kirsch, M.; de Groot, H. *J. Biol. Chem.* **2002**, *277*, 13379-13388.
- (9*) Lymar, S. V.; Shafirovich, V. *J. Phys. Chem. B* **2007**, *111*, 6861-6867.
- (10) Fessenden, R. W.; Meisel, D.; Camaioni, D. M. *J. Am. Chem. Soc.* **2000**, *122*, 3773-3774.
- (11) Merenyi, G.; Lind, J.; Goldstein, S.; Czapski, G. *J. Phys. Chem. A* **1999**, *103*, 5685-5691.
- (12) Benderskii, V. A.; Benderskii, A. V. *Laser Electrochemistry of Intermediates*; CRC Press: Boca Raton, 1995.
- (13) Cook, A. R.; Dimitrijevic, N.; Dreyfus, B. W.; Meisel, D.; Curtiss, L. A.; Camaioni, D. M. *J. Phys. Chem. A* **2001**, *105*, 3658-3666.
- (14) Grätzel, M.; Henglein, A.; Taniguchi, S. *Ber. Bunsen-Ges. Phys. Chem.* **1970**, *74*, 292-298.
- (15) Logager, T.; Sehested, K. *J. Phys. Chem.* **1993**, *97*, 6664-6669.
- (16) Mezyk, S. P.; Bartels, D. M. *J. Phys. Chem. A* **1997**, *101*, 6233-6237.
- (17) Schwartz, S. E.; White, W. H. In *Advances in Environmental Science and Engineering*; Pfafflin, J. R., Ziegler, E. N., Eds.; Gordon and Breach: NY, 1981; Vol. 4, p 1-45.
- (18) Huie, R. E. *Toxicology* **1994**, *89*, 193-216.
- (19*) Funston, A. M.; Lymar, S. V.; Saunders-Price, B.; Czapski, G.; Miller, J. R. *J. Phys. Chem. B* **2007**, *111*, 6895-6902.
- (20*) Cape, J. L.; Lymar, S. V.; Lightbody, T.; Hurst, J. K. *Inorg. Chem.* **2009**, *48*, 4400-4410.
- (21*) Garrett, B. C.; Dixon, D. A.; Camaioni, et al. "Role of Water in Electron-Initiated Processes and Radical Chemistry: Issues and Scientific Advances," *Chem. Rev.*, **2005**, *105*, 355-390.

Spectroscopy of Organometallic Radicals

Michael D. Morse

Department of Chemistry

University of Utah

315 S. 1400 East, Room 2020

Salt Lake City, UT 84112-0850

morse@chem.utah.edu

I. Program Scope:

In this project, we seek to obtain fundamental physical information about unsaturated, highly reactive organometallic radicals containing open d subshell transition metal atoms. Gas phase electronic spectroscopy of jet-cooled transition metal (TM) molecules is used to obtain fundamental information about ground and excited electronic states of such species as the transition metal carbides and organometallic radicals such as CrC_2H , CrCH_3 , and NiCH_3 . Ionic species will become available for investigation when the construction of a new ion trap spectrometer is complete.

II. Recent Progress:

A. Optical spectroscopy of OsC, OsN, and YF

During 2005-2009, we have used resonant two-photon ionization (R2PI) and dispersed fluorescence (DF) spectroscopic methods to investigate the TM carbide, OsC,¹ the TM nitride, OsN, and have also analyzed a spin-forbidden band system in YF.² This work was described in the Abstract for the 2008 CPIMS meeting, and will not be described in this Abstract. Additional work on OsN is proceeding, and this will be included in a publication that will be submitted later this year.

Significant progress has been made this year on some new chemical species, including diatomic CrC. CrC joins MoC and WC as group 6 monocarbides for which spectroscopic data is now available. All of these molecules were first spectroscopically investigated in my research group. Shown below is a qualitative molecular orbital diagram for the transition metal monocarbides, for the specific example of CrC.

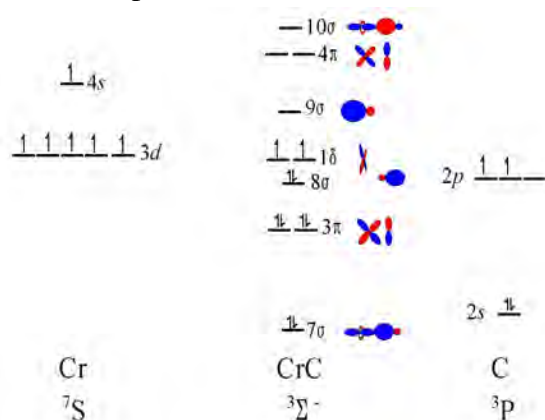


Figure 1. Qualitative MO diagram for the diatomic CrC molecule, showing the arrangement of electrons in the $X^3\Sigma^-$ ground state.

In this diagram, the 7σ orbital is a bonding orbital formed from a $2sp$ hybrid orbital on C and the $3d\sigma$ orbital on Cr and the 3π orbital is a bonding combination of the $2p\pi$ orbital of C with the $3d\pi$ orbital of Cr. The 10σ and 4π orbitals are the corresponding antibonding orbitals. The 8σ orbital is primarily a $2sp$ hybrid on C directed away from the metal atom and is mainly nonbonding, while the 1δ orbital consists purely of the Cr $3d\delta$ orbitals and is nonbonding. Finally, the 9σ orbital is primarily of Cr $4s$ character, and is likewise nonbonding. According to this diagram and several electronic structure calculations, the ground state of CrC is $7\sigma^2 3\pi^4 8\sigma^2 1\delta^2, {}^3\Sigma^-$. This is confirmed in our rotationally resolved spectrum, shown below, which establishes that the ground state of CrC is of ${}^3\Sigma^-$ symmetry, with a bond length of $r_0'' = 1.6188(6)$ Å in the ground state. The excited state reached in this transition is also of ${}^3\Sigma^-$ symmetry, probably deriving from a $9\sigma \leftarrow 8\sigma$ electronic promotion to the $7\sigma^2 3\pi^4 8\sigma^1 1\delta^2 9\sigma^1$ configuration.

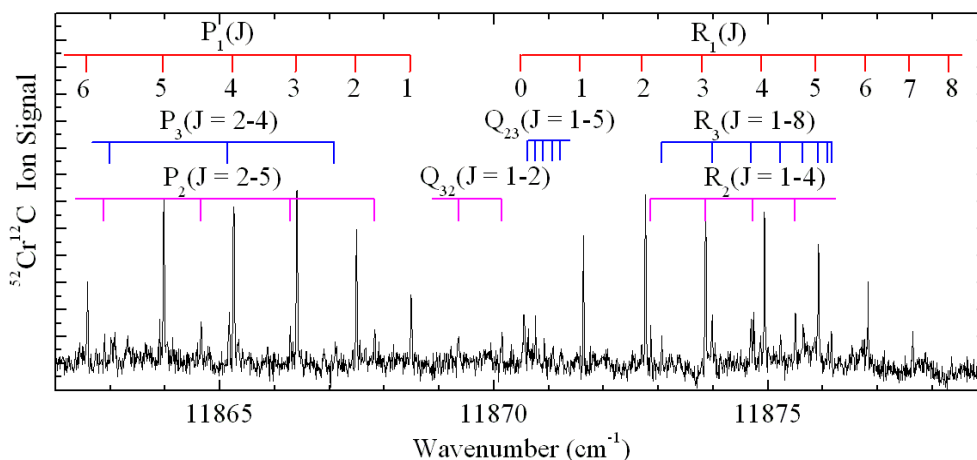


Figure 2. Rotationally resolved spectrum of the 0-0 band of the $[11.9] {}^3\Sigma^- \leftarrow X {}^3\Sigma^-$ band system of CrC. The strong features arise from the $X {}^3\Sigma^-(\Omega = 0^+)$ spin orbit component while the weak features arise from the weakly populated $X {}^3\Sigma^-(\Omega = 1)$ excited spin orbit component.

In other work on organochromium compounds, we have recorded and analyzed rotationally resolved electronic spectra for the CrCCH organometallic radical. The molecule may be considered as arising from a high-spin Cr^+ ($3d^5 4s^0, {}^6S$) atom interacting with a closed shell acetylide ion, $\text{C}\equiv\text{C-H}, {}^1\Sigma^+$, leading to a ground state of the CrCCH molecule of ${}^6\Sigma^+$ symmetry. In this respect the CrCCH molecule is analogous to the well-known CrF, CrCl, and CrH radicals. The observed transition takes the molecule to the an excited ${}^6\Sigma^+$ state lying near $11,100 \text{ cm}^{-1}$. The rotationally resolved spectrum is quite complicated, because each rotational level, specified by N , is split into 6 levels due to the high spin of the molecule ($S = 5/2$). This is true in both the ground state and the excited state, leading potentially to 36 different P branches, 36 different Q branches, and 36 different R branches. In fact, half of these are forbidden by parity rules, so “only” 54 branches (18 of each type) are possible.

We have examined the 1-0 band near 11579 cm^{-1} and have assigned over 300 rotational lines in 33 of the 54 branches. The upper state is clearly perturbed, probably by a nearby ${}^6\Pi$ state that has been observed in CrH and CrF. The ground state, however, displays clean rotational structure, as illustrated in the plots of observed energy levels in Figure 3 below.

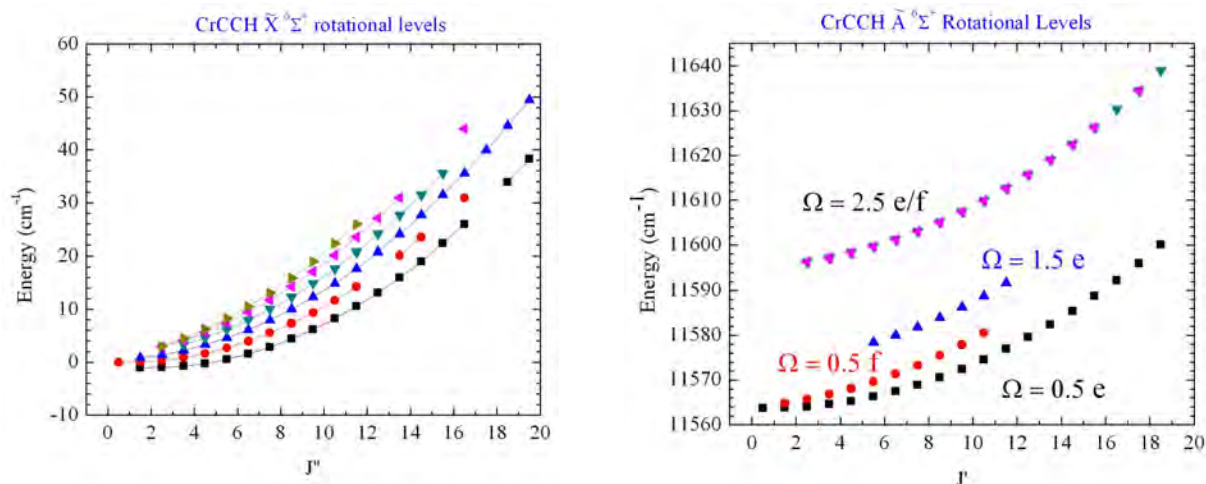


Figure 3. Observed rotational levels in the $\tilde{X}^6\Sigma^+$ state and the excited $\tilde{A}^6\Sigma^+$ state of CrCCH. The ground state displays the energy level pattern expected for a Hund's case (b) molecule while the excited state displays greater spin-orbit splitting, consistent with a Hund's case (a) system.

III. Future Plans

A. R2PI and DF spectroscopy of transition metal carbides and radicals

Projects for the upcoming year include: (1) Completion of the analysis of the spectra of OsN and CrCCH; (2) Collection and analysis of rotationally resolved spectra of VC and TaC, for which some spectra have already been obtained; (3) Analysis of the rotationally resolved spectrum of TiC, using dispersed fluorescence from single rovibronic levels to identify the lines; (4) Attempts to record and analyze the spectra of several transition metal cyanides (or isocyanides) will be made. Species we are considering for investigation include CuCN, AgCN, AuCN, ScNC, YNC, and CrCN.

B. Photodissociation spectroscopy of cold, trapped ions

I am in the process of constructing a new ion photodissociation spectrometer that is designed to record photodissociation action spectra of cryogenically cooled transition metal ion complexes. The procedure will be to generate transition metal ion complexes that can be mass-selected, cooled in a cryogenic trap, irradiated, and photofragmented. The fragment ions will be selectively detected and the spectrum of the cold ion will be recorded by measuring the fragment ion signal as a function of the laser wavenumber.

In January, 2009 I hired an very capable mass spectrometrist, Dr. Sergei Aksyonov, to work in my group. Dr. Aksyonov was tasked with the project of designing and constructing the new instrument. He is being assisted in this work by an undergraduate mechanical engineering student, Eric Allred. The overall design of the instrument is illustrated in Figure 4 below. The instrument is being constructed in stages, with the first pieces being an electron impact ion source and a Daly detector. These two pieces are now complete and are in the process of being tested. When these tests are complete, the first quadrupole mass filter will be inserted between them, and the system will be tested to verify that ions of selected mass can be efficiently transmitted to the detector. Following successful completion of these tests, the cryocooled 22-pole ion trap will be inserted into the instrument and we will work to establish the conditions

needed to successfully trap ions in good yield. Finally, the second mass-selective quadrupole mass spectrometer will be added to the system, followed by integration of the Nd:YAG-pumped dye laser into the system. At that point we will work to verify that the ions are being successfully cooled to cryogenic temperatures by collecting spectra of a test molecule. When this has been accomplished, we will turn our attention to new species, with our initial studies focusing on ions that are readily formed from volatile transition metal carbonyls. Thus, our first studies will focus on species such as FeCO^+ , CoCO^+ , NiCO^+ , CoNO^+ , CrCO^+ , and related species with larger numbers of ligands.

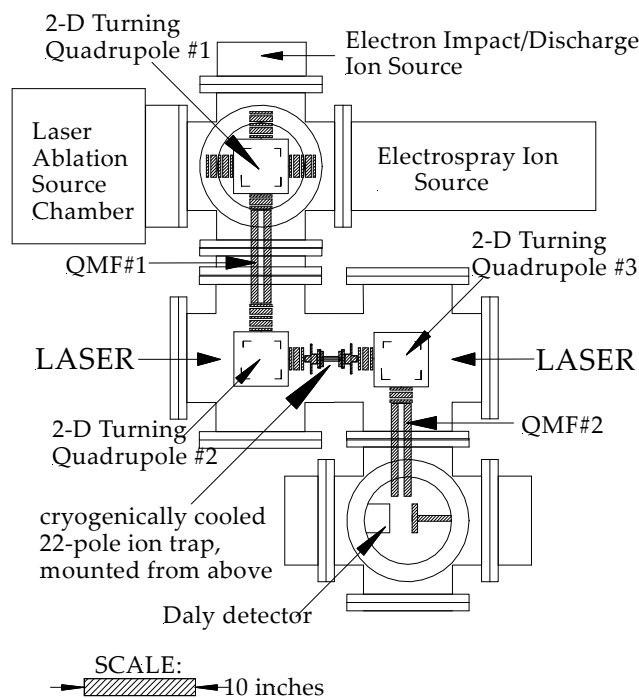


Figure 4. Design plan for the Utah ion trap photodissociation spectrometer.

IV. Publications from DOE Sponsored Research 2005-present:

1. Olha Krechkivska and Michael D. Morse, "Resonant two-photon ionization spectroscopy of jet-cooled OsC ," *J. Chem. Phys.* **128**, 084314/1-9 (2008).
2. Ramya Nagarajan and Michael D. Morse, "Spin-forbidden $c^3\Sigma_1^+ \leftarrow X^1\Sigma^+$ band system of YF ," *J. Chem. Phys.* **126**, 144309/1-6 (2007).
3. Alonzo Martinez and Michael D. Morse, "Infrared diode laser spectroscopy of jet-cooled NiCO , $\text{Ni}(\text{CO})_3(^{13}\text{CO})$, and $\text{Ni}(\text{CO})_3(\text{C}^{18}\text{O})$," *J. Chem. Phys.* **124**, 124316/1-8 (2006).
4. Saeyoung Shin, Dale J. Brugh, and Michael D. Morse, "Radiative lifetime of the $v=0, 1$ levels of the $\text{A}^6\Sigma^+$ state of CrH ," *Astrophys. J.* **619**, 407-11 (2005).

***Ab initio* approach to interfacial processes in hydrogen bonded fluids**

Christopher J. Mundy
Chemical and Materials Sciences Division
Pacific Northwest National Laboratory
902 Battelle Blvd, Mail Stop K1-83
Richland, WA 99352
chris.mundy@pnl.gov

Program Scope

The long-term objective of this research is to develop a fundamental understanding of processes, such as transport mechanisms and chemical transformations, at interfaces of hydrogen-bonded liquids. Liquid surfaces and interfaces play a central role in many chemical, physical, and biological processes. Many important processes occur at the interface between water and a hydrophobic liquid. Separation techniques are possible because of the hydrophobic/hydrophilic properties of liquid/liquid interfaces. Reactions that proceed at interfaces are also highly dependent on the interactions between the interfacial solvent and solute molecules. The interfacial structure and properties of molecules at interfaces are generally very different from those in the bulk liquid. Therefore, an understanding of the chemical and physical properties of these systems is dependent on an understanding of the interfacial molecular structure. The adsorption and distribution of ions at aqueous liquid interfaces are fundamental processes encountered in a wide range of physical systems. In particular, the manner in which solvent molecules solvate ions at the interface is relevant to problems in a variety of areas. Another major focus lies in the development of models of molecular interaction of water and ions that can be parameterized from high-level first principles electronic structure calculations and benchmarked by experimental measurements. *All of the aforementioned studies are performed using novel algorithms based in density functional theory (DFT) in conjunction with high performance computing through a 2008-2009 INCITE award.* These models will be used with appropriate simulation techniques for sampling statistical mechanical ensembles to obtain the desired properties.

Progress Report

Elucidating the role of post-processed dispersion in density functional theory (DFT): Applications to water clusters and bulk aqueous systems: Although DFT holds tremendous promise as an efficient electronic structure theory, applications of DFT to aqueous systems have produced mixed results when attempting to reproduce experimentally determined benchmarks. Although there is no molecular model that can reproduce the full phase diagram of water, the shortcomings of popular exchange-correlation functionals based on the generalized gradient approximation (GGA), *e.g.* BLYP and PBE, are known to underestimate the liquid density and yield a more structured liquid than classical empirical potentials. Moreover, when the results of GGA functionals are compared to high-level *ab initio* methods such as MP2 for the binding energies of water clusters, BLYP and PBE are known to under bind and over bind, respectively relative to the MP2 benchmarks. Although there could be many reasons for these deficiencies in DFT, one major shortcoming is the lack of dispersion interactions in current implementations. Correcting the liquid density at ambient conditions has far reaching implications for use of DFT in studying systems with open boundary conditions, such as liquid-vapor interfaces. To this end we have implemented the correction due to Grimme¹ that amounts to an empirical damped

dispersion interaction that is parameterized to used with both BLYP and PBE. Using CP2K (www.cp2k.berlios.de) we have performed extensive isothermal-isobaric (NpT) molecular dynamics simulations at 330K.[12] Our results have shown that the addition of the empirical correction due to Grimme yields the correct density for liquid water at ambient conditions for both PBE and BLYP. Moreover, the radial distribution functions using the Grimme correction are dramatically improved. Our studies using our novel method of self-consistent polarization (SCP)-DFT also produces have arrived a formulation that accounts for dispersion in a self-consistent manner using empirically determined polarizabilities. The use of SCP-DFT in conjunction with BLYP can reproduce the MP2 binding energies for water clusters up to $n=20$. The connection between Grimme and SCP-DFT is currently being investigated.

Elucidation of novel phases of water using density functional theory (DFT) in conjunction with experiment (with Greg Kimmel and Bruce Kay): It has been speculated that novel hydrogen bonding structures of water could be present in hydrophobic confined geometries such as carbon nanotubes or graphene walls. Elucidation of novel structures through vibrational spectroscopy using DFT reveals subtle shifts in the mid-infrared (IR) region that can be interpreted as dangling hydrogen bonds interacting with the hydrophobic substrate. Experimentally determined temperature programmed desorption on thin films of ice on graphene revealed the presence of a novel bilayer ice structure with an IR finger print, namely the presence of a blue shifted peak in the mid-IR and red shifted peak in the near-IR, that is distinct from cubic or hexagonal ices. Using DFT interaction potentials we constructed an ideal ice bilayer commensurate in 2-dimensions with the two free interfaces interacting with the vacuum (see **Figure 1**). This two-layer ice film was found to be stable under finite temperature molecular dynamics at 150K. Through the calculation of the IR spectrum we were able to reproduce the experimental IR spectrum with near quantitative agreement. Moreover, we were able to assign the blue shifted mid-IR intensities to strained hydrogen bonds from the bridging water molecules comprising the bilayer. This evidence, in conjunction with a experimentally determined LEED pattern, was integral in assigning this novel meta-stable phase of water. Furthermore, we have provided an alternative explanation of the observed blue shifts in the mid-IR spectra for water in confined hydrophobic geometries as being due to strained hydrogen bonding reminiscent of the idealized bilayer structure.[11]

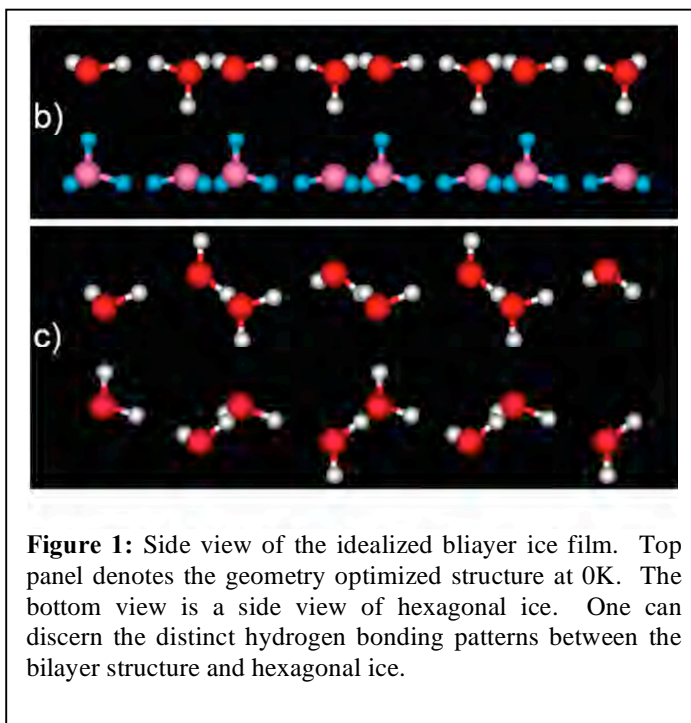


Figure 1: Side view of the idealized bilayer ice film. Top panel denotes the geometry optimized structure at 0K. The bottom view is a side view of hexagonal ice. One can discern the distinct hydrogen bonding patterns between the bilayer structure and hexagonal ice.

This evidence, in conjunction with a experimentally determined LEED pattern, was integral in assigning this novel meta-stable phase of water. Furthermore, we have provided an alternative explanation of the observed blue shifts in the mid-IR spectra for water in confined hydrophobic geometries as being due to strained hydrogen bonding reminiscent of the idealized bilayer structure.[11]

Large-scale density functional theory studies of the free-energies of transfer of OH⁻ from bulk to interface: Although there appears to be a consensus between various theoretical calculations and

experiments on the distributions of several inorganic ions in the interfacial region, there is considerable disagreement of the water ions, specifically, the hydroxide anion and the excess proton, at the air-water interface.² This is problematic, because an accurate knowledge of the propensities of the water ions for the air-water interface is central to our understanding of chemistry at aqueous interfaces. The relative populations of these ions at the interface vs. in bulk neat water determine whether the interfacial region is neutral, as in the bulk, or acidic or basic. Corresponding data for hydroxide could be interpreted in terms of a range of behavior, from slight enhancement to strong repulsion.³ It is clear from the collection of experimental and theoretical data summarized here that more research is needed to resolve the important issue of the acidity/basicity of the water surface. We have weighed in on this critical debate by performing the largest and most extensive DFT (utilizing the Grimme correction¹) studies of the hydroxide anion in water in an interfacial geometry. These calculations were made possible by the 2008-2009 INCITE award and 2008 NERSC large-scale reimbursement program. Our results, presented in **Figure 2** indicate that hydroxide ion has a slight propensity to the liquid-vapor interface on the order of $k_B T$.**[14]**

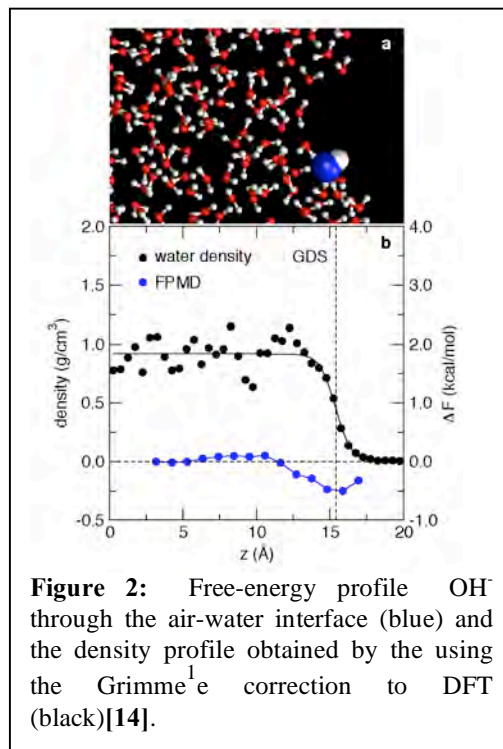


Figure 2: Free-energy profile OH through the air-water interface (blue) and the density profile obtained by using the Grimme correction to DFT (black)**[14]**.

Future directions

1. We plan to extend SCP-DFT to interfacial systems and chemical reactions in aqueous and heterogeneous environments. We also are thinking of ways to provide effective parameterizations for the first two rows of the periodic table and important halide ions to be used within the SCF-DFT formulation.
2. We plan to continue large-scale DFT calculations to determine novel heterogeneous reaction mechanisms in hydrogen bonding fluids. In particular, we will validate the conventional wisdom on the propensity for hydronium at the liquid vapor interface as well as other ions in the Hofmeister series such as iodide and sodium by utilizing DFT interaction potentials that contain *both* polarization and chemistry. In particular we aim to understand the importance of single ion potentials of mean force in determining overall density profiles of electrolytes at finite concentration.

Acknowledgements. This work benefited greatly from active collaborations with D.J. Tobias (UC-I), M.E. Tuckerman (NYU), and I.-F.W. Kuo (LLNL).

Publications from BES support (2007- present)

1. McGrath MJ, Ji Siepmann, I-FW Kuo, and **CJ Mundy**. 2007. "Spatial Correlation of Dipole Fluctuations in Liquid Water." *Molecular Physics* 105(10):1411-1417.
2. **Mundy CJ**, SM Kathmann, and GK Schenter. 2007. "A Special Brew." *Natural History* (Special Issue) 116(9):32-3

3. Glezakou VA, M Dupuis, and **CJ Mundy**. 2007. "Acid/Base Equilibria in Clusters and Their Role in Proton Exchange Membranes: Computational Insight." *Physical Chemistry Chemical Physics* 9(43):5752-5760. DOI:10.1039/b709752b.
4. Wick CD, I-FW Kuo, **CJ Mundy**, and LX Dang. 2007. "The Effect of Polarizability for Understanding the Molecular Structure of Aqueous Interfaces." *Journal of Chemical Theory and Computation* 3(6):2002-2010.
5. **Mundy CJ**, R Rousseau, A Curioni, SM Kathmann, and GK Schenter. 2008. "A Microscopic Approach to Understanding Complex Systems: Computational Statistical Mechanics Using State-of-the-Art Computational Platforms." *Journal of Physics* **125**, 012014 (2008)
6. Kuo IFW, **CJ Mundy**, MJ McGrath, and JI Siepmann. 2008. "Structure of the Methanol Liquid-Vapor Interface: A Comprehensive Particle-Based Simulation Study." *Journal of Physical Chemistry C* 112(39):15412-15418.
7. Kathmann SM, IFW Kuo, and **CJ Mundy**. 2008. "Electronic Effects on the Surface Potential at the Vapor-Liquid Interface of Water." *Journal of the American Chemical Society* 130(49):16556-16561
8. Goldman N, E Reed, IFW Kuo, L Fried, **CJ Mundy**, and A Curioni. 2009. "Ab initio simulation of the equation of state and kinetics of shocked water." *Journal of Chemical Physics* 130(12):Article no. 124517.
9. Baer M, G Mathias, IFW Kuo, DJ Tobias, **CJ Mundy**, and D Marx. 2008. "Spectral Signatures of the Pentagonal Water Cluster in Bacteriorhodopsin." *Chemphyschem* 9(18):2703-2707.
10. Maerzke KA, G Murdachaew, **CJ Mundy**, GK Schenter, and JI Siepmann. 2009. "Self-consistent polarization density functional theory: Application to Argon." *Journal of Physical Chemistry A* 113(10):2075-2085.
11. Kimmel GA, J Matthiesen, M Baer, **CJ Mundy**, NG Petrik, RS Smith, Z Dohnalek, and BD Kay. 2009. "No Confinement Needed: Observation of a Metastable Hydrophobic Wetting Two-Layer Ice on Graphene." *Journal of the American Chemical Society* **131**,12838 (2009)
12. Schmidt J, J VandeVondele, IFW Kuo, D Sebastiani, JI Siepmann, J. Hutter, and **CJ Mundy**. 2009. "Isobaric-Isothermal Molecular Dynamics Simulations Utilizing Density Functional Theory: An Assessment of the Structure and Density of Water at Near-Ambient Conditions." *Journal of Physical Chemistry B* [in press]
13. **Mundy CJ**, KA Maerzke, MJ McGrath, IFW Kuo, G. Tabbachi, and JI Siepmann. 2009. "Vapor-liquid phase equilibria of water modelled by a Kim-Gordon potential." *Chemical Physics Letters* [in press]
14. **Mundy CJ**, IFW Kuo, ME Tuckerman, HS Lee, and DJ Tobias. 2009. "Hydroxide Anion at the Air-Water Interface." *Chemical Physics Letters: Frontiers Article* [in press]

References:

- (1) Grimme, S. *Journal of Computational Chemistry* 2004, 25, 1463.
- (2) Petersen, P. B.; Saykally, R. J. *Chemical Physics Letters* 2008, 458, 255.
- (3) Petersen, M. K.; Iyengar, S. S.; Day, T. J. F.; Voth, G. A. *Journal of Physical Chemistry B* 2004, 108, 14804.

MANIPULATING LIGHT WITH TRANSITION METAL CLUSTERS AND DYES

Serdar Ogut

University of Illinois at Chicago, Department of Physics
845 West Taylor Street (M/C 273), Chicago, IL 60607
ogut@uic.edu

PROGRAM SCOPE: The general goal of this project is to develop and apply state-of-the-art first principles methods based on density functional and many-body perturbation theories to predict structural, electronic, and in particular, optical properties of two systems of significant scientific and technological interest: Transition metal clusters and organic dyes. These systems offer great opportunities to manipulate light for a wide-ranging list of energy-related scientific problems and applications. We will focus our investigations on **(i)** the development and implementation of many-body Green's function method (solving the GW-Bethe-Salpeter-Equation) to examine excited state properties of transition metal clusters, **(ii)** electronic and optical properties of Pt_n, Au_n, and their alloy clusters supported on TiO₂ surfaces, and **(iii)** the applications of static and time-dependent density-functional theories to predict structural, electronic, and optical properties of a set of organic dye molecules (halogenated perylene diimide dyes and their aspartine and glycine derivatives) supported on TiO₂ surfaces, relevant for dye-sensitized solar cell applications.

RECENT PROGRESS:

We have continued our *ab initio* studies on the electronic and optical properties of noble metal (Ag, Au, Cu) clusters and Si_nH_m quantum dots within the framework of time-dependent density functional theory (TDDFT) and GW-Bethe-Salpeter (GWBSE) formalisms. During the last two years, we focused on the following problems:

(1) First Principles Absorption Spectra of Intermediate-Size Ag Clusters:

Owing to their intriguing physical and chemical properties, which are of particular relevance in catalysis, optoelectronics and nanophotonics applications, noble metal clusters merit current research activities. These clusters present challenges to first principles computational methods because of the significant role that the *d* electrons play in determining their structural, electronic, and optical properties. Although the molecular orbitals or bands associated with the *d* electrons in noble metal clusters are completely filled, their close proximity to, and spatial overlap with, *sp* electrons makes it necessary to include them explicitly in computations for a quantitative description. One area which has posed a significant computational challenge is related to the accurate modeling of the dielectric and optical properties of noble metal clusters. For example, although the measured spectra for Ag_n (*n* < 40) have been available since the early 1990s, direct comparisons with predictions from reliable *ab initio* modeling techniques have not been straightforward and lagged significantly.

We have made considerable progress in systematic applications of TDDFT within the local density approximation (TDLDA) to noble metal clusters and in the analysis of the results in terms of the underlying atomic and electronic structures. During the last two years, our studies focused on the optical absorption spectra of Cu_n (*n* = 1- 20), which is still ongoing, and Ag_n clusters (*n* = 10 – 20). For Ag_n clusters, at each size, we performed TDLDA computations for the three lowest-energy isomers. When compared with available experimental data for clusters embedded in Ar matrices, our TDLDA predictions were observed to be rather accurate [Fig. 1(a) and 1(b)]. In some cases, isomer-specific spectra allowed for the corroboration of the theoretically predicted structures and identification of structural forms that contributed to a given experimental spectrum. We have identified that the *d* electrons in Ag_n affect their optical spectra in two ways: First, they quench the oscillator strengths by screening the *s* electrons (on average ~50% of the values characteristic for *s* electrons in alkali metal clusters). Second, they can be directly involved in the low-energy (down to 3 – 3.5 eV) optical excitations. We quantified the role of the *d* electrons in the optical spectra by defining the percent of the *d* electron contributions integrated up to a cutoff energy *E_c* as:

$$\%d = \frac{\sum_{i, \Omega_i < E_c} f_i \sum_{vc} |X_{vc}^i|^2 |\langle d | \phi_v \rangle|^2}{\sum_{i, \Omega_i < E_c} f_i} \times 100$$

where $\langle d | \phi_v \rangle$ is the $l=2$ component of the occupied orbital ϕ_v , f_i is the oscillator strength of the excitation at energy Ω_i , and the double index vc labels the entries of the corresponding TDLDA eigenvector X^i , which is composed of occupied-unoccupied (or “valence-conduction”) Kohn-Sham orbital pairs. The size-dependences of these two main effects of the d electrons are shown in Figure 1. We observe that oscillator strengths per atom integrated up to 6 eV are in reasonable agreement with experimental data, and typically remain much smaller than 1, which is the value expected for alkali metal clusters [Fig. 1(c)]. In Fig. 1(d), we show that the integrated d electron contributions as calculated using the above definition increase almost monotonically with cluster size up to $n \sim 13$, reaching values as high as 70-80% for clusters in the $10 < n < 20$ intermediate-size range.

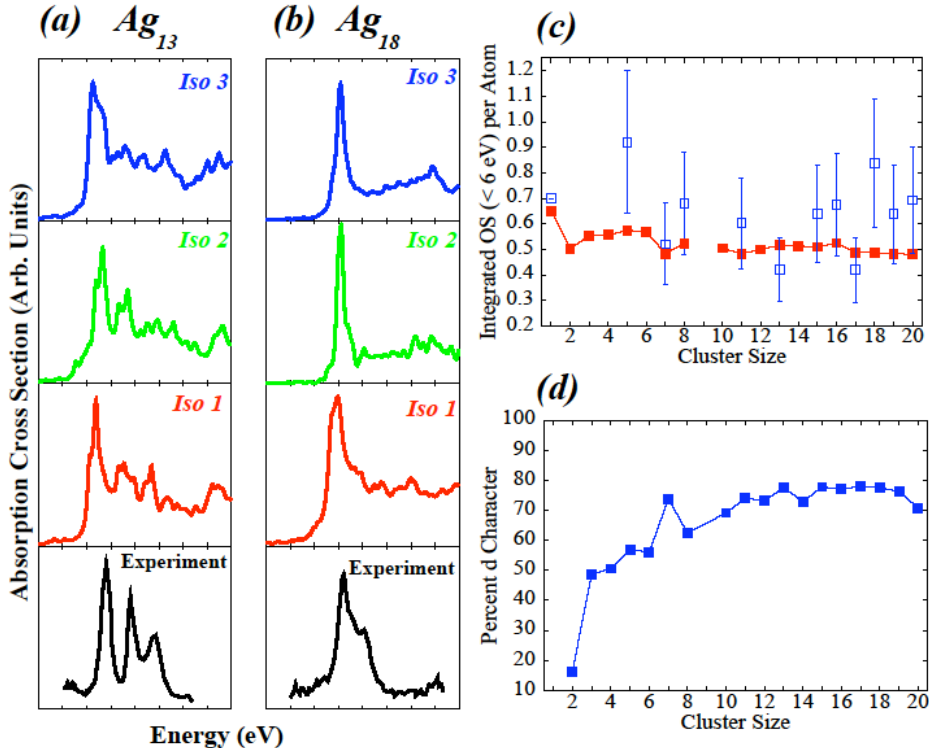


Fig. 1: TDLDA spectra for the three lowest-energy isomers of (a) Ag₁₃ and (b) Ag₁₈ along with experimental data from Ar-matrix spectroscopy. The overall agreement with experimental data is quite good taking into account a small blue-shift of the theoretical spectra, which indicates that quantum confinement due to the surrounding Ar matrix likely plays a role in fixing the positions of the absorption peaks. For Ag₁₃ all three isomers are likely to contribute to the measured spectrum, while for Ag₁₈ the best agreement is observed for the calculated ground state (Iso1) structure. (c) Integrated oscillator strength (below 6 eV) per atom of the lowest-energy Ag_n clusters as a function of n computed from the TDLDA spectra (red filled squares), along with estimates from experimental data (blue empty squares). (d) The percentage of the d character in the optical transitions calculated according to the equation above for the computed ground state structures of Ag_n as a function of size at $E_c = 6$ eV.

(2) Comparisons of TDLDA and GW-BSE Methods for Excitations in Ag Clusters: We have worked on applying the GW-Bethe Salpeter approach in the computations of electronic and optical excitations in Ag_n ($n = 1 - 8$) clusters. We found that the ionization potentials (IPs) and electron affinities (EAs) calculated within the GW approximation are in very good agreement with experimental data [better than those based on the Δ SCF approximation, as shown in Fig. 2(a)]. However, the good agreement is related to the fact that the HOMO and LUMO of Ag_n ($n = 1 - 8$) clusters mostly have sp character with very little d contribution (we have shown this by working with the singly ionized Ag atom, which has the nice feature of having a HOMO with pure d character and a LUMO of pure s character and has reliable experimental data). Our work with Ag⁺ has shown that good agreement with experiment in the GW theory can be achieved, only if the $4s$ and $4p$ semi-core states are included in the construction of the Ag pseudopotential (otherwise, i.e. with standard pseudopotentials for which $4s$ and $4p$ electrons are in the core, the IP of Ag⁺ is underestimated by 2.6 eV). Clearly, the inclusion of semi-core orbitals increases the computational demand enormously, but it is needed for quantitative agreement with experiment. If the $4s$ and $4p$ orbitals are not included in the potential, the resulting BSE optical spectra are also not in good agreement with experiment, since even low-energy optical transitions in Ag_n clusters have appreciable d character. GWBSE enhances the screening of s electrons by the d electrons and over-mixes states of s and d characters. With TDLDA, on the other hand, the agreement with experiment is consistently fairly good even if the $4s$ and $4p$ states are not included in the valence pseudopotentials [Fig. 2(b)-(d)].

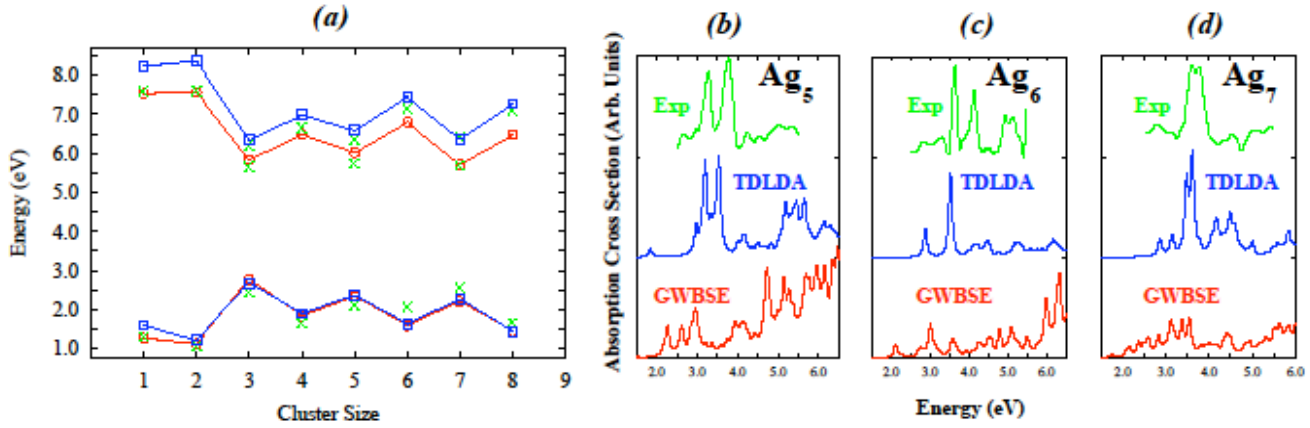


Fig. 2: (a) Ionization potentials (upper lines and points) and electron affinities (lower lines and points) of Ag_n as a function of size calculated within the GW (red circles) and ΔSCF (blue squares) approximation. The experimental data are shown with green crosses. For $n = 3, 5,$ and $7,$ two sets of experimental data are available in the literature. (b)-(d) Calculated GWBSE (lower red curves), TDLDA (middle blue curves), and experimental (top green curves) spectra of $\text{Ag}_5, \text{Ag}_6,$ and $\text{Ag}_7.$

(3) Quasiparticle Gaps and Screening in Si_nH_m Nanoshells: We also investigated from first principles ΔSCF computations the size-dependence of quasiparticle gaps (electron affinities and ionization potentials), and unscreened exciton binding energies in Si_nH_m nanoshells (quantum dots with a cavity inside them). While an empirical model based on the single-band effective mass approximation for impenetrable nanoshells predicts that the quasiparticle gap should depend only on the thickness $t = R_2 - R_1$ of the nanoshell (where R_1 and R_2 are the inner and outer radii, respectively) and scale as t^2 , we found from first principles calculations that the quasiparticle gaps depend on both R_1 (weakly) and R_2 (strongly), as shown in Fig 3(a) below. The dependence of the quasiparticle gap on R_1 (at fixed R_2) and on R_2 (at fixed R_1) is mostly consistent with classical electrostatics of a *metallic shell*. More interestingly, we found that the (unscreened) exciton Coulomb energy (calculated both perturbatively from first principles *and* analytically in the effective mass approximation) in quantum nanoshells has a rather unexpected dependence on the thickness of the nanoshell at fixed R_2 [Fig. 3(b)]. Namely, the Coulomb energy *decreases* as the nanoshell becomes more *confining*, contrary to what one might expect from quantum confinement effects. We showed that this unexpected finding is due to the increase in the average electron-hole distance, which gives rise to reduced Coulomb interaction in spite of the reduction in the confining nanoshell volume.

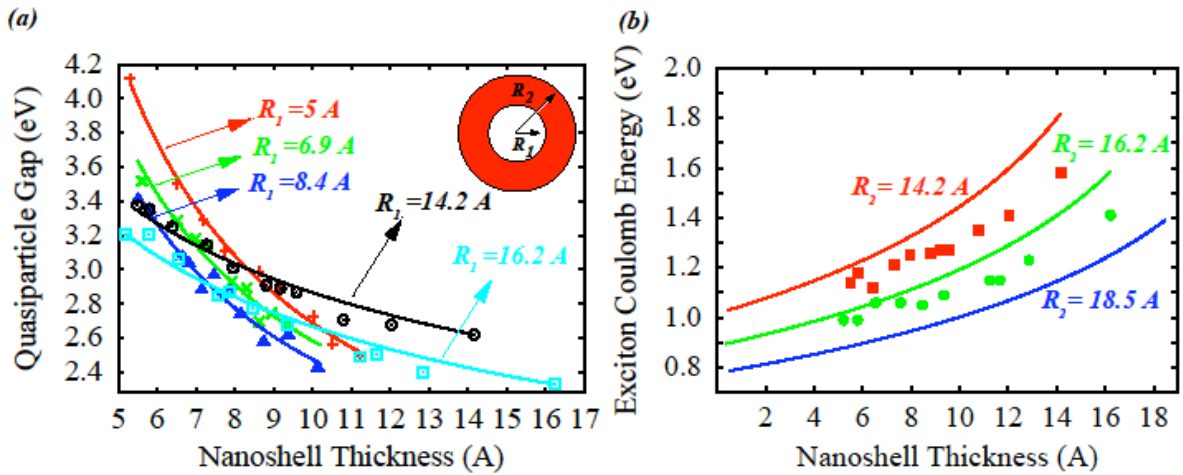


Fig. 3: (a) Calculated first principles quasiparticle gaps as a function of the nanoshell thickness at fixed inner radii of $R_1 = 5 \text{ \AA}, 6.9 \text{ \AA}, 8.4 \text{ \AA}$ and at fixed outer radii of $R_2 = 14.2 \text{ \AA},$ and 16.2 \AA . The solid lines are fitted to the calculated data as power laws of the thickness t . At fixed $R_1,$ the gap scales as $t^1,$ while at fixed R_2 it scales as $t^{1/4}.$ (b) Unscreened Coulomb energy as a function of nanoshell thickness at fixed outer radii of $R_2 = 14.2, 16.2,$ and 18.5 \AA . The solid lines are predictions from the effective mass approximation (EMA). The filled squares and circles are *ab initio* results from direct calculations of the Coulomb energy for $R_2 = 14.2$ and $16.2 \text{ \AA},$ respectively. EMA results are larger than first principles results, since the true wavefunctions decay slowly into the vacuum rather than vanish abruptly at the boundaries.

FUTURE PLANS:

Our ongoing research and future plans in *ab initio* investigations of the optical properties of transition/noble metal clusters and organic dyes include:

- (a) Developing a more robust GWBSE theory that can treat *sp* and *d* electrons on equal footing without the necessity of including semi-core states. This includes possible revisions in the implementation of the theory along lines similar to non-linear-core corrections in total energy and band structure of solids,
- (b) TDDFT and GWBSE computations for the optical spectra of small size *3d* transition metal clusters with partially and fully filled *d* orbitals,
- (c) TDDFT computations for the optical properties of TiO₂-supported transition metal clusters, such as Pt_{*n*} and Au_{*n*}, as well as organic dyes, such as perylene diimide and its glycine and aspartine derivatives, and investigating how substrates affect/modify their optical excitations.

PUBLICATIONS FROM DOE SPONSORED RESEARCH (2005 – Present):

- 1) J. C. Idrobo, S. Ogut, and J. Jellinek, “Size dependence of static polarizabilities and optical absorption spectra of Ag_{*n*} (*n* = 2 – 8) clusters”, Phys. Rev. B **72**, 085445 (2005).
- 2) S. Ogut, J. C. Idrobo, J. Jellinek, and J. Wang, “Structural, electronic, and optical properties of noble metal clusters from first principles”, J. Clus. Sci. **17**, 609 (2006).
- 3) J. C. Idrobo, M. Yang, K. A. Jackson, and S. Ogut, “First principles optical absorption spectra of Si_{*n*} (*n* = 20 – 28) clusters: Time-dependent local-density approximation versus predictions from Mie Theory”, Phys. Rev. B **74**, 153410 (2006).
- 4) J. C. Idrobo, S. Ogut, K. Nemeth, J. Jellinek, and R. Ferrando, “First-principles isomer-specific absorption spectra of Ag_{*11*}”, Phys. Rev. B **75**, 233411 (2007).
- 5) J. C. Idrobo, W. Walksoz, S. F. Yip, S. Ogut, J. Wang, and J. Jellinek, “Static polarizabilities and optical absorption spectra of gold clusters (Au_{*n*}, *n* = 2 – 14, and 20) from first principles”, Phys. Rev. B **76**, 205422 (2007).
- 6) K. Baishya, J. C. Idrobo, S. Ogut, M. Yang, K. A. Jackson, and J. Jellinek, “Optical absorption spectra of intermediate size silver clusters”, Phys. Rev. B **78**, 075439 (2008).
- 7) M. L. Tiago, J. C. Idrobo, S. Ogut, J. Jellinek, and J. R. Chelikowsky, “Electronic and optical excitations in Ag_{*n*} (*n* = 1 – 8): Comparison of density-functional and many-body theories”, Phys. Rev. B **79**, 155419 (2009).
- 8) K. Frey, J. C. Idrobo, M. L. Tiago, F. Reboredo, and S. Ogut “Quasiparticle gaps and exciton Coulomb energies in Si nanoshells: First principles calculations”, submitted to Phys. Rev. B (August 2009).

LASER DYNAMIC STUDIES OF PHOTOREACTIONS ON SINGLE-CRYSTAL AND NANOSTRUCTURED SURFACES

Richard Osgood,

Center for Integrated Science and Engineering, Columbia University, New York, NY 10027, Osgood@columbia.edu

Program Scope or Definition:

Our program focuses our dynamics research on molecular half-collision dynamics and scattering on nanostructured surfaces and, in particular, the surfaces of nanoobjects. In the early stages of the present program, our work first emphasized an STM-enabled study on the formation of uncapped nanocrystals with specific reconstructions and orientations; the particles were formed via reactive layer assisted deposition. We have now extended this work by examining dry alloy-controlled formation of TiO₂ nanocrystals, a process with better control over the size and shape dispersion of the nanocrystals.

We have also begun an effort to examine photo and electron-driven dynamics of dissociation on TiO₂ surfaces. To carry these out, we will first use STM, XPS, and mass-spectroscopy methods with a quadrupole mass spectrometer to explore photoreaction dynamics, i.e. fragment identification, surface ejection distance, and nature of the products on the TiO₂ surface. A second thrust of the research will be to explore fragmentation dynamics on metal nanoparticles, which have plasmon-enhanced-reaction rates. Particle preparation will use gas-phase particle nucleation or deposition on a cryogenic buffer layer such as condensed-phase Xe or D₂O. The research tools will be time-of-flight detection SXPS, STM, standard UHV probes, and theoretical *E&M* (metal nanoparticles) and molecular computational tools. Collaborations with the Surface Dynamics Group and Catalysis Group at Brookhaven National Laboratory are on-going.

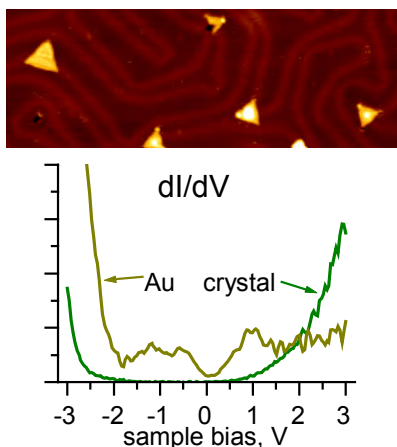


Fig. 1: (top) 50 × 20 nm STM image of TiO₂ crystallites grown by surface-alloy oxidation with 0.1 ML of Ti, oxidized in O₂ at 900 K. (bottom) STS spectra taken over a crystallite and an exposed Au(111) substrate area. The STS spectrum of the crystallite shows a bandgap ~ 3eV, comparable to that of bulk rutile.

From the perspective of energy needs, photoexcitation has been of continuing interest for its importance in photocatalytic destruction of environmental pollutants in several methods of nanotechnology. Our recent work in this program has yielded several new research findings regarding the preparation of nanoparticles, the basic chemical dynamics of surface photofragmentation, and plasmonic surface enhancement and scattering.

Recent Progress:

STM Study of Low-Dispersion Au(111)-Supported TiO₂ Nanocrystals

We have developed a novel approach to low-dispersion TiO₂ nanocrystal growth on single-crystal metal substrates. This method complements the alternative and powerful approach

based on reactive-layer deposition, which was recently reported in an ACS Nano paper. In this method titanium was first evaporated on a clean Au(111) substrate, and the sample was annealed in UHV at 900 K; this process leads to the formation of a Ti-Au surface alloy. Then following a 900 K annealing of this sample in the flow of molecular oxygen, our STM images showed that arrays of ~ 10 nm wide and 0.6 – 2 nm high titania nanocrystals were formed on the Au surface. The majority of the crystallites had hexagonal symmetry and their atomic structure was identified as rutile with their (100) crystal plane parallel to the surface. STS spectra of the crystallites show the presence of a ~ 3 eV band gap that is similar to the bulk rutile value; see Fig. 1. A calculation based on the measured total volume of titania crystallites shows that $\sim 55 - 65$ % of the titanium initially deposited on the surface is pulled out of the bulk by the oxidation process to form titanium oxide. In general, this method of TiO₂ nanocrystal growth from our Au-Ti surface alloy results in a narrower nanocrystallite size distribution and higher structural homogeneity compared to other methods reported in the literature. In particular, O₂-oxidation of Ti deposited on Au(111) surface without preliminary thermal dissolution of titanium in the gold crystal leads to the formation of titania crystallites with generally hexagonal symmetry; thus this crystal form is similar to the results shown here. However, without the alloy formation step these crystallites had a more irregular shape and wider size distribution than the crystallites reported here. Reactive-layer-assisted deposition (RLAD) methods, as described in our ACS Nano publication, also provided somewhat less homogeneity of the crystallites in comparison to those obtained here, although of course (RLAD) does have a chemical “agility” which is greater than shown in the surface alloy approach. With H₂O as a reactive layer, a relatively narrow nanocrystallite size distribution could be achieved but at least 3 different crystallite structures were observed. The fraction of the hexagonal crystallites – the major crystallite structure – in H₂O RLAD work was 60 – 75 % versus ~ 95 % in the present study.

A more detailed discussion of our surface alloy work has recently been published in Nano Letters.

Plasmonic Photochemistry and Surface Probing

Surface plasmon polaritons on surface metal nanostructures have found use in surface chemistry and chemical probing. Because of this importance and because of our recent work in this area, we have initiated a program to understand how new scientific advances in plasmon science can be used to understand surface dynamical phenomena. Thus in our recent work we examined whether propagating plasmon waves themselves can be used to directly generate SHG radiation after interacting with a surface feature. Such interactions could form the basis for a new approach for high-resolution imaging of surface features, investigation of structural properties of colloids, or even a type of plasmon driven surface chemistry. In fact, however, no theoretical prior studies investigating scattered SHG by propagating SPPs are available. To this end, we studied a realistic interaction of plasmon waves with two-dimensional (2D), radially symmetric surface nanodefects. Importantly, our analysis presents an additional complexity that stems from the more intricate polarization properties of the electromagnetic field that is generated near a 2D metallic nanodefekt. This analysis was published this year in Physical Review B.

More recently we have begun a collaboration with a group at University College London to examine new approaches to building arrays of nanoapertures that can be used to form arrays of enhanced field regions for either plasmon-enhanced chemistry or for second-harmonic surface probes of adsorbates. We have examined one design for this structure and will be evaluating it optically during the next few months, including testing it for second-harmonic generation.

Electron-Initiated Dissociation Dynamics on Surfaces.

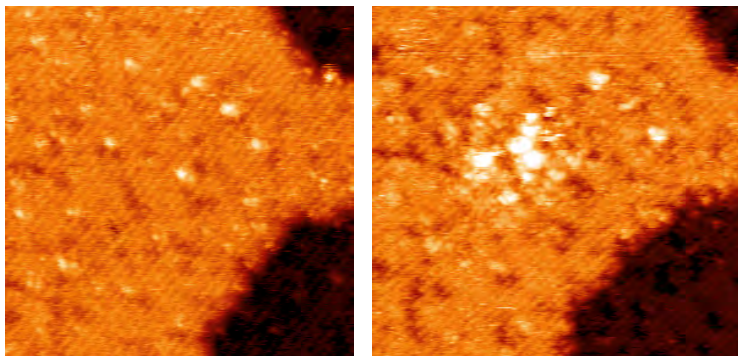


Fig.2. 30 × 30 nm STM image of TiO₂(110) at RT. exposed to 10L of 4-bromobiphenyl (left) before and (right) after a +5V, 2ms pulse from the STM tip.

The central step of many surface photoreactions, such as those in photocatalysis, involves charge transfer from the bulk of substrate to an adsorbed molecule followed by bond cleavage. Scanning tunneling microscopy offers a unique approach to exploration of these molecular dissociation dynamics. Namely, an STM offers, in principle, the possibility to inject an electron or

electrons with a specified energy into a selected molecule on a specific substrate crystal face. This approach, which was examined by the Polanyi Group for semiconductor surfaces, allows dynamical information to be collected including the charge transfer threshold energy of the reaction, the identity of adsorbate states suitable for dissociation, and the nature and adsorption geometry of the products. Recently we have begun to examine the use of this technique on oxide surfaces. In particular, we have initiated investigation of the technique using single-crystal TiO₂ surfaces as model substrates; this work will be followed by work on TiO₂ nanocrystals. Thus far, we have developed a rigorous TiO₂-surface preparation method for our studies; we were aided in this step by useful interactions with the Friend and the PNNL groups. We are now in the process of doing initial experiments with tip-induced reactions using halogenated hydrocarbon (4-bromobiphenyl) adsorbed on this single-crystal TiO₂(110) surface. A recent result of this experiment is shown in Fig. 2, which displays STM images before and after STM irradiation. We have examined electron-dose-dependent changes in the surface adsorbate and examined the range of the dissociation products across the surface. In addition, we are now working on the identification of the reaction products and scaling down of the tip-induced reaction on the single-molecule level.

Future Plans

Our future research efforts are to examine chemical dynamics on TiO₂ surfaces using the very controllable new method using both STM-tip injected electrons and UV irradiation. Both of these experiments involve setting up significantly new instrumenta-

tion in the STM chamber, including a precise evaporator, UV source, and XPS instrumentation; this and other instrumentation upgrades are in progress at present.

Recent DOE-Sponsored Publications

1. Z. Zhu, A. Srivastava, and R.M. Osgood, Jr., "Reactions of Organosulfur Compounds with Si(100)," *J. Phys. Chem. B* **107**, 13939 (2003).
2. A. Srivastava and R.M. Osgood, Jr., "State-Resolved Dynamics of 248 nm Methyl-Iodide Fragmentation on GaAs(110)." *J. Chem. Phys.* **119**, 10298 (2003).
3. K.T. Rim, J.P. Fitts, T. Muller, K. Adib, N. Camillone III, R.M. Osgood, Jr., S.A. Joyce and G.W. Flynn, "CCl₄ Chemistry on the Reduced Selvedge of a α -Fe₂O₃(0001) Surface: A Scanning Tunneling Microscopy Study." *Surf. Sci.* **541**, 59 (2003).
4. K.T. Rim, T. Muller, J.P. Fitts, K. Adib, N. Camillone III, R.M. Osgood, Jr., E.R. Batista, R.A. Friesner, B.J. Berne, S.A. Joyce, and G.W. Flynn, "An STM Study of Competitive Surface Reactions in the Dissociative Chemisorption of CCl₄ on Iron Oxide Surfaces," *Surf. Sci.* **524**, 113 (2003).
5. G. G. Totir, Y. Le and R. M. Osgood, Jr., "Photoinduced-Reaction Dynamics of Halogenated Alkanes on Iron-Oxide Surfaces: CH₃I on Fe₃O₄(111)-(2×2)," *J. Phys. Chem. B* **109**, 8452 (2005).
6. Z. Zhu, T. Andelman, M. Yin, T-L. Chen, S.N. Ehrlich, S.P. O'Brien, R.M. Osgood, Jr., "Synchrotron X-ray Scattering of ZnO Nanorods: Periodic Ordering and Lattice Size," *J. Mater. Res.* **21**, 1033 (2005).
7. Z. M. Zhu, T. Chen, Y. Gu, J. Warren and R. M. Osgood, Jr., "Zinc-oxide Nanowires Grown by Vapor-Phase Transport Using Selected Metal Catalysts: A Comparative Study," *Chem. Mats.* **17**, 4227 (2005).
8. Z. Song, J. Hrbek, R.M. Osgood, Jr., "Formation of TiO₂ Nanoparticles by Reactive-Layer-Assisted Deposition and Characterization By XPS and STM," *Nano. Letts.* **5**, 1357(2005).
9. G.Y. Le, G.G. Totir, G.W. Flynn, and R.M. Osgood, Jr., "Chloromethane Surface Chemistry on Fe₃O₄(111)-(2×2): A Thermal Desorption Spectroscopy Comparison of CCl₄, CBr₂Cl₂, and CH₂Cl₂." *Surf. Sci.* **600**, 665 (2006).
10. N. Camillone III, T.R. Pak, K. Adib, R.M. Osgood, Jr., "Tuning Molecule-Surface Interactions with Sub-Nanometer-Thick Covalently-Bound Organic Monolayers." *J. Phys. Chem B* **110**, 11334 (2006).
11. R.M. Osgood, Jr., "Photoreaction Dynamics of Molecular Adsorbates on Semiconductor and Oxide Surfaces." *Chem. Rev.* **106**, 4379 (2006).
12. L. Cao, N.-C. Panoiu, and R.M. Osgood, Jr., "Surface Second-Harmonic Generation from Surface Plasmon Waves Scattered by Metallic Nanostructures." *Physical Review B* **75**, 205401 (2007)
13. D. Potapenko, J. Hrbek, and R.M. Osgood, Jr., "Scanning Tunneling Microscopy Study of Titanium Oxide Nanocrystals Prepared on Au(111) by Reactive-Layer-Assisted Deposition." *ACS Nano* **2**, 7, 1353-1362 (2008)
14. D. Potapenko and R.M. Osgood, Jr., "Preparation of TiO₂ nanocrystallites by oxidation of Ti-Au(111) surface alloy." *Nano Lett.* **9**, 6, 2378-2383 (2009)
15. L. Cao, N.-C. Panoiu, and R.M. Osgood, Jr., "Surface Second Harmonic Generation from Scattering of Surface Plasmon Polaritons by Radially Symmetric Nanostructures" *Phys. Rev. B*, **79**, 235416 (2009)
16. T.-L. Chen, M.B. Yilmaz, D. Potapenko, A. Kou, N. Stojilovic, R.M. Osgood, Jr., "Chemisorption of Tert-Butanol on Si(100)." *Surf. Sci.* **602**, 21, 3432-3437 (2008)

Optical manipulation of ultrafast electron and nuclear motion on metal surfaces

Hrvoje Petek (petek@pitt.edu)
Department of Physics and Astronomy
University of Pittsburgh
Pittsburgh, PA 15269

We study the unoccupied electronic structure and dynamics of chemisorbed atoms and molecules on metal surfaces by time resolved two-photon photoemission (TR-2PP) spectroscopy, low temperature scanning tunneling microscopy (LT-STM), and theory.¹⁻⁹ Our research concerns simple atomic adsorbates such as alkali and alkaline earth atoms, which provide fundamentally important models for adsorbate-surface interactions, and more complex adsorbates such as fullerenes on noble metals, which illustrate emergent interfacial properties that derive from intrinsic molecular attributes, and molecule-molecule and molecule-surface interactions. Our goal is to understand how these interactions contribute to formation of the interfacial electronic structure, and how thus formed electronic properties affect interfacial phenomena of importance to energy transduction and storage. Moreover, we explore how the interfacial electronic excitation drives dynamical phenomena such as charge transfer and surface femtochemistry.

Electronic structure of a chemisorption interface. We performed systematic studies of the electronic structure of alkali (Li, Na, K, Rb, and Cs) and alkaline earth (Ba) atoms chemisorbed on Cu(111) and Ag(111) surfaces. Surface normal and angle-resolved two-photon photoemission (2PP) spectra were measured with 10 fs, 3.1 eV photon energy laser pulses. At <0.1 monolayer coverage used our experiment, alkali atoms chemisorb in an ionic state. Surprisingly, the unoccupied valence ns resonance of alkali atoms was found to be at 3.0 and 2.8 eV above the Fermi level (E_F) on Cu(111) and Ag(111) surfaces, respectively. This universal behavior was independent of the atomic size and ionization potential within the alkali atom group. We could explain this unexpected behavior with a simple model, which considers the dominant polarization interaction between alkali atoms and metal surfaces. The model we developed should be applicable to predicting the occupied and unoccupied electronic structures of adsorbates on metal surfaces, unless the nature of the interaction has a strong covalent character.

In our model, an alkali atom and a metal surface interact through the Coulomb potential. The conduction electrons in the metal substrate screen the charges of ns valence electron and alkali atom core thereby creating the oppositely charged image charges in the substrate. Thus, the energy of ns valence electron near a metal surface is defined by the Coulomb attraction to the positive core and its image charge, and the repulsion by the image charge of the core. The net repulsive potential destabilizes the ns electron with $1/4z$ dependence, where z is the surface normal distance from the image plane, as alkali atom is brought from vacuum to its chemisorption height R_{ads} above the metal surface. Lifting the ns electron above E_F enables its tunneling into the conduction band of the substrate. The bound state state-continuum interaction between the localized atomic orbitals and the propagating states of the substrate renders the ns level into a σ -resonance ($m=0$, where m is the surface projection of the angular momentum quantum number l) in the unoccupied electronic structure of the interface. The σ -resonance appears as a prominent feature in 2PP spectra of alkali atom covered noble metal surfaces.⁷

We have calculated the σ -resonance energies of alkali atoms on Cu(111) and Ag(111) surfaces using a wave packet propagation procedure and a simple model that simply ascribes them to the $1/4z$ repulsion. Both procedures reproduce the period independent σ -resonance energy, implying that there is an anticorrelation relationship between the atomic ionization potential and R_{ads} . The binding energy of ns electron and R_{ads} are determined by how strongly the core electrons of an alkali atom screen the Coulomb potential of its nucleus. Small atoms with ineffectively screened nucleus (e.g. Li) strongly bind the ns electron and can approach close to the surface to a

distance defined by the Pauli exclusion. The degree of ns electron repulsion, however, also depends on R_{ads} counteracting the strong binding. The correspondingly weak interactions for large alkali atoms result in the period independent σ -resonance energy.

π -resonances. Following the successful explanation of the σ -resonance energy, we reasoned that higher resonances should also be observable for alkali atoms on noble metal surfaces. Therefore, we investigated the angle dependent 2PP spectra in search of $m=1$ resonances arising from the hybridization of the np_x and np_y atomic orbitals. Indeed we found a new resonance at 0.4-0.7 eV above the σ -resonances, when observing emission in the off-normal direction. Figure 1 shows a series of typical angle resolved 2PP spectra of Cs/Cu(111) surface, where the main features are the σ - and π -resonances of Cs. The σ -resonance has maximum intensity near the normal emission, while the π -resonance peaks at ± 15 - 20° from the normal. This difference is explained by their respective $m=0$ and $m=1$ symmetries; the $m=1$ states have zero emission in the normal direction because of nodes in their wave functions. Interestingly, we did not observe π -resonances for Na. Our interpretation is that such resonances exist at higher energies for Li and Na, because for K and larger alkali atoms the hybridization between the np and nd atomic orbitals helps to stabilize the π -resonances.⁸

Ba chemisorption. We also investigated the electronic structure of Ba/Cu(111) surface in order to ascertain the differences between chemisorption of one and two valance electron atoms. Indeed, we observe a prominent σ -resonance at 2.2 eV above E_F in the zero coverage limit. Besides the lower resonance energy, the bandwidth of 0.5 eV is considerably broader than, for example, the σ -resonance of its neighboring element Cs.

In order to gain an understanding of how the alkali and alkaline earth chemisorption differs, we performed electronic structure calculations of both Cs and Ba using an embedding approach with a one-dimensional potential for the surface, which quantitatively reproduces the experiment. The differences between the electronic structures of Cs and Ba on the Cu(111) surface can be attributed to the group dependent screening of the core potentials as manifested by the ionic radii and ionization potentials (alkali vs. alkaline earth). We find that in both cases one $6s$ electron is transferred to the

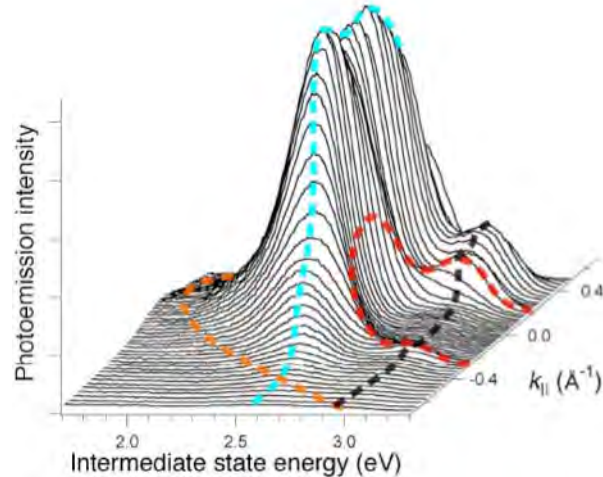


Figure 1. Angle resolved 2PP spectra of Cs/Cu(111). The blue and black dashed lines indicate the σ - and π -resonances.⁸

Figure 2. Spatial distribution of the electronic charge density for Cs/Cu(111) (upper panel) and Ba/Cu(111) (lower panel). The origin (cross) corresponds to the position of the adatom. Vertical lines indicate the image plane position.⁹

substrate, which, in the case of Ba, leaves the second electron still localized on the substrate. The partial charge transfer of Ba valence electrons is responsible for the differences between the calculated electronic charge densities of Cs and Ba on Cu(111), which are shown in Fig. 2. Interestingly, the simple model used to calculate the energy σ -resonances of alkali atoms works equally well for Ba under the assumption that a single electron is transferred to the substrate.⁹

Superatom states of hollow molecules. We used LT-STM and density functional theory to explore the relation between the nearly spherical shape and unoccupied electronic structure of C_{60} molecules adsorbed on copper surfaces. Above the known π^* antibonding molecular orbitals of the carbon-atom framework, starting from 3.5 eV we found atomlike orbitals bound to the core of the hollow C_{60} cage (Fig. 3). These “superatom” states hybridize like the s and p orbitals of alkali atoms into diatomic molecule-like dimers and free-electron bands of one-dimensional wires and two-dimensional quantum wells in C_{60} aggregates. We attribute the superatom states to the central potential binding an electron to its screening charge, a property expected for hollow-shell molecules derived from layered materials. The atomic electron orbitals that underlie molecular bonding originate from the central Coulomb potential of the atomic core. Because the superatom states originate from the image potential of graphene, they are a general feature derived from rolling and wrapping of molecular sheets into hollow molecules.⁵

Future plans. The interaction of alkali atoms with graphitic materials and metal oxides is important in energy storage applications such as rechargeable Li ion batteries. We have therefore initiated a study of the alkali atom electronic structure on HOPG and

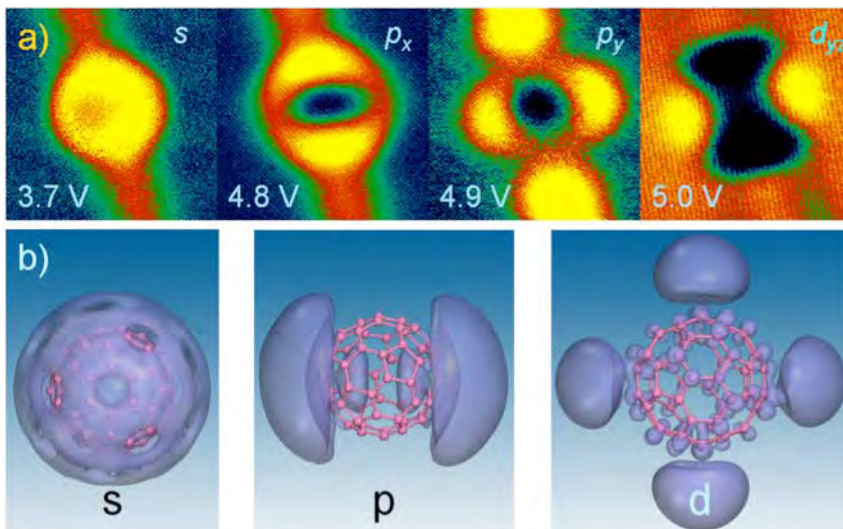
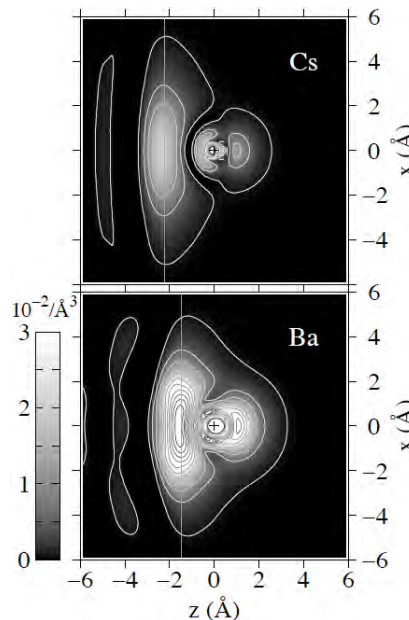


Figure 3. a) The observed s , p , and d superatom orbitals of C_{60} on Cu(110)-O surface. b) the corresponding calculated orbitals from a plane-wave DFT calculation for an isolated C_{60} molecule.⁵

TiO₂. Our preliminary studies for HOPG substrates show evidence for *ns* states of alkali atoms. The samples show complex temperature and alkali atom period dependent behavior that could be related to intercalation or photodesorption. Moreover, we are investigating the effect of endohedral doping of fullerenes on the energy of superatom states. In preliminary measurements on Sc₃N@C₈₀ we have found evidence for the superatom states at higher energy than for C₆₀ (Fig. 4), which is consistent with the endohedral cluster excluding the superatom states from the internal volume.

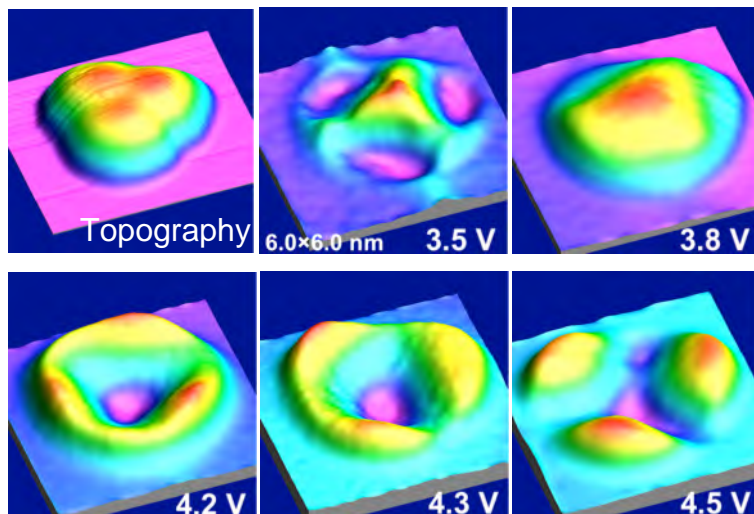


Figure 4. The topography of an equilateral Sc₃N@C₈₀ trimer and dI/dV maps at several representative voltages. The superatom orbitals hybridize into molecular orbitals of the aggregate that resemble those of an alkali atom trimer.

1. M. Fuyuki, K. Watanabe, D. Ino, H. Petek, and Y. Matsumoto, "Electron-phonon coupling at an atomically defined interface: Na quantum well on Cu(111)," *Phys. Rev. B* **76**, 115427-5 (2007).
2. D. B. Dougherty, P. Maksymovych, J. Lee, M. Feng, H. Petek, and J. T. Yates, Jr., "Tunneling spectroscopy of Stark-shifted image potential states on Cu and Au surfaces," *Phys. Rev. B* **76**, 125428-9 (2007).
3. A. Winkelmann, V. Sametoglu, J. Zhao, A. Kubo, and H. Petek, "Angle-dependent study of a direct optical transition in the sp bands of Ag(111) by one- and two-photon photoemission," *Phys. Rev. B* **76**, 195428-11 (2007).
4. M. Feng, J. Lee, J. Zhao, J. T. Yates, and H. Petek, "Nanoscale Templating of Close-Packed C₆₀ Nanowires," *J. Am. Chem. Soc.* **129**, 12394-5 (2007).
5. M. Feng, J. Zhao, and H. Petek, "Atomlike, Hollow-Core-Bound Molecular Orbitals of C₆₀," *Science* **320**, 359-62 (2008).
6. A. Winkelmann, W.-C. Lin, F. Bisio, H. Petek, and J. Kirschner, "Interferometric Control of Spin-Polarized Electron Populations at a Metal Surface Observed by Multiphoton Photoemission," *Phys. Rev. Lett.* **100**, 206601-4 (2008).
7. J. Zhao, N. Pontius, A. Winkelmann, V. Sametoglu, A. Kubo, A. G. Borisov, D. Sanchez-Portal, V. M. Silkin, E. V. Chulkov, P. M. Echenique, and H. Petek, "Electronic potential of a chemisorption interface," *Phys. Rev. B* **78**, 085419-7 (2008).
8. A. G. Borisov, V. Sametoglu, A. Winkelmann, A. Kubo, N. Pontius, J. Zhao, V. M. Silkin, J. P. Gauyacq, E. V. Chulkov, P. M. Echenique, and H. Petek, " π Resonance of Chemisorbed Alkali Atoms on Noble Metals," *Phys. Rev. Lett.* **101**, 266801-4 (2008).
9. S. Achilli, M. I. Trioni, V. Sametoglu, N. Pontius, A. Winkelmann, A. Kubo, J. Zhao, and H. Petek, "Electronic structure of chemisorbed Cs and Ba atoms on Cu(111) from experiment and theory," *Phys. Rev. B* (submitted).

X-ray Spectroscopy of Liquids and their Surfaces

Richard J. Saykally
Department of Chemistry
University of California
and
Chemical Sciences Division
Lawrence Berkeley National Laboratory
Berkeley, CA 94720-1460
saykally@berkeley.edu
<http://www.cchem.berkeley.edu/rjsgrp/index.htm>

Program Scope or Definition

Quantifying the properties of liquid solutions and interfaces defines a current frontier impacting chemical, biological, energy and environmental sciences. The goal of this project is to explore, develop, and exploit novel methodologies for probing the detailed nature of volatile liquids and solutions and their surfaces, employing combinations of liquid microjet technology with synchrotron X-ray and Raman spectroscopies.

Recent Progress

Towards a Predictive Theory of Core-Level Molecular Spectra [20-22]

The development of near edge X-ray absorption fine structure spectroscopy (NEXAFS) of liquid microjets has provided a useful new tool for characterizing the details of solvation for increasingly complex systems. NEXAFS probes the unoccupied molecular orbitals, which are highly sensitive to intermolecular interactions. This new approach to the study of liquids is yielding important insights into the behavior of aqueous systems, but the chemical information that can be extracted from the measurements is currently limited by the reliability of available theoretical methods for computing core-level spectra. In collaboration with LBL scientist David Prendergast, we have used the excited core hole (XCH) method recently developed by Prendergast and Galli to compute the NEXAFS spectra of pyrrole[22] -a prototype aromatic molecule-and compare the results with experimental spectra measured at the ALS. Near edge X-ray absorption fine structure (NEXAFS) spectra of pyrrole measured at the carbon and nitrogen K-edges both in the gas phase and when solvated in water, are compared with spectra simulated using a combination of classical molecular dynamics and first principles density functional theory in the excited state core hole approximation. The excellent agreement enabled detailed spectral assignments. Pyrrole is highly reactive in water and reaction products formed by the autopolymerization of pyrrole in water are identified. The solvated spectra measured at two different temperatures, indicate that the final states remain largely unaffected by both hydration and temperature. This is somewhat unexpected, as the nitrogen in pyrrole can donate a hydrogen bond to water. This study provides a good demonstration of the ability of the XCH method to describe core-level spectra of highly delocalized bonding systems, which are problematic for the methods now commonly used.

As methods of core-level spectroscopy involving X-ray absorption spectroscopy (XAS), near edge X-ray absorption fine structure (NEXAFS), X-ray absorption near edge structure (XANES), or X-ray photoelectron spectroscopy (XPS) mature, they are increasingly being applied to complex molecular systems, including proteins, DNA, large organic molecules, and polymers. However, a major limitation is that deriving molecular information from these measurements usually depends explicitly on comparison with theoretical calculations, which are extremely difficult to perform for such molecules at the accuracy of modern experiments. The accurate description of an absorption event of several hundreds of eV of energy is an ongoing challenge in theoretical chemistry. Our recent study[20] indicates that these calculations are extremely sensitive to the molecular geometries; therefore, in addition to an accurate theoretical formalism to describe the electronic excitation, the molecular geometries and their thermal fluctuations must be correctly sampled.

We reported[21] on the effects of quantized nuclear motion with path integral molecular dynamics PIMD in calculations of the nitrogen K-edge spectra of two isolated organic molecules. S-triazine, a prototypical aromatic molecule occupying primarily its vibrational ground state at room temperature, exhibits substantially improved spectral agreement when nuclear quantum effects are included via PIMD, as compared to the spectra obtained from either a single fixed-nuclei based calculation or from a series of configurations extracted from a classical molecular

dynamics trajectory. Nuclear quantum dynamics can accurately explain the intrinsic broadening of certain features. Glycine, the simplest amino acid, is problematic due to large spectral variations associated with multiple energetically accessible conformations at the experimental temperature. This work highlights the sensitivity of near edge X-ray absorption fine structure NEXAFS to quantum nuclear motions in molecules, and the necessity of accurately sampling such quantum motion when simulating their NEXAFS spectra.

The Liquid Water Surface and the Mechanism of Water Evaporation [7,11,12,18]

The evaporation dynamics of water are crucial elements in the modeling of cloud physics, and thus of atmospheric radiation balance and climate, but remain poorly characterized. Liquid microjet technology affords the opportunity to study the details of water evaporation, free from the obfuscating effects of condensation that have plagued previous studies. Studying small (diameter $< 5 \mu\text{m}$) jets with Raman thermometry, we have found compelling evidence for the existence of a small but significant energetic barrier to evaporation, in contrast to most current models[7,11]. Studies of heavy water indicated a similar evaporation coefficient, and thus an energetic barrier similar to that of normal water[18]. A transition state model developed for this process provides a plausible mechanism for evaporation in which variations in libration and translational frequencies account for the small observed isotope effects[12]. The most important practical result of this work is the quantification of the water evaporation coefficient (0.6), which has been highly controversial, and is a critical parameter in models of climate and cloud dynamics.

Most recently [Drisdell *et al.*, submitted to PNAS], we have measured the effects of added salts on the evaporation dynamics. Using liquid microjets, we measured the cooling rate of 3M ammonium sulfate droplets undergoing free evaporation via Raman thermometry. Analysis of the measurements yields a value of 0.58 ± 0.05 for the evaporation coefficient, identical to that previously determined for pure water. These results imply that sub-saturated aqueous ammonium sulfate, which is the most abundant inorganic component of atmospheric aerosol, does not affect the vapor-liquid exchange mechanism for cloud droplets, despite reducing the saturation vapor pressure of water significantly.

Electrokinetic Energy Conversion in Liquid Water Microjets [14,19]

We have examined the high electrical charging of liquid water microjets that can be effected by metal nozzles, proposing a mechanism based on selective adsorption of hydroxide to the metal surface and subsequent electrokinetic charge separation, and we have demonstrated the use of this “protonic charging” for a novel method of hydrogen generation[14]. Subsequently, we have examined the electrical power generation capabilities of metal nozzle microjets, finding an order of magnitude improvement in efficiency ($\sim 10\%$) over other published results[19]. Recent efforts have addressed the prospects for coupling light energy into the electrokinetic energy conversion process.

Future Plans

1. Continue our exploration of the evaporation of liquid water by Raman thermometry and mass spectrometry, seeking to quantify the effects of salts and surfactants on the evaporation process. We are working with the Chandler group, who is using their elegant TPS methods to deduce the molecular pathways for aqueous evaporation.
2. With LBNL staff scientist David Prendergast, we will continue to develop and test new theoretical methodology for predicting core-level spectra of complex molecules (e.g. biomolecules), for which standard approaches often fail dramatically.
3. Extend our XAS studies of local hydration to important free radical species, generated in liquid water microjets by excimer laser photolysis. Alice England has spent two summers working with the Notre Dame Radiation Lab group to learn techniques for studying free radical chemistry.
4. Extend our studies of amino acid hydration vs. pH to include all natural amino acids. Use the same approach to study hydration of the peptide bonds in small polypeptides, nucleotide bases, nucleosides, and nucleotides, as well as the novel “peptoid” molecules.
5. Measure NEXAFS spectra for pure liquid water, alcohols, and hydrocarbons, seeking to achieve deep supercooling via controlled evaporation. In conjunction with theoretical modeling, we will seek a coherent description of the liquid structure and bonding in these systems.
6. We will continue to explore and compare ion and electron detection of NEXAFS spectra, seeking to obtain a reliable means for characterizing liquid surfaces. Thus far, we have not been able to reproduce the original measurements of the water surface with our newly-designed X-ray spectrometer, and we have shown that the original calculations on which the interpretation of those spectra in terms of “acceptor only” molecules was based

were flawed[16].

7. Complete the XAS study of salt perturbation of local water structure, such that the entire Hofmeister series is ultimately addressed. We seek a comprehensive picture of the effects of both cations and anions on the local structure of water. Raman spectroscopy measurements will also be performed on these systems, the data from which provide complementary insights and aid in the theoretical modeling. We will further develop the use of E-field distributions from simulations to interpret the spectra.

References (DOE supported papers 2005-present) – 22 total

[available at <http://www.cchem.berkeley.edu/rjsgroup/opening/pubs.htm>]

1. B.M. Messer, C.D. Cappa, J.D. Smith, K.R. Wilson, M.K. Gilles, R.C. Cohen, and R.J. Saykally, "pH Dependence of the Electronic Structure of Glycine," *J. Phys. Chem. B* **109**, 5375-5382 (2005). LBNL-56348 *Cover Article.
2. C.D. Cappa, J.D. Smith, K.R. Wilson, B.M. Messer, M.K. Gilles, R.C. Cohen, and R.J. Saykally, "Effects of Alkali Metal Halide Salts on the Hydrogen Bond Network of Liquid Water," *J. Phys. Chem. B* **109**, 7046-7052 (2005). LBNL-56812 *Cover Article.
3. J.D. Smith, C.D. Cappa, B.M. Messer, R.C. Cohen and R.J. Saykally, Response to Comment on "Energetics of Hydrogen Bond Network Rearrangements in Liquid Water," *Science* **308**, 793b (2005). LBNL-57117
4. K.R. Wilson, M. Cavalleri, B.S. Rude, R.D. Schaller, T. Catalano, A. Nilsson, L.G.M. Pettersson, and R.J. Saykally, "X-ray Absorption Spectroscopy of Liquid Methanol Microjets: Bulk Electronic Structure and Hydrogen Bonding Network," *J. Phys. Chem. B* **109**, 10194-10203 (2005). LBNL-56350 *Cover Article.
5. J.D. Smith, C.D. Cappa, K.R. Wilson, R.C. Cohen, P.L. Geissler, and R.J. Saykally, "Unified description of temperature-dependent hydrogen-bond rearrangements in liquid water," *PNAS* **102**, 14171-14174 (2005). LBNL-58789
6. B.M. Messer, C.D. Cappa, J.D. Smith, W.S. Drisdell, C.P. Schwartz, R.C. Cohen, R.J. Saykally, "Local Hydration Environments of Amino Acids and Dipeptides Studied by X-ray Spectroscopy of Liquid Microjets," *J. Phys. Chem. B* **109**, 21640-21646 (2005). LBNL-59184
7. C.D. Cappa, W. Drisdell, J.D. Smith, R.J. Saykally, and R.C. Cohen, "Isotope Fractionation of Water During Evaporation Without Condensation," *J. Phys. Chem. B* **109**, 24391-24400 (2005). LBNL-59505
8. C.D. Cappa, J.D. Smith, B.M. Messer, R.C. Cohen, and R.J. Saykally, "The Electronic Structure of the Hydrated Proton: A Comparative X-ray Absorption Study of Aqueous HCl and NaCl Solutions," *J. Phys. Chem. B* **110**, 1166-1171 (2006). LBNL-59504
9. C.D. Cappa, J.D. Smith, B.M. Messer, R.C. Cohen, and R.J. Saykally, "Effects of Cations on the Hydrogen Bond Network of Liquid Water: New Results from X-ray Absorption Spectroscopy of Liquid Microjets," *J. Phys. Chem. B* **110**, 5301-5309 (2006). LBNL-59955
10. J.D. Smith, C.D. Cappa, B.M. Messer, W.S. Drisdell, R.C. Cohen, and R.J. Saykally, "Probing the Local Structure of Liquid Water by X-ray Absorption Spectroscopy," *J. Phys. Chem. B* **110**, 20038-20045 (2006). LBNL-61736
11. J.D. Smith, C.D. Cappa, W.S. Drisdell, R.C. Cohen, and R.J. Saykally, "Raman Thermometry Measurements of Free Evaporation from Liquid Water Droplets," *JACS* **128**, 12892-12898 (2006). LBNL-61735
12. C.D. Cappa, J.D. Smith, W.S. Drisdell, R.J. Saykally, and R.C. Cohen, "Interpreting the H/D Isotope Fractionation of Liquid Water During Evaporation Without Condensation," *J. Phys. Chem. C* **111**, 7011-7020 (2007). LBNL-62751
13. C.D. Cappa, J.D. Smith, B.M. Messer, R.C. Cohen, and R.J. Saykally, "Nature of the Aqueous Hydroxide Ion Probed by X-ray Absorption Spectroscopy," *J. Phys. Chem. A* **111**, 4776-4785 (2007). LBNL-62752 *Cover Article.
14. A.M. Duffin and R.J. Saykally, "Electrokinetic Hydrogen Generation from Liquid Water Microjets," *J. Phys. Chem. C* **111**, 12031-12037 (2007). LBNL-63475
15. J.D. Smith, R.J. Saykally, and P.L. Geissler, "The Effects of Dissolved Halide Anions on Hydrogen Bonding in Liquid Water," *J. Am. Chem. Soc.* **129**, 13847-13856 (2007). LBNL-63579
16. C.D. Cappa, J.D. Smith, K.R. Wilson, and R.J. Saykally, "Revisiting the total ion yield x-ray absorption spectra of liquid water microjets," *J. Phys.: Condens. Matter* **20**, 205105 (2008). LBNL-189E
17. J.S. Uejio, C.P. Schwartz, A.M. Duffin, W.S. Drisdell, R.C. Cohen, and R.J. Saykally, "Characterization of selective binding of alkali cations with carboxylate by x-ray absorption spectroscopy of liquid microjets," *PNAS* **105**, 6809-6812 (2008). LBNL-894E

18. W.S. Drisdell, C.D. Cappa, J.D. Smith, R.J. Saykally, and R.C. Cohen, "Determination of the Evaporation Coefficient of D₂O," *Atmos. Chem. Phys. Discuss.* **8**, 8565-8583 (2008). LBNL-1182E
19. A. M. Duffin and R. J. Saykally, "Electrokinetic Power Generation from Liquid Water Microjets," *J. Phys. Chem. C* **112**, 17018-17022 (2008). LBNL-1180E
20. J. S. Uejio, C. P. Schwartz, R. J. Saykally, and D. Prendergast, "Effects of vibrational motion on core-level spectra of prototype organic molecules," *Chem. Phys. Lett.* **467**, 195-199 (2008). LBNL-1403E
21. C. P. Schwartz, J. S. Uejio, R. J. Saykally, and D. Prendergast, "On the importance of nuclear quantum motions in near edge x-ray absorption fine structure spectroscopy of molecules," *J. Chem. Phys.* **130**, 184109-184120 (2009). LBNL-1885E
22. C. P. Schwartz, J. S. Uejio, A. M. Duffin, A. H. England, D. Prendergast, and R. J. Saykally, "Autopolymerization and Hydration of Pyrrole Studied by X-ray Absorption Spectroscopy," *J. Chem. Phys.* (accepted 8/16/2009). LBNL-TBA

Molecular Theory & Modeling

Development of Statistical Mechanical Techniques for Complex Condensed-Phase Systems

Gregory K. Schenter
Chemical & Materials Sciences Division
Pacific Northwest National Laboratory
902 Battelle Blvd.
Mail Stop K1-83
Richland, WA 99352
greg.schenter@pnl.gov

The long-term objective of this project is to advance the development of molecular simulation techniques to better understand the relation between the details of molecular interaction and the prediction and characterization of macroscopic collective properties. This involves the investigation of representations of molecular interaction as well as statistical mechanical sampling techniques. Molecular simulation has the promise to provide insight and predictive capability of complex physical and chemical processes in condensed phases and interfaces. For example, the transport and reactivity of species in aqueous solutions, at designed surfaces, in clusters, and in nanostructured materials play significant roles in a wide variety of problems important to the Department of Energy. This includes the design and characterization of catalytic systems for energy storage and conversion.

A detailed understanding of the intermolecular interactions of a small collection of molecules, through appropriate modeling and statistical analysis, will enable us to understand the collective behavior and response of a macroscopic system, thus allowing us to predict and characterize thermodynamic, kinetic, material, and electrical properties. Our goal is to improve understanding at the molecular level in order to address increasingly more complex systems ranging from homogeneous bulk systems to multiple phase or inhomogeneous ones, to systems with external constraints or forces.

To do this effectively, it is necessary to understand the balance between efficiency and accuracy. The evaluation of intermolecular potential energy needs to be efficient enough to allow for effective statistical mechanical and dynamical sampling. At the same time, enough of the underlying physical chemistry and sufficient parameterization needs to be contained in the models of molecular interaction so that the resulting simulation of collective molecular properties are reliable. In addition, it is necessary to understand what level of detail is required to understand a given phenomena. The same potential that is used to describe bulk, homogeneous properties is not necessarily relevant for systems with broken symmetry such as an interface or observables that depend on the quantitative description of electric field fluctuations. This is particularly relevant, as experimental probes are developed to unravel the details of collective molecular response, such as infrared, multidimensional vibrational and x-ray absorption spectroscopies.

In our recent efforts we have noticed that the distinction between methods to describe molecular interaction, such as multipole-polarizable empirical potentials, semiempirical NDDO electronic structure, and density functional theory (DFT) have become blurred and an understanding of the relation between such methods will become more important as mixed methods (such as generalizations of QM/MM, embedding and multilayered methods) are developed. All of these methods require efficient representation of the Coulomb interaction,

$E_{A,B}^{Coul} = \int d\mathbf{r} d\mathbf{r}' \rho_A(\mathbf{r}) \frac{1}{|\mathbf{r} - \mathbf{r}'|} \rho_B(\mathbf{r}')$, between molecular charge densities, $\rho_A(\mathbf{r})$ and $\rho_B(\mathbf{r})$. In

both empirical potentials and NDDO electronic structure such interactions are represented by multipole expansions of the charge density accompanied by appropriate screening at short range as an efficient representation of the explicit expression that is used in DFT. The improvement of accuracy, parameterization and efficiency of such representations is the focus of current and future research efforts. Is it useful to go beyond a dipole expansion in developing empirical potentials? In the NDDO approach what are optimal representations of screening that can be effectively parametrized?

We continue to develop our Self-Consistent Polarization (SCP) method [Refs. a, 1, 12] that enhances the polarization response of an efficient electronic structure method while providing a consistent representation of the dispersive interaction that is based on second-order perturbation theory. This approach may be understood in terms of the enhancement of the base energy functional, $E_0[\rho_0]$, by an auxiliary SCP charge density and functional $E_{SCP}[\rho_{SCP}]$, to give $E[\rho_0, \rho_{SCP}] = E_0[\rho_0] + E_{SCP}[\rho_{SCP}] + E^{Coul}[\rho_0, \rho_{SCP}]$, where the cross-interaction terms, $E^{Coul}[\rho_0, \rho_{SCP}]$, are entirely described by the Coulomb interaction. The energy functional associated with SCP, $E_{SCP}[\rho_{SCP}]$, is based on linear response and requires effective multipole polarizabilities. The associated multipole dispersion interaction is introduced in a ‘‘Casimir-Polder’’ form as $E^{disp} = -\frac{1}{2\pi} \int_0^\infty d\omega \sum_{\alpha < \beta} \sum_{\bar{\alpha} < \bar{\beta}} a_{\alpha, \bar{\alpha}}(i\omega) a_{\beta, \bar{\beta}}(i\omega) (\alpha|\beta) (\bar{\alpha}|\bar{\beta})$, where $a_{\alpha, \bar{\alpha}}(\omega)$ are dynamic multipole polarizabilities (associated with $E_{SCP}[\rho_{SCP}]$) and $(\alpha|\beta)$ are Coulomb integrals over an appropriate basis.

Initial implementations of this approach were used to describe water with NDDO theory. [Ref. 12] We are making progress developing such an approach to describe water with DFT. [Ref. a] We have also tested our SCP-DFT approach on the dispersion-dominated system of the gas, liquid and solid phases of Argon. [Ref. 1] Here, the base DFT is purely repulsive and all of the cohesive interaction is due to dispersion. [See Figure 1.]

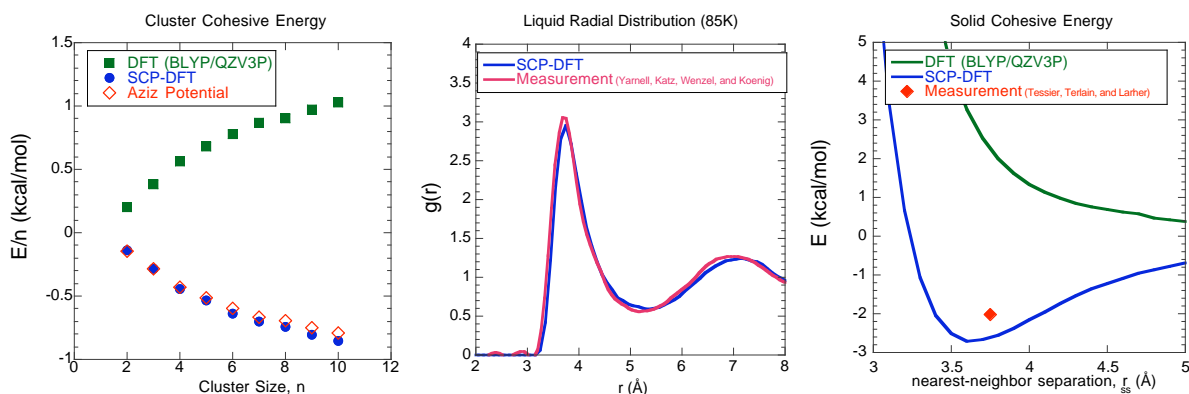


Figure 1. Simulation of cluster, liquid and solid properties of Argon using SCP-DFT.

The SCP-DFT and SCP-NDDO approaches for both cluster and periodic systems have been successfully implemented in the molecular simulation package, CP2K.^b Work continues to enhance the efficiency of the SCP-NDDO periodic electronic structure in order to effectively

treat increasingly larger systems. In Figure 2 we present preliminary results of the radial distribution function of bulk water for the SCP-NDDO model of Ref. 12.

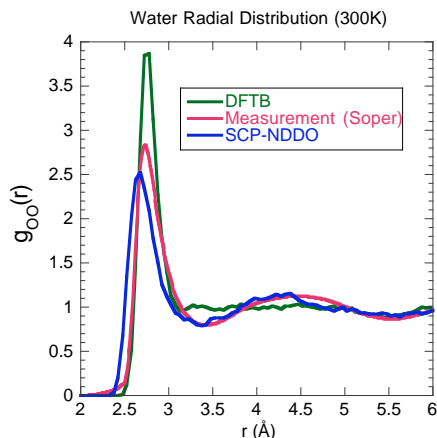


Figure 2. Radial distribution of SCP-NDDO water

Future plans will include expanding the numerical efficiency of both approaches by improving preconditioning of the combined SCP and orbital optimization procedure. With efficient implementations of our SCP approach, we plan to explore solvation in more complex environments. Initial steps have been made to parameterize protonated and hydroxide water clusters. Future efforts will extend the parameterization to aqueous solvation of more complex ions.

In conjunction with these efforts we will continue our analysis of EXAFS measurements as a probe of solvation structure. [Refs. 6, 20 and 24]

From our representation of molecular interaction we will generate ensembles of configurations. From this ensemble, a series of electron multiple scattering calculations are performed using the FEFF8 code^c to generate a configuration averaged EXAFS spectra. In future studies we will consider the influence of molecular interaction between ion pairs. Our challenge is to be able to account for changes in features in EXAFS measurement as a function of solute concentration. In an additional extension of our bulk EXAFS analysis, we will attempt to understand the influence of an interface on the observed ion solvation structure and how it manifests itself in an EXAFS measurement.

Acknowledgements: Direct collaborators on this project include C.J. Mundy and G. Murdachaew. Interactions with B.C. Garrett, S.S. Xantheas, L.X. Dang and S.M. Kathmann have significantly influenced the course of this work.

This research was performed in part using the computational resources in the National Energy Research Supercomputing Center (NERSC) at Lawrence Livermore National Laboratory. Battelle operates Pacific Northwest National Laboratory for the US Department of Energy.

References

- a. G. Murdachaew, C.J. Mundy, and G.K. Schenter, “Self-consistent polarization density functional theory: Application to water,” submitted to J. Chem. Phys.
- b. The CP2K developers group, <http://cp2k.berlios.de/> (2008) J. VandeVondele, M. Krack, F. Mohamed, M. Parrinello, T. Chassaing and J. Hutter, Comp. Phys. Comm. **167**, 103 (2005).
- c. J.J. Rehr, R.C. Albers, S.I. Zabinsky, Phys. Rev. Lett. **69**, 3397 (1992); M. Newville, B. Ravel, D. Haskel, J.J. Rehr, E.A. Stern, and Y. Yacoby, Physica B, **208-209**, 154 (1995); A.L. Ankudinov, C. Bouldin, J.J. Rehr, H. Sims, and H. Hung, Phys Rev. B **65**, 104107 (2002).

References to publications of DOE sponsored research (2006-present)

1. Maerzke, K.A., Murdachaew, G., Mundy, C.J., Schenter, G.K., & Siepmann, J.I., Self-Consistent Polarization Density Functional Theory: Application to Argon. J. Phys. Chem. A **113** (10), 2075-2085 (2009).

2. Kathmann, S.M., Schenter, G.K., Garrett, B.C., Chen, B., & Siepmann, J.I., Thermodynamics and Kinetics of Nanoclusters Controlling Gas-to-Particle Nucleation. *J. Phys. Chem. C* **113** (24), 10354-10370 (2009).
3. Bell, R.C., Wu, K., Iedema, M.J., Schenter, G.K., & Cowin, J.P., The Oil-Water Interface: Mapping the Solvation Potential. *J. Am. Chem. Soc.* **131** (3), 1037-1042 (2009).
4. Mundy, C.J., Rousseau, R., Curioni, A., Kathmann, S.M., & Schenter, G.K., A molecular approach to understanding complex systems: computational statistical mechanics using state-of-the-art algorithms on tera-scale computational platforms. *J. of Phys. Conf. Series* **125**, 012014 (2008).
5. Wang, H.F. et al., Pyroelectricity of water ice. *J. Phys. Chem. B* **112** (20), 6379-6389 (2008).
6. Nichols, P., Bylaska, E.J., Schenter, G.K., & de Jong, W., Equatorial and apical solvent shells of the UO_2^{2+} ion. *J. Chem. Phys.* **128** (12), 124507 (2008).
7. Kathmann, S.M., Schenter, G.K., & Xantheas, S.S., On the determination of monomer dissociation energies of small water clusters from photoionization experiments. *J. Phys. Chem. A* **112** (9), 1851-1853 (2008).
8. Kathmann, S.M., Schenter, G.K., & Garrett, B.C., The impact of molecular interactions on atmospheric aerosol radiative forcing in *Advances in Quantum Chemistry: Applications of Theoretical Methods to Atmospheric Science* (Elsevier Academic Press Inc, San Diego, 2008), Vol. **55**, pp. 429-447.
9. Kathmann, S.M., Palmer, B.J., Schenter, G.K., & Garrett, B.C., Activation energies and potentials of mean force for water cluster evaporation. *J. Chem. Phys.* **128** (6), 064306 (2008).
10. Eustis, S.N. et al., Electron-driven acid-base chemistry: Proton transfer from hydrogen chloride to ammonia. *Science* **319** (5865), 936-939 (2008).
11. Du, S.Y., Francisco, J.S., Schenter, G.K., & Garrett, B.C., Many-body decomposition of the binding energies for $\text{OH} \cdot (\text{H}_2\text{O})_2$ and $\text{OH} \cdot (\text{H}_2\text{O})_3$ complexes. *J. Chem. Phys.* **128** (8), 084307 (2008).
12. Chang, D.T., Schenter, G.K., & Garrett, B.C., Self-consistent polarization neglect of diatomic differential overlap: Application to water clusters. *J. Chem. Phys.* **128** (16), 164111 (2008).
13. Valiev, M. et al., Hybrid approach for free energy calculations with high-level methods: Application to the $\text{S}(\text{N})_2$ reaction of CHCl_3 and OH^- in water. *J. Chem. Phys.* **127** (5), 051102 (2007).
14. Mundy, C.J., Kathmann, S.M., & Schenter, G.K., A Special Brew. *Nat. Hist.* **116** (9), 32-36 (2007).
15. Kathmann, S.M., Schenter, G.K., & Garrett, B.C., Comment on "Quantum nature of the sign preference in ion-induced nucleation". *Phys. Rev. Lett.* **98** (10), 109603 (2007).
16. Kathmann, S., Schenter, G., & Garrett, B., The critical role of anharmonicity in aqueous ionic clusters relevant to nucleation. *J. Phys. Chem. C* **111** (13), 4977-4983 (2007).
17. Du, S.Y., Francisco, J.S., Schenter, G.K., & Garrett, B.C., Ab initio and analytical intermolecular potential for $\text{ClO-H}_2\text{O}$. *J. Chem. Phys.* **126** (11), 114304 (2007).
18. Wick, C.D. & Schenter, G.K., Critical comparison of classical and quantum mechanical treatments of the phase equilibria of water. *J. Chem. Phys.* **124** (11), 114505 (2006).
19. Iordanov, T.D., Schenter, G.K., & Garrett, B.C., Sensitivity analysis of thermodynamic properties of liquid water: A general approach to improve empirical potentials. *J. Phys. Chem. A* **110** (2), 762-771 (2006).
20. Glezakou, V.A., Chen, Y.S., Fulton, J.L., Schenter, G.K., & Dang, L.X., Electronic structure, statistical mechanical simulations, and EXAFS spectroscopy of aqueous potassium. *Theor. Chem. Acc.* **115** (2-3), 86-99 (2006).
21. Garrett, B.C., Schenter, G.K., & Morita, A., Molecular simulations of the transport of molecules across the liquid/vapor interface of water. *Chem. Rev.* **106** (4), 1355-1374 (2006).
22. Fanourgakis, G.S., Schenter, G.K., & Xantheas, S.S., A quantitative account of quantum effects in liquid water. *J. Chem. Phys.* **125** (14), 141102 (2006).
23. Du, S.Y. et al., The OH radical- H_2O molecular interaction potential. *J. Chem. Phys.* **124** (22), 224318 (2006).
24. Dang, L.X., Schenter, G.K., Glezakou, V.A., & Fulton, J.L., Molecular simulation analysis and X-ray absorption measurement of Ca^{2+} , K^+ and Cl^- ions in solution. *J. Phys. Chem. B* **110** (47), 23644-23654 (2006).

Chemical Imaging and Dynamical Studies of Reactivity and Emergent Behavior in Complex Interfacial Systems

Steven J. Sibener

James Franck Institute and Department of Chemistry; GCIS E-215

The University of Chicago, 929 East 57th St., Chicago, IL 60637

Email: s-sibener@uchicago.edu

Program Scope

This new program will explore the efficacy of using molecular-level manipulation and imaging and scanning tunneling spectroscopy in conjunction with supersonic molecular beam gas-surface scattering to significantly enhance our understanding of chemical processes occurring on well-characterized interfaces including structurally-dynamic nanoscale catalytic substrates. The program will focus on the spatially-resolved emergent behavior of complex reaction systems as a function of the local geometry and density of adsorbate-substrate systems under reaction conditions. It will also focus on elucidating the emergent electronic and related reactivity characteristics of intentionally constructed single and multicomponent atom- and nanoparticle-based materials. It will further examine emergent chirality in adsorbed molecular systems where collective interactions between adsorbates and the supporting interface lead to spatial symmetry breaking. In these studies we will combine the advantages of scanning tunneling (STM) and atomic force (AFM) imaging, scanning tunneling local electronic spectroscopy (STS), and reactive supersonic and hyperthermal molecular beams to elucidate precise details of interfacial reactivity that have not been observed by more traditional surface science methods. Using the proposed methods, it will be possible to examine, for example, the differential reactivity of molecules adsorbed at different bonding sites in conjunction with how reactivity is modified by the local configuration of nearby adsorbates. At the core of this proposal resides the goal of significantly extending our understanding of interfacial atomic-scale interactions to create, with intent, molecular assemblies and materials with advanced chemical and physical properties. This ambitious program addresses several key topics in DOE Grand Challenge Science, including emergent chemical and physical properties in condensed phase systems, novel uses of chemical imaging, and the development of advanced reactivity concepts in combustion and catalysis including carbon management. The proposed activities will directly benefit national science objectives in the areas of chemical energy production and advanced materials development.

Recent Progress

This new SISGR program is presently being initiated (Fall 2009). Our vision for this new program is given in the following section on Future Plans.

Future Plans

We begin with a discussion of the first of three themes for this program, namely emergent chemical reactivity at interfaces. Recent exploratory measurements from our group have examined the partial oxidation of condensed phase arenes and unsaturated hydrocarbons on non-catalytic support substrates, and found substantial changes in the reactive potential energy barriers and the product distributions as compared with isolated molecule energetics. This raises a classic issue in the chemical sciences: how does molecular reactivity evolve when going from the single molecule level to the condensed state? Profound changes in electronic structure and

energy relaxation pathways as a function of the local molecular environment lead to such emergent changes in reaction rates and mechanism. In these studies we have seen, for example, markedly different oxidative reaction pathways, activation energies, and product channels for several small hydrocarbons as compared to known gas-phase behavior. These preliminary studies have been done on "thermodynamic ensemble averages", that is, where we have measured reaction rates using molecular beam techniques while varying coverages and temperature without the benefit of local imaging or local electronic spectroscopy. In essence, there remains a remarkably incomplete understanding of molecular reactivity at interfaces as a function of local adsorbate density (coverage), i.e., *local ensemble structure*. This has now changed. In this program we will seek, using scanning probe methods (STM with atomically resolved tunneling spectroscopy) in conjunction with scattering, to directly correlate reactivity with local adsorbate and substrate geometry, and electronic structure. This will allow us to develop a more comprehensive understanding of emergent molecular reactivity with respect to the precise geometry of locally-adsorbed reactants. Such experiments will give us a direct route for elucidating emergent chemical reactivity on a molecule-by-molecule basis, spanning lengthscales from the few molecule limit up to nanoscale systems, and, finally, macroscopic two- and three-dimensional supported films. What, for example, is the relative reactivity of isolated adsorbed molecules versus dimers, trimers, tetramers, extending to 2-dimensional vs. 3-dimensional structures? How do critical rate-determining barrier heights vary depending upon the precise relative placement of such reagents? Related and largely unanswered questions exist about how local defects influence reactivity at specific spatial locations with respect to the defect. The ability to examine, systematically, reactivity using spatially- and temporally-resolved molecular imaging during interfacial reactions will represent a powerful approach to expanding our knowledge of reactivity in condensed phase systems.

Note also that scanning probe techniques offer not only a route for *in situ* imaging, but also a very powerful means of creating local geometries of reagents before reaction *via* atomic and molecular manipulation. The opportunity to examine the differential reactivity of molecules adsorbed at different bonding sites on defined substrates in conjunction with how reactivity is modified by the local configuration of nearby adsorbates represents the next generation of surface science breakthroughs and advances in materials design, and will help bridge the gap from such studies to "Edisonian" real-world catalysis.

In essence, what we are discussing here is that the next level of interfacial studies will come from "*breaking the spatial-temporal average*". During the past few years our group has pioneered such studies, for example examining the atomic-level details of surface restructuring in real-time and real-space using elevated-temperature STM to assess local surface structure and mass transport during metallic oxidation. We have also shown, using an essential combination of imaging and molecular beams, that the $(23 \times \sqrt{3})$ reconstruction of Au(111) persists during the adsorption of self-assembling monolayers until a critical coverage occurs, and how this deconstruction proceeds systematically as a function of adsorbate coverage during oxidation. We are also extending such measurements to complex polymeric and nanoparticle-decorated interfaces. During the past two decades many catalytic, chemical dynamics, and materials growth/erosion studies have focussed on such details as molecular adsorption and reactivity at, for example, near perfect surfaces including unavoidable defects such as steps and kinks. The vast majority of these studies have considered the interface as a locally-stable entity rather than

as a dynamic structure which responds dynamically to local adsorption and chemistry. It is time to move beyond the common paradigm of considering surface structure as a static variable during chemical interactions such as catalytic reactions. Interfaces are clearly dynamic entities, especially in the limit of nanoscale structures where adsorption energetics can strongly influence local physical geometry and hence the local electronic energy landscape. Moreover, many of these prior studies attempted to extract subtle changes in the local electronic potential energy landscape arising from local ensemble structure by systematically varying adsorbate coverages – presenting a major deconvolution problem based on extracting molecular-level information from highly-averaged statistical sampling. The proposed measurements, where we will look "locally", will represent a notable extension and much more direct route to addressing such questions.

The second theme of this program will be to use local probes to interrogate and intentionally assemble atom and nanoparticle-based clusters to form extended ensembles that exhibit emergent electronic and chemical behavior. Using a recently completed liquid helium cooled cryo-STM we have been able to assess the electronic structure of quantum dots (i.e., semiconductor nanoparticles), and will now extend these experiments to include nanoparticle structures adsorbed in different local ensembles. In our initial experiments we will use the STM to locate thermodynamically-formed nanoparticle assemblies spanning single dots to the few dot limit. As part of the proposed program, we will examine, ultimately, supported nanoparticle arrays to see how these systems function as mesoscale electronic systems and catalysts, and how size modification influences reaction energetics. Moreover, chemical physics issues pertaining to adsorption and reaction energetics on nanoparticles are largely unexplored. Tremendous prior effort has been expended to understand activated chemisorption phenomena on single crystal surfaces – at this time one cannot address the shape of adsorption barriers, or even the precise active site location, for nanocatalysts; we seek to address such questions in this new program involving emergent reactivity in complex systems.

The final theme in this proposal deals with emergent chirality in molecularly adsorbed films. Ever since Pasteur first uncovered the direct correlation between the structure of a crystal and the handedness of its component molecules, researchers have been intrigued by the mechanisms of chiral separation. Scanning tunneling microscopy (STM) provides the ultimate technique for determination of the exact structure and chirality of adlayers on a substrate. The structure of an adlayer is the result of a delicate balance of lateral molecule-molecule interactions and adsorbate-substrate forces. The strength of the adsorbate-substrate interaction must be balanced such that adsorbed molecules are mobile enough to self-assemble into an organized array but greater than the adsorbate-adsorbate energy to allow two-dimensional crystallization. We will initially work with metalloporphyrin adlayers on Au(111) as such systems meet these criteria perfectly. They form well-ordered arrays on a variety of surfaces and are highly stable. In addition, they have generated much recent interest because they play an important role in biological processes such as photosynthesis and oxygen transport, which has inspired their use in various technological applications. These porphyrin arrays are especially interesting because they self-assemble at room temperature without the need for annealing, making them a likely candidate for technological applications. We will focus initially on NiTPP (nickel 2,3,7,8,12,13,17,18-octaethyl-21H,23H-porphine) and NiOEP (nickel 5,10,15,20-tetraphenyl-21H,23H-porphine) on Au(111), as well as C₆₀ decoration of these systems. These molecules are achiral when isolated in the gas phase but we find that symmetry is broken when the molecules

adsorb onto a surface in small clusters, where they form local chiral ensembles, Figure 1. Such racemic mixtures contain left- and right-handed domains for both porphyrins, indicating that the interplay of surface-adsorbate and intermolecular interactions induces chirality for the substrate-adsorbate system as a whole. Under the auspices of this program we will pursue not only general rules for the formation of racemic mixtures, but also methods of forcing (guiding) the system to form only one of the two mirror image structures. This might be achieved, for example, by the introduction of a "seed" chiral entity or the use of a high index crystal face.

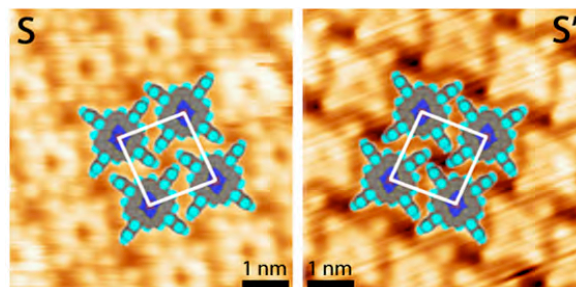


Figure 1. STM images of NiTPP/Au(111) showing two chirally distinct domain conformations with an overlaid structural model. STM tunneling setting: 1.0 nA at 1.0 V.

Our approach for all of the aforementioned activities will build on our continuing development of new and quite general molecular beam techniques for studying the kinetic mechanisms of surface chemical reactions. The proposed research will be carried out using a unique ensemble of molecular beam/scanning probe UHV instruments. In addition to already extant instruments, our group has recently completed a new liquid-He cooled STM facility which can operate over the temperature range 20K to >1000K. It has been designed to couple with a new molecular beam source that will be added under this new program, thereby giving us the ability to conduct studies with real-time/real-space resolution.

References to DOE Sponsored Research 2005-Present

This new program will be launched in Fall 2009, hence there are as of yet no publications. However, we have publications done under prior support with other DOE-BES grants, as noted below:

- Publications with DOE-BES support under a prior grant to SJS (DE-FG02-00ER15089):
 1. Applied Reaction Dynamics: Efficient Single Collision Partial Oxidation of Methane to CO on Rh(111), K.D. Gibson, M. Viste, and S. J. Sibener, *J. Chem. Phys.* **125**, 133401 (2006).
 2. O(³P) Reactions with Small Alkenes Adsorbed on Rh, Au, and Ice, K. D. Gibson and S. J. Sibener, *Surf. Sci. Letters* **600**, L76-L79 (2006).
 3. O-Atom Induced Gradual Deconstruction of the 23 x $\sqrt{3}$ Au(111) Surface, K. D. Gibson and S. J. Sibener, *J. Phys. Chem. A* **111**, 12398 -12401 (2007).
 4. Molecular Beam Induced Changes in Adsorption Behavior of NO on NiO(111)/Ni(111), B. D. Zion and S. J. Sibener, *J. Chem. Phys.* **127** 154720/1-6 (2007).
 5. UV-Photodesorption of Novel Molecular Beam Induced NO Layers on NiO(111)/Ni(111), B. D. Zion and S. J. Sibener, *J. Phys. Chem. C* **112**, 5961-5965 (2008).
- Publication with DOE-BES support in conjunction with the Center for Nanoscale Materials at Argonne National Laboratory (DE-AC02-06CH11357):
 1. Improved Hybrid Solar Cells via *In Situ* UV-Polymerization, Sanja Tepavcevic, Seth B. Darling, Nada Dimitrijevic, Tijana Rajh, and S. J. Sibener, *Small* **5**, 1776-1783 (2009).

Generation, Detection and Characterization of Gas-Phase Transition Metal Containing Molecules

Timothy C. Steimle

Department of Chemistry and Biochemistry

Arizona State University

Tempe, Arizona 85287-1604

E-mail: tsteimle@asu.edu

I. Program Scope

The objective of this experimental project is to produce simple transient, metal containing, molecules and extract from the analysis of their spectra geometric structure, force constants, permanent electric dipole moments, μ_{el} , and magnetic dipole moments, μ_m . This highly quantitative data is used to construct qualitative, molecular-orbital based, bonding models and to evaluate the quantitative predictability of electronic structure calculations performed by others. The established synergism between experiments and theory for these simple molecules guides computations, particularly those based on density functional theory, for more extended chemical systems (e.g. clusters, nanoparticles and surfaces). Studies of *3d* metal dioxides, such as TiO_2 , are being performed to provide benchmark data and to elucidate the catalytic activity of supported metal dioxide clusters. Simple PtX, RhX and IrX (X=OH, NH, CH, H, S, O, F and N) molecules are used to investigate trends in later *4d* and *5d* bonding. Studies of lanthanide and actinide monoxides are performed to glean insight into the role of *f*-orbitals and relativistic effects in bonding.

Visible and near infrared electronic spectroscopy using laser induced fluorescence (LIF) detection is being executed. Small magnetic (Zeeman) and electric (Stark) field induced shifts in the spectra are analyzed to extract experimental values for μ_m and μ_{el} , respectively. Molecular beams of the transition metal containing radicals are produced using either a pulsed laser ablated/reagent supersonic expanding gas or a pulsed d.c. discharge. The molecules are generated with an internal temperature of typically 10 K to minimize spectral congestion and recorded at near the natural line width limit (typically 30 MHz) to maximize the information content.

II. Recent progress

A. Generation and Characterization of Gas-Phase TiO_2

Among the more important of the numerous technological applications of titanium dioxide is its use as a photocatalyst to degrade organic pollutants and to perform other useful chemical transformations. Last year we reported, in collaboration with Prof. J. B. Maier (U. Basel), on the first analysis of the high-resolution optical spectrum of TiO_2 , the results of which are described in publication # 9. A strong band near 18655 cm^{-1} (536 nm) was tentatively assigned as the $\tilde{A}^1B_2 \leftarrow \tilde{X}^1A_1$ (000-000) vibronic transition. The basis for the assignment included: a) the close proximity to the observed neon matrix emission (*J. Chem. Phys.* 1971, **75**, 3243) and the photoelectron spectrum of TiO_2^- (*J. Chem. Phys.* 1997, **107**, 8221); b) the determined ground state parameters match those derived from the analysis of the pure rotational spectrum (*Ap J.* 2008, **676**, 1267); c) the observation of only a symmetric progression in the dispersed fluorescence. It is, however, difficult to explain the presence of intense bands to the red of the 536 nm band seen in the Basel group's mass-selected REMPI spectrum (**Figure 1**). Furthermore, it might be expected that the $\tilde{A}^1B_2 \leftarrow \tilde{X}^1A_1$ (000-000) vibronic transition would be weaker than the 536 nm band due to the expected small Franck-Condon factor. Possible explanations for these REMPI features include that they are: a) $\tilde{a}^3B_2 \leftarrow \tilde{X}^1A_1$ transitions; b) transitions involving linear O=Ti=O; c) hot bands of the $\tilde{A}^1B_2 \leftarrow \tilde{X}^1A_1$ system.

Recently we recorded the low-resolution LIF spectrum in the region from 18100 cm^{-1} to 18900 cm^{-1} (**Figure 1**). The agreement with the mass-selected REMPI spectrum eliminates the

possibility that the unexplained REMPI spectral features are due to hot bands. High-resolution LIF spectra of bands near 18411 cm^{-1} (marked as “♥”) and 18465 cm^{-1} (marked as “♦”) were also recorded (Figure 2). The high-resolution LIF spectra of the “♦” and “♥” bands are radically different from that of the previously analyzed (Publ. #9) band. Combination/differences in the “♦” and “♥” bands revealed that these bands do not have the $\tilde{X}^1A_1(000)$ state as the lower energy terminus, eliminating the possibility that they are $\tilde{a}^3B_2 \leftarrow \tilde{X}^1A_1(v_1 v_2 v_3 - 000)$ transitions. Interestingly, the features of the “♥” do not Stark shift suggesting that the carrier is linear O=Ti=O.

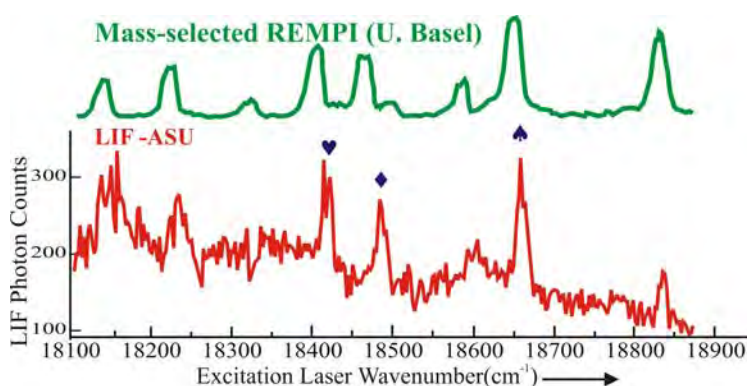


Figure 1. The low-resolution LIF and mass-selected REMPI spectra of TiO_2 . The band system marked “♥” has been assigned as the $\tilde{a}^3B_2(0,0,0) \leftarrow \tilde{X}^1A_1(0,0,0)$ transition and rotationally analyzed. The bands marked “♦” and “♥” have been recorded at high-resolution and selected lines recorded in the presence of an electric field.

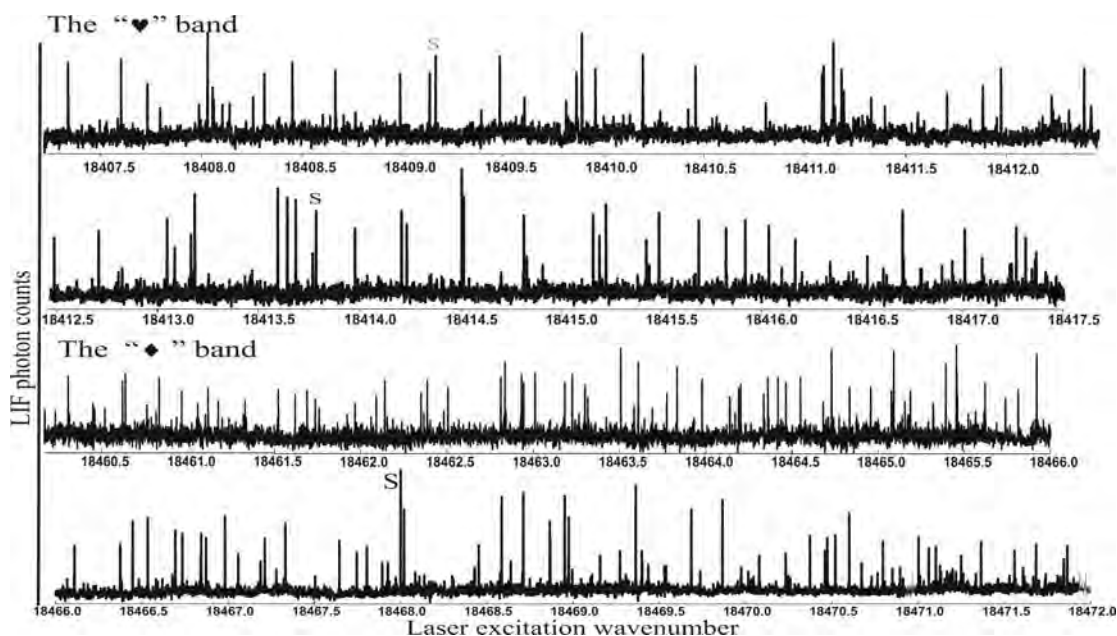


Figure 2. The high resolution LIF spectra of the “♦” and “♥” (Figure 1) bands of TiO_2 . The “♦” band has a considerably higher density of lines and a less recognizable branch structure than the “♥” band. The Stark effect in the lines marked with “S” was determined. Lines in the “♥” band did not exhibit a Stark effect, suggestive of a linear O-Ti-O structure.

B. Properties of IrF

Halogen containing iridium complexes are highly active catalysts for which the variation of the halide produces large changes in the catalytic activity. Prediction of the observed changes, which are electronic and not steric, requires highly accurate theoretical methods.

Simple iridium mono-halides, IrX, are excellent prototypes for investigating the predictive power of computational methodologies, since their molecular properties can be measured with high accuracy. Recently, we have begun a study of the properties of IrF. A portion of the $A^3\Phi_4-X^3\Phi_4(1,0)$ band of ^{193}IrF near the $Q(6)$ branch feature is presented in **Figure 3**. Analysis of the magnetic hyperfine structure, which exhibits an unusually large ^{19}F contribution, is being performed.

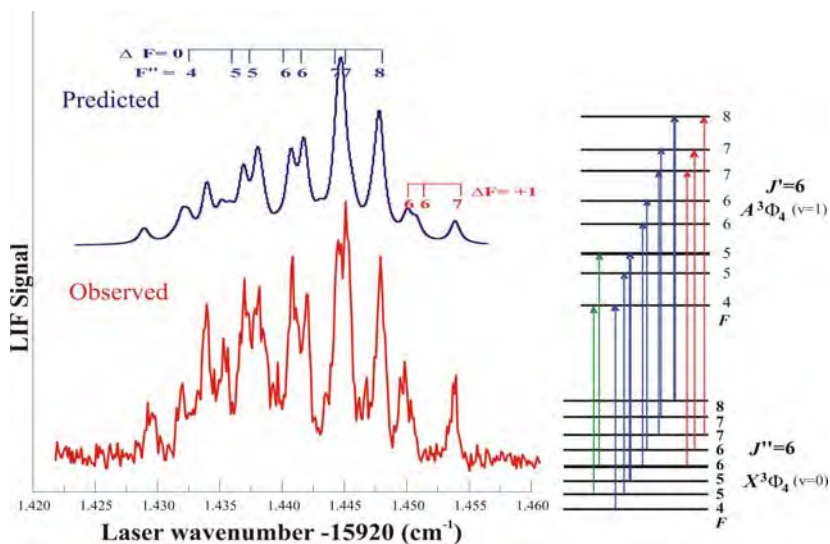


Figure 3 . The high resolution LIF spectrum of the $Q(6)$ branch feature of the $A^3\Phi_4-X^3\Phi_4(1,0)$ band of ^{193}IrF . The spectrum complex because both the $^{193}\text{Ir}(I=3/2)$ and $^{19}\text{F}(I=1/2)$ magnetic hyperfine splitting are large. The predicted spectrum was obtained using our preliminarily determined parameters.

C. Lanthanide and actinide monoxides

Experiments involving the actinides are particularly challenging. Fortunately, it may be possible to gain insight into their chemistry from the properties of the isovalent lanthanides. For example, the μ_{el} value for the ground state of UO was measured as 3.363(26) D and we argued (*J. Chem Phys.* **125** 204314 (2006)) that this should be nearly identical to that of isovalent NdO. Indeed, our recently measured μ_{el} value for the X4 state of NdO is 3.369(13)D(Publ. #8) which is very close to our empirical estimate. Very recently (Publ. # 10 and 11) we recorded and analyzed the optical Stark spectra of PrO and CeO. The determined μ_{el} values are 3.119(8), 3.115(7) and 2.119(8) D for the X_1, X_2, X_3 and $[16.5]_2$ states of CeO, respectively, and 3.01(6) D and 4.72(5) D for the X_2 ($\Omega = 4.5$) and $[18.1]$ ($\Omega = 5.5$) states, of PrO, respectively. A plot of the experimentally derived ground state μ_{el} values for the lanthanide monoxides (**Figure 4**) reveals a smooth trend across the series which can be fit to a 2nd order polynomial as shown in Figure 4. Given that μ_{el} for UO is nearly identical to that of NdO, the same polynomial can be used to predict μ_{el} values for the entire actinide monoxide series.

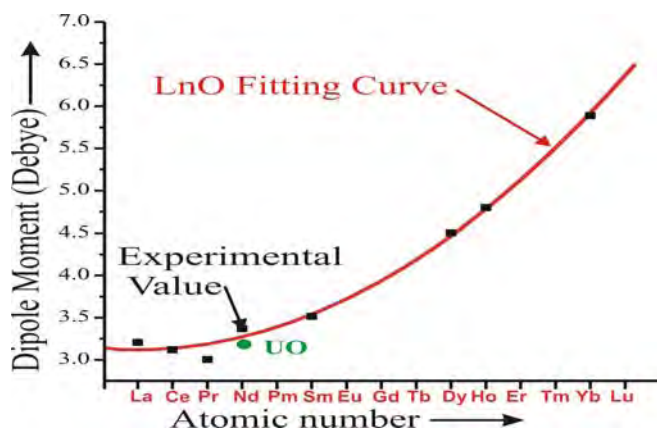


Figure 4 . A plot of the experimentally determined electric dipole moment for the lanthanide monoxide series. The solid line is a fit of our experimentally determined values to a 2nd order polynomial. The determined value for UO is nearly coincident with that of NdO.

III. Future Plans

A. TiO₂

An analysis of the rotational fine structure of the “♦” and “♥” band systems will be undertaken. The resulting rotational constants will be used to determine geometric structure. This should confirm our tentative assignment of linear O-Ti-O as the carrier of the “♥” band. Optical Zeeman spectroscopy of the “♦” and “♥” band systems will also be performed to determine if the electronic states involved are paramagnetic. Bands associated with $\tilde{a}^3B_2 \leftarrow \tilde{X}^1A_1$ transition are predicted to be in the visible regions. Recently we have initiated dispersed LIF measurements of the “♦” and “♥” band, which will characterize the vibrational frequencies of the lower state associated with the “♦” and “♥” bands. Finally, we are collaborating with Prof. John Stanton to predict the nature of the electronic spectrum.

B. LIF studies of late transition of metal containing molecules.

The initiated analysis of the field-free spectrum of IrF will be completed and the optical Stark spectrum recorded and analyzed. Low-resolution LIF scans of the products of ablated Pt, Ir, Pd and Rh with CH₃CH and CH₃OH will be executed in attempts to detect MCN and MOH molecules. Many of the late transition metal (Rh, Pd, Pt, and Ir) containing radicals are proposed to have intense electronic transitions in the near uv (370-460 nm) spectral region. We will use our recently procured external cavity doubler with our cw-dye and Ti:Sapphire lasers in attempts to detect PdC and PdCH.

Publications of DOE sponsored research - 2006-present:

1. “The permanent electric dipole moment and hyperfine interaction in Ruthenium Monofluoride, RuF.” T. C. Steimle, W. L. Virgo and T. Ma, J. Chem. Phys. **124**, 024309-7 (2006).
2. “High Resolution Laser Induced Fluorescence Spectroscopy of the [18.8] $^3\Phi_i - X^3\Phi_i$ (0,0) Band of Cobalt Monofluoride” T.C. Steimle, T.Ma, A.G. Adam, W. D. Hamilton and A. J. Merer, J. Chem. Phys. **125**, 064302-1-064302-9 (2006).
3. “The permanent electric dipole moment and magnetic *g*-factors of uranium monoxide, UO” Michael. C. Heaven, Vasily Goncharon, Timothy C. Steimle, Tongmei Ma, Colan Linton J. Chem Phys. **125** 204314/1-20431/11 (2006).
4. “A Molecular Beam Optical Stark Study of the [15.8] and [16.0] $^2\Pi_{1/2} - X^2\Sigma^+$ (0,0) Band Systems of Rhodium Monoxide, RhO.” Jamie Gengler, Tongmei M, Allan G. Adam, and Timothy C. Steimle, J. Chem. Phys. **126** 134304-11 (2007).
5. “A Molecular Beam Optical Stark Study of Rhodium Mononitride, RhN” Tongmei Ma, Jamie Gengler, Zhong Wang, Hailing Wang and T.C. Steimle, J. Chem. Phys. J.Chem. Phys. J. Chem. Phys. **126** 244312-8 (2007).
6. “A Molecular Beam Optical Stark Study of the [18.1] $^2\Pi_{1/2} - X^4\Sigma_{1/2}^-$, RhS” Tongmei Ma, Hailing Wang and T.C. Steimle, J. Chem. Phys. **127**, 124311-1/6 (2007).
7. “Optical Stark spectroscopy of molybdenum carbide, MoC” Wilton L. Virgo and Timothy C. Steimle, J. Chem. Phys. J. Chem. Phys. **127** 124302-1/6 (2007).
8. “The permanent electric dipole moment and magnetic *g_e*-factors of neodymium monoxide (NdO)” Colin Linton, Tonmei Ma, Hailing Wang and Timothy C. Steimle J.Chem. Phys. 124310/1-5(2008).
9. “Characterization of the $X^1A_1 - A^1B_2$ electronic state of titanium dioxide, TiO₂” Hailing Wang, T. C. Steimle, C. Apetrei and J. P. Maier, Phys. Chem. Chem. Phys. **11** 2649-2656 (2009).
10. “The permanent electric dipole moment of cerium monoxide, CeO” C. Linton, J. Chen, and T.C. Steimle, J. Phys. Chem. (accepted 2009 ; available on line)
11. “The Permanent Electric Dipole Moments and Magnetic *g_e*-Factors of Praseodymium Monoxide (PrO). “ Journal of Physical Chemistry(accepted 2009; available online)

From Charge Transfer to Coupled Charge Transport: A Multiscale Approach for Complex Systems

Jessica M.J. Swanson, jswanson@hec.utah.edu, Center for Biophysical Modeling & Simulation, University of Utah, Department of Chemistry, 315 S. 1400 E. RM 2020, Salt Lake City, UT 84112

The coupled phenomena of electron transfer; proton transport, and redox reactions play a central role in most areas of energy conversion and storage, from biomolecular energy transduction and natural water splitting mechanisms to fuel cells and biomimetic platforms for artificial photosynthesis and photocatalysis. In this work the role of charge transfer in the structure and dynamics of the hydrated proton will be characterized with an *ab initio* energy decomposition analysis. This approach is used to decompose the interactions between H_3O^+ and the surrounding water molecules into physically meaningful components. In conjunction with data from molecular dynamics simulations, it will be shown that the excess proton in bulk water exhibits 1) a large degree of charge transfer between 4 to 10 water molecules, 2) a charge defect that is intrinsically dynamic, 3) dynamic signatures of charge transfer behavior that can be related to IR spectra, and 4) very little resemblance to the classical hydronium ion. The significance of delocalization of the protonic charge defect in condensed phase and biomolecular systems will be discussed.

Additionally, our research proposal on Coupled Charge Transport Molecular Dynamics (CCT-MD), which was recently co-funded by the Theoretical and Computational Chemistry and the Solar Photochemistry Programs, will be described. The aim of this research is to develop a multiscale computational method that dynamically describes electron transfer coupled to proton transport in complex systems and to use this method to gain physical insights into redox-coupled charge transport mechanisms, particularly those most relevant to the conversion of solar energy into storable fuels.

Developing CCT-MD will require incorporating proton transport, which can occur over long distances and inherently involves electronic delocalization over many molecules, electron transfer (both adiabatic and non-adiabatic), and the dynamic motions of condensed-phase aqueous and molecular systems into a single self-consistent multiscale framework. Moreover, it will require treating quantum phenomena which occur on the *femto-* to *pico*-second timescale, within hundred to million atom molecular and biomolecular systems over the *nano-* to *milli*-second time scales. This is a multiscale challenge in both the size and time domains. Overcoming this challenge will require the incorporation of the quantum phenomena into classical simulations, treating nonadiabatic electronic transitions, sampling rare events, and using multiscale approaches to reduce system size and complexity. The primary target of this research will be further characterizing the redox leveling (i.e., charge-balancing) that enables multi-electron chemical reactions, such as water splitting, and providing information that will guide the development of technologies that convert solar energy into storable fuels.

Understanding Nanoscale Confinement Effects in Solvent-Driven Chemical Reactions

Ward H. Thompson

Department of Chemistry, University of Kansas, Lawrence, KS 66045

Email: *wthompson@ku.edu*

Program Scope

It is now possible to synthesize nanostructured porous materials with a tremendous variety of properties including sol-gels, zeolites, organic and inorganic supramolecular assemblies, reverse micelles, vesicles, and even proteins. The interest in these materials derives from their potential for carrying out useful chemistry (*e.g.*, as microporous and mesoporous catalysts with critical specificity, fuel cell electrodes and membranes, molecular sieves, and chemical sensors) and for understanding the chemistry in similar systems found in nature. Despite the advances in synthetic techniques, our understanding of chemistry in solvents confined in nanoscale cavities and pores is still relatively limited. Ultimately, one would like to design nanostructured materials adapted for specific chemical purposes, *e.g.*, catalysis or sensing, by controlling the cavity/pore size, geometry, and surface chemistry. To develop guidelines for this design, we must first understand how the characteristics of the confining framework affect the chemistry. Thus, the overarching question addressed by our work is *How does a chemical reaction occur differently in a nano-confined solvent than in a bulk solvent?*

Solvent-driven reactions, typically those involving charge transfer, should be most affected by confinement of the solvent. The limited number of solvent molecules, geometric constraints of the nanoscale confinement, and solvent-wall interactions can have dramatic effects on both the reaction energetics and dynamics. Our primary focus is thus on proton transfer, time-dependent fluorescence, and other processes strongly influenced by the solvent. A fundamental understanding of such solvent-driven processes in nano-confined solvents will impact many areas of chemistry and biology. The diversity among nanoscale cavities and pores (*e.g.*, in their size, shape, flexibility, and interactions with the solvent and/or reactants) makes it difficult to translate studies of one system into predictions for another. Thus, we are focusing on developing a unified understanding of chemical dynamics in the diverse set of confinement frameworks, including nanoscale silica pores of varying surface chemistry.^{1,2}

Recent Progress

Solvation Dynamics in Nanoconfined Solvents.

Solvation dynamics in nanoconfined solvents are generally marked by dramatic changes relative to the corresponding bulk solvent. In particular, long time scales not seen in the bulk

solvent – often as long as hundreds of picoseconds or several nanoseconds – are observed in the time-dependent fluorescence signal. A number of models have been proposed to explain the origin of this multi-exponential, long-time decay. However, to this point these models have been derived from simulations using atomic or diatomic model dye molecules and/or simplistic confining frameworks. Thus, a direct comparison of theoretical predictions with experimental measurements is lacking as is, by extension, a rigorous test of the models.

To address this issue, we are carrying out simulations of the time-dependent fluorescence confined within ~ 2.4 and 4.5 nm diameter hydrophilic and hydrophobic amorphous silica pores,^{1,2} beginning with the C153 dye molecule, based on a model developed by Maroncelli and co-workers,³ in ethanol. This system is similar to those used in measurements by Baumann *et al.* on C153 in ethanol confined within 2.5 and 5.0 nm sol-gel pores.⁴ In particular, we are aiming to test our own model – also based on simpler dye molecule and confining framework simulations – that attributes the long-time decays in the time-dependent fluorescence signal to diffusive movement of the dye molecule after excitation.⁵

Our preliminary results in ~ 2.4 nm pores indicate that our model is in reasonable agreement with the experimental measurements of Baumann *et al.* The key difference is that faster solvation dynamics is observed in the simulations for both bulk and nanoconfined ethanol. In the case of C153 in ethanol no additional time scales were observed experimentally in the solvation dynamics upon nanoscale confinement⁴ and our simulations find the same result. This suggests a two-state model in which the longer solvation time scales are attributed to surface ethanol molecules while the bulk time scales (arising from molecules away from the surface) survive is not an accurate description. On the other hand, it does not speak as well to our proposed model as we find little solute diffusion after excitation as the position distributions for the solute ground and excited states are similar. This appears to be due to the moderate relative increase in dipole moment from the ground to the excited state; preliminary simulations suggest that other molecules with different ground and excited state charge distributions will act otherwise. We are currently working to understand the interactions involved to develop more general predictions of when and why additional long-time decay would be expected in solvation dynamics of nanoconfined liquids.

Finally, it is important to point out that solvation dynamics in nanoconfined liquids can be an important testing ground for various theories and approximations. In particular, we have investigated the role of entropy in determining solute positions,⁶ confinement effects on conformational dynamics and equilibria,^{2,7} the validity of linear response-type approximations,^{8,9} and Smoluchowski equation descriptions of the solute and solvation dynamics.^{10,11}

Proton Transfer.

We have investigated a number of properties of a model intramolecular phenol-amine proton transfer system in a CH_3Cl solvent confined in a smooth, hydrophobic spherical cavity. We have previously used Monte Carlo and mixed quantum-classical molecular dy-

namics simulations to investigate complex position distributions,¹² free energy curves,¹² vibrationally adiabatic proton transfer reaction dynamics including identification of multiple reaction mechanisms,¹³ and infrared spectra of the proton transfer reaction complex.¹⁴

More recently, we have implemented vibrationally nonadiabatic reactive flux calculations using a classical mapping approach to more accurately describe the proton tunneling in the calculation of the reaction rate constants. The rate constants for the model intramolecular phenol-amine proton transfer system in a CH₃Cl solvent confined in a smooth, hydrophobic spherical cavity have been calculated. These simulations provide insight into the effect of nonadiabatic transitions on the reaction mechanism in nanoconfined solvents and can be straightforwardly extended to more realistic systems.

We have also demonstrated how umbrella sampling can be applied to the vibrational frequency of the proton motion in a proton transfer reaction complex. It is well established that the proton vibrational frequency decreases towards the transition state and thus, this provides a straightforward way to identify transition state configurations without an assumption of a reaction coordinate. It may also permit the construction of the infrared spectrum of proton transfer reaction complexes from purely equilibrium simulations independent of the barrier height.¹⁴

What Drives Changes in Structure and Dynamics upon Nanonconfinement?

We are investigating the relative effects of electrostatics, hydrogen bonding, and hydrophobic effects by comparing the properties of water, methanol, and ethanol in identical model silica pores. In particular, we are determining the equilibrium densities *via* grand canonical Monte Carlo calculations and examining the structure and dynamics using molecular dynamics simulations for these three liquids in nanoscale silica pores of diameter ~ 2.4 nm and varying surface chemistry (hydrophilic and hydrophobic). Preliminary results indicate interesting effects on the reorientation dynamics of these liquids confined in OH-terminated silica pores including multiple additional time scales (relative to the bulk liquid) that can be attributed to a combination of packing effects, electrostatic interactions, and microporosity in the amorphous silica interface.

References

- [1] †T.S. Gulmen and W.H. Thompson, “Model Silica Pores with Controllable Surface Chemistry for Molecular Dynamics Simulations” in *Dynamics in Small Confining Systems VIII*, edited by J.T. Fourkas, P. Levitz, R. Overney, M. Urbakh (Mater. Res. Soc. Symp. Proc. **899E**, Warrendale, PA, 2005), 0899-N06-05.
- [2] †T.S. Gulmen and W.H. Thompson, “Testing the Two-State Model of Nanoconfined Liquids: The Conformational Equilibrium of Ethylene Glycol in Amorphous Silica Pores,” *Langmuir* **22**, 10919-10923 (2006).

- [3] N. Kometani, S. Arzhantsev, and M. Maroncelli, *J. Phys. Chem. A* **110**, 3405-3413 (2006).
- [4] R. Baumann, C. Ferrante, E. Kneuper, F.-W. Deeg, and C. Bräuchle, *J. Phys. Chem. A* **107**, 2422-2430 (2003).
- [5] †W.H. Thompson, *J. Chem. Phys.* **120**, 8125-8133 (2004). “Simulations of Time-Dependent Fluorescence in Nano-Confined Solvents”
- [6] †K.R. Mitchell-Koch and W.H. Thompson, *J. Phys. Chem. C* **111**, 11991-12001 (2007). “How Important is Entropy in Determining the Position-Dependent Free Energy of a Solute in a Nanoconfined Solvent?”
- [7] †J.A. Gomez, A.K. Tucker, T.D. Shepherd, and W.H. Thompson, *J. Phys. Chem. B* **109**, 17479-17487 (2005). “Conformational Free Energies of 1,2-Dichloroethane in Nanoconfined Methanol”
- [8] †B.B. Laird and W.H. Thompson, (in preparation). “Time-Dependent Fluorescence in Nanoconfined Solvents: Linear Response Approximations and Gaussian Statistics”
- [9] †B.B. Laird and W.H. Thompson, *J. Chem. Phys.*, **126**, 211104 (2007). “On the Connection between Gaussian Statistics and Excited-State Linear Response for Time-Dependent Fluorescence,”
- [10] †X. Feng and W.H. Thompson, *Journal of Physical Chemistry C* **111**, 18060-18072 (2007). “Smoluchowski Equation Description of Solute Diffusion Dynamics and Time-dependent Fluorescence in Nanoconfined Solvents”
- [11] †X. Feng and W.H. Thompson, (to be submitted). “Time-dependent Fluorescence in Nanoconfined Solvents. A Smoluchowski Equation Model Study”
- [12] †S. Li and W.H. Thompson, *J. Phys. Chem. B* **109**, 4941-4946 (2005). “Proton Transfer in Nano-confined Polar Solvents. I. Free Energies and Solute Position ”
- [13] †W.H. Thompson, *J. Phys. Chem. B* **109**, 18201-18208 (2005). “Proton Transfer in Nano-confined Polar Solvents. II. Adiabatic Proton Transfer Dynamics”
- [14] †K.R. Mitchell-Koch and W.H. Thompson, *J. Phys. Chem. B* **112**, 7448-7459 (2008). “Infrared Spectroscopy of a Model Phenol-Amine Proton Transfer Complex in Nanoconfined CH₃Cl”

†DOE-sponsored publication.

Structural Dynamics in Complex Liquids Studied with Multidimensional Vibrational Spectroscopy

Andrei Tokmakoff

*Department of Chemistry, Massachusetts Institute of Technology, Cambridge, MA 02139
E-mail: tokmakof@MIT.edu*

Water is a unique liquid due to the fact that it can form up to four hydrogen bonds, creating a structured tetrahedral network of molecules that evolves on ultrafast time-scales as hydrogen bonds break and form. It is the fluctuations of this network that allow water to rapidly solvate nascent charge and to participate in chemical reactions. Moreover, it is predicted that the breakage and rearrangement of hydrogen bonds plays a major role in charge transport in water and is an intrinsic element of proton and hydroxide transport. The goal of our research is to develop ultrafast spectroscopic probes that are sensitive to the fluctuations of water's hydrogen bonding network and to use these probes to obtain a mechanistic understanding of how the rearrangements of water molecules influence aqueous charge transport and reactivity.

As a probe of water's structure, we make use of ultrafast two dimensional infrared spectroscopy (2D IR) of the OH stretch of a solution of dilute HOD in D₂O or of HOD in H₂O. This particular isotopic combination of water is well suited for studies investigating the fluctuations of water's hydrogen bonding network since the OH absorption lineshape is broadened due to distribution of hydrogen bonding environments present in the liquid. Molecules that participate in strong hydrogen bonds absorb at lower frequencies than molecules in strained or broken hydrogen bonds. Thus, if we can excite a water molecule at an initial frequency and then watching how that frequency changes as a function of time we can gain direct information on how water's time dependent structure. 2D IR spectroscopy provides us with this ability to track how different hydrogen bonding environments interconvert over time. A 2D spectrum correlates how a molecule excited at an initial frequency evolves to a final frequency after a given waiting time. By varying the waiting time, we can follow how molecules initially in strong or weak hydrogen bonds exchange environments.

Our work during the past year can be divided into three topics: (1) Reorientational dynamics of hydrogen bonds in water, (2) Temperature-dependent hydrogen bond dynamics in water, and (3) the dynamics of aqueous hydroxide ion transport in water.

Our previous work has suggested that hydrogen bonds in water rearrange in concerted switching events that include large angle excursions in hydrogen bond alignment, and for which the transition state has bifurcated hydrogen bond character. To test the predictions of the orientational dynamics during switching we are performing polarization resolved nonlinear experiments. We have recently measured 2D IR spectra of HOD in H₂O and HOD in D₂O with different polarizations of the exciting fields and using that to calculate a two dimensional anisotropy. This measurement is analogous to the anisotropy decay which can be calculated from 1D pump-probe techniques which report on the reorientation of molecules as a function of time. The advantage of measuring a 2D anisotropy decay over a 1D decay is the ability to correlate both the initial and final frequencies with the degree of rotation of the HOD molecule. Thus, we can determine if a molecule initially at high frequency (weak hydrogen bonding) that moves to lower frequency (strong hydrogen bonding) undergoes a different degree of reorientation than a molecule that remains on either side of the lineshape. Preliminary results of this measurement suggest that molecules initially in strained or broken hydrogen bonds undergo a significant degree of reorientation within 100 fs whereas molecules that remain in strong hydrogen bonds retain memory of their initial orientation but lose this memory if they move toward high frequency. These results are qualitatively similar to those obtained from molecular dynamics simulations and

support the conclusion that the exchange of molecules from one side of the OH lineshape to the other involves molecular reorientation.

In addition, our studies of concerted hydrogen bond rearrangements make certain predictions about the temperature-dependence of hydrogen bond rearrangement dynamics in the liquid. We have recently performed temperature-dependent experiments on HOD in H₂O aimed at describing these dynamics: pump-probe measurements of vibrational lifetime, 2D IR lineshape measurements of the OD frequency dynamics, and pump-probe and 2D anisotropy measurements of reorientational motions. We are currently performing a self-consistent analysis of all experiments to unravel the underlying dynamics.

Over the course of the last year, we have also performed studies to reveal how water participates in the dynamics of hydroxide ion transport. This ion undergoes anomalously fast diffusion due to the ability to accept a proton from neighboring water molecules leading to the translocation of the ion. Simulations have suggested that hydrogen bond rearrangements play a strong role in guiding proton transfer processes involving these ions. However, experimental work that is able to directly capture proton motion is lacking due in large part to the difficulty of finding probes that can measure the timescales predicted for the transfer, which range from 10s of femtoseconds to picoseconds.

We have made 2D IR measurements of solutions of dilute HOD in concentrated NaOD:D₂O solution. Upon the addition of NaOD to HOD:D₂O solution, two new spectral features appear, a new peak at high frequency due to the OH⁻ stretch and a broad shoulder that extends down to very low frequency due to HOD molecules hydrogen bonded to OD⁻ ions. Pump probe and transient grating measurements find that as the NaOD concentration increases, a second vibrational relaxation component appears with an extremely fast timescale of 115 fs. 3PEPS experiments show a large offset with increasing NaOD concentration indicating that long lived static inhomogeneity is present in these solutions. This agrees with the increase in solution viscosity upon addition of NaOD.

Most interestingly though, is the presence of large offdiagonal intensity on the low frequency side of the 2D IR lineshape that disappears on a ~100 fs timescale, which roughly matches the fast decay timescale observed in the pump probe measurements. At longer waiting times a new peak in the 2D spectra which may indicate chemical exchange between OH⁻ and HOD molecules grows in on a ~2ps timescale. In order to better understand these features, we have modeled our experiments using an EVB (empirical valence bond) molecular dynamics simulation model of aqueous sodium hydroxide developed by Todd Martinez's group at the University of Illinois Urbana-Champaign. In order to calculate spectra, we have developed a DFT based electrostatic frequency map which we can use to determine the "instantaneous" OH frequency of a given OH bond for a static configuration of the simulation. We find that in configurations where a proton is significantly shared between two water molecules, all of the transitions within the proton stretching potential undergo significant red shifts, and in particular the OH stretch overtone ($\nu = 2 \leftarrow \nu = 0$) tunes into our experimentally accessible bandwidth. Thus, the rapid loss of intensity in the 2D and pump probe measurements is due to direct excitation of the overtone transition for configurations corresponding to nearly shared protons. As the proton moves to one side of the complex, stabilizing a water molecule, the overtone will blue shift out of our bandwidth, leading to the relaxation we see in the 2D and pump probe spectra.

DOE Supported Publications (2005-2009)

1. "Local hydrogen bonding dynamics and collective reorganization in water: Ultrafast IR spectroscopy of HOD/D₂O," C. J. Fecko, J. J. Loparo, S. T. Roberts and A. Tokmakoff, *Journal of Chemical Physics*, **122** (2005) 054506.

2. "Amide I vibrational dynamics of N-methylacetamide in polar solvents: The role of electrostatic interactions," M. F. DeCamp, L. P. DeFlores, J. M. McCracken, A. Tokmakoff, K. Kwac, and M. Cho, *Journal of Physical Chemistry B*, **109** (2005) 11016.
3. "Upconversion multichannel infrared spectrometer," M. F. DeCamp and A. Tokmakoff, *Optics Letters*, **30** (2005) 1818.
4. "Electric field fluctuations drive vibrational dephasing in water," J. D. Eaves, A. Tokmakoff, and P. L. Geissler, *Journal of Physical Chemistry A*, **109** (2005) 9424.
5. "Hydrogen bonds in liquid water are broken only fleetingly," J. D. Eaves, J. J. Loparo, C. J. Fecko, S. T. Roberts, A. Tokmakoff and P. L. Geissler, *Proceedings of the National Academy of Sciences, USA*, **102** (2005) 13019.
6. "Polarizable molecules in the vibrational spectroscopy of water," E. Harder, J. D. Eaves, A. Tokmakoff and B. J. Berne, *Proceedings of the National Academy of Sciences, USA*, **102** (2005) 11611.
7. "A study of phonon-assisted exciton relaxation dynamics for a (6,5) enriched DNA-wrapped single walled carbon nanotubes sample," S. G. Chou, M. F. DeCamp, J. Jiang, Ge. G. Samsonidze, E. B. Barros, F. Plentz, A. Jorio, M. Zheng, G. B. Onoa, E. D. Semke, A. Tokmakoff, R. Saito, G. Dresselhaus, M. S. Dresselhaus, *Physical Review B*, **72** (2005) 195415.
8. "Single-shot two-dimensional spectrometer," M. F. DeCamp and A. Tokmakoff, *Optics Letters*, **31** (2006) 113.
9. "Spectral signatures of heterogeneous protein ensembles revealed by MD simulations of 2DIR spectra," Z. Ganim and A. Tokmakoff, *Biophysical Journal*, **91** (2006) 2636.
10. "Multidimensional infrared spectroscopy of water. I. Vibrational dynamics in 2D IR lineshapes," J. J. Loparo, S. T. Roberts, and A. Tokmakoff, *Journal of Chemical Physics*, **125** (2006) 194521.
11. "Multidimensional infrared spectroscopy of water. II. Hydrogen bond switching dynamics," J. J. Loparo, S. T. Roberts, and A. Tokmakoff, *Journal of Chemical Physics*, **125** (2006) 194522.
12. "Characterization of spectral diffusion from two-dimensional lineshapes," S. T. Roberts, J. J. Loparo, and A. Tokmakoff, *Journal of Chemical Physics*, **125** (2006) 084502.
13. "2D IR spectroscopy of hydrogen bond switching in liquid water," J. J. Loparo, S. T. Roberts, and A. Tokmakoff, in *Ultrafast Phenomena XV*, ed. by P. Corkum, D. Jonas, R. J. D. Miller, and A.M. Weiner (Springer, Berlin, 2007), p. 341.
14. "Single-shot two-dimensional infrared spectroscopy," M. F. DeCamp, L. P. DeFlores, K. C. Jones, and A. Tokmakoff, *Optics Express*, **15** (2007) 233.
15. "Are water simulation models consistent with steady-state and ultrafast vibrational spectroscopy experiments?" J. R. Schmidt, S. T. Roberts, J. J. Loparo, A. Tokmakoff, M. D. Fayer, and J. L. Skinner, *Chemical Physics*, **341** (2007) 143.
16. "Variation of the transition dipole moment across the OH stretching band of water," J. J. Loparo, S. T. Roberts, R. A. Nicodemus and A. Tokmakoff, *Chemical Physics*, **341** (2007) 218.
17. "Infrared spectroscopy of tritiated water," R. A. Nicodemus and A. Tokmakoff, *Chemical Physics Letters*, **449** (2007) 130.
18. "Shining light onto water's rapidly evolving structure," A. Tokmakoff, *Science*, **317** (2007) 54.

19. "Two-dimensional Fourier transform spectroscopy in the pump-probe geometry," L. P. DeFlores, R. A. Nicodemus, and A. Tokmakoff, *Optics Letters*, **32** (2007) 2966.
20. "Transient 2D IR spectroscopy of ubiquitin unfolding dynamics," H. S. Chung, Z. Ganim, K. C. Jones, and A. Tokmakoff, *Proceedings of the National Academy of Sciences, USA*, **104** (2007) 14237.
21. "Amide I two-dimensional infrared spectroscopy of proteins," Z. Ganim, H. S. Chung, A. W. Smith, L. P. DeFlores, K. C. Jones, and A. Tokmakoff, *Accounts of Chemical Research*, **41** (2008) 432.
22. "The dynamics of aqueous hydroxide ion transport probed via ultrafast vibrational echo experiments" S.T. Roberts, P. B. Petersen, K. Ramasesha, and A. Tokmakoff in *Ultrafast Phenomena XVI*, (Springer, Berlin, in press).
23. "Ultrafast N-H vibrational dynamics of cyclic doubly hydrogen-bonded homo- and heterodimers," Poul B. Petersen, Sean T. Roberts, Krupa Ramasesha, Daniel G. Nocera, Andrei Tokmakoff, *Journal of Physical Chemistry B*, **112** (2008) 13167–13171..
24. "Amide I'-II' 2D IR spectroscopy provides enhanced protein secondary structural sensitivity," Lauren P. DeFlores, Ziad Ganim, Rebecca A. Nicodemus, and Andrei Tokmakoff, *Journal of the American Chemical Society*, 131 (2009) 3385–3391.
25. "Observation of a Zundel-like transition state during proton transfer in aqueous hydroxide solutions," Sean T. Roberts, Poul B. Petersen, Krupa Ramasesha, Andrei Tokmakoff, Ivan S. Ufimtsev, and Todd J. Martinez, *Proceedings of the National Academy of Sciences, USA*, 106 (2009) 15154–15159.
26. "Structural Rearrangements in Water Viewed Through Two-Dimensional Infrared Spectroscopy," Sean T. Roberts, Krupa Ramasesha, and Andrei Tokmakoff, *Accounts of Chemical Research*, in press.

The Role of Electronic Excitations on Chemical Reaction Dynamics at Metal, Semiconductor and Nanoparticle Surfaces

John C. Tully

Department of Chemistry, Yale University, 225 Prospect Street,

P. O. Box 208107, New Haven, CT, 06520-8107 USA

john.tully@yale.edu

Program Scope

Achieving enhanced control of the rates and molecular pathways of chemical reactions at the surfaces of metals, semiconductors and nanoparticles will have impact in many fields of science and engineering, including heterogeneous catalysis, photocatalysis, materials processing, corrosion, solar energy conversion and nanoscience. However, our current atomic-level understanding of chemical reactions at surfaces is incomplete and flawed. Conventional theories of chemical dynamics are based on the Born-Oppenheimer separation of electronic and nuclear motion. Even when describing dynamics at metal surfaces where it has long been recognized that the Born-Oppenheimer approximation is not valid, the conventional approach is still used, perhaps patched up by introducing friction to account for electron-hole pair excitations or curve crossings to account for electron transfer. There is growing experimental evidence that this is not adequate. We are examining the influence of electronic transitions on chemical reaction dynamics at metal and semiconductor surfaces. Our program includes the development of new theoretical and computational methods for nonadiabatic dynamics at surfaces, as well as the application of these methods to specific chemical systems of experimental attention. Our objective is not only to advance our ability to simulate experiments quantitatively, but also to construct the theoretical framework for understanding the underlying factors that govern molecular motion at surfaces and to aid in the conception of new experiments that most directly probe the critical issues.

Recent Progress

Independent Electron Surface Hopping

In the past year of the grant, we have focused on further developing, testing and applying the Independent Electron Surface Hopping (IESH) approach to nonadiabatic dynamics at metal surfaces, using the NO/Au system as a benchmark. The detailed molecular beam experiments of the scattering of vibrationally excited NO molecules from a Au(111) crystal surface by the Wodtke group provide a wealth of quantitative data against which to compare.

Our first step towards this goal was described in our 2008 CPIMS abstract, development of an efficient method for representing a continuous spectrum by discrete states. The second step, also described in the 2008 abstract, was the construction of an electronic Hamiltonian to accurately represent the interactions of the NO molecule with the gold surface, including neutral and negative-ion configurations of NO and a sufficiently large number of levels to adequately represent the electron-hole pair continuum of metallic conduction electron states. This is essential to properly describe electron-hole-pair excitations as required to include electronic friction effects, almost certainly an important source of nonadiabatic behavior. Following the Newns-Anderson

model, we represent the total wave function by a single determinant in which each one-electron orbital is a time-varying linear combination of the diabatic (local adsorbate plus discretized conduction band) electronic states. For our calculations on the NO-Au system, typically 20 electrons distributed among 41 one-electron states were found to satisfactorily represent the electronic space. We note that there are $>10^{11}$ permutations of 20 electrons in 41 orbitals; i.e., we need to carry out surface hopping among 10^{11} adiabatic states.

The third component of our strategy is realistic simulation of the nonadiabatic scattering of the NO molecule from the Au(111) surface, as governed by the enormous numbers of electronic potential energy surfaces (PESs) encompassed in the Newns-Anderson Hamiltonian. We have applied a variation of surface hopping, a stochastic procedure in which trajectories move on a single adiabatic PES, subject to instantaneous transitions to different PESs, with hopping probabilities governed by the evolving amplitudes of each electronic state. This appears to be a daunting task in view of the more than 10^{11} adiabatic states among which to hop in this application. However, it is actually quite feasible, due to the fact that each one-electron orbital of the single determinant Newns-Anderson wave function evolves independently. Surface hops are one-electron events as well, simply involving replacement of a single orbital in the Slater determinant. We implemented this independent electron surface hopping (IESH) method with the standard “fewest switches” surface hopping algorithm developed previously by the PI. The resulting stochastic method is manageable, it accounts for both electronic friction and localized excitations, and it properly resolves the outcomes into final state probabilities. Note that an NO-Au(111) direct scattering event may involve more than 100 surface hops, in contrast to the 2 or 3 typically encountered in nonadiabatic gas phase processes. Details of the IESH algorithm are described in paper 12 cited below.

Dynamics of scattering of NO from Au(111)

We have now carried out extensive simulations of the scattering of NO from the Au(111) surface, comparing our nonadiabatic (IESH) results with adiabatic simulations using the same interaction potential. The IESH calculations reproduce and elucidate many of the observations of the Wodtke group. The most dramatic difference between the adiabatic and surface hopping simulations is in the final vibrational energy distributions of the scattered NO, where adiabatic simulations predict almost no vibrational energy loss whereas IESH predicts a loss of more than 50% of the initial vibrational energy, in accord with the experiments.

The Wodtke group has observed electron emission from a Cs-covered gold surface upon scattering of highly vibrationally excited NO. The electron emission intensity is linearly dependent on the flux of molecules, so it is a single collision event, not heating. The probability of electron emission has a threshold at vibrational quantum number of about $\nu=8$ and increases thereafter with increasing initial ν . (The energy of the $\nu=8$ state is 1.88 eV compared to the work function of the Cs-covered gold surface of 1.6 eV.) These experiments demonstrate that a large fraction of the energy lost from vibration can be deposited into a single electron; the process must occur, at least sometimes, by a multi-quantum vibrational transition, rather than in a stepwise sequence of single vibrational level transitions. Our calculations only address the clean gold surface, so we cannot make any direct comparisons to the Cs-covered gold experiments.

Nevertheless, our surface hopping simulations do predict that multi-quantum vibrational transitions, producing energetic electrons, are quite prevalent.

The Wodtke group recently published the intriguing observation that the electron emission intensity from the Cs – Au surface depends inversely on the incident translational energy of the NO molecule. They point out that this is contrary to the expectation that nonadiabatic transitions become more prevalent at higher energies; gradual motion favors adiabatic behavior. As stated above, we have not carried out scattering simulations on the Cs-covered gold surface. However, we have recorded the final electron energy distribution upon scattering of vibrationally excited NO($v=15$) molecules from the clean gold surface, and find that the computed mean energy of excitation of the electrons decreases with increasing incident velocity. Although the comparison is between different quantities and different systems, the overall trends are similar. We find the underlying mechanism to be the following: at lower translational energy, the NO molecule is steered into the strong nonadiabatic coupling region and remains longer in this region, enhancing the probability of vibration-to-electronic energy transfer.

The IESH results summarized above demonstrate, first, that the approach is computationally feasible; a run of 100 scattering trajectories requires about 15 hours of computational time on a single processor. Second, the method is capable of reproducing the main experimental trends with acceptable accuracy, especially considering the uncertainties in the electronic PESs. Finally, the mechanisms underlying the observed behavior are elucidated quite clearly. We note that, for low vibrational excitation where the system does not undergo significant charge transfer, the surface hopping results should approach those of the electronic friction model. We have demonstrated that this is approximately true for the vibrational lifetime of the $v=2$ level of an adsorbed NO molecule, using the same interaction parameters for both calculations.

Future Plans

The goals of our research program include completing our studies of the NO-Au system and more general investigations of nonadiabatic behavior at metal and semiconductor surfaces. Our plans for the next funding periods include the following:

1. Carry out Ehrenfest dynamics for NO scattering from gold, using the same Hamiltonian employed with IESH, to determine to what extent single average paths can represent the multiple state-specific pathways encountered in IESH.
2. Derive and implement a practical procedure for introducing decoherence in the surface hopping approach, in order to account for the loss of excitation energy via transport of carriers into the bulk metal.
3. Develop improved ab initio methods for computing energies and widths of lifetime-broadened electronic states near metal and semiconductor surfaces, through extension of “constrained density functional theory”. These are the properties that determine the rate and extent of electron transfer as a molecule approaches the surface; i.e., that are required to construct a diabatic or Newns-Anderson Hamiltonian.
4. Carry out ab initio calculations of energies, charge distributions and level widths as input to constructing valence-bond type Hamiltonians for a number of chemical systems, including the CO oxidation reaction on platinum. Somorjai and coworkers have recently demonstrated that hot-electrons are produced as this reaction unfolds.

5. Explore the dynamics of open shell species with metal and semiconductor surfaces, and small metallic clusters. An example is the oxygen molecule where transitions between the ground state triplet and low-lying singlet states may occur without spin-orbit interactions via a two-electron exchange with the conduction band, with major implications to chemical reactivity.

References to Publications of DOE-Sponsored Research: 2006-2009

1. N. Shenvi, H. Z. Cheng and J. C. Tully, "Nonadiabatic dynamics near metal surfaces: Decoupling quantum equations of motion in the wide-band limit", *Phys. Rev. A* **74**, 062902 (2006).
2. N. Shenvi, S. Roy, P. Parandekar and J. Tully, "Vibrational relaxation of NO on Au(111) via electron-hole pair generation", *J. Chem. Phys.* **125**, 154703 (2006).
3. J. C. Tully, "Mode-selective control of surface reactions", *Science* **312**, 1004 (2006). (This paper is an invited "Perspective" commenting on the results of others.)
4. H. Z. Cheng, N. Shenvi and J. C. Tully, "Semiclassical dynamics of electron transfer at metal surfaces", *Phys. Rev. Lett.* **99**, 053201 (2007).
5. X. S. Li and J. C. Tully, "Ab initio time-resolved density functional theory for lifetimes of excited adsorbate states at metal surfaces", *Chem. Phys. Lett.* **439**, 199-203 (2007). (primary support from NSF)
6. C. M. Isborn, X. S. Li and J. C. Tully, "Time-dependent density functional theory Ehrenfest dynamics: Collisions between atomic oxygen and graphite clusters" *J. Chem. Phys.* **126**, 134307 (2007). (primary support from NSF)
7. N. Shenvi, J. R. Schmidt, S. Edwards and J. C. Tully, "Efficient discretization of the continuum through complex contour deformation", *Phys. Rev. A* **78**, 022502 (2008).
8. J. Zwickl, N. Shenvi, J.R. Schmidt and J. C. Tully, "Transition state barriers in multidimensional Marcus theory", *J. Phys. Chem B.* **42**, 10570 (2008).
9. J. R. Schmidt, N. Shenvi and J. C. Tully, "Controlling spin-contamination using constrained density functional theory", *J. Chem. Phys.* **129**, 114110 (2008).
10. N. Shenvi, "Phase-space surface hopping: Nonadiabatic dynamics in a superadiabatic basis", *J. Chem. Phys.* **130**, 124117 (2009).
11. S. Roy, N. Shenvi and J. C. Tully, "Model Hamiltonian for the interaction of NO with the Au(111) surface", *J. Chem. Phys.* **130**, 174716 (2009).
12. N. Shenvi, S. Roy and J. C. Tully, "Nonadiabatic dynamics at metal surfaces: Independent-electron surface hopping", *J. Chem. Phys.* **130**, 174107 (2009).
13. J. E. Subotnik, R. J. Cave, R. P. Steele and N. Shenvi, "The initial and final states of electron and energy transfer processes: Diabatization as motivated by system-solvent interactions", *J. Chem. Phys.* **130**, 234102 (2009) (partial DOE support).
14. S. Roy, N. Shenvi and J. C. Tully, "The Dynamics of Open-Shell Species at Metal Surfaces", *J. Phys. Chem.*, in press.

Reactions of Ions and Radicals in Aqueous Systems

Marat Valiev¹ and Bruce C. Garrett²

¹Environmental Molecular Sciences Laboratory and

²Chemical & Materials Sciences Division

Pacific Northwest National Laboratory

902 Battelle Blvd.

Mail Stop K9-90

Richland, WA 99352

marat.valiev@pnl.gov, bruce.garrett@pnl.gov

The long-term objective of this project is to understand the factors that control the chemical reactivity of atomic and molecular species in aqueous environments. Chemical reactions in condensed phase environments play crucial roles in a wide variety of problems important to the Department of Energy (DOE), (e.g., catalysis for efficient energy use, corrosion in nuclear reactors promoted by reactive radical species such as OH, release of hydrogen from hydrogen storage materials, and contaminant degradation in the environment by natural and remedial processes). The need in all of these areas is to control chemical reactions to eliminate unwanted reactions and/or to produce desired products. The control of reactivity in these complex systems demands knowledge of the factors that control the chemical reactions and requires understanding how these factors can be manipulated to affect the reaction rates. The goals of this research are the development of theoretical methods for describing reactions in condensed phases (primarily aqueous liquids) and their application to prototypical systems to develop fundamental knowledge needed to solve problems of interest to DOE.

Gaining a theoretical understanding of factors that control ground and excited-state properties of chemical systems in condensed phase is a challenging problem requiring simultaneous consideration of the electronic structure of reactive species, collective degrees of freedom associated with the environment, reaction dynamics, and thermal fluctuations. To address these issues, we are developing multi-scale, multi-physics approaches that recognize the advantages of using different theoretical models (multi-physics) to address the natural decomposition of the chemical system into distinct regions (multi-scale). These theoretical models can be associated with different parts of the overall chemical system and/or can coexist in a layered fashion. This flexibility in the system description significantly extends the scope, accuracy, and reliability of ab-initio modeling of ground and excited-state processes in complex systems. Based on this methodology, we are pursuing novel approaches for efficient utilization of high-level electronic structure methods such as coupled cluster (CC) theory in real condensed phase applications.

We recently presented a method for calculating free energy profiles for chemical reactions in solution utilizing high-level ab initio methods (reference 14). We begin with the standard separation of the condensed phase system into a reactive part, which is treated quantum mechanically (QM), and the rest of the system, which is treated by a classical molecular mechanics (MM) model. We use a thermodynamic cycle to take advantage of the state function property of the potential of mean force (PMF), W , and combine simulations of free energy differences with pure MM models that allow sampling to be performed over ensembles, which are sufficiently large to converge statistical averages, with high-level electronic structure calculations for the QM region to accurately predict energetics. This approach has been used to

study the favored configurations in the interaction of chloride ion with OH radical in aqueous solution (reference 24). The potential of mean force (PMF) was calculated for transformation from a hydrogen bonded OH---Cl⁻ species to a hemi-bonded HOCl⁻ species. In the PMF calculation, OH and Cl⁻ represented the QM region and waters were treated with a MM model. The nudged elastic band (NEB) method was used to calculate a sequence of geometries along a reaction path at T = 0K. The approach mentioned above using a thermodynamic cycle takes advantage of MM, DFT, and coupled cluster (CC) methods in the QM regions. The results displayed in Figure 1 show that a subtle interplay of electronic structure and solvation determines the most stable structure. DFT methods commonly used for condensed phase simulations are inadequate for predicting the most stable species. The best estimates of the energies show that the hemi-bonded structure is only about 1 kcal/mol higher than the hydrogen-bonded species and therefore could play an important role in reactions that lead to the formation of Cl₂.

Similar methodology can also greatly improve the description of processes involving excited states where the accuracy of the electronic structure calculations becomes especially problematic. Our current work in this direction involves studies of electronic excitations of the hydrated OH-Cl⁻ species. Optimized geometries, including both the QM and MM regions, were obtained for the hemi-bonded and hydrogen-bonded species and excited-state spectra were simulated for these structures. Figure 2 shows that the hemi-bonded species displays a strong absorption peak at ~350 nm, which is in close agreement with the experimental value, whereas the hydrogen-bonded species has much weaker bands at ~330 and 480 nm. The time dependent (TD)-DFT description of the excited states of hydrated OH-Cl⁻ proves to be unreliable, especially for the hydrogen-bonded species. Future work will explore methods to include thermal fluctuations in the simulations of these spectra. In addition, we are performing simulations to quantify the importance of hemi-bonded interactions between OH and water in condensed phases to understand more clearly the importance of these configurations on the solvation structure around OH and the OH spectra in water.

Collaborators on this project include G. K. Schenter, M. Dupuis, S. S. Xantheas,

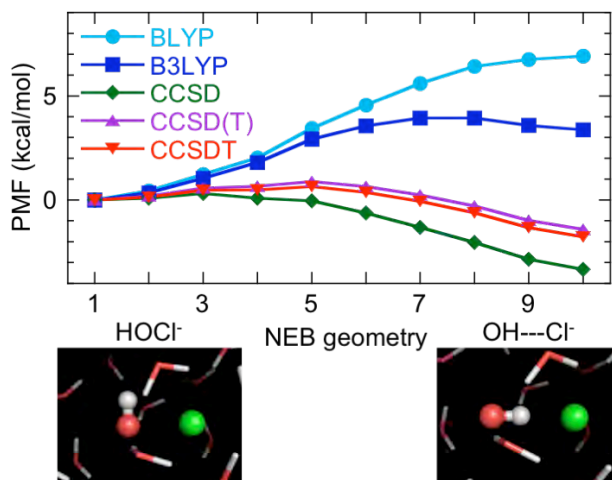


Figure 1: Free energy profile for the transformation from the hemi-bonded HOCl⁻ species to the hydrogen-bonded OH---Cl⁻ species in water. The levels of QM calculations for the QM region include DFT with BLYP (circles) and B3LYP (squares) functionals, and coupled cluster calculations with single and double excitations (diamonds), perturbative triples (triangles) and full triples (inverted triangles).

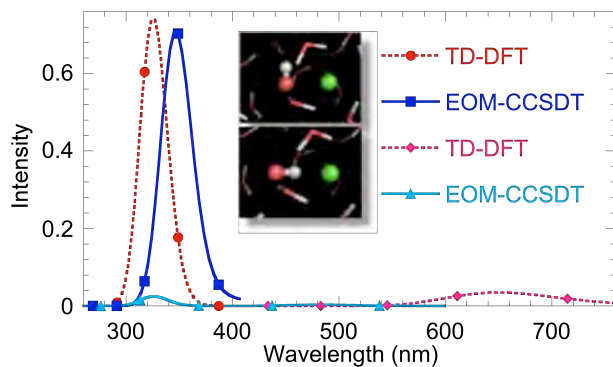


Figure 2: Simulated spectra for optimized geometries (T = 0K) using EOMCCSD and TD-DFT levels of theory for hemi-bonded species (square and circle symbols) and hydrogen-bonded species (triangle and diamond symbols).

Doug Tobias, and Rafaella D'Auria. Some of the work was performed using the Molecular Science Computing Facility in the Environmental Molecular Sciences Laboratory, a national scientific user facility sponsored by the Department of Energy's Office of Biological and Environmental Research, located at Pacific Northwest National Laboratory (PNNL). Battelle operates PNNL for DOE.

References to publications of DOE sponsored research (2005-present)

1. B. C. Garrett, D. A. Dixon, D. M. Camaioni, D. M. Chipman, M. A. Johnson, C. D. Jonah, G. A. Kimmel, J. H. Miller, T. N. Rescigno, P. J. Rossky, S. S. Xantheas, S. D. Colson, A. H. Laufer, D. Ray, P. F. Barbara, D. M. Bartels, K. H. Becker, H. Bowen, S. E. Bradforth, I. Carmichael, J. V. Coe, L. R. Corrales, J. P. Cowin, M. Dupuis, K. B. Eisenthal, J. A. Franz, M. S. Gutowski, K. D. Jordan, B. D. Kay, J. A. LaVerne, S. V. Lyman, T. E. Madey, C. W. McCurdy, D. Meisel, S. Mukamel, A. R. Nilsson, T. M. Orlando, N. G. Petrik, S. M. Pimblott, J. R. Rustad, G. K. Schenter, S. J. Singer, A. Tokmakoff, L. S. Wang, C. Wittig, and T. S. Zwier, "Role of Water in Electron-Initiated Processes and Radical Chemistry: Issues and Scientific Advances," *Chemical Reviews* 105, 355-389 (2005).
2. S. M. Kathmann, G. K. Schenter, and B. C. Garrett, "Ion-Induced Nucleation: The Importance of Chemistry," *Physical Review Letters* 94, 116104 (2005).
3. J. Vieceli, M. Roeselova, N. Potter, L. X. Dang, B. C. Garrett, and D. J. Tobias, "Molecular Dynamics Simulations of Atmospheric Oxidants at the Air-Water Interface: Solvation and Accommodation of OH and O₃," *Journal of Physical Chemistry B* 109, 15876-15892 (2005).
4. B. C. Garrett and D. G. Truhlar, "Variational Transition State Theory," in *Theory and Applications of Computational Chemistry: The First 40 Years*, edited by C. E. Dykstra, G. Frenking, K. S. Kim, and G. E. Scuseria (Elsevier, Amsterdam, 2005), p. 67-87.
5. T. D. Iordanov, G. K. Schenter, and B. C. Garrett, "Sensitivity analysis of thermodynamic properties of liquid water: A general approach to improve empirical potentials," *Journal of Physical Chemistry A* 110, 762-771 (2006).
6. L. X. Dang, T. M. Chang, M. Roeselova, B. C. Garrett, and D. J. Tobias, "On NO₃--H₂O Interactions in Aqueous Solutions and at Interfaces," *Journal of Chemical Physics* 124 066101 (2006).
7. B. C. Garrett, G. K. Schenter, and A. Morita, "Molecular Simulations of the Transport of Molecules Across the Liquid/Vapor Interface of Water," *Chemical Reviews* 106, 1355-1374 (2006).
8. S. Du, J. S. Francisco, G. K. Schenter, T. D. Iordanov, B. C. Garrett, M. Dupuis, and J. Li, "The OH Radical - H₂O Molecular Interaction Potential," *Journal of Chemical Physics* 124, 224318 (2006).
9. D. G. Truhlar and B. C. Garrett, "Variational Transition State Theory in the Treatment of Hydrogen Transfer Reactions," in *Handbook of Hydrogen Transfer*, edited by H. H. Limbach, J. T. Hynes, J. Klinman, and R. L. Schowen (Wiley-VCH, New York, 2007), Vol. 2, pp. 833-875.
10. A. Fernandez-Ramos, B. A. Ellingson, B. C. Garrett, and D. G. Truhlar, "Variational Transition State Theory with Multidimensional Tunneling," in *Reviews in Computational Chemistry*, edited by K. B. Lipkowitz, Cundari, T. R., and D. B. Boyd (John Wiley & Sons, Hoboken, 2007), Vol. 23, pp. 125-232.
11. S. Y. Du, J. S. Francisco, G. K. Schenter, and B. C. Garrett, "Ab initio and Analytical Intermolecular Potential for ClO-H₂O," *Journal of Chemical Physics* 126, 114304 (2007).
12. S. M. Kathmann, G. K. Schenter, and B. C. Garrett, "Comment on "Quantum Nature of the Sign Preference in Ion-Induced Nucleation","" *Physical Review Letters* 98, 109603 (2007).
13. D. G. Truhlar and B. C. Garrett, "Variational transition state theory in the treatment of hydrogen transfer reactions," in *Hydrogen-Transfer Reactions*, Vol. 2, edited by H. H. Limbach, J. T. Hynes, J. Klinman, and R. L. Schowen (Wiley-VCH, New York, 2007), p. 833-875.

14. M. Valiev, B. C. Garrett, M.-K. Tsai, K. Kowalski, S. M. Kathmann, G. K. Schenter, and M. Dupuis, "Hybrid Approach for Free Energy Calculations with High-Level Methods: Application to the S_N2 Reaction of CHCl_3 and OH^- in Water," *Journal of Chemical Physics* **127**, 051102 (2007).
15. S. M. Kathmann, B. J. Palmer, G. K. Schenter, and B. C. Garrett, "Activation Energies and Potentials of Mean Morse for Water Cluster Evaporation," *Journal of Chemical Physics* **128**, 064306 (2008).
16. S. Y. Du, J. S. Francisco, G. K. Schenter, and B. C. Garrett, "Many-Body Decomposition of the Binding Energies for $\text{OH}(\text{H}_2\text{O})_2$ and $\text{OH}(\text{H}_2\text{O})_3$ complexes," *Journal of Chemical Physics* **128**, 084307 (2008).
17. D. T. Chang, G. K. Schenter, and B. C. Garrett, "Self-Consistent Polarization Neglect of Diatomic Differential Overlap: Application to Water Clusters," *Journal of Chemical Physics* **128**, 164111 (2008).
18. M. Valiev, E. J. Bylaska, M. Dupuis, and P. G. Tratnyek, "Combined Quantum Mechanical and Molecular Mechanics Studies of the Electron-Transfer Reactions Involving Carbon Tetrachloride in Solution," *Journal of Physical Chemistry A* **112**, 2713-2720 (2008).
19. S. M. Kathmann, G. K. Schenter, and B. C. Garrett, "The Impact of Molecular Interactions in Atmospheric Radiative Forcing," in *Advances in Quantum Chemistry: Applications of Theoretical Methods to Atmospheric Science*, Vol. 55, edited by M. E. Goodsite and M. S. Johnson (Elsevier, Oxford, 2008), p. 429-447.
20. A. Morita and B. C. Garrett, "Molecular Theory of Mass Transfer Kinetics and Dynamics at Gas-Water Interface," *Fluid Dynamics Research* **40**, 459-473 (2008).
21. D. J. Arseneau, D. G. Fleming, O. Sukhorukov, J. H. Brewer, B. C. Garrett, and D. G. Truhlar, "The muonic He atom and a preliminary study of the $^4\text{He}\mu + \text{H}_2$ reaction," *Physica B* **404**, 946-949 (2009).
22. S. M. Kathmann, G. K. Schenter, B. C. Garrett, B. Chen, and J. I. Siepmann, "Thermodynamics and Kinetics of Nanoclusters Controlling Gas-to-Particle Nucleation," *Journal of Physical Chemistry C* **113**, 10354-10370 (2009).
23. S. L. Mielke, D. W. Schwenke, G. C. Schatz, B. C. Garrett, and K. A. Peterson, "Functional Representation for the Born-Oppenheimer Diagonal Correction and Born-Huang Adiabatic Potential Energy Surfaces for Isotopomers of H_3 ," *Journal of Physical Chemistry A* **113**, 4479-4488 (2009).
24. M. Valiev, R. D'Auria, D. J. Tobias, and B. C. Garrett, "Interactions of Cl $^-$ and OH radical in aqueous solution," *Journal of Physical Chemistry A* **113**, 8823-8825 (2009).
25. S. Y. Du, J. S. Francisco, G. K. Schenter, and B. C. Garrett, "The interaction of ClO radical with liquid water," *Journal of the American Chemical Society* (accepted).

Chemical Kinetics and Dynamics at Interfaces

Gas Phase Investigation of Condensed Phase Phenomena

Xue-Bin Wang & Lai-Sheng Wang

Department of Physics, Washington State University, 2710 University Drive, Richland, WA, 99354 and the Chemical & Materials Sciences Division, Pacific Northwest National Laboratory, P.O. Box 999, MS K8-88, Richland, WA 99352. E-mails: xuebin.wang@pnl.gov; ls.wang@pnl.gov

Program Scope

The broad scope of this program is aimed at microscopic understanding of condensed phase phenomena using clusters as model systems. Our current focus is on the microsolvation of complex anions that are important in solution chemistry. The primary experimental technique is photoelectron spectroscopy of size-selected anions. Unique experimental techniques have been developed by coupling electrospray ionization with photoelectron spectroscopy that allows complex anions, including multiply charged anions and solvated clusters, from liquid phase to be investigated in the gas phase. Experimental studies are combined with *ab initio* calculations to:

- obtain a molecular-level understanding of the solvation of complex anions (both singly and multiply charged) important in solution chemistry
- understand the molecular processes and initial steps of dissolution of salt molecules by polar solvents
- probe the structure and dynamics of solutions and air/solution interfaces

Complexes anions, in particular multiply charged anions, are ubiquitous in nature and often found in solutions and solids. However, few complex anions have been studied in the gas phase due to the difficulty in generating them and their intrinsic instability as a result of strong intramolecular Coulomb repulsion in the case of multiply charged anions. Microscopic information on the solvation and stabilization of these anions is important for the understanding of solution chemistry and properties of inorganic materials or atmospheric aerosols involving these species. Gas phase studies with controlled solvent numbers and molecular specificity are ideal to provide such microscopic information. We have developed a new experimental technique to investigate multiply charged anions and solvated species directly from solution samples and probe their electronic structures, intramolecular Coulomb repulsion, stability, and energetics using electrospray and photoelectron spectroscopy. A central theme of this research program lies at obtaining a fundamental understanding of environmental materials and solution chemistry. These are important to waste storage, subsurface and atmospheric contaminant transport, catalysis, and other primary DOE missions.

Recent Progress (2006-2009)

Development of a low-temperature and temperature-controlled photoelectron spectroscopy instrument: Observation of H_2 physisorption onto negative ions. The ability to control ion temperatures is critical for gas phase spectroscopy and has been a challenge in chemical physics. We have developed a low-temperature photoelectron spectroscopy instrument for the investigation of complex anions

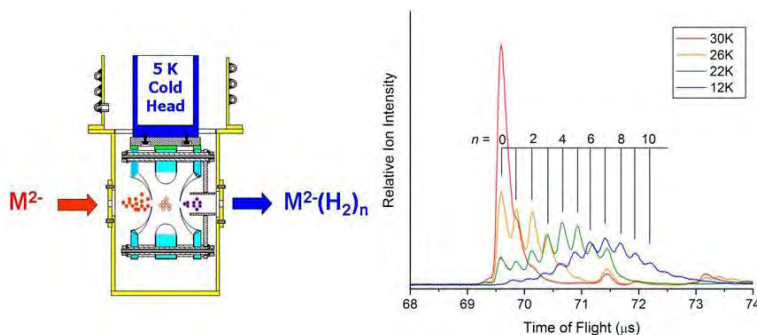


Fig. 1. Schematic view of the cold trap and mass spectra of $^{-}O_2C(CH_2)_{12}CO_2^-(H_2)_n$ physisorbed complexes at different temperatures

in the gas phase, including multiply charged anions, solvated species, and biological molecules. A key feature of the new instrument is the capability to cool and tune ion temperatures from 10 to 350 K in the 3D Paul trap, which is attached to the cold head of a closed-cycle helium refrigerator (Fig. 1, left). Ion cooling is accomplished in the Paul trap via collisions with a background gas and has been demonstrated by observation of complete elimination of vibrational hot bands in photoelectron spectra of various anions ranging from small molecules to complex species. For example, we have observed a remarkable temperature (entropic) effect on conformation changes of complex hydrated clusters, ${}^{-}\text{O}_2\text{C}-(\text{CH}_2)_6-\text{CO}_2{}^{-}$ $(\text{H}_2\text{O})_{14}$. Cold anions result in better resolved photoelectron spectra due to the elimination of vibrational hot bands and yield more accurate energetic and spectroscopic information. Temperature-dependent studies are made possible for weakly-bonded molecular and solvated clusters, allowing thermodynamic information to be obtained.

Further evidence of ion cooling is shown by the observation of H_2 physisorbed anions at low temperatures. Figure 1 shows a set of mass spectra of a doubly-charged anion, ${}^{-}\text{O}_2\text{C}-(\text{CH}_2)_{12}-\text{CO}_2{}^{-}$ (DC^{2-}), when the helium background gas contains 20% H_2 in the ion trap at a total background pressure of ~ 0.1 mTorr. At a trapping temperature of 12 K, more than 10 H_2 molecules can be adsorbed onto DC^{2-} and the maximum adsorbed H_2 decreases with increasing temperature. Photoelectron spectra show that each H_2 molecule can provide on average an electron stabilization energy of 3.3 kJ/mol. Since organic carboxylates are common components in the metal-organic framework hydrogen storage materials, our work may be pertinent to understanding the intermolecular interactions of H_2 in these promising hydrogen-storage materials.

Photoelectron spectroscopy of cold hydrated sulfate clusters : Temperature-dependent isomer populations. Sulfate is an important inorganic anion and its interactions with water are essential to understand its chemistry in aqueous solution. Studies of sulfate with well-controlled solvent numbers provide molecular-level information about the solute-solvent interactions and critical data to test theoretical methods for weakly bonded species. We reported a low-temperature photoelectron spectroscopy study of hydrated sulfate clusters $\text{SO}_4^{2-}(\text{H}_2\text{O})_n$ ($n = 4-7$) at 12 K and *ab initio* studies to understand the structures and dynamics of these unique solvated systems. A significant increase of electron binding energies was observed for the 12 K spectra relative to those at room temperature, suggesting different structural isomers were populated as a function of temperature. Theoretical calculations revealed a competition between isomers with optimal water-solute and water-water interactions. The global minimum isomers all possess higher electron binding energies due to their optimal water-solute interactions, giving rise to the binding energy shift in the 12 K spectra, whereas many additional low-lying isomers with less optimal solvent-solute interactions were populated at room temperature, resulting in a shift to lower electron binding energies in the observed spectra. This study reveals the complexity of the water-sulfate potential energy landscape and the importance of temperature control in studying the solvent-solute systems and in comparing calculations with experiment.

Photoelectron imaging of multiply charged anions: Imaging intra-molecular Coulomb repulsion in multiply-charged anions. Multiply charged anions possess strong intra-molecular Coulomb repulsion (ICR), which not only dictates photoelectron binding energies, but also influence its angular distributions. Using

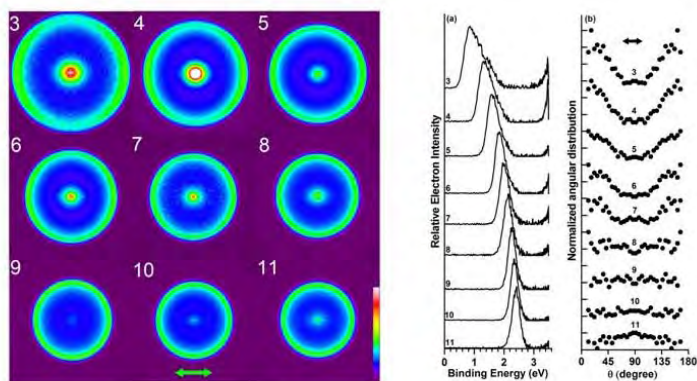


Fig. 2. Left: Photoelectron images of dicarboxylate dianions, ${}^{-}\text{O}_2\text{C}(\text{CH}_2)_n\text{CO}_2{}^{-}$ at 355 nm. Right: Photoelectron spectra obtained from the images and graphical representation of the electron angular distributions.

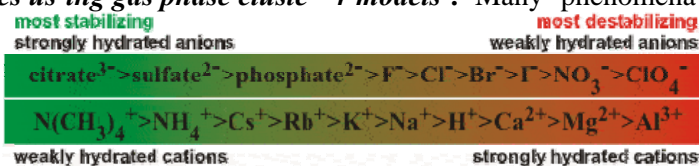
photoelectron imaging, we show the effect of ICR on photoelectron angular distributions for a series of dianions, ${}^{-}\text{O}_2\text{C}-(\text{CH}_2)_n-\text{CO}_2{}^{-}$ (D_n^{2-}) (Fig. 2). The observed photoemission band of D_n^{2-} was due to a perpendicular transition from the charged end group. However, photoemission intensities were observed to peak along the laser polarization for smaller n due to the strong ICR that forces electrons to be emitted along the molecular axis. This emission pattern weakens with increasing n and at D_{11}^{2-} the angular distribution reverses back to peak at the perpendicular direction due to the reduced ICR. We also demonstrated that the anisotropy of photoelectrons is related to the direction of the ICR or the detailed molecular structures, suggesting that photoelectron imaging may allow structural information to be obtained for complex multiply charged anions.

Future Plans

The main thrust of our BES program will continue to focus on cluster model studies of condensed phase phenomena in the gas phase. The experimental capabilities that we have developed give us the opportunities to attack a broad range of fundamental chemical physics problems pertinent to ionic solvation and solution chemistries. In particular, the temperature control will allow us to study different isomer populations and conformation changes as a function of temperature. We will also be able to study physisorption of various gas molecules onto negatively charged anions. The physisorption behaviors of H_2 and CO_2 are of particular interest because of the relevance to identifying potentially H_2 storage materials and CO_2 sequestration by providing fundamental energetic and structural information between H_2 , CO_2 and different types of molecules.

Photoelectron spectroscopic investigation of microsolvation of environmentally important anions under well-controlled temperatures. One of the cornerstones of DOE nuclear cleanup missions and climate research is a fundamental understanding of water and ions, the most common chemical interactions in the environment. We have already investigated the solvation and solvent-stabilization of a variety of simple and complex anions at room temperature previously. As shown above, the newly-developed low-temperature and temperature-controlled technique allows us to significantly expand our research capability to explore important temperature effects in hydration processes. We plan to continue to probe the underlying entropic effects in solvation of complex anions, and to probe the H-bonding structure and dynamics of water interacting with environmentally important anions, such as cyanide, acetate, nitrate, hydroxide, and halides at different temperatures. The obtained detailed energetic and spectroscopic information, with the aid of high level *ab initio* calculations, will provide valuable, specific ion-water interactions, and unravel the vital temperature role in determining solvated structures and dynamics.

Investigation of Hofmeister series using gas phase cluster models. Many phenomena in condensed phases (colloid, polymer, interface and biological science) that involve electrolyte show pronounced ion specificity, generally characterized by the famous Hofmeister series (right). Although such ion specificity has been known for a century, a fundamental molecular-level understanding is still lacking. We propose to use clusters to model such ion specificity in the gas phase via photoelectron spectroscopy and *ab initio* calculations.



Probing H₂, CO₂ physisorption onto negative ions. Because of the light weight and low density of gaseous hydrogen, discovering viable hydrogen storage materials has become a critical step for the application of H_2 as a clean fuel. Understanding the intermolecular interaction between H_2 and different molecular species can provide fundamental information about the H_2 binding affinities of potential hydrogen storage materials. H_2 -adsorbed molecular complexes provide simple model systems for investigating H_2 binding. Our low-temperature ion trap provides an ideal device to produce H_2 complexes

with a variety of ionic species. In particular, for negatively charged ions we can use photoelectron spectroscopy to probe the energetics of the H₂-anion interactions. It has been theoretically shown that H₂ binding can be significantly enhanced on charged species. Thus, we can also probe the dependence of H₂ binding on charge states. Potentially, our technique allows any negatively charged ions to be investigated. We plan to exploit this capability to probe the interaction of H₂ with different anions. Furthermore, we can expand our photoelectron spectroscopic study onto CO₂-physisorbed complex clusters to obtain valuable energetic and structural information about interactions between CO₂ and a variety of anions, which is pertinent to the currently active research field of CO₂ sequestration.

References to Publications of DOE Sponsored Research (FY 2006-2009)

1. "Determination of the Electron Affinity of the Acetyloxy Radical (CH₃COO) by Low Temperature Anion Photoelectron Spectroscopy and *ab initio* Calculations" (X. B. Wang, H. K. Woo, L. S. Wang, B. Minofar, and P. Jungwirth), *J. Phys. Chem. A* **110**, 5047-5050 (2006).
2. "Low-Temperature Photoelectron Spectroscopy of Aliphatic Dicarboxylate Monoanions, HO₂C(CH₂)_nCO₂⁻ (*n* = 1 – 10): Hydrogen Bond Induced Cyclization and Strain Energies" (H. K. Woo, X. B. Wang, K. C. Lau, and L. S. Wang), *J. Phys. Chem. A* **110**, 7801-7805 (2006).
3. "First Steps Towards Dissolution of NaSO₄⁻ by Water" (X. B. Wang, H. K. Woo, B. Jagoda-Cwiklik, P. Jungwirth, and L. S. Wang), *Phys. Chem. Chem. Phys.* **8**, 4294-4296 (2006).
4. "Microsolvation of the Dicyanamide Anion: [N(CN)₂]⁻(H₂O)_n (*n* = 0–12)" (B. Jagoda-Cwiklik, X. B. Wang, H. K. Woo, J. Yang, G. J. Wang, M. F. Zhou, P. Jungwirth, and L. S. Wang), *J. Phys. Chem. A* **111**, 7719-7725 (2007).
5. "Observation of Entropic Effect on Conformation Changes of Complex Systems under Well-Controlled Temperature Condition" (X. B. Wang, J. Yang, and L. S. Wang), *J. Phys. Chem. A* **112**, 172-175 (2008).
6. "Development of a Low-Temperature Photoelectron Spectroscopy Instrument Using an Electrospray Ion Source and a Cryogenically Controlled Ion Trap" (X. B. Wang and L. S. Wang), *Rev. Sci. Instrum.* **79**, 073108-1-8 (2008).
7. "Imaging Intramolecular Coulomb Repulsions in Multiply Charged Anions" (X. P. Xing, X. B. Wang, and L. S. Wang), *Phys. Rev. Lett.* **101**, 083003-1-4 (2008).
8. "Observation of H₂ Aggregation onto a Doubly Charged Anion in a Temperature-Controlled Ion Trap" (X. B. Wang, X. P. Xing, and L. S. Wang), *J. Phys. Chem. A* **112**, 13271-13274 (2008).
9. "Photoelectron Angular Distribution and Molecular Structure in Multiply Charged Anions" (X. P. Xing, X. B. Wang, and L. S. Wang), *J. Phys. Chem. A* **113**, 945-948 (2009).
10. "Photoelectron Spectroscopy of Multiply Charged Anions" (X. B. Wang and L. S. Wang), *Annu. Rev. Phys. Chem.* **60**, 105-26 (2009).
11. "Photoelectron Imaging of Multiply Charged Anions: Effects of Intramolecular Coulomb Repulsion and Photoelectron Kinetic Energies on Photoelectron Angular Distributions" (X. P. Xing, X. B. Wang, and L. S. Wang), *J. Chem. Phys.* **130**, 074301 (2009).
12. "Photoelectron Spectroscopy of Cold Hydrated Sulfate Clusters, SO₄²⁻(H₂O)_n (*n* = 4–7): Temperature-Dependent Isomer Populations" (X. B. Wang, A. P. Sergeeva, J. Yang, X. P. Xing, A. I. Boldyrev, and L. S. Wang), *J. Phys. Chem. A* **113**, 5567-5576 (2009).
13. "Probing the Electronic Stability of Multiply Charged Anions: Sulfonated Pyrene Tri- and Tetraanions" (X. B. Wang, A. P. Sergeeva, X. P. Xing, M. Massaouti, T. Karpuschkin, O. Hampe, A. I. Boldyrev, M. M. Kappes, and L. S. Wang), *J. Am. Chem. Soc.* **131**, 9836-9842 (2009).
14. "Microsolvation of the Acetate Anion [CH₃CO₂⁻(H₂O)_n, *n* = 1-3]: A Photoelectron Spectroscopy and *ab Initio* Computational Study" (X. B. Wang, B. Jagoda-Cwiklik, C. Chi, X. P. Xing, M. Zhou, P. Jungwirth, and L. S. Wang), *Chem. Phys. Lett.* **477**, 41-44 (2009).
15. "Observation of a remarkable temperature effect in the hydrogen bonding structure and dynamics of the CN(H₂O) cluster" (X. B. Wang, J. C. Werhahn, L. S. Wang, K. Kowalski, A. Laubereau, and S. S. Xantheas), *J. Phys. Chem. A* **113**, 9579-9584 (2009).

Surface Chemical Dynamics

M.G. White,^a N. Camillone III,^a and A.L. Harris^b

Brookhaven National Laboratory, Chemistry Department, Building 555, Upton, NY 11973

(mgwhite@bnl.gov, nicholas@bnl.gov, alexh@bnl.gov)

1. Program Scope

This program focuses on fundamental investigations of the dynamics, energetics and morphology-dependence of thermal and photoinduced reactions on planar and nanostructured surfaces that play key roles in energy-related catalysis and photocatalysis. Laser pump-probe methods are used to investigate the dynamics of interfacial charge and energy transfer that lead to adsorbate reaction and/or desorption on metal and metal oxide surfaces. State- and energy-resolved measurements of the gas-phase products are used to infer the dynamics of product formation and desorption. Time-resolved correlation techniques follow surface reactions in real time and are used to infer the dynamics of adsorbate–substrate energy transfer. Planned extensions of this work include investigations of the size-dependence of photoinduced desorption and vibrational dynamics of small molecules on surfaces of supported metal nanoparticles. Complementary efforts use cluster ion beams for studying the structure, dynamics and reactivity of size-selected metal and metal compound nanoclusters in the gas-phase and deposited onto solid supports.

2. Recent Progress

Ultrafast Investigations of Surface Chemical Dynamics. The long-term goal of this aspect of the effort is to follow in real time the evolution of surface chemical processes. Of particular interest are the links between substrate electronic excitations and surface reactivity. Recent experiments and theory have begun to show that diabatic processes cannot be ignored even in descriptions of thermal processes. Thus, it has become increasingly important to understand the role that energy transport due to formal violation of the Born-Oppenheimer approximation plays in surface chemical reactivity.

To understand the dynamics of energy flow, we are working to time-resolve the fundamental steps of surface chemical transformations on the femtosecond timescale and to investigate how the dynamics is impacted by surface morphology and electronic structure. We employ ~ 100 fs near-IR laser pulses to inject energy into adsorbate–substrate complexes, initiating reactions by substrate-mediated processes such as DIMET (desorption induced by multiple electronic transitions) and heating via electronic friction. Time-resolved monitoring of the complex is achieved by a two pulse correlation (2PC) method wherein the surface is excited by a “pump” pulse and a time-delayed “probe,” and a measurement of the product yield as a function of the delay is a measure of the energy transfer rate. We have employed this approach to investigate the dynamics of energy transfer in the desorption of both weakly and strongly-chemisorbed species (O_2 and CO) and in a bimolecular reaction ($O + CO \rightarrow CO_2$) on the surface of Pd.

In particular, our studies of the ultrafast photooxidation of CO in mixed monolayers of O and CO represent an important step in developing our capabilities to time-resolve surface reactions. The subpicosecond 2PC relaxation times are consistent with the reaction taking place between proximate species in the mixed phase, in contradistinction to conditions that prevail during slow thermal excitation where the reactants are known to phase segregate. This suggests that this approach provides the means to take “snapshots” of the reaction by measuring the dynamics from well-defined initial surface structures. In addition, the photooxidation percentage yield is high: the oxidized percentage of the total desorption yield approaches $\sim 40\%$, roughly an order of magnitude greater than prior ultrafast reaction measurements on Ru(001). The high efficiency of the CO_2 channel opens the possibility of time-domain measurements of surface dynamics by time-resolved pump-probe surface spectroscopy.

We have also found that the presence of atomic oxygen strongly affects the photodesorption of CO, providing an attractive opportunity to study the effects of lateral adsorbate interactions. We have compared the CO desorption yield and dynamics for the 0.25 ML O + 0.5 ML CO system to that for pure 0.75 ML CO/Pd(111). The only difference between these two adlayers is the substitution of O for CO at the fcc three-fold hollow. Our measurements reveal a marked ~ 4.5 -fold enhancement in the CO photoyield (Fig. 1), which corresponds to a ~ 7 fold enhancement in the probability of CO desorption when O is present in the adlayer. This is remarkable given the structural similarity of these systems, and points to interesting coadsorbate lateral interactions.

We are currently building a case in support of the conclusion that the interactions responsible for this enhancement must be dynamic in nature and not the result of static changes in binding energy. Thus far we have been able to rule out the simplest explanation, namely that the presence of O destabilizes the CO. Significantly, TPD measurements (data not shown) and DFT calculations (Fig. 2) indicate that the binding at the most labile site—the top site—is not weakened by the presence of O. Thus, we have provisionally concluded that the enhanced desorption must be due to a dynamical increase in the energy coupling to the CO and/or decrease in the barrier to desorption. We hypothesize that the transfer of energy from the substrate to the CO is mediated by O atoms, which are more efficiently excited because they are lighter and more tightly bound. The nature of the energy exchange between the O and CO remains to be elucidated. We are currently considering further calculations simulations.

Pump-Probe Studies of Photodesorption and Photooxidation on $\text{TiO}_2(110)$ Surfaces. Measurements of the final state properties of gas-phase products are being used as a probe of the mechanism and dynamics of photodesorption and photooxidation on well-characterized $\text{TiO}_2(110)$ surfaces. This work is motivated by the widespread use of titania in technological applications where UV photooxidation is used for the degradation of organic materials. Our initial studies on the photodesorption of O_2 on reduced surfaces of $\text{TiO}_2(110)$ attempted to address long standing questions about which O_2 binding sites on the reduced $\text{TiO}_2(110)$ surface are photoactive, and how these are affected by the presence of surface defects and annealing temperature. The O_2 velocity distributions measured as a function of UV excitation energy and surface temperature provide direct evidence for the substrate-mediated hole-capture desorption mechanism and the presence of two photoactive sites of adsorbed oxygen.

Initial photooxidation studies have focused on the small ketones, acetone (CH_3COCH_3) and 2-butanone ($\text{CH}_3\text{CH}_2\text{COCH}_3$), adsorbed on a reduced $\text{TiO}_2(110)$ surface. Recent work by Henderson (PNNL) showed that these molecules are photochemically inactive in the absence of oxygen, but when co-adsorbed with oxygen form a thermally activated intermediate which is postulated to be a diolate species. The photoactive species (thiolate or ketone) decompose via direct ejection of an alkyl radical into the gas

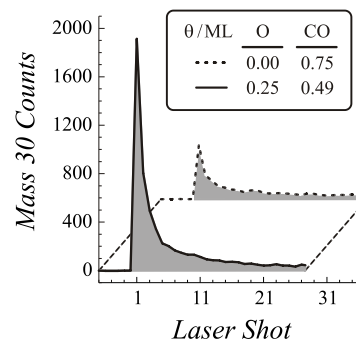


FIG. 1. Raw CO photodesorption data from (CO+O)/Pd(111) (foreground) and CO/Pd(111) showing a dramatic ~ 4.5 -fold increase in the desorption yield.

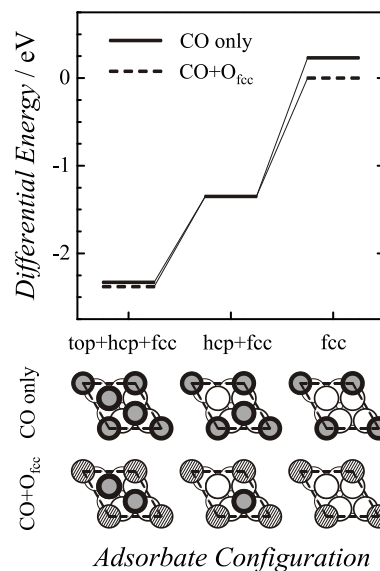


FIG. 2. DFT results for relative energies of CO adsorbed in various configurations with and without coadsorbed O atoms.

phase, e.g., a methyl radical (CH_3^\bullet) from acetone. Pump-probe measurements in our laboratory show that the average translational energy for the CH_3^\bullet from acetone is 0.15 eV which is markedly different than that observed in gas-phase photolysis of acetone (~ 0.6 eV). In the case of 2-butanone, we used a variety of VUV ionization wavelengths to conclusively show that other C_2 hydrocarbon products (ethane or ethylene) suggested by earlier experiments are due to fragmentation of the ethyl radical or background impurities. The translational energy distribution of the ethyl fragment ($\text{CH}_3\text{CH}_2^\bullet$) peaks at relatively low energy ($\langle E_t \rangle \sim 0.05$ eV). The relatively small translational energies observed for the radical products from surface photooxidation are more similar to that derived from dissociative ionization (DI) in the gas-phase, e.g., $\text{CH}_3\text{COCH}_3 \rightarrow \text{CH}_3\text{CO}^+ + \text{CH}_3 + e^-$. A qualitative link between hole-induced, unimolecular decomposition on surfaces and gas-phase DI may provide a useful framework for describing surface photooxidation processes analogous to the connection between $-\text{h}\nu$ electron chemistry on metals and dissociative electron attachment (DEA) in the gas-phase.

Two-Photon Photoemission Studies of Interfacial Electronic Structure. We have recently assembled a tunable ultrafast laser system for performing two-photon photoemission (2PPE) measurements for probing the electronic structure and $-\text{h}\nu$ electron dynamics of molecules and size-selected clusters deposited on surfaces. The strength of 2PPE is its ability to probe both the occupied and unoccupied resonant states of the adsorbate (cluster) and surface, and explore the time evolution of photoexcited states at the interface. For our initial studies, we used 2PPE to probe the valence band structure of chemisorbed thiophene ($\text{C}_4\text{H}_4\text{S}$) and 1,4-phenylenediisocyanide (PDI; $\text{C}\equiv\text{N}-\text{C}_6\text{H}_4-\text{N}\equiv\text{C}$) adsorbed on Au(111) which involve different kinds of molecular linkages to the Au surface (S–Au and $\text{N}\equiv\text{C}-\text{Au}$) that are relevant to charge transfer at molecular device interfaces.

Previous experiments and theory for thiophene and PDI on Au(111), respectively, indicate that the bonding geometries change with increasing coverage, primarily due to π -type intermolecular interactions. Due to the rigid structure of the thiophene ring, changes in the molecular orientation relative to the Au surface in turn modify the S–Au bonding interactions. As the coverage increases, the 2PPE spectra of thiophene/Au(111) show the emergence of a new photoelectron feature (S_u in Fig. 3) that can be assigned to an unoccupied state lying above the E_F . Based on thermal desorption data, the appearance of the S_u level corresponds to the formation of a compressed thiophene layer in which the molecular plane is tilted

further from the surface. Our DFT calculations suggest that the S_u state is mostly a LUMO orbital of the isolated thiophene molecule, which becomes less hybridized with the Au orbitals as the molecule tilts away from the surface. Preliminary 2PPE measurements for PDI/Au(111) show that the work function is strongly dependent on coverage and dosing/annealing temperatures, which clearly signal variations in molecular orientation or ordering. One of the more unusual observations is that a 2PPE feature (unoccupied state) only appears at low temperature (95 K), but only after annealing the PDI/Au(111) surface to room temperature. The annealing and re-cooling is also accompanied by a sharp decrease in the work function. These results point to a thermally induced configurational change of the PDI molecules, which becomes “locked-in” after annealing. We are currently pursuing additional DFT calculations in collaboration with Giulia Galli (UC Davis) to explore these phenomena. Time-resolved 2PPE

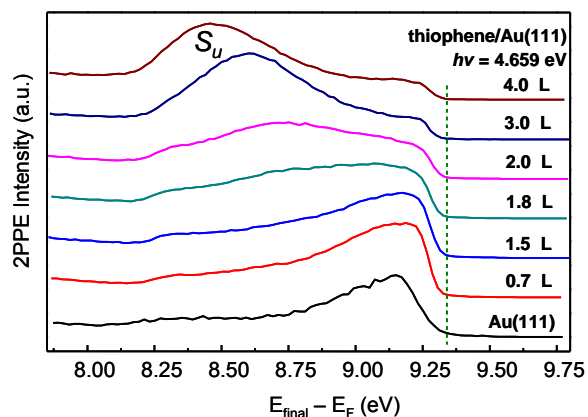


FIG. 3: 2PPE spectra of thiophene adsorbed on a Au(111) surface at 95 K as a function of exposure

measurements are currently underway to explore the time-evolution of the unoccupied levels in thiophene/Au(111) and PDI/Au(111) as a function of coverage and surface temperature.

3. Future Plans

Our planned work develops three interlinked themes: (i) the chemistry of supported nanoparticles and nanoclusters, (ii) the exploration of chemical dynamics on ultrafast timescales, and (iii) the photoinduced chemistry of molecular adsorbates. The investigations are motivated by the fundamental need to connect chemical reactivity to chemical dynamics in systems of relevance to catalytic processes—in particular metal and metal-compound nanoparticles and nanoclusters supported on oxide substrates. They are also motivated by fundamental questions of physical changes in the electronic and phonon structure of nanoparticles and their coupling to adsorbates and to the nonmetallic support that may alter dynamics associated with energy flow and reactive processes.

Ultrafast spectroscopy and photoinduced reaction experiments investigating the dynamics of vibrational energy relaxation as well as molecular desorption from (and reactions on) nanoparticles will address development of a fundamental understanding of the changes in surface reaction dynamics as the size of the metal substrate material is reduced from macroscopic (planar bulk surfaces) to the nanoscale. Size-dependent chemical dynamics will also be the focus of experiments using a cluster beam deposition instrument to prepare a range of supported, size-selected nanoclusters for structure and reactivity studies. The latter will be complemented by ultrafast 2PPE experiments to investigate the electronic structure and dynamics of the nanoclusters and molecular resonances involved in chemistry at their surfaces. Future studies of photoinduced processes on titania surfaces will explore the use of pump-probe techniques for elucidating molecular photooxidation mechanisms on titania and other oxide photocatalysts.

DOE-Sponsored Research Publications (2006–2009)

1. P. Liu, J.M. Lightstone, M.J. Patterson, J.A. Rodriguez, J.T. Muckerman and M.G. White, —Gas-phase interaction of thiophene with the $\text{Ti}_8\text{C}_{12}^+$ and Ti_8C_{12} met-car clusters,” *J. Phys. Chem. B*, **110**, 7449 (2006).
2. J. M. Lightstone, M. J. Patterson, P. Liu and M. G. White, —Gas-phase reactivity of the $\text{Ti}_8\text{C}_{12}^+$ met-car with triatomic sulfur-containing molecules: CS_2 , SCO , and SO_2 ,” *J. Phys. Chem. A*, **110**, 3505 (2006).
3. N. Camillone III, T. Pak, K. Adib, K.A. Khan and R.M. Osgood, Jr., —Tuning molecule-surface interactions with nanometer-thick covalently-bound organic overlayers,” *J. Phys. Chem. B*, **110**, 11334 (2006).
4. P. Szymanski, A.L. Harris and N. Camillone III, —Adsorption-state-dependent subpicosecond photoinduced desorption dynamics,” *J. Chem. Phys.*, **126**, 214709 (2007). (Note: Selected for the July 2007 issue of the *Virtual Journal of Ultrafast Science*.)
5. P. Szymanski, A.L. Harris and N. Camillone III, —Temperature-dependent electron-mediated coupling in subpicosecond photoinduced desorption,” *Surf. Sci.*, **601**, 3335 (2007).
6. P. Szymanski, A.L. Harris and N. Camillone III, —Temperature-dependent femtosecond photoinduced desorption in $\text{CO}/\text{Pd}(111)$,” *J. Phys. Chem. A*, **111**, 12524 (2007).
7. M. Lightstone, M. Patterson, J. Lofaro, P. Liu and M. G. White, —Characterization and reactivity of the Mo_4S_6^+ cluster deposited on $\text{Au}(111)$,” *J. Phys. Chem. C*, **112**, 11495 (2008).
8. M. Patterson, J. M. Lightstone and M. G. White, —Structure of molybdenum and tungsten sulfide M_xS_y^+ clusters: experiment and DFT calculations,” *J. Phys. Chem. A*, **112**, 12011 (2008).
9. P. Szymanski, A.L. Harris and N. Camillone III, —Efficient subpicosecond photoinduced surface chemistry: The ultrafast photooxidation of CO on palladium,” *J. Phys. Chem. C*, **112**, 15802 (2008).
10. D. Sporleder, D. Wilson, R. J. Beuhler and M. G. White, —Dynamics of O_2 photodesorption from $\text{TiO}_2(110)$,” *J. Phys. Chem. C*, **113**, 13180 (2009).

^a Principal Investigator; ^b Collaborating Investigator

Ionic Liquids: Radiation Chemistry, Solvation Dynamics and Reactivity Patterns

James F. Wishart

Chemistry Department, Brookhaven National Laboratory, Upton, NY 11973-5000

wishart@bnl.gov

Program Definition

Ionic liquids (ILs) are a rapidly expanding family of condensed-phase media with important applications in energy production, nuclear fuel and waste processing, improving the efficiency and safety of industrial chemical processes, and pollution prevention. ILs have low volatilities and are combustion-resistant, highly conductive, recyclable and capable of dissolving a wide variety of materials. They are finding new uses in chemical synthesis, catalysis, separations chemistry, electrochemistry and other areas. Ionic liquids have dramatically different properties compared to conventional molecular solvents, and they provide a new and unusual environment to test our theoretical understanding of primary radiation chemistry, charge transfer and other reactions. We are interested in how IL properties influence physical and dynamical processes that determine the stability and lifetimes of reactive intermediates and thereby affect the courses of reactions and product distributions. We study these issues by characterization of primary radiolysis products and measurements of their yields and reactivity, quantification of electron solvation dynamics and scavenging of electrons in different states of solvation. From this knowledge we wish to learn how to predict radiolytic mechanisms and control them or mitigate their effects on the properties of materials used in nuclear fuel processing, for example, and to apply IL radiation chemistry to answer questions about general chemical reactivity in ionic liquids that will aid in the development of applications listed above.

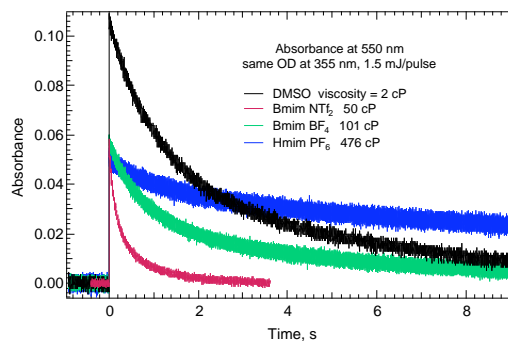
Very early in our radiolysis studies it became evident that the slow solvation dynamics of the excess electron in ILs (which vary over a wide viscosity range) increase the importance of pre-solvated electron reactivity and consequently alter product distributions and subsequent chemistry. This difference from conventional solvents has profound effects on predicting and controlling radiolytic yields, which need to be quantified for the successful use under radiolytic conditions. Electron solvation dynamics in ILs are measured directly when possible and estimated using proxies (e.g. coumarin-153 dynamic emission Stokes shifts or benzophenone anion solvation) in other cases. Electron reactivity is measured using ultrafast kinetics techniques for comparison with the solvation process.

Methods. Picosecond pulse radiolysis studies at BNL's Laser-Electron Accelerator Facility (LEAF) are used to identify reactive species in ionic liquids and measure their solvation and reaction rates. IL solvation and rotational dynamics are measured by TCSPC and fluorescence upconversion measurements in the laboratory of E. W. Castner at Rutgers Univ. Investigations of radical species in irradiated ILs are carried out at ANL by I. Shkrob and S. Chemerisov using EPR spectroscopy. Diffusion rates are obtained by PGSE NMR in S. Greenbaum's lab at Hunter College, CUNY and by Castner's group at Rutgers. Professor Mark Kobrak of CUNY Brooklyn College performs molecular dynamics simulations of solvation processes. A collaboration with M. Dietz at U. Wisc. Milwaukee is centered around the properties and radiolytic behavior of ionic liquids for nuclear separations. Collaborations with C. Reed (UC Riverside), D. Gabel (U. Bremen) and J. Davis (U. South Alabama) are aimed at characterizing the radiolytic and other properties of borated ionic liquids, which could be used to make fissile material separations processes inherently safe from criticality accidents.

Ionic liquid synthesis and characterization. Our work often involves novel ILs that we design to the requirements of our radiolysis and solvation dynamics studies and are not commercially available. We have developed in-house capabilities and a network of collaborations to design, prepare and characterize ILs in support of our research objectives. Cation synthesis is done with a CEM microwave reactor, resulting in higher yields of purer products in much shorter time than traditional methods. We have assembled an instrumentation cluster including DSC, TGA, viscometry, AC conductivity and Karl Fischer moisture determination. The cluster serves as a resource for our collaborators in the New York Regional Alliance for Ionic Liquid Studies and other institutions (Penn State, ANL). Our efforts are substantially augmented by student internships from the BNL Office of Educational Programs, particularly the FaST program, which brings collaborative faculty members and their students into the lab for ten weeks each summer. Since 2003, a total of 27 undergrads, two graduate students, one pre-service teacher, one high school student and three junior faculty have worked on IL projects in our lab.

Recent Progress

Cage escape and recombination in ILs. Another aspect of photoinduced reactivity in ILs is relevant to the general case of bimolecular reactions. With Prof. V. Strehmel (U. Potsdam) and D. Polyanskiy (BNL), we measured cage escape yields and geminate recombination rates of lophyl radicals formed by the photolysis of *ortho*-chloro-hexaarylbisimidazole (*o*-Cl-HABI) in ionic liquids of varying viscosities and compared them with the well-characterized case of *o*-Cl-HABI in DMSO. The figure shows that cage escape (indicated by the initial absorbance of the lophyl radical) is reduced in the ILs compared to DMSO, indicating longer cage retention times in the ILs, which facilitate recombination. As expected, recombination in the ILs gets slower with increasing viscosity, yet comparison of the kinetics for butylmethylimidazolium NTf₂ with DMSO (25x less viscous) indicates that lophyl radical recombination seems to be promoted by the IL environment, possibly through transition state stabilization. Further work is underway.



Dissociative electron attachment in ionic liquids. In collaboration with Prof. Yusuke Heijima (Kanazawa U.), rates of halide ion detachment subsequent to electron capture were measured for a series of aryl halides. The rate constants were similar to or up to 2x faster than in 1-methyl-2-pyrrolidone. It was found that C4mpyrr dicyanamide is an effective IL solvent for the suppression of hole-derived transients and the investigation of electron-derived species. Also, in C4mpyrr NTf₂, the ultrafast DEA process in 2-bromobiphenyl allows the electron to be irreversibly scavenged without the creation of an absorbance feature in the visible, while at the same time producing 2-bromobiphenyl radical cations from hole capture. This will permit the quantification of hole yields and make it easier to follow their subsequent chemistry. One of our objectives in fundamental IL radiation chemistry is to be able to control the yields of oxidizing and reducing species to facilitate broader studies of chemical reactivity in ILs, in the same way that water radiolysis was converted into an experimental tool decades ago.

Potential formation of imidazole radical dimers in ionic liquids. In our earlier collaborative work with I. A. Shkrob of ANL, the radiolysis of imidazolium ILs yielded EPR spectra that did not agree with the theoretical spectrum of the imidazolium cation electron adduct Rmim•. Subsequent calculations suggested that Rmim• develops a strong distortion from planarity and may form a dimer radical cation (Rmim)₂^{•+} by attachment to an imidazolium cation. This reactivity would help explain some products identified by ESI/MS analysis of γ -irradiated ILs by the French CEA group studying ILs for nuclear separations. Experiments at LEAF revealed two intermediate species in the radiolysis of C₂mim NTf₂ that had not been observed previously for lack of time resolution. Our calculations predict Raman and IR spectra for the radical dimer cation and we hope to use our developing vibrational spectroscopy capabilities at LEAF to identify the observed intermediates.

Future Plans

Electron solvation and pre-solvated reactivity in ionic liquids. The competition between the electron solvation and electron capture processes in ionic liquids will be explored to test the validity of pre-solvated electron scavenging mechanisms advanced in the literature and to learn how these reactivity patterns can be controlled or exploited for diverse purposes. Electron solvation dynamics in several families of ILs will be measured by Vis-NIR pulse-probe radiolysis and optical fiber single-shot spectroscopy (OFSS) detection developed at BNL by Andrew Cook. However, electron solvation in some interesting families of ionic liquids cannot presently be studied by those methods because the ILs are too viscous to flow for pulse-probe and OFSS detection capability in the NIR awaits the acquisition and installation of appropriate area detectors.

Therefore, solvation phenomena in ionic liquids is also being investigated through the time-resolved absorption spectral shift of the highly solvatochromic benzophenone anion as well as time-resolved fluorescence Stokes shifts of solvatochromic dyes (e.g. coumarin 153). The spectral range of the presently operational OFSS system is well suited for the benzophenone experiments. In preliminary work, OFSS was used to observe benzophenone anion solvation in C₄mpyrr NTf₂ and MeBu₃N NTf₂ at selected wavelengths. The trend of solvation being slower in the higher-viscosity ionic liquid is seen in the neighboring graph, but quantification of the solvation dynamics requires a full spectral analysis from future experiments. Planned technical improvements to the OFSS system will facilitate

these measurements. Our experimental work will be supported by molecular dynamics simulations performed by Profs. Mark KobraK of CUNY and Claudio Margulis of U. Iowa.

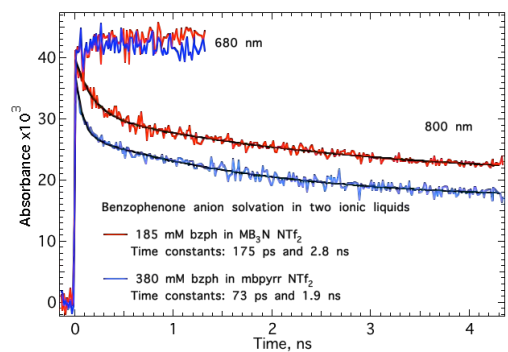
In a parallel series of experiments, scavengers will be added to measure the kinetics of pre-solvated electron capture directly when the ultrafast radiolysis techniques can be applied and indirectly by product yields when they cannot. The characterization of electron solvation dynamics referred to above is essential to proper interpretation of the scavenging kinetics data.

It is well known from work in molecular solvents that many scavengers, for example SeO_4^{2-} and NO_3^- to name two extremes, have widely different reactivity profiles towards pre-solvated and solvated electrons. The solubility characteristics of ionic liquids will permit direct comparison of inorganic and organic scavengers that are not normally soluble in the same solvent system at high enough concentrations to scavenge pre-solvated electrons.

In preliminary experiments we used OFSS to monitor electron capture by benzophenone, Cd^{2+} and NO_3^- at varying concentrations in $\text{C}_4\text{mpyrr NTf}_2$. As the concentrations of benzophenone or Cd^{2+} increase the spectral blue shift associated with the electron solvation process disappears, indicating that these scavengers react efficiently with pre-solvated electrons. In contrast, NO_3^- does not show that effect. By quantitative measurement of the scavenging profiles of many reactants, we seek to provide a mechanistic basis for understanding excess electron scavenging that can be applied to real-world applications such as predicting radiolytic product distributions during the processing of radioactive materials and guiding the deliberate addition of reactants to reduce radiolytic damage, or conversely, to maximize yields of desired products.

EXAFS studies of structure and reaction dynamics in ionic liquids. In collaboration with R. Crowell, D. Polyanskiy and R. Musat, we are using Br EXAFS to study IL structure and Br^- ion solvation environment in neat and diluted bromide ionic liquids and the effect of solutes. We will use photoionization coupled with time-resolved EXAFS to probe the solvation dynamics of Br^0 atoms in ILs and the effect of the ionic liquid environment on the $\text{Br}^- + \text{Br}^0 \rightarrow \text{Br}_2^-$ reaction. The results can be applied to understanding related iodide systems of interest in solar photoconversion.

Development of Vibrational Spectroscopies at LEAF. Until recently the detection of short-lived species generated by pulse radiolysis at LEAF has relied primarily upon absorption or emission spectroscopy in the UV-visible-NIR regions. Although these methods afford excellent kinetic information, structural identification of intermediates for the elucidation of reaction pathways can be inconclusive in many cases. Time-resolved vibrational spectroscopic (TRVS) detection methods (both IR and Raman) offer highly specific molecular and structural characterization. We are therefore in the process of implementing time-resolved infrared (TRIR) and time-resolved resonance Raman (TR^3) detection systems for pulse radiolysis. The successful coupling of these techniques with pulse radiolysis will add a powerful new dimension to our research and enable a wide variety of investigations (in collaboration with A. Cook, D. Polyansky, D. Grills, J. Preses and K. Iwata).



Publications on ionic liquids

1. *Radiation Chemistry of Ionic Liquids* J. F. Wishart, A. M. Funston, and T. Szreder in "Molten Salts XIV, Proceedings of the 2004 Joint International Meeting of the Electrochemical Society, Honolulu, HI, 2004", R. A. Mantz, et al., Eds.; The Electrochemical Society, Pennington, NJ, 2006, pp. 802-813. (ISBN 1-56677-514-0)
2. *Tetraalkylphosphonium polyoxometalates: electroactive, "task-specific" ionic liquids* P. G. Rickert, M. R. Antonio, M. A. Firestone, K.-A. Kubatko, T. Szreder, J. F. Wishart, and M. L. Dietz *Dalton Trans.* **2006**, 529-531 (2006).
3. *The Physical Chemistry of Ionic Liquids (Editorial for Special Issue)* J. F. Wishart, and E. W. Castner, *J. Phys. Chem. B*, **111**, 4639-4640 (2007).
4. *Tetraalkylphosphonium Polyoxometalate Ionic Liquids: Novel, Organic-Inorganic Hybrid Materials*, P. G. Rickert, M. P. Antonio, M. A. Firestone, K.-A. Kubatko, T. Szreder, J. F. Wishart, and M. L. Dietz, *J. Phys. Chem. B*, **111**, 4685-4692 (2007).

5. *Intermolecular Interactions and Dynamics of Room Temperature Ionic Liquids that have Silyl- and Siloxy-Substituted Imidazolium Cations* H. Shirota, J. F. Wishart, and E. W. Castner, Jr., *J. Phys. Chem. B*, **111**, 4819-4829 (2007) DOI: 10.1021/jp067126o. *17th Most-Cited Article for 2007, *J. Phys. Chem. B*.
6. *Nuclear Magnetic Resonance Study of the Dynamics of Imidazolium Ionic Liquids with $-CH_2Si(CH_3)_3$ vs $-CH_2C(CH_3)_3$ Substituents* S. H. Chung, R. Lopato, S. G. Greenbaum, H. Shirota, E. W. Castner, Jr. and J. F. Wishart, *J. Phys. Chem. B*, **111**, 4885-4893 (2007).
7. *Fluorescence Probing of Temperature-Dependent Dynamics and Friction in Ionic Liquid Local Environments* A. M. Funston, T. A. Fadeeva, J. F. Wishart, and E. W. Castner, *J. Phys. Chem. B*, **111**, 4963-4977 (2007) DOI:10.1021/jp068298o. *Fifth Most-Cited Article for 2007, *J. Phys. Chem. B*.
8. *The Initial Stages of Radiation Damage in Ionic Liquids and Ionic Liquid-Based Extraction Systems* I. A. Shkrob, S. D. Chemerisov, and J. F. Wishart, *J. Phys. Chem. B*, **111**, 11786-11793 (2007).
9. *Intermolecular Dynamics, Interactions and Solvation in Ionic Liquids* E. W. Castner, Jr., J. F. Wishart, and H. Shirota, *Acc. Chem. Res.* **40**, 1217-1227 (2007).
10. *Physical Properties of Ionic Liquids Consisting of the 1-Butyl-3-Methylimidazolium Cation with Various Anions and the Bis(trifluoromethylsulfonyl)imide Anion with Various Cations* H. Jin, B. O'Hare, J. Dong, S. Arzhantsev, G. A. Baker, J. F. Wishart, A. J. Benesi, and M. Maroncelli *J. Phys. Chem. B* **112**, 81-92 (2008).
11. *Trialkylammonio-Dodecaborates: Anions for Ionic Liquids with Potassium, Lithium and Proton as Cations* E. Justus, K. Rischka, J. F. Wishart, K. Werner and D. Gabel, *Chem. Eur. J.*, **14**, 1918-1923 (2008).
12. *Kinetic Salt Effects on an Ionic Reaction in Ionic Liquid/Methanol Mixtures - Viscosity and Coulombic Screening Effects* K. Takahashi, H. Tezuka, T. Sato, Y. Katsumura, M. Watanabe, R. A. Crowell, and J. F. Wishart, *Chemistry Letters*, **38**, 236-237 (2009).
13. *Charge trapping in imidazolium ionic liquids* I. A. Shkrob and J. F. Wishart, *J. Phys. Chem. B*, **113**, 5582-5592 (2009).
14. *Energy applications of ionic liquids* J. F. Wishart, *Energy Environ. Sci.*, **2**, 956 - 961 (2009).
15. *Synthesis, characterization and radiolytic properties of bis(oxalato)borate containing ionic liquids* S. I. Lall-Ramnarine, A. Castaño, G. Subramaniam, M. F. Thomas, and J. F. Wishart, *Radiat. Phys. Chem.*, **78**, 1120-1125 (2009).
16. *Photo-detrapping of solvated electrons in an ionic liquid* K. Takahashi, K. Suda, T. Seto, Y. Katsumura, R. Katoh, R. A. Crowell, J. F. Wishart, *Radiat. Phys. Chem.*, **78**, 1129-1132 (2009).
17. *Recombination of Photogenerated Lophyl Radicals in Imidazolium-Based Ionic Liquids* V. Strehmel, J. F. Wishart, D. E. Polyansky, and B. Strehmel, *ChemPhysChem* **10**, in press (2009).
18. *The radiation chemistry of ionic liquids and its implications for their use in nuclear fuel processing*, J. F. Wishart and I. A. Shkrob in "Ionic Liquids: From Knowledge to Application," Rogers, R. D.; Plechkova, N. V.; Seddon, K. R., Eds. *ACS Symp. Ser.*, Amer. Chem. Soc.: Washington, in press.
19. *Radiation Chemistry and Photochemistry of Ionic Liquids*, K. Takahashi and J. F. Wishart in "Charged Particle and Photon Interactions with Matter" Y. Hatano, Y. Katsumura and A. Mozumder, Eds. Taylor & Francis, in press.

Publications on other subjects

20. *Reactivity of Acid Generators for Chemically Amplified Resists with Low-Energy Electrons* A. Nakano, T. Kozawa, S. Tagawa, T. Szreder, J. F. Wishart, T. Kai and T. Shimokawa, *Jpn. J. Appl. Phys.*, **45**, L197 (2006).
21. *Pulse radiolysis and steady-state analyses of the reaction between hydroethidine and superoxide and other oxidants* J. Zielonka, T. Sarna, J. E. Roberts, J. F. Wishart, B. Kalyanaraman, *Arch. Biochem. Biophys.*, **456**, 39-47 (2006).
22. *Conformational Analysis of the Electron Transfer Kinetics across Oligoproline Peptides Using N,N-dimethyl-1,4-benzenediamine Donors and Pyrene-1-sulfonyl Acceptors* J. B. Issa, A. S. Salameh, E. W. Castner, Jr., J. F. Wishart and S. S. Isied, *J. Phys. Chem. B*, **111**, 6878-6886 (2007).
23. *Tools for radiolysis studies*, J. F. Wishart in "Radiation chemistry: from basics to applications in material and life sciences" Spothem-Maurizot, M., Douki, T., Mostafavi, M., and Belloni, J., Eds.; L'Actualité Chimique Livres, Paris, (2008) Ch. 2, pp. 17-33.

Electronically non-adiabatic interactions in molecule metal-surface scattering: Can we trust the Born-Oppenheimer approximation in surface chemistry?

Alec Wodtke, Dept. of Chem. Biochem., UCSB, Santa Barbara CA 93106
wodtke@chem.ucsb.edu

Program Scope or Definition

Today, we can expect that research and development aimed at improving heterogeneous catalysis will lead to important new technologies with potentially profound energy implications. Within this context, developing a predictive understanding of heterogeneous catalysis is one of the most exciting challenges of modern chemical research. A detailed, accurate and predictive understanding will require a first principles theory of chemical reactions and molecular interactions at interfaces, especially gas/solid and liquid/solid interfaces, which represent the important atomistic processes underlying heterogeneous catalysis. Much progress has been made in recent years using electronically adiabatic electronic structure theory usually combining Density Functional Theory with quantum or classical dynamics and more recently using first principles derived micro-kinetic reaction rates. Essential to the electronically adiabatic picture of molecular events at interfaces is the concept of the potential energy surface (PES), first demonstrated by H. Eyring and M. Polanyi, which relies on the Born-Oppenheimer Approximation (BOA). In this approach one assumes that electronic excitation does not occur due to the (much slower time-scale) motion of heavy nuclei. The limits of the BOA are well-tested for gas-phase reactions and at least for some situations, like conical intersections and avoided crossings, theoretical approaches to treating BOA breakdown are well worked out. In other gas-phase cases where the BOA is good, the electronically adiabatic approach has led to spectacular quantitative agreement between experiment and theory. Our ability to treat BOA breakdown in gas surface collisions is not so well worked out or heavily studied. Furthermore, there is growing evidence that BOA break-down can be quite important for molecular interactions at metal surfaces.

Our laboratory has been responsible for producing some of the most compelling evidence of BOA break-down in gas surface interactions. Highly vibrationally excited NO($v=15$) undergoes multi-quantum vibrational relaxation in direct scattering collisions with Au(111) producing NO($v=8$) with highest probability but scatters predominantly in the vibrationally elastic channel from LiF - an insulator.. Vibrationally excited NO can promote electron emission from a low work function solid when the vibrational energy exceeds the work function and the probability of electron emission increases rapidly with decreasing NO velocity, suggesting vibrational promotion of electron excitation may be important for surface adsorbates. Also in NO-Au collisions, vibrational relaxation results in less rotational excitation than vibrationally elastic channels, an observation that has been taken as indicative of an orientation effect in electronically nonadiabatic coupling.

Recent Progress

We have successfully implemented an IR-UV double resonance methodology into our DOE funded surface scattering experiment. This significantly improves our experimental capability as it allows true state-to-state experiments to be carried out revealing among other things the translational inelasticity of the collision, i.e. the amount of translational energy taken up by the surface in molecule surface collisions. For the case of HCl scattering from Au(111), an infrared pulse of laser light excites a molecular beam cooled sample of HCl from $v=0$ to $v=2$ via the R(0) line, exclusively producing HCl($v=2, J=1$). After scattering from the surface, the state distribution of the HCl is probed by REMPI. Rotational redistribution is easily seen by probing the rotational quantum levels of HCl($v=2$). We configure a quantum-state resolved velocimeter by separating the PUMP and PROBE laser beams by a known distance and varying the delay time between the two pulses. A set of two alignment jigs mounted to

translation stages allows us to rapidly switch back and forth between a configuration for measuring the incident velocity of the molecular beam and one for measuring the velocity of scattered HCl molecules.

This experimental configuration allows a number of interesting experiments. For example, vibrational relaxation and the associated translational energy release can be seen simply by tuning the REMPI laser to detect HCl($v=1, J$). State-to-state scattering angular distributions can be obtained by moving the REMPI laser beam parallel to the surface at a finite distance. Perhaps most importantly, state-to-state time-of-flight (TOF) measurements can be carried out, which reveal the translational inelasticity associated with each quantum state resolved scattering channel. Translational inelasticity is by definition, the amount of initial translational energy transferred to excitation of the solid or internal excitation of the molecule. For state-to-state experiments, the internal excitation is known and we can deduce the energy transferred to excitation of the solid. This is the underlying physical quantity governing trapping and for molecules, it cannot be measured without a true-state-to-state experiment like the one presented here.

Using different seed ratios and carrier gases, we could vary the incidence energy from $0.25 \text{ eV} \leq E_i \leq 1.25 \text{ eV}$. Translationally inelastic scattering measurements were then made for a variety of final rotational and vibrational states. These experiments point out several interesting facts. First, the experimentally derived translational energy distributions are more energetic than a Maxwell-Boltzmann translational energy distribution at the surface temperature. This result is consistent with a direct scattering mechanism for which there is copious additional evidence. Second, for both vibrationally elastic as well as inelastic (relaxation) channels, a large fraction of the incidence energy is missing, having been converted to excitations of the solid. Third, the translational energy distribution of the vibrationally inelastic channel is only slightly more energetic than that of the vibrationally elastic channel; it is also slightly broader. Fourth, a perhaps naïve expectation that all of the vibrational energy release would appear as additional translation beyond that exhibited by the vibrationally elastic channel is not even approximately fulfilled. Results like these were obtained for seven incidence energies and (for two incidence energies) at several surface temperatures between 200 and 1000 K. In all cases, the four points just described also apply. The rotational state and surface temperature dependence measured for $E_i = 0.52 \text{ eV}$ were found to be both weak and no further discussion is necessary.

These experiments indicate that for both the vibrationally elastic and inelastic relaxation scattering channels, an average of 56% of the translational energy of incidence is transferred to the surface. Furthermore, this efficient translational excitation of the solid extends over the entire range of incidence energies studied. The “extra” translational energy appearing due to vibrational relaxation corresponds to only ~26% of the vibrational energy released. Interestingly, we see that the vibrational energy being liberated to translation when HCl vibrationally relaxes in a ($v=2 \rightarrow 1$) transition, is independent of the incidence energy.

Translational inelasticity can also be measured for the vibrational ground state employing a simple experimental insight. Consider a molecular beam of HCl incident upon a Au(111) surface. Prior to the collision, essentially all of the molecules are in the $v=0, J=0$ state. After collision with the surface, rotational redistribution is the highest probability process producing significant population in all rotational states up to about $J=8$, depending on the incidence energy. If we use the infrared laser to excite HCl($v=0 \rightarrow 2$) via, for example, the R(4) line at the proper time, we selectively excite vibrational ground state molecules that have collided with the surface and suffered a $J=0 \rightarrow 4$ collisional transition. If we probe the HCl($v=2, J=5$) molecules downstream with REMPI, we selectively obtain the TOF of those molecules. Indeed we can use this “trick” to measure the velocity of any rotational channels in the $v=0-0$ vibrationally elastic channel.

This allows us to directly compare the translational elasticity of the $v=2-2$ channel to the $v=0-0$ channel. It is notable that there is no experimentally meaningful difference in the translational inelasticity for these two vibrational channels. We may also compare the translational energy distributions to two limiting models: The “simple” and “attractive” Baule model. The simple Baule model removes all Au-Au interactions in the solid and considers the translational energy transfer in a purely impulsive zero-impact parameter collision between an HCl molecule of mass $m_1=36$ and a Au atom of mass $m_2 = 198$.

$$E_s = \frac{(m_1 - m_2)^2}{(m_1 + m_2)^2} E_I$$

This is equivalent to the well-known impulsive cube model with an effective surface mass set to a single surface atom. The maximal influence of the attractive interaction well between the HCl and Au(111) can be included in an “attractive” version of the Baule model. Here one assumes that the molecule is accelerated by an energy equal to the well depth, before the impulsive collision with an isolated gold atom.

$$E_s = \frac{(m_1 - m_2)^2}{(m_1 + m_2)^2} E_I - \left[1 - \frac{(m_1 - m_2)^2}{(m_1 + m_2)^2} \right] D_0$$

This model provides an estimate of the upper limit to the mechanical energy transfer possible between an HCl molecule and a solid gold target. The experiments reveal that a large fraction of the HCl collisions transfer more translation energy into the solid than can be explained by this limiting mechanical picture. This is strong albeit indirect evidence that translational excitation of electron-hole pairs is important to defining the translational inelasticity in HCl - Au(111) collisions.

We have also successfully applied this IR-UV double resonance approach to the state-to-state scattering of NO from Au(111). Here, we prepare single ro-vibrational quantum levels of NO in $v=3$. Scattering from Au(111) is followed by 1+1 REMPI detection. Figure 6 shows the derived translational energy distributions for the vibrationally elastic (open circles) and inelastic (closed circles) channel, respectively. Similar to HCl/Au scattering, both channels exhibit large translational inelasticity suggesting the importance of translational excitation of electron hole pairs in the metal. We also see that the extra translational energy released in the vibrational relaxation channel is small – ~7% of the vibrational energy loss. The efficiency of conversion of vibrational to translational energy is even lower here than in HCl. More extensive studies will be performed on this in the near future.

Also, during this funding period we have carried out preliminary measurements of multi-quantum vibrational excitation in NO collisions with Au(111). Here a molecular beam of NO with an incidence energy of ~1 eV is scattered from a Au(111) surface at a controlled and variable temperature. We detect vibrationally excited molecules recoiling from the surface in $v=1, 2$ and 3. Figure 7 shows the surface temperature dependence of the vibrational excitation probability obtained in our lab. The results are plotted on an Arrhenius-type plot and the effective activation energy is seen to increase dramatically with the increasing energy of the vibrational state produced in the collision. These results are entirely different than previous work of Kay et al. where multi-quantum vibrational excitation of the low frequency umbrella mode in NH_3 was observed and attributed to a mechanical mechanism. In that work vibrational up-pumping was nearly independent of surface temperature and theoretical simulations assuming an electronically adiabatic mechanism were able to capture the key experimental observables.

Future work

The major intention of work funded under this grant has been to examine the underlying assumptions of modern theoretical surface chemistry and to stimulate more sophisticated approaches to electronically non-adiabaticity. Recently, Tully has described a new approach called independent electron surface hopping – IESH. This is a mixed quantum classical approach which allows electronic excitation (and de-excitation) to be treated quantum mechanically as “hops” between electronic adiabats, while heavy atom motion – including adsorbate and surface atoms – is treated classically.

Initial applications of this theory show reasonable agreement with experimental observations and the results are sufficiently encouraging that predictions of this theory should be taken seriously and tested experimentally. A major part of the next three years’ efforts will be to perform experiments that test key

predictions of the IESH theory. In particular a means to test the predictions of importance of steric effects in the NO Au(111) scattering system using Fourier transform limited pulsed laser excitation will be developed and implemented. Testing the provocative prediction that NO($v=15$) does not trap at any incidence energy is another fascinating part of the next funding period's efforts.

References

1. *Direct translation-to-vibrational energy transfer of HCl on Gold: Measurement of absolute vibrational excitation probabilities*, Qin Ran, Daniel Matsiev, Daniel J. Auerbach, Alec M. Wodtke, Proceedings of the 16th International Workshop on Inelastic Ion-Surface Collisions; Nuclear Instruments and Methods in Physics Research, Section B: Beam Interactions with Materials and Atoms (NIMB) **258**(1) 1-6 (2007)
2. *Change of vibrational excitation mechanism in HCl/Au collisions with surface temperature: transition from electronically adiabatic to non-adiabatic behavior*, Q. Ran, D. Matsiev, D. J. Auerbach, A. M. Wodtke, Physical Review Letters **98**(23), 237601 (2007)
3. *An advanced molecule-surface scattering instrument for study of vibrational energy transfer in gas-solid collisions*, Qin Ran, Daniel Matsiev, Daniel J. Auerbach, Alec M. Wodtke Rev. Sci. Instr. **78**, 104104 (2007)
4. *Energy Transfer and Chemical Dynamics at Solid Surfaces: The Special Role of Charge Transfer*, Alec M. Wodtke, Daniel Matsiev, Daniel J. Auerbach, invited review for Progress in Surface Science, **83**(3), 167-214 (2008).
5. *Efficient vibrational and translational excitation of a solid metal surface: State-to-state time-of-flight measurements of HCl ($v=2, J=1$) scattering from Au (111)*, Igor Rahinov, Russell Cooper, Cheng Yuan, Xueming Yang, Daniel J. Auerbach, Alec M. Wodtke, J. Chem. Phys. **129** 214708 (2008)
6. *Efficient translational excitation of a solid metal surface: State-to-state translational energy distributions of vibrational ground state HCl scattering from Au(111)* Russell Cooper, Igor Rahinov, Cheng Yuan, Daniel J. Auerbach, Xueming Yang, Alec M. Wodtke, J. Vac. Sci. Tech. A **27**(4) 907-912, (2009) DOI 10.1116/1.3071971

Molecular level understanding of hydrogen bonding environments

Sotiris S. Xantheas

Chemical & Materials Sciences Division, Pacific Northwest National Laboratory
902 Battelle Blvd., Mail Stop K1-83, Richland, WA 99352
sotiris.xantheas@pnl.gov

The objective of this research effort is to develop a comprehensive understanding of the collective phenomena associated with aqueous solvation. The molecular level details of aqueous environments are central in the understanding of important processes such as reaction and solvation in a variety of homogeneous and heterogeneous systems. The fundamental understanding of the structural, thermodynamic and spectral properties of these systems is relevant to the solvation in aqueous solutions, the structure, reactivity and transport properties of clathrate hydrates, in homogeneous catalysis and in atmospheric processes.

The motivation of the present work stems from the desire to establish the key elements that describe the structural and associated spectral features of simple ions in a variety of hydrogen bonded environments such as bulk water, aqueous interfaces and aqueous hydrates. In particular, solid hydrates of salts containing a fixed ratio of water molecules in their crystal structures have attracted special interest due to their importance in geology, chemistry, and physics. The quest for deciphering the properties of hydrogen bonds makes those materials ideal candidates for studying the spectral signatures of water in different, well-defined environments with varying bonding partners and distances.

We have carried out molecular dynamics simulations with polarizable interaction potentials in order to understand the solvation structure of chloride and iodide anions in bulk and interfacial water, showing qualitative similarities between the first solvation shell structures at the interface and bulk. For the more polarizable iodide, its solvation structure was more anisotropic than chloride, and this trend persisted at both the interface and in the bulk (see Fig. 1). The anisotropy of the solvation structure correlated with polarizability, but it was also found to inversely correlate with anion size. When polarizability was reduced to near zero, a very small anisotropy in the water solvation structure around the ion still persisted. Polarizable anions were found to have on average an induced dipole in the bulk that was significantly larger than zero. This induced dipole resulted in the water hydrogen atoms having stronger interactions with the anions on one side of them, in which the dipole was pointing at. In contrast, the other side of the anions, in which the induced dipole was pointing away from, had fewer water molecules present and, for the case of iodide, was rather devoid of water molecules all together at both the interface and in the bulk. This region formed a small cavity in the bulk, while at the air-water interface was simply part of the air interface. In the bulk, this small cavity may be viewed as somewhat hydrophobic, and the need for the extinction of this cavity may be one of the major driving forces for polarizable anions to reside at the air-water interface.

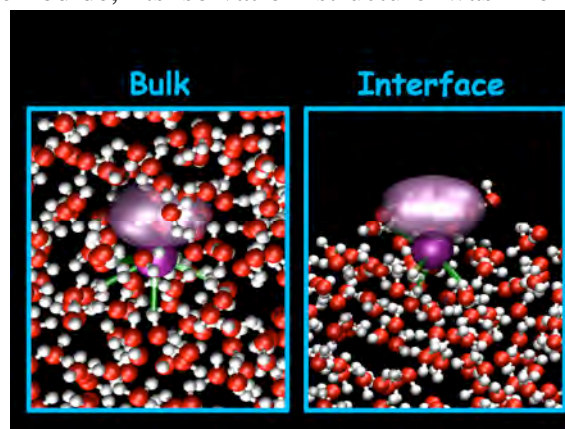


Figure 1: The asymmetric solvation of Iodide in the bulk and the aqueous interface

We plan to extend the development of the family of TTM potentials to describe interactions between water and metal (Li^+ , Na^+ , K^+ , Rb^+ , Cs^+) as well as halide (F^- , Cl^- , Br^- , I^-) ions. The ion-water interactions will be parametrized from high level electronic structure calculations following the same protocol that was previously used for the water-water interactions. Special emphasis will be paid on reproducing the experimentally measured IR spectra in the hydrogen bonded stretching region. We plan to simulate the IR spectra of hydrates of aqueous salts (measured at the group of Prof. Laubereau in the TU of Munich at Garching) with the obtained potentials.

Hydrate crystal structures are water scaffolds held together by hydrogen bonds acting as ‘host’ lattices that can trap ‘guest’ molecules such as H_2 , Cl_2 , Br_2 , SO_2 , H_2S and CH_4 within their cages via weak van der Waals interactions. The potential importance of clathrate hydrates – the combination of the host lattice and the guest molecules – as inclusion compounds relevant to renewable energy (i.e. molecular hydrogen storage devices) has been recently emphasized. A bottleneck in the modeling of those networks lies with the existence of a plethora $[(3/2)^N]$ of possible isomers satisfying the Bernal-Fowler ice rules based on the position of the Hydrogen atoms. For example, for the pentagonal dodecahedron (5^{12}) isomer of the $(\text{H}_2\text{O})_{20}$ water cluster (D-cage), Singer and co-workers have previously enumerated a total of 30,026 networks for a fixed position of the oxygen atoms. However, there has been no work to-date regarding the 3,043,836 networks of the larger tetrakaidecahedron (T-cage, $5^{12}6^2$) $(\text{H}_2\text{O})_{24}$ cluster that together with the D-cage constitute the unit cell of structure I (sI) hydrate lattice.

We employed a four-step hierarchical procedure to determine the global minimum and the low-energy networks of the T-cage $(\text{H}_2\text{O})_{24}$ cluster: (i) all possible 3,043,836 symmetry-distinct configurations were classified using the Strong-Weak Effective Bond (SWEB) discrete model into groups depending on the maximum number of the strongest hydrogen bonds. For the T-cage $(\text{H}_2\text{O})_{24}$ cluster there are 321 symmetry-distinct isomers of with a maximum number of 9 ‘strong’ H-bonds, (ii) the relative energies of those 321 low-lying candidates predicted with the SEWB model were refined via geometry optimizations with the TIP4P, TTM2.1-F and TTM3-F interaction potentials for water, (iii) the lowest 66 networks obtained from the classical water potential results were refined by full geometry optimization at the density functional theory (DFT) level with the B3LYP functional (B3LYP) and (iv) the final list of low-energy networks was determined by full geometry optimization of the first 18 low-lying DFT minima at the second order Møller-Plesset perturbation (MP2) level of theory with Dunning’s augmented correlation-consistent basis set of double- (aug-cc-pVDZ) and triple- ζ

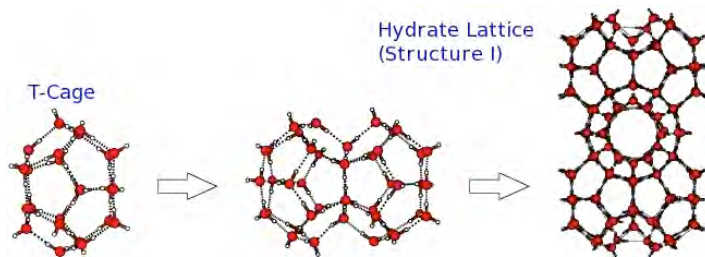


Figure 2: Procedure for constructing periodic unit cells of structure I (sI) hydrate lattice starting from any of the low-lying energy networks of the constituent T-cage.

This ‘bottom-up’ procedure allows for the identification of low-lying networks of the T-cage which can be used for constructing 3-D periodic networks of the (sI) hydrate lattice starting from any of the low-energy networks of the T-cage (see Fig. 2).

We plan to initiate work on identifying the low-lying networks of the larger hexakaidecahedron (H-cage, $5^{12}6^4$) $(\text{H}_2\text{O})_{28}$ cluster and use them to construct unit cells of the structure II (sII) hydrate lattice. These periodic networks of the (sI) and (sII) hydrate will be used

as models for the accommodation of host molecules (such as H₂, CH₄, CH₃OH and H₂S) using both classical potentials and periodic density functional based electronic structure calculations.

Acknowledgements: This research was performed in part using the computational resources of the National Energy Research Supercomputing Center (NERSC) at Lawrence Livermore National Laboratory and the Molecular Sciences Computing Facility (MSCF) at the Environmental Molecular Sciences Laboratory, a national scientific user facility sponsored by the Department of Energy's Office of Biological and Environmental Research located at Pacific Northwest National Laboratory. Battelle operates PNNL for the US Department of Energy.

References to publications of DOE sponsored research (2006-present)

1. G. S. Fanourgakis and S. S. Xantheas, "The flexible, polarizable, Thole-type interaction potential for water (TTM2-F) revisited" *Journal of Physical Chemistry A* **110**, 4100 (2006)
2. G. S. Fanourgakis and S. S. Xantheas, "The bend angle of water in ice Ih and liquid water: The significance of implementing the non-linear monomer dipole moment surface in classical interaction potentials" *Journal of Chemical Physics* **124**, 174504 (2006). Featured in the *Virtual Journal of Biological Physics Research*.
3. K. A. Ramazan, L. M. Wingen, Y. Miller, G. M. Chaban, R. B. Gerber, S. S. Xantheas and B. J. Finlayson-Pitts, "New Experimental and Theoretical Approach to the Heterogeneous Hydrolysis of NO₂: Key Role of Molecular Nitric Acid and Its Complexes", *Journal of Physical Chemistry A* **110**, 6886 (2006)
4. T. A. Blake, S. S. Xantheas, "The Structure, Anharmonic Spectra and Puckering Barrier of Cyclobutane: A Theoretical Study", *Journal of Physical Chemistry A* **110**, 10487 (2006)
5. S. S. Xantheas, "Anharmonic vibrational spectra of hydrogen bonded clusters: Comparison between higher energy derivative and mean-field grid based methods", Roger E. Miller memorial issue (invited), *International Reviews in Physical Chemistry* **25**, 719 (2006)
6. G. S. Fanourgakis, G. K. Schenter and S. S. Xantheas, "A quantitative account of quantum effects in liquid water", *Journal of Chemical Physics* **125**, 141102 (2006). Featured in the *Virtual Journal of Ultrafast Science*, November 2006
7. S. Bulusu, S. Yoo, E. Aprà, S. S. Xantheas, X. C. Zeng, "The lowest energy structures of water clusters (H₂O)₁₁ and (H₂O)₁₃", *Journal of Physical Chemistry A* **110**, 11781 (2006)
8. G. S. Fanourgakis, V. Tipparaju, J. Nieplocha and S. S. Xantheas, "An efficient parallelization scheme for molecular dynamics simulations with many-body, flexible, polarizable empirical potentials: Application to water", *Theoretical Chemistry Accounts* **117**, 73 (2007)
9. T. Pankewitz, A. Lagutschenkov, G. Niedner-Schatteburg, S. S. Xantheas, Y.-T. Lee, "The Infrared Spectrum of NH₄⁺(H₂O): Evidence for mode specific fragmentation", *Journal of Chemical Physics* **126**, 074307 (2007)
10. M. N. Slipchenko, B. G. Sartakov and A. F. Vilesov, S. S. Xantheas, "A study of NH stretching vibrations in small ammonia clusters by infrared spectroscopy in He droplets and *ab-initio* calculations", Roger E. Miller memorial issue (invited), *Journal of Physical Chemistry A* **111**, 7460 (2007)
11. L. Rubio-Lago, D. Zaouris, Y. Sakellariou, D. Sofikits and T. N. Kitsopoulos, F. Wang and X. Yang, B. Cronin and M. N. R. Ashfold, S. S. Xantheas, "Photofragment slice imaging studies of pyrrole and the Xe⁺pyrrole cluster", *Journal of Chemical Physics* **127**, 064306 (2007)
12. T. A. Blake, E. D. Glendening, R. L. Sams, S. W. Sharpe and S. S. Xantheas, "High Resolution Infrared Spectroscopy in the 1200 to 1300 cm⁻¹ Region and Accurate Theoretical Estimates for the Structure and Ring Puckering Barrier of Perfluorocyclobutane", Thom H. Dunning Jr. Festschrift (invited), *Journal Physical Chemistry A* **111**, 11328 (2007)
13. G. S. Fanourgakis and S. S. Xantheas, "Development of Transferable Interaction Potentials for Water: V. Extension of the flexible, polarizable, Thole-type Model potential (TTM3-F, v. 3.0) to describe the vibrational spectra of water clusters and liquid water", *Journal of Chemical Physics* **128**, 074506 (2008)

14. S. M. Kathmann, G. K. Schenter and S. S. Xantheas, “On the Determination of Monomer Dissociation Energies of Small Water Clusters from Photoionization Experiments”, *Journal of Physical Chemistry A*, **112**, 1851 (2008)
15. M. V. Kirov, G. S. Fanourgakis and S. S. Xantheas, “Identifying the Most Stable Networks in Polyhedral Water Clusters”, Frontiers article (invited), *Chemical Physics Letters* **461**, 180 (2008). Journal cover
16. M. L. Lipciuc, F. Wang, X. Yang and T. N. Kitsopoulos, G. S. Fanourgakis and S. S. Xantheas, “Cluster-Controlled Photofragmentation: The Case of the Xe-Pyrrole Cluster”, Communication to the Editor, *ChemPhysChem* **9**, 1938 (2008)
17. S. S. Xantheas, “Dances with Hydrogen Cations” *Nature* **457**, 673 (2009). Invited *News & Views* article
18. S. S. Xantheas, G. A. Voth, “Aqueous Solutions and their Interfaces”, *Journal of Physical Chemistry B* **113**, 3997 (2009)
19. C. D. Wick and S. S. Xantheas, “Computational Investigation of the First Solvation Shell Structure of Interfacial and Bulk Aqueous Chloride and Iodide Ions”, Special Issue on Aqueous solutions and their Interfaces (invited), *Journal of Physical Chemistry B* **113**, 4141 (2009). Journal cover
20. S. Yoo, M. V. Kirov and S. S. Xantheas, “Lowest energy networks of the T-cage (H₂O)₂₄ cluster and their use in constructing unit cells of the structure I hydrate lattice”, Communication to the Editor, *Journal of the American Chemical Society* **131**, 7564 (2009). Highlighted in the “Science Concentrates” section, Chemical & Engineering News, June 1st (2009). Selected for DOE National Impact feature article
21. S. Yoo, X. C. Zeng and S. S. Xantheas, “On the phase diagram of water with density functional potentials: the melting temperature of ice I_h with the Perdew–Burke–Ernzerhof and Becke–Lee–Yang–Parr functionals”, Communication to the Editor, *Journal of Chemical Physics* **130**, 221102 (2009). Featured in the *Virtual Journal of Biological Physics Research*. 3rd most downloaded paper in July 2009
22. X.-B. Wang, J. Werhahn, L.-S. Wang, K. Kowalski, A. Laubereau and S. S. Xantheas, “Observation of a remarkable temperature effect in the hydrogen bonding structure and dynamics of the CN⁻(H₂O) cluster”, Letter to the Editor, *Journal of Physical Chemistry A* **113**, 9579 (2009). Journal cover
23. N. Hontama, Y. Inokuchi, T. Ebata, C. Dedonder-Lardeux, C. Jouvet, and S. S. Xantheas, “The structure of the Calix[4]arene-(H₂O) cluster, *world’s smallest cup of water*”, *Journal of Physical Chemistry A*, ASAP article: DOI:10.1021/jp902967q (2009)
24. F. Paesani, S. S. Xantheas and G. A. Voth, “Infrared Spectroscopy and Hydrogen-Bond Dynamics of Liquid Water from Centroid Molecular Dynamics with an Ab Initio-Based Force Field”, *Journal of Physical Chemistry B*, ASAP article: DOI: 10.1021/jp907648y (2009)
25. X. Sun, S. Yoo, S. S. Xantheas, L. X. Dang, “The reorientation mechanism of hydroxide ions in water: A molecular dynamics study”, Frontiers article (invited), *Chemical Physics Letters*, ASAP article: DOI: 10.1016/j.cplett.2009.09.004 (2009)
26. E. Aprà, R. J. Harrison, W. A. deJong, A. P. Rendell, V. Tipparaju, S. S. Xantheas, “Liquid Water: Obtaining the right answer for the right reasons”, *SC’09: Proceedings of the 2009 ACM/IEEE conference on Supercomputing* (accepted). Considered in the final round for the Gordon-Bell price (2009)
27. S. Yoo and S. S. Xantheas, “The role of hydrophobic surfaces in altering the water-mediated peptide-peptide interactions in an aqueous environment”, *Physical Chemistry Chemical Physics* (submitted)
28. S. Yoo, S. S. Xantheas, X. C. Zeng, “The melting temperature of Bulk Silicon from *Ab initio* Molecular Dynamics Simulations” *Chemical Physics Letters* (submitted)
29. S. Pandelov, J. C. Werhahn, B. Pilles, S. S. Xantheas, and H. Iglev, “A simple criterion governing the formation of aqueous salt hydrates”, *Angewandte Chemie International Edition* (submitted)
30. J. R. Hammond, N. Govind, K. Kowalski, J. Autschbah, S. S. Xantheas, “Accurate dipole polarizabilities for water clusters $n=2-12$ at the Coupled Cluster level of theory and benchmarking of various density functionals” *Journal of Chemical Physics* (submitted)

The Quest for Ultimate Sensitivity in Nonlinear Optical Imaging

Sunney Xie, Wei Min, Christian Freudiger, Brian Saar, Sijia Lu, Shasha Cong, Gary Holtom

Department of Chemistry and Chemical Biology, Harvard University
12 Oxford Street, Cambridge, MA 02138
e-mail: xie@chemistry.harvard.edu

Label-free chemical contrast is highly desirable in molecular imaging. Spontaneous Raman microscopy provides specific vibrational signatures of chemical bonds, but is often hindered by low sensitivity. We reported a three-dimensional multiphoton vibrational imaging technique based on stimulated Raman scattering (SRS) [3]. The sensitivity of SRS imaging is significantly greater than that of spontaneous Raman microscopy, which is achieved by implementing high-frequency (megahertz) phase-sensitive detection. SRS microscopy has a major advantage over previous coherent Raman techniques, such as CARS, in that it offers background-free and readily interpretable chemical contrast. We have shown a variety of applications of this new imaging modality.

Many chromophores absorb but have undetectable fluorescence because the spontaneous emission is dominated by their fast nonradiative decays. Yet their absorption is too weak to be detected by an optical microscope. We have made the chromophores detectable by a new contrast mechanism for optical microscopy based on stimulated emission, which competes effectively with the nonradiative decay [1]. In a dual-beam pump-probe experiment, upon photo-excitation by a pump pulse, the sample is stimulated down to the ground state by a time-delayed probe pulse, the intensity of which is concurrently increased. Similar to SRS microscopy, we extract the miniscule intensity increase with shot-noise-limited sensitivity by using a lock-in amplifier and intensity modulation of the pump beam at a high megahertz frequency. In contrast, conventional one-beam absorption measurement exhibits low sensitivity, lack of three-dimensional sectioning capability, and complication by sample scattering. We have demonstrated a variety of applications of stimulated emission microscopy, for which the sensitivity is orders of magnitude higher than for spontaneous emission or absorption contrast, permitting nonfluorescent reporters for molecular imaging.

Publications of DOE/BES Sponsored Research

1. Min, Wei; Lu, Sijia; Chong, Shasha; Roy, Rahul; Holtom, Gary R.; Xie, X. Sunney, "Imaging chromophores with undetectable fluorescence by stimulated emission microscopy," *Nature*, in press.
2. Min, Wei; Xie, X. Sunney; Bagchi, "Role of Conformational Dynamics in Kinetics of an Enzymatic Cycle in a Nonequilibrium Steady State," *J. Chem. Phys.*, **131**, 065104 (2009).
3. Freudiger, Christian W.; Min, Wei; Saar, Brian G.; Lu, Sijia; Holtom, Gary R.; He, Chengwei; Tsai, Jason C; Kang, Jing X.; Xie, X. Sunney "Label-Free Biomedical Imaging with High Sensitivity by Stimulated Raman Scattering Microscopy," *Science*, **322**, 1857-1861 (2008).
4. Min, Wei; Xie, X. Sunney; Bagchi, Biman "Two-Dimensional Reaction Free Energy Surfaces of Catalytic Reaction: Effects of Protein Conformational Dynamics on Enzyme Catalysis," *J. Phys. Chem. B*, **112**, 454 (2008).
5. Luo, Guobin; Wang, Mina; Konigsberg, William H.; Xie, X. Sunney "Single-molecule and Ensemble Fluorescence Assays for a Functionally Important Conformational Change in T7 DNA Polymerase," *PNAS*, **104**, 12610 (2007).
6. Min, Wei; Gopich, Irina V.; English, Brian P.; Kou, Sam C.; Xie, X. Sunney.; Szabo, Attila "When Does the Michaelis-Menten Equation Hold for Fluctuating Enzymes?" *J. Phys. Chem. B*, **110**, 20093 (2006).
7. Luo, Guobin; Andricioaei, Ioan; Xie, X. Sunney; Karplus, Martin "Dynamic Distance Disorder in Proteins Is Caused by Trapping," *J. Phys. Chem. B*, **110**, 9363 (2006).
8. Min, Wei; Xie, X. Sunney "Kramers Model with a Power-law Friction Kernel: Dispersed Kinetics and Dynamic Disorder of Biochemical Reactions," *Phys. Rev. E*, **73**, 010902 (2006).
9. Min, Wei; Jiang, Liang; Yu, Ji; Kou, S.C.; Qian, Hong; Xie, X. Sunney "Nonequilibrium Steady State of a Nanometric Biochemical System: Determining the Thermodynamic Driving Force from Single Enzyme Turnover Time Traces," *Nano Lett.*, **5**, 2373 (2005).
10. Min, Wei; Luo, Guobin; Cherayil, Binny J.; Kou, S.C.; Xie, X. Sunney "Observation of a Power-Law Memory Kernel for Fluctuations within a Single Protein Molecule," *Phys. Rev. Lett.*, **94**, 198302 (2005).
11. Min, Wei; English, Brian P.; Luo, Guobin; Cherayil, Binny J.; Kou, S.C.; Xie, X. Sunney "Fluctuating Enzymes: Lessons from Single-Molecule Studies," *Acc. Chem. Res.*, **38**, 923 (2005).

*Author Index
and
List of Participants*

Author Index

Ahmed, M.....	5	Khalil, M.....	143
Anderson, S.	9	Kimmel, G	145
Balasubramanian, K	13	LaVerne, J.	149, 153, 23
Bartels, D.....	17, 23	Leone, S.	5
Baruah, T.....	21	Liu, D.-J.....	77
Beck, K	111	Lu, H.P.....	157
Bentley, J.....	17	Lu, S.	239
Camillone, N.	223	Lymar, S.V.	161
Carmichael, I	23, 153	Meisel, D.	153
Carter, E.....	1	Miller, J.R.....	43
Castleman, Jr., A	27	Min, W.....	239
Ceyer, S.	31	Morse, M.	165
Chandler, D.	35	Mundy, C.....	169
Chipman, D.	39, 17, 23, 153	Ogut, S.....	173
Cong, S.	239	Osgood, R.	177
Cook, A.R.....	43	Petek, H.....	181
Cowin, J.....	47	Petrik, N.....	145
Crowell, R.A.....	51	Raghavachari, K	127
Dang, L.....	55	Rossky, P	3
Dohnálek, Z.....	139	Saar, B.	239
Duncan, M.....	59	Saykally, R.....	185
Dupuis, M.....	63	Schenter, G.	189
Eisenthal, K.	65	Smith, R. S.....	139
Ellison, G.B.....	69	Sibener, S.J.	193
El-Sayed, M.....	73	Steimle, T.....	197
Evans, J.....	77	Swanson, J.M.J.	201
Fayer, M.	81	Thompson, W.	203
Fernandez-Serra, M.V.	85	Tokmakoff, A.	207
Freudiger, C.	239	Tully, J.	211
Fulton, J.	89	Valiev, M.....	215
Garrett, B.....	215	Wang, L.-S.....	219
Geissler, P.L.	93	Wang, X.-B.....	219
Gordon, M.	97	White, M.G.	223
Harris, C.	101	Wilson, K.	5
Harris, A.L.....	223	Wishart, J.....	227
Harrison, I.....	105	Wodtke, A.....	231
Hayden, C.....	107	Xantheas, S.	235
Hess, W.	111	Yang, H.....	107
Hirata, S.....	115	Xie, S.	239
Ho, W.	119		
Holtom, G.....	239		
Jackson, B.....	123		
Jarrold, C.	127		
Johnson, M.	131		
Joly, A.	109		
Jordan, K.	129		
Kathmann, S.	133		
Kay, B.....	137		

Participants

Musahid Ahmed
Lawrence Berkeley National Laboratory
MS 6R-2100, 1 Cyclotron Road
Berkeley, CA 94720
Email: mahmed@lbl.gov
Phone: 510-486-6355

Krishnan Balasubramanian
California State University, East Bay
25800 Carlos Bee Blvd.
College of Science
Hayward, CA 94542
Email: kris.bala@csueastbay.edu
Phone: 925-422-4984

Tunna Baruah
University of Texas at El Paso
Dept. of Physics
500 W. University Avenue
El Paso, TX 79968
Email: tbaruah@utep.edu
Phone: 915-747-7529

Ian Carmichael
Notre Dame Radiation Laboratory
University of Notre Dame
Notre Dame, IN 46556
Email: carmichael.1@nd.edu
Phone: 574-631-4502

Michael Casassa
DOE/Office of Basic Energy Sciences
19901 Germantown Road
Germantown, MD 20874
Email: michael.casassa@science.doe.gov
Phone: 301-903-0448

Sylvia Ceyer
MIT
77 Mass Ave, 6-217
Cambridge, MA 02139
Email: stceyer@mit.edu
Phone: 617-253-4537

Daniel Chipman
Notre Dame Radiation Laboratory
University of Notre Dame
Notre Dame, IN 46556
Email: chipman.1@nd.edu
Phone: 574-631-5562

Scott Anderson
University of Utah
Chemistry Department
315 S. 1400 E.
Salt Lake City, UT 84112
Email: anderson@chem.utah.edu
Phone: 801-585-7289

David Bartels
Notre Dame University
Radiation Laboratory
Notre Dame, IN 46556
Email: bartels.5@nd.edu
Phone: 574-631-5561

Nicholas Camillone
Brookhaven National Laboratory
Chemistry Department
Building 555
Upton, NY 11973
Email: nicholas@bnl.gov
Phone: 631-344-4412

Emily Carter
Princeton University
Olden Street, Equad
Suite D404A
Princeton, NJ 08544
Email: eac@princeton.edu
Phone: 609-258-5391

A. Welford Castleman
Penn State University
104 Chemistry Building
University Park, PA 16802
Email: awc@psu.edu
Phone: 814-865-7242

David Chandler
University of California, Berkeley
Department of Chemistry
Berkeley, CA 94720
Email: chandler@cchem.berkeley.edu
Phone: 510-643-6821

Andrew Cook
Brookhaven National Lab
Bldg. 555 Chemistry
Upton, NY 11973
Email: acook@bnl.gov
Phone: 631-344-4782

Participants

James Cowin
Pacific Northwest National Laboratory
3335 Q Ave
Richland, WA 99354
Email: jp.cowin@pnl.gov
Phone: 509-371-6167

Robert Crowell
Brookhaven National Laboratory
PO Box 5000
Upton, NY 11973
Email: crowell@bnl.gov
Phone: 631-344-4515

Liem Dang
Pacific Northwest National Laboratory
PO Box 999, K1-83
Richland, WA 99352
Email: liem.dang@pnl.gov
Phone: 509-375-2557

Michael Duncan
University of Georgia
Department of Chemistry
Athens, GA 30602
Email: maduncan@uga.edu
Phone: 706-542-1998

Michel Dupuis
Pacific Northwest National Laboratory
PO Box 999, K1-83
Richland, WA 99352
Email: michel.dupuis@pnl.gov
Phone: 509-375-2617

Kenneth Eisenthal
Columbia University
3000 Broadway MC 3107
New York, NY 10027
Email: kbe1@columbia.edu
Phone: 212-854-3175

Barney Ellison
University of Colorado
Department of Chemistry & Biochemistry
Boulder, CO 80309
Email: barney@jila.colorado.edu
Phone: 303-492-8603

Mostafa El-Sayed
Georgia Tech
579 Westover Dr
Atlanta, Ga 30305
Email: melsayed@gatech.edu
Phone: 404-352-0453

James Evans
Ames Laboratory USDOE
315 Wilhelm Hall, Iowa State University
Ames, IA 50011
Email: evans@ameslab.gov
Phone: 515-294-1638

Michael Fayer
Stanford University
Department of Chemistry
Stanford, CA 94305
Email: fayer@stanford.edu
Phone: 650-723-4446

Maria Victoria Fernandez-Serra
Stony Brook University
Physics and Astronomy Dept.
Stony Brook, NY 11794
Email: maria.fernandez-serra@stonybrook.edu
Phone: 631-632-8244

Gregory Fiechtner
DOE/Office of Basic Energy Sciences
19901 Germantown Road
SC-22.11 Germantown, MD 20874
Email: gregory.fiechtner@science.doe.gov
Phone: 301-903-5809

John Fulton
Pacific Northwest National Laboratory
PO Box 999, K2-57
Richland, WA 99352
Email: john.fulton@pnl.gov
Phone: 509-375-2091

Bruce Garrett
Pacific Northwest National Laboratory
PO Box 999 (K9-90)
Richland, WA 99352
Email: bruce.garrett@pnl.gov
Phone: 509-372-6344

Participants

Phillip L. Geissler
Lawrence Berkeley National Laboratory/UC Berkeley
207 Gilman, MS: 1460
Berkeley, CA 94720
Email: geissler@cchem.berkeley.edu
Phone: 510-642-8716

Jeffrey Guest
Center for Nanoscale Materials
Argonne National Laboratory
9700 S. Cass Ave
Lemont, IL 60439
Email: jrguest@anl.gov
Phone: 630-252-7073

Charles Harris
University of California
Department of Chemistry
Berkeley, CA 94720
Email: cbharris@berkeley.edu
Phone: 510-642-2814

Carl Hayden
Sandia National Laboratories
P. O. Box 969, MS 9055
Livermore, CA 94551
Email: cchayde@sandia.gov
Phone: 925-294-2298

So Hirata
University of Florida
P.O. Box 118435
Gainesville, FL 32611
Email: hirata@qtp.ufl.edu
Phone: 352-392-6976

Bret Jackson
UMass Amherst
Dept. of Chemistry
Amherst, MA 01003
Email: jackson@chem.umass.edu
Phone: 413-545-2583

Mark Johnson
Yale University
P.O. Box 208107
New Haven, CT 06520
Email: mark.johnson@Yale.edu
Phone: 203-432-5226

Mark Gordon
Ames Laboratory
201 Spedding Hall - Iowa State University
Ames, IA 50011
Email: mark@si.msg.chem.iastate.edu
Phone: 515-294-0452

Alexander Harris
Brookhaven National Laboratory
Chemistry Department
Building 555, PO Box 5000
Upton, NY 11973
Email: alexh@bnl.gov
Phone: 631-344-4301

Ian Harrison
University of Virginia
Dept of Chemistry
Charlottesville, VA 22904
Email: harrison@virginia.edu
Phone: 434-924-3639

Wayne Hess
Pacific Northwest National Lab
902 Battelle Blvd
Richland, WA 99352
Email: wayne.hess@pnl.gov
Phone: 509-371-6140

Wilson Ho
University of California, Irvine
4129 Frederick Reines Hall
Irvine, CA 92697
Email: wilsonho@uci.edu
Phone: 949-824-5234

Caroline Jarrold
Indiana University
Department of Chemistry
800 E. Kirkwood Avenue
Bloomington, IN 47405
Email: cjarrold@indiana.edu
Phone: 812-856-1190

Kenneth Jordan
University of Pittsburgh
Pittsburgh, PA 15260
Email: jordan@pitt.edu
Phone: 412-624-8690

Participants

Shawn Kathmann
Pacific Northwest National Laboratory
PO Box 999, K1-83
Richland, WA 99352
Email: shawn.kathmann@pnl.gov
Phone: 509-375-2870

Munira Khalil
University of Washington
Department of Chemistry
Box 351700
Seattle, WA 98195
Email: mkhalil@chem.washington.edu
Phone: 206-543-6682

Jay LaVerne
University of Notre Dame
314 Radiation Laboratory
Notre Dame, IN 46556
Email: laverne.1@nd.edu
Phone: 574-631-5563

Sergei Lymar
Brookhaven National Laboratory
Chemistry Department
Upton, NY 11973
Email: lymar@bnl.gov
Phone: 631-344-4333

Dan Meisel
University of Notre Dame
Radiation Lab
Notre Dame, IN 46556
Email: dani@nd.edu
Phone: 574-631-5457

John R. Miller
Brookhaven National Lab
Bldg. 555 Chemistry
Upton, NY 11973
Email: jrmiller@bnl.gov
Phone: 631-344-4354

Christopher Mundy
Pacific Northwest National Laboratory
PO Box 999, K1-83
Richland, WA 99352
Email: chris.mundy@pnl.gov
Phone: 509-375-2024

Bruce Kay
Pacific Northwest National Laboratory
K8-88, PO Box 999
Richland, WA 99352
Email: bruce.kay@pnl.gov
Phone: 509-371-6143

Greg Kimmel
Pacific Northwest National Laboratory
MSIN K8-88
Chemical & Materials Sciences Div.
Richland, WA 99352
Email: gregory.kimmel@pnl.gov
Phone: 509-371-6134

H. Peter Lu
Bowling Green State University
Department of Chemistry
Center for Photochemical Sciences
Bowling Green, OH 43403
Email: hplu@bgsu.edu
Phone: 419-372-1840

Diane Marceau
Department of Energy
170 Poinsett Lane
Frederick, MD 21702
Email: diane.marceau@science.doe.gov
Phone: 301-360-9873

John Miller
DOE/Office of Basic Energy Sciences
1000 Independence Ave., SW
SC-22.1 Germantown Bldg
Germantown, MD 20585
Email: john.miller@science.doe.gov
Phone: 301-903-5806

Michael Morse
University of Utah, Department of Chemistry
315 S. 1400 East, Room 2020
Salt Lake City, UT 84112
Email: morse@chem.utah.edu
Phone: 801-581-8319

Serdar Ogut
University of Illinois at Chicago
845 West Taylor Street (M/C 273)
Chicago, IL 60607
Email: ogut@uic.edu
Phone: 312-413-2786

Participants

Richard Osgood
Columbia University
345 Quaker St.
Chappaqua, NY 10514
Email: osgood@columbia.edu
Phone: 212-854-4462

Hrvoje Petek
University of Pittsburgh
Department of Physics and Astronomy
Pittsburgh, PA 15260
Email: petek@pitt.edu
Phone: 412-624-3599

Larry Rahn
DOE/Office of Basic Energy Sciences
19901 Germantown Road
Germantown, MD 20874
Email: Larry.Rahn@science.doe.gov
Phone: 301-903-2508

Peter Rossky
University of Texas at Austin
1 University Station, A5300
Austin, TX 78731
Email: ROSSKY@MAIL.UTEXAS.EDU
Phone: 512-471-3555

Gregory Schenter
Pacific Northwest National Laboratory
PO Box 999, K1-83
Richland, WA 99352
Email: greg.schenter@pnl.gov
Phone: 509-375-4334

Wade Sisk
DOE/Office of Basic Energy Sciences
1000 Independence Ave. SW
Washington, DC 20585
Email: wade.sisk@science.doe.gov
Phone: 301-903-5692

Jessica Swanson
University of Utah
315 S. 1400 E., RM. 2020
Salt Lake City, UT 84112
Email: jswanson@hec.utah.edu
Phone: 801-581-5419

Mark Pederson
DOE/Office of Basic Energy Sciences
1000 Independence Ave., SW
SC-22.1 Germantown Bldg
Germantown, MD 20585
Email: Mark.Pederson@science.doe.gov
Phone: 301-903-9956

Krishnan Raghavachari
Indiana University
800 E. Kirkwood Avenue
Bloomington, IN 47405
Email: kraghava@indiana.edu
Phone: 812-856-1766

Eric Rohlfing
Department of Energy
19901 Germantown Road
Germantown, MD 20874
Email: eric.rohlfing@science.doe.gov
Phone: 301-903-8165

Richard Saykally
University of California, Berkeley
Department of Chemistry
D31 Hildebrand Hall
Berkeley, CA 94720
Email: saykally@berkeley.edu
Phone: 510-642-8269

Steven Sibener
University of Chicago
James Franck Institute, GCIS-E215
929 East 57th Street
Chicago, IL 60637
Email: s-sibener@uchicago.edu
Phone: 773-702-7193

Timothy C. Steimle
Arizona State University
Department of Chemistry and Biochemistry
Tempe, AZ 85287
Email: TSteimle@asu.edu
Phone: 480-965-3265

Ward Thompson
University of Kansas
Department of Chemistry
Lawrence, KS 66045
Email: wthompson@ku.edu
Phone: 785-864-3980

Participants

Andrei Tokmakoff
Massachusetts Institute of Technology
77 Mass. Ave., Room 6-213
Cambridge, MA 02143
Email: tokmakof@mit.edu
Phone: 617-253-4503

John Tully
Yale University
225 Prospect Street
New Haven, CT 06520
Email: john.tully@yale.edu
Phone: 203-432-3934

Marat Valiev
Pacific Northwest National Lab
902 Battelle Blvd, PO Box 999, K8-91
Richland, WA 99352
Email: marat.valiev@pnl.gov
Phone: 509-371-6459

Lai-Sheng Wang
Brown University
Department of Chemistry
Providence, RI 02912
Email: ls.wang@pnl.gov
Phone: 509-371-6138

Xue-Bin Wang
Pacific Northwest National Lab
Chemical & Materials Sciences Division
902 Battelle Boulevard, P. O. Box 999, MS K8-88
Richland, WA 99352
Email: xuebin.wang@pnl.gov
Phone: 509-371-6132

Michael White
Brookhaven National Laboratory
Chemistry Department
Upton, NY 11973
Email: mgwhite@bnl.gov
Phone: 631-344-4343

James Wishart
Brookhaven National Laboratory
Chemistry Department
Upton, NY 11973
Email: wishart@bnl.gov
Phone: 631-344-4327

Alec Wodtke
UC Santa Barbara
Dept of Chemistry and Biochemistry
Santa Barbara, CA 93106
Email: wodtke@chem.ucsb.edu
Phone: 805-893-8085

Sotiris Xantheas
Pacific Northwest National Laboratory
PO Box 999, K1-83
Richland, WA 99352
Email: sotiris.xantheas@pnl.gov
Phone: 509-375-3684

Xiaoliang Sunney Xie
Harvard University
12 Oxford Street
Cambridge, MA 02138
Email: xie@chemistry.harvard.edu
Phone: 617-496-9925

Hua-Gen Yu
Brookhaven National Laboratory
Chemistry Department
Upton, NY 11973
Email: hgy@bnl.gov
Phone: 631-344 4367